VACUUM

The International Journal and Abstracting Service

for

VACUUM SCIENCE AND TECHNOLOGY

Vol.
9
959/60

VOLUME 9

(1959-60)

PERGAMON PRESS

OXFORD · LONDON · NEW YORK · PARIS

VACUUM

The International Journal and Abstracting Service for Vacuum Science and Technology and their Applications in Research and Industry

BOARD OF EDITORS

Mr. A. S. D. BARRETT, Finsbury Pavement House, 120, Moorgate, London, E.C.2.

Mr. A. H. BECK, Engineering Laboratories, University of Cambridge, Trumpington Street, Cambridge.

Mr. B. B. DAYTON, Technical Director, Consolidated Vacuum Corp., 1775, Mt. Read Blvd., Rochester 3, N.Y., U.S.A.

Dr. J. M. DUNOYER, École Nationale Supérieure de Mécanique de Nantes, Université de Rennes, 3, rue Marechal-Joffre, Nantes, France.

Professor Dr. R. JAECKEL, Physikalisches Institut der Universität, Abt. Vakuum, Nussallee 6, Bonn, Germany.

Mr. W. G. MATHESON, Sylvania Electric Products, Inc., 60, Boston Street, Salem, Mass., U.S.A.

Mr. P. A. REDHEAD, National Research Council, Radio and Electrical Engineering Division, Ottawa, Canada.

Professor Dr. E. THOMAS, École Royale Militaire, Centre des Sciences Nucléaires, 30, Avenue de la Renaissance, Bruxelles 4, Belgium.

Mr. J. YARWOOD, Head of the Department of Mathematics and Physics, The Polytechnic, 309, Regent Street, London, W.1.

Secretary to the Board of Editors: G. E. SATTERTHWAITE

HONORARY INTERNATIONAL EDITORIAL ADVISORY BOARD

E. N. DA C. ANDRADE (London)
C. H. BACHMAN (Syracuse)
C. BALAKRISHNAN (Bombay)
J. BLEARS (Manchester)
R. N. BLOOMER (Aldermaston, Berks)
J. R. BOWMAN (Evanston)
H. L. J. BURGESS (London)
J. H. CARMICHAEL (New Hyde Park, N.Y.)
K. DIELS (Köln)
L. DUNOYER (Paris)
H. EBERT (Braunschweig)
F. D. EDWARDS (Crawley—*Joint Chairman*)
A. J. GALE (Burlington, Mass.)
C. L. GOULD (Brookhaven)
A. GUTHRIE (San Francisco)
W. HAENLEIN (Nürnberg)
C. HAYASHI (Tokyo)
K. C. D. HICKMAN (Rochester, N.Y.—*Joint Chairman*)
H. KLUMB (Mainz)
W. H. KOHL (Los Altos, Calif.)
J. H. LECK (Liverpool)
G. LEWIN (Princeton, N.J.)
A. LORENZ (Hainau-am-Main)
C. LOVINFOSSE (Bruxelles)
I. R. MAXWELL (Publisher)
C. R. MEISSNER (Atlanta, Georgia)
G. L. MUNDAY (Genève)
H. NAKAGAWA (Tokyo)
N. OCHERT (Israel)
G. W. OETJEN (Köln)
J. POLLARD (Baldock, Herts)
P. DELLA PORTA (Milano)
L. E. PREUSS (Detroit)
W. PUPP (Giessen)
L. RIDDIFORD (Birmingham)
N. W. ROBINSON (Salford)
D. J. SANTELER (Schenectady)
K. SCHAEFER (Frankfurt-am-Main)
R. F. STRICKLAND-CONSTABLE (London)
E. A. TRENDELENBURG (Balzers)
A. H. TURNBULL (Harwell)
H. VON UBISCH (Sweden)
A. VENEMA (Eindhoven)
M. W. WELCH (Chicago)
O. WINKLER (Liechtenstein)

Publishing Offices: Headington Hill Hall, Oxford (Oxford 64881)

Annual subscription (including postage) :

(A) For libraries, government establishments and research institutions £10 ($28.00)

(B) For individuals who write directly to the publisher and certify that the journal is for their personal use £5 5s. ($15.00)

Copyright © 1960 Pergamon Press Ltd.

PERGAMON PRESS LTD

Headington Hill Hall, Oxford

122 East 55th Street, New York 22, N.Y.

Vo 9 1959

CONTENTS OF VOLUME 9

Number 1

page

J. BOUNDEN and J. ROTBLAT : Vacuum in Medicine .. 1

O. S. HEAVENS, M. M. BROWN and V. HINTON : The Structure and Density of Iron Films formed by Thermal Evaporation .. 17

N. S. VERMA and T. W. G. ROWE : The Breakage of Glass Ampoules during Freeze-drying .. 21

F. SCHOSSBERGER and K. D. FRANSON : Adhesion of Evaporated Metal Films .. 28

L. DUNOYER : Les Bases Expérimentales de la Théorie Cinétique des Gaz .. 36

E. N. DA C. ANDRADE : The History of the Vacuum Pump .. 41

N. W. ROBINSON and F. BERZ : Initial Pumping and Recovery of Ionization Gauges .. 48

A. VENEMA : The Production of Ultra-high Vacua by Means of a Diffusion Pump .. 54

W. H. KOHL : Design Approaches for Electron Devices Operating in Critical Environments, Especially Ceramic-envelope Tubes for High-temperature Operation .. 58

C. L. GOULD : Vacuum System for a Thirty Billion Electron Volt Particle Accelerator .. 63

Book Review

" Optics of Thin Films ", by A. VAŠÍČEK (Reviewed by E. Wolf) .. 69

Abstracts of Communications presented at the First International Congress on Vacuum Techniques .. 70

Vol. 9 959/60

Number 2

D. ALPERT : Recent Advances in Ultra-high Vacuum Technology .. 89

R. G. HERB : Evapor-ion Pump Development at the University of Wisconsin .. 97

M. L. LYUBIMOV, K. P. SHAKHOV and YA. A. YUKHVIDIN : Experience in Designing and Manufacturing All-Metal Vacuum Systems .. 108

I. A. KALJABINA and YA. A. YUKHVIDIN : Experience in Using Mass-Spectrometric Methods in Electro-Vacuum Technology .. 117

P. C. BANBURY, G. A. BARNES, D. HANEMAN and E. W. J. MITCHELL : The Attainment of Clean Surfaces by Breaking Crystals in Ultra-high Vacuum .. 126

R. C. MARKER : Vacuum Techniques and Components used for a Continuously Pumped Linear Electron Accelerator 128

A. M. SAMARIN and L. M. NOVIK : Vacuum Treatment of Molten Steel—A New Way of Improving Converter Steel Production .. 134

T. TURBADAR : Oblique Reflectance and Transmittance Measurements on Aluminium Films .. 139

G. SIDDALL and G. SMITH : A Thin Film Resistor for Measuring Strain .. 144

Letters to the Editor

P. I. P. KALMUS : A Simple Flexible Vacuum Joint .. 147

W. R. LAMB, F. A. RHOADS and P. S. APPLEBAUM : A Shutter for Use between Source and Work during Vacuum Evaporations .. 147

Conferences and Symposia .. 149

Classified Abstracts .. 152

Papers to be published in future issues .. 170

Numbers 3/4

W. STECKELMACHER, J. M. PARISOT, L. HOLLAND and T. PUTNER : Apparatus for the Controlled Deposition of Optical Film Systems .. 171

S. VEIS : The Measurement of the Pressures of Various Gases by means of a Pirani Gauge .. 186

G. CARTER : Electrical Clean-up of Gases in Hot Cathode Discharge Tubes .. 190

S. A. VEKSHINKY, M. I. MENSHIKOV and I. S. RABINOVICH : High-Vacuum Pumps and Units for Accelerators .. 201

E. THOMAS, R. SERVRANCKX and R. LEYNIERS : On the Choice of Units of Pressure and of Flow in Vacuum Technique 207

R. JAECKEL : Die Diffusionspumpe ihre Physik und Technik .. 209

C. G. J. JANSEN and A. VENEMA : A McLeod Manometer with Prescribed Volumes for Use as a Standard Instrument 219

page

Letters to the Editor
E. MENDOZA : Application of the Air Pump .. 231
L. D. MILLER and P. N. PETERSEN : Automatic Level Control for Liquid Nitrogen Trap .. 231
C. E. ANTHONY and L. E. PREUSS : On the Production of Silver Apertures by the Vacuum Evaporation Technique 232
L. E. PREUSS : Vacuum Distillation Source Image Formation by Surface Sensitization .. 233
Classified Abstracts .. 234
Papers to be published in future issues .. 253

Numbers 5/6

Biographical Notes : EMILE THOMAS .. 255
E. THOMAS : The International Organization for Vacuum Science and Technology .. 256
D. J. PACEY : A Piezoelectric Oscillator Manometer .. 261
N. C. BALCHIN and B. L. MORDIKE : Semi-Automatic Control of Vacuum Pumping Systems .. 264
P. T. STROUD : Cathodic Etching in a Penning Cold Cathode Discharge .. 269
G. SIDDALL : Vacuum Deposition of Dielectric Films for Capacitors .. 274
D. S. STARK : Measurements on the Properties of a Simple Omegatron .. 288
Book Review
" Vacuum Metallurgy ", edited by R. F. BUNSHAH (Reviewed by A. G. QUARRELL) .. 295
Vacuum Notes .. 295
Conferences and Symposia .. 296
Classified Abstracts .. 306
Papers to be published in future issues .. 316

Vo
9
1959

AUTHOR INDEX Volume 9 (1959-60)

(B.R.) denotes a Book Review

Alpert, D. p. 89
Andrade, E. N. da C. p. 41
Anthony, C. E. p. 232
Applebaum, P. S. p. 147
Balchin, N. C. p. 264
Banbury, P. C. p. 126
Barnes, G. A. p. 126
Berz, F. p. 48
Bounden, J. p. 1
Brown, M. M. p. 17
Carter, G. p. 190
Dunoyer, L. p. 36
Franson, K. D. p. 28
Gould, C. L. p. 63
Haneman, D. p. 126
Heavens, O. S. p. 17
Herb, R. G. p. 97
Hinton, V. p. 17
Holland, L. p. 171
Jaeckel, R. p. 209
Jansen, C. G. J. p. 219
Kaljabina, I. A. p. 117
Kalmus, P. I. P. p. 147
Kohl, W. H. p. 58
Lamb, W. R. p. 147
Leyniers, R. p. 207
Lyubimov, M. L. p. 108
Marker, R. C. p. 128
Mendoza, E. p. 231
Menshikov, M. I. p. 201
Miller, L. D. p. 231
Mitchell, E. W. J. p. 126
Mordike, B. L. p. 264
Novik, L. M. p. 134
Pacey, D. J. p. 261
Parisot, J. M. p. 171
Petersen, P. N. p. 231
Preuss, L. E. pp. 232, 233
Putner, T. p. 171
Quarrell, A. G. p. 295 (B.R.)
Rabinovich, I. S. p. 201
Rhoads, F. A. p. 147
Robinson, N. W. p. 48
Rotblat, J. p. 1
Rowe, T. W. G. p. 21
Samarin, A. M. p. 134
Schossberger, F. p. 28
Servranckx, R. p. 207
Shakhov, K. P. p. 108
Siddall, G. pp. 144, 274
Smith, G. p. 144
Stark, D. S. p. 288
Steckelmacher, W. p. 171
Stroud, P. T. p. 269
Thomas, E. pp. 207, 256
Turbadar, T. p. 139
Weis, S. p. 186
Vekshinsky, S. A. p. 201
Venema, A. pp. 54, 219
Verma, N. S. p. 21
Wolf, E. p. 69 (B.R.)
Yukhvidin, Ya. A. pp. 108, 117

INDEX TO ABSTRACTS

OF VOLUMES 9-10

IN VOLUME 10

VACUUM

The International Journal and Abstracting Service

for

VACUUM SCIENCE AND TECHNOLOGY

Vol.
9.
959/60

VOLUME 9

(1959-60)

CLASSIFIED SUBJECT INDEX

PERGAMON PRESS

OXFORD · LONDON · NEW YORK · PARIS

NUMERICAL LIST OF PAPERS PUBLISHED

	page	article
J. BOUNDEN and J. ROTBLAT : Vacuum in Medicine	1	1
O. S. HEAVENS, M. M. BROWN and V. HINTON : The Structure and Density of Iron Films formed by Thermal Evaporation	17	2
N. S. VERMA and T. W. G. ROWE : The Breakage of Glass Ampoules during Freeze-drying	21	3
F. SCHOSSBERGER and K. D. FRANSON : Adhesion of Evaporated Metal Films	28	4
L. DUNOYER : Les Bases Expérimentales de la Théorie Cinétique des Gaz	36	5
E. N. DA C. ANDRADE : The History of the Vacuum Pump	41	6
N. W. ROBINSON and F. BERZ : Initial Pumping and Recovery of Ionization Gauges	48	7
A. VENEMA : The Production of Ultra-high Vacua by Means of a Diffusion Pump	54	8
W. H. KOHL : Design Approaches for Electron Devices Operating in Critical Environments, Especially Ceramic-envelope Tubes for High-temperature Operation	58	9
C. L. GOULD : Vacuum System for a Thirty Billion Electron Volt Particle Accelerator	63	10
D. ALPERT : Recent Advances in Ultra-high Vacuum Technology	89	11
R. G. HERB : Evapor-ion Pump Development at the University of Wisconsin	97	12
M. L. LYUBIMOV, K. P. SHAKHOV and YA. A. YUKHVIDIN : Experience in Designing and Manufacturing All-Metal Vacuum Systems	108	13
I. A. KALJABINA and YA. A. YUKHVIDIN : Experience in Using Mass-Spectrometric Methods in Electro-Vacuum Technology	117	14
P. C. BANBURY, G. A. BARNES, D. HANEMAN and E. W. J. MITCHELL : The Attainment of Clean Surfaces by Breaking Crystals in Ultra-high Vacuum	126	15
R. C. MARKER : Vacuum Techniques and Components used for a Continuously Pumped Linear Electron Accelerator	128	16
A. M. SAMARIN and L. M. NOVIK : Vacuum Treatment of Molten Steel—A New Way of Improving Converter Steel Production	134	17
T. TURBADAR : Oblique Reflectance and Transmittance Measurements on Aluminium Films	139	18
G. SIDDALL and G. SMITH : A Thin Film Resistor for Measuring Strain	144	19
P. I. P. KALMUS : A Simple Flexible Vacuum Joint	147	20
W. R. LAMB, F. A. RHOADS and P. S. APPLEBAUM : A Shutter for Use between Source and Work during Vacuum Evaporations	147	21
W. STECKELMACHER, J. M. PARISOT, L. HOLLAND and T. PUTNER : Apparatus for the Controlled Deposition of Optical Film Systems	171	22
S. VEIS : The Measurement of the Pressures of Various Gases by means of a Pirani Gauge	186	23
G. CARTER : Electrical Clean-up of Gases in Hot Cathode Discharge Tubes	190	24
S. A. VEKSHINKY, M. I. MENSHIKOV and I. S. RABINOVICH : High-Vacuum Pumps and Units for Accelerators	201	25
E. THOMAS, R. SERVRANCKX and R. LEYNIERS : On the Choice of Units of Pressure and of Flow in Vacuum Technique	207	26
R. JAECKEL : Die Diffusionspumpe ihre Physik und Technik	209	27

VO 9 1959

	page	article
C. G. J. JANSEN and A. VENEMA : A McLeod Manometer with Prescribed Volumes for Use as a Standard Instrument	219	28
L. D. MILLER and P. N. PETERSEN : Automatic Level Control for Liquid Nitrogen Trap	231	29
C. E. ANTHONY and L. E. PREUSS : On the Production of Silver Apertures by the Vacuum Evaporation Technique	232	30
L. E. PREUSS : Vacuum Distillation Source Image Formation by Surface Sensitization	233	31
E. THOMAS : The International Organization for Vacuum Science and Technology	256	32
D. J. PACEY : Piezoelectric Oscillator Manometer	261	33
N. C. BALCHIN and B. L. MORDIKE : Semi-Automatic Control of Vacuum Pumping Systems	264	34
P. T. STROUD : Cathodic Etching in a Penning Cold Cathode Discharge	269	35
G. SIDDALL : Vacuum Deposition of Dielectric Films for Capacitors	274	36
D. S. STARK : Measurements on the Properties of a Simple Omegatron	288	37

Classified Subject Index

Volume 9

The numbers refer to the papers in the Numerical List of Papers Published

Absorption and Adsorption
4, 7, 11, 21, 24

Aluminium
16, 18

Analysis of Gases
14, 17

Automatic Control
34

Biophysics
1

Calibration of Gauges
23, 28

Cathodes
14, 35

Cathodic Etching
35

Cathode Ray Tube
24

Ceramics
9, 12

Ceramic to Metal Seals
9

Coaters and Coating
22

Degassing
14

Diffusion
27

Diffusion Pumps
8, 15, 16, 25, 27, 29

Distillation
1, 31

Drying
1

Ejector Pump
27

Electrical Circuits
19, 22, 23, 29, 33, 34

Electron Beam
11

Electron Diffraction
2

Electron Microscope
1, 4

Electron Tubes
9

Electronics
7

Environmental Testing
9

Evaporation of Metals
2, 4, 12, 21, 22, 30

Vol. 9 959/60

Evaporation of Non-metals
36

Films
2, 4, 18, 22, 36

Flow of Gases
27

Freeze Drying
3

Furnace, Electron Bombardment
2

Gates
25

Gauges
Pirani 23
Piezolectric 33
Ionization 7, 11, 15
McLeod 28

Getter-ion Pumps
10, 11, 12

Glass
3, 7, 24, 36

Indium
15

International Units
26

International Organization
32

Iron and Steel
2, 13, 17

Joints
13, 20

Kinetic Theory
5, 27

Mass Spectrometer
14

Metals
22

Metallurgy
17, 35

Molecular Beams
5, 22

Nickel
19

Omegatrons
37

Particle Accelerators
10, 16, 25

Photosensitive Layers
15

Plastics
21

Pumps
(general) 6
oil vapour 25

Radiation
18, 22

Resistors
19

Semiconductors
15

Silver
30

Sealing and Seals
12, 13

Solders
12

Sputtering
22, 35

Surface Phenomena
15, 31

Thermodynamics
5, 36

Titanium
10, 11, 12

Traps
13, 25, 29

Ultra-high Vacuum Systems
8, 11, 15

Vacuum Production
6

Vacuum Systems
10, 16, 17, 22, 34

Vacuum Techniques
17, 30, 31, 36

Valves
13

Vapour Pressure
36

X-Rays
1

Vo
9
1959

Vacuum in Medicine

J. BOUNDEN and J. ROTBLAT

St. Bartholomew's Hospital Medical College, London

The authors give a survey of the scope and actual applications of vacuum engineering in the medical field. After remarks on the direct application of suction in the early days of history, the authors discuss the preparation of pharmaceutical materials and in this connexion mention various forms of distillation and freeze-drying. The main part of the article is devoted to an appreciation of the electron microscope and subsidiary techniques such as specimen preparation, the importance of X-rays and technical aspects connected with it as well as the preparation and uses of isotopes.

Vol. 9 959/60

Introduction

The high standard of modern medicine is to a large extent the result of the rapid adoption of new methods and techniques and of the application to clinical and practical medicine of almost every discovery or improvement in science and technology. The great achievements in electronics, in atomic and nuclear physics, and in microscopy, have all been immediately taken up by the medical profession and used either as an aid to diagnosis, as a means of therapy, or for the better understanding of the working of the human body. It is not surprising, therefore, that vacuum techniques, which have played such a tremendous role in the progress of science, have also proved to be of great importance to medicine. These techniques are used in medicine either directly, or indirectly by employing apparatus which require some degree of vacuum for their operation. In this article the most important of these applications are reviewed with the aim of giving the reader an idea of the scope and variety of the uses of vacuum equipment and techniques in medicine.

Suction in ancient and modern times

Long before vacuum pumps were invented the advantage

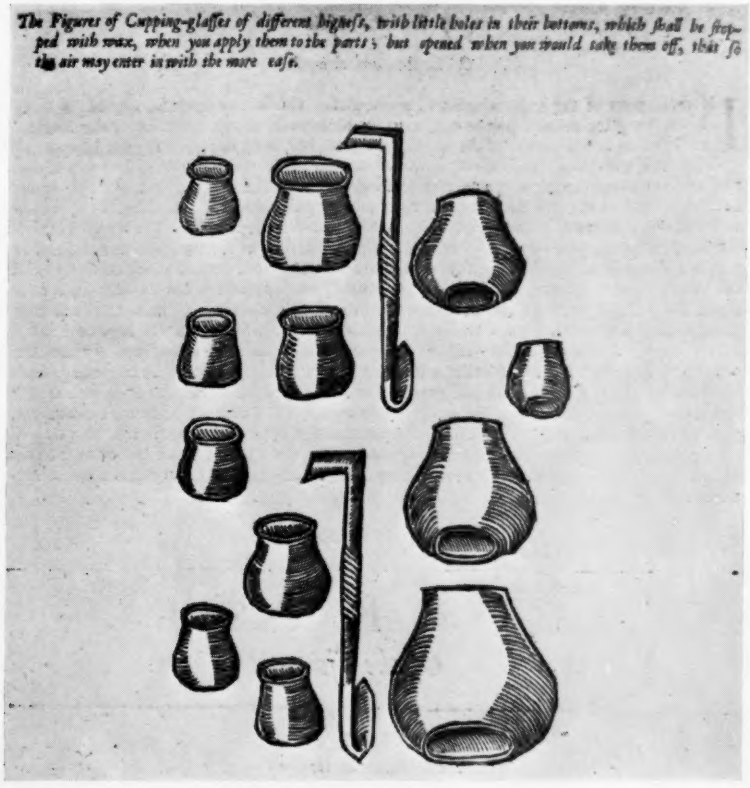
The Figures of Cupping-glasses of different bigness, with little holes in their bottoms, which shall be stop-
ped with wax, when you apply them to the parts; but opened when you would take them off, that so
the air may enter in with the more ease.

FIG. 1. Cupping glasses used in medicine.

of even a slight reduction in atmospheric pressure has been appreciated and regularly been made use of in medicine. Still today a multitude of procedures are based on the effects of a slightly reduced pressure.

It was known throughout the ages that an infected wound would heal much more readily if it was kept open and allowed to drain freely, and also that boils would terminate more quickly if heat and suction were applied in the treatment. One of the earliest appliances used for this purpose was the " cupping glass ", see Fig. 1, a device which is still employed in many countries. It consists of a hemispherical vessel which is first filled with boiling water and then emptied and clapped over the affected part of the body. When in position cold water is poured over the glass and the resultant condensation of the steam inside the glass creates a slight vacuum which sucks the exposed part of the skin into the cup causing the capillaries in the skin surface to become congested with blood around the infection. At the same time infected matter is drawn to the surface or out through the wound.

During the long period in history when " bleeding " was the principal method of treating diseases, the causes of which were unknown, or which would not yield to the limited range of remedies available, cupping glasses and leeches were the chief resources of the physician and barber surgeon. A whole class of illnesses attributable to high blood pressure, in many cases resulting from over-indulgence, responded very well to this treatment. As is often the case, a remedy which was specific and successful for some diseases was soon applied to others in the hope that " something would happen", an attitude not unknown at the present time.

However archaic the cupping glass appears to us today, it must be remembered that it had great success in the past and

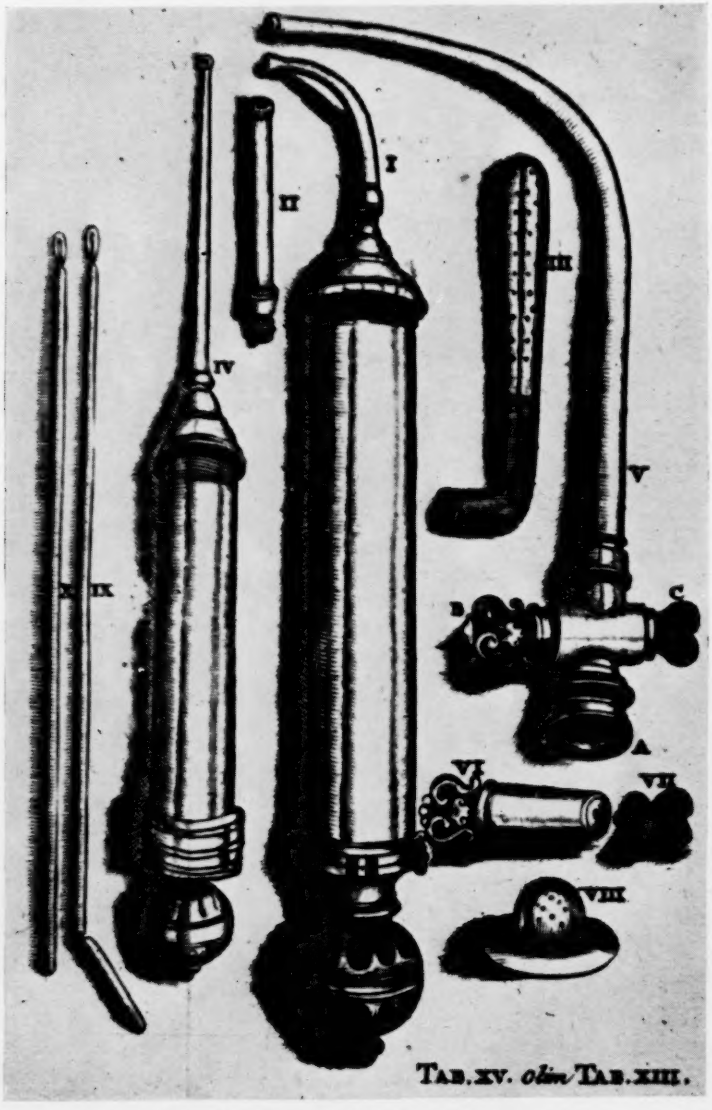

FIG. 2a. Syringes used in the Middle Ages.

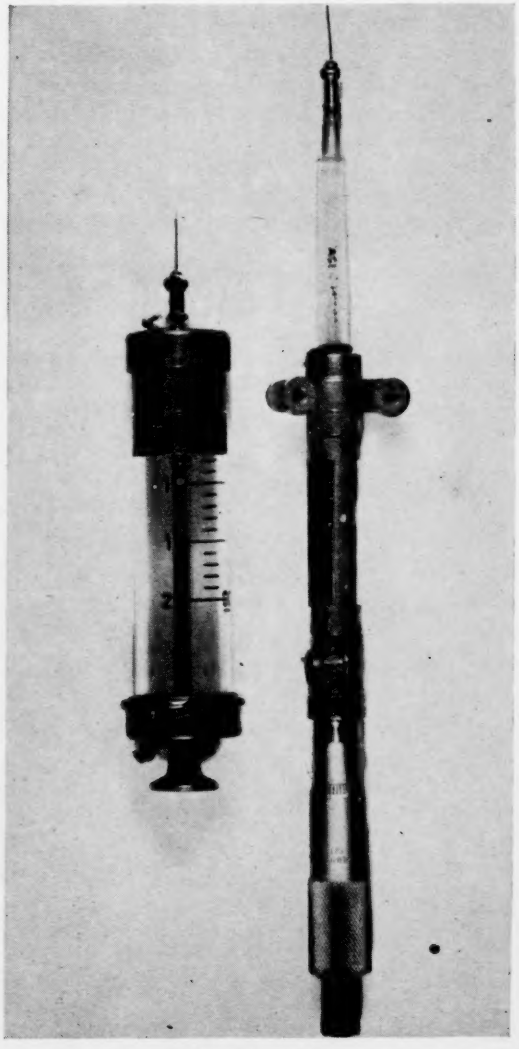

FIG. 2b. Modern syringe with micrometer adjustment.

that even now it is the first remedial means sick people resort to in countries where medical care is under-developed. In these areas it represents a favourite treatment for chills and pneumonia, and is also used to cure headaches and migraine. Twenty or more glasses are applied to the back and spine of the patient and left in position for a few minutes, whereupon, it is claimed that relief is obtained. The treatment of stubborn boils by a hot bottle used in this manner is common in some country districts. The plight of the patient when it comes to removing the bottle can well be imagined, as the suction is strong enough to draw a considerable amount of flesh into the neck of the bottle.

Another example is the syringe. The use of syringes of various kinds in surgery came at a time when major operations had become an established routine rather than a last resort. Instances are known, however, from records dating back to Roman times of the use of syringes (see Fig. 2a) and crude piston pumps for the irrigation and drainage of wounds. Pictures of the early surgical instruments show that their construction changed little for a long time. But nowadays, the hypodermic syringe, for instance, is a precision instrument, and the smallest version of it is fitted with a micrometer attachment which allows extremely small amounts of solution to be administered (see Fig. 2b).

Suction pumps of various kinds are used in many branches of medicine, ranging from the simple aspirator which the dentist uses to keep the mouth free of saliva, to a large-volume pump for the operation of the artificial lung. Mechanical pumps which circulate saline solution and irrigate wounds are in common use. The most remarkable instance is an apparatus which, to a large extent, takes over the action of the heart. Blood is drawn from a main vessel, passed through an oxygenation stage and then pumped back into the patient, thus allowing the surgeon to perform complicated operations in the interior of the heart (see Fig. 3). Such

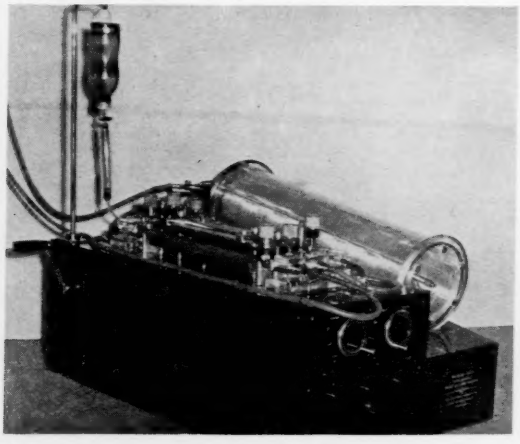

FIG. 3. Heart and lung machine.

procedures are as yet in the experimental stage, but have already made possible great achievement in surgical treatment of the heart.

Another important application of suction is the iron lung (see Fig. 4). The body of the patient is completely enclosed in a metal cylinder, and a rubber collar at the neck seals the

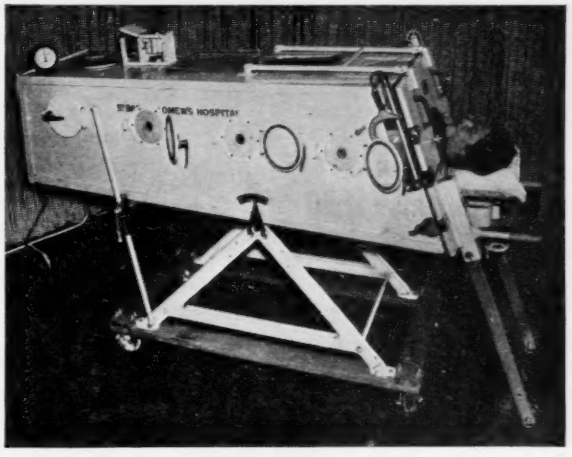

FIG. 4. An iron lung.

chamber, allowing the pressure within to be reduced. Air flows into the passively dilated lungs of the patient and is expelled when the pressure is returned to normal. Thus, by means of pumps operating at the correct rate, the function of breathing becomes independent of muscular power and a patient in whom this function is impaired can be kept alive until the muscles regain their ability to perform the breathing process unaided.

Vacuum in the preparation of pharmaceutical materials

Vacuum distillation

The boiling point of a liquid depends on the pressure prevailing above the surface of the liquid. A reduction of this pressure enables the liquid to be vaporized at a correspondingly lower temperature. This method of distillation has found many applications in the preparation of drugs and other biological materials ; for instance, it is an essential condition for the successful isolation and purification of vitamins, or for the successful separation of steroids, that the temperature at which distillation is carried out is as low as possible.

If a distilling vessel, the upper part of which is designed to serve as the condenser, is filled with liquid, evacuated and heated; then as vaporization proceeds the pressure above the liquid surface will become higher than that existing at the surface of the condenser. This is particularly pronounced if the diameter of the vessel is small and the distance between the liquid and the condenser is large. It is the aim of distilling *in vacuo* to keep this pressure built up immediately above the liquid as low as possible. Other important requirements are some means of continuously replenishing the distilland surface during treatment and smooth facilities for the removal of the fractions. Brief mention is made below of a number of commercial apparatus, by and large meeting the needs of the biochemist and medical worker engaged in distillation work.

Vol. 9 959/60

The alembic still—Distillation has been one of the most widely used techniques throughout the ages and the alembic in particular could almost be classed as the hallmark of the alchemist. It is still in use and Figs. 5 and 8 give an opportunity of comparing the alchemist's tool with modern designs.

CHAP. V.

Of what fashion the Vessels for the distilling of Waters ought to be.

FOr the distilling of any kind of Waters, two kind of Vessels are necessary, which are comprehended under this original name of an Alembick. They call one of them the body, or containing Vessel, the other the head, that is, the cap or top, wherein the ascending vapours are condensated or turned into water. It is called the head, because it stands over the body, like as an head; from the head there comes out a pipe or nose, whereby the distilled liquor flows drop by drop into the Receiver, as you may see by the Figure.

The parts of an Alembick.

Of what fashion the Vessels for the distilling of Waters ought to be.

A *Shews a brass Kettle full of Water.* B *The cover of the Kettle perforated in two places to give passage forth to the Vessels.* C *A Pipe or Chimney added to the Kettle, wherein the fire is contained to heat the water.* D *The Alembick consisting of his body and head.* E *The Receiver wherunto the distilled liquor runs.*

L l l 3 The

FIG. 5a. Ancient stills.

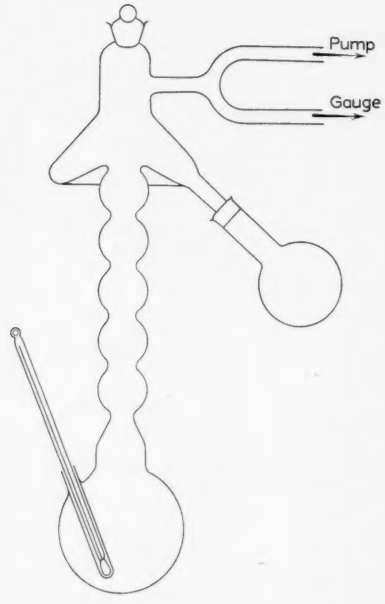

FIG. 5b. High-vacuum column still.

The alembic still is essentially used for the distillation of viscuous liquids and consists of a squat vessel fitted with one or more receivers cooled by ice or solid carbon dioxide. Its operational pressure ranges from 0.1 to 0.001 mm Hg. When distilling highly viscuous liquids there is the constant danger of rapid impoverishment of the liquid at the surface and the provision of means of stirring the liquid is essential. One common method is to admit air through a fine capillary tube dipping just below the surface of the liquid, air being passed in a quantity sufficient to produce bubbles keeping the liquid in motion but not large enough to raise noticeably the pressure in the vessel. The alembic still is suitable for the treatment of substance such as vitamin E, most of the sterols and some hormones.

The molecular still—The method of molecular distillation is particularly suitable for the treatment of heat sensitive materials. The basic principle comprises an arrangement whereby the evaporator and the condenser surfaces are positioned at a distance not exceeding the mean free path of the evaporated molecules of the distillant and operating at a pressure of the residual permanent gases not exceeding 10^{-3} mm Hg, i.e. evacuating the still to a pressure which obviates any collisions between the vaporized molecules and molecules of the residual gas atmosphere in the still. For details of this method the reader is referred to the article on p. 113 of Vol. VI which is devoted to a critical examination of all aspects of that technique. There are broadly speaking three types of molecular stills ; the pot-still, the falling-film still and the centrifugal still.

The essential design features of a small molecular pot still are shown in Fig. 6. Cooling of the condenser is effected by water, ice or solid carbon dioxide. The operational pressure

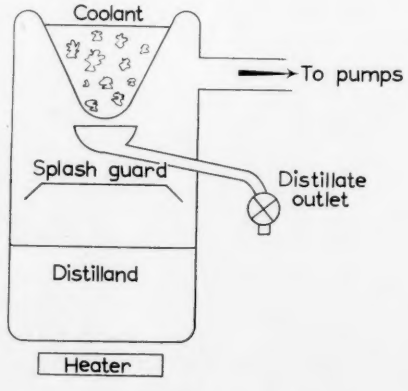

FIG. 6. Short-path molecular still.

is 10^{-4} mm Hg. Removal of the condensate can be effected without breaking the vacuum and thus the still can be operated continuously until the charge is exhausted.

The hazard of thermal decomposition of any given substance increases not only with temperature but also with time of exposure. This consideration lead to the development of the falling-film technique. Stills of the latter kind have a great advantage in that heat is supplied only to a thin layer of liquid and this layer is constantly renewed. The falling-film molecular still is to date the type of high-vacuum distillation apparatus most universally applied and the basic features of this type of still are shown in Fig. 7. The material to be

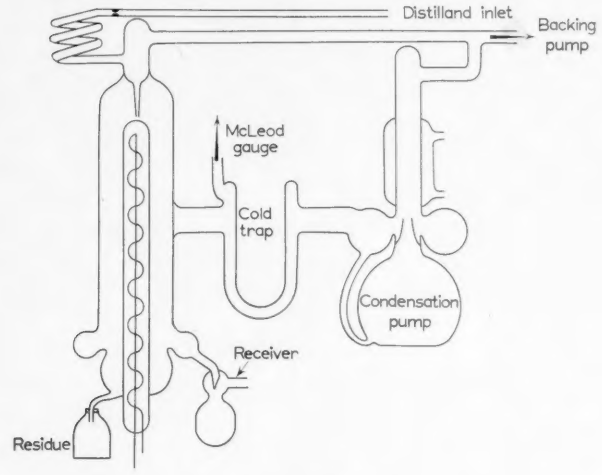

FIG. 7. Falling film still.

processed is fed on to the walls of a heated vertical cylinder surrounded by a jacketed cylinder, cooled by suitable means. In order to increase the evaporation rate the surface of the cylinder is at times ruffled up or machined with a spiral groove in order to increase the area presented to the liquid. The residue is collected at the base of the column and either recirculated immediately or stored for recycling later.

In the case of the centrifugal still a thin film of liquid is obtained by releasing the solution at the centre of a rapidly

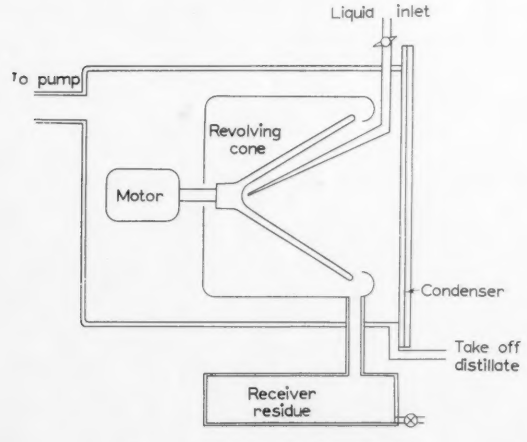

FIG. 8. Centrifugal molecular still.

revolving heated disk or cone over which the distilland film spreads by the action of the centrifugal force (see Fig. 8). The processed material is thrown from the edge of the rotating disk, is caught by a gutter and removed from the still.

A feature inherent in the operational conditions of molecular distillation is the absence of a properly defined boiling point. Distillation will take place whenever there is a temperature difference between evaporator and condenser. However, Embree and Hickman devised a method for the planning of operations in a molecular still introducing the concept of the elimination maximum of the compound to be treated as a substitute to boiling point. Briefly the substance under investigation is dissolved in a constant yield glyceride oil and then subjected to repeated distillation in a cyclic batch still under standard conditions in each cycle except for increasing the temperature in each subsequent cycle. The fractions obtained at each cycle are then analysed for the constituents of interest and the yields obtained are plotted against the temperature of the cycle. Thus the temperature at which each constituent reaches maximum yield is well defined, and the relative position of the maximum affords a good measure of comparing the quasi-boiling points of the various components.

The molecular still is expensive in construction, extravagant in the consumption of heat and dependent for its operation on somewhat costly vacuum plant. In spite of all this it is widely applied in the separation of oil-soluble vitamins from fish liver and other oils. Many of the commercially produced vitamins A and E are prepared in this way.

Special purpose laboratory apparatus—Vacuum distillation is used in the laboratory mainly for the separation and purification of mixtures and for the identification of materials. Apart from the commercial types of machines described above, many instances arise in research work when stills are constructed in the laboratory for specific purposes (see Fig. 9). In some applications a rotary vacuum pump

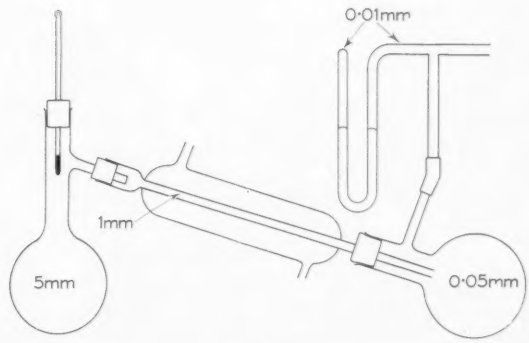

FIG. 9. Laboratory vacuum distillation apparatus. Numbers represent probable pressures at different points during a typical distillation.

unit of high speed is sufficient; in others, where a higher vacuum is required, diffusion pump units must be used. In all cases appropriate gauges and traps must be provided, the traps for the removal of condensable vapours are normally charged with phosphorus pentoxide, other types of vapours are removed in traps cooled by liquid air or a mixture of

Vol. 9 959/60

crushed solid carbon dioxide in acetone, or alcohol. In one example of an apparatus of this type purification of a compound is carried out by successive sublimation from one vessel to another. A row of test tubes is used, sealed to the main vacuum line, with the substance which is to be purified in the first tube of the row. The tube next to that is cooled and the sample gently heated until the successive fractions are transferred to the next tube. By continuing this process along the line of tubes, separation and purification of the substance into its components can be achieved.

Freeze drying

Another vacuum development of considerable importance to the industrial pharmacist and practising surgeon alike is the freeze-drying method. The process makes it possible to store organic material in a dehydrated condition for long periods—extending over several years in many cases—at room temperature and to reconstitute it when required for use simply by the addition of water. Thus the need for refrigerated storage is avoided. The latter is expensive, requires a substantial storage area when large quantities of material are involved and is not always practicable. In applied medicine the freeze-drying method is established for the preservation of a variety of materials. Blood plasma for example is commonly freeze-dried, facilitating bulk storage in a state where it can be readily made available for transfusions. In the same manner fragments or whole bones and arteries are freeze-dried and kept in readiness for grafting. In biological research freeze-drying offers the major advantage of effecting a rapid cessation of all cellular activity and of enabling embedding of the specimen without resort to chemical reagents which cause diffusion, dissolution and distortion. The method is most valuable for cytochemical and cytomorphological research.

In principle the method consists of two distinct operational phases, freezing and drying, which in one particular variety of the method are combined by providing for evaporative freezing. The materials treated may be either in the form of a liquid (solutions or suspensions) or in solid form such as tissue or organs. The state of the material has a considerable bearing on the temperature applied in freezing. The critical temperature is −40°C. Above that temperature the ice formed has a crystalline nature, and below that temperature the ice is in an amorphous state. Thus when treating liquid materials, the freezing temperature employed can be above −40°C and is essentially governed by considerations of effecting the freezing of the specimen within a conveniently short space of time. But in the case of solid material, such as living tissue, for instance, the freezing temperature must be below −40°C in order to avoid any serious damage to the structure of the specimen. Further, when freezing tissue for biological research it is essential to do so rapidly. Therefore temperatures as low as −160°C are commonly used in this sphere of applications.

Drying of the frozen material is carried out under vacuum in order to facilitate sublimation, i.e. the passing of the ice directly from the solid state into the vapour state. There are various methods of dealing with the rising water vapours, for instance, by providing suitable desiccants such as phosphorus pentoxide. In the case of liquids the end-product has a porous sponge-like appearance. Generally speaking, frozen liquids can be successfully treated at moderately reduced pressures, i.e. at pressures of the order of ½–1 mm Hg. The material may be heated without causing any harm to the substance during the drying period up to a temperature below that of the melting point of the ice, and this has the advantage that the rate of drying is considerably accelerated. But in the case of frozen organs where it is important to retain the cellular structure the temperature, for reasons explained above, must never rise above −40°C. Thus, in view of the low vapour pressures of the ice, drying of solid components must be carried out at very much lower pressures than drying of frozen liquids, i.e. in the proper high vacuum range, if a reasonably fast rate of drying is to be achieved.

The basic features of the freeze-drying method remain the same, but actual procedures do vary to an extent depending on the material processed. This explains why commercially available freeze-drying units differ in their construction according to the purpose for which they are designed. Generally speaking, the drying follows established lines, but it may be worth while to add a few more detailed comments on the various freezing systems in use. It is beyond the scope of this article to give great detail, and the reader is referred to a contribution published on p. 89 of Vol. VI dealing in greater detail with the freeze-drying technique. Within the sphere of medicine and biology it suffices to distinguish between two states of the material to be treated : (1) solutions and suspensions and (2) tissue.

Solutions and suspensions—The material may be frozen prior to the application of a vacuum, or alternatively by evaporative freezing during the initial stages of pumping down. There are three methods of pre-freezing : (a) shell freezing, (b) vertical spin freezing and (c) shelf freezing.

In method (a) the material is fed into bottles, the bottles are partially immersed in a freezing mixture and are rotated slowly about an almost horizontal axis. Due to the centrifugal force the liquid spreads over the walls of the bottle and a large surface area of the material is exposed to the refrigerant. This facilitates both a fast rate of freezing and of drying. The method was given the name of " shell-freezing " because of the fact that the liquid freezes in the form of a hollow shell.

Method (b) represents a modification of (a). Here the bottles are in a vertical position and totally immersed in the freezing mixture. The speeds of rotation are appreciably higher and processing times are shorter, mainly because of the total immersion of the bottle in the freezing mixture.

Method (c) provides for the bottles to be placed on refrigerated shelves. When freezing is completed the bottles are connected to a vacuum manifold and the water-vapour is removed during pumping. Externally, the bottles are exposed to atmospheric pressure and temperature, and during drying there is a rapid transfer of heat from the exterior to the interior of the bottles, causing the contents of the bottles to melt at times. To avoid this the bottle can be appropriately insulated. On completion of the process a dry inert gas is fed into the vacuum system until atmospheric pressure is

Vo
9
1959

reached. At this stage the bottles are removed and sealed immediately.

Freezing by evaporation under vacuum is a very rapid and efficient method. However, violent foaming of the liquid occurs when freezing under reduced pressure unless it is controlled by low speed centrifugation, a method evolved by Dr. R. I. N. Greaves of Cambridge University.

The liquid material in its container is centrifuged at about 800 r.p.m. and this has the double advantage of suppressing the foaming and throwing the liquid to the side of the container, where it freezes in a wedge shape of very reduced thickness and large surface area. Under these conditions drying is very rapid.

Also, up to 20 per cent of the water content of the liquid material evaporates during the freezing period of about 10 min. Freeze drying continues from the frozen state by sublimation.

Tissue—Specimens to be freeze-dried for cytochemical and cytomorphological research purposes are invariably pre-frozen. In that case freezing must be rapid and homogenous as possible. This is achieved by restricting the dimensions of the tissue specimen (e.g. to a thickness of no more than 1 mm) and by immersing the specimen directly in the refrigerant which must have a very low melting point. The refrigerating fluid is held at a temperature just above its melting point by keeping it in a vessel which is surrounded by a second vessel containing another refrigerant which has an even lower melting point. To quote an example, combinations of refrigerants of this type may consist of isopentane (melting point −160°C) and liquid nitrogen (about −190°C). The vessels containing these refrigerants are preferably Dewar flasks. The outer flask is lagged but both are open at the top.

On completion of the freezing process the tissue is conveyed rapidly to the vacuum chamber and in order to prevent ice crystals from forming within the tissue the chamber temperature is kept below −40°C. Generally the temperature employed in the chamber range from −70°C to −50°C and are obtained by surrounding the chamber with a mixture of acetone and carbon dioxide ice. The pressure in the chamber during drying is reduced to about 0.001 mm Hg. Water-vapour is removed either by absorption, employing phosphorous pentoxide, or by means of a liquid air trap. Under such conditions drying takes about 3 days. In some cases the temperature difference between the tissue specimen and the chamber walls is made as great as possible by heating electrically the specimen holder, but, to avoid damage to the tissues, never to a temperature exceeding −40°C. As a result the water-vapour condenses more readily on the colder walls of the chamber from where it can be removed by the desiccant.

On completion of the drying process the tissue is embedded in paraffin-wax or some other suitable medium. This process is carried out *in vacuo*, the wax being previously placed on the specimen holder before the latter is charged with the frozen tissue. To melt the wax for the purposes of embedding, the chamber is heated to about 60°C. Finally, air is let into the system and the tissue is removed in an embedded condition. Subsequently the tissue is sectioned, the wax is dissolved away and the specimen is ready for examination directly by phase-contrast or interference microscopy.

Vacuum in support of medical practice and research

The electron microscope

The optical microscope has for many years been one of the most important and indispensible tools of medicine. The cellular nature of living matter and the small size of microbes make microscopic examination one of the most valuable methods of diagnosing disease and following-up results of treatment. The optical microscope is, however, restricted in its scope. The nature of light limits its resolving power to about 2000 Å for visible light. By the use of ultra-violet light, the resolving power can be raised to about 800 Å, but this is still not sufficient for all purposes. Many objects of interest in medical science are of a size much less than 100 Å, and for the study of some cytological details far greater resolutions are required.

For applications in that range the electron microscope has become an invaluable tool for research. According to wave-mechanics the wavelength associated with a beam of electrons of mass m and velocity v, is given by $\lambda = h/mv$. For an electron beam accelerated through a potential V, and neglecting the relativistic correction, this formula becomes

$$\lambda = \frac{h}{\sqrt{(2meV)}} = \sqrt{\frac{150}{V}}$$

where V is in volts and λ is in angströms. Thus, for a beam of electrons accelerated by a potential difference of 60 kV, the wavelength is 0.05 Å, giving a theoretical resolution about 100,000 times greater than for the optical microscope.

Two different techniques can be employed in operating the electron microscope, the transmission and the reflection techniques. For the purposes of this article, we will restrict ourselves to a discussion of the former only. In practice 40–100 kV are required to ensure that the electron beam penetrates the specimen, and also that focusing of the beam is adequate.

In a general way a direct comparison can be made between electron and optical microscope systems, as can be seen from Fig. 10 and the following description. The only major differences are that in the electron microscope (1) the image cannot be viewed directly, but is made visible through the intermediary of a fluorescent screen or, where fine detail is required, by means of photographic records, and (2) that the "focal length" of the electromagnetic lenses can be changed *ad libitum* by varying the magnetizing current.

Fig. 10 shows the body of the instrument. At one end of a highly evacuated metal tube is the electron gun, consisting of a tungsten filament serving as the electron emitter, and the anode with a small hole in the centre allowing a fine pencil of electrons to emerge. This beam is concentrated by passing through an aperture which is negatively charged with respect to the filament. The beam then reaches what is, in effect, the electrical analogue of the condenser lens in an optical microscope, i.e. a variable coaxial magnetic field which

Vol. 9 959/60

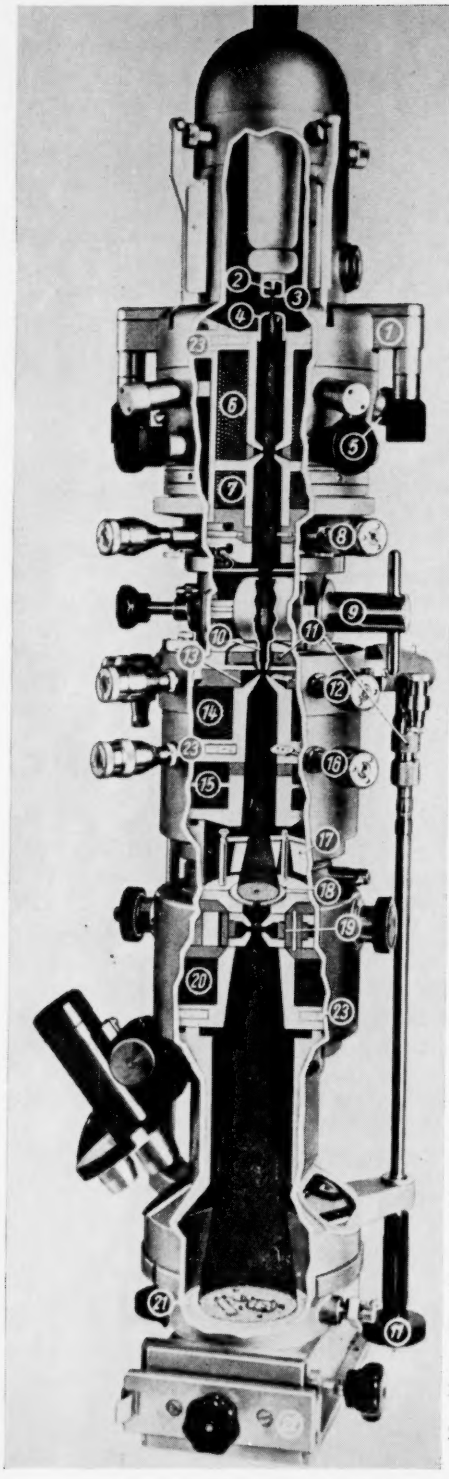

1. Beam adjusting device.
2. Cathode.
3. Control electrode.
4. Anode.
5. Control knobs of electron gun.
6. Condenser coil No. 1.
7. Condenser coil No. 2.
8. Condenser-diaphragm control.
9. Airlock handle.
10. Specimen cartridge.
11. Object stage and adjustment.
12. Aperture-diaphragm control.
13. Location of stigmator.
14. Objective coil.
15. Intermediate-lens coil.
16. Control of intermediate-lens diaphragm.
17. Mirror for intermediate image.
18. Intermediate-image screen.
19. Pole-piece drum and control.
20. Projector coil.
21. Final fluorescent screen.
22. Camera.
23. Water cooling.

FIG. 10. Modern electron microscope.

controls the divergence and the amount of " illumination " falling upon the specimen. After penetrating the specimen, the electrons enter into the field of a magnetic objective lens of short focal length. Since the specimen is situated just in front of the focal plane of the latter an enlarged image is formed which is arranged to be in the focal plane of another, a high-power projector lens, which throws an image on to the fluorescent screen or photographic plate. Focusing is effected by varying the magnetic field of the objective lens, and magnification is changed by altering the field of the projector lens. To counteract distortion the projector lens usually consists of two or more sections of different strengths. At the same time by varying the relatively weak lenses in this combination, the magnification can be changed. In some microscopes the range is 2000–160,000. If no projector lens is provided the range of magnification is lower, i.e. usually 200–20,000.

The amount of detail resolved in the image depends on the differential scattering of the electrons conveyed by the beam to the specimen, in different parts of the specimen. At an accelerating voltage of 100 kV the penetration of the beam in biological material is 0.25 μ. Since most objects consist of sections of varying density, the corresponding difference in the transmission of electrons will result in variations of contrast in the image, the loss of electrons depending on the amount of matter in the path of the beam. The image depicts thus the distribution of matter in the specimen in a way analogous to the results obtained when using staining techniques in light microscopy. Actually, the electron micrograph is more comparable with the image seen in a phase contrast microscope, since in that instrument the phase delay is determined by the length of the optical path in the specimen, i.e. the product of thickness and refractive index, the same as in the electron microscope.

The thickness of the specimen is limited by the penetrating power of the electrons. This is small even at high accelerating voltages. As a result of inelastic scattering some of the electrons are slowed down, which is comparable to a loss of monochromatism in light systems.

Associated with this is the fact that electron lenses suffer from chromatic aberration if fluctuations of the accelerating potential occur and the electrons in the beam are not all of the same energy. At a potential of 50 kV the maximum permissible thickness of a biological specimen is 1000 Å ; at 100 kV this thickness can be doubled. As a rough guide, the resolution is about one-tenth of the specimen thickness. This, however, is probably a conservative estimate and the resolution may approach one-twentieth of the specimen thickness. The overall thickness of biological specimens (not including the supporting film) is usually about 300 Å and the resolution obtained is in the range of 10–20 Å at 80 kV.

Very low pressures in the microscope tube are an imperative requirement, not least for the reason of reducing to a minimum air scattering of the electrons issuing from the electron gun. In addition, operation of the instrument makes it necessary that certain parts of the microscope are opened repeatedly to the atmosphere, i.e. the specimen chamber, the film or plate holder and the electron gun. This means not only that there should be adequate and reliable sealing facilities and air locks, but also that the vacuum pumps should be capable of producing the

operational pressure in as short a time as possible. A typical exhaust unit, pumping down the system in a matter of minutes, consists of an oil diffusion pump with a speed of the order of 120 l/s backed by a rotary pump of 150 l/min. Incidentally, this does not take into account the manipulation of wet specimens which are usually pre-pumped in a separate vessel. Further details of vacuum interest relating to the design of electron microscopes can be readily found in the literature and will not be discussed here.

The mounting of solid specimens—In passing through the specimen the electron beam conveys a charge and transmits energy to the specimen. As a result the specimen is heated and electrostatic forces are built up. In most cases the specimen is good enough an electrical conductor to allow the charges to leak away to earth, but sections of biological material which are embedded in a non-conductor such as methacrylate (which is commonly employed) must be in contact with a good conductor to prevent internal damage by the electrostatic charge. This condition is fulfilled if copper grids are used to support the specimen. The grids also serve to dissipate the heat. In addition a copper cooling ring is required if the biological sections are very thin. Another means of reducing the heating effect is to keep the illumination as low as possible, consistent with reasonable viewing conditions.

Vol. 9 959/60

A support grid of metal mesh (about 200 per in.) in the form of a disc $\frac{1}{8}$ in. in diameter of copper or stainless steel, provides the specimen mounting. The grids form a square or rectangular pattern and the supporting film is placed upon it. Whatever the pattern of the grid, it is usual for the centre to have a hole of different contour in order to facilitate the positioning and identification of other parts of the specimen.

The conventional supporting films are made from collodion or formvar. The films must be very thin (150–200 Å) and uniform in thickness. Collodion films are prepared from a 2 per cent solution of cellulose nitrate in amyl acetate, a drop of which is fed from a fine pipette on to the surface of clean distilled water. The solution spreads across the water surface and as the solvent evaporates a thin film of collodion remains. Details of the transfer of the collodion film to the support grids have been frequently described in the literature. It is important to note that the film should always be formed from a single drop of solution, a number of drops causing film overlap and variation in thickness. The strength of the solution is so adjusted that a single drop will give a film of the required thickness, without allowing it to touch the sides of the vessel holding the water.

Formvar films are prepared by pouring a 1 per cent solution of formvar in chloroform over a clean glass slide which is then stood on end to drain. When dry, the slide is slowly immersed in water at an angle of about 30° to the surface of the water, and the film comes away from the glass and floats on the surface. Films formed in this way are found to be thicker at the edge from which the solution was drained, but the greater part of the film area is of a reasonably uniform thickness.

Carbon supporting films—Carbon, owing to its great stability under the electron beam, has now largely superseded the use of formvar and collodion. Carbon films are prepared by the evaporation of carbon *in vacuo*. For this purpose the end of a carbon rod is ground to a moderately fine point. The end of a second carbon rod is also tapered although not to the same extent. The tapered ends of the two rods are placed in contact with each other under slight pressure. Either clean glass slides or copper grids coated with collodion or formvar beforehand are positioned beneath the carbon rods at a distance of about 10 cm. A picture of the arrangement can be seen in the article in Vol. V (p. 109). Finally, a bell jar is placed over the electrode system and the air is removed. On passing a current through the carbon rods heating takes place at the point of contact, reaching a temperature sufficiently high for the carbon to be evaporated.

One particular evaporating unit, specially designed for the purpose, is fitted with a large manifold so that both pumps can be switched off during the actual evaporation process. In this way all vibration is eliminated and an even deposit of carbon is obtained. Evaporation is carried out at 10^{-4} mm Hg. The plant contains two transformers; one supplies 60 A at 30 V and the other 20 A at 10 V. For carbon evaporation the first transformer is used and the duration of the process is controlled by a press button switch. Thin carbon films can be readily stripped from glass slides, but in order to obtain a satisfactory thin film it is advisable to cut down the voltage available from the transformer to two-thirds by means of a regulator. Deposition takes about 10 sec.

If the carbon is deposited directly on to a glass slide the film can be detached by immersing the slide at an angle in distilled water. If the film is deposited on a grid previously coated with collodion or formvar then the latter are removed by means of a chemical solvent or by the application of heat.

Evaporation units of the kind just described have other useful functions in the field of electron microscopy. For instance, they provide the only simple method by which certain small components of the microscope, such as objective apertures, can be cleaned. Further, the vacuum manifold can be used for the dehydration of the photographic plates before they are placed in the microscope.

Shadow casting—Shadow casting of the specimen affords a useful means of increasing contrast of surface detail in the micrograph but requires that the deposit should be as thin as possible consistent with sufficient differentiation. Shadow casting equipment is very simple, consisting essentially of a bell jar of 12 in. × 14 in., a diffusion pump unit of 100 l/s speed and a Philani Model I type gauge. Several filaments for the evaporation of different metals, or of the same metal from various directions, are usually incorporated, these being spiral, boat shaped or V-shaped, depending on the type of metal to be evaporated. Tantalum, beryllium and chromium are some of the metals employed in shadow casting, and in addition it is useful to have provision for the evaporation of silica for replica work.

Evaporation is carried out with the specimen at a distance of at least 10 cm from the evaporation source in order to avoid damage by radiant heat and to ensure uniformity of the deposit over a fairly large area. The angle at which the evaporated metal atoms strike the specimen is varied for

differing specimens, i.e. 20°–30° for general work and 10°–15° for plant viruses and macromolecules. Under average conditions the deposit should have a thickness of 10–20 Å.

The pressure should be reduced to 10^{-4} mm Hg or lower and this pressure should be maintained for $\frac{1}{2}$ h or more before actual deposition, to remove oil and contaminating vapours generally present on the metal surfaces. After switching on the filaments a large quantity of gas is evolved from the heated parts. To avoid the specimen becoming recontaminated small shutters should be provided which are placed between the source and the specimen during the initial heating period.

Remarks on liquid specimens—Liquid suspensions are applied to the grid from a small pipette, and in the case of mixed particles of differing sizes a series of centrifuge operations enables those above a certain size to be removed from the solution. Aggregation of the particles may cause trouble but this can be overcome by the addition of dispersing agents, variation of the pH or by supersonic vibration. Bacteria and viruses are diluted and deposited on the supporting film in the same way, but here clumping may present a serious obstacle to obtaining a satisfactorily dispersed sample. To prevent damage during preparation fixation of the organisms is carried out in the culture medium or directly after removal from it, usually in 5 per cent formalin or by exposure to the vapour of osmium tetroxide.

These and other techniques, specific to the type of work being undertaken, provide the research worker with an increasing variety of refinements and make the electron microscope one of the most useful tools for fundamental research in biology.

X-Rays

X-rays are electromagnetic waves of very short wavelength. They are produced when a beam of fast electrons hits a target of high atomic number. Because of their short wavelength the interaction of the rays with matter is different from that of light rays. In particular, they possess the ability of penetrating solid matter, the degree of penetration depending on the atomic number of the material. This property of X-rays forms the basis of their diagnostic use in medicine, and was established soon after their discovery by Roentgen in 1895. In fact, only a few months later photographs of the interior of the human body were taken by doctors as an aid in the diagnosis of disease. Incidentally, the first of these photographs caused a wave of indignation and fears on the possible consequences of the existence of rays which made the body visible and from which clothing was not a protection.

Nowadays X-ray radiographs, as well as direct screening, are an integral and indispensable part of medical practice. They are used not only to detect bone fractures, dental cavities and foreign bodies, but also to observe the action of the heart, lungs and other organs, to study pathological changes, infections and neoplasms, and to help the surgeon during operations. Indeed, it is difficult to imagine how modern medicine could carry on without X-rays.

The shorter the wavelength, the " harder " the X-rays, i.e. the greater their penetration ability, e.g. in tissue. At a given voltage applied to an X-ray tube, the X-rays produced form a continuous spectrum of wavelengths, the lower limit of which is well defined. This shortest wavelength λ is related to the voltage V applied to be tube by

$$\lambda = \frac{he}{eV} = \frac{12{,}396}{V}$$

where V is entered in volts and λ in Ångstroms (h is Planck's constant, c is the velocity of light and e is charge of the electron). Thus, to obtain X-rays of great penetration ability, high voltages must be used.

Early X-ray tubes—Vacuum plays an important part in the production of X-rays since X-rays can only be generated in a vessel kept at very low pressure. The earlier X-ray tubes relied for their action on a small amount of residual gas, usually at a pressure of about 10^{-4}mm Hg, left deliberately in the tube on evacuation. These tubes were known as " gas tubes " and the electrons required for X-ray generation were produced by ionization of the residual gas.

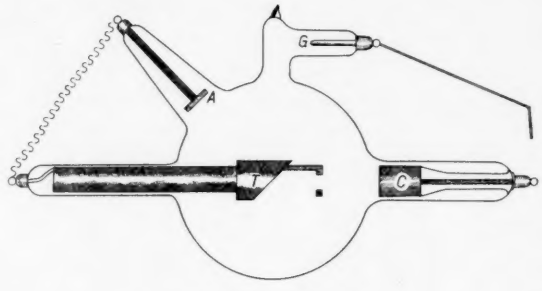

FIG. 11. Gas-filled X-ray tube.

Fig. 11 shows a diagram of such a tube. As can be seen, its essential components are a cathode C which is concave and, opposite to it, an anti-cathode or target T. The latter is electrically connected to the anode A, the location of which in the tube is not of great significance. These tubes are run with a potential difference of 20–50 kV between the electrodes. As a result free electrons in the residual gas are accelerated in the electric field and produce fresh electrons by ionizing collisions with the atoms of the residual gas. This process continues resulting in an electron avalanche, facilitating the build-up of a large electron current. The actual magnitude of the current, as well as the energy which the electrons can acquire, depends on the pressure of the residual gas. At 10^{-3} mm Hg, collisions are so frequent that the current is very large, of the order of 100 mA. But the electrons have only a very low energy, and consequently the X-rays produced are soft, i.e. of long wavelength. At 10^{-5} mm Hg the electrons will acquire the maximum energy corresponding to a given tube voltage and the X-rays are hard, but there are so few electrons produced that the intensity of the X-ray beam is extremely low. In practice, it was found that the optimum pressure is about 10^{-4} mm Hg when both high current and high energy can be obtained. Varying the gas pressure around that value affords a convenient means of regulating the voltage and the current.

Experience with pumpless gas tubes, which were nearly

always used in medical work, showed that the pressure gradually decreased with time, owing to the adsorption of the gas by the glass and metal surfaces. To overcome this difficulty, the tube was provided with a " gassifier ", of asbestos or glass wool, which released gas when a discharge was passed through it by applying a voltage to electrode *G*.

Although gas tubes are no longer used in medicine, they are still employed for diffraction work. However, the later types are continuously pumped and fitted with a leak-in valve to regulate the pressure.

Modern X-ray tubes—In modern X-ray tubes the principle of generating the electrons by ionization of a residual gas atmosphere is abandoned and the source of electrons is a heated filament, as in the case of radio valves. The pressure inside the tube is the lowest obtainable in practice. The cathode filament (see Fig. 12) comprises a conical spiral of tungsten wire, positioned inside a metal cap, shaped so that the electrons emitted from the filament are focused on to the target or anode. The intensity of the electron beam is regulated by variation of the current passing through the filament, and very intense beams of X-rays can be obtained, particularly at high tube voltages. Thus, the energy of the electrons, and consequently of the X-rays produced, depends only on the voltage applied to the tube and on the nature of the target.

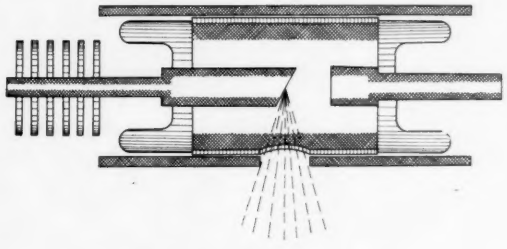

FIG. 12. X-ray tube with air cooling.

At tube voltages of the order of 100 kV only about 1 per cent of the energy of the electrons is converted into X-rays ; 99 per cent of the energy is dissipated in the form of heat which is generated in the focal spot of the target. With a current of about 10 mA, this heat dissipation amounts to about 1 kW. Therefore, the anode would get white-hot in a very short time, unless some method of cooling is provided. For short exposures, or low-power tubes, the copper rod supporting the tungsten target is connected to an external radiator in the form of fins for air cooling (see Fig. 12). Another method is to rotate the target ; in this case the rod carrying the target operates as the rotor of an induction motor, the windings of which are outside the tube. The target in this design is a tungsten disc, only a small area of which is bombarded by electrons at any given time.

Normally, modern diagnostic X-ray tubes are run at voltages of about 60–80 kV, the maximum being 120 kV. These voltages ensure the best contrast obtainable between tissues of different densities. At lower voltages, the soft X-rays are readily absorbed in superficial tissues, thus increasing the potential risk of damage to these tissues without contributing to the quality of the radiograph. At higher energies the difference in absorption between various tissues decreases, so that the contrast is diminished.

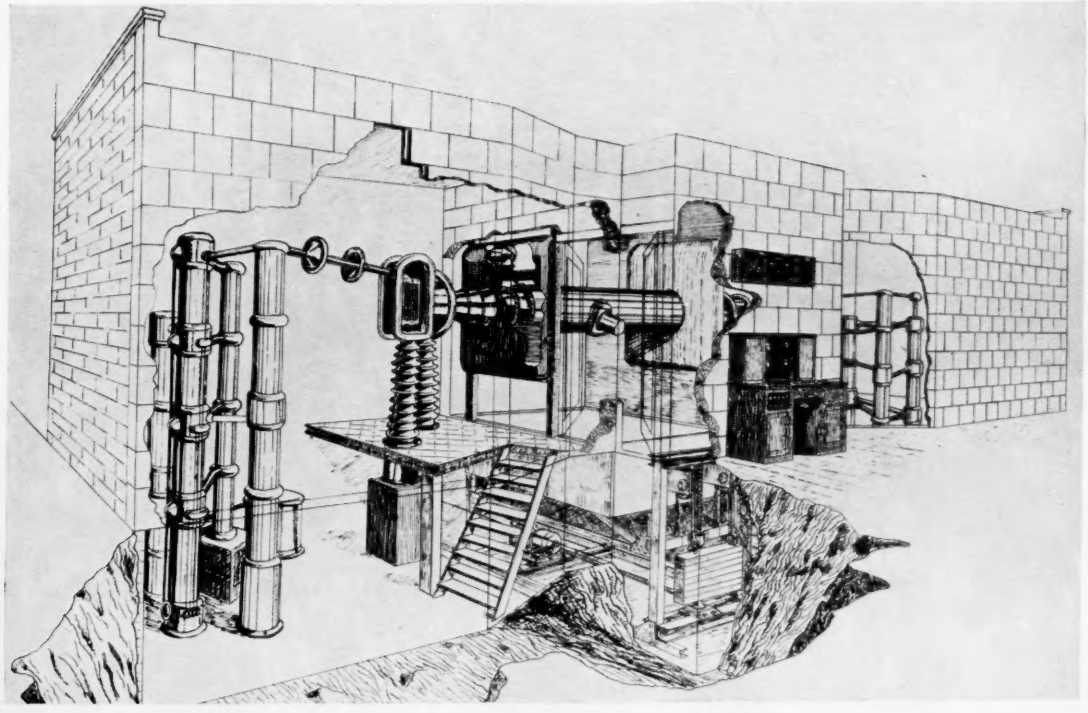

FIG. 13. One million volt X-ray set at St. Bartholomew's Hospital.

Vol. 9 959/60

X-rays are also used in medicine for the treatment of disease. X-rays, in common with all ionizing radiations, have the property of destroying living tissue through which the rays have passed. The actual mechanism by which this destruction occurs is not yet known, but it has been established that when living tissue is exposed to ionizing radiation a certain number of the cells are destroyed, this number depending on the dose absorbed. The effect is made use of to destroy diseased tissue, such as cancer cells. X-ray tubes operating at various voltages, but mainly at 250 kV, are now commonly employed for the treatment of cancer.

Although different cells show a different sensitivity to radiation, and although it is sometimes possible to increase the radio-sensitivity of cancer cells, for example by increasing the oxygen tension, the destructive action of ionizing radiations does not, on the whole, discriminate between healthy and cancer tissue. This puts a limitation on the therapeutic use of X-rays, because in the process of killing cancer cells many healthy cells are also destroyed. The damage suffered by the patient may, therefore, prove to be greater than the cure attempted. This is particularly true in the case of the treatment of deep-lying tumours, since owing to the attenuation of the X-rays in passing through tissue, a much bigger dose is delivered to the skin and superficial tissues than to the tumour.

In the method of multiple-field therapy, or of rotation therapy, where the dose is given from different directions, the overall damage suffered by the healthy tissues is spread over a wider area. This reduces but does not remove the basic difficulty. A more promising approach is the use of high-energy X-rays. With such X-rays not only is the attenuation smaller but, more important still, secondary electrons moving in the forward direction cause a build-up effect such that the maximum dose occurs not at the surface but at a depth of say a few centimetres, depending on the voltage. For this reason the emphasis in X-ray therapy has shifted towards higher voltages in recent years, and tubes are now employed which operate in the million volt range.

The first machine of this kind in Europe was installed at St. Bartholomew's Hospital in 1936 and is still in use today (see Fig. 13).

The high tension is produced by means of two Cockcroft–Walton units, each generating 500,000 V. The units are installed at each end of the X-ray tube, one feeding the cathode and the other the anode. For treatment purposes the X-ray beam can be brought out in the desired direction by rotating a lead shutter about the axis of the tube. The patient is stationed underneath the beam exit port at a distance which can be adjusted by raising or lowering the floor of the treatment room. The X-ray tube is continuously pumped by means of two 8 in. diffusion pumps. (Incidentally, during the 20 years of using the machine the oil in the diffusion pumps has been changed only once.)

Note on radiation hazards—It has recently come to light

Vo
9
1959

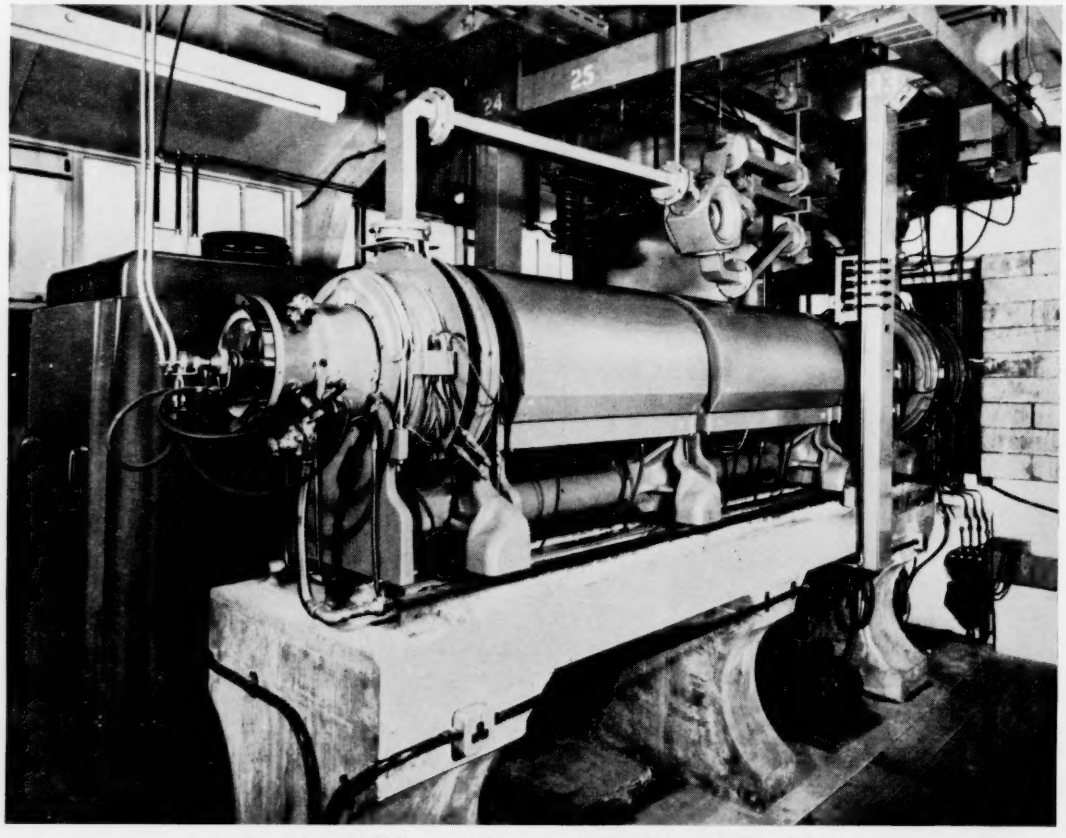

FIG. 14. 15 MeV linear accelerator at St. Bartholomew's Hospital.

that the widespread use of X-rays for diagnostic purposes may be an important factor in contributing to the genetic damage to the population resulting from radiation. It has been found that in Great Britain and in the United States, the population receives on an average as large a dose from diagnostic X-ray examinations as from all the natural sources of radiation together. Steps are being taken to reduce this dose, not only by avoiding unnecessary X-ray photographs or screening, but also by providing filters to the X-ray tubes to stop the useless soft X-rays. Further, certain devices such as image intensifiers, are coming into use, which produce a bright picture although an X-ray beam of comparatively low intensity is employed.

Accelerators—The expansion of radiotherapy into the range of megavolt radiation was greatly helped by the development of various types of particle accelerators for the purposes of research in nuclear physics. Many of the new electron accelerators have found their way into hospitals. Those most frequently used are the electrostatic generator of the Van de Graaff type, which usually operates at 2 MeV, and the betatron and the synchrotron operating at electron voltages up to 70 MeV. These machines offer the additional advantage of using the beam of electrons directly for therapy. Electrons of an energy of, say, 15 MeV penetrate tissue to a depth of about 3 in., and there are a number of clinical conditions where electron therapy is of greater benefit than X-rays.

One of the most recent types of accelerator for radiotherapy, which appears to be favoured in Great Britain, is the linear accelerator. A pulsed electromagnetic wave, at a frequency of 3000 Mc/s, is generated in a magnetron and travels along a corrugated waveguide, i.e. a tube containing a series of diaphragms, the inner diameter of which increases in the direction of travel. This increase of aperture dimensions results in a rising speed of the wave travelling along the wave-guide. Electrons emitted from a heated tungsten filament and accelerated at 50 kV are injected into the waveguide in phase with the radio-frequency supply. The electrons are then carried along the waveguide at the speed of the wave. Thus, by the use of a potential of only 50 kV, electrons are obtained of the same energy as would be obtained by the direct use of a potential of several millions of volts.

In the linear accelerator recently installed at St. Bartholomew's Hospital (see Fig. 14) the waveguide is 20 ft long and the electron velocity reaches ultimately 99.95 per cent of that of light ; the energy is then about 15 MeV. The system is pumped continuously. A 10 in. oil diffusion pump unit is used. The working pressure is 10^{-5} mm Hg or less.

After emerging from the accelerating waveguide, see Fig. 15, the electron beam is bent through 90° and passes into the air via a 0.002 in. window of copper–beryllium alloy. The beam can then either be used directly for electron therapy, or can be conveyed to a water-cooled gold target to produce an intense beam of X-rays. The X-ray head can be rotated through an angle of 140°, making it possible to send the beam in any direction required for treatment. The cross-sectional size of the X-ray beam is determined by four thick lead shutters forming a variable aperture which

FIG. 15. X-ray head of linear accelerator at Bart's.

defines the area exposed for treatment at 1 m distance from the target. The maximum area is 20 × 28 cm.

The intensity of the X-ray or electron beam is controlled by varying the current passing through the tungsten filament ; this also results in some variation of the electron energy obtained. The frequencies are 100, 200, 400 and 500 pulses/sec. A special device makes it possible to run the machine at any given number of pulses.

With the high-intensity beam obtained in this type of machine some peculiar radiation effects have been encountered which have a bearing on the vacuum engineering aspect. In the linear accelerator at Bart's the " O "-rings were found to become exceedingly hard in the course of time as a result of exposure to scattered radiation. In some cases they could only be removed from the locating grooves by applying a chisel. Similar effects could be noticed in the magnet employed for deflection. Here the insulation of the windings deteriorated, sometimes leading to a breakdown.

Treatment with high-energy accelerators—Brief mention may be made of the use of another accelerator for radiotherapy, i.e. the large 184 in. cyclotron at Berkeley, which was employed for the ablation by radiation of the pituitary gland. In this case use is made of the fact that the proton beam from the cyclotron which has an energy of 400 MeV, is very well defined and undergoes very little scattering in tissue. By accurate positioning of the patient it is possible to direct the proton beam so as to produce the therapeutic effect where desired, without damaging vital organs in the immediate vicinity.

Vol. 9 959/60

Radioactive isotopes

The large-scale production of radioactive isotopes, which mainly stems from the development of nuclear reactors, has had a great influence on medical research and practice. The exceedingly high sensitivity with which radioactivity can be detected, and the fact that radioactive isotopes behave biologically in a fashion identical to that of the stable isotopes of the same element, have opened the possibility of studying metabolic processes, and particularly the rate at which such processes occur in the body, without upsetting its normal functioning. Radioactive isotopes have found very wide applications both in fundamental studies of metabolic processes and as an aid in the diagnosis of disease. Diverse detecting apparatus associated with isotope work, such as Geiger counters, scintillation counters, pulse analysers and rate meters, are now a normal item of equipment of a hospital and of many a physiology or biochemistry department. There are several aspects of isotope work for which vacuum equipment is essential; these concern mainly the use of gaseous isotopes.

Uses and preparation of radon—The first radioactive gas to be used was radon, the daughter product of radium. Long before the discovery of artificial radioactivity in 1934, radium and its derivatives have been used in cancer therapy as a supplement to X-ray treatment, and often with much better results owing to the different properties of the radiations and the greater convenience in application. Radon was found to be particularly useful at the time because (a) a high activity could be obtained in a small volume by compressing the gas in the container, (b) containers of almost any shape and size could be employed and (c) the container with the charge could be inserted into the body of the patient and left there permanently. The latter possibility arises from the fact that the half-life of radon is only 3.8 days, and thus the amount of radon to be used in an applicator can be properly assessed to deliver the desired dose during the period of its complete decay.

Due to the relatively short half-life of radon new supplies have to be regularly obtained from a given amount of radium. Solid radium does not easily emanate radon gas and for this reason a solution of radium chloride or bromide in hydrochloric acid is used. While radon gas is evolved from the solution other gases are also produced, incidentally, in quantities appreciably larger than that of radon gas. Essentially these are hydrogen and oxygen formed by the decomposition of water under the action of the radiation, but there are also organic vapours, carbon dioxide, etc. All these gases have to be removed before the radon is collected in the tubes or " seeds " for treatment.

An apparatus for the purification of radon is shown in Fig. 16. In operation the apparatus is evacuated to about 10^{-6} mm Hg while the radium solution is sealed off by the mercury column *M*. The gas mixture above the radium solution is then admitted into the apparatus and is cooled at *D* with solid carbon dioxide and acetone to freeze out water and other vapours. A spark through *S* removes the hydrogen and oxygen. The partly purified gas is then transferred by means of a Toepler pump to the capillary *T* which is cooled with liquid air. The radon is frozen and the volatile gases

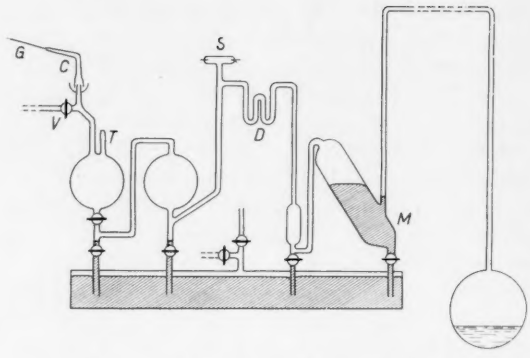

FIG. 16. Plant for the purification of radon.

are pumped off through the tap *V*. The liquid air is removed and the radon passed into tube *C*, the walls of which are coated with fused KOH and heated to remove carbon dioxide. Finally the radon reaches capillary *G*, made of glass or gold. Short portions or " seeds " of this tube are sealed off and used as applicators.

One of the difficulties encountered with a radon plant is that under the action of radiation the glass becomes brittle and develops leaks which are difficult to seal. Owing to the hazards involved when working near strong radiation sources, radon plants went out of general use as soon as artificial radioactive isotopes came into being, but they are still in existence in a number of hospitals.

Uses and detection of tritium and carbon-14—Tritium and carbon-14 are two radioactive isotopes very frequently employed in medical studies and research. Both isotopes emit low energy β-rays and special Geiger counters are used to detect their presence and to assess the intensity of their radiation.

Fig. 17a gives a diagrammatic sketch of a common form of

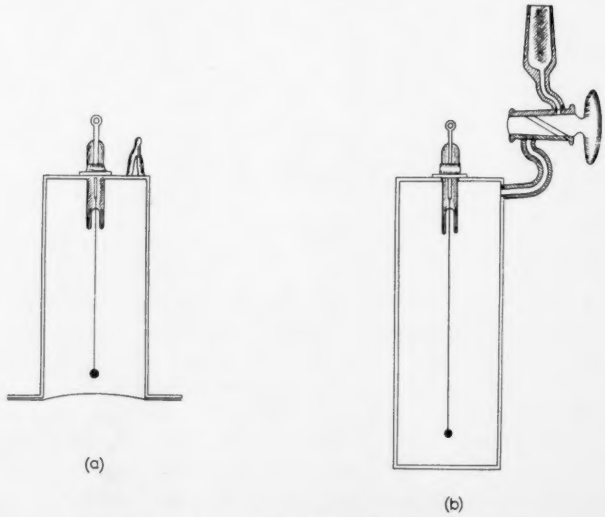

FIG. 17. A sealed off tube and refillable Geiger counter.

Geiger counter. For details of their production and operation reference should be made to recent publications made in various technical periodicals. Essentially the counter

consists of a fully enclosed envelope initially evacuated and finally filled with an argon–alcohol mixture in the proportion of 9 : 1 at a total pressure of about 9 cm Hg. The argon will facilitate the spontaneous initiation of a discharge at a potential of less than about 2000 V and the alcohol will act as the gas quenching the discharge.

Geiger counters are available in various designs to suit the counting of α-, β- or γ-radiation. Those for the counting of α-particles are usually fitted with thin mica windows, those for β-particles with thin aluminium windows and those for efficient counting of γ-rays have a cathode of a particular type.

The radiation from tritium or carbon-14 is too weak to permit penetration even through a thin mica window. For that reason a Geiger counter of the conventional design is unsuitable for that purpose. Fig. 17b shows a counter design suitable for the detection of low-energy β-emitters such as tritium and carbon-14 in gaseous form. As can be seen the counter is fitted with a stopcock-controlled inlet which permits the addition of the sample to the standard filling of the tube. In the particular case of tritium the latter may be attached to an organic molecule such as methane, ethane, acetone, ether, benzene, etc., and may be assayed after introducing a compound of this nature into the counter. Carbon-14 is usually assayed in the form of carbon dioxide and in that case the Geiger counter tube is filled with a mixture of carbon dioxide at a pressure of 20 mm Hg and 5 per cent carbon disulphide which acts as the quenching gas, omitting the standard filling altogether. In the case of tritium, background counting is taken care of by adding ordinary hydrogen in the same proportion as tritium to the mixture. A different form of counting device has to be applied where the isotopes are to be assayed in solid form. Fig. 18 illustrates the type of counter employed for the assay

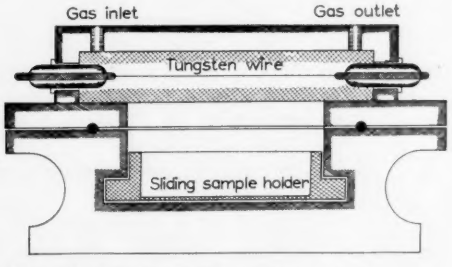

FIG. 18. Continuous gas flow in Geiger counter.

of low-energy β-emitting isotopes in solid form. As can be seen the metal casing is designed to permit continuous circulation of the gas through the casing. The sample is placed in a tray immediately below the horizontally arranged counter cylinder. Helium is used as the counting gas and is bubbled through alcohol before it enters the counter casing, the alcohol vapours serving as the quenching agent. Counters of this kind are operated at atmospheric pressure.

The biosynthesis of tritium labelled antibody—This process may serve as a typical example of the uses of tritium in hospital techniques.

Antibodies labelled with a radioactive isotope were required for a biological investigation.

A rabbit was immunized against bovine albumen by three intramuscular injections of alum-precipitating antigen. Sixteen days after the last injection the rabbit was injected intraperitoneally with DL[$\alpha\beta$-^{3}H] valine (200 mg ; 3 mc), and a sample of blood was drawn from the ear 7.5 h later. The blood was allowed to clot and the serum dialysed to remove any free valine that might have been circulating in the rabbit's plasma.

The vital serum proteins were precipitated and the antibody then isolated from the serum. Radioactivity measurements were made in a windowless flow-type counter by using 10 mg samples mixed with 10 mg of graphite. (The precipitate was assumed to contain 5/6 of the weight of antibody.) The results are given in Table I. If the total circulating plasma volume of the rabbit is assumed to be 140 ml and the protein concentration 7 per cent, 9.8 g of plasma protein will be circulating. Thus, at 7.5 h the total radioactivity incorporated into the plasma protein was 49 μc, or 1.6 per cent of the radioactivity administered.

TABLE I

	Observed activity (counts/min)	Specific activity (μC/g)
Radioactivity of total serum protein ..	363	5.0
Radioactivity of γ-globulin fraction ..	244	3.4
Radioactivity of antibody to bovine albumen	110	1.5

Stable isotopes

The detection of isotopic constituents—In spite of the large number of radioactive isotopes readily available in these days, there are still many chemical and biological problems which cannot be successfully studied by the means of normal radioactive tracer technique. This applies in particular to research problems on materials consisting essentially of nitrogen and oxygen, since the radioactive isotopes of these elements have too short a half-life to be of use in a long-term study. There are also certain cases where a radioactive isotope with a long half-life such as carbon-14 may be unsuitable. Thanks to the existence of the mass spectrometer, research work which otherwise would be limited by the availability of available radioactive isotopes can be extended by employing stable isotopes. The mass spectrometer makes it possible to analyse the isotopic constituents of stable elements and therefore such instruments are in use in several hospitals and medical research institutions.

It is beyond the scope of this article to describe in detail the design and operation of mass spectrometers, reference should be made to the article on mass spectrometers published in a previous issue of this journal. But it will be remembered that the Nier-type mass spectrometer, which is the type frequently used, facilitates selective collection of the ions originating from the ionized sample by deflecting the ions in a magnetic field of constant strength ; consequently the curvature of the path of the ion will vary according to their mass. Needless to say that the working principle of this

Vol. 9 959/60

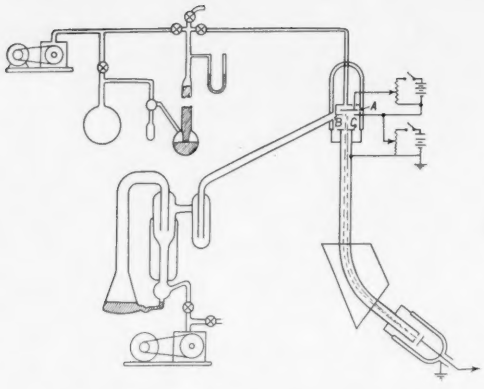

FIG. 19. Principle of Nier–Harper mass spectrometer.

instrument depends for its functioning on the provision of a vacuum of the highest order.

In this form of mass spectrometer the material under investigation must be in a gaseous state so that ionization may be effected at normal temperatures. The samples are prepared in a vacuum manifold attached to the instrument. Purification by fractional distillation, freeze-drying or special devices to conduct reactions under reduced pressure are but some of the facilities made available in attachments to apparatus of this kind.

Examples of the uses of stable isotopes in medical research—The discovery that nitrogen mustard and sulphur mustard inhibit cell division, suggested the possibility of using these compounds for the treatment of certain forms of cancer such as leukaemia. To facilitate the work the nitrogen mustard was enriched with the isotope nitrogen-15. The study was carried out *in vitro* and involved observations on the action of nitrogen mustard with respect to certain protein molecules. These experiments were facilitated by examining and analysing the end-products in a mass spectrometer.

Another line of research was the investigation of a condition known as hyperoxaluria, a disease characterized by the secretion of oxalic acid. The isotopes nitrogen-15 and carbon-13 were employed in the study which extended to an investigation of the metabolism of glycine, a possible precursor in the formation of oxalic acid.

Both these examples serve as good illustrations for the type of research which is facilitated by the existence of the mass spectrometer. It has proved a most valuable supplementary instrument facilitating in certain instances the extension of the study of metabolic processes, a sphere of activities which has acquired almost unlimited possibilities with the discovery of radioactive isotopes.

Vo
9
1959

The Structure and Density of Iron Films formed by Thermal Evaporation

O. S. HEAVENS, M. M. BROWN and V. HINTON

Royal Holloway College, University of London, Englefield Green, Surrey

The densities have been determined of iron films of thickness 800–1600 Å. deposited on the cleavage faces of rocksalt crystals maintained at 470°C. The films are monocrystalline, as shown by electron diffraction, and appear continuous when examined in the electron microscope. The values obtained for the densities are found not to differ significantly from that for the bulk metal.

Vol. 9 959/60

Introduction

As a necessary preliminary to the study of the magnetic properties of single-crystal thin films of iron, the structure and densities of such films have been investigated. The films were formed by evaporation on to cleavage faces of rocksalt, maintained at temperatures up to 470°C. The structure has been determined by electron diffraction and electron microscopy. Film thicknesses were measured by multiple-beam Fizeau fringes[1] and the masses of the films by a microchemical technique.

Film structure

The general features of the structure of iron films, from electron diffraction observations, have been described earlier by Collins and Heavens[2]. Films formed at a rate of deposition of ~50 Å/sec on the (001) face of a rocksalt substrate at room temperature are found to be polycrystalline with random orientation of crystallites. As the temperature is raised, the crystallite size increases and at about 350°C the crystallites tend to sit on (111) faces, resulting in fibre orientation. As the temperature is further raised, three-dimensional ordering develops with the (001) face of the iron crystals lying parallel to the (001) rocksalt face. Either of two orientations of the iron may form or, in some cases, a mixture of the two. The [100] direction of the iron lattice aligns itself either along the [100] NaCl axis or along the [110] direction. Fig. 1 shows the pattern obtained from a film ~700 Å thick deposited at 400°C. Although mainly polycrystalline, definite signs of orientation are present. At 470°C, orientation is complete, as is shown by the orderly array of diffraction spots in Fig. 2. Care is necessary in control of the substrate temperature if appreciable oxidation is to be avoided. Fig. 3 was obtained from a film grown at 500°C. Most of the additional rings in this pattern are due to disoriented oxide on the film surface. It is interesting to note that whereas films which are allowed to oxidize at 470°C generally show the oxide to grow epitaxially on the metal surface,[2] more rapid oxidation at the higher temperature results in a disoriented layer. The pressure in the evaporation system was maintained at $> 3 \times 10^{-5}$ mm Hg.

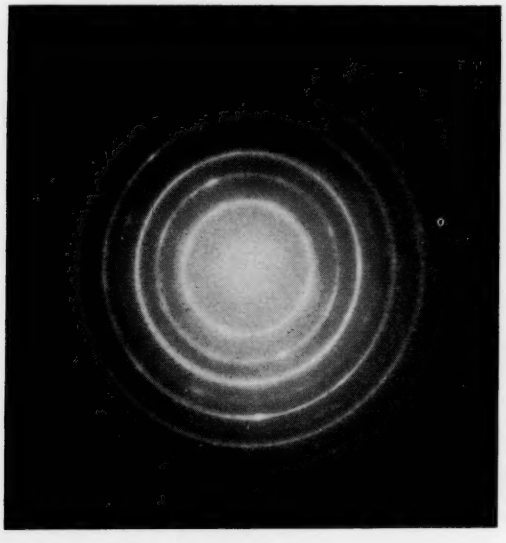

FIG. 1. Electron diffraction pattern of iron film ~700 Å thick, deposited at 50 Å.sec^{-1} on rocksalt substrate at 400°C.

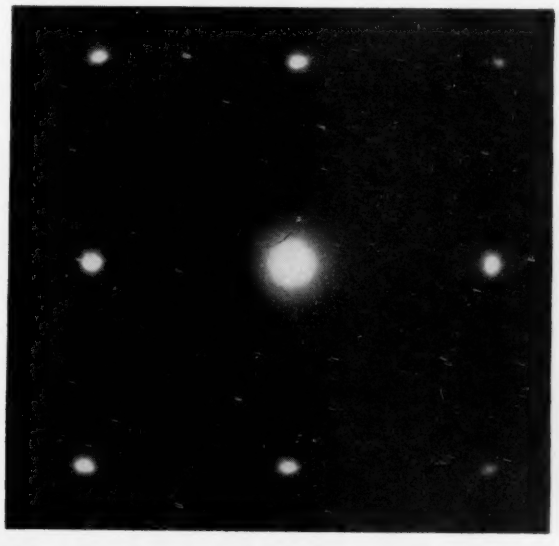

FIG. 2. Pattern from a similar film formed on rocksalt at 470°C.

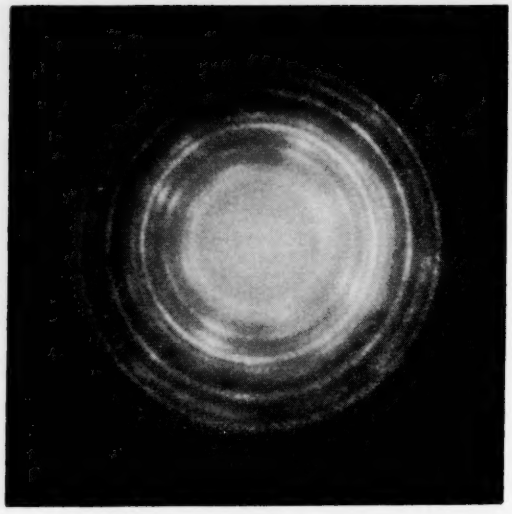

FIG. 3. Pattern showing considerable oxide on film formed at 500°C.

Film density measurement

Preparation of films—The evaporation of iron was effected by electron bombardment of a pendant drop (Kelly[3], Heavens[4]). The arrangement is shown in Fig. 4. The

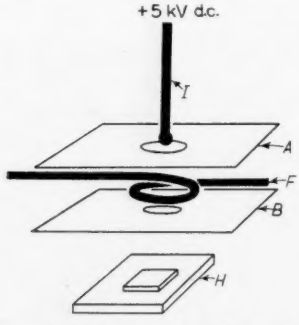

FIG. 4. Arrangement for the evaporation of iron by electron bombardment.

shield *A*, connected to the molybdenum filament *F*, serves for rudimentary focusing of the electrons from *F* on to the end of the iron rod *I*. A similar shield *B* is arranged so that the specimen, on the hotplate *H*, cannot see the filament. With a rod of diameter 3 mm, an electron current of ~15 mA sufficed to form a stable drop ~5 mm in diameter. The bombarding current is conveniently controlled by varying the filament current. It is convenient to arrange that the position of the rod *I* can be adjusted from outside the system.

Thickness measurements—Rocksalt cleavage surfaces are not sufficiently flat microscopically to enable thickness measurements to be made *in situ*. The films were therefore removed from the rocksalt by solution of the underlying crystal and picked up on a glass flat. The edge of the film was then silvered and Fizeau fringe measurements made in the usual way. Previous measurements by Heavens and Pandeya[5] have confirmed the validity of this procedure.

Mass determination—The masses of the films were determined by a standard microchemical colorimetric procedure using Tiron[6] (1 : 2-dihydroxybenzene-3 : 5-disulphonic acid. Sodium salt.) The experimental details are given since it has proved possible to make commendably accurate measurements with simple apparatus.

The film is dissolved in 2 ml of 7 per cent HCl. Equal volumes are taken of the iron solution, Tiron reagent (0.0075 M), 8 per cent ammonia solution and sodium phosphate/sodium hydroxide buffer, the latter serving to bring the pH of the solution to 9.5. A pink coloration results. A blank solution is made with distilled water substituted for the test solution. The transmissions of the solutions are measured using a colorimeter arranged as shown in Fig. 5.

FIG. 5. Schematic arrangement of colorimeter for microchemical determinations.

Light from a filament lamp is collimated and passes through a Wratten 28 filter *F*. The shutter *S* enables either cell to be selected ; the light falls on a barrier-layer photocell *P*. Even with identical solutions in the two cells, the photocell outputs for the two shutter positions are generally slightly different, partly on account of non-uniformity of illumination and partly due to variation of sensitivity across the photocell surface. Measurements are first made with blank solutions in each cell thus enabling the ratio of overall transmissions to be obtained. The readings for this case are designated θ_{0a} and θ_{0b}. Test solutions are then measured in cell *A* whilst measurements on the blank solution in cell *B* serve to indicate any changes due, e.g. to changing light output or changing photocell sensitivity with ambient temperature. In practice, with the circuit arrangements given below, these changes amount to at most a few parts in 10,000 over periods of several minutes. If the readings for cell *A* (test solution) and cell *B* (blank solution) are θ_a and θ_b then the density of the test solution is given by :

$$\log \left\{ \frac{\theta_{0a} \times \theta_b}{\theta_{0b} \times \theta_a} \right\}$$

Calibration is effected by using solutions of known concentration and the density is plotted against concentration. Fig. 6 shows the calibration so obtained. A micro-cell with a volume of 0.3 ml and a path length of 1 cm was used.

The usual precautions are needed to ensure stability of the lamp current. The circuit shown in Fig. 7 served to keep fluctuations to below the limit of measurement of the photocell output (2–3 parts in 10^4) over periods large compared with the time required to take pairs of readings. It was found advisable slightly to under-run the lamp (0.43 A instead of 0.5 A). Before connecting the 200 V/d.c., *M* is short-circuited and the manganin resistance *R* is adjusted until the required current is obtained. The 200 V supply is then connected and the rheostat adjusted until the same current is registered. The batteries then serve to supply

only the small difference current occasioned by a variation in the main d.c. supply.

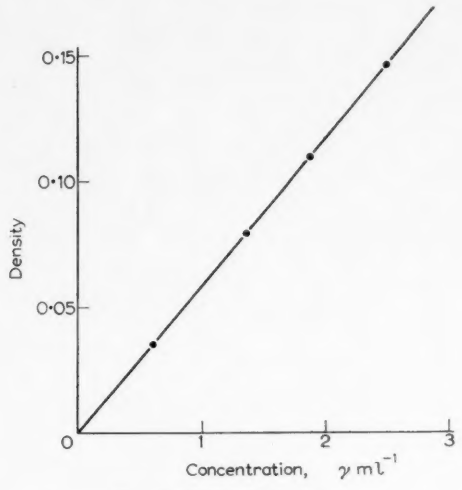

FIG. 6. Calibration curve.

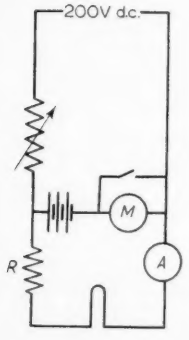

FIG. 7. Simple circuit for stabilizing lamp current.

The output from the barrier-layer photocell was measured with the usual zero-impedance circuit (Fig. 8). The photocell

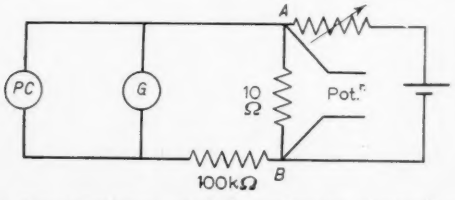

FIG. 8. Zero-impedance circuit for measuring photocell output.

current was determined by measuring the p.d. across *AB* with a potentiometer. Readings to five significant figures are made, their repeatability being such that the mean of a half-dozen readings is reliable to better than 0.05 per cent. This enables the concentration of a solution containing 10^{-6} g.ml^{-1} $\equiv 1$ μg.ml^{-1} to be determined to within ± 1 per cent, a noise level of 10^{-8} g.ml^{-1}. Beer's Law was found to be accurately obeyed up to concentrations of ~ 3 μg.ml^{-1}.

Results of density measurements

The accuracy of the density measurements is limited, for the most part, by the uncertainties in the film thicknesses. The rather drastic treatment of removing and re-mounting the film results in a slight deterioration in fringe definition. For films of thickness around 800 Å the thickness measurements are estimated to be reliable to ± 20 Å.

The results obtained are summarised in Table I below. The rate of deposition was found to vary over a factor of about 2, even for constant electron bombarding current. It is unlikely that variation over this small range will affect the results.

TABLE I

Density of Films grown epitaxially on Rocksalt at 470°C

Film thickness (Å)	Rate of deposition (Å/sec)	Density (g.cm^{-3})
840 ± 20	40	7.8_8
936	50	7.8_2
1120	20	7.8_8
1180	39	7.9_0
1210	40	7.8_2
1670	25	7.6_2
1670	25	8.1_9

The density quoted[7] for iron is 7.85–7.88 g.cm^{-3}. It appears therefore that films grown epitaxially on rocksalt possess the bulk density, within the accuracy of these determinations. This conclusion is supported by electron micrographs of the films, which show no sign of voids or of grain boundaries. Typical structures of films deposited cold on amorphous substrates (Sennett and Scott[8]) show a considerable extent of voids. These may be compared with Fig. 9, taken of a

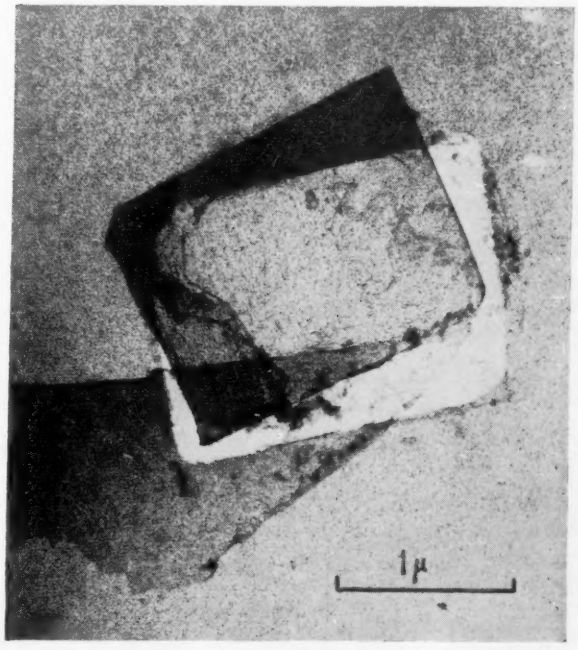

FIG. 9. Electron micrograph of damaged iron film showing (100) cleavage.

film ~300 Å thick. Part of this film is seen to be broken away, the film having cleaved along [100] directions. Whether the break at 45° in one corner is a genuine [110] cleavage is uncertain.

Conclusions

The method of evaporation employing a pendant drop heated by electron bombardment is found to be highly satisfactory for iron. The mass of iron films can be determined by microchemical colorimetric techniques using simple apparatus and circuitry. An accuracy of ±1 per cent is attained for the mass of a film of area 0.5 cm^2 and of thickness 50 Å on the assumption that the density is the same as that of the bulk metal. Measurements of the density of films grown epitaxially on the (001) cleavage face of rocksalt at 470 °C yield a mean value 7.93 ± 0.15 $g.cm^{-3}$ compared with the bulk figure of 7.86 $g.cm^{-3}$. Electron diffraction examination shows such films to be in a crystallographically ordered state and electron micrographs show no voids or grain boundaries.

Acknowledgments

Thanks are due to Dr. P. Holt for guidance in the microchemical work and for the loan of a colorimeter : and to A. Grant and J. Henley for their assistance in the design and construction of an improved instrument.

References

[1] S. Tolansky ; *Multiple Beam Interferometry*, Oxford University Press (1948).
[2] L. E. Collins and O. S. Heavens ; The epitaxial growth and oxidation of nickel, iron and cobalt on rocksalt, *Proc. Phys. Soc* **B70**, 265–281 (1957).
[3] O. S. Heavens and D. C. Pandeya ; Thickness measurement of epitaxially grown films, *Nature, Lond.* **181**, 1394 (1958).
[4] J. C. Kelly ; An electron bombardment apparatus for vacuum evaporation, *J. Sci. Instrum.*, in press.
[5] O. S. Heavens ; The evaporation of metals by electron bombardment, *J. Sci. Instrum.*, in press.
[6] Hopkins and Williams, Monograph No. 28 (1956).
[7] *Handbook of Chemistry and Physics* (31st Ed.) Chemical Rubber Publishing Co. (1949).
[8] R. S. Sennett and G. D. Scott ; The structure of evaporated metal films and their optical properties, *J. Opt. Soc. Amer.* **40**, 203–211 (1950).

Vo
9
1959

The Breakage of Glass Ampoules during Freeze-drying

N. S. VERMA and T. W. G. ROWE

Freeze Drying Research Laboratory, Edwards High Vacuum Ltd., Crawley, Sussex

It is shown that the nature of the material (its eutectic point and the concentration of the eutectic mixture), the quantity of material in each ampoule and adhesion of frozen material to the glass wall play important roles in causing breakage of glass ampoules during centrifugal evaporative freezing. Other factors are also discussed.

Vol. 9 959/60

Introduction

Centrifugal freeze-drying, introduced by Greaves[1], has become popular in recent years. The method is based on the evaporative freezing in the drying chamber of the substance to be freeze-dried. The material is contained in ampoules which are centrifuged at low speed to prevent frothing while the pressure is reduced before freezing occurs ; centrifuging also disposes the material in the ampoules in the form of wedges. Breakage of the ampoules during freezing is sometimes observed. Its frequency appears to vary with the nature of the fluid : solutions of albumen in distilled water, or distilled water alone, causing extensive damage which may be reduced if the quantities dispensed in the ampoules are small. Breakage is undesirable as it may lead to the loss of valuable material and contamination of the apparatus with infectious materials.

The writers can find no published record of the breakage of ampoules during freeze-drying. Their object was to investigate the factors causing it and to propose a remedy.

Material and methods

Ampoules of neutral glass from the stock of Messrs. Edwards High Vacuum Limited were used in the investigation. These correspond closely to the British Standard Specification for ampoules to be used in freeze-drying. Some data relating to them are given in Table I.

TABLE I

Capacity for freeze drying (ml)	Average thickness of glass (mm)	Average internal diameter of ampoule (mm)
0.5	0.85	5.7
2.5	0.80	13.6
10.0	nearly 0.50	22.0

An Edwards 3PS Centrifugal Freeze Dryer was used in all the experiments. The duration of the tests was 15 min from the commencement of evacuation from atmospheric pressure in all cases unless otherwise stated. Usually this time was sufficient to permit complete freezing of the test material.

Experimental procedure

(a) *Susceptibility to breakage*—To see whether a proportion of ampoules in a batch was more prone to breakage than the remainder, a number of 10 ml ampoules containing tap water only were used repeatedly, the survivors from a previous test being employed in the subsequent one. Not only was it found that the breakage occurred in a similar way in each test, but that approximately the same proportion of ampoules broke on each occasion.

(b) *Effect of varying the volume of ampoule content*—As before, tap water was used. The results are given in Table II.

TABLE II

Ampoule (ml)	Quantity of water used (ml)	Total no. of ampoules used	Average breakages (%)	Ice in bottom
0.5	0.3	200	1.5	About ½ full
	0.4	100	38.0	½ full
	0.5	250	78.5	Over ½ full
	0.7	100	80.0	Full
2.5	2.5	120	3.3	½ full
	3.0	120	5.8	Over ½ full
	3.5	120	20.8	¾ full
10.0	5.0	60	10.0	Less than ½ full
	8.0	60	8.3	About ½ full
	10.0	60	28.3	Over ½ full
	12.0	60	78.3	¾ full

(c) *Effect of altering the inclination of the ampoules*—Ampoules are usually inclined towards the axis of rotation at an average angle of 7° from the vertical. This inclination varies depending upon differences in ampoule diameters. If the ampoules are arranged more nearly vertically in the carrier assembly, the wedge of material extends into the neck and, in extreme cases, it may spill out of the ampoule. Inclining ampoules further from the vertical produces a shorter and thicker wedge of material extending beyond the axial plane and causing a higher proportion of breakages.

The results are as in Table III.

(d) *Effect of adhesion of ice to the glass*—The ice formed during evaporative freezing adheres strongly to the glass.

TABLE III

Ampoule used	Quantity of water used	Breakage with normal inclination (%)	Breakage with increased inclination (%)	Remarks
10 ml	10 ml	28.3	75.0	Bottom of wedge extending across the ampoule

To reduce this, ampoules were coated internally with a silicone preparation (Repelcote) manufactured by Hopkins & Williams, London. The results obtained, using tap water in 0.5 ml ampoules, are recorded in Table IV.

TABLE IV

Quantity of water used (ml)	Breakage among uncoated ampoules* (%)	Breakage among silicone coated ampoules† (%)
0.3	1.5	0
0.4	38.0	0
0.5	78.5	0
0.7	80.0	0

* Ice adhered strongly to the glass surface.

† No adhesion of ice to the glass surface.

(e) *Effect of eutectic point of material*—A number of solutions having known or measurable eutectic points were evaporatively frozen in 0.5 ml ampoules. The results are given in Table V.

TABLE V

Solution	Quantity in each ampoule (ml)	Eutectic point (°C)	Breakage (%)
Tap water	0.7	—	80.0
0.1% Sodium sulphate	0.7	−1.1*	80.0
0.1% Sodium carbonate	0.7	−2.2*	30.0
0.1% Ammonium chloride	0.7	−16*	0.0
0.1% Sodium chloride	0.7	−21.2*	1.3
0.1% Potassium iodide	0.7	−23*	0.0
0.1% Calcium chloride	0.7	−51*	0.0
Serum	0.7	−60†	0.0

* Perham[2]

† Greaves[1]

It will be seen from the above table that substances having a higher eutectic point cause more breakage than those with a lower eutectic.

(f) *Effect of concentration of substances*—Sodium chloride solutions of varying concentrations were evaporatively frozen in 0.5 ml ampoules (the eutectic point of sodium chloride in water is −21.2°C). The results are shown in Table VI.

TABLE VI

Sodium chloride solution (% w/v)	Quantity in each ampoule (ml)	Breakage (%)
0.01	0.5	50
0.02	0.5	50
0.03	0.5	12
0.05	0.5	13
0.1	0.5	3
0.2	0.5	0
0.85	0.5	0

(g) *Effect of position of the ampoule in a centrifugal carrier*—10 ml ampoules, of which sixty could be accommodated in holes arranged on four concentric circles, were used. The variations of breakage according to position and content were noted. The results shown in Table VII indicate that the position of the ampoule does not significantly affect the breakage figures.

TABLE VII

Quantity of water in each ampoule (ml)	Breakage (%)			
	Inner row	Inner central	Outer central	Outermost
5	10	0	10	15
8	0	20	10	5
10	70	30	15	20
12	100	100	75	60
Average breakage	45	37.5	27.5	25

Apparent causes of breakage

The above results indicate collectively that ampoule breakage may be reduced by a number of expedients. These are (1) to reduce the quantity of material dispensed into each ampoule ; (2) to change the composition of the material to be dried, either basically by using an alternative suspending medium, or by adding substances to reduce the eutectic ; (3) to coat the ampoule internally with a water-repelling substance to reduce adhesion of the ice. Pre-freezing of the ampoule obviates the difficulty, but also discards the advantage of evaporative freezing. Increasing the wall thickness or altering the composition of the glass of the ampoule might also solve the problem, but would introduce manipulative difficulties, e.g. in vacuum sealing.

The effect of composition of the material on breakage

It seemed that a satisfactory answer to the problem lay in further study of the effect of the composition of the substance on breakage, or in the employment of a water-repellant coating. The following substances were, therefore, investigated and the results tabulated as in Table VIII.

(a) *Distilled water*—See experiment (b) in part I.

(b) *Human plasma*—The plasma for this purpose was obtained by reconstitution of freeze-dried product.

Vo 9 1959

TABLE VIII

Ampoule (ml)	No. of ampoules used	Quantity in each ampoule (ml)	Breakage (%)	Remarks
0.5	100	0.5	0	No cracks in ice
	100	0.6	4	,,
		0.7	11	,,
2.5	100	2.5	0	,,
10.0	40	10.0	0	,,

(c) *Partially skimmed milk*—Results are tabulated in Table IX.

TABLE IX

Ampoule (ml)	No. of ampoules used	Quantity in each ampoule (ml)	Breakage (%)	Remarks
0.5	50	0.5	0	No cracks in ice
	50	0.6	0	,,
	50	0.7	0	,,
10.0	40	10.0	0	,,

(d) *Glucose solution in distilled water*—Glucose solutions of various concentrations were prepared by dissolving glucose B.P. in distilled water. 0.5 ml ampoules were used (Table X).

TABLE X

Glucose (% w/v)	No. of ampoules used	Quantity in each ampoule (ml)	Breakage (%)	Remarks
0.2	50	0.5	56	Cracks in ice
	50	0.7	64	,,
	50	1.0	78	,,
0.25	50	0.5	24	,,
	50	0.7	52	,,
		1.0	52	,,
0.3	50	0.5	4	Some cracks in ice
	50	0.7	4	,,
	50	1.0	4	,,
0.4	50	0.5	0	No cracks in ice
	50	0.7	0	,,
	50	1.0	0	,,
0.5	50	0.5	0	,,
	50	0.7	0	,,
	50	1.0	0	,,
1.0	50	0.5	0	,,
	50	0.7	0	,,
	50	1.0	0	,,
7.5	50	0.5	0	,,
	50	0.7	0	,,
	50	1.0	0	,,

(e) *Gelatin solution in distilled water*—Gelatin (B.D.E.) solutions of various concentrations were prepared in distilled water by dissolving the powder with the aid of heat in a water bath. 0.5 ml ampoules were used (Table XI).

TABLE XI

Gelatin solution (% w/v)	No. of ampoules used	Quantity in each ampoule (ml)	Breakage (%)	Remarks
1	50	0.5	46	Many cracks
	50	0.7	94	,,
	50	1.0	100	,,
5	50	0.5	0	No visible cracks
	50	0.7	6	,,
		1.0	14	,,

(f) *Mixed contents of infertile eggs in* 0.5 ml *ampoules*—The contents of several fresh infertile eggs except membrane and shell were well mixed and diluted with distilled water as required. The results of breakage are noted in Table XII.

TABLE XII

Solution (% v/v)	No. of ampoules used	Quantity in each ampoule (ml)	Breakage (%)	Remarks
5	50	0.5	28	Cracks in ice
	50	0.7	66	,,
25	50	0.5	0	Some cracks
	50	0.7	28	,,
	50	1.0	74	,,
50	50	0.5	0	No cracks in ice
	50	0.7	4	,,
	50	1.0	20	,,
Undiluted	50	0.5	0	,,
	50	0.7	0	,,
	50	1.0	0	,,

(g) *Egg yolk in* 0.5 ml *ampoules*—After removing the white from fresh infertile eggs, the yolk was pooled in a beaker and well homogenized. It was diluted with distilled water as required. The results are recorded in Table XIII.

TABLE XIII

Solution (% v/v)	Ampoules used	Quantity in each (ml)	Breakage (%)	Remarks
10	75	0.5	4	No visible cracks
	75	0.7	27	,,
	25	1.0	20	,,
Undiluted	20	0.5	0	,,
	20	0.7	0	,,
	20	1.0	0	,,

(h) *Egg white in* 0.5 ml *ampoules*—Egg white from several fresh infertile eggs was collected in a beaker and well mixed. It was diluted with distilled water when required. Results are noted in Table XIV.

(i) 10 *per cent egg white with sodium chloride in* 0.5 ml *ampoules*—Results are given in Table XV.

Vol. 9 959/60

TABLE XIV

Solution (% v/v)	No. of ampoules	Quantity in each (ml)	Breakage (%)	Remarks
10	50	0.5	56	Many cracks in ice
	50	0.7	98	,,
	50	1.0	94	,,
50	25	0.5	0	Some cracks in ice
	35	0.7	56	,,
	10	1.0	90	,,
Undiluted	10	0.5	0	No visible cracks
	20	0.7*	5	,,
	10	1.0*	50	,,

* Evaporative freezing was carried out for 30 min.

TABLE XV

NaCl in 10% egg white (%)	No. of ampoules	Quantity in each (ml)	Breakage (%)	Remarks
0.05	50	0.5	44	Some cracks in ice
	50	0.7	100	,,
	50	1.0	100	,,
0.5	25	0.5	0	No cracks in ice
	10	0.7	0	,,
	10	1.0	0	,,
0.85	50	0.5	0	,,
	25	0.7	0	,,
	25	1.0	0	,,

(j) *Glycerin solution in distilled water in* 0.5 ml *ampoules*—Results are shown in Table XVI.

TABLE XVI

Glycerin solution (%)	No. of ampoules	Quantity in each	Breakage (%)	Remarks
0.05	50	0.5	22	Cracks in ice
	50	0.7	80	,,
	50	1.0	96	,,
0.1	50	0.5	6	Some cracks in ice
	50	0.7	4	,,
	50	1.0	4	,,
0.2	50	0.5	0	,,
	50	0.7	0	,,
	50	1.0	0	,,
0.25	50	0.5	0	,,
	50	0.7	0	,,
	50	1.0	0	,,
0.3	50	0.5	0	,,
	50	0.7	0	,,
	50	1.0	0	,,
0.4	50	0.5	0	,,
	50	0.7	0	,,
	50	1.0	0	,,
0.5	100	0.5	0	,,
	100	0.7	0	,,
	100	1.0	0	,,
5.0	100	0.5	0	,,
	100	0.7	0	,,
	100	1.0	0	,,

(k) *Sodium chloride solution in distilled water in* 0.5 ml *ampoules*—Results are given in Table XVII.

TABLE XVII

NaCl solution (%)	No. of ampoules	Quantity in each (ml)	Breakage (%)	Remarks
0.01	50	0.5	50	Cracks in ice
	50	0.7	86	,,
	50	1.0	96	,,
0.02	100	0.5	50	,,
	100	0.7	53	,,
	100	1.0	39	,,
0.03	100	0.5	12	,,
	100	0.7	9	,,
	100	1.0	7	,,
0.05	100	0.5	13	,,
	150	0.7	19	,,
	150	1.0	31	,,
0.1	150	0.5	3	No visible cracks
	150	0.7	1	,,
	150	1.0	7	,,
0.2	50	0.5	0	,,
	50	0.7	2	,,
	50	1.0	14	,,
0.85	50	0.5	0	,,
	50	0.7	0	,,
	50	1.0	0	,,

(l) *Bovine serum in* 0.5 ml *ampoules*—Results are given in Table XVIII.

TABLE XVIII

No. of ampoules used	Quantity in each ampoule (ml)	Breakage (%)	Remarks
50	0.5	0	No cracks in ice
50	0.7	0	,,

Effect of the prevention of adhesion on breakage

If a water-repellant is to be used it is first necessary to establish its efficacy in preventing breakage when a range of substances are to be evaporatively frozen. A number of such substances were investigated, but in each case only Repelcote was employed for treating the ampoules. Clean and dry ampoules were filled with Repelcote and immediately emptied and drained. For convenience some ampoules were forced-dried with compressed air and others were dried normally before use. The results are tabulated in Table XIX.

Resistance of Repelcote to washing

A further problem in connexion with the use of silicone coating is its resistance to washing. A 10 per cent solution of egg white in distilled water was evaporatively frozen in 100 Repelcote-treated ampoules of 0.5 ml nominal capacity. To increase the stringency of the test, 0.7 ml of solution was dispensed into each ampoule. When 0.5 ml of this solution is employed in untreated ampoules the breakage is as high as 98 per cent. The treated ampoules were used successively for six experiments, being washed thoroughly with tap and distilled water after each test. The results are given in Table XX.

Vo 9 1959

TABLE XIX

Comparative Breakage Among Uncoated and Silicone-coated Ampoules

Material	Ampoule (ml)	Quantity in each ampoule (ml)	Breakage in uncoated ampoules (%)	Breakage in silicone-coated ampoules (%)
Tap water	0.5	0.3	1.5	0
		0.4	38.0	0
		0.5	78.5	0
		0.7	80.0	0
	2.5	2.5	3.3	0
		3.0	5.8	0
		3.5	20.8	0
		4.0	—	0
	10.0	5.0	10.0	0
		8.0	8.3	1.6
		10.0	28.3	3.3
		12.0	78.3	15.0
02.% Glucose	0.5	0.5	56.0	4.0
		0.7	64.0	0
		1.0	78.0	0
0.05% Glycerin	0.5	0.5	22.0	0
		0.7	80.0	0
		1.0	96.0	0
5% Mixed egg contents in distilled water	0.5	0.5	28.0	0
		0.7	66.0	0
Egg white	0.5	0.5	0.0	0
		0.7	5.0	0
		1.0	50.0	40
10% Egg white in distilled water	0.5	0.5	56.0	0
		0.7	98.0	4
		1.0	94.0	2
10% Egg yolk in distilled water	0.5	0.5	4.0	0
		0.7	24.0	0
		1.0	20.0	0
1% Gelatin in distilled water	0.5	0.5	46.0	2
		0.7	94.0	4
		1.0	100.0	6

TABLE XX

Ampoule	Quantity in each (ml)	No. of washing	No. of ampoules used	Breakage (%)
0.5 ml	0.7	—	100	4.1
	0.7	1st	90	1.1
	0.7	2nd	80	5.0
	0.7	3rd	75	10.6
	0.7	4th	60	10.0
	0.7	5th	50	10.0

It can be seen from the above that the Repelcote-treated ampoules could be used three times before a significant increase in the rate of breakage occurred. For most applications, however, the ampoule is used only once.

Effect of Repelcote treatment on the viability of bacteria—A final factor influencing the choice of Repelcote is its effect on the viability of bacteria.

In experiments involving the investigation of bacterial survival the treated ampoules were sterilized by autoclaving or in a hot air oven.

Bacterial counts were done by the surface counting method of Miles and Misra. The virus of Newcastle disease was titrated in developing eggs by injecting 0.1 ml of various dilutions in the allantoic cavity. Results are given in Tables XXI to XXVI.

TABLE XXI

NCTC 8001 *Suspended in Normal Horse Serum**

Time	Normal	Tubes coated with Repelcote	Tubes coated with Repelcote + treated paper
Before drying	5×10^6	5×10^6	5×10^6
After drying	25×10^2	80×10^3	35×10^3
After 1 month ..	45×10^4	50×10^3	35×10^4
After 3 months.. ..	35×10^4	40×10^4	80×10^4

* Private communication by Dr. S. T. Cowan (1956), the Curator of National Collection of Type cultures, London, N.W.9.

TABLE XXII

Pasteurella boviseptica Suspended in "Mist desiccans"

Time	Normal	Tubes treated with Repelcote
Before drying	3425×10^6	3425×10^6
After drying	2975×10^6	2900×10^6
After 2 months.. ..	1350×10^6	1250×10^6
After 11 months at 4°C..	1220×10^6	1380×10^6

TABLE XXIII

A Virulent Anthrax Vaccine Strain (34F2)

Time	Normal	Tubes treated with Repelcote
(a) *Suspended in "mist desiccans"*		
Before drying	400×10^6	400×10^6
After drying	40×10^6	40×10^6
(b) *Suspended in 0.5% yeast extract*		
Before drying	28×10^6	28×10^6
After drying	7×10^6	10×10^6
After 10½ months at 4°C	6.8×10^6	7.8×10^6

TABLE XXIV

Brucella abortus Strain 99 Suspended in Rabbit Serum

Time	Normal	Tubes coated with Repelcote
Before drying	5800×10^6	5800×10^6
After drying	192×10^6	392×10^6
After 10½ months at 4°C	148×10^6	122×10^6

Vol. 9 959/60

TABLE XXV

Coliform Organism D201H *Suspended in* " *Mist desiccans* "

Time	Normal	Tubes coated with Repelcote
Before drying	455×10^6	455×10^6
After freeze drying ..	270×10^6	395×10^6
After $10\frac{1}{2}$ months at 4 °C	86×10^6	89×10^6

The Newcastle disease virus was grown in chick embryos and an emulsion of embryo, membranes and fluids was prepared in a Waring Blendor. This emulsion was freeze dried. Titration of the virus was done in living chick embryos using five eggs for each titration. Each inoculated dead egg was subjected to H.A. test.

TABLE XXVI

Newcastle Disease Virus (*Mukteswar Vaccine Strain*)

Time	L.D.50 titre in normal tubes	L.D.50 titre in tubes treated with Repelcote
Before drying	$10^{-8 \cdot 63}$	$10^{-8 \cdot 63}$
After drying	$10^{-7 \cdot 62}$	$10^{-7 \cdot 67}$
After 11 months at −20 °C	$10^{-7 \cdot 74}$	$10^{-7 \cdot 74}$

The above experiments show that Repelcote treatment of the glass ampoules does not show any perceptible toxicity towards the viability of the bacteria or viruses used.

Discussion

It is clear that the nature of the material, the quantity in each ampoule and adhesion of the frozen material to the glass surface influence the breakage of glass ampoules during centrifugal evaporative freezing.

The nature of the material to be frozen and freeze-dried determines not only its adhesion to glass but also the crystalline form and degree of expansion on freezing. It has been observed that when materials giving rise to a high rate of breakage are frozen, the solid appears to be hard and shows cracks. Conversely, the materials which do not cause much breakage present a smooth appearance and are free from cracks after freezing. The " hardness " of the frozen material depends on the eutectic point of the mixture or solution and also on the concentration of any solid which it contains. The variation in the breakage of ampoules due to the eutectic point of the material and concentration of the eutectic mixture is illustrated by the experiments.

These facts are explained by Perham[2] as follows :

" If a solution of a concentration less than the eutectic, at a temperature above 32 °F, is cooled it will not solidify at 0 °C but will continue to cool as a liquid. The ice crystals of pure water begin to form accompanied by removal of their latent heat thereby increasing the concentration of the solution. As the temperature is lowered these crystals continue to form and the mixture of ice crystals and brine solution form a slush and later the liquid freezes at eutectic concentration ".

The temperature resulting from evaporative freezing is not always below −20 °C, hence solutions having a eutectic point below this will never be " hard " frozen, thereby causing less breakage of the ampoules. Those having eutectic points above this will be " hard " frozen, as in the case of sodium sulphate solution, and cause higher breakage. Again the hardness of the frozen mass also depends on the concentration of the eutectic mixture. As the concentration of salt or salts in the mixture decreases the proportion of pure ice crystals will increase. Thus the " hardness " of the frozen mass depends on the proportion of ice crystals formed, and the breakage of ampoules will increase with the increase in " hardness " of the frozen mass.

Reduced breakage obtained with smaller quantities of material is due to the fact that a thin layer is formed which freezes throughout almost instantaneously. If the quantity of the material in the ampoule is increased, the frozen wedge of ice is considerably thicker in the lower portion. In this case, superficial layers of the material freeze first and become attached at the edges to the glass wall. Expansion of the remaining trapped fluid sets up strain which, if not released by rupturing, or if the surface on becoming detached cannot move into a volume of expanding cross-section, fractures the glass. The site of the fracture is always associated with the thickest layer of material. The above reasoning is supported by the fact that breakage can be increased by increasing the thickness of the wedge by altering the angle of inclination of the ampoule from the vertical.

As it may not be possible to change the position of the ampoule to be dried by adding certain substances to bring down the eutectic point or, more drastically, to change the suspending medium ; and as the advantage of evaporative freezing is lost if the contents of ampoules are pre-frozen, only two courses remain. One is considerably to decrease the quantity of material in the ampoule so that only a thin layer is formed which freezes homogeneously. The other is to coat the ampoule with a water-repellant, e.g. silicone, to prevent the adhesion of ice to the glass surface.

Silicone water-repellants are used nowadays for various purposes and on a large scale. In pharmaceutical manufacture and distribution, they are now being used on glass ampoules and vials containing penicillin and similar aqueous suspensions or emulsions. Glass laboratory apparatus so treated gives improved release of liquids which results in more accurate transfer (Gilbert[3]). In a similar way glassware for the handling of blood is treated with chlorosilanes to form a siliconized surface (Clark *et al.*[4]). The clotting time of blood in treated glassware is considerably increased. Artificial kidneys have been constructed using silicone-coated rubber grids for supporting the dializing membranes (Skeggs and Leonards[5]).

Conclusions

Treatment of glass ampoules with Repelcote (Hopkins & Williams) significantly reduces the breakage during centrifugal

evaporative freezing. The coating is fairly resistant to washing and exerts no toxicity towards various bacteria and the virus of Newcastle disease. Use of this substance obviates the necessity for altering the composition of the material to be freeze-dried.

The authors are grateful to the Food and Agriculture Organization of the United Nations, Rome, and Messrs. Edwards High Vacuum Ltd., Manor Royal, Crawley, Sussex, England for providing facilities for the work. They also acknowledge with thanks the communication of work on the viability of NCTC 8001 culture by Dr. S. T. Cowan, Curator of National Collection of Type Cultures, Public Health Laboratories, London.

They are also indebted to Sri P. G. Pande, Director of Animal Husbandry, U.P. and Sri K. Govinda Rau, Deputy Director i/c Biological Products Section, Badshahbagh, Lucknow, U.P. (India) for permission to carry out the bacteriological work in the section.

The above work was carried out partly in the Drying and Distillation Laboratory of Messrs. Edwards High Vacuum Ltd., Manor Royal, Crawley, Sussex, England, and partly at the Biological Products Section, Badshahbagh, Lucknow, U.P. (India).

References

1 R. I. N. Greaves ; *Biological applications of Freezing and Drying* (Edited by R. J. C. Harris), p. 95, Academic Press, New York (1954).

2 D. E. Perham ; *Air Conditioning Refrigerating Data Book* (8th Ed.), pp. 9–03, 9–09, American Society of Refrigerating Engineers (1953–54).

3 P. T. Gilbert ; *Science* **114**, 637 (1951).

4 L. C. Clark, F. Gollan and V. B. Gupta ; *Science* **111**, 85 (1950).

5 L. T. Skeggs and J. R. Leonards ; *Science* **108**, 212 (1948).

R. I. N. Greaves ; Centrifugal vacuum freezing : its application to the drying of biological materials from the frozen state, *Nature, Lond.* **153**, 485 (1944).

R. de R. Barondes, W. D. Judge, C. G. Towne and M. L. Baxter ; *Military Surgeon* **106**, 379–387 (1950).

H. Koffler and M. C. Goldsmidt ; *Industr. Engng. Chem.* **42**, 1819 (1950).

Vol.
9
959/60

Adhesion of Evaporated Metal Films

F. SCHOSSBERGER and K. D. FRANSON

Armour Research Foundation of Illinois Institute of Technology, Technology Center, Chicago 16, Illinois

An abrasion-resistivity test was developed to study the adhesion of vacuum-deposited aluminum films on glass surfaces. The test consists of measuring the electrical resistance of the metal film during abrasion by a stream of fine silicon carbide particles. An analysis is given of the anticipated test results on homogeneous and nonhomogeneous metal films and on effects near the interface.

Differences in the plating and annealing conditions of evaporated aluminum films were detected by the abrasion-resistivity test. Poorest adhesion was found on platings made on unclean surfaces and platings made at a slow rate of evaporation of the metal. The optimum substrate temperature for good adhesion was determined to be 175°C. Annealing of the aluminum film resulted in formation of a surface oxide layer and development of an interlayer compound at the interface.

I. Introduction

The improvement of the adherence of an evaporated metal film on solid surfaces requires a test that will yield information about the chemical and mechanical characteristics of the film throughout its depth and particularly at the interface between the film and substrate.

A brief examination of the literature[1, 2] confirmed the magnitude of the problem of measuring adherence of thin evaporated metal films. Several tests such as an adhesive tape test, a bonding test, and scratch tests of various degrees of refinement are described, but all are essentially qualitative and not reproducible. In none is it clear that the bonding strength " measured " is that at the interface between the film and the substrate.

The need for a quick test led to the idea of measuring the electrical conductivity of the film while its thickness was being reduced by abrasion. In such a test, the resistance of the film being abraded should constantly increase, but the rate of increase will be governed by the abrasive resistance and conductivity of the material being removed. Thus, if the thickness can be reduced layer by layer, the test should identify layers of differing density, composition and hardness throughout the depth of the film and indicate the relative bonding strength at the interface.

II. Abrasion-resistivity test

The essential idea of the abrasion-resistivity test is measurement of resistance of a metal film while its thickness is being reduced in a uniform manner. The thickness of the film was reduced by allowing uniformly distributed silicon carbide (SiC) particles to fall a constant distance, under gravity, on to an unmasked part of the aluminum surface. The variation of resistance with time between two contacts on unmasked areas can be derived for an ideal model, and the effect of a number of possible departures from the ideal can be shown.

A. *Ideal model*

For the purposes of this analysis, the ideal film is taken to be a conducting planar film homogeneous in all its properties. The film is subjected to a constant abrasive action. Since the abrasion rate is constant and the resistance changes inversely with the thickness, the resistance as a function of time is given by :

$$R = \frac{rl}{a(d-kt_0)} \tag{1}$$

where R = resistance (Ω), r = resistivity (Ωcm), l = length (cm), a = width (cm), k = abrasion rate (cm/h), d = original thickness at $t_0 = 0$ (cm), t_0 = time (h)
or

$$R = \frac{rl}{akt} \tag{2}$$

where $t = d/k - t_0$.

The inverse time, t, in equation (2) may be regarded as the time required to build up a film of thickness kt, starting from infinite resistance. Equation (2) is hyperbolic in R and t, and, if r, l, a and k are constant, it will plot on log–log coordinate paper as a straight line with a slope of -1.

B. *Anticipated effects of some film defects*

On the basis of the above simple model the effects of some possible nonideal film characteristics on the resistance–time relation can be predicted.

The abrasion of any homogeneous metal film should give a resistance–time curve such that the slope on log–log paper is -1. Differences in resistivity, thickness and hardness of

homogeneous films will be shown by displacement of the curves. Measurement of thickness and resistance before abrasion will allow determination of the resistivity of the film material, and the total time of abrasion to infinite resistance will give the abrasion rate. Since $\log R + \log t = \log (rl/ak)$, homogeneous films are the family of lines with intercepts at $\log t = 0$ and $\log R = \log (r_i l/ak_i)$, where r_i = resistivity of film i and k_i = abrasion rate of film i.

1. *Effects of nonhomogeneous films*—Nonhomogeneity with depth is expected in an evaporated aluminum film because of the nonuniformity of the plating process. Release of gases from the filament and the aluminum to be evaporated, occlusion of gases in the evaporated aluminum and gettering action of the metal vapors are likely to occur in the initial phases of the plating process. This suggests that impurities will be concentrated in the layers of film close to the substrate. Near the interface the film may also have a different structure due to surface forces influencing the order of the deposited metal atoms. This condition is similar to a chemical reaction between the substrate and the metal.

Nonhomogeneity in laminar or continuous structures or compositions should be detected as a change in the slope of the log–log plot, with a higher sensitivity for effects near the substrate. Fig. 1 shows the abrasion characteristics of a film with a hard layer located near the interface.

Vol. 9 959/60

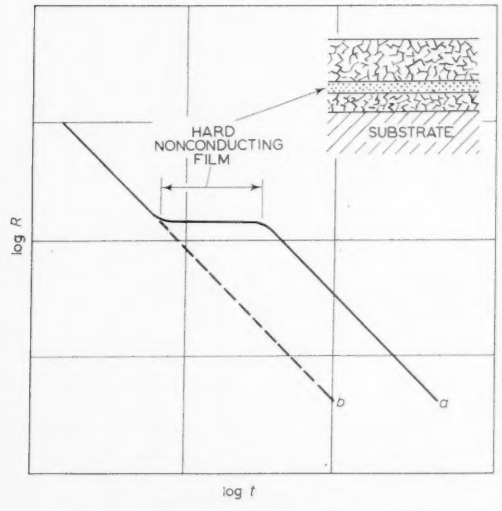

FIG. 1. Abrasion characteristics of a homogeneous film with a hard nonconducting interlayer near the interface.

2. *Effects at the interface and surface of the film*—During the abrasion test, a transition is made from a finite resistance to an open circuit at the interface. Here the bond between the substrate and the bulk of the film is ultimately broken. The nature of this bond is extremely important in understanding the phenomenon of adhesion. It is of great interest then to analyze this test in terms of what interfacial characteristics can be anticipated and what their effects will be.

The film may have the composition and properties of pure aluminum at the boundary where the aluminum is held by physical adsorption. Adhesion of the film may be produced through formation of aluminum–glass compounds at the interface by reaction of aluminum and glass with gases, such as water and oxygen, adsorbed on the substrate. Or, adhesion may be produced by the formation during evaporation of an intermediate compound, such as aluminum oxide (Al_2O_3), which adheres to the substrate and to the bulk of the film. Or, the film may be bonded to the substrate by van der Waal's forces ; under this condition a discontinuous change in composition exists across the interface.

When the bonding is weak, the resistance should reach infinity abruptly from a relatively low value. When the bonding is strong, a condition exists approaching compound formation between the film and the substrate ; and therefore the slope of the log–log curve should change due to decreased abrasion rates before the abrupt jump from low resistance to open circuit. Any interlayer compound which can be imagined will have a resistivity intermediate between that of the aluminum film and the dielectric substrate. Hence, it is anticipated that abrasion will indicate transition from the low resistance of the film through the high resistance of the intermediate compound to the extremely high resistance of the clean dielectric glass surface.

In actual tests resistance–time curves closely corresponding to the ideal model cannot be expected. Real films are undoubtedly not uniform on a microscale, as assumed above. However, the abrasion is an average process, and the ideal model can be used as a guide for the interpretation of the test results.

The abrasion test, then, shows promise of yielding information which can be interpreted in terms of surface preparation, plating conditions, and subsequent treatment of the deposited film. It should be possible to verify such interpretations by plating experiments conducted under carefully controlled conditions.

III. Apparatus

The abrasive-handling system consisted of a hopper, a flow restricting orifice, two screens, and chain-driven buckets to recycle the abrasive as shown in Fig. 2. Uniform flow was achieved by causing the particles to fall from the hopper through a flow-restricting orifice. The stream was broken up on a coarse screen, and the particles then fell through a length of 13 mm glass tubing on to a fine screen, which made the distribution uniform over the sample. The distance between the fine screen and the plated surface is the height of free fall of the particles.

Total abrasion time and control of flow are the factors which determined the choice of abrasive particle size. It was observed that under a given set of conditions, the larger the particle size the shorter the abrasion time. With very fine particles it was found that the handling system would not give uniform flow because the orifice tended to clog. For films about 0.2 μ thick, 150–200 mesh particles gave abrasion

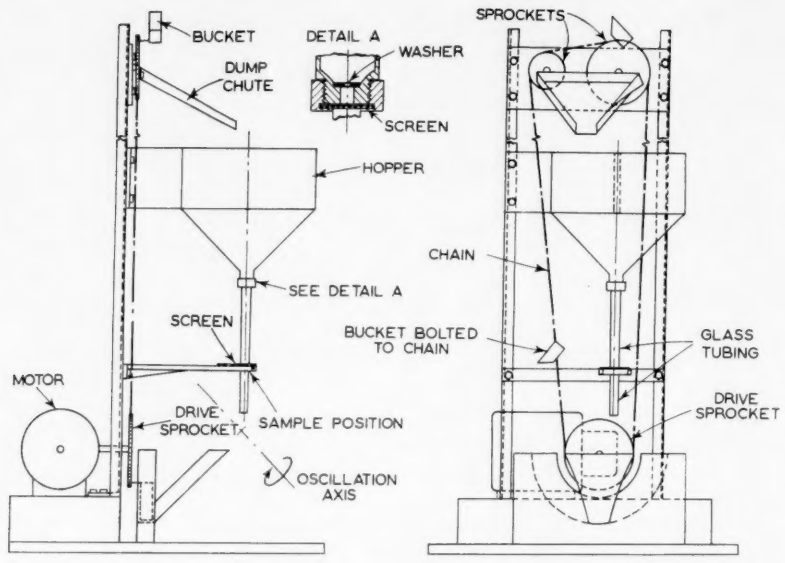

FIG. 2. Abrasive-handling system.

times sufficiently long to record details of the process. No difficulty in maintaining uniform flow of particles of this size range was encountered.

The substrate was mounted on a table directly beneath the stream of falling particles and was inclined at an angle of 45° to the horizontal to permit the particles to fall off. To minimize the effect of the inclination and any azimuthal dependence of abrasion on the height of fall, the table was oscillated between 290° limits. Figs. 3 and 4 show the mounting table, specimen and oscillator.

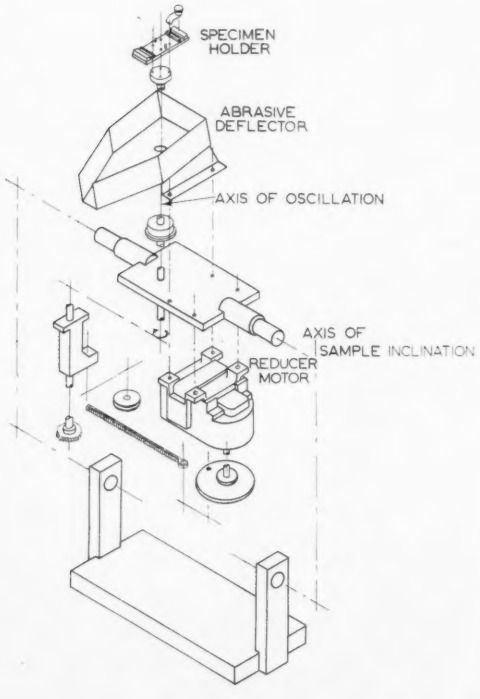

FIG. 3. Oscillating mechanism.

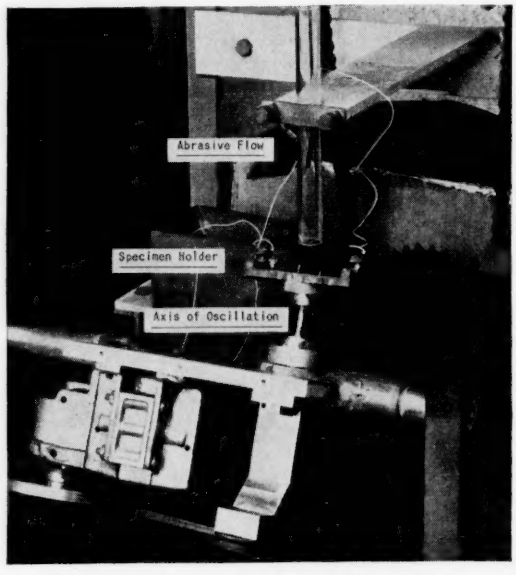

FIG. 4. Oscillating mechanism.

Electrical contacts with the film were made as shown in Fig. 5. Copper wire (30 gage) was bent in the shape shown

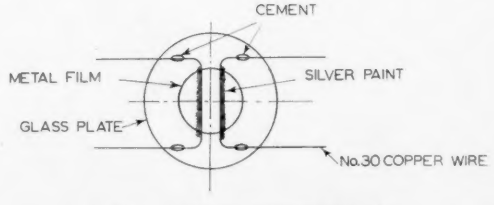

FIG. 5. Electrical contacts with film.

and layed on the film, leaving a gap of 2 mm between electrodes. The electrodes were bonded with cement to the unplated border of the substrate, and electrical contact to the film was insured by applying silver paint between the wire and metal film on the side away from the gap. Upon hardening, all the film except the gap was masked with a thin coat of cement. This contact proved to be reliable. Since the electrodes were firmly attached to the substrate, their interference with the fall of the abrasive can be neglected.

The resistance of the metal film between the electrodes was measured as a function of time by means of an Esterline Angus recording milliammeter. This meter has an internal resistance of 1400 Ω and registers full-scale deflection for 1 mA. The chart speed used was 3 in/h, and the average abrasion time for the platings tested was 7 h. A simple series circuit was used. This consisted of a dry cell power source, the meter, a current-limiting resistor and the metal film. Provision was made for calibration with a decade box. With this circuit, resistances between 100 and 100,000 Ω were measurable.

IV. Plating experiments

The plating variables investigated were rate of evaporation, substrate temperature, and annealing of the aluminum film. Glass plates were used as substrates, and a vacuum of about 5×10^{-5} mm Hg was maintained in the plating chamber. A jig for holding and masking the plates during evaporation was wired with Nichrome wire as shown in Fig. 6, so that

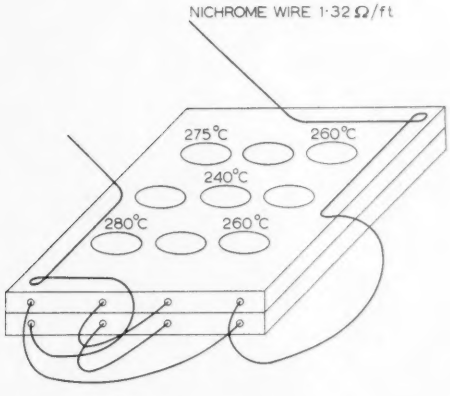

FIG. 6. Heating wiring of jig.

the nine plates in the jig could be heated uniformly up to 300°C. To test the temperature distribution, thermocouples were attached to the surfaces in the jig with Sauereisen cement, and the jig was heated in a vacuum system. Representative temperatures are shown in Fig. 6.

The quantity of aluminum deposited on the plates under various conditions was analyzed chemically, and an effective thickness was determined from the bulk density of aluminum. The aluminum analysis[3] consisted of dissolving the aluminum in nitric acid, forming the aluminum salt of 8-hydroxyquinoline in buffered acetic acid (pH 6.0 ± 1), extracting with chloroform, reading the resultant color in a colorimeter, and comparing it with a standard curve. The sensitivity of this method was about 0.001 mg aluminum, or 0.01 μ film thickness, for glass plated on one side only.

To permit description of the distribution of the evaporating metal, a single aluminum source on a tungsten filament was chosen as the means of evaporation. The source distance required to obtain uniform distribution over the nine plates in the jig was determined experimentally to be 9.5 cm. The aluminum charge was adjusted to give a film thickness of 0.2 μ. The arrangement of source and jig for the plating experiments is shown in Fig. 7.

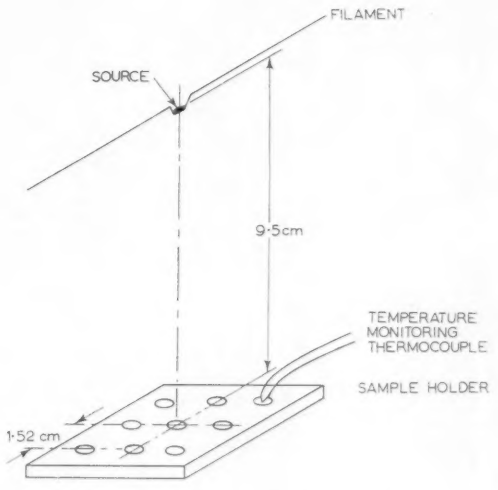

FIG. 7. Arrangement of jig and evaporation source in vacuum system.

Preliminary experiments indicated that when the substrate surfaces were not cleaned and the vacuum during evaporation was poor, the film was destroyed immediately in the abrasion test. Therefore, in the final plating experiments, a set of glass plates was cleaned in a uniform manner and stored in a desiccator. The cleaning process included washing in a detergent, suspension in condensing solvent vapor, dipping in dilute hydrochloric acid, and final rinsing in triple-distilled water. The conditions of the plating experiments and descriptive results of the abrasion tests are given in Table 1.

When the substrate temperature was below 175°C and the evaporation time greater than 1½ min, as in experiments 1–3, test results were unsatisfactory. Complete removal of the film from the surface occurred in less than 10 min. The effect of the abrasive in breaking the circuit through the film was instantaneous, and no resistance between 100 Ω and open circuit was recorded. This behavior is believed to have been due to poor adhesion.

Vol. 9 959/60

In experiments 5 and 6 (Figs. 8 and 9), however, where the substrate temperature was 175°C and evaporation time

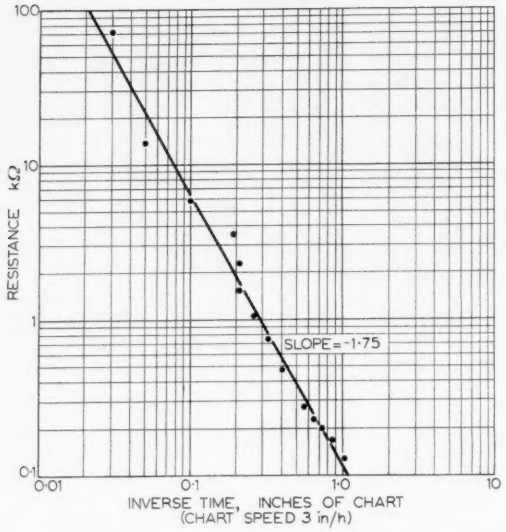

FIG. 8. Log–log curve, Plate 5.

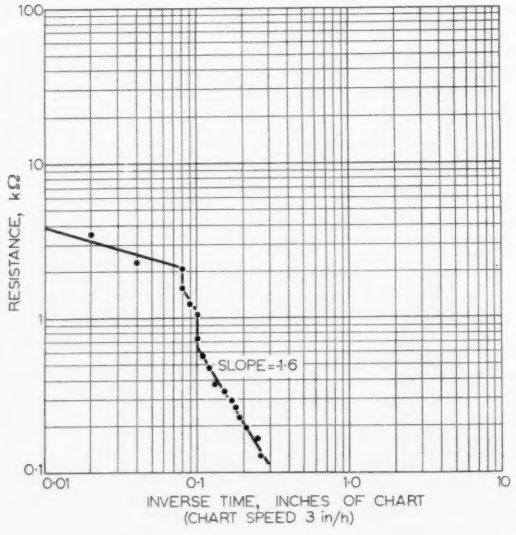

FIG. 9. Log–log curve, Plate 6.

1½ min, test results indicated good adhesion. The plating conditions in experiments 5 and 6 were not identical. In 5, the surfaces were plated from an aluminum charge which had been previously degassed by fusion. In 6, the plating operation was performed with a charge which had not been degassed. The intention, of course, was to detect the influence of contaminations near the interface due to volatile matter from the aluminum charge and filament. The differences in final resistance, shape of the log–log curve, and time at 100 Ω between samples 5 and 6 are significant.

The ideal model predicts a slope of −1 for the log–log curve of resistance vs. inverse time for homogeneous film. However, the slopes in experiments 5 and 6 (Figs. 8 and 9) were −1.75 and −1.6, respectively. At least a partial explanation for the high slopes is found by considering the effect of film thickness on resistivity. As the film thickness approaches the magnitude of the mean free path of an electron, the resistivity of the conductor increases due to electron scattering at the film boundaries. Assessment of this effect and of the extent to which it affects the ideal model involves assuming values for the final thickness at which the film ceases to conduct electricity and for the mean free path of an electron in aluminum.

According to the Planck–Weale equation[4] relating resistivity to film thickness,

$$r_{\text{film}} = r_{\text{bulk}} [1 + (4L_T/\pi d)]$$

where L_T = the electron mean free path at T°K, d = thickness.

By assuming that aluminum conducts at a thickness of 10^{-7} cm and that the mean free path of an electron is 10^{-5} cm, the log–log curve of resistance vs. time for a constant abrasion rate is found to have a maximum slope of −2.0. The slope approaches −1 only at a thickness greater than 1 μ. Thus, it is apparent that the ideal model of Section IIA is oversimplified, and, for the uniform abrasion of a homogeneous film, one should anticipate a slope between −1 and −2 rather than a slope of −1.

It is also of interest to consider the reasons for the magnitude of the final resistances listed in Table I. A

TABLE I

Abrasion Test of Films Plated under Various Conditions

Expt. no.	Plating conditions		Film thickness (μ)	Abrasion test results	
	Evaporation time (min)	Substrate temp. (°C)		Final resistance (Ω)	Slope of log–log curve
1	10	30	0.20	Not measurable	
2	10	100	0.10	Not measurable	
3	5	100	0.09	Not measurable	
4	5	175	0.13	Not tested	
5	1½	175	0.2*	100,000	−1.75
6	1½	175	0.2*	4,000	−1.6

* Estimated.

reasonable thickness limit for conduction of electricity by an aluminum film is 10^{-7} cm. An aluminum film of this thickness having the bulk resistivity of aluminum and the planar dimensions used in the abrasion tests would have a resistance of about 5 Ω. Even when the effect of electron scattering at this thickness is considered, the final resistance may reach 1000 Ω. Higher final resistances can only be explained by a high resistivity due to either composition or structure of the films. Possible mechanisms for the high

resistivity are poor contact between crystallites of aluminum, interspersion of a nonconducting compound such as aluminum oxide, or inclusion of a portion of the aluminum in the lower layers in interfacial compounds.

V. Film uniformity determinations

Experiments were performed to determine the uniformity of platings by using abrasion time as the criterion.

A. *Unannealed films*

Seven films were evaporated simultaneously in the heated jig. Since there was no assurance that abrasion time would be proportional to film thickness if adhesion were poor, plating conditions were chosen to insure good adhesion. Hence the sample holder centrally located 9.5 cm beneath the aluminum source, was heated to 175 °C and the evaporation performed at a fast rate. Without further treatment the seven plated surfaces were subjected to the abrasion test. Fig. 10 shows these abrasion curves, and Table II summarizes

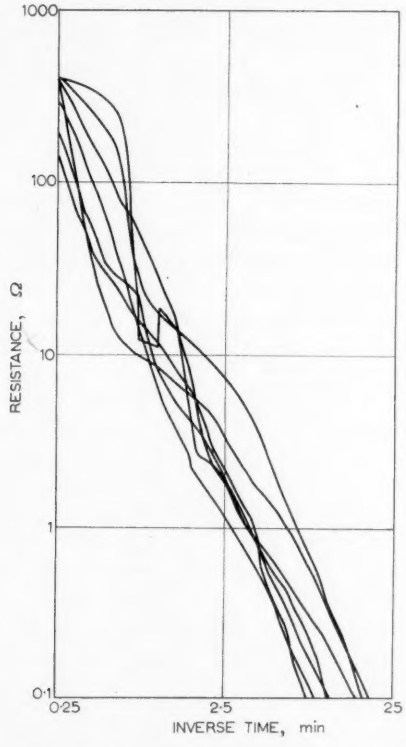

FIG. 10. Abrasion of unannealed aluminum film.

data taken from the curves. Minor fluctuations in the abrasion curves are interpreted as circuit noise.

The maximum deviation in thickness between the unsymmetrically arranged plates should be less than 5 per cent, if evaporation from a point source is assumed. It is significant that the abrasion times showed variation of ±8 per cent. Part of the deviation in abrasion time must be assigned to the test method and film variations due to factors other than the geometry of evaporation. If abrasion time were a function of thickness only, a distribution pattern should be distinguishable in the array of samples. However, abrasion times appeared to be random. Although a pattern of distribution could not be detected, an element of certainty in the abrasion test is derived from the relatively small dispersion of data.

TABLE II

*Abrasion Test of Unannealed Films**

Abrasion time (min)	Slope of log–log curve	Final resistance (k Ω)
78	−2.3	400
71	−2.8	150
73	−2.2	300
73	−1.8	400
82	−2.2	200
70	−2.5	400
75	−2.0	400

* Substrate temperature 175 °C, evaporation time 1 min.

B. *Annealed films*

Annealing was done in oxygen in a tubular furnace, with the control thermocouple inside the Vycor tube downstream from the samples being annealed. Four films were annealed in two groups of two each. In the first annealing, the temperature was raised immediately to 500 °C and held there for 1 h. In the second annealing, the 500 °C temperature was maintained for 16 h. In both cases, oxygen was flushed through the tube at a rate of about 1 l/min. The abrasion test results of these six samples are shown in Fig. 11 and

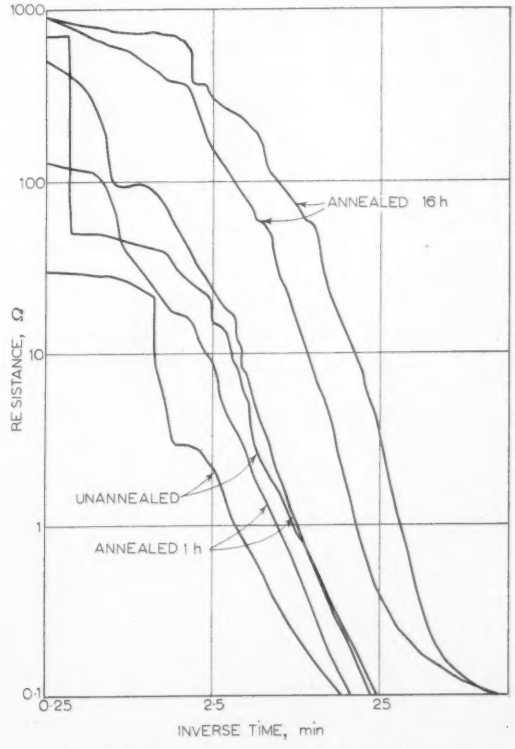

FIG. 11. Abrasion of aluminum films annealed in oxygen.

Vol. 9 959/60

TABLE III

Abrasion Test of Films Annealed in Oxygen*

Abrasion time (min)	Annealing time at 500 °C (h)	Slope of log–log curve	Resistance (Ω)	
			Initial	Final
75	0	−2.7	<100	50×10^3
91	0	−2.1	<100	30×10^3
96	1	−2.8	<100	500×10^3
98	1	−2.8	<100	130×10^3
132	16	−3.8	100	980×10^3
137	16	−3.7	100	950×10^3

* Substrate temperature 175 °C, evaporation time 1 min.

Table III. It is apparent from the data that total abrasion time, final resistance, and the slope of the log–log curve increased with annealing time.

Hass[5, 6] reported that an oxide film 15 to 20 Å thick forms rapidly on a fresh aluminum surface exposed to air. Further growth is slow, and a limiting film thickness of about 45 Å (90 Å if the underlying aluminum is granular) is reached after about 30 days. Temperature influences the rate of oxidation only slightly until 475 °C is reached. Here the oxidation rate increases sharply, and transition of the amorphous oxide layer to crystalline gamma aluminum oxide begins to take place. The limiting thickness of oxide film also increases at high temperatures. Gulbranson and Wysong[7] reported that at 600 °C, the stable oxide thickness is 2000 Å. They also reported that the oxidation reaction rate is dependent only on temperature, although in their experiments they did not reduce the oxygen pressure below 0.01 atm or study the effect of water.

In our experiments it was observed that the 16 h annealed films became transparent to visible light, whereas both the unannealed and the 1 h annealed films appeared opaque. From the rates at 500 °C given by Hass[5, 6] it is estimated that the oxide film on the samples annealed for 1 h and abraded was about 60 Å thick, while the film on the 16 h samples was about 660 Å thick. The transparency of the films annealed for 16 h is due to formation of the oxide at the expense of the aluminum. Walkenhorst[8] showed that aluminum becomes opaque when the film thickness reaches 400 Å. The transparency observed on the 16 h films indicates oxidation reduced the aluminum thickness to less than this value. The reduction in conductivity after annealing is a result of the decrease in the thickness of aluminum after surface oxidation.

The 16 h annealed samples yielded abrasion curves with several novelties. These samples were the only ones which had measurable resistances before abrasion was started. The shape of curves in the initial stages indicates the presence of an abrasion-resistant surface layer. It may be assumed that this layer is relatively thick and nonconducting. The increase in abrasion time indicates that the abrasion resistance of this surface layer was somewhat greater than that of the unannealed films. The slope above 100,000 Ω indicates that an abrasion-resistant cohesive layer was present beneath the bulk of the aluminum.

Electron micrographs of the unabraded and abraded film surface are shown in Figs. 12(a) and 12(b), respectively. The

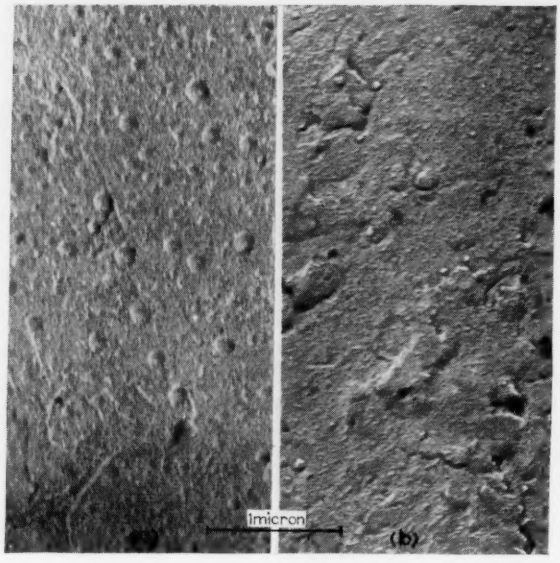

FIG. 12. Electron micrographs of aluminum film on glass (23–7): (a) evaporated and annealed ; (b) abraded.

film was annealed at 500 °C for 1 h and showed an abrasion time of 98 min and a final resistance of 130×10^3 Ω (see Table III). The abraded surface shows large residual particles of adherent aluminum metal and occasional fracture defects. In Figs. 12(a) and 12(b), 3 cm = 1 μ.

Electron diffraction diagrams taken from the surfaces of unannealed and annealed aluminum films showed that surfaces of polycrystalline aluminum were transformed to amorphous aluminum oxide after annealing. The existence of a surface oxide layer implies that the aluminum film is dense on the surface of the plate and not porous to the extent that oxygen can diffuse into the film to coat each crystallite.

Oxidation is, of course, not the only effect of annealing. It is probable, although there was no confirming evidence, that recrystallization occurs in the aluminum. The improvement in continuity and adhesion noted at the interface in the abrasion test of the samples annealed for 16 h also indicates that the bonding strength between the film and substrate was increased during annealing. This phenomenon cannot be attributed to oxidation at the surface if it is accepted that the film is dense. Formation of an interlayer is indicated.

The annealed aluminum film was removed from the surface by dissolving it in 20 per cent hydrochloric acid, and an electron micrograph was taken of the surface (Fig. 13a). A pitted surface, with pits of about 500 Å in diameter, can be observed. No such pits are present on a surface not previously plated with aluminum metal (Fig. 13b).

The pits observable in Fig. 13(a) are therefore the places where the aluminum or aluminum oxides reacted with the silica of the substrate to form acid-soluble aluminum silicates. Such reactions take place when aluminum metal in close contact with the glass surface is heated in an oxidizing

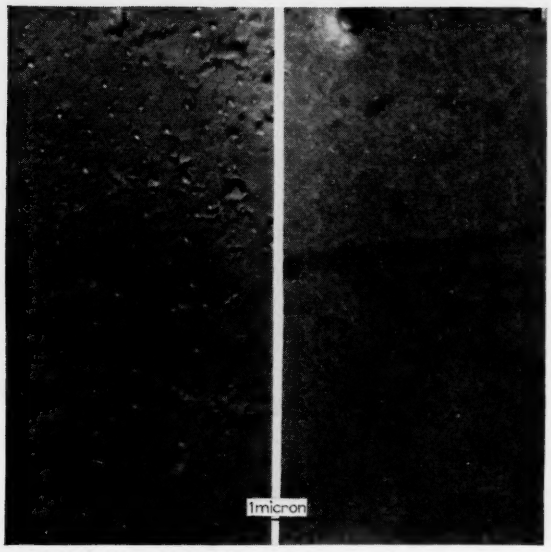

FIG. 13. Electron micrographs of glass surface : (a) after dissolving annealed aluminum film in hydrochloric acid ; (b) unplated.

atmosphere. On the point of contact where bonds are developed, the metal is oxidized to aluminum oxide and subsequently reacts or dissolves in the silicate base material to form aluminum silicates. The reaction, however, does not proceed at the same rate at all points of contact. Reactive spots exist on solid surfaces. As the solubility, heat content, vapor-pressure, adsorption, and catalytic activity are all higher on these spots, they show an increase in the rate of reaction with adsorbed surface atoms. The number and the distribution of the reactive spots depend upon the cleanliness and the crystal structure of the surface. It can be assumed that the pits which became detectable after the hydrochloric acid treatment are the sites of the reactive spots on the glass surface. Their reaction with aluminum or aluminum oxide constitutes part of the interlayer and improved the adhesion, as indicated by the abrasion test.

Vol. 9 959/60

VI. Summary

An abrasion-resistivity test was developed to study adhesion of vacuum-deposited aluminum films on glass surfaces. The test measures the resistance of the metal film during abrasion by a stream of fine silicon carbide particles.

Differences in the plating and annealing conditions of evaporated aluminum films were detected by an abrasion-resistivity test. Poorest adhesion was found on platings made on unclean surfaces and platings made at a slow rate of evaporation of the metal. The optimum substrate temperature for good adhesion was determined to be 175°C. Annealing of the aluminum film resulted in formation of a surface oxide layer and development of an interlayer compound at the interface.

VII. Acknowledgment

The authors wish to thank the sponsor of this work, Motorola, Incorporated, for helpful discussions and permission to publish this paper.

References

[1] R. C. Williams and R. C. Bakus ; *J. Appl. Phys.* **20**, 98 (1949).
[2] S. Bateson ; *Vacuum* **2**, 365 (1952).
[3] S. A. Wiberly and L. C. Basset ; *Analyt. Chem.* **21**, 609 (1949).
[4] L. Holland ; *Vacuum Deposition of Thin Films.* John Wiley, New York (1956).
[5] G. Hass ; *Z. anorg. Chem.* **254**, 95 (1947).
[6] G. Hass ; *J. Opt. Soc. Amer.* **39**, 532 (1949).
[7] E. A. Gulbransen and W. S. Wysong ; *J. Phys. Colloid Chem.* **51**, 1087 (1947).
[8] W. Walkenhorst ; *Z. tech. Phys.* **22**, 14 (1941).

Les Bases Experimentales de la Theorie Cinetique des Gaz*

L. DUNOYER

Paris, France

Encore au début du siècle la théorie cinétique des gaz n'était que le développement déductif de très anciennes hypothèses sur l'existence des molécules et de leurs mouvements. Ce développement mathématique conduisit à des possibilités de vérifications expérimentales sur la viscosité et la conductibilité calorifique. Le succès de ces vérifications donna grand crédit à la théorie, mais elles ne peuvent évidemment pas en être considérées comme des bases *expérimentales.*

L'auteur rappelle que les faisceaux moléculaires fournissent une vérification directe des hypothèses fondamentales et peuvent par suite servir réellement de bases expérimentales à la théorie. Il montre en outre que l'emploi des faisceaux en résonance optique peut fournir des indications précieuses et directes sur le comportement des molécules dans leur choc sur une paroi, ou dans leurs collisions avec les molécules différentes d'une atmosphère raréfiée (vapeur de mercure, hydrogène).

Il signale cette anomalie que, si les faisceaux moléculaires ont donné lieu dans les pays Anglo-saxons à de très nombreux et très importants travaux (montrant qu'ils constituent un instrument de recherche puissant), ils ont été peu étudiés en France où pourtant, ils ont été observés pour la première fois.

1. Personne ne sera surpris, je pense, qu'une des communications faites en un congrès consacré aux techniques du vide ait le sujet évidemment théorique qu'indique son titre. Mais il n'en a pas toujours été ainsi, et il peut y avoir quelque profit à rappeler un état d'esprit fort répandu au début du siècle.

La théorie cinétique des gaz était alors considérée souvent plus comme un jeu de l'esprit que comme un chapitre nécessaire de la physique. Dès le milieu du XVIIIe siècle, Daniel Bernoulli avait développé d'une manière précise une theorie déjà fort suggestive. Les choses, pourtant, en restèrent là jusqu'après 1850. Durant la seconde moitié du XIXe siècle, les travaux de Clausius, puis de Maxwell et de Boltzmann vinrent préciser la théorie d'une manière considérable en prédisant que le coefficient de viscosité et la conductibilité calorifique d'un gaz devaient être indépendants de la pression. Ces deux prévisions importantes, assez surprenantes au premier abord, se sont trouvées vérifiées par l'expérience, ce qui fit grandir considérablement le crédit de la théorie.

On peut donc prendre ces vérifications expérimentales comme des justifications de la théorie mais non comme des bases expérimentales. La filiation allant de la conception antique de l'individualité des molécules, et de leurs mouvements rectilignes entre deux collisions, aux résultats en question restait bien complexe et lointaine. Pour le sujet que nous nous proposons de traiter aujourd'hui, nous remarquons d'ailleurs que les déductions dont il s'agit ne font intervenir en rien la technique du vide. D'après ce que nous savons maintenant, la vérification de l'indépendance des coefficients de viscosité et de conductibilité par rapport à la pression aurait au contraire nettement échoué si les expériences avaient été faites sous de trop basses pressions. C'est ce qu'ont montré les célèbres travaux de Knudsen, qu'il faut considérer comme l'un des pères de la théorie moderne et de la technique du vide. Dans son excellent ouvrage *Kinetic Theory of Gases* (1927), Léonard B. Loeb s'exprime ainsi : " telle qu'elle a été laissée par Kelvin et Boltzmann, la théorie ne restait rien de plus qu'une hypothèse, en dépit du nombre des accords entre la théorie et le comportement du gaz, aucune preuve n'ayant été obtenue de l'existence distincte d'atomes et de molécules, ni aucune réelle démonstration de leurs continuels mouvements calorifiques. La théorie cinétique restait donc une très intéressante curiosité, mais c'était tout." Elle était d'ailleurs fortement battue en brèche par le groupe des thermodynamiciens.

Cette situation fut complètement modifiée par le célèbre travail de Jean Perrin sur le mouvement brownien en 1908, bien que ce travail portât sur les liquides et non sur les gaz. La " réalité moléculaire " et celle des mouvements rectilignes d'une collision à la suivante, furent dès lors incontestées, quoique pas toujours profondément assimilées. J'ai souvenir d'un mémoire d'un très éminent physicien qui chauffant dans un tube réfractaire relié à une pompe à vide un morceau de métal relativement volatil, admettait que la vapeur de ce métal devait s'écouler lentement vers les extrémités froides comme un liquide visqueux. Il est clair que pareille opinion était en désaccord complet avec les notions de base de la théorie des gaz.

2. Au contraire, les faisceaux moléculaires, découverts

* Paper presented at the First International Congress on Vacuum Techniques, Namur, 10–13 June 1958.

Vo
9
1959

en 1911[1] apportèrent une confirmation éclatante des idées de base de la théorie cinétique.

Considérons un récipient divisé en trois parties par deux cloisons dans lesquelles sont percées deux petits trous A et B

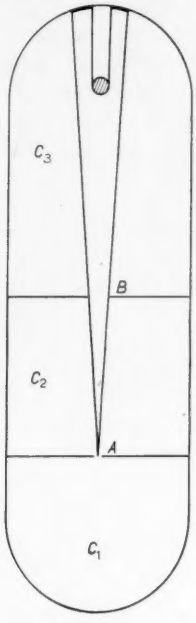

FIG. 1.

(Fig. 1). Imaginons qu'on entretienne un excellent vide dans les compartiments C_2 et C_3 et qu'au contraire une atmosphère gazeuse existe dans le compartiment C_1. Pendant un intervalle de temps donné il existe, d'après l'hypothèse de base de la théorie cinétique, des molécules du compartiment C_1 dont les vitesses sont dirigées vers le trou A. Si elles n'en rencontrent aucune autre avant d'atteindre cet orifice, elles doivent le traverser et continuer ensuite en ligue droite dans le compartiment C_2 sans faire de nouvelles rencontres puisque ce compartiment est vide. Celles de ces molécules dont les vitesses ont des directions qui passent par l'orifice B le traverseront donc et continueront en ligne droite dans le compartiment C_3 jusqu'à ce qu'elles rencontrent la paroi, si éloignée soit elle, puisque le vide y règne aussi. Les deux orifices A et B définiront donc dans le volume C_3 un faisceau de rayons moléculaires (ou atomiques), exactement comme ces orifices définiraient un faisceau de lumière. Dans le volume délimité par le faisceau il existe bien une masse gazeuse ; mais, à l'inverse d'un gaz ordinaire, aucune des molécules qui la composent n'a tendance à en sortir, puisque les directions de leurs vitesses ne traversent pas la surface latérale du faisceau.

3. On peut mettre en évidence l'existence de ce faisceau de bien des manières. La plus simple consiste à choisir pour le gaz contenu dans le compartiment C_1 une vapeur dont les molécules se fixent sur la paroi C_3 au point où elles la rencontrent. On peut alors y observer, au bout d'un certain temps, un dépôt exactement délimité à la section par cette paroi du faisceau moléculaire géométriquement défini par les orifices. Dans " l'ombre " d'un obstacle interposé sur le trajet du faisceau aucun dépôt de matière ne se produit. On peut aussi,[2] quand les molécules ou les atomes présentent

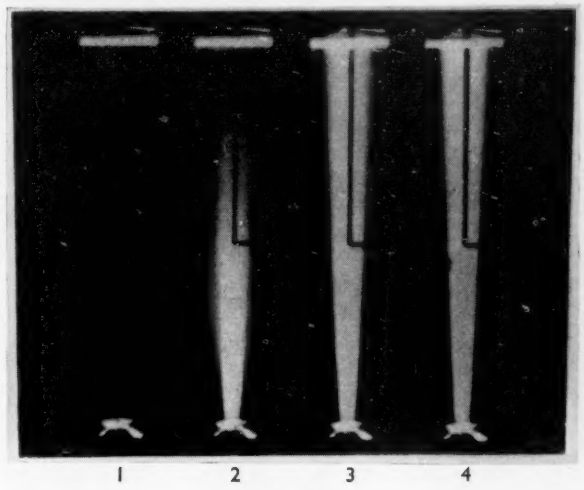

FIG. 2.

le phénomène de la résonance optique, rendre visible le faisceau tout entier en l'éclairant avec la radiation pour laquelle se produit cette résonance. La Fig. 2 reproduit la photographie de trois faisceaux atomiques de sodium rendus visibles par résonance optique en les éclairant avec une lampe à vapeur de sodium, faisceaux obtenus dans des conditions de vide différentes.

On voit, à la partie inférieure de la figure, quatre images de l'orifice B de la Fig. 1. Le faisceau se propage de bas en haut et arrive à la partie supérieure sur une plaque de verre plane formant le fond d'un tube dans lequel on peut verser de l'air liquide. Pour la pose 1, à gauche, le sodium n'était pas encore chauffé ; on ne voit aucun faisceau ; on n'aperçoit que l'orifice et aussi, en regardant attentivement, la trace d'une tige vue en bout, éclairée de gauche à droite par la lumière d'une lampe à vapeur de sodium. Pour les trois autres poses le sodium du compartiment C_1 était chauffé à 360 °C environ (tension de vapeur 0,1 mm Hg). Pour la pose 2 l'appareil à faisceau moléculaire était relié à une pompe à diffusion à vapeur de mercure, qui y réduisait la pression des gaz autres que la vapeur de mercure au millième de micron de Hg, la pression de cette vapeur étant elle-même de l'ordre du micron de Hg. Pour la pose 3 le vide était fait de la même manière, mais en outre on versait de l'air liquide dans un piège intercalé entre la pompe et l'appareil, ce qui éliminait la vapuer de mercure dans celui-ci. Enfin, pour la pose 4 on versait en outre de l'air liquide dans le tube sur le fond plat duquel venait frapper le faisceau moléculaire. Les aspects du faisceau sont nettement différents dans les trois cas, ainsi que l'aspect de l'ombre produite dans le faisceau par la baguette perpendiculaire à celui-ci et vue en bout par l'objectif photographique. Le patite ombre horizontale qu'on voit dans le faisceau est celle de la baguette pour la lumière excitatrice. On remarque :

(1°) Qu'en présence de la vapeur de mercure, le faisceau s'atténue beaucoup plus vite qu'en l'absence de cette vapeur. L'interprétation est évidente : les collisions des atomes de

Vol. 9 959/60

sodium du faisceau avec ceux de la vapeur de mercure font sortir les premiers du faisceau et le rendent plus diffus ;

(2°) qu'en même temps les atomes de sodium ainsi sortis du faisceau forment une atmosphère bien visible autour de sa partie moyenne ; cette atmosphère a disparu pour les poses 3 et 4 ;

(3°) que l'ombre de la baguette dans le faisceau atomique, c'est-à-dire la région qu'elle protège de l'arrivée d'atomes de sodium, reste plus longtemps parfaitement noire, même jusqu'au choc du faisceau sur la plaque de verre supérieure. Cet aspect est beaucoup plus marqué lorsque celle-ci est refroidie par l'air liquide (pose 4) que lorqu'elle est à la température ordinaire (pose 3), ce qui semble montrer qu'à cette température certains atomes de sodium ne restent pas fixés sur la plaque dès leur premier choc, tandis qu'ils y restent à la température de l'air liquide.

4. Il parait évident que l'expérience qui vient d'être décrite fournit un base expérimentale directe à la théorie cinétique des gaz. Ce n'est pas ici le lieu d'entrer dans le détail des calculs à partir de cette base : j'en indiquerai seulement les premières étapes. On calculera d'abord le libre parcours moyen et le nombre de molécules (ou d'atomes) traversant par seconde une section droite du faisceau, nombre qui définit son intensité. Pour la mesure de cette intensité on a usé de divers procédés. Le plus ancien consiste à peser le dépôt de matière—quand il y a dépôt—formé en un temps donné sur la surface où la condensation a eu lieu. Mais ce procédé, qui d'ailleurs exclut les gaz non condensables, n'a qu'une médiocre sensibilité. Depuis longtemps déjà on lui en a substitué un autre infiniment plus sensible, qui consiste à faire traverser le faisceau par un fil fin légèrement chauffé, comme dans une jauge de Pirani. Dans certains cas on peut même augmenter encore la sensibilité, comme l'ont montré Taylor et Stern, en utilisant l'ionisation superficielle qui se produit à la surface d'un fil fin de tungstène recouvert d'une couche d'un métal alcalin ; on mesure alors le courant produit par les ions positifs formés.

De la mesure directe des vitesses moléculaires, on conçoit qu'on ait pu passer facilement à l'étude de la répartition des vitesses. La loi de distribution de Maxwell a reçu ainsi une vérification expérimentale directe. De même Estermann et Stern ont pu vérifier directement la relation fondamentale de Louis de Broglie en faisant diffracter un faisceau moléculaire d'hydrogène ou d'hélium sur une face naturelle d'un cristal de LiF. Mais il ne peut être question d'entrer dans plus de détails et nous devons nous contenter de renvoyer à l'excellent ouvrage de Ronald Fraser (*Molecular Rays*, 1931) ou au volume beaucoup plus développé de Norman Ramsey (*Molecular Beams*, 1956). Nous nous bornerons à quelques indications sur des expériences, malheureusement incomplètes, effectuées par nous-même de 1942 à 1944 sur des faisceaux moléculaires de sodium en résonance optique.[3]

5. Dans les expériences en question, le faisceau moléculaire (ou atomique) de sodium a été rendu visible sur tout son parcours en l'éclairant avec la lumière fournie, dans des conditions convenables, par une lampe à vapeur de sodium. L'appareil à faisceau moléculaire était notablement plus perfectionné que celui qui a servi pour obtenir la photographie de la Fig. 2. Nous ne le décrirons pas ici, en renvoyant pour les détails de construction au mémoire 1. La fente pupille définissant l'origine du faisceau, avait seulement 0,135 mm de largeur parallèle à l'axe photographique, tandis que la fente lucarne, définissant l'ouverture angulaire du faisceau, avait 1 mm de largeur et 6 mm de longueur. Nous nous limiterons à l'examen de quelques photographies et aux remarques qu'elles suggèrent. Toutes les poses étaient de 4 minutes et l'examen visuel du faisceau était facile. Les points sur lesquels porteront nos remarques sont :

(1°) Le comportement des atomes ou des molécules au voisinage d'une paroi solide ; (2°) la propagation du faisceau à travers une atmosphère de vapeur de mercure ; (3°) sa propagation à travers une atmosphère d'hydrogène.

6. Comportement des atomes de sodium au choc sur une paroi solide

Les faisceaux moléculaires de sodium ont été originairement observés grâce aux dépôts miroitants qu'ils formaient sur la paroi de verre qu'ils rencontraient paroi à la température ordinaire. Avec d'autres métaux Knudsen a montré qu'il existait pour un métal donné une température critique de la paroi de verre au dessus de laquelle aucun dépôt n'apparaissait ; on a d'ailleurs constaté que cette température critique était d'autant plus basse que le faisceau était moins intense.

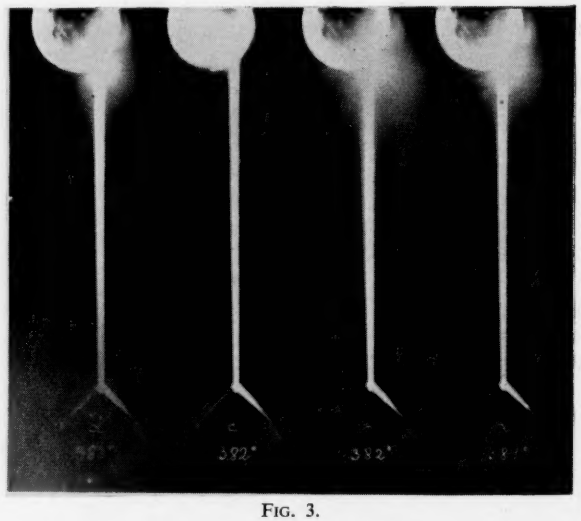

FIG. 3.

Dans cet ordre d'idées la photo de la Fig. 3 montre que le faisceau moléculaire est très visible par résonance longtemps avant qu'on puisse observer aucun dépôt. Cette photo a été prise dans les conditions suivants : température de la vapeur de sodium d'où sort le faisceau 381°C (pression de cette vapeur 0,25 mm Hg) ; la paroi de verre sur laquelle vient frapper le faisceau est à la température ordinaire pour les poses *a*, *b*, *d*, et à la température de l'air liquide pour la pose ; *c* pour les poses *a* et *b* la paroi frappée est vierge de dépôt de sodium ; pour la pose *c* un dépôt de sodium se forme instantanément dès qu'on verse de l'air liquide dans le tube fermé en bas par la glace de verre ; après la pose *c* on a laissé

l'air liquide s'évaporer et la glace revenir à la température ordinaire : la pose *d* a alors été prise, mais cette fois, à la différence des poses *a* et *b*, le faisceau bombardait, non pas le verre, mais le dépôt de sodium formé pendant la pose *c*. On remarque :

(α) le nuage de sodium réémis par la paroi de verre frappé par le faisceau. Comme le bombardement a été poursuivi constamment jusqu'au momment de commencer la pose *c* *sans qu'il apparaisse aucun dépôt*, soit pendant une durée de *33 minutes*, il parait bien probable qu'aucun atome de sodium n'a été fixé ; il n'y a eu sur la paroi *aucune adsorption de sodium*.

(β) Le nuage réémis pendant la pose *d* indique que la réémission produite sur la couche de sodium formé pendant la pose *c* avait presque autant d'intensité que sur la paroi de verre nu (poses *a* et *b*). Mais de l'ensemble des expériences analogues que j'ai faites il résulte que cette réémission diminue beaucoup lorsque l'épaisseur du dépôt augmente.

(γ) Sur le cliché original, on voit nettement qu'après les poses *a* et *b* il aparait une lueur diffuse dans le ballon. Elle est évidemment due aux atomes de sodium qui ont rebondi sur la paroi ou ont été réémis par elle.

(δ) En première approximation le nuage réémis parait bien symétrique autour de la normale à la paroi bombardée. Il conviendrait évidemment d'explorer la lueur réémise au microphotomètre ; le cliché avait été préparé dans ce but, mais il ne m'a pas été donné de remplir ce programme. La lueur réémise doit très vraisemblablement obéir à la loi du cosinus, comme dans les expériences de Knudsen.

7. Comportement des faisceaux dans une atmosphere de vapeur de mercure

La Fig. 4 permet de montrer ce comportement. La pose *a* a été faite avant que le four à sodium fût chauffé, pour contrôler l'absence de luminosité du fond photographique. La pose *b* a été faite un quart d'heure environ après le commencement du chauffage du four ; la température de la vapeur source était alors 372 °C ; le piège à air liquide placé entre l'appareil à faisceau et la pompe à vapeur de mercure *n'etant pas* garni d'air liquide, de sorte que la température de l'appareil étant d'environ 22 °C, la pression de la vapeur de mercure y était d'environ 0,002 mm Hg. Pour la pose *c* on commençait par verser de l'air liquide dans le piège de la pompe. Enfin avant de faire la pose *d* on versait de l'air liquide dans le tube récepteur.

Si l'on compare, surtout sur le cliché original, les poses *b* et *c* on constate que :

(α) La présence de la vapeur de mercure ne diminue pas la netteté des bords du faisceau, dont la forme ne change pas, ce qui indique que la décroissance de l'intensité est le même sur tous les rayons. Il semble donc qu'après le choc d'un atome de sodium du faisceau sur un atome de mercure, la vitesse ne conserve aucun " souvenir " de sa valeur avant le choc.

(β) La comparaison des poses *b* et *c* montre que si l'introduction d'air liquide dans le piège de la pompe à mercure a pour effet presqu'immédiat de rendre le faisceau moléculaire beaucoup moins rapidement décroissant, elle ne semble pas avoir d'effet sur la lueur diffuse, qui entoure le faisceau, ce qui parait surprenant au premier abord. L'interprétation de ce fait me parait être la suivante : que le piège à air liquide de la pompe soit froid ou non, le faisceau moléculaire apporte constamment de nouveaux atomes de sodium, tandis que le piège, s'il est froid, retient les atomes de mercure qui viennent de la pompe ; de sorte qu'au bout de peu de temps il n'y a plus dans l'appareil d'atomes de mercure, tandis qu'il y arrive toujours autant d'atomes de sodium qui, après réémission sur le récepteur, viennent enrichir la lueur diffuse entourant le faisceau.

(δ) Il est à noter que la lueur diffuse observée sur les poses

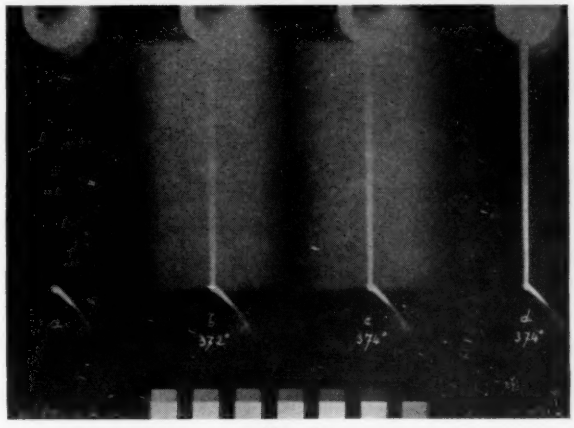

FIG. 4.

b et *c* de la Fig. 4 est d'autant plus intense qu'on approche d'avantage de la surface d'impact. C'est bien conforme à l'hypothèse que cette lueur est due, pour une part importante au moins, aux atomes réémis par cette surface ; le reste de la lueur serait due à des atomes du faisceau primaire après collison avec des atomes de mercure.

8. Comportement du faisceau moleculaire dans une atmosphere d'hydrogene

Quand on introduit dans l'appareil pendant l'émission du faisceau moléculaire, une très petite quantité d'hydrogène, de manière à produite une pression d'hydrogène de quelques microns de mercure, on constate aussitôt que le faisceau se raccourcit considérablement, sans d'ailleurs devenir plus ouvert. C'est à quoi l'on pouvait s'attendre ; mais peu à peu, en quelques secondes si la pression de l'hydrogène introduit est assez petite, en quelques minutes si elle est plus grande, la longueur du faisceau réaugmente. La mesure de la pression montre en même temps que celle-ci diminue. La durée de la pose de 4 minutes employée dans toutes les expériences précédentes est beaucoup trop longue pour que la photographie du faisceau traduise exactement ce que l'on voit ; la Fig. 5 en donnera seulement quelque idée. La température du four à sodium réglé à 379 °C et le piège de la pompe ainsi que le récepteur étant garnis d'air liquide, de l'hydrogène était introduit au moyen d'un osmo-régulateur pendant 3 minutes ; la pression était alors de 6,70 μ Hg, et le faisceau presque complètement disparu, comme rentré dans la fente lucarne. La pose *a* était alors commencée. Pendant la pose (de 4 minutes), le faisceau réapparaissait de

Vol. 9 959/60

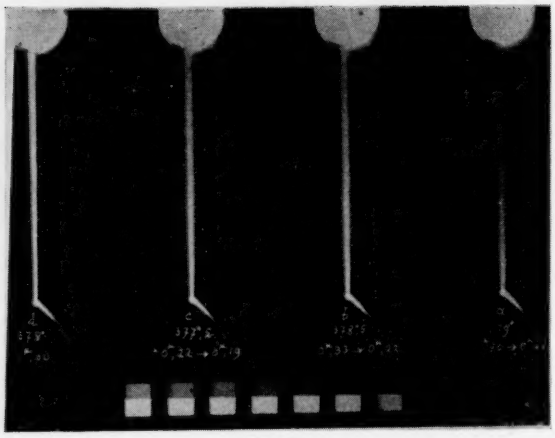

FIG. 5.

mieux en mieux, comme s'il poussait à partir de la fente lucarne ; à la fin de la pose il atteignait de nouveau le récepteur ; il était net, auréolé cependant d'une légère gaine. La pose *a* de la figure ne donne donc qu'un aspect moyen. La pression d'hydrogène, mesurée aussitôt après la fin de la pose, n'était plus que de 0,33 μ Hg. La pose *b* était alors commencée et, pendant cette pose de 4 minutes, la pression diminuait encore de 0,22 à 0,19 μ Hg. Après avoir rouvert le robinet de communication avec la pompe, on effectuait la pose *d*. Malgré le petitesse de la pression correspondant à la pose *c*, on remarque sur la pose *d* (tout du moins sur le cliché original) la forte augmentation d'intensité du faisceau moléculaire produite par l'élimination de cette atmosphère gazeuse résiduelle. A la fin de l'expérience on constatait l'existance sur le cylindre récepteur, d'un léger dépôt blanc, très probablement formé de l'hydrure de sodium HNa. Ce dépôt blanc disparut quand on laissa le récepteur revenir à la température ordinaire ; en même temps la pression réaugmentait. Cette formation d'hydrure peut surprendre au premier abord, si l'on compare les pressions réalisées dans l'appareil et les valeurs de la tension de dissociation de l'hydrure (355 mm Hg à 400 °C, 62 mm Hg à 350 °C). Mais il ne faut pas oublier que dans les expériences classiques de dissociation les conditions sont tout autres ; le faisceau moléculaire produit un effet du même genre qu'un tube " chaud et froid " de Sainte-Claire-Deville. Si les atomes de sodium du faisceau, rencontrant des molécules d'hydrogène, les dissocient pour former des molécules d'un hydrure, ces molécules d'hydrure, une fois sorties du faisceau, se trouve dans une atmosphère très rarifiée où, ne subissant que de très rares collissions, elles n'ont plus d'occasions de se dissocier, jusqu'à ce qu'elles se condensent sur le piège à air liquide, où elles se dissocient quand la température remonte.

9. Conclusion

Je prie le congrès de m'excuser de ne lui avoir présenté que des parties du'un travail inachevé. Il me semble pourtant que mes résultats, si imcomplets qu'ils soient, pourraient être le point de départ de nouvelles recherches sur les faisceaux moléculaires qui, observés pour la première fois en France, il y a presqu'un demi-siècle, ont donné lieu dans les pays anglo-saxons, à de nombreuses découvertes, même en physique nucléaire, comme en témoigne l'important volume de M. Norman Ramsey, paru en 1956 et qui donne plus de 600 références bibliographiques.

Références

[1] L. Dunoyer ; *C.R. Acad. Sci., Paris* **152**, 593 (1911). *Le Radium* **8**, 162 (1911).

[2] L. Dunoyer ; *C.R. Acad. Sci., Paris* **157**, 1068 (1913) ; **178**, 145 (1924).

[3] L. Dunoyer ; *Le Vide* Juil–Août, 172–189 (1956).

The History of the Vacuum Pump*

By E. N. DA C. ANDRADE

Imperial College of Science and Technology, London, United Kingdom

The first man to make a vacuum pump was Guericke, somewhere about 1654. It was a crude pump, with joints kept airtight by water immersion. Soon after Boyle produced a much improved piston pump, made by Robert Hooke. About the same time the Accademia del Cimento used the vacuous space in the enlarged head of a mercury barometer to carry out experiments : this may be considered as a one-stroke mercury pump. Pumps on the Boyle pattern were made by Huygens, Papin and Senguerd.

In 1682 Boyle described a two-cylinder pump, in which the pressure of the atmosphere on one piston did most of the work required to raise the other. A much improved pump of this type was made by Haukesbee about 1705 and this remained essentially the pattern of cylinder vacuum pumps until the end of the nineteenth century, when Fleuss introduced the cylinder oil pump. For producing high vacua for the classic research on discharge in gases, pumps of the Geissler and Toepler type, based on continuous repetition of Torricelli's experiment, were used, which were extremely slow in action.

A new era was initiated in 1905, when Kaufmann introduced a continuously rotating mercury pump, which was almost at once superseded by Gaede's much speedier rotary mercury pump. Fore pumps of box type, the prototypes of which were water-pumps of the sixteenth and seventeenth century, were brought in by Gaede and others. In 1912 Gaede invented a pump based on a fundamentally new principle, that a surface moving rapidly parallel to itself drags with it gas molecules. This so-called molecular pump produced extremely low pressures. The last inventive step was also made by Gaede, when in 1915 he utilized the carrying along of gas molecules by a jet of mercury vapour to effect a high vacuum. These vapour-stream pumps, oil and mercury, have been developed on an enormous scale of recent years.

Vol. 9 959/60

THE first vacuum pump, in the sense of a machine by which air could be progressively removed from a closed vessel, was undoubtedly that invented by Otto von Guericke somewhere about 1650, but before that, in 1644, Evangelista Torricelli had carried out his famous experiment with the barometer tubes, showing that the mercury stood at the same height whether the upper end of the tube had the ordinary form or was blown out to a sphere. From this, he correctly concluded that the space above the mercury was empty. This method was some 20 years later used to produce a vacuous space for experiment, as shown in Fig. 1, which is taken from the *Saggi di Naturali Esperienzi*, published by the Accademia del Cimento in 1667. In (a) a small ball of bitumen is being heated by sunlight concentrated by a concave mirror, to show that smoke falls *in vacuo* ; in (b) where the evacuated space is closed by a glass lid, another innovation, it is shown that a tied lamb's bladder, containing a trace of air, swells out to a sphere *in vacuo*. This method which, comparing it with the mercury pumps of the nineteenth century, may be called a one-stroke mercury pump, was used in 1786 by Rumford to create a vacuum for investigating " the propagation of heat in various substances." He specified that the mercury had been previously freed of air and moisture by boiling. Properly handled, the method is clearly capable of giving a much better vacuum than the early cylinder pumps, with water-saturated washers and such like, but it is not easy to evacuate large spaces by this means, and the space must not contain constructions of metals or other substances either fragile or attacked by mercury.

Guericke's pump was first described in Kaspar Schott's *Mechanica Hydraulica-Pneumatica*, 1657, as figured in Fig. 2. It consisted simply of a cylindrical tube with two valves one at *H*, halfway along it, which opened outwards to the atmosphere under internal pressure and one at *I*, the lower end of the cylinder, opening when the piston was withdrawn and closing when it was returned. This is clearly not good design, even if the valves were efficient—and we are not told how they were made. A tap *E* could be used to shut off the evacuated vessel, which could then be removed, as shown in the background. Water was freely used to make the joints air-tight.

Guericke himself first published an account of his work much later, in 1672, in his famous book *Experimenta Nova* (*ut vocantur*) *Magdeburgica de Vacuo Spatio* (The New, commonly called Magdeburg, experiments on Empty Space) generally referred to as *De Vacuo Spatio*. The pump figured

* Paper presented at the First International Congress on Vacuum Techniques, Namur, 10–13 June 1958.

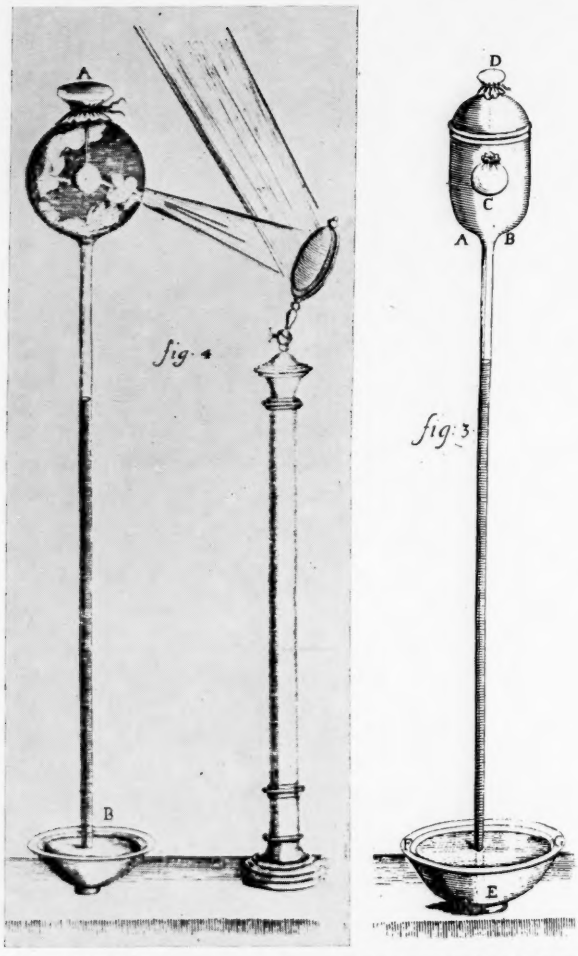

FIG. 1(a) & (b). The vacuum experiments of the Accademia del Cimento.

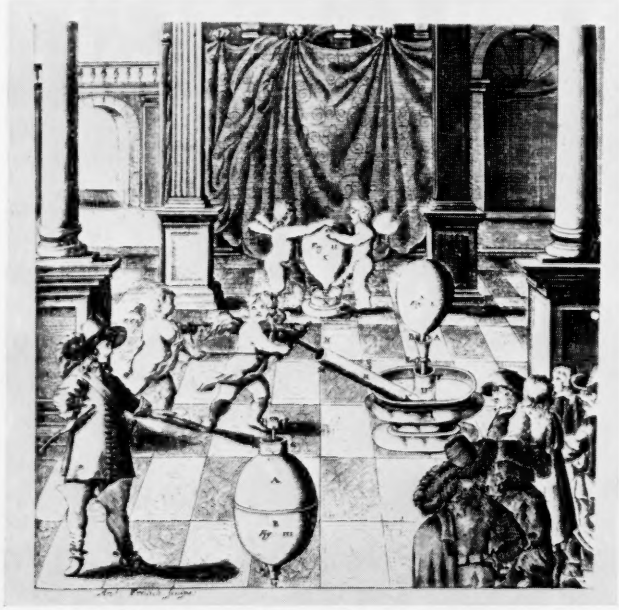

FIG. 2. Schott's representation of Guericke's early pump.

there (Fig. 3) is of much better design and probably much later construction than that figured by Schott. The essential cylinder, *gh*, was supported by a tripod : it is shown separately in "Fig. III". The piston running in this cylinder was of wood, made air-tight with wet string. For use in the early stages of pumping, a leather valve, *z*, closed by a spring, was provided. When the pressure of the air to be expelled became too low to force it open, use was made of the peg, *m*, taken out by hand during the upstroke and replaced during the downstroke. Essential was the tap, *gr*, used as in Boyle's pump, to be next described. It must be remembered that the account of Boyle's pump appeared in a Latin edition in 1661, 11 years before *De Vacuo Spatio* and that Guericke may well have seen it. The conical vessel, *xx*, at the upper end of the cylinder and that shown in "Fig. VI", designed to be hung so as to enclose the lower end of the cylinder, were to be filled with water, which was relied on to make the joints air-tight. The spherical glass receiver *L* was cemented to the brass attachment carrying the tap. The famous Magdeburg experiment with the two hemispheres enclosing an exhausted space, which two teams of horses could not pull apart, was carried out in 1654, probably with the type of pump figured by Schott.

Robert Boyle's pump, of which he published an account, with the illustration reproduced in Fig. 4, in 1660, was actually made by Robert Hooke, which accounts for the excellent design and workmanship, evidenced by the fact that there was no need of water to keep the joints tight. In the vertical brass cylinder ran a "sucker", "4 4" in the diagram, which

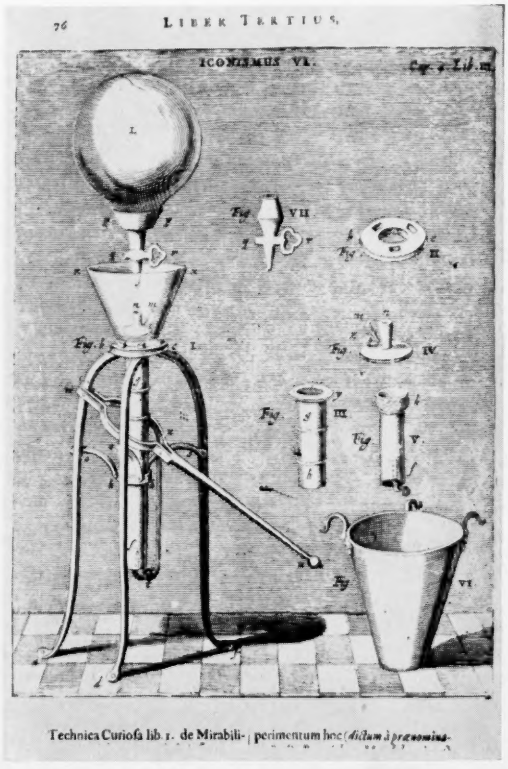

FIG. 3. Guericke's pump, from *De Vacuo Spatio*.

was presumably of wood, since a disc of oiled leather was nailed to it, for air-tightness. This was driven up and down by a rack and pinion. Oil, or an emulsion of oil and water, was put on the piston for easy running. The receiver was a large glass sphere with an opening at the top, cemented into which was a brass ring made to receive a brass cover, shown in detail at the upper right-hand corner. All this bespeaks excellent handicraft.

Essential for the working was the hole at the upper shoulder of the piston, shown closed by a peg. To operate the pump, the tap below the receiver was closed, the peg removed and the piston run up, expelling the air. The peg was then replaced, the tap opened and the piston withdrawn, sucking air from the receiver. The tap was then closed, the peg removed and the process repeated. This is how Guericke's last pump operated. It is clear that this pump of Boyle's was an excellent instrument, well adapted for experiment.

Boyle's second pump, described in a book published in 1669, is shown in Fig. 5. The single cylinder was of the type of the first pump, the peg being on the end of the long stick shown on the right of the rack : the whole was immersed in water for air-tightness, no doubt because, Hooke being no longer in Boyle's service, the workmanship was not up to standard. Today it is hardly necessary to stress the importance of perfection of finish in a mechanical pump. The advantageous new feature was the flat plate to which the bell-jar for experiment could be cemented, a feature anticipated in a pump made by Huygens, of which, however, he published no account, so that possibly Boyle's innovation was an independent one.

Just as Hooke had worked for Boyle, so Denis Papin, also a genius, worked for Huygens and made, to Huygens' design, a pump, similar in many respects to Boyle's first pump, with a plate for the receiver, of which he published an account in 1674. At the same time he described a pump of his own design, shown in Fig. 6, remarkable for having a two-way tap, *G*, drawn separately to the right. One channel was an ordinary hole at right-angles to the axis of the turning part, the other a groove along *aa* for communication with the air. The stirrup was another novel feature : with these early pumps with wide cylinders it required considerable force to overcome the atmospheric pressure.

This trouble was avoided by providing two cylinders, the pressure of the atmosphere on one piston helping to withdraw the other. The first such pump, illustrated in Fig. 7, was described by Boyle in 1682, but he clearly stated that it was the invention of Papin, who was working for him at the time.

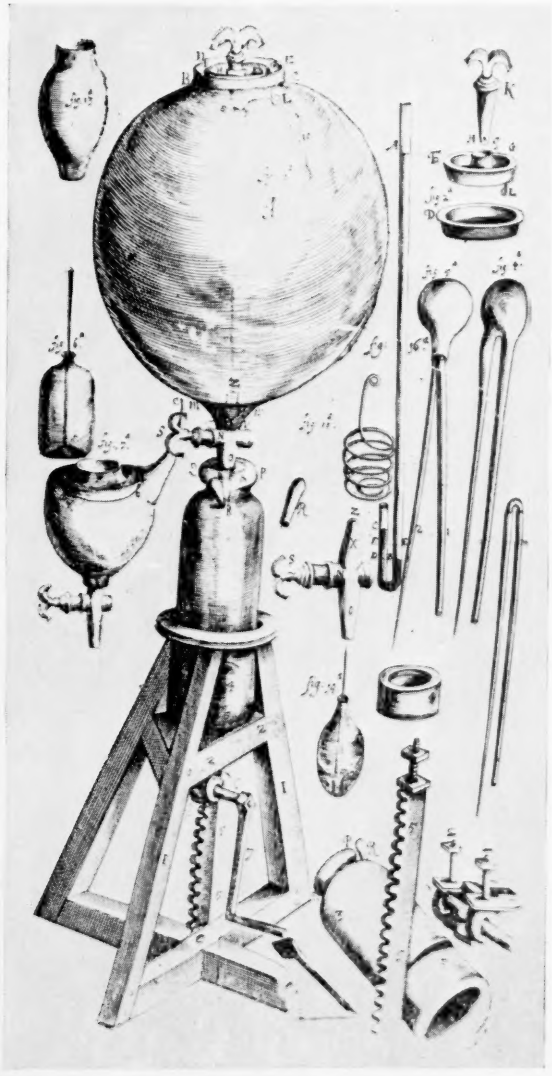

FIG. 4. Robert Boyle's first pump.

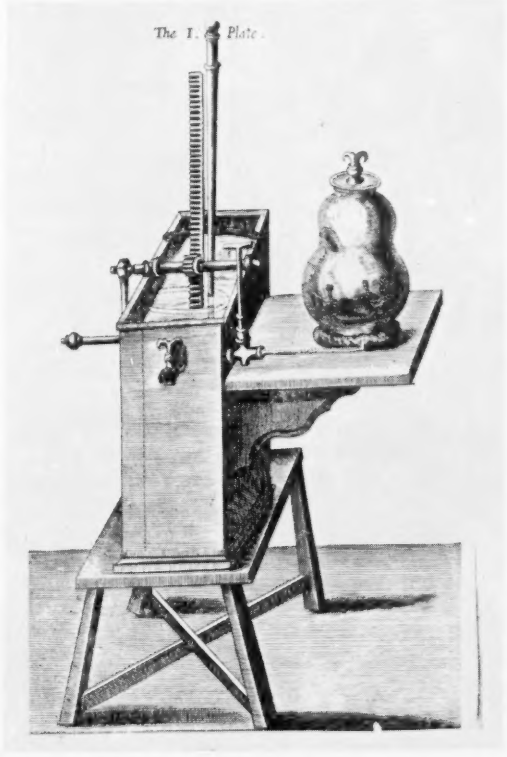

FIG. 5. Boyle's second pump.

Vol. 9 959/60

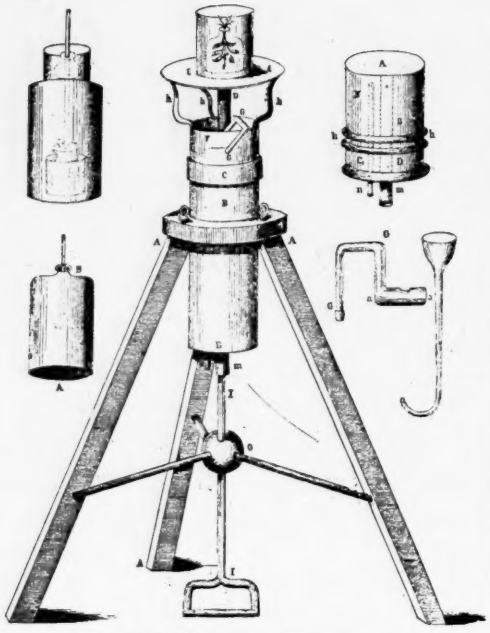

FIG. 6. Papin's pump with two-way tap.

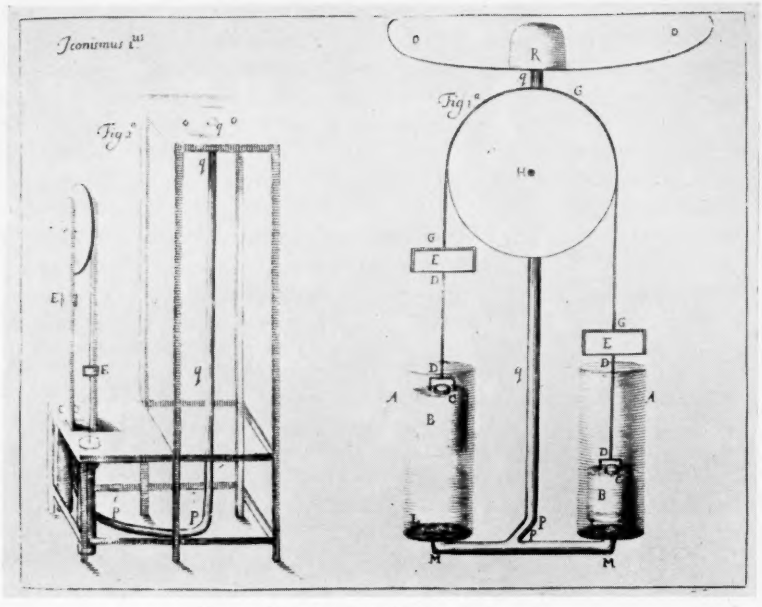

FIG. 7. Boyle's two-cylinder pump.

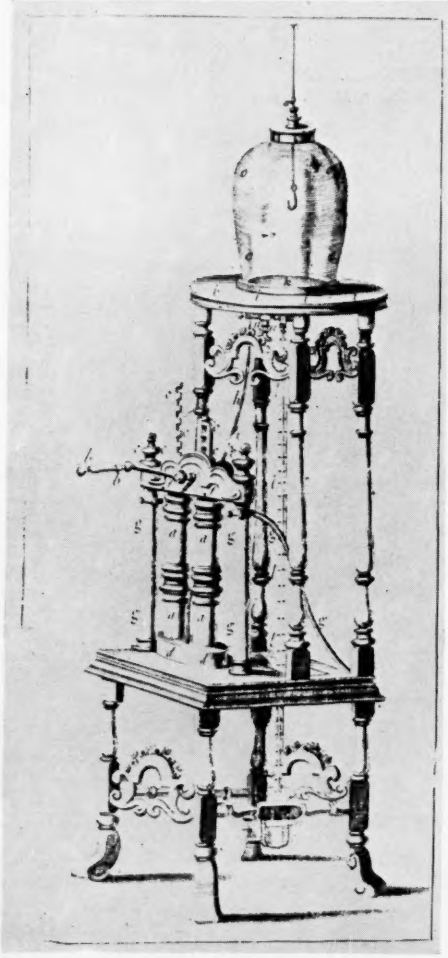

FIG. 8. Francis Hauksbee's pump.

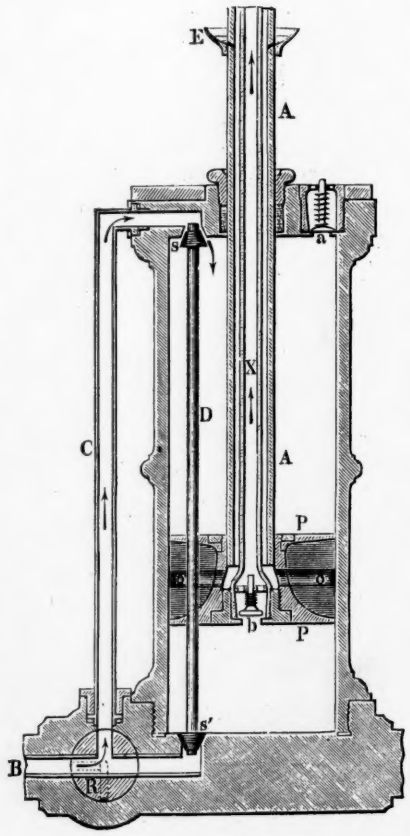

FIG. 9. Bianchi pump.

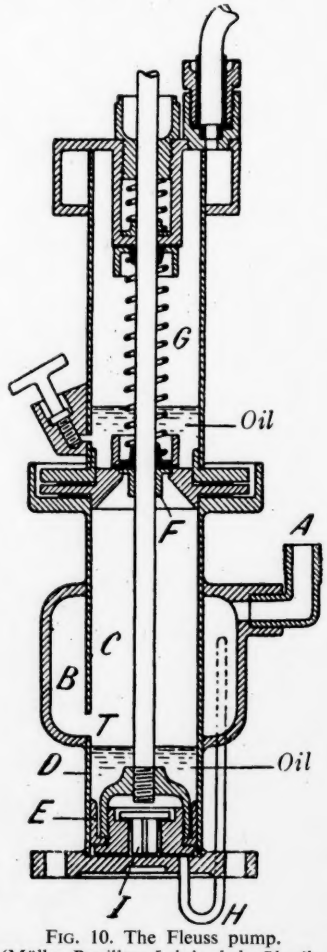

FIG. 10. The Fleuss pump.
(Müller–Pouillet : *Lehrbuch der Physik*, vol. 1, 1906, Fig. 514, Vieweg.)

The pistons were coupled together by a cord passing over a pulley wheel. A two-cylinder pump of much better design was produced by Francis Hauksbee and described in 1709. His illustration, reproduced in Fig. 8, corresponds exactly to a pump still in the possession of the Royal Society. The two pistons are worked by rack and pinion, so arranged that as one descends the other ascends. The valves were made of bladder. The arrangement of the bell-jar, with a mercury column manometer directly beneath it, was a very convenient one. This pump, when put in order some years ago according to Hauksbee's description, gave a vacuum within about 1 in. of mercury of perfect, better than which, as wet leather was used for certain washers, could not be expected.

Hauksbee's design remained, in principle, unchanged until well on in the nineteenth century : in fact, pumps of this type, with small modifications and improvements, were still being made at the end of that century. In 1856, Bianchi introduced a pump with a single cylinder, Fig. 9, so designed that the air from the receiver was drawn in alternately above and below the piston as it played in the cylinder, with the effect that, as far as the mechanical work was concerned, the pressure difference in both up and down stroke was negligible. This pump does not seem to have come into general use, perhaps on account of difficulties of construction.

Vol. 9 959/60

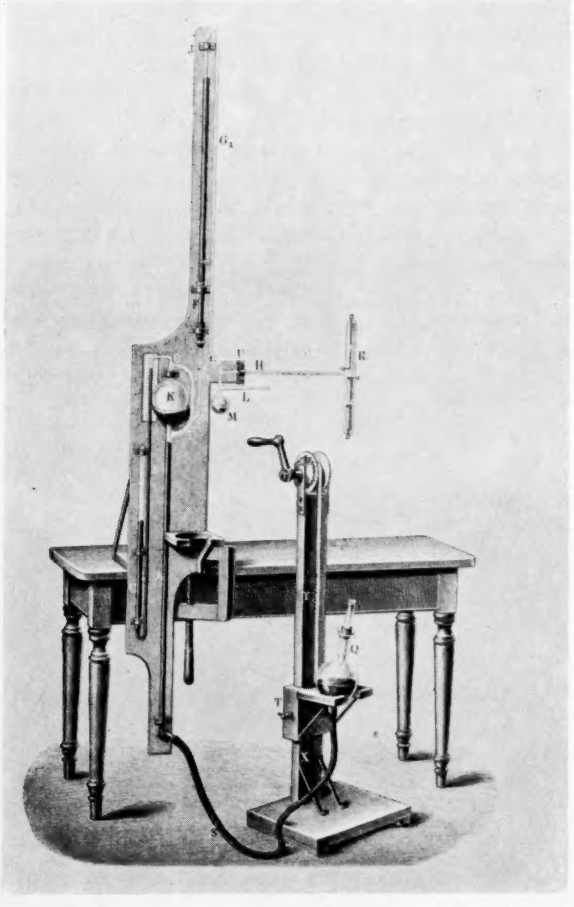

FIG. 11. Töpler pump, as used towards the end of the nineteenth century. (Müller–Pouillet ; *Lehrbuch der Physik*, vol. 1, 1906, Fig. 527.)

A substantial improvement in the vacuum produced by cylinder pumps was made by Fleuss in 1892 with what he called the Geryk pump, in honour of the Magdeburg pioneer. The new feature was that the dead space which is still left when the piston has advanced to the end of the cylinder was filled with oil, whence these pumps were sometimes called oil pumps. As shown in Fig. 10, halfway up the cylinder there is a partition, supporting a spring-controlled valve through which the piston-rod passes. Oil is contained above this and above the piston. At the end of its upward stroke, the piston, with its superincumbent oil and air, lifts the valve and forces out the air. The valve does not close until the piston has descended a short distance, which ensures a correct distribution of the oil. A special oil, of low vapour pressure, although not as good as the modern apiezon oils, was used and it is claimed that pressures as low as 0.0002 mm mercury were attained. In any case, these pumps were at one time widely used in the electric lamp industry.

In the middle of the nineteenth century, when high vacua—which in those times might mean a few times 10^{-3} mm of mercury—were required for electrical discharge tubes, the mercury pump began to be developed. That used by Geissler in 1855, said to be a modification of one devised in principle by Swedenborg, was the first of a large class. It consisted of a bulb connected by a flexible tube to an open reservoir of mercury, this bulb being provided with a two-way tap by means of which it could be connected either to the outside air or to the vessel to be exhausted. The tap being turned so as to give passage to the air and to cut off the vessel, the reservoir was raised until all the air had been expelled from the bulb : the tap was then turned so as to cut off passage

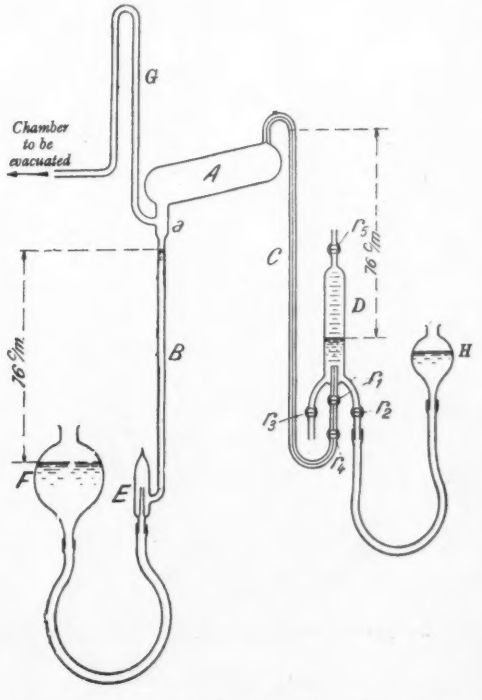

FIG. 12. Improved form of Töpler pump. (Dunoyer ; *Vacuum Practice*. G. Bell, 1926, Fig. 1.)

to the air and to connect to the vessel and the reservoir lowered. The process was repeated as often as desired. The vessel was thus effectively connected to a Torricellian vacuum at each stroke, the fraction of air removed depending upon the relative volume of bulb and vessel to be exhausted.

A great improvement was effected in 1862 by Töpler, who retained the mercury reservoir and flexible tube but substituted for the tap an arrangement of tubes by which passage was made for the air to be expelled, and the vessel to be exhausted was connected to the Torricellian vacuum, automatically at the appropriate position of the mercury level. This went through improvements at the hands of Neesen and Bessel–Hagen which brought it to the form shown in Fig. 11. *R* is the vessel to be exhausted (a Geissler tube), *K* is the bulb in which the Torricellian vacuum is produced, *P* is the joint at which the rising mercury cuts off connection of *K* and *R*, *OBC* the tube through which the air is expelled. *M* is a bulb containing phosphorus pentoxide. It was with pumps of this general type that exhaustion was effected for many of the early classical experiments on cathode rays, Röentgen rays and electronics in general. The latest type, which was in use well into the present century, is illustrated in Fig. 12. One advantage of this pattern is the cylindrical inclined bulb, *A*, in place of the old spherical bulbs. This gives a big volume for a small vertical displacement and also lessens the mechanical shock of the rising, uncushioned mercury when the pressure is low. Anyone who has used one of the old Töpler pumps systematically knows how easy it was to knock the head off, if the mercury reservoir was raised without due caution.

Mention must be made of the Sprengel mercury pump, invented in 1873, which was also extensively used by the classic experimenters on the electric discharge. In this, the air was carried away by a succession of falling mercury pellets, between which it was trapped. It was with an improved form of this pump, devised by Gimingham and having a number of tubes for the mercury fall instead of one, that William Crookes, one of the most skilled workers on vacuum physics in the second half of the nineteenth century, carried out, for instance, his classic work on the radiometer. He used phosphorus pentoxide to absorb water vapour, precipitated sulphur to stop mercury vapour and reduced copper to stop the sulphur vapour entering his evacuated space. He claims to have reduced the pressure to 0.4×10^{-6} atm, say 3×10^{-3} mm of mercury, and says, " Formerly, an air-pump, which would diminish the volume of air in the receiver 1000 times, was said to produce a vacuum ", adding that the Sprengel pump had already rarified air a few hundred thousand times, which in those days was very good performance.

In 1905, a new period was ushered in by the invention of the rotary vacuum pump of W. Kaufmann, in which a continuous rotation, effected by an electric motor or by hand, carried away the air. It is illustrated in Fig. 13. It needed a backing pump, to reduce the pressure to 2 cm of mercury or so, a feature of all modern high-vacuum pumps. The principle is clear : the air is trapped by the mercury in the inclined Archimedean spiral and delivered to the roughly evacuated space. Only a relatively few of such pumps were, however, made, for at the end of the same year, Gaede produced his rotary mercury vacuum pump, which, on account of its simplicity and speed of working, was an immediate success.

The general scheme is shown in Fig. 14, *G* is a cast-iron cylindrical container, with a thick glass front *B*, within which a porcelain drum, shown in section, rotates. This drum consists of three similar compartments. With rotation in a counter-clockwise direction, the air in W_2 is displaced by the mercury along the passage between the walls Z_1 and Z_2, until it is delivered into the space above the mercury in the outer container. Here it is removed, through s_2, by the backing pump, which produces the low pressure, 1 cm of mercury or so, needed if the mercury level inside and outside the drum is not to be too large. As the drum rotates, the

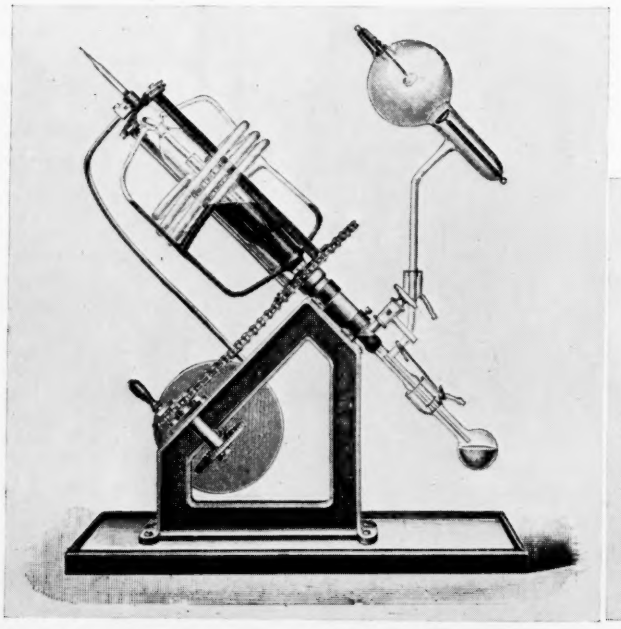

FIG. 13. The Kaufmann pump. (Müller–Pouillet ; *Lehrbuch der Physik*, vol. 1, 1906, Fig. 537.)

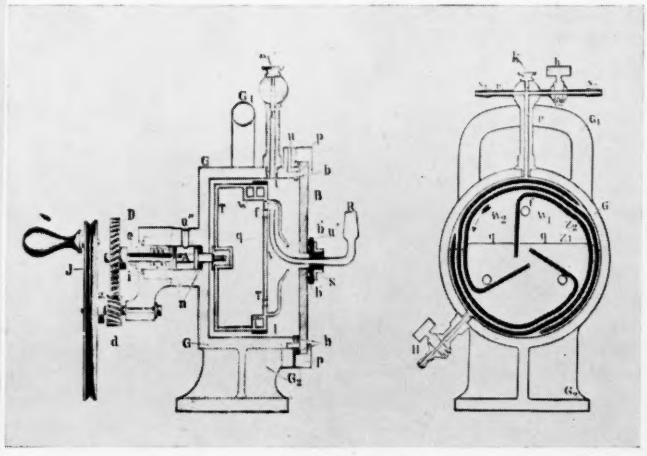

FIG. 14. Gaede's rotary vacuum pump.

volume of air in W_1, entering through the passage f, from the vessel to be exhausted, increases, to be expelled in its turn by further rotation, and so on. By 1910 such pumps were to be found in constant use in every continental laboratory devoted to vacuum physics. They could produce a vacuum of 10^{-6} mm of mercury.

For backing pump a mechanical rotary pump was generally used. Gaede's so-called *Kapselpumpe*, or box pump, is shown in cross-section in Fig. 15. There is an eccentrically-

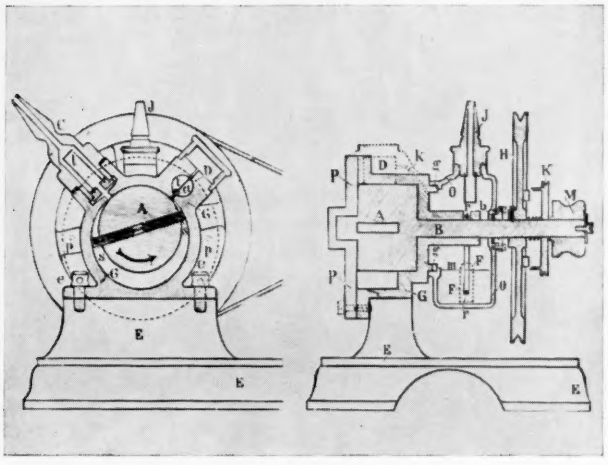

FIG. 15. Gaede's box-pump.

mounted rotating cylinder, with vanes maintained in contact with the wall of the container by springs : the mode of operation is clear. There was nothing new about the general

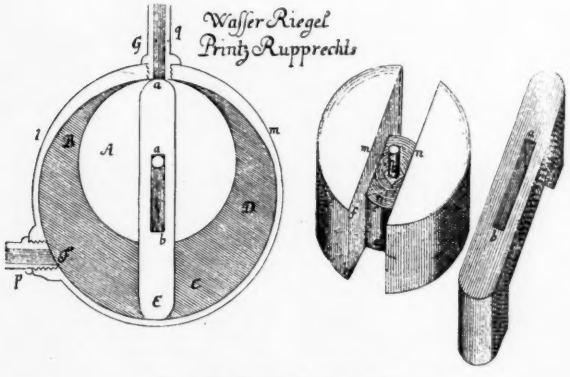

FIG. 16. Rupert's water-bolt.

design, as can be seen by comparing Fig. 15 with Fig. 16, which shows Prince Rupert's " Water-Bolt," a water pump invented some 250 years earlier, and itself not unlike a device figured by Ramelli in 1588. Gaede's early box pump was the forerunner of a large range of recent pumps of this general pattern. It produced a vacuum of about 0.01 mm of mercury : the new pumps, with improved design and special oils, can do somewhat better than that.

In 1912, Gaede made another fundamental advance by his invention of the molecular pump. This depends for its action on the peculiar properties of gases at pressures so low that the mean free path is larger than the width of the passage that is under consideration : in this connection it may be recalled that the mean free path of the nitrogen molecule at a pressure of 0.001 mm of mercury is about 7 cm. At the low pressures in question, the molecules striking a wall behave as if the gas condensed on the wall and evaporated again. If, therefore, the wall is moving in its own plane, the velocity of the wall must be added to that of the molecules. In Gaede's molecular pump, which demanded a comparatively high fore-vacuum, a cylinder rotating at high speed gave the rapid surface movement required. A number of grooves in the cylinder, each divided by a tongue projecting from the housing, were connected in series, to increase the effect. The pump had the advantage that it dealt with condensable vapours as well as with ordinary gases.

The construction demanded a very high degree of mechanical skill and it was, in consequence, expensive. It never came into general use because in 1915 Gaede invented the vapour stream pump, which is simple to make and very efficient. A form of the molecular pump devised by Holweck, which was somewhat simpler to make, is, however, in its modern form used for certain purposes.

The history of the vapour stream pump of Gaede and its development by Langmuir and many others to the position which it now occupies is too recent a story, and one too familiar to all present, to be included in this brief sketch. I should like to conclude with a tribute to Gaede, who originated so much, if not all, of the modern equipment for winning a vacuum. He combined deep theoretical knowledge with clear physical insight and a genius for design. Lenard in 1926 wrote to him telling him that he had proposed him for the Nobel prize : " Denn, mein lieber Gaede, was wären wir alle ohne Sie?" It would have been an award which would have given pleasure to many physicists. With his inventive genius Gaede combined a character of singular courage and probity. He was of old German descent, but he was denounced by the Nazis as politically unreliable and friendly to Jews, was removed from his university post and, in general, shamefully treated for his open desire for decency. He died in 1945 of diphtheria and undernourishment. All honour to his memory.

Vol. 9 959/60

Initial Pumping and Recovery of Ionization Gauges*

N. W. ROBINSON and F. BERZ

Mullard Research Laboratories, Salfords, United Kingdom

Measurements have been made on the pressure decrease in a closed glass system when an ion gauge pumps and also of the recovery of pressure when pumping is stopped after a short period. The pressure decrease may be represented by an equation of the type

$$p - p_1 = C_1 e^{-a_1 t} + C_2 e^{-a_2 t}$$

where p and p_1 are the pressure after any time t and the "final" pressure, respectively. C_1, C_2, a_1, a_2 are parameters depending upon the nature of the gas and surfaces. For pumping a_1 and a_2 contain terms depending upon the electron current. For recovery a_1 is determined by the sticking time of pumped molecules on the glass and a_2 by a glass characteristic. Average sticking times are found to increase from about 10 s *to* 2000 s *as the temperature of the system increases from* 22 *to* 450°C *with consequent change in heats of adsorption from* 18 *to* 40 kcal/mole *approximately. The increase in sticking times are attributed to changes in residual gas composition.*

THERE have been many theories put forward for the pumping of ionization gauges by Meyern[1], Schwartz[2], Bloomer and Haine[3] and more recently Young[4]. In addition Varnerin and Carmichael[5] studied the pumping and re-emission of trapped helium atoms in an ion gauge enclosed in a molybdenum cage. It is thought that pumping is the result of two effects ; the trapping of charged atoms or molecules of gas on the glass surface enclosing the normal gauge and the re-emission of atoms or molecules which have lost their charge and are free to re-enter the space. The later experiments have elaborated theories in which the number of re-emitted particles is proportional to the number of particles pumped and equations are derived on this basis. The present paper amplifies a theory which was first suggested by Dickey[6] with the addition of a re-emission term depending upon the properties of the glass or other surfaces included in the ionization gauge.

The theory is the result of practical experiments in which two ionization gauges Mullard Type IOG 1 (Kodial glass) were mounted on one stem and one gauge was used with small electron current solely for pressure measuring, while the other was made to pump at will. The pressure in the system was continuously recorded during pumping and also during the subsequent recovery of pressure after the pumping current was switched off. It was found that the pressure in the system was very sensitive to temperature changes so that the filament temperature in both the ionization gauges was kept constant and the electron current in the pumping gauge was switched on and off by means of potentials applied to an auxiliary grid concentric with the accelerating grid.

The arrangement is shown in Fig. 1.

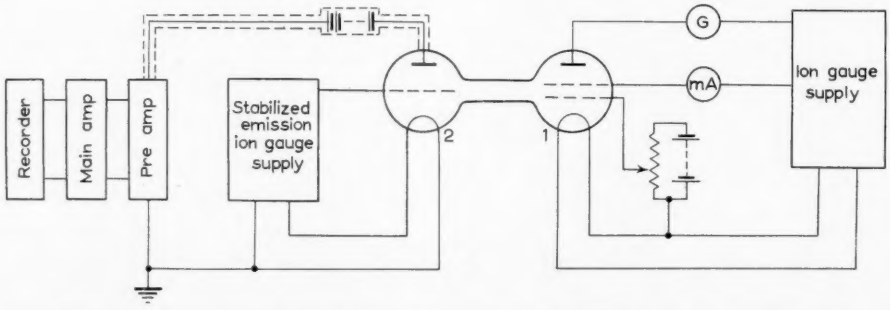

FIG. 1. Schematic arrangement of measuring circuits. 1. Pumping gauge 2. Measuring gauge.

The pumping and recovery records were taken with the tubes in an oven whose temperature could be controlled. At about 260°C leakage conductance of the glass gave currents comparable with the measured ion currents so that this temperature marks the upper limit of measurements. For one set of tubes the measuring gauge was kept at room temperature while the pumping gauge was heated.

The pumping curves showed a rapid pressure fall in a few seconds followed by a quasi-equilibrium pressure.

* Paper presented at the First International Congress on Vacuum Techniques, Namur, 10–13 June 1958.

Pumping was then stopped and recovery followed. Thus, the experiments consider only short-term pumping and it is found that during recovery the pressure almost returns to its original value.

Records were of the form shown inset in Fig. 2 where the pressure symbols are defined.

On the same figure are shown the normalized pumping and recovery curves at a variety of temperatures and pumping

It will be noticed that there is a singularity in the neighbourhood of 150 °C which will be considered later.

Another feature of the pumping curves is illustrated in Figs. 4 a and b where the pumping factor, i.e. $(p_0 - p_1)/p_1$ is plotted against temperature and also against current from which

$$(p_0 - p_1)/p_1 = ki. \tag{2}$$

It is seen that the pumping effect is proportional to the

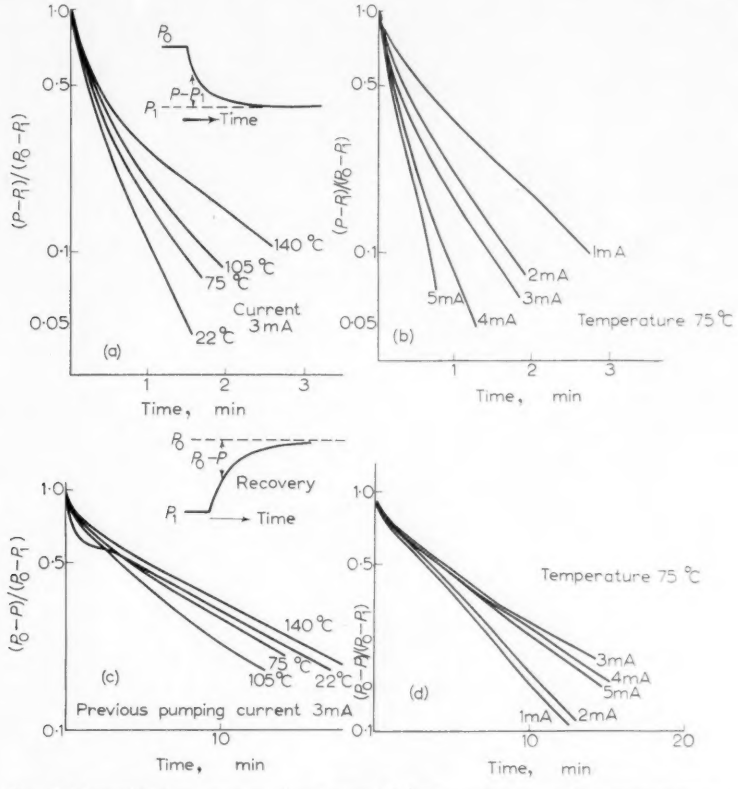

FIG. 2 Normalized pressure vs. time curves (a) for pumping at various temperatures. Electron current constant at 3 mA. (b) For pumping at various currents at constant temperature 75 °C. (c) For recovery at various temperatures after pumping at constant current, 3 mA. (d) For recovery after pumping with various currents at constant temperature 75 °C.

currents drawn on semi-logarithmic paper. The curves in general can be represented by an equation of the form

$$p - p_0 = C_1 \exp(-a_1 t) + C_2 \exp(-a_2 t) \tag{1}$$

where C_1, C_2, a_1, a_2 may be obtained graphically or by a method described by Prony[7].

The Prony method is very laborious and gives the various coefficients to little better accuracy than the graphical method. In the latter method the final straight line portion of the curve is produced backwards and C_2 is given by intercept with the pressure axis and a_2 by the slope. The exponential $C_1\exp(-a_1 t)$ is obtained by plotting the difference between the asymptotic straight line and the curve. The intercept of the resulting straight line with the pressure axis gives C_1 and again the slope gives a_1.

The way in which the constants vary with temperature and current is shown in Figs. 3 a and b.

pumping current but it does not depend in a simple fashion on temperature. The singularity shown in Fig. 3 is manifest in these pumping curves also. A minimum in pumping occurs at a temperature somewhere between 100 and 200 °C.

The form of the recovery curves is similar to that for the pumping curves and to distinguish them the constants will be named C_1^*, C_2^*, a_1^*, a_2^*.

Theory

In order to analyse the results further a tentative theory is outlined here. In a closed system such as the two ion gauges there is a fixed number of atoms and molecules, some of which form the solid lattice of the structures and can be ignored in the theory, while there is a number which takes part in the dynamic exchanges in the tube, some particles are adsorbed, some desorbed, some ionized and some deionized,

Vol. 9 959/60

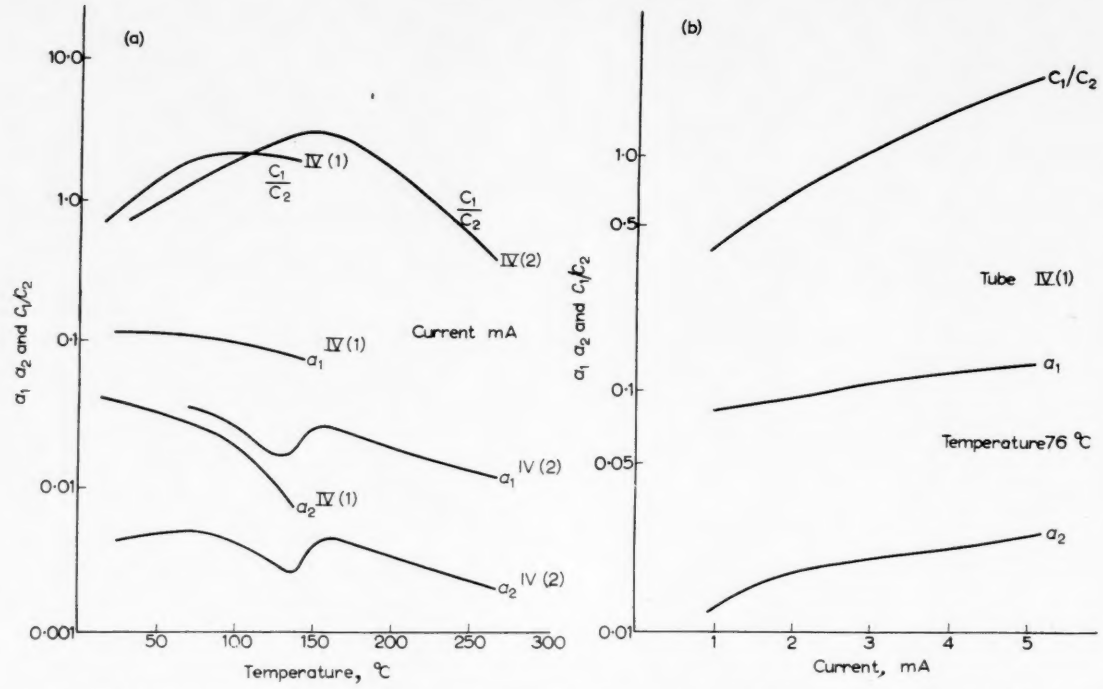

FIG. 3 (a) Values of a_1, a_2, C_1/C_2 for tubes IV (1) and IV (2) vs. temperature at constant current 3 mA. (b) Values of a_1, a_2 and C_1/C_2 with current at constant temperature 76 °C.

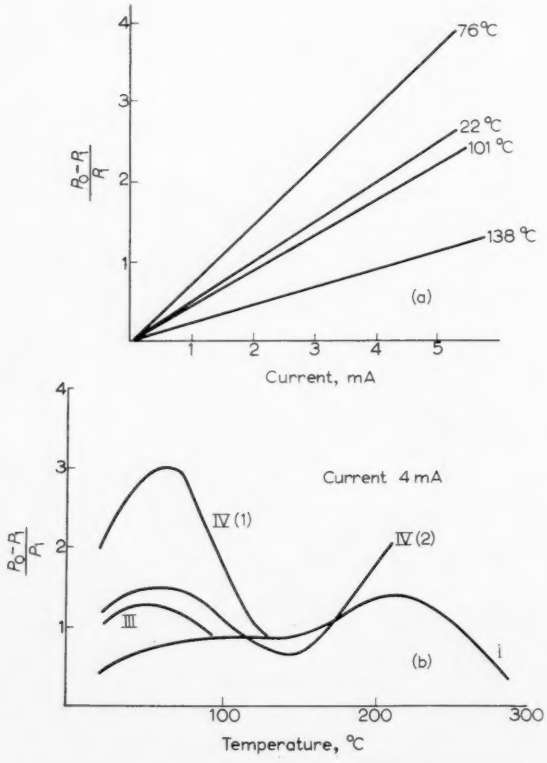

FIG. 4 (a) Values of $(p_0-p_1)/p_1$ vs. current at various temperatures.
(b) Values of $(p_0-p_1)/p_1$ vs. temperature at constant current.

but at any instant there is dynamic equilibrium. The only factor allowed to disturb this equilibrium is to start and stop pumping. The change in pressure is due to electrical and non-electrical effects which are considered separately.

Electrical effects

During pumping the rate at which molecules are removed from the space is assumed to be proportional to the electron current i and the number N of particles in the space and can therefore be represented by aiN, where a is a constant.

The pumped particles can be considered in two groups, those which disappear permanently from the space and those, forming a proportion γ/a which are re-introduced into the space after a finite sticking time $1/\beta$.

Thus

$$dN_a/dt = -aiN + \beta W, \quad (3)$$

$$dW/dt = -\beta W + \gamma iN, \quad (4)$$

where dN_a/dt is the overall rate of variation of the number of particles in the space due to electron pumping, and W is the number of electrically pumped particles which are adsorbed on the walls for a short time. These two equations were given by Dickey.

Non-electrical effects

Two kinds of effects are to be taken into account (a) the desorption factor, and (b) chemical pumping. The latter effect is due to chemical reaction of residual gases with a hot tungsten filament. It has been noted by Langmuir who investigated the reaction with water vapour. The effect increases with increased temperature so that in these experiments the tungsten filaments have been run at the lowest temperature possible. It is thought therefore that this effect is small. The desorption effect is due to the presence on the

surface of the glass of a very extensive reservoir of gas molecules. If the pressure in the space is reduced there is a desorption from the glass surface tending to restore equilibrium. The desorption occurs whenever the pressure is decreased by any means whatsoever. It also takes place if the glass is heated as was shown by Schrader[8] when he found that the pressure in an evacuated glass vessel increased by an amount larger than required by the gas laws.

As a first approximation the rate of change of gas molecules in the space due to desorption and to a less extent by chemical pumping, can be represented by

$$dN_b/dt = \delta(N_0 - N), \tag{5}$$

where N_0 is the number of particles at equilibrium and δ is a constant. It is assumed that the reservoir of gas particles on the surface is so large that the fraction desorbed is small even though it may have a great influence on the pressure.

Combined effects

The total rate of change in the number of particles N is given by the sum of equations (3) and (5) together with (4). Thus

$$\left.\begin{aligned} dN/dt &= -\alpha i N + \beta W + \delta(N_0 - N), \\ dW/dt &= -\beta W + \gamma i N. \end{aligned}\right\} \tag{6}$$

These equations are valid for pumping when $i \neq 0$ and for recovery when $i = 0$ in which case β and δ must be replaced by β^* and δ^* to take into account any change due to the absence of electrical fields. The solution of these equations is given below :

Pumping

$$N = N_1 + C_1 \exp(-a_1 t) + C_2 \exp(-a_2 t)$$

$$N_0/N_1 = 1 + \frac{\alpha - \gamma}{\delta} i,$$

where N_0 is the value of N before pumping,
and N_1 is the value of N after pumping,
a_1 and a_2 are the roots of the equation
$x^2 - [\alpha i + \beta + \delta]\, x + \beta\,[(\alpha - \gamma)\, i + \delta] = 0.$

Recovery

$$N = N_0^* - C_1^* \exp(-\beta^* t) - C_2^* \exp(-\beta^* t)$$

$$C_1^* = \frac{\gamma i}{\beta} \frac{\beta^*}{\beta^* - \delta^*} N_1^*$$

$$C_2^* = N_0^* - N_1^* - \frac{\gamma i}{\beta} \frac{\beta^*}{\beta^* - \delta^*} N_1^* \tag{7}$$

N_1^* is the value of N at the beginning of recovery,
N_0^* is the value of N after recovery.

Analysis of experimental results

From the above equations we see that for pumping

$$k = \frac{p_0 - p_1}{p_1 i} = \frac{(\alpha - \gamma)}{\delta} \tag{8}$$

$$a_1 + a_2 = \alpha i + \beta + \delta, \tag{9}$$

$$a_1\, a_2 = \beta\delta\left(\frac{\alpha - \gamma}{\delta}\, i + 1\right) = \beta\delta\, \frac{p_0}{p_1} \tag{10}$$

The parameters a_1, a_2 and k can be determined experimentally. For recovery

$$a_1^* = \beta^* \quad \text{and} \quad a_2^* = \delta^*. \tag{11}$$

Recovery. Values of β^* and δ^*

The values of β^* and δ^* are shown in Fig. 5. The figure contains data on tubes number I, II, III, IV (1) and IV (2). Tubes I, II and III were heated to 450°C for 14 h before

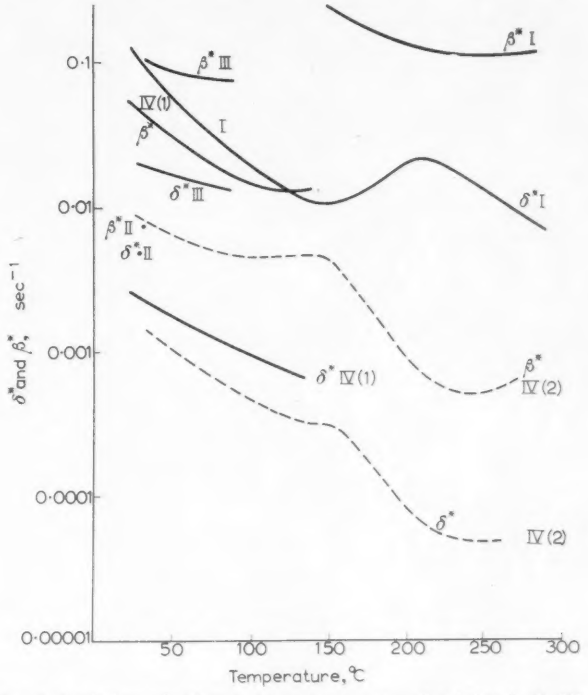

FIG. 5. Variation of β^* and δ^* vs. temperature for tubes I, II, III, IV(1) and IV(2).

sealing off, while tubes IV (1) were heated for three periods of 14 h. while tubes IV (2) denote experiments on tubes IV (1) after long continued heating to 250°C and continuous ion pumping. The order of pressures in the tubes was as follows : tubes I, 10^{-8} mm Hg, tubes II, 3×10^{-7} mm Hg, tubes III, 7×10^{-8} mm Hg, tubes IV (1), 4×10^{-9} mm Hg, tubes IV (2), 3×10^{-9} mm Hg.

It is seen that β^* decreases with increased temperature with a drastic change in the rate of decrease for Tube IV (2) at a temperature of 150°C. The decrease in β^* denotes an increase in the sticking time with temperature. This is contrary to the normal behaviour of sticking time with temperature since the surface activity of a solid-gas interface should increase and tend to reduce the sticking time. The effect obtained here may be due to two factors, one due to the change in the nature of the residual gases with temperature and the other due to the physical change in the solid surfaces. As the temperature increases, the residual gases become richer with gases of long sticking times, which at lower temperatures are held so tightly by the glass that they do not contribute to pumping or recovery. The presence of such gases tends to increase the average sticking time. More precise mass-spectroscopic evidence obtained in these

Vol. 9 959/60

laboratories shows that these gases can be divided into two groups—below 150–200 °C comparatively lightly held gases are driven away, whereas well above these temperatures one finds gases of higher mass number which are due to cracked oil vapour and glass decomposition. This might possibly explain the knee in the β^* and δ^* curves of Fig. 5 in the neighbourhood of 150 °C.

The second factor may be due to changes in the surface structure of the glass. Douglas[9] has found rearrangement of glass structure occurring in some glasses at relatively low temperatures.

The singular pumping curves shown in Figs. 4 a and b are also evidence of some effect which may be a consequence of new surface conditions, or changes in the gas composition.

Frenkel 1924 derived the relation between sticking time and heat of adsorption for a gas on a surface

$$\tau = \tau_0 \exp(Q/RT),$$

where Q is the heat of adsorption, R is the gas constant and T the temperature on the absolute scale, τ is the sticking time and τ_0 the vibration time of the surface lattice usually assumed 10^{-13} s. The heat of adsorption of residual gases on glass is given on Fig. 6. The values range from 18–20 kcal/g at room

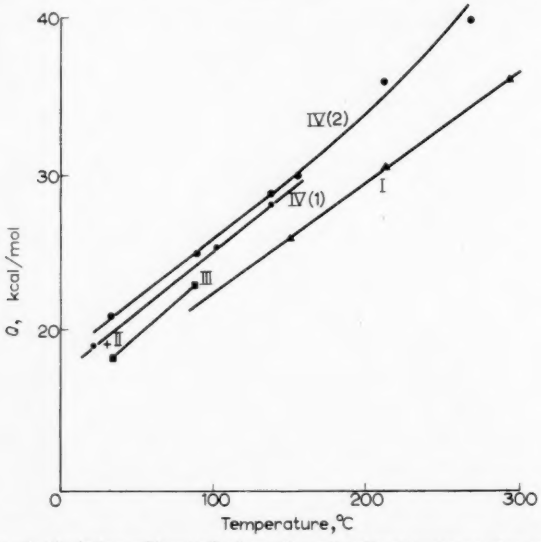

FIG. 6. Variation of heat of adsorption of residual gases on glass with temperature for tubes I, III, IV (1) and IV (2).

temperature, the higher values being associated with tube IV (2) which had the most rigorous baking. These values are in the region of weak chemisorption.

Referring again to Fig. 5, the values of the desorption factor also show the same kind of variation with temperature as β^*, but are usually one order less in value. Again, the tube having had the most rigorous baking showed the lowest desorption factor. This is in accordance with expectation, since it is probable that the reservoir of molecules in the desorbing skin may have been depleted.

Pumping. Values of α, β, and δ

Theoretically α, β and δ may be obtained from the equations given in (9) and (10). The value of α may be obtained from the slope of the straight lines obtained by plotting $a_1 + a_2$ against the electron current i. The intercept of the line at $i = 0$ also gives $\beta + \delta$. These curves are plotted on Fig. 7. The method depends upon graphical solutions and the accuracy is reduced by cumulative errors. The results do, however, show a trend to decrease with increasing temperature. It is not expected that δ will differ substantially from δ^*, since the desorption factor is not very dependent on electric fields.

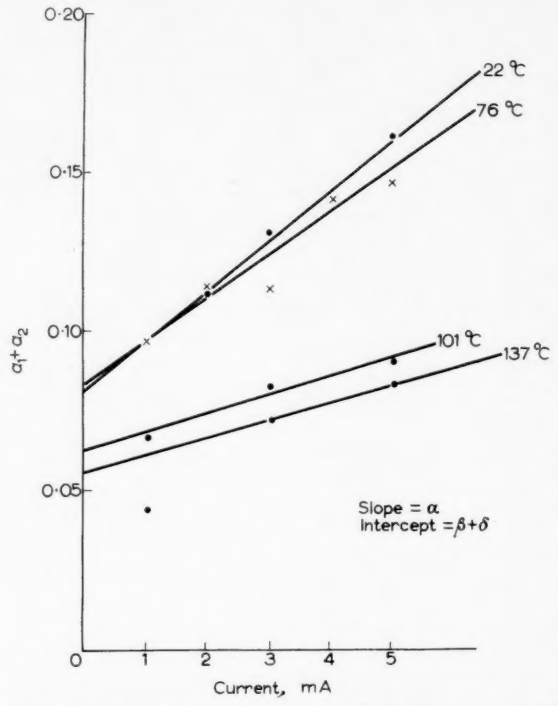

FIG. 7. Variation of $a_1 + a_2$ vs. current at various temperatures. The slope is a measure of α and the intercept on the ordinate $(\beta + \delta)$.

Glass coated with titanium

The experiments have been repeated before and after the glass surface of the pumping tube was covered with evaporated titanium. The titanium was interleaved with one of the tungsten heaters in the pumping ion gauge and could be evaporated by heating the tungsten. No special precautions were taken to pump the tubes to low pressures, since the main object of the experiment was to measure the effectiveness of the system as an evapor-ion pump. The experiments were done first with the unsputtered bulb pumping and the standard ion gauge measuring. The functions of the two tubes were interchanged and the measurements repeated. The titanium was then sputtered on to the walls of the pumping tube and the experiments repeated. Again the functions of the bulbs were interchanged and pumping and recovery records made.

Considering first the normal arrangement of measurement, the results are given in Fig. 8. It is seen that the initial pumping factor $[(p_0 - p_1)/p_1]$ has a value of 7.5, and the initial equilibrium pressure is 8.9×10^{-5} mm Hg. After evaporating the titanium the pressure has dropped to 2×10^{-7} mm Hg and the pumping factor is now only 1.3.

The pumping curve finally changed from a double exponential with $a_1 = 0.17$ and $a_2 = 0.027$ to a single exponential in which $a = 0.68$.

The recovery curve also shows a change from a double exponential with $\beta^* = 0.035$ and $\delta^* = 0.005$ to a single exponential with $\beta^* = 0.185$. The heat of adsorption corresponding to the latter value of β^* is 18.3 kcal/mol.

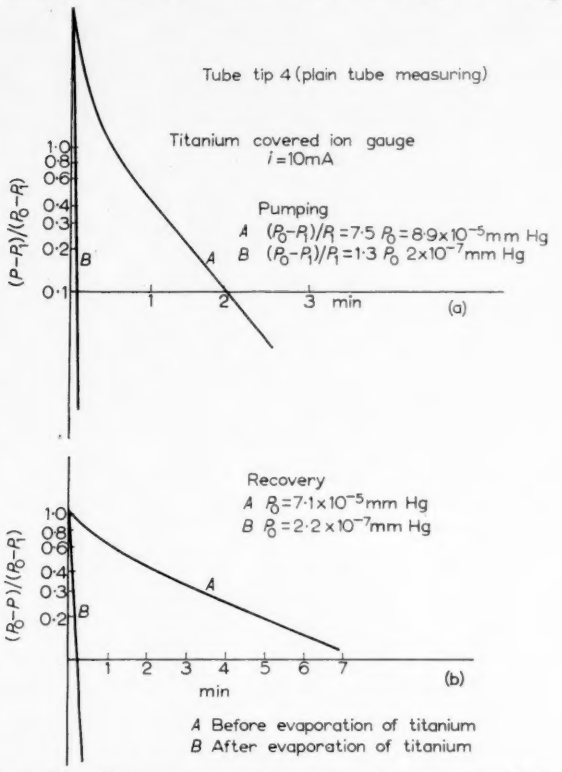

FIG. 8. Normalized pressure vs. time curves. For pumping *A* before and *B* after covering the ion gauge with titanium. Plain gauge measuring. (b) For recovery *A* before and *B* after covering the ion gauge with titanium. Plain gauge measuring.

The effects observed are probably the results of change in the nature of the residual gases and also due to the metallic film on the glass.

With the measuring and pumping tubes interchanged the results are given in Fig. 9. It is found that again the double exponential pumping curves with $a_1 = 0.09$, $a_2 = 0.009$ were converted to single exponential curves with $a = 0.185$.

The recovery curve, which before evaporating the titanium, was a double exponential no longer followed the usual pattern, but showed the pressure rising to a maximum and then decreasing. The effect appears to be due to the gettering action of the titanium adsorbing some of the gas released from the glass during normal recovery after pumping.

The analysis of the results on evaporated film in ion gauges is not complete, but it promises to afford some interesting information on the adsorption of gases on metallic surfaces.

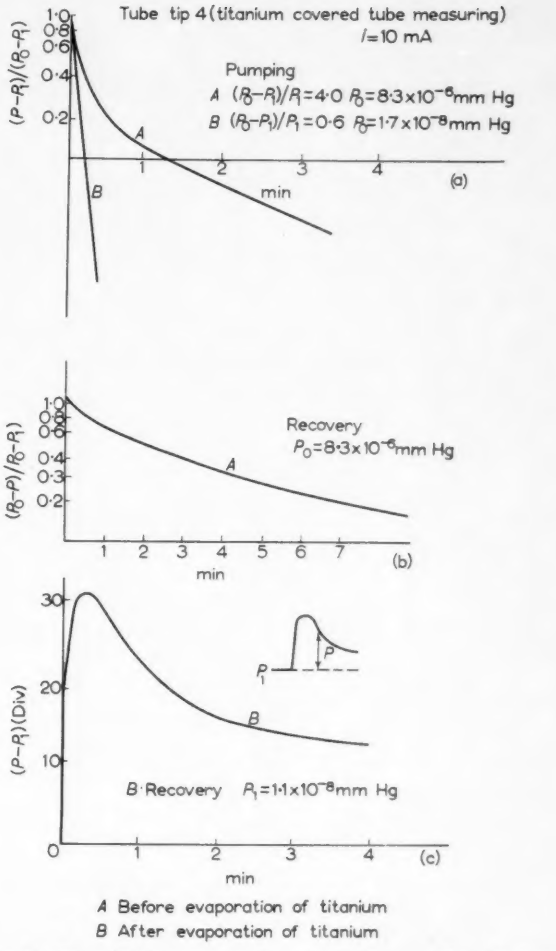

FIG. 9 (a). Normalized pessure vs. time curves for pumping *A* before and *B* after covering the ion gauge bulb with titanium. Plain gauge pumping. (b). Normalized pressure vs. time curves for recovery before covering the ion gauge bulb with titanium. (c). $(p-p_1)$ vs. time curves for recovery of plain gauge after the ion gauge had been sputtered with titanium.

Acknowledgment

The authors wish to thank the Director of Mullard Research Laboratories and the Directors of Mullard Radio Valve Co. Ltd. for permission to publish this paper.

References

1 W. von Meyern ; *Z. Phys.* **84**, 531 (1933).
2 H. Schwarz ; *Z. Phys.* **117**, 23 (1940) ; *Z. Phys.* **122**, 437 (1943).
3 R. N. Bloomer and M. E. Haine ; *Vacuum* **3**, 128 (1953).
4 J. R. Young ; *J.O.A.P.* **27**, 926 (1956).
5 L. J. Varnerin and J. H. Carmichael ; *J.O.A.P.* **28**, 913 (1957).
6 D. H. Dickey ; *Quart. Prog. Rep., M.I.T.* (July 1954).
7 E. T. Whittaker and G. Robinson ; *The Calculus of Observations*, Blackie and Son (1940).
8 J. E. Schrader ; *Phys. Rev.* **13**. 434 (1919) ; (S. Dushman. *Vacuum Techniques*, 516. John Wiley 1949).
9 R. W. Douglas ; *G.E.C. J.* 21 (1954).

Vol. 9 959/60

The Production of Ultra-high Vacua by Means of a Diffusion Pump*

A. VENEMA

Philips Research Laboratories, N.V. Philips' Gloeilampenfabrieken, Eindhoven, Netherlands

The result of a measurement of the so-called ultimate pressure of a diffusion pump is often not only determined by the pump itself, but also by the additional apparatus necessary for making this measurement. An analysis will be given of the gases which may be present at the pump mouth and the factors determining the pressure of those gases will be treated. A discussion of the methods which can be used for making these pressures as small as possible results in a design of a pump apparatus. A description of this apparatus, which includes a mercury diffusion pump with cooling traps, will be given. With the apparatus a pump speed at the recipient of 5–10 l./s *for the common gases is obtained and an ultimate pressure lower than* 10^{-12} mm Hg *is reached.*

1. Introduction

The use of ultra-high vacuum equipment has steadily increased in recent years. The sort of vacuum system which has to be used in a particular case will depend on the demands which are made. This holds for vacuum systems in the normal high-vacuum region down to pressures of about 10^{-7} mm Hg ; the same holds, however, for systems which have to supply vacua of the order of 10^{-11} mm Hg or higher. General considerations have led to the development of a system which differs from the one usually employed for the ultra-low pressure region. The system has been in use for some years now. A number of investigations have been made with it and it has proved to be very valuable. After some general considerations which hold for all vacuum systems in which Knudsen flow is predominant, a description will be given of this system which allows the production of pressures below 10^{-12} mm Hg with a pump speed at the vacuum chamber of 5–10 l./s. The pump which is used in the apparatus is a glass mercury diffusion pump. The backing-pump is a metal mercury diffusion pump which in its turn is backed by a rotary pump.

2. General considerations on the evacuation process

It will be assumed that the temperature in the system is constant and equal everywhere. To determine a certain amount of gas it is sufficient to give the product of volume and pressure. First, it will be assumed that only one sort of gas is present. The volume will be denoted by V, the pressure by p, starting with p_0 at the time zero. The gas production per second in the system is Q. A pump is used which gives at the vacuum chamber a pump speed S. This speed becomes zero at the ultimate pressure p_u which is determined by the pump and the connection between the pump and the chamber. This limiting pressure is reached when the amount of gas A_1 which escapes from the chamber in 1 s is equal to the amount which re-enters it from the pump side A_2. It will be assumed that A_2 is independent of A_1 which is usually the case.

One can always write

$$A_1 = S^*p \tag{1}$$

S^* being the pump speed of the escaping gas. The net amount of gas which disappears from the chamber can be written Sp. Obviously

$$Sp = S^*p - A_2 \tag{2}$$

At the limiting pressure p_u, the speed S is zero and $S^*p_u = A_2$, so (2) can be written as

$$Sp = S^*p - S^*p_u,$$

$$\text{or} \quad S = S^*\left(1 - \frac{p_u}{p}\right) \tag{3}$$

In the time dt the pressure change is dp and we have the relation

$$Q\,dt = S^*(p - p_u)\,dt + V\,dp. \tag{4}$$

If Q varies only slowly with time which is usually true, the solution of (4) is

$$p = p_0 e^{-(S^*/V)t} + (p_u + Q/S^*)\,(1 - e^{(S^*/V)t}) \tag{5}$$

The first term determines the pressure in the very first part of the pumping process, the second term is predominant when the time t becomes of the order of several minutes and longer. For large values of t

$$p = p_u + (Q/S^*). \tag{6}$$

When p_u is small as compared with p, S^* is equal to S which is then a constant.

A low pressure p is reached when p_u is low, when Q is small and S is large. When several gases are present, which is generally the case, the argument given above still holds for each gas, however, with different values of p_u, Q and S^*. The total pressure will be the sum of the partial pressures.

3. Special requirements

The system generally used in ultra-high vacuum techniques is the one first described by Alpert. It is a closed system with all metal or glass taps and pumped with an ionization

* Paper presented at the First International Congress on Vacuum Techniques, Namur, 10—13 June 1958

gauge. For many applications this system is very favourable. The components can be outgassed very efficiently so Q can be made very small. If the amount of gas taken up by the gauge is small, the ultimate pressure p_u will also be low. The speed S, however, is not very large. For the active gases like oxygen which is taken up by the filament the speed can be of the order of 1 l./s. For inactive gases it is only of the order of 10–100 cm^3/s.

If now an experiment has to be made at a very low pressure, with a material which can not be outgassed so well, this pressure can only be reached when the pump speed is made high enough. Another example of an experiment which can hardly be realized with ion gauge pumping, is the production of a pure atmosphere of low pressure, e.g. 10^{-9} mmHg with an impurity level of 1 per cent or lower. Either, one has to stop the pump process after admission of the desired gas and then the impurity level will rise continuously, or one proceeds with pumping and the impurity level may rise due to the liberation of gas which has been pumped before. Also, in the case that helium diffusion through the glass is a disturbing factor, a larger pump speed is wanted. A solution may be found by using an open system with a moderate pump speed. A speed of about 5–10 l./s for air was aimed at and the possibility of using a diffusion pump was investigated. With such a system a pure atmosphere of low pressure can easily be obtained by a continuous-flow method. In addition, an open-pump system which yields a pressure in the 10^{-10} mm Hg range might be a valuable tool for special valve pumping.

Vol. 9 959/60

4. The diffusion pump

There is no problem in obtaining a sufficient high pump speed with a diffusion pump. The major problem is the ultimate pressure p_u. The limiting pressure at the vacuum chamber is determined by (a) the gas production and pump speed in the tube system connecting the pump and the chamber (b) the gas production from the pump itself. Item (a) is governed by the requirement of a small Q and a large S as we have seen. We shall now deal with item (b), the gas coming from the pump itself. In a diffusion pump there are four sources of gas flow through the pump mouth in reversed direction :

(a) The vapour of the pump fluid and the decomposition products of this fluid. The vapour pressure of the oils usually employed is not low enough at room temperature. Cooling would be necessary, but experiment shows that it is not possible to freeze out with liquid nitrogen all decomposition products formed during boiling of the oil. For this reason mercury was chosen as pump fluid.

(b) Back diffusion from the fore-pump side through the vapour. This diffusion can be made small by decreasing the pressure at the outlet of the pump. Therefore, a diffusion pump is used as a backing-pump. Measurements showed that the pressure at the pump mouth is more than a factor 10^6 lower than the pressure at the outlet, the latter being usually below 10^{-6} mm Hg.

(c) Gas production from the walls of the pump in the vicinity of the mouth. The upper part of the mercury pump can be outgassed so as to make this production as small as possible.

(d) Gas dissolved in the cold condensated pump liquid which is transported again to the upper jet. This effect was not further investigated.

For the sake of convenience the whole system was made of hard glass. Fig. 1 shows the pump which was constructed for this purpose. It is a two-stage pump with a pump speed of 60–70 l./s.

FIG. 1. Two-stage glass mercury diffusion pump.

5. The pumping system

The pumping system consists of a metal mercury diffusion pump as a backing-pump, the glass mercury diffusion pump

and two or three cooling traps of special design. Three traps are needed when it is necessary to maintain pressures in the region of 10^{-11}–10^{-12} mm Hg for a period of about 24 h. A photograph of the trap is given in Fig. 2. It has a conductance for air of 25 l./s and a great cooling efficiency. It is necessary to keep the level of the liquid nitrogen constant. Therefore, an automatically working device as described by Feld and Klein[1] is used.

FIG. 2. Cooling trap of special design. The gas coming from one side and the mercury vapour from the other have to pass the space between the two walls at liquid nitrogen temperature.

The system has been built with the idea that the vacuum chamber, where the pump speed has its lowest value, had to be outgassed for the longest time. Fig. 3 shows the complete system. The upper part of the glass diffusion pump (with the nozzles) is situated above the top of a table. Underneath this table is placed the metal diffusion pump, a vacuum reservoir to back this diffusion pump when almost all the gas has been pumped off, a rotary oil pump and the safety device. Above the glass diffusion pump one can see the three cooling traps and an ionization gauge. This gauge is of the Bayard and Alpert type. It has an ion-collector of 25 μ tungsten wire. At 150 V anode voltage the X-ray current corresponds to 5×10^{-11} mm Hg. An estimation of the pressure is possible to 10^{-12} mm Hg.

A cylindrical oven can be placed over the glass system, so that it rests on the table. Outgassing of the system is done at 450°C and usually overnight. The metal diffusion pump is in action during this operation. The next step is to lift the oven so far that the glass pump can be used. The rest of the system stays in the oven at 450°C and is now outgassed much more efficiently. The pump speed is about a factor of 50 greater and the pressure is lower. After a few hours the oven is again lifted and the first trap is put into action. Then with intervals of some hours the other traps are cooled.

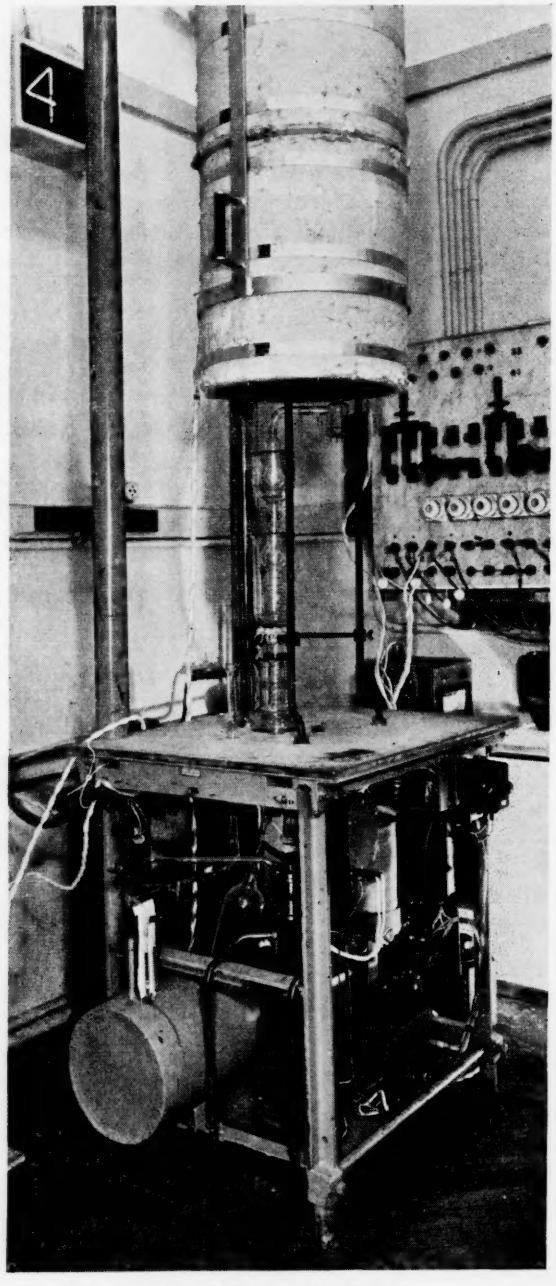

FIG. 3. The pumping system.

Vo
9
1959

While the chamber and the gauge are still hot the components are thoroughly outgassed by electron bombardment or radio-frequency heating. Finally, they are also allowed to cool down. Using only the ion gauge as the vacuum chamber a pressure is now obtained which can no longer be measured by the gauge. This means that it was below 10^{-12} mm Hg.

In those cases where mercury must be excluded from the chamber the glass pump and the first trap cannot be heated. Only the other traps, the chamber and the gauge are treated as mentioned before.

It goes without saying that this vertical arrangement is only an example of a variety of possibilities. Other designs according to the same idea could be made with more ovens.

The quite high pump speed for all gases at the chamber (about 5–10 l./s) is obtained with a rather large glass area. It is not immediately evident that a real gain in pressure is achieved as compared with ion gauge pumping. where a smaller pump speed is combined with a small glass area. A calculation shows, however, that the system with the diffusion pump can produce pressures which are more than a factor 400 lower than those with an ion gauge. It is assumed in this case that it is the gas production from the walls which determines the ultimate pressure.

Reference

[1] M. Feld and F. S. Klein : *J. Sci. Instrum.* **31**, 474 (1954).

Vol.
9
959/60

Design Approaches for Electron Devices Operating in Critical Environments, Especially Ceramic-envelope Tubes for High-temperature Operation*

W. H. KOHL†

Electronics Research Laboratory, Stanford University, Stanford, California (U.S.A.)
Presented by J. V. Lebacqz, Microwave Laboratory, Stanford University

On the basis of several surveys conducted for the Armed Services and in the light of current trends in the industry, a review is presented of developments aiming toward reliable components for operation in critical environments where temperatures of the order of 500 °C, high shock and vibration levels, and nuclear flux densities are encountered. The construction of high-vacuum tubes for such service presents unique problems of which many have been overcome in recent years. The different design approaches will be briefly described and illustrated, and still existing limitations pointed out.

Introduction

The increasingly rapid advances of our technology in the military and civilian domains have imposed new concepts of reliability on the design of electronic devices in order to make them survive in critical environments where high temperature, severe shock and vibration, as well as nuclear radiation are encountered. Components of electronic systems comprise a variety of elements such as resistors, connectors, capacitors, transformers, inductors, semi-conductor diodes, transistors, ferrite cores, and vacuum tubes. Bearing in mind the main topic of this Congress, it is the last item of this list of components, i.e. vacuum tubes, which will be the principal subject in the following discussion ; some remarks, however, will apply to components in general.

Even for ordinary, non-critical applications, vacuum tubes have been shown to be the least reliable component in spite of the great improvements that have been made in recent years in the reliability of glass envelope tubes.[1, 2] The various causes of failure have been analyzed and are under continuous survey by government and industry in many countries. Very impressive results can be achieved if a consistent effort is made to avoid these causes of failure by careful design and processing of the tubes. An equally careful analysis of the circuit and all its other components, as well as their environmental conditions in service is necessary.

The several submarine telephone cable systems installed recently by the American Telephone and Telegraph Company employ several hundred tubes in their repeaters, and the failure of any one tube would put a particular cable out of commission for several weeks during which time the cable would have to be lifted from the ocean floor for replacement of the faulty repeater. No such need has arisen to date, and over ten million tube hours of service have been accumulated. On the basis of most exhaustive tests over a period of many years, the life expectancy of the tubes is estimated to be 20 years.[3]

The design philosophy applied to the development of reliable computers at the Lincoln Laboratory of the Massachusetts Institute of Technology also demonstrates the high degree of reliability that can be realized for complex systems comprising as many as 20,000 circuits and containing many vacuum tubes. Operating lifetime of over 100,000 hr has been achieved for a typical circuit, including its tube.[1]

In both these examples, success depended on the most painstaking analysis of the effect of any one variable on the performance of the component in question and its effect on the system as a whole. The details of this method of " marginal checking " have been described in the literature ;[1] suffice it to say that derating of commercial operating parameters was found necessary in order to gain the wider tolerances required for safe, long-term operation. Bulb temperatures for tubes were held to the range of 80 to 100 °C, cathode loading to not more than 60 mA/cm² for d.c. operation and about ten times this value for short-pulse operation ($<10\ \mu$s) and low-duty cycles (<10 per cent). Submarine cable tubes have a cathode loading of about 1 mA/cm² at an operating cathode temperature of 670 °C (true temp.).[3]

On the basis of this experience it can be stated that highly reliable tubes of conventional design can be made for operation in controlled, static environments where no unusual conditions prevail. The effort required to achieve this end is very great and the cost accordingly high.

High-temperature tubes

It has been recognized for a long time that one of the causes for the gradual deterioration of vacuum tubes is the

* Paper presented at the First International Congress on Vacuum Techniques, Namur, 10–13 June 1958.

† Present address : Senior Engineering Specialist, Microwave Components Laboratory, Sylvania Electric Products Division, Inc., Mountain View, California.

release of gas from the internal structural components and the envelope during operation of the tube in its circuit. A thorough outgassing procedure on the pump, and preferably a separate outgassing of the components before they are assembled, is thus required. The conventional soft-glass envelope imposes a limit to the temperature at which bake-out can be safely carried out. This upper bake-out temperature can be raised from 350 to 450°C when conventional hard glasses are used. A further increase to the 700°C level is possible by using aluminosilicate glasses which can be sealed to molybdenum.[4, 5, 6] Each of these steps, replacing soft glass by harder and harder glasses, makes the mass production of such tubes more difficult and requires the development of new process techniques and at least modified equipment for the handling of these tubes in quantity production. To prevent corrosion of the metal at high bake-out temperature, a first recourse would be to provide a non-oxidizing atmosphere within the oven, but permeation of gases from such atmospheres through the tube envelope, particularly the metals, makes the use of a protective vacuum necessary. For this reason, the use of this design approach has been restricted to special tubes made on a laboratory scale. Seals as large as 5 cm in diameter were made at Stanford, using glass type C-37 (B.T.H.) and molybdenum. All-silica transmitting tubes (Type TN-77) were made in England for the British Admiralty as early as World War I and could be operated in service well above 500°C.

The trend indicated by these developments points in two directions which, after some detours, finally merge into one avenue of approach to the goal of reliable, high-temperature tubes. Rigorous processing on the pump dictated the introduction of high-temperature-resistant materials for the tube structure and its envelope and resulted in a greatly improved quality of the tube under ordinary operating conditions. Service at higher temperatures was a natural outcome of this development, but resistance to shock and vibration and elimination of the many causes for catastrophic failure and slow deterioration of the tube required a more drastic revision of conventional structures. The stacked ceramic tube promises to fulfil all these requirements.

Ceramic tube structures

Ceramic-envelope receiving-type tubes were first produced on a fairly large scale by Telefunken, A.G., in Germany during World War II. The experience gained in this program became available to other countries after the cessation of hostilities and served as a basis for evaluation and further development, particularly in the United States. Beginning in 1952, the Armed Services sponsored long-range programs in several industrial establishments with the original objective to obtain a complement of receiving-type tubes that were characterized by high reliability and could be produced by automatic machinery. Reliability in normal environments was later extended to critical environments of high temperature (500°C), severe shock and vibration as well as nuclear radiation. The status of these programs has recently been described in published reports and symposia.[7, 8] For the purpose of orientation, Figs. 1–4 portray some typical structures which are representative of two design approaches, Types A and B, that have been successfully developed and are in the pilot plant production stage.

Type A (Fig. 1) consists of a number of high-alumina ceramic rings of accurate dimensions which are separated from each other by thin metallic members, the electrodes of the internal tube structure, and brazed together in a hydrogen atmosphere furnace. At the right of the figure is an end view showing the anode of this double-ended triode,

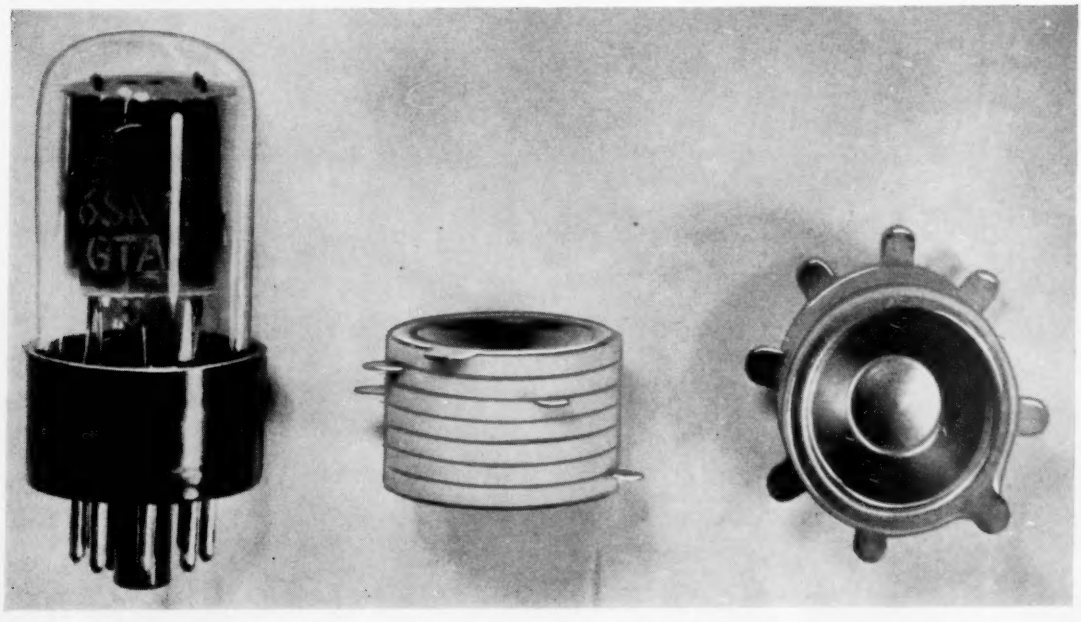

FIG. 1.

Vol. 9 959/60

Type 6SN7, of which the glass prototype is shown on the left. The metallic lugs protruding from the cylindrical structure can readily be seen ; permanent electrical connections are made to these lugs. Fig. 2 shows a cross-section of this tube. It is evident that the active elements extend through the wall and that their alignment and spacing from each other depend on the dimensions of the ceramic rings and the thickness of the metalizing coating on their surfaces.

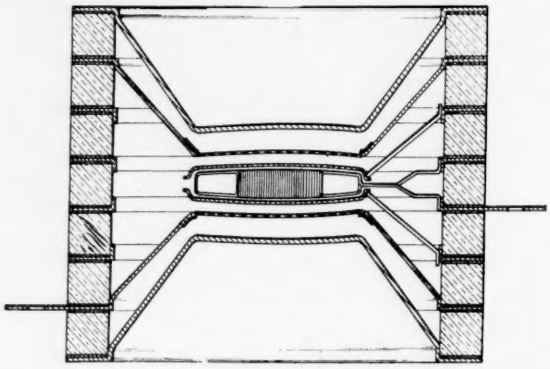

FIG. 2.

Figure 3 illustrates structure Type B where a separate ceramic envelope is brazed onto a ceramic header on which the structure is mounted as shown in Fig. 4. Again, the same prototype, Type 6SN7, is shown, but the stacking of the active elements and ceramic spacers results in a separate mount that is readily inspected for possible faults before the envelope is brazed to the header. A more conventional arrangement of the electrical connections results ; base pins permit use of standard sockets at low temperature where corrosion is less of a problem ; flying leads can be attached to the pins and soldered to printed-circuit boards.

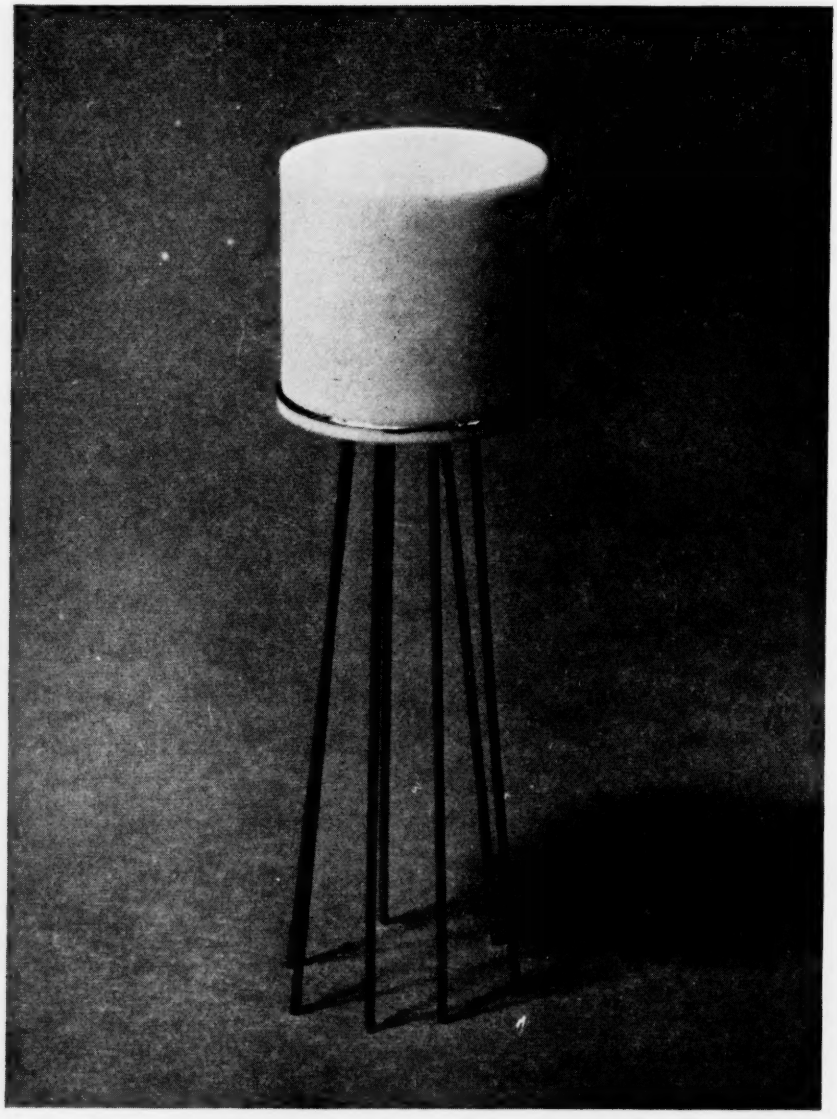

FIG. 3.

Vo
9
1959

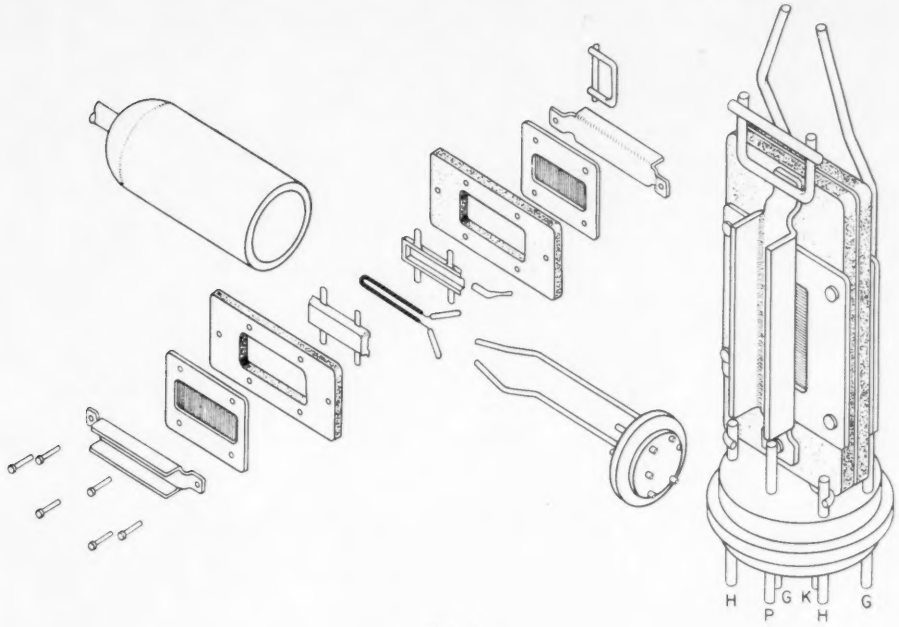

FIG. 4.

Vol. 9 959/60

In many of the stacked-mount structures, evacuation takes place in a bell jar before the final braze is made *in vacuo* ; when a separate ceramic envelope is used, as in Type B, a copper tubulation can be brazed into the dome and pinched off after conventional machine exhaust. The physical size of the tube will in large measure determine the most practical approach to the exhaust problem. Some of these ceramic tubes are smaller than the eraser of a lead pencil ; in such cases, the use of a tubulation would obviously be impractical. It should be mentioned, in passing, that very large ceramic tubes, where the diameter of the ceramic cylinders reaches 25–30 cm, have been in commercial production for a number of years.

Problems and limitations

It might appear that the rate of progress toward the realization of ceramic-type receiving tubes has been slow when the very substantial sums of money are considered which have been invested in this program during the past 16 years by government and industry. However, the problems which had to be overcome were manifold indeed. Not the least of these was the *procurement of high-quality, electronic-grade ceramics*, generally of the high-alumina type, although forsterite bodies are also being used in some cases. To overcome this difficulty, several tube manufacturers in U.S.A. established their own ceramic production facilities, where the processes could be sufficiently closely controlled to guarantee the required quality and uniformity of the product. This supply problem has now been solved, and the need for ceramic production by tube makers has essentially disappeared. In close co-operation with the electronic industry, ceramic producers have learned how to apply their experience in this field to the very exacting demands of the tube industry. Unified standards of test are now being worked out, and research continues in the remaining problem areas of which there are quite a few. The trend is toward the use of alumina ceramics of higher and higher purity, approaching 100 per cent, and several of these bodies are now commercially available. The avoidance and, if present, the discovery of locked-in strains in such ceramics remains a major problem ; the control of shrinkage in dimension on firing, or the production of bodies with zero shrinkage, is another. The desorption of gases at elevated temperature, and the permeation of gases from the atmosphere are under investigation.

Joining ceramics to metals is a technique which is of paramount importance to the successful construction of ceramic tubes. The procedures originally developed for this purpose by Siemens and Telefunken during World War II still apply in principle, but have been extended and supplemented by other processes in recent years.[7] Here again, success depends on the meticulous attention given to many details. A particular metalizing technique successfully applied to one type of ceramic body may have to be modified to suit another. The most commonly used procedures require one or more high-temperature firing cycles in the 1000–1400 °C range to effect a tight bond between ceramic and metal. In the sintered-metal process, a layer of finely divided refractory metals, principally molybdenum and manganese, is first fired onto the ceramic surface in a hydrogen atmosphere, and a film of nickel or copper subsequently applied by electroplating, or oxide reduction, and also sintered in hydrogen to the base, at about 1000 °C. A conventional braze with any suitable filler metal finally produces the seal between the mating surfaces of metalized ceramic and metal or alloy. The so-called active alloy technique achieves this end in one firing operation near 1000 °C in pure hydrogen, rare gas, or vacuum by the simultaneous application of active metal or alloy, i.e. Ti, Zr and

Ni, with the brazing alloy. One or the other technique is favored by different manufacturers, and many modifications or combinations of both exist.

Diffusion seals at relatively low temperature have been made between copper-plated steel and large ceramic cylinders by subjecting the abutting members to high pressure.[7] A similar approach is under development by another manufacturer who achieves a bond in this manner between the metal body and the ceramic bearing a sintered-metal coating. At the Stanford Electronics Laboratory, we have recently produced successful seals for high-temperature service by electroplating copper around gold-plated metalized ceramics that were separated by copper disks which were part of the active circuit. Any number of such ceramic cylinders separated by disks can be stacked up on a mandrel and electroformed while some mechanical pressure is applied to the assembly. The excess copper which accumulates near the joints is then machined off. Fig. 5 shows such an assembly made in a conventional manner by induction sealing. The successive heat shocks imposed on preceding seals made it very difficult to get twenty tight seals, while the new approach by electroforming gives good results.[9] Repeated heat shocks at 700°C given the finished stacked mount caused no leaks detectable with a helium leak detector.

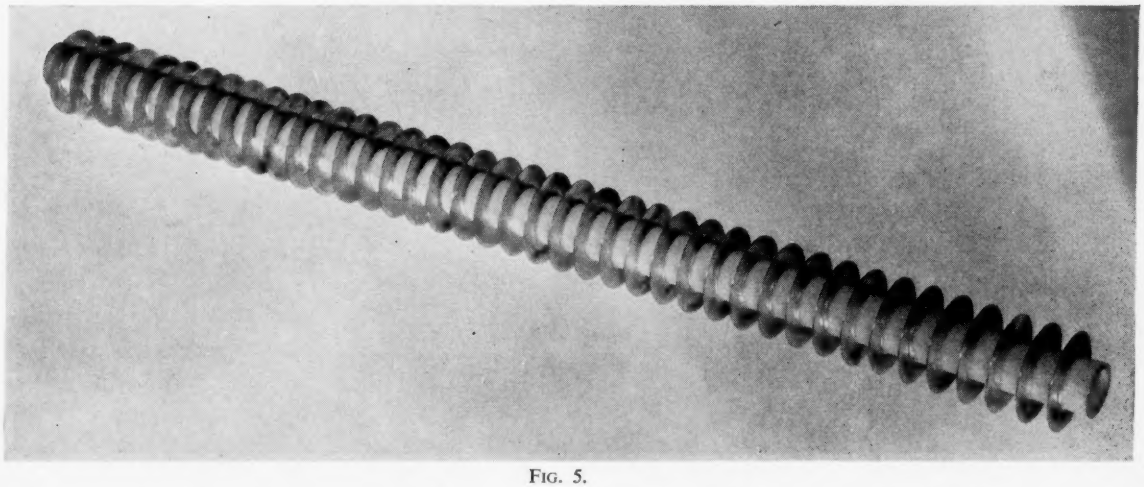

FIG. 5.

The lossy nature of the metalizing compounds should be borne in mind when seal areas are exposed to radio-frequency fields. It has recently been demonstrated that effective radio-frequency attenuators can be obtained by coating ceramic rods with some of the metalizing compounds and sintering them onto these rods in the usual way.

A problem which is particularly related to high-vacuum technology is the failure of conventional barium getters in high-temperature operation.[7] The cerium-thorium (Ceto) getters seem to be the only available substitute and they have been used with considerable success on some of the ceramic tube programs. Suppression of primary and secondary emission at elevated temperature also is a limiting factor which deserves further study.[7] Conventional gold coatings on grid wires cease to be effective at about 350°C and furthermore suffer from the disadvantage of becoming saturated with barium or its compounds after prolonged operation. Chrome vanadate coatings are presently under investigation at Stanford.

Conclusion

While it was possible to touch on only a few highlights in this short review, it is the hope of the author that the art of making reliable components will be advanced by having a wider circle made aware of the problems encountered. By far the larger part of this work has been sponsored by the Armed Services,[8] and the U.S. Air Force[7] in particular. By having been involved in two major surveys under such sponsorship, the author had the opportunity of gaining first-hand information and he wishes to acknowledge these opportunities.

References

[1] N. H. Taylor ; Designing for reliability, *Proc. Inst. Radio Engrs.* **45**, 811–822 (1957).

[2] G. W. A. Dummer ; Component reliability research in the United Kingdom, *Proc. 1958 Electronic Components Conf.*, Los Angeles, April 22–24, pp. 138–147. Engineering Publishers, New York (1958).

[3] J. O. McNally, G. H. Metson, E. A. Veazie and M. F. Holmes ; Electron tubes for the transatlantic cable system, *Bell Syst. Tech. J.* **36**, 163–188 (1957).

[4] R. L. Bell and M. Hillier ; High melting point aluminosilicate glasses in microwave valves, *Services Electronic Res. Lab. Tech. J.* **4**, 1–9 (1954).

[5] R. L. Bell and M. Hillier ; An 8 mm Klystron power oscillator, *Proc. Inst. Radio Engrs.* **44**, 1155–1159 (1956).

[6] M. Hillier and R. L. Bell ; Aluminosilicates and the high-temperature processing of microwave vacuum tubes, *Brit. J. Appl. Phys.* **9**, 94–97 (1958).

[7] W. H. Kohl and P. J. Rice, Jr. ; Electron tubes for critical environments, Final Report by Stanford Research Institute, Menlo Park, California to United States Air Force, Wright Air Development Center (Contract AF 33(616)–3460) ; *WADC Tech. Rep.* 57–434 (1957). U.S. Department of Commerce, Office of Technical Services, Washington 25, D.C. PB 131852. Astia No. AD 151158.

[8] J. O. McNally ; Status Report on the ceramic receiving tube development, *Proc. 1958 Electronic Components Conf.*, Los Angeles, April 22–24. Engineering Publishers, New York (1958).

[9] M. D. Hare, R. F. Keller and H. A. Meneses; Electroformed ceramic-to-metal seal for vacuum tubes, *Tech. Rept.* No. 453–3 (Nov. 17, 1958), Electron Devices Lab., Stanford Electronics Laboratories, Stanford University, Stanford, California.

Vacuum System for a Thirty Billion Electron Volt Particle Accelerator*†

C. L. GOULD

Brookhaven National Laboratory, N.Y., U.S.A.

A vacuum system is being developed for a Thirty Billion Electron Volt Particle Accelerator. The vacuum chamber is a torus one-half mile in circumference with a cross-section of 3 in. *by* 7 in. *Approximately fifty getter-ion type pumps will be used on the ring to give the required pressure of* 2×10^{-6} mm Hg.

A linear accelerator yielding fifty million electron volts protons will be used as the injector. The vacuum chamber of this accelerator is 110 ft *long and* 3 ft *in diameter. It will be evacuated to* 1×10^{-6} mm Hg *by eleven getter-ion pumps.*

The choice of getter-ion pumps has permitted a departure from conventional vacuum system design and operation. Details of some new concepts of initial evacuation, steady state operation, and simplicity of control of a system of this nature will be given.

Vol. 9 959/60

BROOKHAVEN National Laboratory is midway in the construction stage of the world's largest atom smasher. The entire building complex for this Alternating Gradient Synchrotron is now complete and earth shielding has been placed on the tunnel ring which houses the magnets and vacuum chamber. Fig. 1 is an aerial photograph taken a few months ago showing the linear accelerator injector, the ring, the target building and the research laboratories and offices. This strong-focusing synchrotron will accelerate protons to the energy range of 25–30 BeV. The application of the strong focusing principle permits the use of a small aperture in the vacuum chamber ; in marked contrast to the Cosmotron at Brookhaven, the Bevatron at Berkeley and the Synchrophasotron in the U.S.S.R.

FIG. 1.

* Paper presented at the First International Congress on Vacuum Techniques, Namur, 10–13 June 1958.

† Work done under the auspices of the U.S. Atomic Energy Commission.

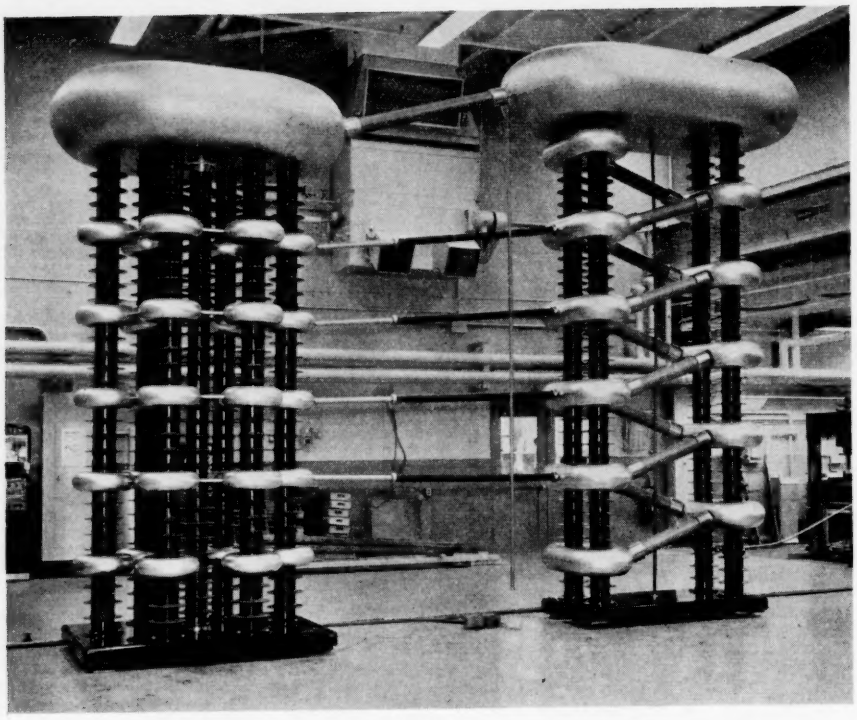

FIG. 2.

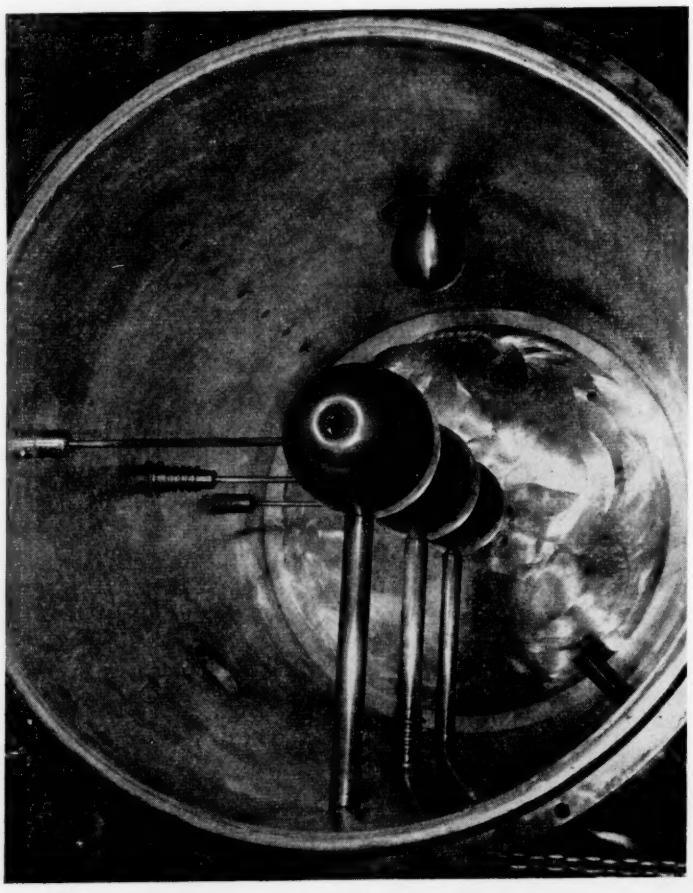

FIG. 3.

Before discussing the ring vacuum chamber, however, it would be best to start where the protons originate and trace the several distinct vacuum systems which must be coordinated in this machine.

Fig 2 shows the Cockcroft–Walton generator designed and fabricated by Philips of Eindhoven. This emits 750,000 eV protons from its accelerating tube. The vacuum system for the accelerating tube consists of two titanium evapor-ion pumps mounted in parallel, only one of which is used at one time. The ion source gas load for these pumps is hydrogen at a rate of 600 l./s at 1×10^{-5} Torr. One pump is kept on ion pump standby, that is, no wire being evaporated, and it will be put in full operation when the titanium wire is exhausted in its mate. Valves separate these pumps from each other to permit removal for maintenance. One oddity in the physical arrangement of these pumps is dictated by lack of space. They are mounted one above the other and one pump has its high vacuum entry on top as usual. The other, stacked above it, pumps through its lower opening.

From the Cockcroft–Walton the protons are injected into a linear accelerator, there to be raised to an energy of 50 MeV. Unlike other linacs, the vacuum enclosure and the r.f. cavity are combined in a single copper plated steel cylindrical tank. This tank is separated into eleven flanged sections each about 10 ft long and 3 ft diameter. The volume of the linac is therefore about 800 ft^3 and the required pressure is 2×10^{-6} Torr.

Fig. 3 shows a scale model for r.f. power experiments using model accelerating drift tubes. It is 4 ft long and 3 ft diameter. This model has been in operation for over a year with an rf power input of 200 kW at 200 Mc/s. An evapor-ion pump has been in constant use on this model and except for the initial outgassing period when the power was first applied, it has kept the pressure below 2×10^{-6} Torr, often using no titanium at all, only the ion pump.

While the conductance of the linac tank is practically infinite, it is not the vacuum engineer's dream that it appears as far as designing a pumping system is concerned. The X-ray level of a linear accelerator is extremely dependent upon the oil migration from the vacuum pumps. For this reason mercury diffusion pumps are most often recommended for use on linacs. However, the evapor-ion pumps do not even need a baffle to produce a clean vacuum and so it has been decided to use them on the linac.

Fig. 4 is a schematic of the linac vacuum system. It should be noted that the only mechanical pumps used are the roughing pumps. These consist of two sets of Roots type booster pumps backed by standard piston type oil sealed pumps. There is no reason to utilize a foreline manifold since the evapor-ion pumps require no backing and certainly the tank itself serves as an excellent roughing manifold. To take full advantage of the fact that an evapor-ion pump need not be isolated from the tank in event of catastrophe, no automatic valves are used except in the roughing lines.

The start-up procedure for the linac is as follows. All valves are open except the foreline valves on the evapor-ion pumps. The mechanical pumps are then started. In 30 min the pressure in the tank and evapor-ion pumps should be 1×10^{-4} Torr. At that time, depending upon the previous condition of the electrodes in the evapor-ion pumps, the titanium wire can be evaporated and the roughing valves closed and rough pumps turned off. If the evapor-ion pump has been opened for a long while and is gassy, it may be necessary to fire a primer charge for a minute or so before starting the main titanium wire feed. However, in 1 h from atmospheric start-up the tank pressure should be 1×10^{-5} Torr and in 2 h should be 5×10^{-6} Torr at which time r.f. power can be introduced. Twenty evapor-ion pumps have been shown on this schematic. All may be necessary during the first six months of operation to handle the large outgassing caused by r.f. bombardment. It is contemplated that ten of these will be removed at a future date.

When a pump needs maintenance such as replacing a spool of titanium wire, its manual isolation valve is closed and it is removed from the system. Then a replacement is installed and roughed out with a portable, small, piston pump and Roots pump combination. As soon as the titanium is evaporating, these rough pumps are removed and the isolation valve opened.

After ejection from the linac, the protons are directed through a 3 in. diameter tube 130 ft long leading to the ring accelerator vacuum chamber. This injection tube is maintained under vacuum by two titanium pumps along its length. The ring vacuum chamber is intersected by this injection tube tangentially at the injection section and the protons are then started on a 160,000 mile trip around the ring vacuum chamber.

Fig. 5 shows one typical ring vacuum chamber section. There are 240 similar sections, each located with precision

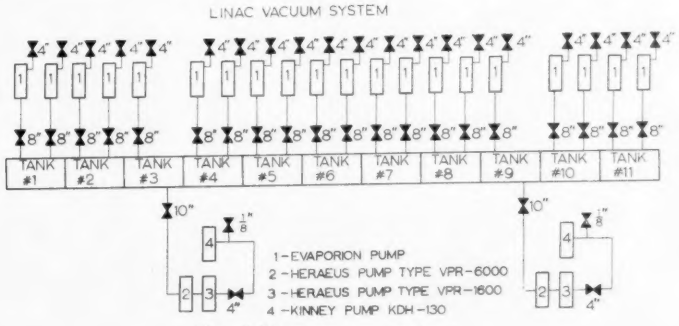

FIG. 4 Linac vacuum system.

Vol. 9 959/60

in a magnet as shown in Fig. 6. Each chamber is approximately 10 ft long and the cross-section is 7 in. by $3\frac{1}{4}$ in. These sections are fabricated of Inconel "X", a high nickel alloy with an electrical resistivity of 120 $\mu\Omega$cm. This is an advantage over the stainless steels at 70 $\mu\Omega$cm, since these chambers are in a changing magnetic field and the eddy currents cause field perturbations inside the chambers. The sections are formed in two halves and welded longitudinally at top and bottom. The wall thickness is 0.078 in. with a tolerance of 0.0025 in.

The 240 chamber sections are joined to each other by short expansion joints which permit some assembly flexibility (Fig. 7). However, these expansion joints must provide lateral motion as well as axial motion and thermal expansion.

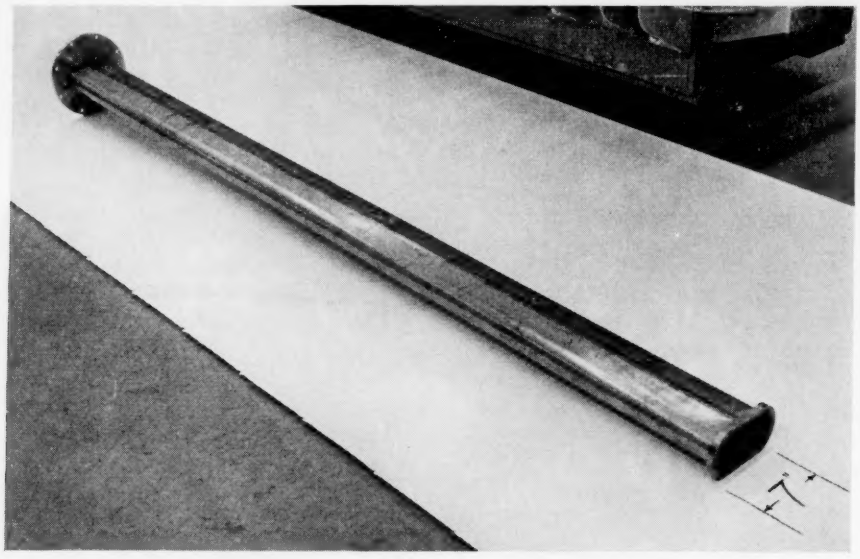

FIG. 5.

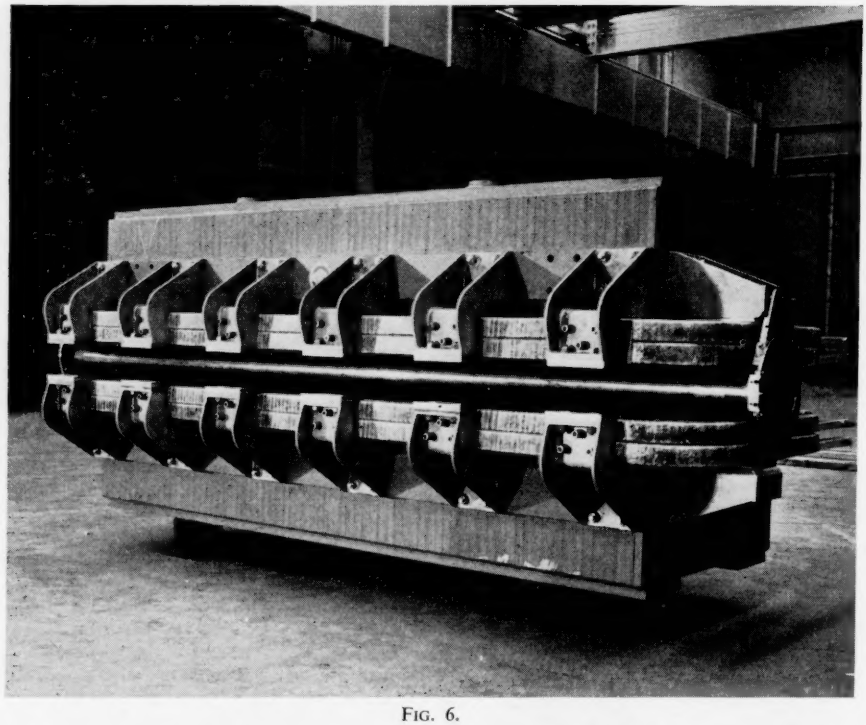

FIG. 6.

It is contemplated that several magnets may be moved to permit orbit corrections. This movement will be in the range of ± 0.040 in. and the bellows must allow this motion with no strain being placed on the vacuum chambers.

In addition to the bellows, there are twenty-four vacuum chamber straight sections 10 ft long available for r.f.

Vo
9
1959

acceleration and target chambers. Also, there are seventy-two straight sections 5 ft long available for quadrupole and sextupole correcting magnets. Summing up, the ring

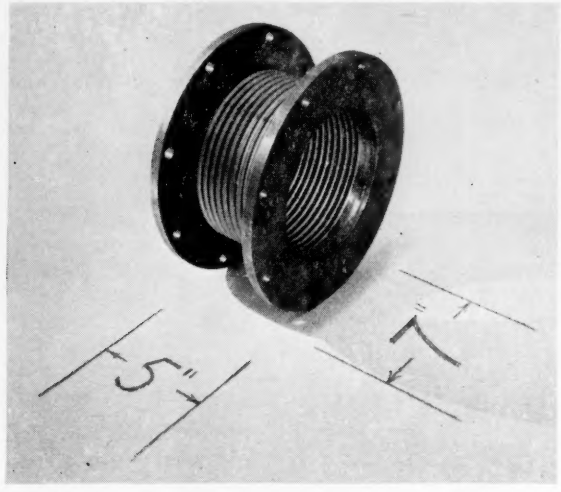

FIG. 7.

chamber is a large torus made up of 480 separate flanged sections. Its circumference is over 2600 ft with a conductance equivalent to a 5 in. diameter tube. The required pressure throughout the ring is 2×10^{-6} Torr.

In a previous paper on this subject it was shown that the vacuum system for a chamber of this geometry should be a compromise between outgassing, conductance and the number and location of pumps. The calculated optimum separation is 55 ft between pumps for a total of 48 pumps. Experimental data confirm this value. Fig. 8 is a schematic of one-fourth of the ring vacuum system. It will be noted that there are four pump systems in a group with a sectionalizing valve between each group. Within these groups only one evapor-ion pump has a mechanical pump combination associated with it. There are, therefore, twelve pumps with roughing systems and thirty-six without. The evacuation procedure using this arrangement is somewhat unconventional.

First, the twelve evapor-ion pumps with roughing systems are roughed out with their high vacuum valves closed. As soon as their wire feed can be started, the foreline valves are closed and the mechanical pumps are switched to roughing out the ring and the rest of the evapor-ion pumps using the ring as a manifold. When the pressure in the ring is 10^{-2} Torr, the high vacuum valves of the twelve operating titanium pumps can be opened and the mechanical pumps turned off. Shortly thereafter the thirty-six titanium pumps will be at a pressure where their titanium feed can be started and all pumps will now be evacuating the ring. This entire procedure will take one and a half hours from atmosphere to 5×10^{-6} Torr.

Fig. 9 shows an early model of a typical pump station. The evapor-ion pump pictured here has operated continuously for nine months with no shutdown for any reason. It should be noted that there is no baffle, no foreline, no mechanical pump, no automatic valve. The foreline gate valve is similar to the type, that, in 6 in. size will be used to sectionalize the ring and also serve as a high vacuum valve for these pumps. They are cast aluminium and are only 4 in. in the axial dimension.

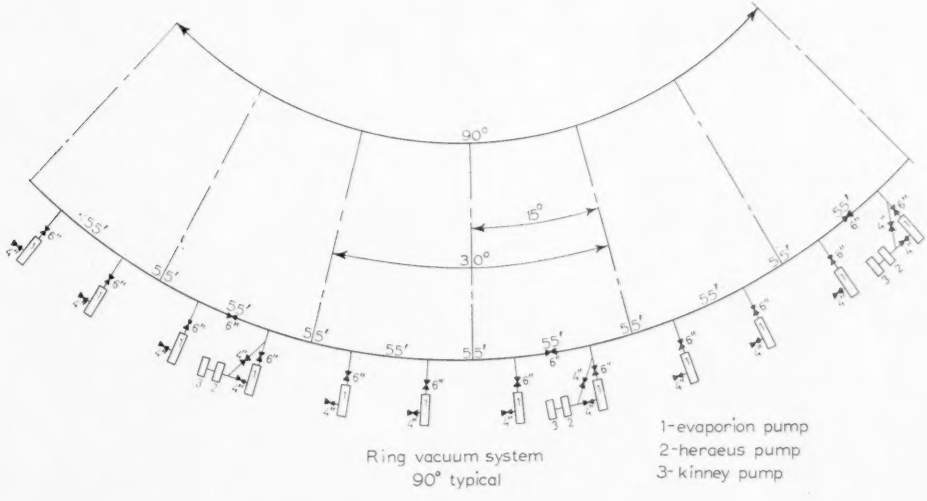

FIG. 8 Ring vacuum system 90° typical.

The gaskets throughout the entire accelerator will be a fluorocarbon elastomer which has been available for the last year. This gasket material has all the mechanical properties of rubber but retains the vapor pressure of the fluorocarbons, about 10^{-8} Torr. The compression set is 5 per cent at 20°C.

Vol. 9 959/60

The hardness is about 40 durometer. Pressure measurements on this machine will be done with conventional ionization gages and thermocouple gages.

Summing up, it is seen that two completely dissimilar vacuum chambers must be designed and systems developed to evacuate them. One is a large volume, high conductance cylindrical tank. The other is a very long, low conductance circular torus. The titanium getter-ion pump lends itself well to the pumping of both these chambers with the minimum complexity of associated equipment.

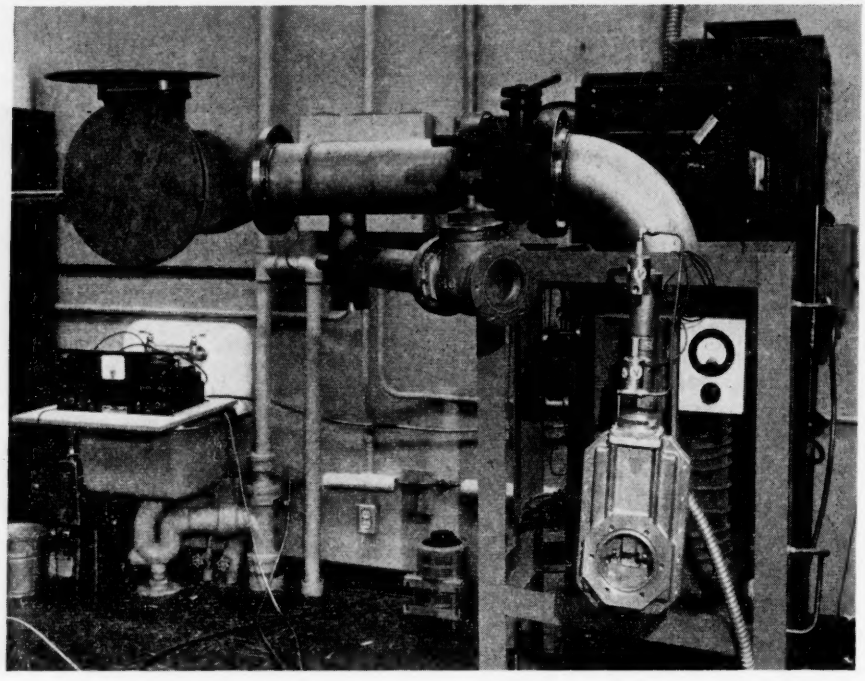

FIG. 9.

Book Review

A. VAŠÍČEK : **Optics of Thin Films.** Czechoslovak Academy of Sciences, Prague, 1956. 354 pp. (in Czech).

THIS monograph is the first part of a two-volume work on optics of thin layers. The present volume is mainly theoretical, whilst the second (which was published in Prague in 1957) is concerned with measurements and production.

The monograph is divided into the following sections : (1) Introduction, (2) Reflection and refraction on the interface of two or more dialectrics, (3) Reflection and refraction on a single layer, (4) Reflection and refraction on two or more layers, (5) Thin dielectric layers on a metal. Thin metallic layers, (6) Influence of thin layers on polarization of light by total reflection, (7) Conclusion. The monograph also contains a list of symbols and a list of references.

The introductory section summarizes the main properties of light and is followed by a brief discussion of Maxwell's equations for isotropic dielectric media. This part also includes a thorough discussion of polarization of plane waves (in parts following closely the presentation of BORN's *Optik*) and of Fresnel's formulae for refraction and reflection. Later sections are concerned mainly with the applications of the general theory to the basic problem arising in the optics of thin films, namely to find expressions for the reflection and refraction coefficients of a system of layers. Some of the treatment is based on the original investigations carried out by the author over a period of almost 20 years, but accounts of methods developed by other authors are also presented.

The monograph may be regarded as a small handbook for workers concerned with the optics of thin films. The treatment is thorough and systematic and most cases of practical interest are discussed. The printing is excellent. All the formulae are well displayed and the results are illustrated by many well-drawn diagrams. Although today several more extensive treatments of the subject are available (e.g. H. MAYER'S *Physik Dünner Schichten*), this little volume serves a useful purpose by presenting the most important formulae in a compact manner. It is to be hoped that Prof. Vašíček's book will be translated into some of the languages with which scientists outside Czechoslovakia are more familiar.

E. WOLF.

Vol.
9
959/60

Notice

Symposium on
" Current Developments in the Production of High Vacua "

THE Institute of Physics announces that it is arranging a one-day symposium entitled " Current developments in the production of high vacua " to take place in London on 17 April 1959.

There will be three sessions :

(a) Chemical and ionic pumping in kinetic vacuum systems.

(b) Problems in the production of high vacua in large equipment.

(c) Analysis of residual gases in kinetic vacuum systems.

The symposium is intended mainly for persons working with high vacua. Abstracts (but not preprints) will be circulated before the symposium, the proceedings of which will not be published in full.

All communications regarding the symposium should be sent to the Secretary, The Institute of Physics, 47 Belgrave Square, London, S.W.1.

Abstracts of Communications Presented at the First International Congress on Vacuum Techniques

(Namur 10–13 June 1958)

* Articles marked thus will appear in full elsewhere in the journal.

* A.1. **Les Bases Expérimentales de la Théorie Cinétique des Gaz :** L. DUNOYER. Paris, France.

* A.2. **The History of the Vacuum Pump :** E. N. DA C. ANDRADE. Imperial College of Science and Technology, London, United Kingdom.

* A.3. **Die Diffusionspumpe ihre Physik und Technik :** R. JAECKEL. Universität Bonn, Deutschland.

* A.4. **Recent Advances in Ultrahigh Vacuum Technology :** D. ALPERT. University of Illinois, U.S.A.

A.5. **l'Apport de la Technique du Vide à la Science et à l'Industrie:** ROBERT CHAMPEIX. Laboratoires d'Electronique et de Physique Appliquées, Paris, France.

La contribution que la Technique du Vide a apporté aux autres domaines scientifiques, peut se classer en trois catégories :

1. Sur le plan théorique, la nécessité qu'elle a créée d'approfondir la théorie cinétique des gaz, a puissamment aidé à ouvrir la voie à la physique corpusculaire et a constitué tout naturellement une entrée en matière aux théories statistiques modernes, qui sont à la base de l'Electronique et de l'Atomistique.

2. Sur le plan technique, et en ne rappelant que brièvement les divers usages des effets mécaniques de la pression (correspondance pneumatique, béton sous vide, etc.) elle a permis la réalisation des tubes électroniques qui sont les éléments essentiels des télécommunications, de l'automatisme et es appareils de mesure et de contrôle modernes.

Elle a aussi puissamment contribué au développement des sciences nucléaires, grâce aux accélérateurs de particules. Il n'est pas jusqu'à la Chimie et l'Industrie pétrolière, qui n'utilisent intensivement la distillation moléculaire. Quant à l'evaporation sous vide, on sait l'usage qu'en fait l'optique.

3. Mais il est un aspect non moins important des services rendus à la science expérimentale par la technique du vide : elle a été une école infiniment précieuse dans la recherche du " phénomène pur ", c'est-à-dire débarrassé de toutes réactions parasites. Que l'on songe aux soins méticuleux qu'exige la fabrication des tubes électroniques et les dépôts de couches minces par évaporation.

---

* B.1. **Evapor-Ion Pump Development at the University of Wisconsin :** R. G. HERB. University of Wisconsin, Madison, U.S.A.

B.2. **Neuere Untersuchungen zu Problemen der Vakuumphysik und der Vakuum-Messtechnik :** H. KLUMB. Johannes Gutenberg Universität, Mainz, Deutschland.

B.3. **Education in Vacuum Technology :** J. YARWOOD. The Polytechnic, London, United Kingdom.

In view of the importance of vacuum technology in experimental science, it is considered that more attention should be devoted to its study in schools, universities and colleges of technology.

Four types of course are considered : (a) for pupils studying physics in the sixth-form of a grammar school (i.e. students of 16 to 18 years) ; (b) for university students in physics and engineering ; (c) for technicians or laboratory assistants ; (d) specialist courses, primarily for graduates.

In general, courses (a), (b) and (c) should preferably be undertaken as part of a training in physics because to obtain a good appreciation of vacuum technology demands the concurrent study of such topics as the kinetic theory of gases, heat conduction, electric circuitry, properties of materials, ion physics, etc. Under (d) courses in vacuum technology for such specialities as electronic, nuclear and chemical engineering and metallurgy are more and more required.

The content and approach to lectures and laboratory work in such courses is considered.

Two slides will be used in the lecture, one giving details of a typical course in vacuum technology for a physics student at a college of technology and the other details of the accompanying laboratory course in vacuum practice.

If time is available, it is hoped to show a film (35 mm sound) " Vacuum Practice ", recently made by Mullard Ltd. in conjunction with the Educational Foundation for Visual Aids, with the author as adviser. This film is suitable for assisting the instruction of grammar school pupils in the elementary principles, and also indicates the scope of vacuum technology.

10.1. **International Cooperation on Vacuum Standards and Literature Abstracting :** B. B. DAYTON. Consolidated Electrodynamics Corp., Rochester, N.Y., U.S.A.

The exchange of information on standards for nomenclature, units, symbols, flanges, and measuring techniques which has already occurred between the Standards Committee of the American Vacuum Society and similar standards groups in England, Germany, France and Japan will be reviewed. The areas in which international cooperation might be profitable will be examined and proposals will be made for reaching as much agreement as possible before releasing final standards in the cooperating countries. Problems of abstracting and indexing the periodical literature on vacuum technology will be mentioned in connection with standardization of nomenclature.

10.2. **Zur Frage der Einheiten in der Vakuumtechnik :** K. SCHAEFER. Edwards Hochvakuum GmbH, Frankfurt-am-Main, Deutschland.

Die Entwicklung der Vakuumtechnik während der letzten Jahrzehnte von einer reinen Laboratoriumstechnik, an der nur einige Spezialisten interessiert waren, zu einer bedeutenden industriellen Technik, die heute in vielen Fertigungszweigen eine wichtige Rolle spielt, lässt es ratsam erscheinen, zu einer internationalen Vereinbarung über die Einheiten und Messbereiche der Vakuumtechnik zu kommen. Der I. Internationale Kongress der Vakuumtechnik scheint die geeignete Gelegenheit, um eine solche internationale Vereinbarung anzuregen. Es wird daher vorgeschlagen, die Einheit " Torr " mit ihren Unterteilungen " Millitorr " und " Mikrotorr ", die bereits in die Normvorschläge bzw. Empfehlungen verschiedener nationaler Normenkomitees Eingang gefunden haben, in möglichst breitem Umfang in der Praxis anzuwenden. Es werden die Gründe auseinandergesetzt, die für diesen Vorschlag sprechen und verschiedene neuerdings erhobene Einwände diskutiert. Die Verwendung dieser Einheiten bringt die einfache Möglichkeit zur Definition von Mess-bzw. Arbeitsbereichen in der Vakuumtechnik, die anstelle älterer, weniger eindeutiger Bezeichnungen treten können.

* 10.3. **Sur le Choix des Unités de Pression et de Débit en Techniques du Vide :** E. THOMAS, R. SERVRANCKX et R. LEYNIERS. Institut Interuniversitaire des Sciences Nucléaires, Belgique.

VO
9
1959

10.4a. **Standard for Vacuum Flanges in Japan :** K. HISANO. President, Vacuum Engineering Society of Japan, Associate Director, Electrotechnical Laboratory, Tokyo, Japan.

(a) The types of flanges are classified into two groups, i.e., plain type and grooved type.

(b) The standard shapes and dimensions for twenty-five species are specified, outside diameter of the pipe ranging 15 to 1040 mm.

(c) Applications of two types are determined as follows.

(1) For all pumps, grooved type shall be used.

(2) For all valves, plain type shall be used.

(3) For all pipe connexions, it is customary to use the grooved one on the side facing the normal direction of flow in these pipes.

(d) As the reference of this standard, gaskets are specified in shapes, dimensions, materials, etc.

10.4 b. **Standard for Performance Rating of Mechanical Vacuum Pumps in Japan :** K. HISANO. President, Vacuum Engineering Society of Japan, Associate Director, Electrotechnical Laboratory, Tokyo, Japan.

(a) The pumping speed must comply with the following equation :

$$S_e = Q_m/(P_m - P_0)$$ where, S_e = pumping speed
Q_m = measured throughput
P_m = pressure measured in the test dome
P_0 = ultimate pressure

(b) The volume of the test dome should be more than twice as much as displacement per revolution.

(c) The vacuum gauge used for measurement of the pumping speed must be a McLeod gauge and a U-tube manometer.

(d) The electric power consumption is to be measured for several inlet pressures.

10.4 c. **Standard for Performance Rating of Vapour Pumps in Japan :** K. HISANO. President, Vacuum Engineering Society of Japan, Associate Director, Electrotechnical Laboratory, Tokyo, Japan.

(a) The test dome for measuring the pumping speed is decided by taking Dayton's principle into consideration, and by determining the dimensions in detail, especially, in making the diameter of pump mouth the same as that of the test dome to make it free from entrance effect.

(b) The definition of pumping speed is same as that of the rotary oil pump, viz.

$$S_e = Q_m/(P_m - P_0)$$

(c) The vacuum gauge to be used should be calibrated in compliance with the " standard for vacuum gauge calibration method ", now under deliberation, and have no errors greater than $\pm$ 5 per cent.

(d) The backing pressure when the fine vacuum side pressure is increased by just 10 per cent is defined as the critical backing pressure.

10.5. **" Anwendungsgebiete der Höchstvakuumtechnik " :** K. DIELS. E. Leybold's Nachfolger, Köln, Deutschland.

Durch die Ultra-Hochvakuumtechnik sind eine Reihe von physikalischen Prozessen erleichtert und zum Teil sogar erst möglich geworden. Es wird die Anwendung der Ultra-Hochvakuumtechnik für verschiedene Gebiete, wie z.B. Halbleiter, Molekularstrahlphysik, Dünne Schichten usw. beschrieben.

10.6. **Endpartialdrucke Verschiedener Pumpentypen :** H.-G. NOELLER. E. Leybold's Nachfolger, Köln, Deutschland.

Nachdem in einer Arbeit über Endpartialdruckanalysen mit dem Omegatron bei Öl-Diffusionspumpen berichtet worden war, liegen nunmehr auch Messungen mit Quecksilber-Diffusionspumpen mit Kühlfallen für flüssige Luft bzw. Kohlensäure sowie über Rootspumpen und ölüberlagerten Rotationspumpen vor.

10.7. **Vacuum Process Evaluation :** D. J. SANTELER. General Electric Co., Schenectady, N.Y., U.S.A.

Vacuum Process Evaluation is a new technique to (1) Determine the outgassing occurring within a vacuum system as a continuous function of time, and (2) analyse the resulting curve to obtain information as to the source and nature of the outgassing. The report describes this technique and its application in determining the optimum combination of such parameters as temperature, time, materials, restrictions, and pumps on such processes as electron tube exhaust and cellulose dehydration. Vacuum process evaluation has also been used to study such phenomena as the outgassing characteristics of insulating materials and vacuum gauges, the flow of gases through orifices and short tubes, and the gettering action of various materials. A digital computer and data reduction facilities have been incorporated to eliminate the detailed hand calculations and plotting. This has resulted in a rapid and inexpensive method for the study of vacuum engineering problems.

10.8. **La Technique du Vide et des Hautes Pressions :** L. DEFFET. Institut Belge des Hautes Pressions, Bruxelles, Belgique, et E. THOMAS, Ecole Royale Militaire, Bruxelles.

On rappelle d'abord brièvement l'origine de la technique des hautes pressions et de la technique du vide.

On met ensuite en évidence quelques similitudes entre ces deux techniques et l'on recherche si les moyens et les méthodes utilisés pour l'obtention et le maintien des vides élevés ne pourraient être appliqués davantage aux hautes pressions et vice versa.

10.9. **The Potential and Application of the Radioactive Isotopes in Vacuum Research and Technology :** LUTHER E. PREUSS. Physics Department, Edsel B. Ford Institute for Medical Research, Detroit 2, Michigan, U.S.A.

A brief outline of the uses, to date, of the radioactive nuclide in basic vacuum research and routine application illustrates that the tracer tool's initial emphasis, in vacuum work, has been predominately in the realm of distillation phenomena. Specific examples of the radiotracer system, as applied to vacuum evaporation, are given. The available synthetic radioactive isotopes are reviewed, along with the parameters imposed on their use in vacuum study by their characteristics of half-life, radiation type, specific activity, etc. The methodology and examples of health-physics procedures, vacuum system alteration and essential techniques of radiotracer work, as they are applied to vacuum studies, are dealt with. The use of ancillary techniques, such as the autoradiographic method, are discussed. A brief outline is made for the potential of the radiotracer technic, and its attendant sensitivity, for specific vacuum studies.

10.10. **Outlook on New Trends in Vacuum Physics :** H. J. SCHWARZ. Project leader at Radio Corporation of America, Industrial Advanced Development, Camden 2, New Jersey, U.S.A. (Professor of Applied Physics, on leave from University, Rio de Janeiro, Brazil).

General remarks on techniques of production and measurement of vacuum. Weak points of the techniques used up to now. Are there any new means possible for obtaining and measuring high vacuum ?

Possible trends will be outlined. Specially the conception of an " ultrasonic molecular high vacuum pump " will be given.

10.11. **Massenspektrometrische Gasanalyse schneller Vorgänge im Hochvakuum :** H. J. SCHÜTZE und P. F. VÁRADI. Telefunken, Ulm, Deutschland.

Eine Reihe dynamischer Vorgänge der Vakuumtechnik ist mit Druckänderungen verbunden, die in der Grössenordnung von Minuten ablaufen. Die Untersuchung derartiger Erscheinungen, wie z.B. die Gasaufzehrung durch Getter und die Gasabgabe von Röhrenbauteilen erfordert ausser der Messung des Totaldruckverlaufes auch die gleichzeitige Erfassung der Partialdruckkomponenten. Die hierfür notwendigen verschiedenen Anforderungen an die Vakuum-apparatur, die Analysenmethode, die Registrierung und deren Auswertung werden diskutiert. Ergebnisse, die mit einem für diesen Zweck geeigneten HF-Massenspektrometer gewonnen wurden, werden gezeigt.

10.12. **Étude des Phénomènes Eléctriques dans un Vide très Poussé :** A. BLÁHA. Slovenskà vysoká škola techniká, Bratislava, Tchécoslovaquie.

Vol. 9 959/60

Il s'agit de l'étude des phénomènes électriques dans le haut vide (10^{-2}–10^{-5} mm Hg) sans champ magnétique. Dans ce domaine, trois groupes de théories existent :

1. La théorie de la décharge électrique de Langmuir-Tonks-Kljarfeld avec chute libre des ions positifs (Freifallsäule).
2. La théorie du vacuomètre à ionisation de Kaufmann-Serovy-Morgulis.
3. La théorie de la pompe à ionisation de Schwarz.

Ces trois catégories de théories, exprimant des phénomènes comparables, ont des points de départ assez différents. Cette divergence existe surtout au point de vue de la considération de la structure du mouvement des ions positifs. Tandis que dans les théories du premier groupe, les ions positifs ont une composante importante du mouvement radial en chute libre dans le champ électrique radial, dans les théories du deuxième groupe, le mouvement des ions positifs est latéral rectiligne et dans la troisième théorie, le mouvement des ions positifs est chaotique.

En partant de cette confrontation, l'auteur a élaboré une théorie qui serait capable de concilier quelques-unes de ces suppositions divergentes. Cette théorie prend pour base la superposition des phénomènes cités plus haut du mouvement chaotique et du mouvement dirigé des particules électriques.

11.1. **The Measurement of Noise in the Production Testing of Mechanical Vacuum Pumps :** W. STECKELMACHER. Edwards High Vacuum Ltd., Crawley, United Kingdom.

An instrument has been developed for measuring the noise produced by a rotary pump against the background noise and vibration produced under industrial testing conditions. A vibration pick-up transducer is mounted directly on the pump under test, the electrical signals from which are in the form of regular bunched audio-frequency impulses produced during every pump cycle. Details are given of an electrical system selectively sensitive to the test pump noise only, so that a standard of acceptable noise having been set in relation to an electrical signal defective pumps can be readily detected and the type of noise defect determined.

11.2. **Industrielle Anwendung von Rootspumpen :** H. MOESTA. E. Leybold's Nachfolger, Köln, Deutschland.

Rootspumpen sind heute—wenige Jahre nach ihrer Einführung in die Vakuumtechnik—im gesamten Druckbereich vom Grobvakuum bis zu Drucken von einigen 10^{-7} Torr eingesetzt. Für jeden Druckbereich wird mit einem charakteristischen Anwendungsbeispiel Betriebsart und Leistung der Rootspumpe gezeigt. Besondere Beachtung gilt hierbei dem Feinvakuumbereich und dem Bereich höherer Drucke, in dem Rootspumpen, Ölluftpumpen und Strahlsauger in den Betreibskosten und der Betriebssicherheit überlegen sind.

11.3. **The Axial Flow Compressor as a High Vacuum Pump :** H. HABLANIAN. NRC Equipment Corporation, Newton Highlands, Mass., U.S.A.

To determine the extent of pumping action produced by an axial flow compressor at very low pressures, a small ten-stage compressor was tested in series with an oil-sealed rotary piston vacuum pump. The performance of the compressor is similar to that of the Roots blower used in the same manner, except that the region of higher pressure ratios occurs at lower inlet pressures. Ultimate vacuum of 3×10^{-4} mm Hg and pressure ratios as high as 70 were obtained at moderate rotor tip velocities. Design features of a high vacuum turbocompressor are outlined and use of such machines for high capacity vacuum pumping systems is discussed.

11.4. **Über eine Neue Molekularpumpe :** W. BECKER. Firma Arthur Pfeiffer, Wetzlar, Deutschland.

Eine Molekularpumpe, die von den seither bekannten Konstruktionen wesentlich abweicht, wird in ihrem Aufbau und ihrer Wirkungsweise erläutert. Bei dieser Konstruktion ist der sonst übliche Luftspalt von einigen 1/100 Millimetern vermieden, wodurch eine grosse Betriebssicherheit erreicht wird. Ein weiterer Vorteil der Konsrtuktion ist eine grosse Sauggeschwindigkeit der Pumpe. Trotz der hohen Sauggeschwindigkeit wird auch ein hohes Druckverhältnis erzielt. Das Endvakuum wird praktisch nur durch Undichtigkeiten der Apparatur und Gasabgabe der Wände begrenzt. Das Verhalten der Pumpe bei verschiedenen Vorpumpen wird in Diagrammen vorgeführt. Ausserdem wird auf die Anwendungsgebiete dieser Pumpen näher eingegangen.

11.5. **Mechanische Vakuumpumpen :** A. LORENZ. W. C. Heraeus, Hanau/Main, Deutschland.

Die mechanischen Pumpen sind als meist gebrauchte Vakuumpumpen von besonderer Wichtigkeit für die Vakuumtechnik. Es werden verschiedene Besonderheiten der 3 wichtigsten mechanischen Vakuumpumpen, rotierende Ölpumpen, Rootspumpen, Wasserringpumpen, besprochen.

Die meisten Vakuumprozesse erfordern die Kombination mehrerer Pumpen. Rootspumpen und Wasserringpumpen sind besonders dann am Platze, wenn ein Anwendungsfall vorliegt, bei dem viel Staub oder viel Wasserdampf auftritt. In vielen Fällen werden sogar keine Staubabscheider oder Baffles benötigt. Pumpstände bis zu 25,000 cbm pro Stunde sind gebaut worden. Durch Hintereinanderschaltung mehrstufiger Rootspumpen und einer Wasserringpumpe können Vakuumanlagen von Atmosphärendruck bis auf Hochvakuum ausgepumpt werden.

Es wurde eine neue Bauform der Drehkolbenpumpe entwickelt. Die verschiedenen Pumpengrössen werden aus den gleichen Konstruktionselementen zusammengebaut und unterscheiden sich nur in der Länge. Durch eine besondere Anordnung der Kolben sind sie in hohem Masse von dynamischer Unwucht frei.

11.6. **Purification of Vacuum Pump Lubricating and Sealing Oils :** M. KUNSTENAAR. European Operations of The Hilliard Corporation, Elmira, U.S.A.

Lubricating oil used in rotary high-vacuum pumps can be maintained continuously at new oil values by means of a purification system consisting primarily of a filtering section—for the removal of solids and oil oxidation products ; in series with a heated vacuum vaporizer—for the removal of volatile contaminants.

Practical and economic advantages of vacuum pump oil purification include increased production, reduced vacuum pump maintenance, and reduced oil consumption.

12.1. **Der Einfluss von Verunreinigungen auf den Totaldruck über Öl-Diffusionspumpen :** W. BÄCHLER. E. Leybold's Nachfolger, Köln, Deutschland.

Es wird über eine Anordnung berichtet, mit deren Hilfe die Auswirkung von in jedem Vakuumprozess auftretenden Verunreinigungen auf den Totaldruck untersucht werden kann. Die möglichen Gegenmassnahmen, mit denen man die Verunreinigungen mehr oder weniger unwirksam machen kann, werden erläutert.

Anschliessend wird anhand von Versuchserbebnissen gezeigt, wie eine gute Selbstreinigung des Treibmittels den nach einer bestimmten Pumpdauer erreichbaren Totaldruck bei vorgegebenen Verunreinigungen verbessert.

12.2. **A Continuous Distillation Method for High Grade Diffusion Pump Fluids, Checking the Ultimate Vacuum of the Distillates :** H. ISHII. Electrotechnical Laboratory, Tokyo, Japan.

A new high vacuum continuous distillation apparatus which is made of glass and composed of five tandem batch stills and two falling film type molecular stills was investigated. Using this apparatus, high grade diffusion pump fluids could be obtained from commercial plasticizers, i.e. di-2-ethylhexyl phthalate (EHP) and di-2-ethylhexyl sebacate (EHS) respectively.

Peculiarities of this apparatus are : (1) the stills themselves have pumping action ; (2) the ultimate vapor pressure of the last stage still is that of the distillate itself and (3) the ultimate vacuum indicated by anionization gauge can be used as monitor of the distillation rate and quality.

Vo
9
1959

Under conditions such as a distillation rate of 29 cc/hr and a yield of 76 per cent of crude oil in the distillation process of EHP at 184°C, the equilibrium pressure indicated by the ionization gauge is 4.2×10^{-6} mm Hg. The minimum ultimate pressure of this apparatus using EHP is 4×10^{-7} mm Hg at room temperature of 15°C and a last stage still temperature of 178°C. At a distillation rate of 32 cc/hr, a still temperature of 192°C and a yield of 70 per cent the equilibrium pressure of EHS is $4 \sim 5 \times 10^{-7}$ mm Hg. The minimum ultimate vacuum is 1.2×10^{-7} mm Hg at the room temperature of 25°C and the still temperature of 180~185°C. Furthermore, the fractionating capacity of this apparatus was studied with binary mixtures of EHP and EHS.

12.3. **The Experimental Research on the Back-Streaming of Oil Vapor of an Oil Diffusion Pump :** S. KOBAYASHI and H. OTAKE. Tokyo Shibaura Electric Co., Ltd., Tokyo, Japan.

In this paper, the authors treat the problem of the back-streaming of oil vapor toward fine pressure side in an oil diffusion pump and analyse the sources in four causes of back streaming. These are :

(1) the drains on the jet surface,
(2) the vaporization of cold oil drains on the upper wall of a pump cylinder,
(3) the scattering of oil vapor stream,
(4) the reflection of oil vapor stream.

To measure the back-streaming of oil vapor, the authors employ metal probes located in the radial direction of the cylinder at the pump head, and determine the quantity of the back-streaming by the weights of the oil condensed on these probe surfaces in the unit time.

The authors concluded experimentally that the extremely large parts of the back-streaming of oil vapor is caused by the oil drain on the jet surface, and the scattering, reflection and evaporation of cold oil drain affects only few parts respectively.

Using some baffles, the evaporation of oil from the cold surface can be measured, but the scattering and reflection are not separated from each other ; nevertheless, the amount of the oil back-streaming caused by the scattering and reflection is only three times as large as that caused by the evaporation from the cold surface.

12.4. **Study on the Oil Ejector Pump with High Speed, High Tolerable Backing Pressure :** S. KOMIYA and T. IHEDA. Tokuda Seisakusho Co., Ltd., Tokyo, Japan.

Experiment of an oil ejector pump which has high tolerable backing pressure (1–10 mm of mercury) is described. The linear relation between a critical backing pressure and a quantity of oil vapor passing through a nozzle to a diffuser is obtained.

" Double critical backing pressure " and " double throughput " phenomena for higher air discharge are discussed.

Maximum throughput appears near an " equivalent pressure " which means intake air pressure is equal to vapor jet pressure at nozzle outlet. The pumping speed per unit area of annular clearance between the nozzle outlet and diffuser is almost constant at this " equivalent pressure " in our study.

12.5. **An Unusual Mercury Ejector Pump :** B. D. POWER and N. T. M. DENNIS. Edwards High Vacuum Ltd., Crawley, United Kingdom.

A three-stage mercury ejector pump will be described which has a throughput for air of 20 l. mm/sec at 1 mm Hg when working against a backing pressure of 100 mm Hg. The permanent gas ultimate of the pump when working against 100 mm Hg being less than 10^{-3} mm Hg.

13.1. **Problems Arising in the Attainment of Low Pressure by Fractionating Vapour Pumps in Large Demountable Systems :** B. D. POWER and D. J. CRAWLEY. Edwards High Vacuum Ltd., Crawley, United Kingdom.

In any large-scale vacuum system the time taken to pump down to a given pressure, and the ultimate pressure attainable, cannot be predicted from a knowledge merely of the performance of the pumping unit, and the dimensions of the system, since the effects of outgassing are usually incalculable.

This paper describes some work done to measure on a small scale the effects of outgassing from gasket materials and metallic surfaces, and presents some typical pumping data for a large system to demonstrate the magnitude of such effects in practice. The importance is also shown of other factors whose influence on pump-down time does not seem to have been sufficiently emphasized.

13.2. **The Important Role of the Vapour Booster Pump in Large-scale Vacuum Operations :** A. S. D. BARRETT and N. T. M. DENNIS. Edwards High Vacuum Ltd., Crawley, United Kingdom.

The performance characteristics of the vapour booster pump designed for the large gas throughputs associated with industrial vacuum processing in the range 10^{-4} to 1 mm Hg are discussed. Their initial and running costs are compared with those of other types of pumps which can be used in this pressure range and reveal definite economic optimum applications within the range. Vapour booster pumps have proved to be extremely reliable under difficult industrial pumping conditions and examples of their successful applications will be described.

13.3. **Zur Konstruktion von Pumpständen und Pumpsätzen :** J. MOLL. Leybold — Hochvakuum — Anlagen, Köln, Deutschland.

Auf Grund der wichtigsten Anwendungen von Hochvakuumpumpständen werden die verschiedenen Anforderungen diskutiert. Einige wesentliche Gesichtspunkte, wie Sicherheit, Wirtschaftlichkeit und Betriebsbereitschaft werden herausgestellt und Konstruktionsprinzipien erörtert. Insbesondere wird der Einsatz der verschiedenen Kombinationen von mechanischen Pumpen mit Hochvakuumpumpen abgewogen.

14.1. **Détection des Fuites :** R. JEAN. Compagnie Générale de T.S.F., Corbeville par Orsay, France.

Introduction : Généralité et intérêt des contrôles d'étanchéité. Nécessité de définir une fuite limite et de mesurer les fuites. Exemples. Définition d'une fuite : 3 types : trou ou fissure, porosité et diffusion. La diffusion n'intéresse que les gaz et est extrêmement rare.

Unités : Elles sont tres nombreuses. Avantage à adopter une unité convenable pour les gaz et liquides : le cm^3/sec.

Étude des fuites cylindriques : Les fuites naturelles ont une structure complexe, mais l'étude des fuites cylindriques permet de déduire les lois fondamentales de l'écoulement des fluides dans les fuites. Calcul sur les fuites de longueur unité, régime d'écoulement.

Fuites de liquides : Incompressibles. Formules de débit. Limitations dues à la tension de surface. Evaporation.

Fuites de gaz sous pression : Régime. Formules de débit. Mélanges de gaz. Cas où la fuite débite dans un liquide.

Fuites de gaz dans les enceintes vidées : Régime. Formules de débit. Exemples de débits en fonction du diamètre et de la nature du gaz. Cas des mélanges de gaz. Fractionnement dans les fuites laminaires.

Fuites de liquides dans les enceintes vidées : Beaucoup de liquides se vaporisent sous vide. Complexité du problème. Bouchage des fuites par les liquides.

Relation entre les débits des fuites dans les différents cas : Détermination du débit d'une fuite dans les conditions d'utilisation à partir de la valeur de la fuite mesurée avec la méthode de détection choisie. Mêmes relations avec les conséquences sur la facilité de détection des fuites. Variation du débit lorsqu'un liquide remplace un gaz à l'entrée d'une fuite.

Temps de transit : Calcul. Son importance en détection de fuites. C'est le temps de transit qui limite la possibilité de détecter des porosités. Le temps de transit est indépendant de la pression extérieure dans les essais sous vide. Temps de débouchage des fuites remplies de liquide. Conclusion.

Vol. 9 959/60

14.2. **l'Helitest Détecteur de Fuites a l'Hélium Calcul et Performances de la Cellule d'Analyse :** G. MONGODIN. Laboratoire des Basses Pressions, Argenteuil (S. et O.), France.

Description d'un spectromètre de masses conventionnel à séparation magnétique, destiné à la recherche de fuites à l'hélium.

Description détaillée de la cellule d'analyse d'une réalisation technologique inédite : source d'ions dégazable ce qui élimine les pertes de sensibilité filament toujours maintenu dans un vide poussé, lame de gaz ionisée à haute pression (jusqu'à 1/2 Torr) sans aucune apparition de claquages électriques, visée optique du filament au travers de l'alignement des électrodes, aimant de déflexion incorporé.

Calculs de la source d'ions et de la concentration électronique. Calcul de la lentille de focalisation. Evaluation du pouvoir séparateur.

La sensibilité du détecteur permet de déceler des fuites de l'ordre de 10^{-7} lusec.

14.3. **Détection de Fuites par Spectrométrie de Masse à Helium :** S. CHOUMOFF et J. LAPLUME. Compagnie Française Thomson-Houston, Paris, France.

La recherche des fuites a pris une importance de plus en plus grande, due notamment au développement de l'industrie atomique. Le spectromètre de masse à hélium représente un type de détecteur particulièrement perfectionné, son emploi se généralise de plus en plus, il est maintenant réalisé d'une manière industrielle en Europe : La description d'un tel détecteur fabriqué sous licence du C.E.A. est fournie ; les principes généraux de détection sont envisagés, ainsi que des exemples concrets d'utilisation, avec indication des performances obtenues. Les problèmes posés par la définition des caractéristiques, et de l'étalonnage sont abordés.

14.4. **The Silica Gel Leak Detector :** TH. P. J. BOTDEN. Philips Research Laboratories, Eindhoven, Holland.

The silica gel leak detector consists of a sensitive Penning-manometer (Philips vacuum gauge) connected to a tube filled with grains of silica gel.* The silica gel, cooled at liquid air temperature, is a good absorbant for air, while hydrogen and some inert gases are but little absorbed. A system to be tested is connected to the detector. When a leak is present, air entering the tube is absorbed by the silica gel before reaching the vacuum gauge. When hydrogen is sprayed around the tube, the ionization current will increase due to a rise in pressure in the vacuum gauge by the hydrogen which is not absorbed by the silica gel. Leaks down to about 10^{-9} cc.mm Hg/sec. can be detected by this rather simple method. Results will be given of measurements on sensitivity, the dependence of the latter on the amount of absorbed air in the silica gel, the current as a function of the leak rate and also some examples of leak-measurements.

*J. A. van Leeuwen and H. J. Oskam, *Rev. Sci. Instr.*, **27**, 328, 1956.

14.5. **A Differential Pirani Type Leak-Detector with a Charcoal Trap :** HIROSHI ISHII. Electrotechnical Lab., Tokyo, Japan.

The differential Pirani type leak-detector with cold trap is not convenient for use at any place and at any direction on the vacuum system for it requires to prepare liquid air or liquid nitrogen.

In this investigation, we used a charcoal trap in one of the arms of Pirani tube so that we were free from such troubles as in the case of using a cold trap, and moreover we could improve the sensitivity and convenience by means of a.c. amplifier and audible alarm in the circuit.

The minimum detectable leak in the case of a 2 l volume metal dome evacuated by oil diffusion pump and proved by butane gas is $1—3 \times 10^{-6}$ l mm Hg/sec.

It is not difficult to detect some leaks as large as about 10^{-5} l mm Hg/sec when this detector is used in an ordinary bell jar type coating system. The range of pressure in which this detector has enough sensitivity is from about 10^{-5} mm Hg to 1 mm Hg.

In these respects, this detector is superior to an ionization gauge used for leak detection when the vacuum of the system is lower than 10^{-3} mm Hg.

14.6. **Leak Test of Rubber Gaskets :** S. KOBAYASHI and K. YADA. Tokyo Shibaura Electric Co., Ltd., Tokyo, Japan.

The relations between the compression ratio and the leak of some rubber gaskets having practical dimensions were investigated by a helium leak detector. As the materials of the samples were used acrylenitrile-butadiene, chloroprene, natural and silicone rubber.

Testing was tried for 3 different kinds of cross-section : circular, square and semicircular ; and also for the gaskets of 7 different Shore hardness from 30 to 90. Five jointless pieces for each kind of sample, 420 pieces in total, are made as samples to be tested.

There are 2 kinds of leak in a gasket, namely " usual leak " and permeation. The former is a leak through the space between the surface of gasket and that of a gasket seat, and the latter is a leak through the gasket material itself. These two kinds of leak can be distinguished clearly by experiment. The former leak can be made less than 1×10^{-9} mm Hg/sec when rubber of any kind is compressed by 10–15 per cent. The latter leak can be diminished only when the surface area of the gasket exposed to both vacuum and atmosphere is made small.

14.7. **La Détection des Fuites et l'Analyse de Mélanges Gazeux au Moyen du Spectromètre de Masse à Résonance d'Ions du Type Omégatron :** R. J. WARNECKE, JR. Compagnie Générale de T.S.F., Paris, France.

Après avoir rappelé brièvement le principe de l'Omégatron, l'auteur expose les possibilités de ce spectromètre utilisé soit comme détécteur de fuits, soit comme analyseur de masses.

(a) Détection des fuites : apres description rapide d'un détecteur de fuites du type à Omégatron qui se distingue des autres appareils existant actuellement par le fait qu'il permet l'utilisation de plusieurs gaz d'épreuve, en particulier l'argon, des résultats expérimentaux sont fournis qui montrent que la sensibilité de l'Omégatron est comparable à celle des spectromètres classiques à champs constants. C'est ainsi qu'en régime dynamique, l'argon étant utilisé comme gaz témoin, des fuites de l'ordre de 10^{-4} mm3 atm/h, soit 2.10^{-8} lusecs peuvent être détectés rapidement sur des enceintes de volumes très divers. Par construction, l'Omégatron se prête à un dégazage poussé ce qui permet de procéder par accumulation pour la recherche des très faibles fuites ; de cette façon des fuites de l'ordre de 10^{-8} mm 3 atm/h, soit 2.10^{-12} lusecs peuvent encore être décelées dans des temps raisonnables.

(b) Analyse de gaz : l'Omégatron est un spectromètre particulièrement bien adapté à analyse de mélanges gazeux contenant des constituants légers tels que H, He, O, O_2, CO, CO_2, N_2... Avec un champ magnétique de 3000 oersteds, le pouvoir de résolution a une valeur acceptable dans un domaine de masse compris entre $m = 1$ et $m = 100$ u.m.a. Sa sensibilité est telle que des pressions partielles de 10^{-10} Torr sont mesurables. Des spectres de masses sont présentés et des chiffres sont donnés concernant la précision et la stabilité des mesures.

14.8. **Spectromètre de Masse pour la Détection des Fuites, Fonctionnant avec un Mélange à Faible Teneur en Hélium :** N. WARMOLTZ. Philips Research Laboratories, Eindhoven, Holland.

On décrit un détecteur des fuites à si grande sensibilité qu'on peut utiliser comme test-gaz un mélange d'hélium et d'air et déceler encore des fuites aussi faibles qu'on peut trouver normalement avec de l'hélium pur. Cette sensibilité a été atteinte grâce à l'utilisage d'un multiplicateur d'électrons comme détecteur des ions.

Maintenant l'approvisionnement de l'hélium pour détecteurs de fuites n'est plus un problème en Europe.

15.1. **Über Vakuummessung mit dem McLeodschen Vakuummeter :** H. EBERT. Phykalisch-Technische Bundesanstalt, Braunschweig, Deutschland.

Das 1874 von McLeod eingeführte Messgerät ist auch heute in der Vakuumtechnik noch eines der wichtigsten Instrumente.

Vo
9
1959

Es ist daher immer wieder Gegenstand besonderer Untersuchungen hinsichtlich der Bedingungen des Richtigzeigens (ideales Gasgesetz, Adsorption, Absorption) und der Erweiterung seines Messbereichs (neueste Vorschläge von Moser—Poltz).

15.2. **A Modified McLeod Gauge for Low Pressure Measurements:** L. J. GRIFFITHS. Royal College of Science and Technology, Glasgow, United Kingdom.

A McLeod gauge employing low vapour pressure oil and a modified method of gas compression is described. The gas to be compressed is contained in a vertical glass cylinder open at its lower end and fitted at its upper end with a capillary tube. The compression is achieved by lowering this cylinder vertically into an oil reservoir by means of an external magnet.

The gauge is robust and compact and is not difficult to construct. Large compressions may be obtained without difficulty. A pressure of 5×10^{-5} mm of mercury can be measured with a vessel volume of about 200 cm³ when the compressed gas occupies 1 cm length of capillary of bore diameter 1.5 mm. No liquid air trap is required for the gauge but it must be kept permanently at a pressure below about 10^{-2} mm of mercury if absorption and subsequent degassing of the oil is to be avoided.

15.3. **On the Standard of Vacuum Installed in the Electrotechnical Laboratory. The Standard McLeod Gauge and the Calibration of Ionization Gauges to it :** M. GOTO. Electrotechnical Laboratory, Tokyo, Japan.

As the industrial and scientific importance of high vacua increased, it became necessary to measure high vacua accurately and to establish the high vacuum standard.

In the present stage, we have chosen the McLeod gauge as the standard one for the absolute pressure and hot cathode type ionization gauges as the substandards. The standard McLeod gauge is constructed with a bulb of 1 l volume and a pair of capillaries, 1.110 ± 0.002 mm in internal diameter, having a roughened inside surface. The accuracy is about $\pm$ 3 per cent at 10^{-4} mm Hg and less than $\pm$ 1 per cent at 10^{-3} mm Hg. The substandard ionization gauge tube is an ordinary cylindrical ion collector type, but is specially designed and has sensitivity of about $20\mu A/mA/\mu Hg$ for nitrogen gas and linear sensitivity up to $1\mu Hg$.

The calibration system, composed of glass, works on the principle of constant throughput and stationary evacuation by a large mercury diffusion pump and maintains a constant pressure. The whole system is set in a removal furnace which can heat to outgas the system including the McLeod gauge and traps up to 400°C.

At the present stage of the investigation, we can calibrate commercial ionization gauges within the accuracy of $\pm$ 5 per cent to the absolute with a substandard gauge attached to a metal calibration dome which is evacuated by an oil diffusion pump.

15.4. **Highly Sensitive Hot Cathode Ionization Gauge :** S. KOBAYASHI. Tokyo Shibaura Electric Co., Ltd., Tokyo, Japan.

To improve the sensitivity of the ionization gauge, it is necessary to enlarge the flying path of electrons.

From this standpoint, locating the filament near the ion-collector in the gauge, the author could enlarge the flying path of electrons about twice that in which the filament is located in the center of collector. In the case of cylindrical collector, if the diameter of the cylinder is 25 mm, the sensitivity K of the gauge is about 40 for air ; if 38 mm, the K is about 80 ; and if 50 mm, the K is 130.

15.5. **Membran-Manometer für Vakuumdruckmessungen :** H. W. DRAWIN. Atlas-Werke, Bremen, Deutschland.

Sobald geringere Drucke gemessen werden sollen, zeigen die meisten der heute verwendeten. Druckmessgeräte eine Abhängigkeit von der Gas-oder Dampfart. Diesen Nachteil besitzen Membran-Manometer nicht. Sie messen den Totaldruck unabhängig von der Gas-oder Dampfart. Ihre Eichkurve ist weitgehend linear. Sie sind bei entsprechender Konstruktion ausheizbar.—Es wird über Konstruktionsprinzipien empfindlicher Membran-Manometer berichtet, die sich sowohl für Vakuumdruckmessungen (Absolutdruck) als auch für Differenzdruckmessungen bei beliebigen Absolutdrucken eignen. Es werden die Eigenschaften des Membran-Mikro-Manometers Type MMM (Druckbereich 10^{-5}–2.10^{-1} mm Hg) und des Membran-Kapazitäts-Torrmeters Type MCT (Druckbereich 1.10^{-1}–30 Torr) beschrieben. Dann wird auf die Verwendung dieser Membran-Manometer in Forschung und Betriebskontrolle eingegangen.

15.6. **La Mesure des Basses Pressions à l'Aide des Thermistances :** M. VARIĆAK et B. SAFTIĆ. Faculté des Sciences et Institut Rugjer Bošković, Zagreb, Yougoslavie.

Des considérations théoriques sur la conduction thermique à travers les gaz ont conduit à la construction d'un système formé d'une thermistance perle fixée au centre d'une feuille métallique mince et circulaire (*C.R. Ac. Sci.* **245**, 1956 *Il Nuovo Cimento* **6**, 1957 ; *J. Phy. et Rad.* **18**, 1957).

Les recherches récentes ont pourtant montré que la sensibilité de ce système, pour les mesures des basses pressions, augmente si on utilise deux thermistances en forme de petites plaques, au lieu d'une thermistance perle. On a trouvé que pour chaque matériau il existe une proportion optimum entre la hauteur de la plaque et le diamètre de sa base.

La construction d'un manomètre thermique, basée sur ces recherches, est décrite. On discute la possibilité de compenser l'influence de la température ambiante à l'aide d'un tube compensateur classique ou à l'aide de deux systèmes thermistance, placés dans l'enceinte où la pression des gaz est à mesure. On trouve que les meilleurs résultats sont obtenus, si le système de mesure et le système compensateur sont faits de matériaux ayant des caractéristiques électriques différentes. De cette manière, on peut profiter de la sensibilité et de la stabilité maximum du pont de mesure. Cette jauge à vide permet la mesure exacte des pressions de gaz de 1 mm Hg jusqu'à 10^{-6} mm Hg.

15.7. **Le Manomètre Thermique à Compression :** J. GROSZKOWSKI. Université Technique, Varsovie, Pologne.

La communication concerne un manomètre thermique dans lequel on a étendu la gamme de mesure aux pressions plus basses en employant le principe de compression. Pour mesurer la pression, on se sert d'une thermistance (une résistance à fil ou un thermistor). La thermistance a les dimensions les plus petites possible, et est placée dans une chambre de volume très réduit V_1. La compression est obtenue à l'aide d'un réservoir à volume variable, le volume peut être changé d'une valeur maximum V_{max} jusqu'à une valeur minimum V_{min}.

Le réservoir de compression est constitué de deux plaques métaliques rondes, legèrement concaves, soudées à leur circonférence. Une des plaques, en cuivre, est massive, l'autre—en bronze, est mince et élastique. Dans la position correspondant au volume minimum, la plaque élastique adhère strictement à la plaque massive. Dans la position correspondant au volume maximum, la plaque élastique devient convexe, le réservoir prenant la forme d'une lentille. Pendant le passage d'une position à l'autre a lieu une petite déformation de la plaque élastique. Le réservoir de compression communique par une canalisation métallique avec la chambre à thermistance et—par l'intermédiaire d'un robinet (sans graisse)—avec l'espace à pression mesurée, le volume V_2 de la canalisation (jusqu'au robinet) est aussi très petit. De cette façon, en employant une construction convenable, on peut obtenir pour le coefficient de compression, donné par l'expression

$$K = \frac{V_{max} + V_1 + V_2}{V_{min} + V_1 + V_2} \approx \frac{V_{max}}{V_{min} + V_1 + V_2},$$

la valeur de l'ordre de 1000. Cela permêt d'étendre la limite des pressions $10^{-1} + 10^{-3}$ Torr normalement mesurées par la manomètre à thermistance, jusqu' à $10^{-4} + 10^{-6}$ Torr.

Le même appareil peut être utilisé avec le principe de décompression, c'est qui permet d'étendre la region de mesure vers les pressions plus hautes, p. ex. 100 + 1 Torr.

Vol. 9 959/60

La comparaison du manomètre thermique à compression avec la jauge de McLeod (vapeur de mercure) et avec la jauge à ionisation (*clean-up effect*) montre ses avantages.

15.8. **Une Jauge Radiométrique Pratique pour la Mesure des Vides Élevés :** Madame J. BAILLEUL-LANGLAIS. La Radiotechnique Suresnes, France.

Nous présenterons une jauge radiométrique pour la mesure absolue des pressions comprises entre 5.10^{-4} et 10^{-7} mm Hg. Les valeurs de la pression totale se calculent d'après les dimensions de l'appareil indépendamment de la nature des gaz.

La jauge est en verre dur, étuvable à 450°C, d'encombrement très réduit (cylindre de 25 mm de diamètre et 70 mm de longueur), relativement peu fragile (suspension mobile interchangeable), facilement transportable et adaptable par simple soudure sur cristallerie.

La période d'oscillation de l'équipage mobile est de l'ordre de la seconde, mais le système doit être amorti et protégé des vibrations parasites.

La mesure d'une valeur de la pression dure 1 min au plus, mais nous insisterons sur le fait qu'une jauge radiométrique de ce type ne saurait être un appareil de mesures continues, la fréquence des measures devant être peu élevée (1 mesure tous les quarts d'heure environ).

15.9. **Mesure du Vide dans les Valves par la Méthode de la Tension de Paschen :** P. ANDRÉ. La Radiotechnique Suresnes, France.

On mesure la tension d'amorçage V_a de la décharge obscure entre les deux électrodes et on détermine expérimentalement la fonction ψ du champ réduit $V_a = \psi(E/p)$. On est alors en état d'annoncer le degré de vide dans un tube à froid.

Le domaine des pressions inférieures à celles correspondant au minimum de Paschen à été exploré. On trouve le coefficient d'ionisation par volt η une expression de la forme :

$$\eta = A(E/p)^{-2} \log B\,(E/p) \quad (A \text{ et } B \text{ constantes}).$$

Si les conditions géométriques et le coefficient d'émission secondaire sont connus, η est lié à la tension de Paschen, de sorte que l'on à avec une bonne approximation $V_a p =$ constante; c'est-à-dire que la tension d'amorçage est proportionnelle au libre parcours moyen électronique, cela en accord avec l'expérience.

Le dispositif de mesure est décrit et de nombreux résultats communiqués pour différents gaz.

15.10. **Un Manomètre à Membrane à Échelle Linéaire pour des Pressions entre 10^{-5} et 10 mm Hg :** J. J. OPSTELTEN et N. WARMOLTZ. Philips Research Laboratories, Eindhoven, Holland.

On décrit un double manomètre à membrane, démontable, construit presque complètement en acier inoxydable. La sensibilité est égale pour la plupart des gaz. On peut aussi mesurer la pression des gaz polaires qui sont absorbés dans l'appareil, par un changement de circuit.

Le manomètre peut fonctionner à une température de 150°C ou même plus élevée.

15.11. **Sur les Vacuomètres à Viscosité :** A. BLÁHA. Slovenská vysoká škola techniká, Bratislava, Tchécoslovaquie.

Dans la catégorie des vacuomètres utilisant pour la mesure des basses pressions l'action dynamique du milieu raréfié et dont les vacuomètres à viscosité sont un représentant typique, nous avons plusieurs possibilités de réalisations :

I. Le milieu en mouvement agit sur une vanne légère.
II. Une vanne légère, actionnée par un micromoteur, agit sur le milieu.
1. L'action de la surface de la vanne et l'action du milieu sont perpendiculaires.
2. L'action de la surface de la vanne et l'action du milieu sont tangentielles.
(a) Le mouvement résultant est continu (par ex. rotatif).
(b) Le mouvement résultant est avec vibrations forcées.
(c) Le mouvement résultant est avec oscillations apériodiques.

En combinant ces différents procédés, nous avons 12 possibilités de construction de vacuomètres dont quelques-unes seulement sont jusqu'ici utilisées dans la pratique.

Les cas I, II, 1, 2, se distinguent au point de vue théorique. Par exemple dans le domaine du haut vide (10^{-2}–10^{-5} mm Hg), l'action I du milieu mouvement que l'on peut considérer comme trés lent, se manifeste par la pression $p = 1/4.$ nc. 2 mc, qui ne dépend pas de la masse du milieu. Au contraire l'action II de la vanne se traduit par une pression dynamique $p_d = p.$ (4 u/c), qui dépend de la masse du milieu.

D'autre part, l'action 1 perpendiculaire se manifeste dans toutes les catégories des pressions.

Au contraire, l'action 2 tangentielle ne se manifeste que dans le vide fin et dans le haut vide.

Nous avons ainsi, parmi les 12 possibilités de construction des vacuomètres utilisant l'action dynamique du milieu, 4 cas différents :

1. Les cas non sélectifs au point de vue de la masse du milieu.
2. Les cas sélectifs au point de vue de la masse du milieu.
3. Les cas non sélectifs au point de vue de la catégorie des pressions.
4. Les cas sélectifs au point de vue de la catégorie des pressions.

Cet examen critique peut être utile dans le choix de la construction des vacuomètres utilisant l'action dynamique du milieu.

L'auteur a jugé qu'il est profitable de combiner les principes II, 1, (b). Avec un système de deux fils parallèles recouverts d'une toile légère, il a réalisé un appareil mesurant la pression depuis la pression atmosphérique jusqu'à la pression 10^{-4} mm Hg. Le système est actionné par deux systèmes galvanométriques avec courant alternatif. Le changement de sensibilité se fait par une variation de la tension des fils.

16.1. **Les Debitmeters :** J. AMOIGNON. Laboratoire des basses Pressions, Argenteuil (S. et O.), France.

L'un des moyens permettant de mesurer commodément une vitesse de pompage, consiste à employer la méthode dite à pression constante.

On introduit en permanence de l'air dans l'installation et on en mesure le débit à la pression atmosphérique. On a :

$$S = \frac{V}{t} \cdot \frac{h}{p}$$

La mesure du débit de gaz à la pression atmosphérique n'offre aucune difficulté si l'on a à sa disposition un débitmètre approprié.

On se propose, dans cet exposé, de décrire et discuter différentes formes de débitmètres utilisés dans les laboratoires.

16.2. **Mesure du Débit des Pompes :** D. A. DEGRAS. Compagnie Générale de Radiologie, Paris, France.

L'auteur rappelle les procédés de mesure de débit exposés dans la littérature récente pour les pompes à jet de vapeur. Il fait ensuite l'analyse comparée sous l'angle de la précision et de la commodité.

La connaissance du débit d'une pompe ne constitue qu'exceptionnellement une fin en soi. Par contre, c'est un paramètre essentiel parmi tous ceux qui définissent une installation à basse pression. C'est dans cet esprit que l'auteur montre combien est nécessaire un standard de mesure de débit et il propose un procédé déjà utilisé par plusieurs constructeurs de pompes.

Les valeurs physique et industrielle du procédé sont étudiées, en liaison avec l'exposé sur les débimètres de Monsieur J. Amoignon.

16.3. **The Effect on the Test Dome in the Measuring of the Speed of an Oil Diffusion Pump :** S. KOMIYA. Tokuda Seisakusho Co., Ltd., Tokyo, Japan.

In measuring of the speed of an oil diffusion pump by Dayton's method, the speed measured with a test dome of larger diameter than that of the pump mouth shows smaller value than the one obtained with test dome of the same diameter as the pump mouth. The reason for this is considered to be that the former conductance is smaller than the latter, while the distance between

VO 9 1959

the pump mouth and the measuring position is smaller than a mouth diameter of the pump. We measured pressure distribution in an axial and a radial direction within a test dome, and determined the conditions in the test dome for speed measurement.

16.4. **Caractéristiques d'une Pompe à Diffusion de Mercure Contrôle Industriel des Manèges de Pompage :** Madame J. BAILLEUL-LANGLAIS. La Radiotechnique Suresnes, France.

I : Insuffisance des definitions et du choix des grandeurs caractéristiques classiques.

(1) Plutôt que la " vitesse de pompage ", nous préférons souvent considérer la " puissance d'aspiration " qui est le volume débité par une pompe pendant l'unité de temps, ce volume étant mesuré à la pression unité. Cette grandeur est homogène à une puissance et nous montrerons qu'elle rend mieux compte des possibilités d'une pompe.

(2) Au lieu de la " pression d'amorçage " ou " la pression maximum de refoulement ", nous considérerons la " pression primaire limite de bon fonctionnement ", car une pompe commence à donner des signes de mauvais fonctionnement (diminution et instabilité des valeurs de la vitesse de pompage) pour des pressions inférieures à la pression dite " de désamorçage ".

II : Mesure de la puissance d'aspiration par la méthode du capillaire.

III : Description d'un controleur inspiré de certains débitmètres, permettant de vérifier rapidement la constance de la puissance d'aspiration des pompes montées sur un manège de pompage automatique.

17.1. **Le Problème des Vannes en Technique du Vide :** J. MOREAU. Laboratoire des Basses Pressions, Argenteuil, (S. et O.), France.

Dans toutes les installations devant travailler sous vide, la vanne, élément indispensable, joue un rôle qui ne pourrait être négligé.

Nous nous proposons, dans cet exposé, de mettre en évidence les différentes fonctions que les vannes peuvent avoir à remplir sur les installations sous vide.

Pour cela, nous sommes ammenés à poser et à discuter ce que nous appelerons les qualités d'une vanne, tant sur le plan technique du vide que sur le plan mécanique.

Après avoir énuméré quelques procédés permettant de donner à une vanne toutes les qualités énoncées, nous décrirons une vanne pouvant solutionner le problème posé.

17.2. **Zur Charakterisierung der Eigenschaften von Oelfaengern :** G. ZINSMEISTER. Gerätebau-Anstalt, Balzers, Fürstentum Liechtenstein, Deutschland.

Ueblicherweise werden Oelfänger (Baffles) durch die von ihnen verursachte Verringerung der Oelrückströmung (Abschirmfaktor) und Drosselung der Sauggeschwindigkeit charakterisiert.

An Stelle der Drosselung wird vorgeschlagen, zur Beurteilung den spezifischen Leitwert anzugeben. Der Abschirmfaktor ist aus messtechnischen Gründen zur Zeit nur von wenigen Oelfängern bekannt. Deshalb wird die Beurtailung der Abschirmwirkung durch qualitative Angaben über den Verlauf der Oelrückströmung, die auf der Arbeit von J. Ruf und O. Winkler basieren, ergänzt.

In einer Zusammenstellung aller gebräuchlichen Oelfänger werden diese nach den angeführten Kriterien untersucht und verglichen. Ausserdem werden die Bedingungen für das optimale Verhältnis der Grössen von Oelfänger, Pumpe und Plattenventil angegeben.

17.3. **Recherches sur l'Efficacite d'un Baffle :** M. MALTAGLIATI. Officine Galileo, Firenze, Italia.

Mesure de l'efficacité d'un piège pour pompe à vide à diffusion de vapeur d'huile. Les mesures sont exécutées en utilisant une modification de la méthode de Langmuir comme système de comparaison. Examen de l'importance du refroidissement du piège.

20.1. **Ultra-high Vacuum Investigations :** N. A. FLORESCU. New South Wales University of Technology, Sydney, Australia.

This communication is concerned with the various requirements for obtaining reliable results with a conventional ultra-high vacuum system, and the improvement of the speed of the ion pump.

After pointing out that the problem of ultra-high vacuum was clearly outlined as far back as 1924, the general relationship between the factors involved in the performance of a vacuum system is discussed. Such a formula is useful in checking the validity of the various experimental results.

Further, a critical survey is presented of the results so far published on the production of ultra-high vacuum. From the curve giving the decrease in pressure with time it is concluded that the initial speed of the clean-up pump for active gases decreases and reaches a constant value at pressures below 10^{-7} Torr. The various values previously reported do not represent the speed of the clean-up pump in the ultra-high vacuum range.

After giving an account of ultra-high vacuum valves an improved design of a closing valve is described.

Finally, a suggestion is made of using glass fibres to increase the active area. A clean-up pump in which the grid is surrounded by loosely packed glass fibres shows an increased pumping speed.

20.2. **Diffusionskoeffizienten und Löslichkeiten von Helium und Wasserstoff in Verschiedenen Gläsern :** H. L. ESCHBACH. Physikalisches Institut der Universität Bonn, Bonn, Deutschland.

Aus dem Anhaufvorgang des Diffusionsprozesses wurden die Diffusionskoeffizienten und die Löslichkeiten von Helium und Wasserstoff in Gläsern unterschiedlicher Zusammensetzung bestimmt. Die Messungen wurden in Abhängigkeit von der Temperatur durchgeführt. Es konnten so die für den Diffusionsvorgang massgeblichen Aktivierungswärme bei sechs verschiedenen Gläsern ermittelt werden. Es wurde eine deutliche Abhängigkeit der Aktivierungswärmen von der Glaszusammensetzung festgestellt.

*20.3. **Initial Pumping and Recovery of Ionization Gauges :** N. W. ROBINSON. Mullard Research Laboratories, Salford, United Kingdom.

20.4. **Factors Limiting Ultimate Pressure in Ultra-high Vacuum Systems :** J. P. HOBSON and P. A. REDHEAD. National Research Council, Ottawa, Canada.

A summary will be made of the phenomena encountered in recent experiments at pressures below 10^{-10} mm Hg.

*20.5. **The Production of Ultra-high Vacua by Means of a Diffusion Pump :** A. VENEMA. Philips Research Laboratories, Eindhoven, Holland.

20.6. **Rôle de l'Aéronomie et de l'Astrophysique dans l'Étude des Processus Physico-chimiques à Très Basses Pressions :** B. ROSEN. Institut d'Astrophysique de l'Université de Liège, Belgique.

Les techniques du vide les plus perfectionnées sont encore très loin de permettre l'obtention au laboratoire de pressions aussi basses que celles qui règnent dans l'espace interstellaire, dans les couches extérieures de certains objets cosmiques encore facilement accessibles à l'étude spectroscopique, ou dans la haute atmosphère terrestre.

Même si ces pressions pouvaient être réalisées au laboratoire, l'étude des processus physico-chimiques dans les gaz extrèmement raréfiés serait entravée par les chocs sur les parois des récipients et par la faible intensité des émissions spectrales due à la densité négligeable et au volume limité.

Vol. 9 959/60

L'absence des parois, l'extrême rareté des chocs multiples, le nombre restreint de chocs simples dans certaines atmosphères cosmiques (y compris la haute atmosphère terrestre) permettent de mieux dégager les aspects des processus physico-chimiques primaires qui peuvent y avoir lieu ; il est, en particulier, possible de se rendre mieux compte du rôle joué dans ces processus par les radocaux libres (ou par des ions), dont la durée de vie à pression suffisamment basse est pratiquement illimitée. La nature des processus, dont l'étude peut être facilitée par des observations aeronomiques ou astrophysiques, est illustrée par deux exemples caractéristiques : la haute atmosphère terrestre et les atmosphères des cométes.

21.1. **Das Omegatron als Partialdruckmesser :** A. KLOPFER. Allgemeine Deutsche Philips Industrie, Aachen, Deutschland.

Es wird ein Omegratron aus Edelmetallelektroden beschrieben, bei dem es durch Anlegen eines geeigneten elektrostatischen Feldes und bei Verwendung einer zweckmässigen Kathode gelingt, Partialdrucke von Gasen und Dämpfen im Druckbereich unter 10^{-5} mm Hg mit einer Genauigkeit von 10% zu messen. Die Empfindlichkeit der Röhre bleibt auch bei längerem Einwirken von unedlen Gasen und Dämpfen, wie H_2O, CO_2 und CH_4 zeitlich konstant und ist unabhängig von dem jeweiligen Exemplar, solange die geometrischen Abmessungen eingehalten werden. Ein Vergleich der aus der Literatur bekannten Ionisierungswahrscheinlichkeiten mit denen aus den Eichkurven des Omegatrons berechneten Werten zeigt, dass praktisch alle vom Elektronenstrahl gebildeten Resonanzionen am Fonenkollektor aufgefangen werden. Die dafür notwendige Einstellung der Betriebsdaten ist im allgemeinen unabhängig von der Masse.

Die Einflüsse der Betriebsdaten auf den Fonenstrom werden mitgeteilt.

21.2. **Einfluss von Gasreaktionen in Vakuumsystemen auf die Zusammensetzung des Restgases :** E. BARONETZKY und A. KLOPFER. Allgemeine Deutsche Philips Industrie, Aachen, Deutschland.

Restgase in Vakuumsystemen können sowohl durch gegenseitigen Umsatz als auch durch Reaktion mit vorhandenen Bauteilen oder auch zufälligen Verunreinigungen ihre Zusammensetzung ändern. Diese wird gerade von der üblichen Messmethode oft stark beeinflusst. Daher ist bei der Beurteilung solcher Messergebnisse Vorsicht geboten. An Hand von einigen Beispielen wird gezeigt, wie sich Einflüsse von Druck und Temperatur geltend machen. Messungen über die Kinetik des Methanzerfalls an verschiedenen Kathoden werden wiedergegeben.

21.3. **Restgasanalysen mit dem Omegraton :** S. GARBE. Allgemeine Deutsche Philips Industrie, Aachen, Deutschland.

Der Vorteil des Omegatrons gegenüber anderen Massenspektrometern liegt in der Möglichkeit, in einem relativ kleinen, von der Pumpe abgeschlossenen Volumen bei sehr niedrigen Drucken Gasanalysen durchführen zu können. Der Aufbau einer Höchstvakuumapparatur aus Glas mit Metallhähnen für Gasabgabemessungen und Partialdruckanalysen wird beschrieben. Für permanente Gase können Gasabgabegeschwindigkeiten von einigen 10^{-10} Torr L/Min gemessen werden. Die Schwierigkeit, geringe Mengen stark adsorbierender Gase zu ermitteln, wird am Beispiel des Wassers erläutert. Wegen chemischer Reaktionen an heissen Oberflächen ist die Art der im Omegatron und auch in Ionisationsmanometern verwendeten Kathoden von ausschlaggebender Bedeutung auf das Analysenergebnis. Als Beispiel einer Restgasanalyse wird gezeigt, wie sich das Restgas über dem Bariumgetterspiegel einer Vakuumröhre mit L-Kathode im Betrieb ändert.

21.4. **Pressure Measurements at Ultra-high Vacuum (10^{-8} to 10^{-14} mm Hg) :** P. A. REDHEAD. National Research Council, Ottawa, Canada.

The techniques of pressure measurement in the range 10^{-8} to 10^{-14} mm Hg will be discussed. The construction and operating characteristics of a cold-cathode magnetron gauge will be described which can measure pressures in the range 10^{-4} to 5.10^{-14} mm Hg. This gauge has a linear relation between ion current and pressure and a sensitivity of 10 A/mm Hg (fifty times the sensitivity of a Bayard–Alpert gauge). Pressures of 5.10^{-14} mm Hg have been obtained in glass systems by the use of a liquid helium cold trap.

21.5. **Measurement of Ultra-high Vacua :** J. SCHUTTEN. Laborortorium voor Massaspectrografie, Amsterdam, Holland.

A review is given on the circuitry of methods to measure the pressure in high and ultra-high vacuum systems. One electronic circuit is dealt with in detail.

In an Alpert type of hot-cathode ionization gauge, the quotient of ion current over emission current is proportional to the pressure below 10^{-3} mm Hg. By measuring this quotient, the need for an emission stabilizer is eliminated, and no switching of high ohmic resistors is required in the normal range of 10^{-4} to 10^{-10} mm Hg.

22.1. **Erfahrungen mit Titan-Ionenpumpen :** A. KLOPFER und W. ERMRICH. Allgemeine Deutsche Philips Industrie, Aachen, Deutschland.

An Hand von Gasanalysen mit dem Omegatron wurde die Eignung der Titan-Ionenpumpen als Höchstvakuumpumpe untersucht. Zur Erreichung sehr niedriger Drucke erwires es sich dabei als notwendig, das gleiche Prinzip der Entgasungstechnik zu benutzen, wie es für Ionen- und Hg-Diffusionspumpen erforderlich ist. Einflüsse, die den erreichbaren Enddruck und die Auspumpzeit bestimmen, werden mitgeteilt.

22.2. **A Barium Getter-Ion Pump :** S. SIBATA, Japan Vacuum Engineering Co., Ltd., Tokyo, Japan ; C. HAYASHI, Japan Vacuum Engineering Co., Ltd., Tokyo, Japan ; H. KUMAGAI, Professor, Tokyo University, Tokyo, Japan.

A new type of getter-ion pump, using barium as a getter material, is developed. This pump consists of a main getter chamber (14 in. in diameter and 40 in. long) in which a barium evaporation source and gas-exciting electrodes are mounted, and a vacuum-distillation chamber in which barium is outgassed and distilled.

Barium is vacuum-distilled in the distillation chamber, flows through a thin tube into the crucible in the main chamber and evaporates at a rate of 5–10 μg/min.

The vacuum obtained is 1×10^{-4} μHg or better. The pumping speed for pure oxygen is about 5000 l/sec or larger. Its characteristics for various gases are also discussed.

22.3. **Characteristics of Titanium Evapor-Ion Pump :** H. KUMAGAI, Professor, Tokyo University ; C. HAYASHI, Japan Vacuum Engineering Co., Ltd., Tokyo ; Y. ISHIBE, Scientific Research Institute of Japan ; N. DOGI, Tokyo University ; G. TOMONAGA, Assis. Prof., Tokyo University ; H. SIBATA, Japan Vacuum Engineering Co., Ltd ; K. KANEKO, Tokyo University ; A. KATAYAMA, Scientific Research Institute of Japan ; K. SHINMA, Scientific Research Institute of Japan.

This paper describes some improvements on the design of the titanium evapor-ion pump originally designed by Prof. Herb. This also describes some experimental results obtained by the pump, which show the characteristics of the reaction of titanium on the gas in the pump. A slight change in the pump design brought a more stable operation of the pump—a few hundred hours without repair. Titanium easily reacts on oxygen and hydrogen without excitation. Water vapor and perhaps also nitrogen are more efficiently sorbed by titanium with the aid of excitation or dissociation caused by energized electron current in the space.

22.4. **Pompe Getter à Piège à Très Basse Température :** P. PRUGNE et P. GARIN. C.E.N. Saclay, France.

Présentation d'une pompe à évaporation de getter équipée d'un piège à très basse température.

Une série de courbes de vitesses de pompagne pour différents gaz et pour l'air est donnée.

Une application de cette pompe est décrite.

VO 9 1959

22.5. **Ionen-Getterpumpe für Niedrige Drucke :** G. REICH. E. Leybold's Nachfolger, Köln, Deutschland.

An Ionen-Getterpumpen, die beispielsweise für grosse Kernmaschinen eingesetzt werden sollen, werden zwei wesentliche Forderungen gestellt :

(1) Niedriger Enddruck.

(2) Betriebssichere Arbeitsweise über mehrere Monate.

Es wird eine grosse Pumpe mit Sauggeschwindigkeiten zwischen 500 und 5000 l/s beschrieben, die diese Forderungen dadurch erfüllt, dass der Gettermetallvorrat vor Inbetriebnahme ausgeheizt wird und dass durch eine automatische druckabhängige Steuerung des Verdampfers der Gettermetallverbrauch auf ein Minimum herabgesetzt wird.

Es wird weiter über Ergebnisse eingehender Untersuchungen über den Aufzehrmechanismus berichtet, die durch Partialdruckanalysen mit dem Omegatron gewonnen wurden.

22.6. **Sur un Principe Nouveau de Réalisation de la " Pompe à Évaporation de Titane " :** A. SCHRAM. Compagnie Générale de Radiologie, Paris, France.

L'évaporation de titane dans une pompe pose des problèmes difficiles et dont les solutions apportées jusqu'aujourd'hui restent plus ou moins délicates, en particulier : le creuset ou le support sur lequel le titane s'évapore, le système d'alimentation en fil de titane, et le système de chauffage du titane.

A partir des systèmes à cathode froide, on peut obtenir des décharges électriques si intenses et si courtes qu'une cible massive de titane soit portée superficiellement, sans échauffement notable de la masse, à des températures dépassant de loin le point de fusion.

De telles décharges périodiques permettent d'obtenir une importante évaporation de titane, sans qu'aucun élément soit porté à haute température, sans creuset et en utilisant du titane sous forme massive, en cylindre ou plaques par exemple.

Par un tel procédé, une evaporation de 15 mg de titane par min avec 200 W a été obtenue.

23.1. **Adsorption and Desorption of Positive Ions on Glass and Metal Surfaces :** J. H. LECK. University of Liverpool, Liverpool, United Kingdom.

Observations have been made of the amount of the inert gases adsorbed on to glass and metal surfaces in high vacuum systems. In the case of the metals adsorption was brought about by bombarding the surfaces with ions of the inert gases with energies up to 5000 eV. Subsequently the surfaces were degassed by heating. The total quantity of gas desorbed was measured by using a mass-spectrometer as the detecting element. The mass-spectrometer enables accurate measurements of small desorption transients to be made against a large and fluctuating background pressure.

Results obtained for tungsten, nickel and platinum show the total quantity of gas taken up to increase with increasing energy of the bombarding ions to such a value as to be equivalent to a complete surface layer for an energy of 5000 eV. Temperatures of the order of 800°K are required to remove the gas, thus showing binding energies much higher than for physical adsorption. It has also been noted that the ions can dislodge, and take the place of, molecules already adsorbed at the surface. The ion bombardment was also found to allow the release of impurities such as potassium and sodium from the metal targets. This was especially true for tungsten, where after a bombardment of ions a subsequent heating produced a short burst of potassium and sodium positive ions from the target surface.

No quantitative measurements of the intensities or energies of the incident ions on to glass surfaces have yet been undertaken ; all the measurements have been made at the glass envelope of the Bayard–Alpert type ionization gauges. It has been shown, however, that stable adsorption takes place, again with a comparatively large binding energy, which does not appear to be constant over all the adsorption sites. For example, for argon, in order to release all the inert gas molecules from the surface baking temperatures in the range 500–600°K must be used.

*23.2. **The Attainment of Clean Surfaces by Breaking Crystals in Ultra-high Vacuum :** P. C. BANBURY, G. A. BARNES, D. HANEMAN and E. W. J. MITCHELL. University of Reading, Reading, United Kingdom.

23.3. **Hydrogen Adsorption and its Effect on the Resistance of Evaporated Nickel films—An Application of Ultra-high Vacuum :** T. ICHIMIYA and Z. ODA. Nippon Telegraph and Telephone Public Corporation, Tokyo, Japan.

The gas adsorption phenomena on metal surfaces are very sensitive to the cleanliness of the surface. Therefore, in order to investigate the interactions between gas and metal surface fundamentally, it was required to attain the ultra-high vacuum and carry out the experiment in it. As an example of the application of ultra-high vacuum technique, the change of electric resistance of evaporated nickel films due to the adsorption of hydrogen under various conditions is investigated.

By gas adsorption the resistance increases on very clean films, while it decreases on contaminated films. Experiments show that this decrease is due not to the oxygen pre-adsorbed on the surface, but to that which has diffused into nickel lattice. There are two sorts of reversal in resistance change during adsorption : one occurs on a very clean film at −183°C and the other on a film containing a small amount of oxygen at 0°C. The former is considered to be an inherent property on nickel film connected to adsorption mechanism, while the latter is a spurious one due to oxygen. The degree of vacuum which can guarantee the cleanliness of the film will be discussed.

31.11. **Factors Controlling the Ultimate Pressures Obtainable in Large Nuclear Physics Vacuum Systems :** J. BLEARS, E. J. GREER and J. NIGHTINGALE. Metropolitan-Vickers Electrical Co., Manchester, United Kingdom.

The paper presents new data on the rates of degassing and thermal decomposition of the more commonly used high vacuum materials, including synthetic resins. It gives an account of an investigation of the relative performance of large cold traps, activated carbon and alumina adsorption traps and refrigerated baffles. Observations on transient pressure changes following changes in system temperature are compared with analogous phenomena observed during the baking of vacuum gauges.

31.12. **Some Vacuum Problems at Low Temperatures :** R. BUDDE. CERN, Geneva, Switzerland.

There will be discussed some sealing techniques for metal-metal and metal-glass seals that have been developed and tested for the use at high vacuum and low temperatures. Hand- and pneumatically-operated valves for liquefied gases have been designed, and are now in use in a vacuum system. Some equipment industrially available has been used with or without having been adapted, and will be discussed, as well as the properties of some materials which were found to be useful in the vaccum-low temperature range.

31.13. **Vacuum Techniques in Mass Spectrometry :** J. BISHOP. United Kingdom Atomic Energy Authority, Capenhurst, United Kingdom.

This paper gives a survey of some of the vacuum techniques used and experience gained in a laboratory engaged on design, operation and development of high-precision mass spectrometers. The performance of the mass spectrometer is critically dependent on both the quantity and the type of the residual gases in the vacuum system and the developments in vacuum techniques have been aimed at reducing these. Illustrations are given of types of gaskets which can permit brake-out temperatures of the vacuum system to be extended up to 450°C, together with a suitable copper analyser tube. Designs of improved baffles for the reduction of back-streaming from mercury pumps and of greaseless seals for rotating shafts are given.

31.21. **Automatische Steuerung in der Hochvakuumtechnik :** K. H. MIRGEL. E. Leybold's Nachfolger, Köln, Deutschland.

Vol. 9 959/60

Es wird über Erfahrungen berichtet, die bei der Sicherung und beim automatischen Betrieb von Hochvakuumpumpständen gemacht wurden.

Bei den Störungsursachen, gegen die ein Pumpstand gesichert werden muss, wurde untershieden zwischen Störungen, die schnelle und schwerwiegende Auswirkungen zeigen, und solchen, die nur langsam wirksam werden. Ferner wird berichtet über die Erfahrungen mit der Schaltgeschwindigkeit verschiedener Stellglieder (Ventile). Abschätzung der notwendigen Schaltgeschwindigkeit zur Verhütung grösserer Schäden in Pumpständen.

*31.22. **Vacuum Techniques and Components used for a Continuously Pumped Linear Electron Accelerator :** R. C. MARKER. Applied Radiation Corporation, Walnut Creek, Cal., U.S.A.

31.23. **The CERN Proton Synchrotron Vacuum System. Part I :** G. L. MUNDAY. CERN, Geneva, Switzerland.

The vacuum problems of the alternating gradient proton synchrotron are discussed.

The system to be pumped is a tube whose conductance varies along its length and in which a mean pressure of 10^{-5} Torr or less must be achieved.

Questions related to the vacuum chamber are outlined and their solutions are discussed.

31.24. **The CERN Proton Synchrotron Vacuum System. Part II :** B. MONNIER. CERN, Genève, Suisse.

En relation avec les données du Synchrotron à Protons du CERN, en particulier avec les impératifs en pression et dans le dessin de la chambre à vide, le choix du système de pompage sera expliqué. Le nombre, la répartition, et la composition des groupes de pompage, le système de controle seront successivement commentés.

31.25. **Calculation of Pressures in Toroidal Vacuum Chambers :** J. BLEARS. Metropolitan-Vickers Electrical Co., Manchester, United Kingdom.

A general numerical treatment is given for the problem of rapidly calculating the partial pressures due to degassing and leakage in toroidal vacuum chambers pumped at two or more stations.

31.26. **Zur Automatisation von Hochvakuumanlagen unter besonderer Berücksichtigung der bei einem Zirkular-beschleuniger vorliegenden Verhältnisse :** R. HAEFER. Gerätebau Anstalt Balzers, Fürstenstum Liechtenstein.

Es wird zunächst die Wirkungsweise einer Reihe von neu entwickelten und für die Automatisation von Pumpständen notwendigen Kontrollorganen, insbes. Vakuumwächtern für den Hoch- und für den Feinvakuumbereich beschrieben. Am Beispiel eines Pumpstandes für einen Zirkularbeschleuniger wird dann gezeigt, wie durch das Zusammenspiel dieser Kontrollorgane mit pneumatischen bzw. magnetischen Ventilen (1) ein vollautomatischer Ablauf des gesamten Pumpvorganges und (2) ein Schutz der Anlage vor Unfällen verschiedener Art erreicht werden kann. Die elektrische Schaltung ist dabei so beschaffen, dass der automatische Ablauf auch ausser Kraft gesetzt werden und eine willkürliche Betätigung der einzelnen Bauelemente möglich ist.

*31.27. **Vacuum System for a Thirty Billion Electron Volt Particle Accelerator :** C. L. GOULD. Brookhaven National Laboratory, N.Y., U.S.A.

31.28. **Groupes de Pompage Automatiques pour Accélérateurs de Particules :** H. MEYER. Firenze, Italie.

Exposition des critères pour l'application de dispositifs automatiques pour le fonctionnement des installations de vide destinées aux accélérateurs de particules élémentaires.

Ces dispositifs doivent respecter trois exigences fondamentales :

La possibilite de faire fonctionner les installations de façon automatique, d'après un programme préétabli, basé sur une seule commande initiale.

La nécessité d'avoir—sur place ou à distance—la signalisation automatique d'alarme qui prévient d'une avarie éventuelle, en indique la nature et la localisation, et signale en même temps la " mise en défense " ou protection du système.

La nécessité de prévoir ces dispositifs automatiques d'une manière universelle et adaptable à tous les cas, de façon qu'il soit possible de les appliquer à tous les types d'accélérateurs en tenant compte des exigences particulières de chaque installation.

31.31. **Die Anwendung der Vakuumtechnik bei der Herstellung von Reaktor-Baustoffen :** H. HARDUNG-HARDUNG. Degussa, Wolfgang, Deutschland.

Die hohen Reinheitsforderungen bei der Herstellung und Verarbeitung von Reaktorbaustoffen sowie die besonderen Eigenschaften einiger Reaktormetalle machen besondere Dimensionierungen bei den in einigen Verfahrensstufen notwendigen Vakuum-Apparaturen notwendig. Für das Schmelzen und Giessen von Reaktormetallen werden sowohl spezielle Induktions—wie auch Lichtbogenöfen verwendet. Die Vakuum-Sublimation von Reaktormetallen erfordert beim Apparatebau Berücksichtigung der Dampfdruckkurven von unerwünschten Verunreinigungen. Beim Sintern von Reaktorwerkstoffen sind die Verunreinigungsmöglichkeiten durch abdampfendes Heizleitermaterial sowie eine unüblich hohe Temperatur-Konstanz zu berücksichtigen. Für chemische Reaktionen, die der Herstellung von Reaktorwerkstoffen dienen, finden Spezialöfen Verwendung, die wegen der hohen Temperaturen vielfach mit Stützvakuum arbeiten.

31.32. **Application de la Technique du Vide à la Préparation et à la Purification de Certains Fluorures, Notamment du Tétrafluorure de Zirconium :** C. DECROLY, J. GÉRARD et D. TYTGAT. Centre d'Étude de l'Énergie Nucléaire, Mol, Belgique.

Les auteurs donnent un bref aperçu d'un mode de préparation du tétrafluorure de zirconium pur. On montre notamment comment on a tiré parti des avantages offerts par la technique du vide en vue de la purification de ce tétrafluorure.

En outre, on décrit certaines dispositions auxquelles on a jugé nécessaire d'avoir recours pour protéger le matériel à vide contre l'action corrosive de certains des produits mis en oeuvre.

31.33. **Diode pour Essais de Transmission de Chaleur :** C. BEERNAERT et B. BLANC. Commissariat à l'Energie Atomique, Saclay, France.

But : L'étude des éléments combustibles exige la réalisation de barreaux chauffants où l'on essaie de réaliser les gradients de température qui seront rencontrés en pile. Les flux calorifiques à obtenir sont donc très importants et il est nécessaire d'utiliser un moyen de chauffage puissant, facilement réglable, et acceptant des températures élevées de combustible. L'appareil décrit répond à ces 3 impératifs.

Principe : Le barreau est chauffé intérieurement par bombardement électronique.

Description de l'appareillage : Circuits de pompage et caractéristiques électriques—mesures thermiques.

Exemples d'applications : Détermination de la chute au contact barreau-gaine. Etude de l'évolution du gainage type contact lors des cyclages. Etude de corrosion sous flux importants.

31.34. **Soudure par Bombardement Électronique :** J. A. STOHR et J. BRIOLA. Commissariat à l'Energie Atomique, Saclay, France.

Ce procédé de soudage a été récemment mis au point au Commissariat à l'Energie Atomique en France. Il consiste à utiliser, pour fondre les lèvres des pièces à souder, l'impact d'un faisceau d'électrons produit par un canon à électrons. Le soudage s'effectue sous un vide de 10^{-4} à 10^{-6} mm Hg.

La machine à souder se compose schématiquement :

(a) d'une enceinte métallique où l'on fait le vide.

Vo 9 1959

(b) d'une cathode émettant des électrons,
d'un générateur H.T. permettant d'accélérer ces électrons,
d'un dispositif de focalisation.

Advantages de ce procédé :

(1) possibilité de souder les métaux trés oxydables (ex. zirconium),
(2) réalisation de " containers " métalliques fermés sous vide poussé,
(3) obtention de profondeurs de soudure considérables.

Ce nouveau procédé est donc particulièrement intéressant pour l'énergie atomique, la fabrication des tubes électroniques et en général toutes les industries utilisant des métaux très spéciaux.

31.35. **Fusion sous Vide de l'Uranium :** Y. ORTEL et H. OLLIER. Commissariat à l'Energie Atomique, Saclay, France.

Fusion et coulée sous vide de l'uranium : description et mode de fonctionnement de l'appareillage utilisé ; description du groupe de fonderie proprement dit, qui comporte un inducteur alimenté en moyenne fréquence et placé à l'extérieur de la chambre de fusion. Brève description des auxiliaires : pompes, groupes d'alimentation et leurs possibilités de couplage, appareils de mesures diverses : électriques, thermiques et de vide.

Principe : description, utilisation de dispositifs destinés à améliorer l'utilisation du groupe de fonderie, tant au point de vue rendement qu'efficacité :

(a) vanne à clapet détachable permettant de tripler l'utilisation,
(b) dispositif de double coulée permettant un dégazage considérablement amélioré,
(c) système de déclenchement de la coulée par rupture de membrane, cette commande pouvant s'effectuer de divers points.

31.36. **The Application of High Vacuum Techniques to the Production of Special Materials of Interest to Nuclear Reactors :** L. R. WILLIAMS. Research and Development Branch UKAEA/IG, Salwick, Nr. Preston United Kingdom.

Considerable attention has been devoted during recent years to the development of materials capable of withstanding the severe operational conditions pertaining in the central core of nuclear reactors. This has resulted in the development of production and fabrication techniques for a number of unusual metals, some of which were formerly in the category of metallurgical curiosities. The paper discusses some of the more interesting applications of vacuum techniques associated with the metallurgical processing of both fuels and canning materials. Particular attention is devoted to the vacuum requirements associated with the sintering and fabrication of the two refractory metals niobium and vanadium. The paper concludes with a brief survey of future trends in this field.

32.11. **Überblick über die derzeitige Anwendung der Vakuumtechnik in der Metallurgie :** W. H. Scheibe. Degussa Wolfgang, Deutschland.

In einem kurzen Überblick werden die vakuumtechnischen Mittel besprochen, die heute bei der Herstellung und Verarbeitung von Metallen sowie in der Metallforschung eingesetzt werden.

32.12. **Effect of Ambient Pressure on the Oxygen Content of Nickel, Iron, and their Alloys at Vacuum Melting :** K. MURAMATSU. Tokyo Shibaura Electric Company, Kawasaki, Japan.

In the cases of the vacuum melting of nickel, iron, and their alloys, relation between oxygen content of their ingots and ambient air pressure at melting has been studied. The melting was carried out in an alumina crucible in a reduced atmosphere whose pressure was varied in the range between 10^{-5} and 10^{1} mm Hg, and each melt of 2.5 kg was poured into a water-cooled copper mould at a temperature approximately 50°C above the melting point.

The rate of decrease in oxygen content with reducing oxygen partial pressure is great in nickel, but little in iron. For example, the oxygen content in the case of melting at 5×10^{-5} mm Hg was 0.002 and 0.07 wt.% in nickel and iron respectively, while at 5×10^{-2} mm Hg it was 0.007 and 0.08 wt.%

Oxygen contents in Fe–Ni alloys of various constituents melted at 5×10^{-5} or 5×10^{-2} mm Hg were measured, but strict linear relation was not found.

32.13. **Über den Einfluss von Sauerstoff, Stickstoff und Kohlenstoff auf die mechanischen Eigenschaften von Nickel- und Chromstählen :** W. H. SCHEIBE. Degussa Wolfgang, Deutschland.

In seither veröffentlichten Arbeiten konnten die Kerbschlagzähigkeit und die Härte von Eisen-Chrom-Legierungen nicht in eine eindeutige Beziehung zum Sauerstoffe-, Stickstoff- und Kohlenstoffanteil gebracht werden, da andere Legierungsbestandteile z.B. Silizium und Mangan zu stark variierten.

Durch saubere Versuchsführung mit hoher Analysengenauigkeit konnten die direkten Abhängigkeiten ermittelt werden.

32.14. **Die Entgasung von Stahl durch das Vakuum-Giessstrahlverfahren :** W. COUPETTE. Bochumer Verein, Bochum, Deutschland.

Die Aufteilung des Strahles in Tröpfchen beim Vakuumblockguss und Durchlaufentfasung. Die Grösse der Tröpfchen und ihre Grössenbestimmung. Erreichung der Wasserstoffwerte nach dem Sievert'schen Gesetz in kürzester Zeit. Durch Senkung des Wasserstoffgehaltes Erzielung von Flockenunempfindlichkeit bei Schmiedestücken und Halbzeug. Bei beruhigtem Stahl wesentliche Verringerung der oxydischen Einschlüsse, bei unberuhigtem Stahl Senkung des Sauerstoffgehaltes bis zu 1/10 des Ausgangswertes. Zugabe von Desozydationsmitteln und Legierung im Vakuumgefäss. Bewegliche Anlage. Kontinuierliche Entgasung. Aufteilung des Entgasungsvorganges in zwei oder mehrere Druckstufen. Wesentliche Einsparung von Pumpenleistung durch Abführung von Gasen bei höheren Drücken. Hierbei Erreichung von Drücken in der Endstufe in der Grössenordnung des Vakuum-Schmelzofens. Gute Möglichkeiten von Wärmezufuhr und metallurgischen Schlackenreaktionen in der Vorstufe. Guss von kleinen Blöcken bei Stufenentgasung unter Vakuum.

32.15. **Über den Reaktionsablauf bei der Vakuumentgasung von Flüssigem Stahl :** O. WINKLER und T. KRAUS. Gerätebau-Anstalt, Balzers, Fürstentum Liechtenstein, Deutschland.

Bei der Vakuumentgasung von Stahl steht die Entfernung des Wasserstoffs zur Verringerung der Flockenanfälligkeit und die Sauerstoffentfernung zur Verringerung der oxydischen Einschlüsse im Vordergrund.

Es ist bekannt, welche Lösungsgleichgewichte bei einem gegebenen Partialdruck dieser Gase erzielt werden können. Diese geben aber keine Aussage darüber, welche Werte mit den heute gebräuchlichen Entgasungsverfahren tatsächlich erriechbar sind.

Es wird untersucht, welche Faktoren für den Reaktionsablauf geschwindigkeitsbestimmend sein können, und auf Grund der entwickelten Vorstellungen über den Transport-Mechanismus abgeschätzt, welche Gasgehalte theoretisch erreichbar sein müssten. Sie werden den Werten gegenübergestellt, die in der Praxis, insbesondere beim Vakuum-Induktionsschmelzen und bei der Durchlaufentgasung, erreicht werden.

32.16. **Anlagen zum Sintern im Vakuum :** A. BUSSARD. W. C. Heraeus, Hanau/Main, Deutschland.

Übersicht über die verschiedenen Beheizungsarten sowie Abgrenzung der Verwendungsbereiche, direkte Widerstandserhitzung, indirekte Widerstandserhitzung, sowie Induktionserhitzung mit direkter Ankopplung und mit Hilfselementen.

Übersicht über die vakuumtechnischen Gesichtspunkte unter Berücksichtigung der Betriebserfahrungen, Abgrenzung der Anwendungsbereiche verschiedener Pumpsysteme bezüglich Sauggeschwindigkeit und Verschmutzungsanfälligkeit.

Gaskinetische Gesichtspunkte bei der Auslegung von Sinter- und Glühtiegeln sowie Hilfszylindern.

Praktische Ausführungsbeispiele.

Vol. 9 959/60

32.17. **Behandlung von Stahl im Vakuum :** L. BANGERT. W. C. Heraeus, Hanau/Main, Deutschland.

Qualitätsverbesserungen von Stählen durch Vakuumbehandlung beruhen auf zwei Erscheinungen :

1. Der Gasgehalt wird reduziert, dies bezieht sich in erster Linie auf die Gase Wasserstoff, Sauerstoff, Stickstoff.
2. Durch die den Erfordernissen der Vakuumtechnik agepasste Versuchsführung erhält man bereits ein Gussgefüge, das sich von dem Gefüge der auf herkömmliche Weise vergossenen Stahlblöcke unterscheidet. Der wohl entscheidende Parameter ist die meist erhöhte Erstarrungsgeschwindigkeit, die sich auf die Primärkorngrösse und auf die Ausscheidung der intermetallischen Phasen sowie der Karbide und Nitride günstig auswirkt.

Als Beispiel für die erste Gruppe wird ein Stahlentgasungsverfahren beschrieben, bei dem die Gasentfernung in der Giesspfanne vorgenommen wird bzw. in einer in sie eintauchenden Vakuumapparatur. Das Verfahren zeichnet sich durch apparative Einfachheit, bequeme Einbaumöglichkeit in den Arbeitsablauf eines Stahlwerkes sowie durch wirksame Entgasung aus. Der Giessvorgang erfolgt aus der Pfanne in herkömmlicher Weise.

Als Beispiel für die zweite Gruppe werden die Qualitätsverbesserungen beschrieben, die man beim Umschmelzen von hochwarmfesten Stählen im Vakuum-Lichtbogenofen erzielt. Neben der Gasentbindung im Lichtbogen selbst (hohe Temperaturen) und im Schmelzsee, erhält man, bedingt durch die schnelle Abkühlung, ein Erstarrungsgefüge, das sich durch Feinkörnigkeit und homogene Verteilung der intermetallischen Phasen sowie der Karbide und Nitride auszeichnet. Diese Gefügeausbildung bewirkt eine wesentlich verbesserte Schmiedbarkeit im Vergleich zu den an Luft in Kokillen vergossenen Blöcken.

Abschliessend soll über orientierende Versuche berichtet werden, die mit dem Ziel angelegt wurden, oxydische Einschlüsse aus Kugelager bzw. Wälzlagerstahl zu entfernen, sowie plastische Einschlüsse, wie z.B. Sulfide, feiner zu verteilen.

32.31. **High Vacuum Furnace for Laboratory Use :** T. NAGASHIMA. Electrotechnical Laboratory, Tokyo, Japan.

The vacuum furnace described in this paper is capable of melting the metals by ordinary radio-frequency induction-heating from the outside of the furnace, and of casting the melt in vacuum. The furnace consists of 2 rooms, one for melting and the other for casting. When a metal was melted down and degassed in a silica tube, the crucible which is hung with 2 steel wires is wound up by a pair of pulleys and brought into the upper casting-room. Then the crucible is rotated by a rotating system and the melt is poured into a mould placed in a suitable position. Such a mechanism makes it very easy to melt and cast in high vacuum ($\sim 3 \times 10^{-5}$ mm Hg) within a short time ($\sim$1 hr). The pumping system consists of 4 in. oil diffusion pump of 200 l/sec and a mechanical pump of 400 l/min. The electric power is supplied by a 5 kW radio oscillator with 400 kc. The maximum melting capacity may be as large as 1 kg.

For larger capacities over 3 kg, some modifications were done, especially in the moving system of the crucible. In this furnace, instead of hanging the crucible with wires, the crucible is supported with a rigid rod which can be moved vertically.

The furnace was shown to be very convenient and useful for laboratory use, and we have got metals having excellent workability, improved magnetic properties, and other interesting properties.

32.32. **The Effect of some Heat Insulators as an Element of a High Temperature Vacuum Furnace :** S. YASAKAWA. Tokuda Seisakusho Co., Ltd., Tokyo, Japan.

Two methods of heat insulation in high temperature vacuum furnace are discussed. One is metal reflector system and another is powder insulation method. Either a single or a complex method is used according to the purpose.

On application of heat insulation for large vacuum furnace of industrial scale, it is very important to select the best suitable materials to economize the operation costs.

It is advisable to use the metal reflector in temperature below 1500°C. However, over the temperature 2000°C the powder insulation method is more effective and economical.

Experiments have been carried out in several industrial vacuum furnaces to consider the properties of the graphite powder as an insulator in high temperature, artificial graphite for electrodes, as well as the heat shield effect of metal reflector.

32.33. **Neuentwicklungen bei technischen Lichtbogenöfen :** H. GRÜBER und H. SCHEIDIG. W. C. Heraeus, Hanau/Main, Deutschland.

Bedeutung und Verwendung des Vakuum-Lichtbogenschmelzens bei reaktiven Metallen. Vakuum-Lichtbogenschmelzen in der Stahl-Industrie. Vergleich mit anderen Vakuumverfahren für Stahl. Technische Entwicklungstendenzen. Möglichkeiten der Reduzierung der Schmelzkosten.

32.34. **Fours de Traitement Sous Vide Continus et Discontinus Résultats Obtenus pour le Frittage des Métaux Ordinaires :** M. EUDIER. Conservatoire National des Arts et Métiers, Paris, France.

La communication comprend une étude des types principaux de fours sous vide discontinus, et de leurs caractéristiques. Ils sont comparés aux fours à atmosphère controlée tant au point de vue économique qu'au point de vue des résultats en métallurgie des poudres.

Il résulte de cette étude que les fours actuels sont souvent peu économiques lorsqu'ils rendent des services comparables aux autres fours. Il est possible de les améliorer en les adaptant à des conditions de travail précises particulièrement en fonction de la température d'utilisation.

Les fours continus constituent un progrès considérable. Les difficultés de construction sont largement compensées par l'amélioration du rendement. Quelques types de fours continus sont étudiés à cet égard et quelques résultats sont donnés sur les propriétés mécaniques que l'on peut obtenir par frittage dans de tels fours.

Ces propriétés, qui sont très voisines de celles des métaux coulés et forgés et même leur sont parfois supérieures, ne seront utilisables que par l'adoption de méthodes nouvelles pour la fabrication des outillages.

32.41. **Application de la Méthode de Fusion Sous Vide à l'Étude des Gaz Occlus dans les Métaux :** B. ROSEN. Institut d'Astrophysique de l'Université de Liège, Belgique.

A la méthode chimique usuelle d'analyse des gaz libérés par la fusion sous vide, l'auteur a substitué une méthod spectroanalytique, basée sur l'excitation électrique de bandes moléculaires appropriées. Pour le dosage de l'oxygène en particulier, on peut utiliser les bandes de l'oxyde de carbone qui se forme par suite de la réaction de l'oxygène libéré avec les parois du creuset en graphite. L'intensité des bandes appartenant aux différents systèmes de CO varie d'une façon inégale en fonction de la pression. La détermination du rapport d'intensité des bandes appartenant aux différents systèmes, permet par conséquent de doser l'oxygène libéré des échantillons. L'utilisation de filtres optiques et de dispositif électronique de mesure permet un dosage rapide et précis, ne nécessitant pas de spectrographe.

32.42. **Coulée Sous Vide de l'Acier pour Pieces de Forge à la S.A. Cockerill-Ougree—Equipments—Premiers Résultats Obtenus :** J. LEVAUX et L. HANNON. S. A. Cockerill-Ougrée, Seraing, Belgique.

Les gaz contenus dans l'acier liquide ont une influence néfaste sur la qualité des pièces de forge. La coulée sous vide de l'acier permet d'abaisser les teneurs en gaz en dessous des niveaux dangereux.

Dans cette technique, on vise avant tout l'élimination de l'hydrogène. Cette élimination permet au forgeron de raccourcir ses traitements thermiques. L'acier obtenu de cette façon permet de fabriquer des pièces de forge plus compactes et de meilleure qualité.

Vo
9
1959

La S. A. Cockerill-Ougree utilise couramment ce procédé pour la fabrication de ses pièces de forge et de certains de ses aciers spéciaux.

33.11. **Residual Gases in Vacuum Systems and their Effects on Oxide Cathodes :** N. W. ROBINSON. Mullard Research Laboratories, Salford, United Kingdom.

An experimental examination has been made of the gases desorbed from tungsten in a glass envelope at pressures of 10^{-10} mm Hg. Two gas phases are found at desorption temperatures of 100°C and 250°C respectively and two phases at 1000°C approximately. One of the gases desorbed at 1000°C is not adsorbed by the glass while the other three are evident for a few seconds only since they are readily adsorbed by the glass. The heats of adsorption have been measured. An oxide cathode on a tungsten base was poisoned by the gases given off at the higher temperatures but not those at the lower temperatures. The poisoning persisted for an appreciable time after the gas had been adsorbed. It is thought that the poisoning due to transient gases desorbed from metals in vacuum-tubes is one of the contributory causes shortening the lives of oxide cathodes.

33.12. **Electrical Clean-up Phenomena in Electron Tube :** K. M• YAZAWA. Matsuda Research Laboratory, Tokyo Shibaura Electric Co., Ltd., Japan.

The electrical clean-up phenomena as well as the gettering phenomena of active metals have been measured. The electrical clean-up phenomena are more striking than the gettering ones in the high vacuum ($<10^{-4}$ mm Hg).

The effect of electrical clean-up depends on the anode current, vacuum degree and electron path fixed by the voltage of electrodes. The rate of clean-up accords with the value of calculation in the low vacuum region (10^{-2} — 10^{-4} mm Hg), but it does not accord with the line calculated, decreasing in the high vacuum (10^{-5} — 10^{-6} mm Hg).

The differences of values (litre-micron Hg) between the calculation and measurement are nearly equal at each stage. So, these differences seem to show gases desorbed from the wall, and the vacuum degree of tube is fixed as result of equilibrium of sorption and desorption. The gases cleaned-up are not found on the surfaces of the cathode and positive electrode, and the small quantity of gases are found at the negative electrode, the gases are sorbed on the surface of the decontaminated glass bulb by which there are many electron paths.

33.13. **Erfahrungen über den bypass-losen Betrieb von Hochvakuum-Pumpständen :** R. HAEFER. Gerätebau Anstalt Balzers, Fürstenstum Liechtenstein.

Es werden Ergebnisse mitgeteilt über das Verhalten verschiedener Typen von bypass-losen Pumpständen, wie sie z.B. bei der Aluminiserung von TV-Röhren, als Troley in der Röhrenfabrikation, bei Bedampfungsanlagen und in der Höchstvakuumtechnik üblich sind.

33.14. **Conditions Optima pour le Pompage des Tubes à Vide :** Madame J. BAILLEUL-LANGLAIS. La Radiotechnique Suresnes, France.

Si tout technicien du vide sait prendre un queusot, une pompe à diffusion, une pompe à palettes pour vider un tube, il ne sait pas toujours choisir ces éléments de la façon la plus judicieuse. Il ne pense souvent qu'à la première partie de l'opération qui consiste à amener la pression à l'intérieur du tube, de la pression atmosphérique jusqu'à " un bon vide ", se souciant peu des valeurs atteintes pendant la deuxième partie du pompage. Or, il apparait aujourd'hui bien plus important de pomper rapidement les gaz au cours de la décomposition des carbonates que d'atteindre une basse pression finale.

Cette nouvelle conviction peut amener les fabricants de tubes à revoir leurs conceptions en matière de systèmes de pompage. Nous étudierons donc rapidement comment il faut concevoir rationnellement un système à vide en fonction des débits demandés au système et nous appliquerons ces considérations au cas du pompage d'un tube à vide.

*33.15. **Design Approaches for Electron Devices Operating in Critical Environments, Especially Ceramic-Envelope Tubes for High-Temperature Operation :** W. H. KOHL. Electronics Research Laboratory, Stanford University, Stanford, California, U.S.A.

33.21. **The Structure and Sorption of Barium Getter Films :** T. ICHIMIYA, Y. MIZUSHIMA and Z. ODA. Nippon Telegraph and Telephone Public Corporation, Tokyo, Japan.

The electrical resistance and nitrogen sorption at −183°C were measured for Ba films evaporated and heat-treated under various conditions. The conditions which controlled the properties of the film were :

1. Temperature of the tube wall during deposition ;
2. Temperature of annealing, and
3. Pressure of residual gas during deposition.

Comparing the temperature variation of electrical resistance with sorption property for nitrogen, it was confirmed that the lattice imperfections as well as grain boundary can contribute to the enlargement of adsorption capacity.

33.22. **Ein neuartiger, metallischer Getterstoff :** E. BARONETZKY. Allgemeine Deutsche Philips Industrie, Aachen, Deutschland.

Durch Zusatz von Silber und anderen edleren Metallen kann man die gasaufzehrenden Eigenschaften von Thoriumaluminiumlegierungen bei Raumtemperatur, insbesondere die autokatalytische Wasserstoffgetterung nach vorheriger Oxydation mit reinem Sauerstoff, und die Aufzehrung von Kohlenmonoxyed beträchtlich steigern. Es wird versucht, eine Deutung des Effekts des Silberzusatzes zu geben. Im System Th_2[Al, Ag] bilden Th_2Al und Th_2Ag eine lückenlose Reihe von Mischkristallen.

33.23. **On the Flashing of Barium Alloy Getter :** K. M. YAZAWA. Matsuda Research Laboratory, Tokyo Shibaura Electric Co., Ltd., Japan.

As results of measuring the rate of sublimation or evaporation of simple metal getters (i.e. Ba, Mg, or Al), the values obtained by experiments accord with the values induced by calculation in the high temperature region, but in the lower temperature region the former is very small. This is due to the stable thin film existing on the metal surface that prevents the sublimation of metal. It is possible to remove the film beforehand by mechanical or chemical polishing. Soon after the metal covered with a film boils in a vacuum up to above its melting point, the film splits and then from the splits the fresh metal flashes suddenly.

Many intermetallic compounds are used generally as alloy getters, because of their stable character in the atmosphere. The melting point of intermetallic compound (e.g. $BaAl^4$) is higher than that of each component, so flashing temperature will increase over is melting point of alloy. It seems to be at the flashing that the alloy becomes liquid perfectly, and the active metal atoms diffuse out easily to the surface and evaporate immediately. The vapor pressure of metal component in the alloy decreases more than that of simple metal in accordance with the quantity of the other component, and the reasonable value is gained by employing Raoult's equation.

Notwithstanding that the addition of the third metal to the alloy decreases the melting point of the alloy, if the vapor pressure of the active metal component is maintained considerably, the new alloy will serve as a flash getter that forms the active deposit having an amorphous construction. Because its flashing temperature is a little lower, the deposit metal has a little kinetic energy, and the wall is not heated by the radiation from the getter source.

33.24. **Essais quantitatifs des Getters :** Madame J. BAILLEUL-LANGLAIS. La Radiotechnique Suresnes, France.

(1) Nous définirons les grandeurs essentielles à considérer : absorption totale, puissance d'absorption, vitesse d'absorption. (2) Nous énumérerons les paramètres dans l'étude de l'absorption des getters : ceux qui sont dûs au getter, ceux qui sont dûs au gaz à pomper. (3) Nous rappellerons très brièvement les

Vol. 9 959/60

méthodes de mesure insistant particulièrement sur les conditions de travail à réaliser pour que les valeurs obtenues soient absolument indépendantes de l'appareillage de mesure. (4) Nous donnerons quelques résultats d'adsorption, en fonction principalement de la température du getter, de la pression du gaz au-dessus du getter, de la pression de flash du getter.

33.25. **Ion Induced Re-emission of Noble Gases from a Nickel Surface*** : E. A. TRENDELENBURG† and J. H. CARMICHAEL. Westinghouse Research Laboratories, Pittsburgh 35, Pennsylvania, U.S.A.

Each of the noble gases, He, Ne, A, and Kr, has been ionically pumped with an energy of about 100 eV into a nickel target and has been subsequently released by a similar bombardment using a different noble gas. As described by Brown and Leck‡ a mass spectrometer permitted the measurement of both the re-emission of the trapped atoms and the trapping of the bombarding particles. The re-emission mechanism is described in terms of a simple model which assumes that the trapped atoms are released by the bombarding particles through a mechanism of sputtering of either the target material or the trapped gas or a combination of both. The experimental results are in agreement with the model. A direct replacement of a trapped atom from its trapping site by a bombarding particle is shown to be a relatively unimportant factor in the re-emission process. Measurements of the re-emission rates of the trapped atoms have yielded information concerning the depth distribution of the trapped atoms in the nickel target. In particular, saturation of the depth distribution has been observed for Ne, A, and Kr, at concentrations below one equivalent monolayer while He showed no such effects at the highest concentrations used, which corresponded to approximately 15 equivalent monolayers.

33.26. **Present Stage of the Researches on the Adsorption of Gases by the Getters Evaporated from Barium Alloys** : DELLA PORTA. Societe Apparecchi Elettrici e Scientifici, Milan, Italy.

The methods and the techniques employed for the study of the adsorption of gases by barium getters are outlined. The development of the researches in this field from the almost empirical measurements of the adsorption capacity and gettering rate up to the present strictly chemical-physical perspective of the problem is emphasized.

The method of the Knudsen flow can yield fully informative data on the nature and the course of this process. The value of the method is greatly enhanced when tests are carried out at a constant pressure on the evaporated metallic film : the experimental curve shows directly the variations of the sticking probability and fully demonstrates the evolution of the process particularly in regard to its dependence on the fraction of surface covered.

Some results obtained with this method relating to the influence of the pressure, the temperature and the getter evaporation conditions on the adsorption of gases are illustrated as well at the influence of the subesquent treatment of the evaporated film.

The case of nitrogen is examined in detail and discussed.

33.31. **Problems Related to Very High Power Windows at Microwave Frequencies** : J. JASBERG and J. V. LEBACQZ. Stanford University, Stanford, U.S.A.

It has been difficult to obtain satisfactory output windows for those microwave tubes which operate in the multi-MW range.

Although such high-power tubes may be used for a number of purposes, this paper considers only the experience gained during the past five years with a number of large klystrons which are used to supply rf power to the Stanford Mark III linear electron accelerator. This machine is used for research in nuclear physics, and it is driven by 20 klystrons operating at approximately 2850 Mc, and each delivering a peak power of 15 to 20 MW, and an average power of a few kW watts. The windows in these tubes are used to isolate the klystron vacuum from the poorer vacuum existing in the accelerator. The results obtained with a number of different window designs have been inconsistent, and generally poor. However, in recent years, a high-alumina, ceramic disk window has been used, and a reasonably satisfactory average window life of 2000 hr has been obtained. Toward the end of increasing this life, perhaps to 5000 hr, studies have been made of the mechanism of window failure. This paper presents a discussion of the kind of failure to which such windows are subject, and also a description of some of the phenomena which are observed at the window, both during and after operation.

33.32. **Versuche zur Bestimmung von Cäsiumdampfdruck bei der Herstellung von Sb-Cs und Ag-O-Cs Photokathoden** : E. KANSKY and S. JERIC. Institut za electroniko, Ljubljana, Jugoslavija.

Sb-Cs und Ag-O-Cs Photokathoden entstehen bei der Reaktion von dünnen Antimon und Silberoxydschichten mit Cäsiumdampf im Vacuum. Für das theoretische Studium und eine zweckmässige Führung des Herstellungsprozesses ist es sehr wichtig den Dampfdruck über der Schicht während des Formierens zu kennen. Dieser Druck hängt von der Zuströmungsgeschwindigkeit des Cäsiumdampfes, der Kinetik der Bildung von Cäsiumverbindungen in der Schicht und vom Zersetzungsdampfdruck dieser Verbindungen ab. Es wurden Versuche gemacht diesen Druck bei dem Formieren der Sb-Cs und Ag-O-Cs Kathoden zu bestimmen.

Die Resultate wurden mit den thermodynamisch geschätzten Werten vergliechen.

33.33. **Probable Explanation for the Composition of Residual Gases in Electronic Valves** : F. H. R. ALMER, H. J. R. PERDIJK and P. G. VAN ZANTEN. Philips' Gloeilampenfabrieken, Eindhoven, Netherlands.

In electronic valves containing a barium getter mirror sometimes a small gas pressure is observed after storing during some weeks. This gas consists mainly of CH_4 which gas quickly disappears without having harmful effects when the valve is put into use. The source of this gas is not very well known. Although it might be explained by assuming that the valve had not been properly heated during pumping and that some gassy organic material is still present afterwards, an alternative explanation is thought to be more likely.

This explanation is based on experiments made during investigations on efficiencies of barium getter mirrors for CO. It will be shown that barium carbide will be formed. With the aid of a mass-spectrometer the reaction of getter mirrors (partly saturated by CO) and water vapour has been studied and in many cases CH_4 has been detected.

Afterwards the occurrence of CO and water vapour in commercial valves will be discussed.

33.34. **Testing of Minute Oxidation of the Base Metal for Oxide Cathode** : Y. TACHIHARA, T. HATA and M. ONIZUKA. Engineering Laboratory, Mitsubishi Electric Mfg. Co., Ltd., Amagasaki, Hyogo, Japan.

Electron emission of the oxide-coated cathode is sharply affected by slight oxidation of impurities contained in the nickel core metal. This minute oxidation occurs during ingot melting, rolling, annealing, forming and tube exhausting. A new method was developed for testing of the cathode base metal without using the thermionic emission test through electronic tubes. This new method makes use of the fact that the corrosion rate of metals in acid or alkaline solution is markedly affected by minute oxidation.

The extent of oxidation, the depth of oxidation and the oxidation resisting power of the metal for cathode core can be estimated from the curve of time and the weight of metal specimen in an acid solution.

Tube exhausting process can also be checked.

*This work was supported by the U.S. Atomic Energy Commission under Contract AT(11–1) 570.

†Present Address : Gerätebau-Anstalt Balzers, Principality of Liechtenstein.

‡*Brit. J. Appl. Phys.* **161**, 6 (1955).

33.35. **Eine Feinfokus-Fernfokus-Röntgenröhre für Körperhöhlenaufnahmen :** E. B. Bas und F. Gaydou. Institut für Technische Physik an der ETH, Zürich, Schweiz.

In der Dental-Diagnostik wird der Film in die Mundhöhle eingeführt und durch eine ausserhalb angeordnete Röntgenquelle belichtet. Für die Übersichtsaufnahmen des Gesamtgebisses ist es zweckmässiger, die Röntgenquelle innerhalb der Mundhöhle und den Film ausserhalb anzuordnen. Die Realisierung einer Röntgenröhre, welche diese Art von Durchleuchtung ermöglicht, bietet elektronenoptische und röhrentechnologische Probleme, welche kurz besprochen werden. Es werden Aufnahmen mit einer solchen Röntgenröhre gezeigt.

33.36. **Materialbearbeitung mit Elektronen im Hochvakuum :** E. B. Bas. Institut für Technische Physik an der ETH, Zürich, Schweiz.

Beschleunigte Elektronen besitzen grosse kinetische Energie, welche in den meisten Elektronengeräten an der Auftreffstelle der Elektronen unangenehme Wärmeableitungsprobleme mit sich bringt. Man kann aber diese Wärmeentwicklung bewusst zum Schmelzen und Verdampfen von Materialien ausnützen. Die Möglichkeiten werden kurz erläutert und die an das Elektronenstrahl–Erzeugungssystem zu stellenden Bedingungen diskutiert. Ein für robusten praktischen Betrieb geeignete Elektronenkanone wird besprochen und eine Versuchsapparatur für Schmelzen und Bohren mit Elektronen kurz beschrieben. Einige Versuchsresultate werden mitgeteilt.

33.37. **Ziehen von Einkristallen im Vakuum :** H. Bumm. Leybold—Hochvakuum—Anlagen, Köln, Deutschland.

In den letzten Jahren sind grosse Anstrengungen gemacht worden, geeignete technische Apparaturen zur Herstellung reinster Einkristalle zu entwickeln, da in der Halbleiter-Technik aus physikalischen Gründen Einkristalle verwendet werden müssen. Die meisten Kristallziehöfen arbeiten unter Schutz- oder Edelgasen ; erst seit kurzem werden auch Hochvakuum-Apparaturen gebaut, die grosse Vorteile gegenüber den unter Gas-Atmosphäre arbeitenden brachten. Eine Ganzmetall-Produktions-Apparatur, in der nicht nur Halbleiter-(Germanium oder Silicium), sondern auch andere Metall-Kristalle in höchster Reinheit geschmolzen und gezogen werden können, wird beschrieben und einige Messergebnisse von gezogenen Si-Kristallen werden mitgeteilt.

34.1. **Distillation Apparatus for Compounds having a High Melting Point :** K. Hashimoto. Japan Vacuum Engineering Co., Tokyo, Japan.

Vacuum distillation is adopted for the purification of an organic compound having a high boiling point, such as phenol, naphthol, etc. The distillate is generally kept in a molten state in a container.

But this has two defects : first, the compound, especially in a molten state, is easily decomposed, and therefore becomes impure and its colour changes ; second, the distillate in the container re-evaporates and the vapor travels towards the pump, sticking to the inner wall of the pipe, finally blocking the pipe altogether.

These defects, however, can be completely corrected by using a rotating condenser. The rotating condenser has a mechanism which is similar to a flaker. The material is fed in vapor phase instead of liquid phase and the product is obtained in flakes or in powder form.

34.2. **The Performance of the Falling Film Molecular Still :** H. Nakagawa. Nippon Rika Kogyo Co., Ltd., Tokyo, Japan.

During the past 12 years, more than 30 sets of industrial molecular distillation equipments were constructed in Japan and are now being operated successfully for the concentration of vitamin A from fish liver oil, for instance. But all of them are of the falling film type, because some difficulties obstruct the construction of a centrifugal type still.

The running performances of several of these stills will be introduced, especially the relations between concentration of distillate, total recovery, vacuum, flow rate of distillation (i.e. thickness of the film) and distillating temperature.

Because many complicated factors must be considered, the theoretical analysis of these relations is very difficult, but some trials were made to approach exact settlement, and we intend to present them here.

34.3. **A Laboratory Molecular Still with Improved Fractionating Power :** P. R. Watt. Walton Oaks Experimental Station, Tadworth, United Kingdom.

A laboratory moving-film molecular still is described, for the fractional molecular distillation of thermolabile materials.

Amounts as small as 3 g may be handled in the apparatus. There are five successive stages in counter-current, and the overall fractionating power is considerably better than that of the normal laboratory pot-still or single stage falling-film still, while thermal hazard is reasonably low. The total hold-up in the apparatus does not normally exceed 300–400 mg.

35.11. **Technik und Anwendungen der Gefriertrocknung in der Biologie :** K. Buob. Charles Pfister S.A. Secfroid, Lausanne, Schweiz.

Es wird ein kurzer Überblick über die physikalischen Phänomene bei der Gefriertrocknung gegeben und über neue konstruktive Verbesserungen berichtet, durch die das Verfahren vereinfacht und die Trocknungszeiten verkürzt werden können.

Im besondern werden hierauf praktische Erfahrungen mit der Gefriertrocknung in der biologischen Forschung, in der Histologie und der Chirurgue bekannt gegeben.

35.12. **Mess- und Regelprobleme bei der Gefriertrocknung :** K. H. Neumann. Leybold—Hochvakuum—Anlagen, Köln, Deutschland.

Es wird über ein neues Verfahren berichtet, welches bei der Gefriertrocknung eine ständige Temperaturkontrolle im Trockengut erlaubt. Messungen mit Thermoelementen sind hierfür aus mehr als einem Grunde unzureichend. Von diesem neuen Messverfahren ausgehend lassen sich Steuer- und Regelorgane entwickeln, mit deren Hilfe es gelingt, die optimale Temperatur in den verschiedenen Schichten des Gutes während der Haupttrocknung und der Nachtroknung auch tatsächlich einzuhalten. Sie erlauben ferner, gegen Ende der Trocknung mit guter Genauigkeit den Grad der Restfeuchtigkeit zu erkennen und die Trocknung dementsprechend zum geeigneten Zeitpunkt abzubrechen. Es gelingt, die Gesamtheit dieser Mess- und Regelorgane zu einer automatisch arbeitenden Steuerung zu verbinden (" Tempomatik–Leybold "), die die selbsttätige Einhaltung der gewünschten Trocknungsbedingungen von Beginn bis zum Abschluss der Gefriertrocknung besorgt. Mit Hilfe dieses Steuerprinzips kann der Gefeiertrocknungsprozess um 30 bis 50 per cent beschleunigt werden. Die Wirtschaftlichkeit der Gefriertrocknung wird damit auf eine neue Basis gestellt.

35.21. **Application Nouvelle du Vide dans l'Industrie des Conserves de Poissons :** J. M. Dunoyer. Faculté des Sciences de Rennes, France.

On décrit quelques expériençes faites pour utiliser le refroidissement produit sur des sardines, par une très légère dessiccation sous vide, pour porter ces poissons à une température de quelques degrés centigrades, suffisante pour assurer leur conservation pendant la durée de la pêche.

35.22. **Le Vide Poussé dans l'Industrie Alimentaire :** C. Morand. Charles Pfister S.A., Secfroid, Lausanne, Suisse.

1. Introduction.
2. Historique du séchage sous vide des produits alimentaires.

Brève rétrospective de cette technique et de son évolution au cours des dernières décennies.

3. Séchage sous vide et transfert de chaleur.

Importance du transfert de chaleur, méthodes de chauffage, réalisations pratiques.

4. Réalisations aux Etats-Unis et en Europe.

Vol. 9 959/60

Qualité des produits obtenus, installations en service, derniers developpements.

5. Conclusion.

35.31. **Dispersion of Metals in Glucose Powder by Vacuum Evaporation for Medical Use :** Y. MORIYA. Tokyo Shibaura Electric Co., Ltd., Tokyo, Japan.

A new method for producing colloidal solutions is described. Soon after glucose powder (300 mesh) containing various substances dispersed by vacuum deposition is dissolved in water, colloidal solutions are produced. As these solutions do not contain protecting colloids, they are very unstable, but they may be injected into human blood vessels without injury. If the metal dispersed is Sb (antimony), this treatment has then proved very effective in case of trypanosoma diseases.

35.32. **Analysis of Drying Process during Freeze-Drying of Biological Materials Using a Recording Vacuum Torsion Balance :** T. NEI, C. YOSHIMOTO and S. CHIBA. The Institute of Low Temperature Science, Hokkaido University, Sapporo, Japan.

A recording vacuum torsion balance was designed for the investigation of the freeze-drying process of biological materials. It consists of a lever attached to the center of a phosphorous-bronze strip suspended horizontally by two flat springs. The container of the material to be investigated is hung to the lever by a fine wire, and the whole system is enclosed in a glass vacuum housing. As the ice contained in the material sublimes, the deflexion of the strip is recorded optically on sheet of photographic paper through the window of the vacuum housing. From the " dehydration-time curve " which was recorded by making use of this apparatus and which indicated the change in weight of the biological material during freeze-drying, the " rate of drying-time curve " and the " rate of drying-residual moisture content curve " were obtained by drafting and calculation.

The results obtained through analysis of these curves are as follows :

(1) The freeze-drying process of rabbit serum is made up of five stages : Preparatory stage, stage of increasing rate of drying, stage of constant rate, the first stage of decreasing rate and the second stage of decreasing rate.

(2) These stages make their appearance separately or jointly, lasting long or short according as the contributing factors are varied. No definite type of freeze-drying has been observed.

(3) Also in the freeze-drying (i.e. sublimation) process of pure ice there appear various drying stages as described above. The mechanism of appearance of these stages, however, comes out essentially different from that of rabbit serum.

(4) In the freeze-drying process of bacterial suspension of E. coli, there appears a third stage of decreasing rate of drying, where a little moisture barely escapes from the material. It is to be considered that this stage corresponds to the period of dehydration from the bacterial cells and has some biological significance.

35.33. **Les Applications de la Lyophilisation dans les Collections de Types Microbiens :** P. HAUDUROY et J. D. PIGUET. Centre de Collections de Types Microbiens, Lausanne, Suisse.

Le développement récent des Collections de Types Microbiens a rendu nécessaire l'emploi d'une technique simple et économique de conservation des êtres microscopiques. La dessication après congélation est employée à l'heure actuelle à peu près universellement. A Lausanne, on utilise dans le Centre International de Collections de Cultures un appareil, construit il y a plus de 10 ans, permettant de lyophiliser 200 ampoules à la fois. La réfrigération est obtenue au moyen d'un mélange neige carbonique–acétone. La sublimation de la glace se fait grâce à des vides de l'ordre de 10^{-3} à 10^{-4} mm Hg obtenus par un système de deux pompes, l'une à palettes et l'autre à diffusion, entre lesquelles set intercalé un condensateur maintenu à $-70°C$. La chaleur de vaporisation est prise dans la pièce où se trouve l'appareil, pièce dont la température est maintenue entre 20°C et 22°C. Après scellage sous vide, les ampoules sont contrôlées quant à leur étanchéité. Ainsi lyophilisées, les bactéries se conservent plusieurs années sans perdre aucune de leurs qualités biochimiques et physiologiques.

35.34. **The Use of Dielectric Heating in the Drying of Biological Materials from the Frozen State :** A. L. HOPKINS. Western Reserve University, Cleveland, Ohio, U.S.A.

The rate of vacuum drying of biological materials from the frozen state may be extremely slow due to the lowering of the vapor pressure which results from evaporative cooling. Present means of supplying heat involve the danger of localized damage due to overheating at the surface. This can be avoided by the use of radio frequency (1000 Mc/s) energy from a radar generator. These wavelengths are not absorbed by dry proteins and thus the dielectric heating occurs only in that part of the material still containing water. Microscopic examination of tissues dried in this way revealed no evidence of localized overheating or other changes due to exposure to radio energy.

In operation, a small antenna is placed next to the sample holder and the temperature, as indicated by a thermocouple in the material, is controlled by adjusting the power to the radar generator. The amount of power needed to produce a given amount of heating is a function of the rate at which vapor can escape from the material as well as the dielectric properties of the material itself. When all water has been removed, no further heating can be produced.

36.11. **Herstellung und Eigenschaften von Mehrkomponentenschichten durch Vakuumbedampfung :** W. HÄNLEIN and K. G. GÜNTHER. Siemens-Schuckertwerke, Nürnberg, Deutschland.

Es werden Methoden besprochen, die zur Herstellung von Mehrkomponentenschichten durch Vakuumbedampfung geeignet sind. Nach einer kurzen Betrachtung des Kondensationsvorganges wird die sogenannte Mehrfachstrahlbedampfung näher erläutert, die unter gewissen Voraussetzungen die Bildung von Schichten mit exakt stöchiometrischer Zusammensetzung ermöglicht. Neben der Steuerung der einzelnen Verdampfertemperaturen ist hierzu eine geeignete Wahl der Temperatur der Kondensationsfläche notwendig. Die Anwendbarkeit des Verfahrens wird am Beispiel dünner Glasschichten sowie Halbleiterschichten vom Typ der A_{III}-B_V-Verbindungen gezeigt.

36.12. **Adhesion of Thin Films :** C. WEAVER. Royal College of Science and Technology, Glasgow, United Kingdom.

A survey of the nature of adhesion forces and their influence on the structure and properties of thin evaporated films. Calculations and measurements of absorption energy and practical methods of measuring film adhesion and durability are critically reviewed. Time effects have been observed in measuring adhesion of metallic films, particularly with double layers such as aluminium on chromium.

36.13. **Spezielle Probleme der Hochvakuum-Bedampfung :** W. REICHELT. W. C. Heraeus, Hanau/Main, Deutschland.

Die konventionelle Technik der Hochvakuum-Bedampfung stellt Schichten mit dicken $\leqslant 1\ \mu$ her. Der Anwendungsbereich des Verfahrens kann wesentlich erweitert werden, wenn es gelingt, auch dickere Schichten herzustellen, wofür Möglichkeiten und Grenzen aufgezeigt werden. Erforderlich ist die Entwicklung leistungsfähiger Dampfquellen, mit denen es gelingt, grosse Mengen Metall über lange Zeiten hinweg zu verdampfen. Derartige Verdampfer sind z.B. von ausschlaggebender Bedeutung für kontinuierliche Bandbedampfungsanlagen.

Die für wirtschaftliche Arbeitsweise notwendige kurze Evakuierungszeit ist das zweite Problem bei Bandbedampfungsanlagen. Während man zunächst Einkammer- und Zweikammer-Maschinen baute, wendet sich heute das Interesse solchen Anlagen zu, bei denen fast das ganze zu bedampfende Material sich in Räumen von Atmosphärendruck befindet und nur jeweils kleinere Teile zwecks Bedampfung über Druckstufen durch die Hochvakuumkammer geleitet werden. Es werden

Beobachtungen und Messungen an solchen Druckstufen mitgeteilt.

36.21. **Evaporation of Aluminium by Graphite Evaporator :** Y. MORIYA. Tokyo Shibaura Electric Co., Ltd., Tokyo, Japan.

The desirable properties of graphite for evaporation of aluminium were determined as follows :

1. Apparent density >1.80 per cent ;
2. True density >2.15 per cent ;
3. Ashes <0.05 per cent.

The destruction of graphite usually occurs at 1200°–1300°C but it can be prevented by heating it at above 1500°C.

36.22. **Application à la Métallisation sous Vide du Chauffage Électronique :** J. SOMMERIA et R. GRIFFOUL. Cie Générale de Radiologie, Paris, France.

Les traitements thermiques, la fusion et la vaporisation sous vide de substances de plus en plus réfractaires et de grande pureté exigent des méthodes de chauffage à énergie très concentrée et ne provoquant pas de pollution.

Le bombardement électronique, qui ne fait intervenir aucun support, répond à ce problème. La Compagnie Générale de Radiologie a réalisé un canon à électrons destiné spécialement à l'application de dépôts sous vide par vaporisation.

Une puissance de 500 W concentrée sur 3 mm² permet de vaporiser toutes les substances réfractaires et notament le carbone. L'appareil forme un ensemble facilement adaptable sur une enceinte à vide.

36.23. **The Effects of a Glow Discharge on Glass and Organic Materials :** L. HOLLAND. Edwards High Vacuum Ltd., Crawley, United Kingdom.

The effects are described of exposing glass and organic materials to the bombardment of electrons and ions formed in a glow discharge. Contaminants are removed from glass surfaces by ion bombardment, whereas bombardment by high velocity electrons from the cathode dark space produces contaminant films if hydrocarbon vapours are present. Positive ions accelerated on to a glass surface may remove constituents of the glass leaving the surface porous thereby lowering its refractive index. Ion bombardment also removes hydrocarbon decomposition products from surfaces previously exposed to electron bombardment. Electron irradiated hydrocarbon vapours form polymerized coatings which are optically absorbing, whereas decomposed silicone vapours form optically adsorbing coatings which have surface properties similar to those of clean glass.

Plastic materials exposed to a glow discharge are invariably degraded. Electron bombardment produces damage similar to that obtained by thermal means whereas bombardment by air or argon ions may, in certain cases, remove material and etch the surface. This is further evidence that ion bombardment cleans glass, etc. by sputtering the outer contaminant layers.

Electrode systems specially designed to overcome the undesirable effects described are dealt with.

36.31. **Eine universell verwendbare Kleinst-Vakuumapparatur für die elektronenmikroskopische Präparationstechnik :** R. HAEFER. Gerätebau Anstalt Balzers, Fürstenstum Liechtenstein.

Es wird eine Kleinst-Vakuumapparatur beschrieben, mit der alle derzeit in der Elektronenmikroskopie üblichen und ein Vakuum benötigenden Präparationsverfahren routinemässig möglich sind : Schräg- und Kegelbedampfung, Verdampfung von Kohlespitzen Glimmentadung in einer Kohlenwasserstoffatmosphäre.

37.1 **Fabrication d'Éléments de Canaux Chantier Neto (Italie) :** CENTRE SCIENTIFIQUE INTERNATIONAL BILLNER. Paris, France.

Des éléments de canaux dits éléments porteurs sont utilisés pour la distribution d'eau en canal d'irrigation découvert.

Ces éléments sont préfabriqués en longuer de 7.50 m et sont précontraints longitudinalement. Leur préfabrication s'effectue dans une position retournée c'est-à-dire avec la concavité vers le bas sur des moules intérieurs métalliques, le coffage extérieur étant équipé pour l'application du traitement par le vide.

Dès la fin du traitement qui ne dure que quelques minutes, les coffrages extérieurs peuvent être enlevés pour être réutilisés immédiatement. Les éléments de canaux eux-mêmes restent en position pendant un temps suffisant pour assurer le durcissement du béton et permettre la précontrainte.

37.2. **Octopus pour la Manutention de Carpettes Asphaltiques Destinées au Revêtement du Canal de Funa Congo Belge :** CENTRE SCIENTIFIQUE INTERNATIONAL BILLNER. Paris, France.

Un engin spécial de manutention par le vide appelé " Octopus " est utilisé pour la manutention de ces carpettes asphaltiques tant au chantier de fabrication qu'à la pose.

Cet engin qui comporte de nombreuses ventouses à amorçage automatique est en fait le seul qui permet d'effectuer le transport des carpettes sans leur faire subir des efforts qu'elles ne seraient pas en mesure de supporter.

La mise en place des éléments sur les berges est rendue facile par un réglage de l'octopus qui amène la carpette avec l'angle exact du talus.

37.3. **Fabrication de Tuyaux Précontraints pour l'Adduction d'eau de la Ville d'Athènes, Grèce :** CENTRE SCIENTIFIQUE INTERNATIONAL BILLNER. Paris, France.

Pour la première fois une canalisation importante est réalisée par les procédés Vacuum Concrete en tuyaux en béton à âme d'acier.

Les tuyaux ont un diamétre intèrieur de 1.27 m et 6 m de long. Ils sont fabriqués en position verticale le béton étant coulé entre un moule vacuum rétractile intérieur et l'âme en tôle. Ce moule intérieur est libéré dès la fin du traitement. Après une période de durcissement le tuyaux (noyau) est " frêtté " en vue de mettre le béton en précontrainte et une couche de protection de 3 cm est coulée à l'extérieur pour enrober les spires. Cette couche est elle-même traitée par le vide.

37.4. **Das Vakuum Concrete-Verfahren bei der Fabrikation von langen, verwindbaren Stahlbeton-Hohlbalken als ALWEG-Fahrbahn in Kurven und geraden Strecken :** K. ROSENBAUM. Alweg-Forschung, Köln, Deutschland.

1. Einleitende Worte, bezogen auf den Tragkörper der ALWEG-Bahn, mit Übergang auf die Schalungskammer. 2. Erklärung der wichtigsten Merkmale der Schalungskammer mit Übergang auf das Vakuum Concrete-Verfahren in Verbindung mit dem Balken als Hohlkörper und die Möglichkeit, Kurvenbalken bzw. verwindbare Balken herzustellen. 3. Aufzeichnung der Vorteile bzw. Anwendung des Vakuum Concreet-Verfahrens. 4. Transport und Montage der ALWEG-Fertigteile. 5. Neue Wege über Verwendung der Schalungskammer 6. Schlussworte mit Kurzbericht über ALWEG-Weiche.

38.1. **Entlüftung von Dampfturbinenkondensatoren mit Rootspumpen :** R. THEES. E. Leybold's Nachfolger, Köln, Deutschland.

Die in eine Kondensations-Dampfturbine durch Undichtigkeiten einströmende Luftmenge muss am Absaugstutzen des Hauptkondensators abgepumpt werden. Während die bisher als Luftpumpen eingesetzten Strahlsauger eine Luftmenge von 15 kg/h bei einem Druck von einigen Torr mit einem Leistungsverbrauch von 800 kg/h Dampf—entsprechend etwa 80 kW—pumpen, ergibt sich für die gleiche Förderleistung beim Einsatzab einer Gasballastpumpe mit Hilfskondensator eine Gesamtantriebsleistung von 14 kW. Der Einsatz des Hilfskondensators erfordert allerdings Kühlwasser mit einter Temperatur, die um mindestens 10°C unter der Temperatur des Kühlwassers zu dem Hauptkondensator liegt. Universell einsetzbar für Fluss- und Rückkühlkraftwerke wird erst der Rootspumpsatz, der ausserdem mit einer Gesamtantriebsleistung von 8 kW auch der wirtschaftlichste Pumpsatz ist.

Vol. 9 959/60

Die Arbeitsweise eines solchen Rootspumpsatzes wird anhand der Ergebnisse einer Versuchsreihe in einem Grosskraftwerk erläutert. Die Ergebnisse ermöglichen es, Rootspumpsätze für beliebige Luftmengen und beliebige Ansaugdrucke zu berechnen.

38.2. **Untersuchungen über die Verdampfungsgeschwindigkeit von Heizleitern für Vakuum-Glühanlagen :** G. ZINSMEISTER. Gerätebau-Anstalt, Balzers, Fürstentum Liechtenstein.

Die üblichen Heizleitermaterialien für Vakuum-Glühanlagen sind Mo, Ta, W und Graphit. Es bestehen aber viele Anwendungsgebiete, bei denen Temperaturen im Bereich von 1000–1400°C gefordert werden, so dass billige Materialien wie Eisen, Kanthal, Ni-Cr-Legierungen usw. in Frage kommen.

Es wird ein einfaches Verfahren zur Bestimmung der Verdampfungsgeschwindigkeit beschrieben Dieses Verfahren, das auf einer Absorptionsmessung von aufgedampften Schichten beruht, ermöglicht die Verdampfungsgeschwindigkeit in einfacher Weise zu bestimmen. Es werden die erhaltenen Ergebnisse für Ni Cr (80/20) sowie für Kanthal in Abhängigkeit der Voroxydation angegeben.

38.3. **A Vacuum Insulated Transfer Line for Liquified Gases :** F. FARRAR. The British Oxygen Research and Development, Ltd., London, United Kingdom.

This paper analyses the problems involved in applying a powder filled vacuum insulation to a liquid transfer line, and how these problems may be overcome.

The line was designed and constructed for the movement of liquified gases at temperatures of 77°K. The design is described in detail, showing how, by the choice of materials and construction, it is possible to eliminate flexible bellows, and flexible joints in both the inner and outer tubes throughout a complete assembly.

Data compiled from tests carried out over a period of three months is included, showing how an experimental line withstood accelerated operational cycles.

Slides will be shown indicating constructional details experimental procedure, and experimental data.

38.4. **Neue Methoden zur Messung des Fremdgasdruckes in Pumpenlosen Quecksilberdampf-Stromrichtern :** G. PECHE und W. SCHMALENBERG. Siemens-Schuckertwerke, Berlin-Siemensstadt, Deutschland.

Die Betriebssicherheit grosser abgeschweisster Quecksilberdampf-Stromrichter und Ignitrons hängt wesentlich von ihrem Fremgasdruck ab, so dass ihre Dichtigkeit nach Beendigung des Entgasungsprozesses geprüft werden muss. In Excitrons ist die Diffusion von Quecksilberionen aus einer im Kathodenraum brennenden Hilfsentladung zu einer möglichst weit entfernten negativen Elektrode, so weit die mittler freie Weglänge merklich kleiner als die Gefässdimension ist, umgekehrt proportional dem Fremdgasdruck. In Ignitrons wird die Absorption der im Kathodendampfstrahl mit geführten Quecksilberionen im Fremdgas zur Druckmessung benutzt. Bei Impulsentladungen des Zündstiftes ist hierbei der Ionenstrom an der negativen Anode proportional exp(-Druck), sofern die mittlere freie Weglänge kleiner als die Entfernung Kathode-Anode ist. Ferner ist die Laufzeit der Ionen von Kathode zur Anode ein Mass für den Fremdgasdruck. Die Absorption des Quecksilberdampfstrahles sowie die Diffusion der Quecksilberionen ist von der Art des Fremdgases abhängig. In Verbindung mit Brennspanungsmessungen ist in einfachen Fällen eine Gasanalyse möglich. Im interessierenden Bereich on 0,5 bis 100 mTorr erlauben diese Methoden eine sichere Beurteilung des Fremdgasdruckes, ohne dass zusätzliche Einbauten in den Gefässen angebracht werden müssen. Insbesondere ässt sich die Dichtigkeit der Quecksilberdampf-Stromrichter und Ignitrons gegenüber der atmosphärischen Luft überwachen.

38.5. **Évaporation de Tungstène en Atmosphère Argon-Azote :** R. DE KÖVESLIGETHY. Ranelagh, Buenos Aires, Argentine.

Les équations caractéristiques des lampes électriques sont presentées en fonction de la température de la spirale. En supposant que chaque lampe cesse de fonctionner au moment où le même pourcentage de sa spirale s'est évaporé, on peut exprimer la vitesse d'évaporation du tungstène sous une forme relativement simple, ou l'exposant est une fonction de la température de la spirale.

On ajoute quelques tableaux numériques, calculés selon les équations données, entre autres le log $Mx10^{-6}$ pour l'intervalle de 2302–2886°C de température, correspondant à une efficacité lumineuse de 8.00–30.00 Lumens W. M est l'évaporation de tungstène en mg/cm²h. Les équations sont représentées aussi graphiquement.

38.6. **Force Measurements in Low Density Hypersonic Air Flows :** G. J. MASLACH. Institute of Engineering Research, University of California, Berkeley, California, U.S.A.

In recent years several wind tunnels have been designed to operate at a pressure level of approximately 0.1 mm Hg absolute pressure. The problems associated with the measurement of low aerodynamic pressures of this order has been the subject of many publications. The problem of measuring forces, both lift and drag, has not received as much attention. This paper describes a single component force balance capable of measuring either lift or drag forces up to 100 g. The balance, by the use of various quartz springs, may be used for the measurement of forces as low as 100 mg with a sensitivity of 0.1 mg.

38.7. **Chargenzeiten in modernen Trocken- und Imprägnier-Anlagen :** M. BEYER. Leybold—Hochvakuum—Anlagen, Köln, Deutschland.

Bei der Fertigung von Kabeln, Kondensatoren, Messwandlern und Transformatoren hat man durch Anwendung geringerer Drucke bei der Trocknung und der anschliessenden Imprägnierung mit weitgehendst getrockneten und entgasten Ölen eine wesentliche Verbesserung der elektrischen Eigenschaften erreicht.

Durch zum Teil besondere Heizverfahren und den Einsatz der in den letzten Jahren entwickelten Pumpanordnungen mit sehr hohen Saugleistungen bei tiefen Drucken können nunmehr auch günstige Chargenzeiten für die Trocknung bei sehr niedrigen Betriebsdrucken erzielt werden.

Über die verschiedenen Trocknungs- und Imprägnierverfahren bei der Fertigung derartiger elektrischer Erzeugnisse und die dabei möglichen Char enzeiten wird im einzelnen berichtet.

VO
9
1959

Vol.
9
959/60

VACUUM

Recent Advances in Ultra-high Vacuum Technology*

D. ALPERT
University of Illinois, U.S.A.

The two major directions for advances in ultra-high vacuum technology are (1) the attainment and measurement of pressures below 10^{-10} mm Hg, and (2) the development of large ultra-high vacuum systems. New vacuum components have recently been introduced which are of great value in both of these directions. Of particular interest are the development of ionization gauges capable of reading pressures below 10^{-12} mm Hg and the design of systems several orders of magnitude larger than those heretofore described. Contributions of a number of workers in this field are briefly discussed. One of the most important recent developments is the "getter-ion" pump as a means of achieving both lower pressures and higher pumping speeds. It has been shown that very simple "getter-ion" pumps are possible which can replace diffusion pumps to achieve pressures down to the 10^{-10} mm Hg region. Despite this achievement there are many unanswered questions involving the underlying mechanisms of sorption and desorption for neutral and activated molecular gases. Preliminary experiments have been made on the sticking probability of certain gases on titanium and the effect of an adjacent ionizing electron beam.

1. Introduction

The large number of papers on ultra-high vacuum offered at this Congress clearly demonstrates the widespread research in this field during the past few years. This great interest is evidence, I believe, that we recognize the importance in broad areas of electron, atomic, and surface physics of a technology which allows the use of extremely pure gases or atomically clean surfaces. I shall not take much of the limited time available this afternoon to list the many experiments which have been made possible by the introduction of ultra-high vacuum technology in various phases of pure and applied electron physics. I will, however, call attention to the important fact that even the nuclear physicists[1] have taken a great interest in ultra-high vacuum in connection with a number of applications and have thus introduced a new need—that of very *large* ultra-high vacuum systems. My discussion this afternoon will include an important emphasis of this phase of ultra-high vacuum technology.

Shortly after World War II a number of developments in the means for measuring pressures and evacuating a vessel resulted in the development of a technology which within a few years had become more or less "standard" in the U.S.A. and elsewhere. While there are a number of variations, such a system has been described in the literature[2] and is shown in Fig. 1. Using such systems and other recently evolved techniques a very sizeable number of experimenters have in the last few years embarked on research programs intended to examine the underlying scientific questions and to investigate new means for achieving ultra-high vacuum. Many of these researches have not yet reached the publication stage and I see from the program that a number will be reported at this Congress for the first time. My first purpose in coming here to Namur was, therefore, to hear these papers and learn about the various researches now in progress. My second, but more immediate purpose, is to try to describe, at least by title, some of the scientific problems which are being worked on and to indicate some of the questions which are yet to be answered. In addition, I shall try to describe very briefly a few of the specific advances in ultra-high vacuum which have come forth in the most recent past.

2. Basic high-vacuum parameters

To introduce my discussion, let me write a simplified version of the general pumping equation for any system of volume V and any pump of effective speed S. The rate of change of pressure is given by the expression

$$V(dp/dt) = -Sp + Q, \tag{1}$$

where Q is the total influx and is the sum of the separate influx rates due to leaks, to back diffusion from the pumps, to desorption from the walls, etc. In general, S and Q vary with pressure and time. However, if we assume that they are constants, as is often the case, the solution to the above equation is an exponential with a characteristic time $\tau = V/S$ (time required to evacuate the system to $1/e$ of its initial value). When the system comes to its equilibrium pressure, i.e. $dp/dt = 0$, the above equation gives

$$P_e = (Q/S). \tag{2}$$

The problem of achieving ultra-high vacuum is summarized by the statement that the ratio of total influx Q divided by the pumping speed S must be made small compared to 10^{-8} mm Hg. The pumping speeds of various pumps are easily measured. What are the chief sources of influx? This is obviously not a simple question, since even the same

* Paper presented at the First International Congress on Vacuum Techniques, Namur, 10–13 June 1958.

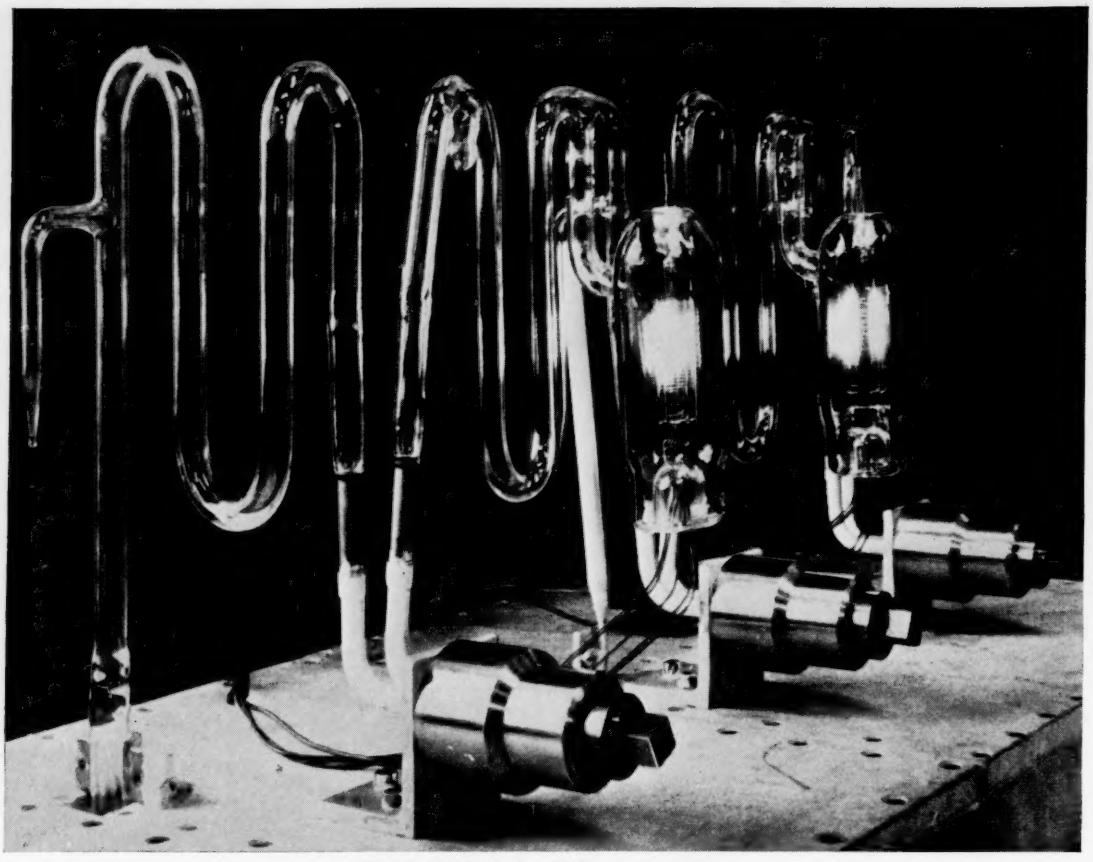

FIG. 1. Standard ultra-high vacuum system.

system may have widely different rates under different conditions. However, we can make certain general comments under the categories listed below :

(1) *Influx due to leaks*

A good helium leak detector can detect a leak with an influx rate of 10^{-9} to 10^{-10} mm.l/s. If a system of moderate complexity were to be tested only by such a leak detector one might expect several such leaks resulting in total leak rates of 10^{-8} to 10^{-9} mm.l/s. To achieve pressure of 10^{-10} against such leaks would require pumping speeds of 10 to 100 l/s. In standard ultra-high vacuum systems of a few liters in volume, the total leak rate is of the order of 10^{-12} mm.l/s even in demountable systems. Clearly then, it is possible to reduce leak rates to very low values, several orders of magnitude below those barely detectable by a helium leak detector.

(2) *Back-streaming and back-diffusion from pumps*

There is not ample time to present a critical review of this rather complicated problem. For either oil or mercury diffusion pumps, manufacturers have in the past paid little attention to this problem, having been content to attain maximum speeds in the 10^{-5} to 10^{-7} mm range. Their published curves show a large maximum in this region with the " speed " dropping to very low values below this point. There is little evidence to indicate an actual reduction of pumping speed at very low pressures. On the contrary, it seems clear that the low values of measured speeds at pressures below 10^{-8} mm Hg are due to sizeable values of gas influx—either coming continuously from the pumps or from the pumping fluids originating therein which have condensed within the system. These two effects are different—yet both are due to inadequate baffling or to poor pump design.

Typical values of influx due to the pumps at 10^{-8} mm Hg range from 10^{-6} mm.l/s for a 25 l/s pump to 3×10^{-3} mm.l/s for a 1000 l/s pump. These values are obviously many orders of magnitude greater than those due to leaks. As the speed of the diffusion pumps increases, the effect of back-streaming is usually greater. To achieve ultra-high vacuum it is apparent that a central problem is the elimination of this source of influx.

At the present time, considerable effort and thought is going into the development of ion pumps of various designs to get away from the large back-streaming from diffusion pumps. In this case there is still a mechanism comparable to back-streaming, that is, the re-emission of gases from the surfaces to which they have been attached. Work is now in progress at various laboratories to evaluate such effects and to understand the physical processes involved, which fall into the third category.

(3) *Gas desorption from walls*

It is well known from work originating with Langmuir[3] and continued by many researchers that the gas physically

adsorbed at the surfaces of a vacuum system constitutes a major source of influx into the system volume. In addition, gas may diffuse from within the envelope walls or arise as a result of interactions at the surface. To present a quantitative value for gas influx from the walls requires an understanding of the mechanism by which each individual gas may arise in each of the types of surfaces used in vacuum enclosures. Such a discussion is clearly beyond the scope of this paper[4] though such studies are essential to the scientific understanding of the problem.

It is, however, useful to give some very approximate estimates for the rates of gas influx to be found in typical vacuum systems. We list in Table I a few values for the

TABLE I.

Specific Influx for Various Systems

Type of system	Gas	Envelope material	Specific influx at room temperature (mm. l.) (s./cm²)
1. Baked ultra-high vacuum	H_2O	Borosilicate glass	3×10^{-18}
2. Baked ultra-high vacuum	Helium	Borosilicate glass	10^{-15}
3. Baked stainless steel	Mostly CO	Stainless steel	5×10^{-15}
4. Unbaked stainless steel	Molecular gases	Stainless steel	10^{-7}
5. Unbaked ultra-high vacuum system	Molecular gases	Glass and metal valves	10^{-8}

specific influx, i.e. the rate of influx in mm.l/s per cm² for several types of vacuum systems.

Consider a 10 l. volume system with a surface area of 3000 cm² (it is the surface area which is important here). To achieve a pressure of 10^{-10} mmHg with a specific influx of 10^{-15} mm.l/s per cm² requires a pumping speed of only 0.03 l/s. This is consistent with the original results found in our laboratory[5, 6] in which we showed that for a system in which all of the components were baked at 400 °C the required speeds were very small and were readily obtained by the ion-pumping of a Bayard–Alpert gauge. On the other hand, if the specific influx is 10^{-7} mm.l/s, the pumping speed required to achieve 10^{-10} mmHg is 3,000,000 l/s. While such a speed is clearly out of range of present-day developments, I mention it because we are beginning to think of evacuating volumes with comparable influx rates.

Having described some of the important parameters, let us proceed to discuss two of the major directions in which work is now being actively attacked : (1) to achieve pressures in relatively small systems below 10^{-10}, and (2) to achieve pressures of 10^{-9} to 10^{-10} in much larger systems.

3. Attainment of extremely low pressures

Varnerin and White[7] showed that one could achieve pressures lower than those observable on a Bayard–Alpert gauge (estimate $<10^{-11}$ mmHg) by enclosing one vacuum system completely within another. Here the ion-pumping of an ionization gauge was used and the influx of helium eliminated completely.

Alpert and Carmichael[8] also demonstrated that one could reach pressures below those measurable with a Bayard–Alpert gauge—by utilizing the substantially higher pumping speed of an oil diffusion pump to reduce the helium pressure in conjunction with a copper trap which reduced the backstreaming from the diffusion pump.

These papers indicated the limitation of the Bayard–Alpert gauge for reading pressures below 10^{-10} mm or even estimating them below $2\text{–}3 \times 10^{-11}$ mm Hg.

Houston[9] proposed a new ultra-high vacuum gauge which has a lower limit several orders of magnitude below that of the Bayard–Alpert gauge. As shown in Fig. 2, it utilizes a

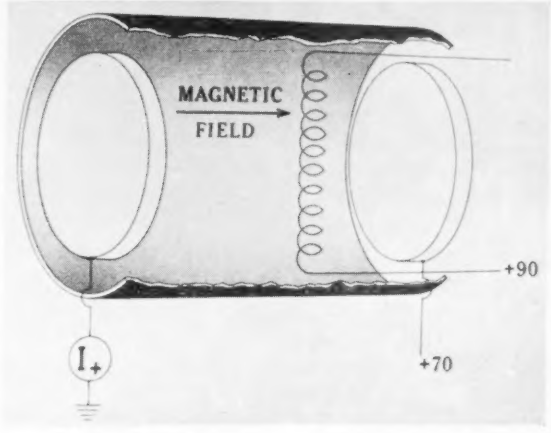

FIG. 2. Houston ion gauge.

combination of electric and magnetic fields not too different from those in a Penning gauge,[10] but with a very fine hot tungsten filament as the electron source. Since the electrons are trapped in the field, they traverse a much longer path before striking the collecting and give a sensitivity which is at least an order of magnitude greater than that for a Bayard–Alpert gauge. This characteristic provides the gauge with an ionic pumping speed which is considerably greater than that for the Bayard–Alpert gauge, and Houston has used it to achieve and measure pressures as low as 2×10^{-12} mm Hg.

Hobson and Redhead[11] have described another ionization gauge which traps electrons in a combined electric and magnetic field. In their gauge the electrons are drawn from the cold cathode by field emission ; this current is prevented from submerging the ion collector current by the use of an auxiliary cathode which shields the ion collector from the high fields. In this case, the ionizing electron current *per se* is not measured ; rather it is determined by a type of space charge effect and it is stated that the ion current varies almost linearly with pressure. While there are a number of questions which are not clearly understood, these authors have reason to believe that they have achieved pressures as low as 10^{-13} mm Hg. In their case they immerse a portion of their system into liquid helium at 4.2 °K and have observed very

Vol. 9 959/60

interesting properties of the pumping characteristics of a refrigerated surface.

Thus, at least two variations of the Penning gauge have been proposed to increase the ratio of the sensitivity to X-ray current over that of the Bayard–Alpert gauge.

As one reaches lower and lower pressures in various investigations it becomes increasingly evident that it is necessary to measure not only the total pressures below 10^{-9} mm Hg, but the partial pressures of the various gas constituents. A number of investigators have laid major emphasis on this endeavor as the next step in the measurement of ultra-high vacuum. Alpert and Buritz[12] reported a simplified version of the omegatron[13] with a capacity for measuring partial pressures of approximately 10^{-10} mm Hg (resolution approximately 1/40). With this instrument they were able to demonstrate the influx of atmospheric helium into an ultra-high vacuum system and also to demonstrate the relatively large concentration of CO (approximately 10^{-9} mm Hg) in the system in the presence of the omegatron. Similar instruments have been designed and used by Edwards[14] and Wagener and Marth[15]. Lange[16] converted a commercial cycloidal mass spectrometer (Consolidated Electrodynamics Corporation Model MS 21-620) into a bakeable design with a minimum detectable peak of 10^{-11} mm Hg. Special mass spectrometers with high resolution and even greater sensitivities have been built by Reynolds[17] and Fox[18], but their instruments were designed with other researches in mind.

It would seem to me that the most obvious need in this field is a mass spectrometer of even greater sensitivity and of relatively simple construction which does not introduce impurities large compared to those it is intended to measure. Here again, I look forward with pleasure to hearing papers at this Congress on this very subject.

4. Large ultra-high vacuum systems

In the studies I have mentioned involving the achievement of pressures below 10^{-10}, the systems have been relatively small in size (of the order of 1 l.) and the pumping speeds required have been less than 1 l./s. In the recent past a considerable effort has been applied to the problems of achieving ultra-high vacuum in much larger systems.

Without going into too much detail it is quite clear from experience in standard systems that certain components are required, in particular :

(1) demountable joints for large systems, capable of bakeout at 400 °C ;
(2) vacuum valves, capable of bakeout at 400 °C ;
(3) pumping systems of substantially higher speed.

With regard to demountable joints, Hickam[19] had shown some time ago that fine wire O-ring gaskets made of gold were eminently successful when mounted between flanges of stainless steel, monel, or almost any suitable harder material.

A number of workers[20, 21] had also demonstrated the effectiveness of flat copper gaskets when clamped between knife-edged ridges of a harder material (Fig. 3). Lange and Alpert suggested a much simpler design[22], the so-called step-type demountable joint which makes a very easily machined

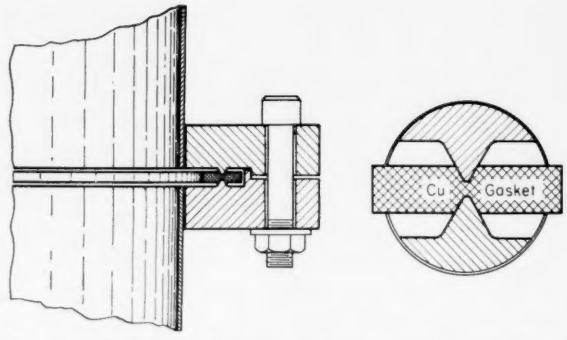

FIG. 3. Typical knife-edge flange arrangement utilizing a flat copper gasket.

but dependable joint with copper gaskets of large diameters (Fig. 4). Gaskets of both the gold O-ring type and the

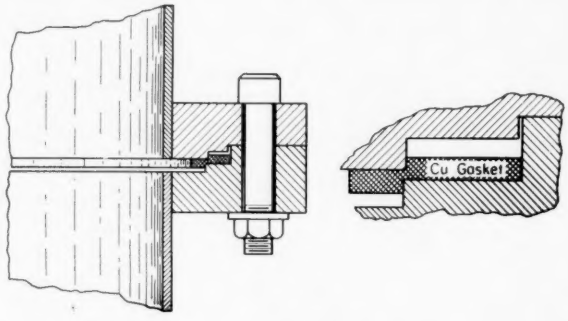

FIG. 4. Step type demountable vacuum joint.

copper step-type flange have been made in diameters of 30 cm or more with excellent reproducibility and with essentially zero leak rates. Thus bakeable demountable systems with conductances of tens of thousands of l./s are possible.

The problem of designing a bakeable valve for isolating one portion of a vacuum system from another is rather more formidable. Lange[23] has designed a valve which is basically a scaled up version of the low conductivity valves used in standard systems. I show in Fig. 5 a cross-section of such a

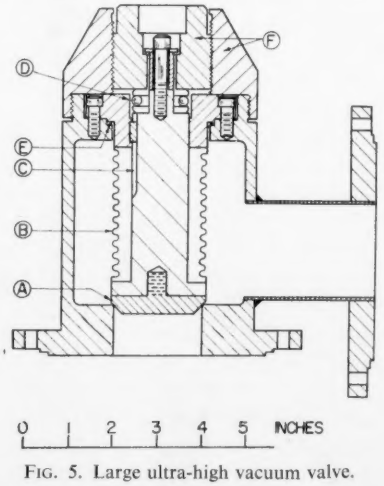

FIG. 5. Large ultra-high vacuum valve.

valve which contains a flexible bellows and a metal-to-metal nose to seat arrangement. Such valves have been made with conductances of the order of 100 l./s and one can visualize scaling them up to perhaps several hundred or 1000 l./s. However, it is difficult to visualize a direct scale-up of such valves to even larger sizes.

Reynolds[24] has suggested a large valve which utilizes an indium seat which in effect forms an internal solder joint capable of being opened and closed many times. Lange, Milleron and others are now working on designs which could be scaled up to very large sizes.

It is in the study of pumps for large ultra-high vacuum that perhaps the greatest challenge lies in this field. As mentioned before, Carmichael and I have shown that with adequate baffling to reduce back diffusion, oil diffusion pumps (speeds approximately 20 l./s) could be used to achieve pressures below 10^{-10}. This was accomplished with copper traps of a design shown in Fig. 6 and described some

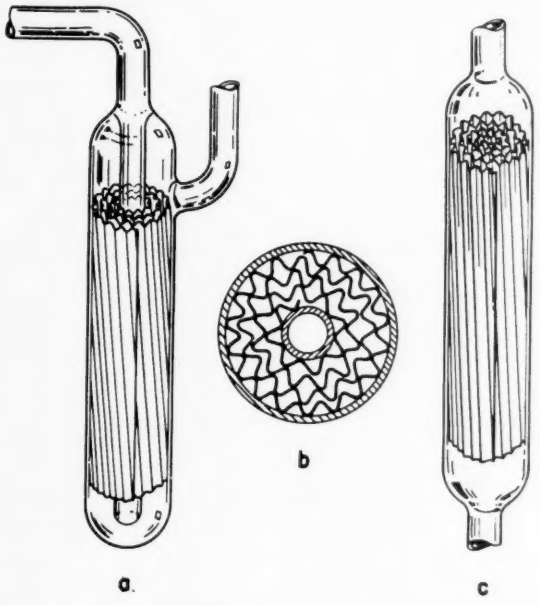

FIG. 6. Copper-foil trap.

years ago.[25] Such traps operate at room temperature to isolate oil diffusion pumps from the system. With small glass diffusion pumps, such traps are effective for periods of a month or more before saturation.

Little is understood about the physical and chemical mechanism by which such traps operate. One of my colleagues, W. J. Lange, at the Westinghouse Research Laboratories has begun a study of the mechanism by which such traps operate utilizing a bakeable mass spectrometer to see if similar copper traps can be utilized for pumps one or two orders of magnitude faster (see Fig. 7). Thus far, the results are too fragmentary to suggest a design for larger traps. One can state first of all that with a small trap of about 1 l./s conductance it is possible to prevent back diffusion from either a glass or a larger metal pump. The only gases in the system found by the mass spectrometer are CO and

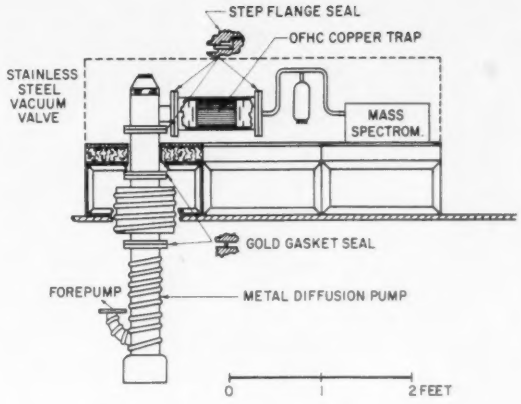

FIG. 7. 100 l./s pumping system.

H_2. This perhaps suggests some sort of adsorption and cracking of the organic molecules at the copper surface. But little more can be said at this time. We look forward with anticipation to an understanding of the mechanism which may allow us to design large room temperature baffles of this type.

The question arises, is there any other way of reducing the back-streaming from a large pump to an acceptable minimum? The answer seems to be yes. If one constructs a liquid nitrogen trap which assures that a given organic molecule would have to be reflected several times from a refrigerated surface, it has been shown by a number of experimentalists that one can achieve ultra-high vacuum with oil diffusion pumps with apertures from 4 to 9 in. in diameter.

As to how many reflections are required, we still cannot give quantitative answers—further experiments are necessary on sticking probabilities under a wide variety of conditions.

A similar statement can be made about mercury diffusion pumps. There is every reason to believe that large pumps can be used if sufficient baffling at liquid-nitrogen temperatures is included. Among traps which have been proposed are those by R. F. Post (Fig. 8) and E. Thomas (Fig. 9).

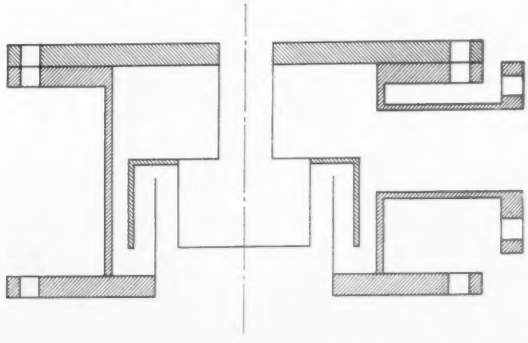

FIG. 8. Schematic diagram of trap, designed by R. F. Post.

Which of these fluids is to be preferred in large systems—oil or mercury? This question has been raised numerous times—first with high vacuum and now with ultra-high vacuum. At this time there is no obvious preference. Both

Vol. 9 959/60

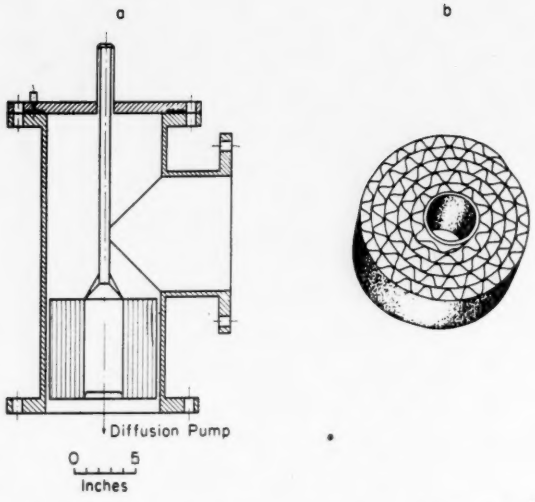

FIG. 9. Stainless-steel liquid-nitrogen trap, designed by E. Thomas.

require liquid-nitrogen traps to achieve pressures below 10^{-8} mm Hg. Each has certain advantages which are too well known from high-vacuum experience to review here. One comment should be made. As Blears[26] demonstrated, even a mercury diffusion pump can be a source of organic vapor unless care is taken to isolate or eliminate the usual mechanical pump.

Further work is required both in the design of baffles and in the redesign of diffusion pumps to reduce back-streaming.

5. Getter-ion pumps for the production of very low pressures

I have mentioned the use of ion-pumping to achieve very low pressures. A number of workers[27] have investigated the use of active metals as " getters " to evacuate a system. And in recent years a number of groups[28, 29, 30] starting with Prof. Herb's group at Wisconsin have combined the two mechanisms in such pumps as the " Evapor-Ion Pump " utilizing freshly evaporated titanium. In an interesting utilization of magnetic fields as in the Penning gauge, Hall[30] has shown, perhaps for the first time, that such devices are capable of operating in the ultra-high vacuum region. This field contains some of the most exciting prospects for the future—especially in the development of very high pumping speeds. At the same time it contains many unknowns, and much work must be done to understand the ultimate limitations in speed and equilibrium pressure.

Some of the most interesting questions are related to the process of " gettering " or adsorption in the absence of an electronic discharge. This interest arises not only from the need to understand these processes in designing pumps, but also in understanding the rates of influx due to desorption from other metallic surfaces.

Despite the voluminous references in the field, very little work relevant to our subject has been done, i.e. at low pressures and with clean surfaces. Thus, the vast bulk of data in the literature refers to gettering rates for an active surface which has already been exposed at relatively high pressures and thus has previously adsorbed large quantities of molecular gas.

Some of the best quantitative work has been done recently by Becker and Hartman, Ehrlich, Eisinger,[31, 32] and Hagstrum for the adsorption of molecular gases on tungsten and molybdenum. These people find the result that gases like N_2, O_2 and H_2 have a very large sticking coefficient on tungsten. A particularly interesting feature is that until a complete monolayer has been formed this sticking coefficient is essentially independent of the coverage of the surface as shown in Fig. 10. This result is quite different from what

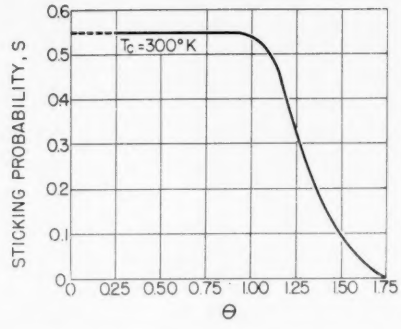

FIG. 10. Variation of sticking probability of N_2 on W with θ.

one would be led to expect by Langmuir's adsorption hypotheses.

Ehrlich[33] and Kisliuk[34] have put forth models to explain this behavior ; but further work remains to be done before we have an adequate physical picture of the process.

For some of the more typical gettering materials, sticking probabilities and rates of desorption are far less well known. Wagener[35] has measured the sticking probability of various gases on freshly evaporated barium. For H_2 and N_2 he observed a sticking probability of 10^{-3} for hydrogen on barium and 3×10^{-4} for nitrogen on barium. Stout and Gibbons[36] have measured the sticking coefficient of hydrogen on outgassed titanium metal to be only 1.6×10^{-5}. They attribute this very low value to the previous formation of titanium oxide on the surface which effectively seals it from the hydrogen. In the light of the extremely high pumping speeds quoted for various evapor-ion pumps, the sticking coefficients for a freshly evaporated surface would seem to be far larger, but few quantitative data are available. We also know relatively little about desorption rates from such surfaces at very low pressures. Finally, we must examine carefully the action of an ionizing electron beam in the vicinity of a freshly evaporated surface.

Recently, at the University of Illinois, Mr. Alan Blankfield and I have undertaken a series of experiments to determine sticking coefficients of various gases on freshly evaporated titanium surfaces. At this time I can only present some preliminary results for nitrogen on titanium.

The experimental arrangement for this experiment is shown in Fig. 11. The titanium is evaporated to the walls of a Bayard–Alpert gauge in which the usual ion collector has been replaced by a tungsten rod on which titanium wire

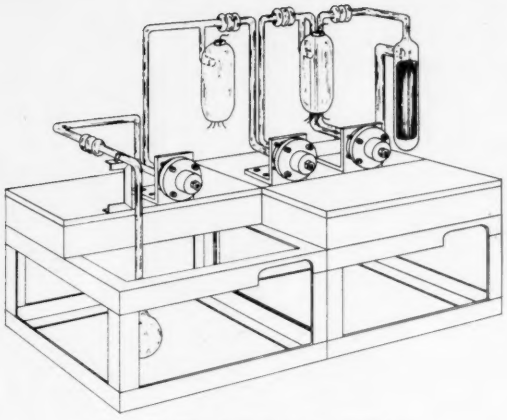

FIG. 11. Titanium pumping experiment.

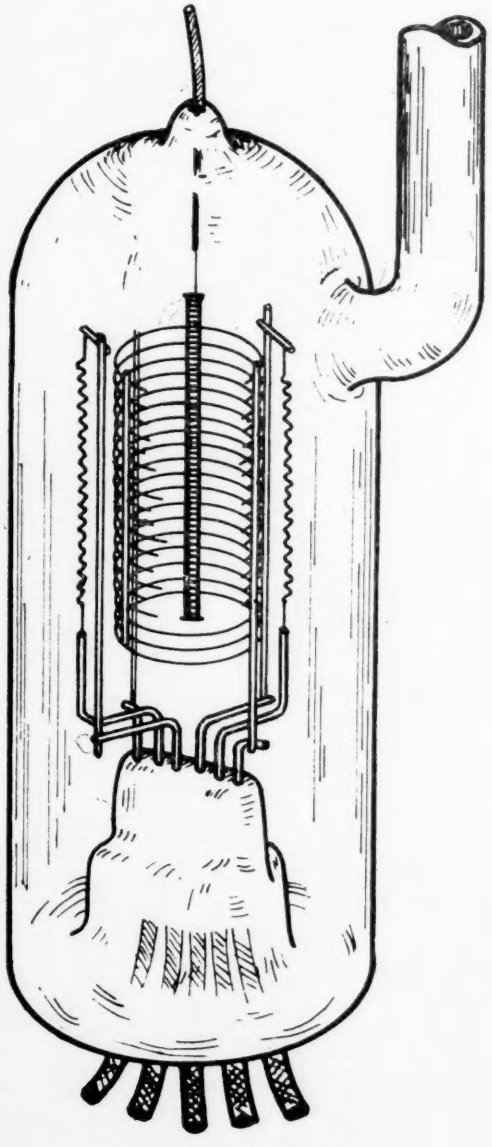

FIG. 12. Titanium ion pump.

has been wound as shown in Fig. 12. By bombarding the collector wire with electrons (20–30 mA at approximately 1000 eV) it is easy to deposit 10–100 monolayers of titanium in a few minutes.

A schematic diagram and typical data for several pump-down runs are shown in Fig. 13. Immediately after flashing

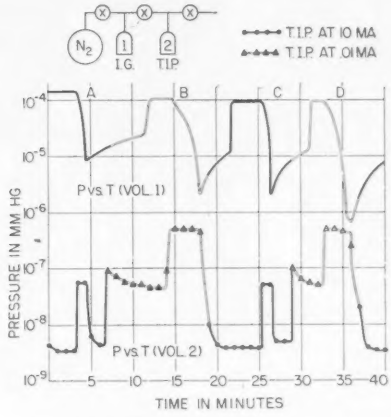

FIG. 13. Data from titanium pumping experiment.

the getter, the pressure in the titanium ion pump is approximately 3×10^{-9} mm Hg. Valve 2 is then opened sufficiently to maintain a constant chosen pressure in the pump and the rate of influx is obtained from the change in pressure in volume 1. The curves shown were taken consecutively to establish the difference in pumping speed with and without an appreciable electron beam. Curves *A* and *C* were taken with an electron emission of 10 mA ; *B* and *D*, 0.01 mA. In this manner the " pumping speed " with and without appreciable ionizing current can be measured. The sticking probability is obtained by estimating the surface area of freshly evaporated titanium and comparing the measured pumping speed with the theoretical maximum assuming a sticking coefficient of unity. While the area cannot be measured accurately, it can readily be estimated to within 25 per cent and the overall accuracy is of this order. From these curves we also can obtain values for the desorption rates of nitrogen at room temperature.

A preliminary estimate of the sticking coefficient thus obtained is approximately 4×10^{-4} for coverage of less than 0.2 monolayers. While this is comparable to Wagener's value for nitrogen on barium, it seems very low when compared with the pumping speeds of the titanium pump. However, when the voltages and an emission current of 10 mA are applied to the ionization gauge, the measured pumping speed of the " pump " is increased by a factor of 40! That is, a Bayard–Alpert gauge with titanium evaporated to the walls has a pumping speed of at least 20 l./s! This is 100 times greater than would be expected if every nitrogen ion formed were to be removed, and is also 100 times greater than any pumping speed which has been measured for an ionization gauge. I must caution you on the fact that these are very preliminary results ; nevertheless, they are very interesting and emphasize that we still don't know how a titanium pump works.

Vol. 9 959/60

This use of an ion gauge as a pump in the immediate vicinity of an evaporated layer of titanium is very similar to that described by King and Zacharias.[37] The results bear out their optimism for such a device and, further, demonstrate its unique effectiveness for ultra-high vacuum. Figure 14 shows a system in which the usual oil diffusion

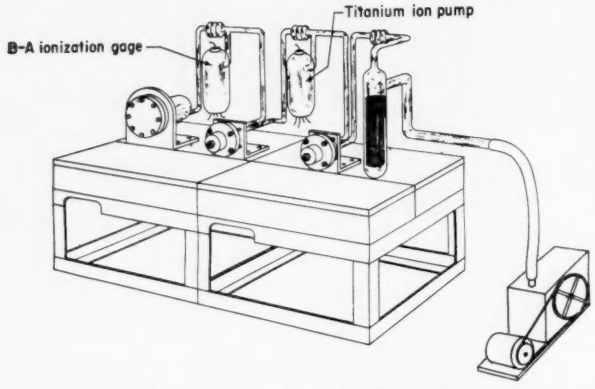

FIG. 14. Titanium ion pump system.

pump of the standard ultra-high vacuum system has been completely eliminated. The roughing pump in this case is a conventional rotary mechanical pump which is isolated during initial bakeout by a copper trap immersed in liquid nitrogen. Immediately after bakeout the vacuum valve between the titanium pump and mechanical pump is closed and the titanium is flashed briefly. Thereafter the system is pumped quickly to $3\text{–}4 \times 10^{-10}$ mm Hg. The simplicity of the system is self-evident. The pump is not more difficult to make than the standard Bayard–Alpert ionization gauge and may be operated with a standard supply. It should be emphasized, however, that the pump does not operate at pressures below 10^{-8} mm Hg unless the electron beam is turned on.

6. Summary

In summary, then, I have tried to outline some of the advances in ultra-high vacuum technology which have taken place in the past few years. It is clear that significant changes are in the making, both in the degree of vacuum which can be achieved and in the size of system which can be evacuated. The "getter-ion" pump seems at this time to offer the prospect of both high speed and very low pressures. At the same time there is a strong need for further studies of the physical and chemical interactions of neutral and activated molecules with surfaces.

References

[1] See, for example, D. W. Kerst *et al* ; *Phys. Rev.* **102**, 590 (1956), and G. K. O'Neill ; *Phys. Rev.* **102**, 1418 (1956).
[2] D. Alpert ; " New developments in the production and measurement of ultra-high vacuum," *J. Appl. Phys.* **24**, 860 (1953).
[3] I. Langmuir ; *J. Amer. Chem. Soc.* **40**, 1361 (1918).
[4] For a general discussion see D. Alpert, Production and measurement of ultra-high vacuum, *Handbuch der Physik*, Springer-Verlag, Berlin, in press.
[5] D. Alpert ; New developments in the production and measurement of ultra-high vacuum, *J. Appl. Phys.* **24**, 860 (1953).
[6] D. Alpert and R. S. Buritz ; " Ultra-high vacuum II. Limiting factors on the attainment of very low Pressures," *J. Appl. Phys.* **25**, 202 (1954).
[7] L. J. Varnerin and D. White ; " Ultimate vacuum in a vacuum-enclosed ionization gauge," *J. Appl. Phys.* **25**, 1207 (1954).
[8] D. Alpert ; Experiments at very low pressure, *Science* **122**, no. 3173, 729 (1955).
[9] J. M. Houston ; " New ultra-high-vacuum ionization gauge," *Bull. Amer. Phys. Soc. II*, **1**, no. 6, 301 (1956).
[10] *Philips Tech. Rev.* **2**, 201 (1937).
[11] J. P. Hobson and P. A. Redhead ; Operation of an inverted-magnetron gauge in the pressure range 10^{-3} to 10^{-12} mmHg, *Canad. J. Phys.* **36**, 271 (1958).
[12] D. Alpert and R. S. Buritz ; *J. Appl. Phys.* **25**, 202 (1954).
[13] Sommer, Thomas and Hipple ; *Phys. Rev.* **82**, 697 (1951).
[14] Edwards ; *J. Appl. Phys.* **6**, 44 (1955).
[15] J. S. Wagener and P. T. Marth ; *J. Appl. Phys.* **28**, 1027 (1957).
[16] W. J. Lange ; private communication.
[17] J. H. Reynolds ; *Rev. Sci. Instrum.* **27**, 928 (1956).
[18] R. E. Fox ; private communication.
[19] W. M. Hickam ; *Rev. Sci. Instrum.* **20**, 472 (1949).
[20] H. H. Pattee ; *Rev. Sci. Instrum.* **25**, 1132 (1954).
[21] P. J. Van Heerden ; *Rev. Sci. Instrum.* **26**, 1130 (1955).
[22] W. J. Lange and D. Alpert ; *Rev. Sci. Instrum.* **28**, 726 (1957).
[23] W. J. Lange ; *Rev. Sci. Instrum.* (in press).
[24] F. L. Reynolds ; *Vacuum Symposium Transactions* (1955).
[25] D. Alpert ; *Rev. Sci. Instrum.* (1953).
[26] Blears ; *Rev. Sci. Instrum.* **28**, 36 (1951).
[27] See W. Espe, M. Knoll and M. P. Wilder ; *Electronics* **23**, 80 (1950) and Dushman ; *Vacuum Technique*, Chapter 11, Section 2, for surveys of this field.
[28] Herb, Davis, Diviata and Saxon ; *Phys. Rev.* **89**, 897 (1953).
[29] A. M. Gurewitsch and N. F. Westendorp ; *Rev. Sci. Instrum.* **25**, 389 (1954).
[30] L. D. Hall ; *MIT Conference on Physical Electronics* (1958).
[31] *Bull. Amer. Phys. Soc.* **3**, 193.
[32] For a discussion see J. A. Becker ; *Advances in Catalysis Vol.* 7, Academic Press, New York City (1955).
[33] Ehrlich ; *J. Phys. Chem. Solids* **1**, 3 (1956).
[34] Kisliuk ; *J. Phys. Chem. Solids* **3**, 95 (1957).
[35] S. Wagener ; *Proc. Inst. Elect. Engrs* Pt. III **99**, 135 (1952).
[36] V. L. Stout and M. D. Gibbons ; *J. Appl. Phys.* **26**, 1488 (1955).
[37] J. G. King and J. R. Zacharias ; *Advances in Electronics and Electron Physics Vol.* 8, Academic Press, New York (1956).

Evapor-ion Pump Development at the University of Wisconsin*

R. G. HERB

Evapor-ion pumps have been developed at the University of Wisconsin for a variety of applications. The largest of these pumps has a diameter of 24 in. *It is used in connection with a hydrogen negative ion source and gives a pumping speed for hydrogen of approximately 15,000* l/s *at pressures in the region of* 5×10^{-6} mm Hg. *Several pumps of 12* in. *diam. and of 8* in. *diam. are now being used. For other applications pumps of 1* in. *diam. and 2* in. *diam. have been developed. Evaporation techniques, starting techniques, and general operational characteristics of these pumps will be given.*

Vol. 9 959/60

Introduction

Since early in the 1930's an active development program has been maintained at the University of Wisconsin toward improvement of high voltage electrostatic generators. A series of generators was built culminating in 1940 in a machine which operated up to 4.5 million volts. Attempts to improve on these machines at many laboratories throughout the world have been relatively unrewarding. Each of these machines must be equipped with an accelerating tube. This tube must be evacuated to permit acceleration of ions. Nearly all generators of this type now in operation are limited in voltage by electrical breakdown in the accelerating tube.

Experience at Wisconsin had indicated that vapors in the accelerating tube played a role in electrical breakdown. A program was initiated in the late 1940's toward development of techniques for an all metal and ceramic accelerating tube. This program was successful. By the use of titanium hydride painted on to high alumina porcelain, disks of Kovar were soldered to cylinders of porcelain with a solder consisting of the eutectic mixture of silver and copper. Vacuum seals between removable joints in the vacuum system were made by compressing rings of copper or aluminum wire between flat Kovar or steel surfaces. The remaining source of vapor was from the oil diffusion pump and the forepump. A program was then initiated leading toward a new vapor-free pumping system.

Early attempts along a number of lines were unsuccessful. With the first successful evaporation of titanium the pumping action achieved was spectacular and the direction of the program was determined.

Some of the early evapor-ion pumps and principles of operation have been described in previous publications.[1–3] During the past few years more than twenty Evapor-ion pumps have been built for use in our laboratory. They range in size from an inner diameter of 24 in. to an inner diameter of 1 in. Many different arrangements have been tried for evaporation of titanium and other gettering materials and for ionization to provide for pumping of inert gases. A few of the more interesting pumps are described in this paper and some operational results are given.

Principles of operation

In order to review the basic principles of Evapor-ion pumps a brief description will first be given of the first successful pump, which is shown in Fig. 1. Titanium wire of 0.020 in.

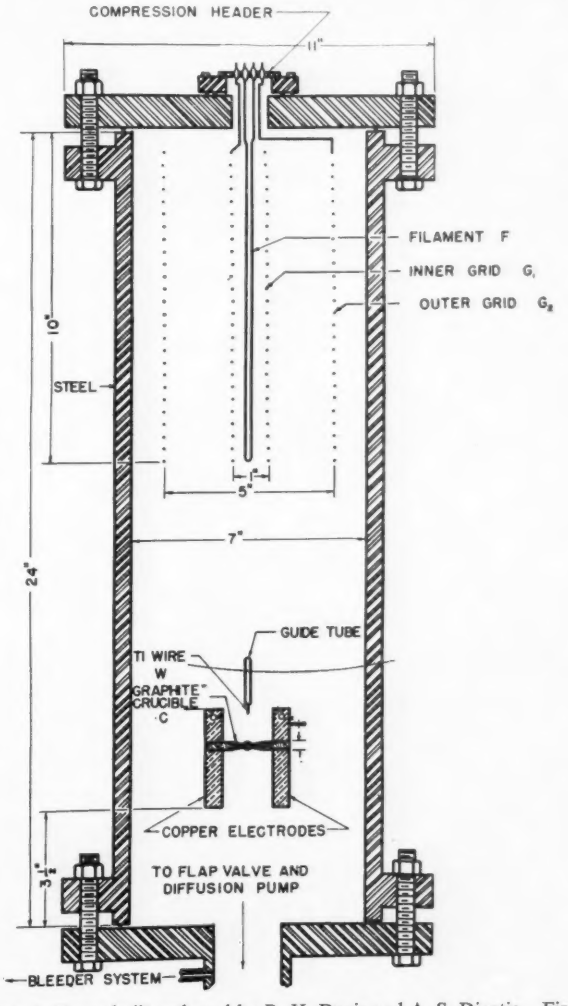

FIG. 1. Pump built and used by R. H. Davis and A. S. Divatia. First pump to include ionization. Conduction-heated crucible, heating current approximately 600 A. Described in paper by Davis and Divatia[2].

* Paper presented at the First International Congress on Vacuum Techniques, Namur, 10–13 June 1958.

diameter is fed from a spool inside the pump through a guide tube which directs it towards the evaporator. The evaporator in this pump was a graphite rod into which a vertical radial hole was formed to provide a cavity. The graphite rod was heated by conduction current to where titanium was melted and evaporated. It condensed on to the inner walls of the cylindrical container. Active gases such as oxygen, nitrogen and hydrogen became attached to this surface. They became permanently bound and were later buried by further condensed titanium. To pump inert gases such as the noble gases, electrons from filament F, which is near ground potential, were accelerated by grid G_1 G_2 which is at a positive potential of about 500 V. Grid geometry and potentials were chosen to give electrons a long mean-free path. Positive ions formed in the high potential region were driven into the wall where they were buried by successive layers of titanium.

Evaporation techniques

The graphite evaporator of the pump shown in Fig. 1 was limited to an operational life of only a few days. Other techniques were tried. Fine titanium wires were exploded by condenser discharge. Arcs were struck between titanium wire and other electrodes. Titanium wire was directly bombarded by electrons to where evaporation appeared to take place from a molten ball at the tip. Sputtering from titanium was tried. Rods made from tantaloy, an alloy of tantalum and tungsten, were heated by conduction current to give evaporation of titanium. All of these above methods were relatively unsuccessful, some because of poor operational life, others, such as the direct bombardment of titanium[7]wire, because of relatively inefficient pumping.

Best performance has been obtained from an evaporator consisting of a cylindrical rod of tantaloy heated by electron bombardment. Promising results have also been obtained recently utilizing stranded wire heated directly by electron bombardment.

Pumps for electrostatic generator

Fig. 2 shows the pump which has been used for the past two years for evacuation of the accelerating tube of our electrostatic generator. In this application the pumping

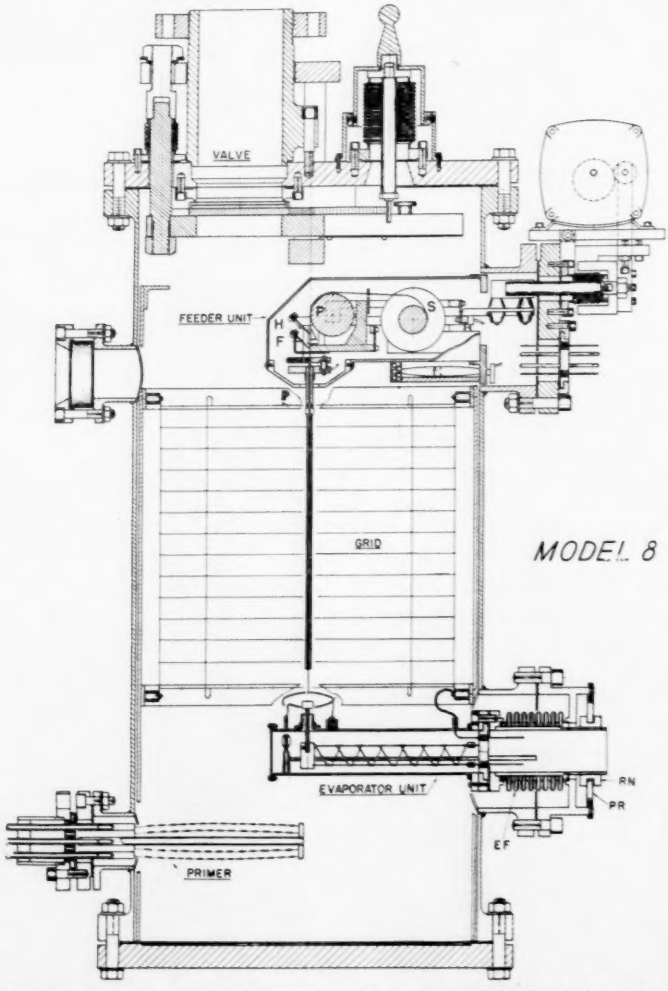

FIG. 2. Pump for large electrostatic generator. Major responsibility for design and construction taken by D. J. Knecht. This pump has a 12 in. diameter and can be separated from the vacuum system of the high-voltage generator by a 3½ in. all-metal valve.

speed requirements are low and the relatively large pump diameter (12 in.) was chosen because our experience at the time this pump was designed had been principally with pumps of this size. Dependable trouble-free operation was the chief requirement. Wire is stored on a spool toward the top. The evaporator near the bottom of the pump utilizes a tantaloy cylinder $\frac{3}{8}$ in. in diameter by $\frac{3}{8}$ in. high mounted on a tungsten rod of $\frac{1}{16}$ in. diameter. The tungsten filament which supplies electrons to heat the tantaloy cylinder also furnishes electrons to the grid for the pumping of inert gases.

Titanium is fed to the evaporator every few days when the electrostatic generator is not in operation and about twice per day when the generator is running. Pressures of a few times 10^{-8} mm Hg are obtained when the system is leak-free.

Fig. 3 shows the pump which now evacuates the electrostatic analyzer and target region. This pump has an 8 in. diameter. The wire feeder and evaporator are in this case mounted as a single unit and upper regions of the pump are left clear for the grid. The wire feeder and guide tube are adjustable in position through the same metal bellows that provides for wire-feeding motion. The tip of the guide tube moves through a vertical distance of approximately $\frac{1}{2}$ in. and during each stroke the titanium wire is advanced approximately $\frac{1}{16}$ in. These feeding mechanisms have been termed " dipping duck feeders ". They are convenient to install and to service and they minimized trouble due to the wire sticking to the tantaloy post.

Experimental pumps

Figure 4 shows a pump which has been used for the study of ion pumping problems. A dipping duck feeder is used similar to the feeder in the pump of Fig. 4. The evaporator consists of a tantaloy pill above which is mounted a " reflector ". Wire is fed through a hole in the reflector and titanium evaporated from the tantaloy pill is re-evaporated and directed downward by the heated reflector. A wide variety of grid arrangements has been tried in this pump. The grid illustrated consists of a cylindrical array of tungsten wire of 0.002 in. diameter spaced $\frac{1}{4}$ in. apart. Top and bottom are closed by disk-shaped arrays of wire similarly

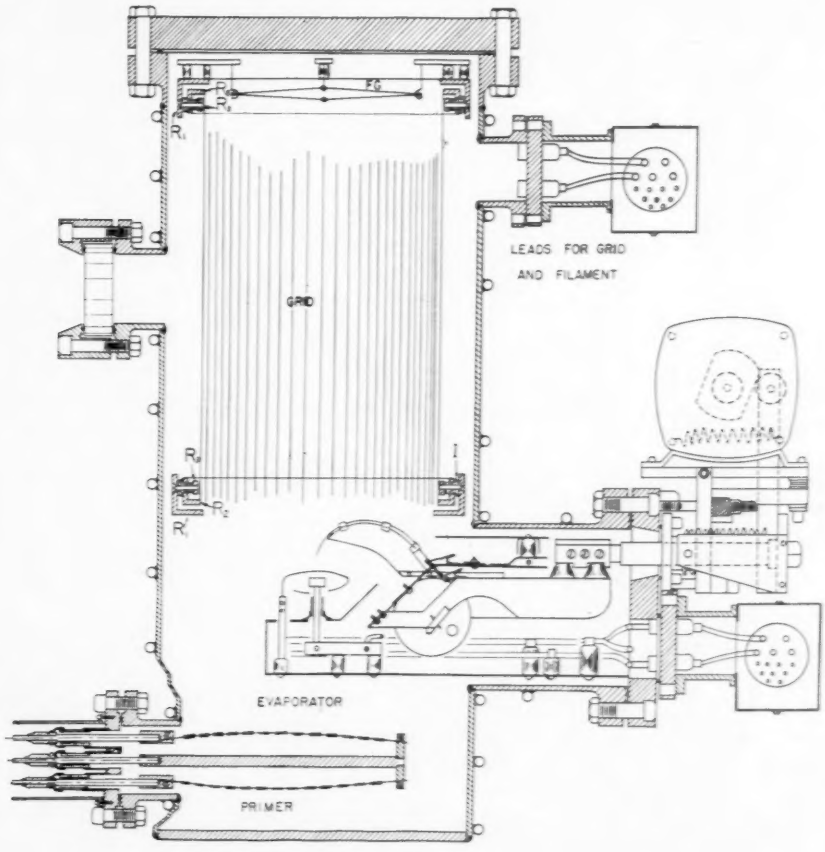

FIG. 3. Pump for target region of electrostatic generator. Major responsibility for design and construction assumed by D. J. Knecht. This pump has an 8 in. diameter and is equipped with a " dipping duck " feeder. The grid shown in the drawing has been replaced by one of simpler design.

Vol. 9 959/60

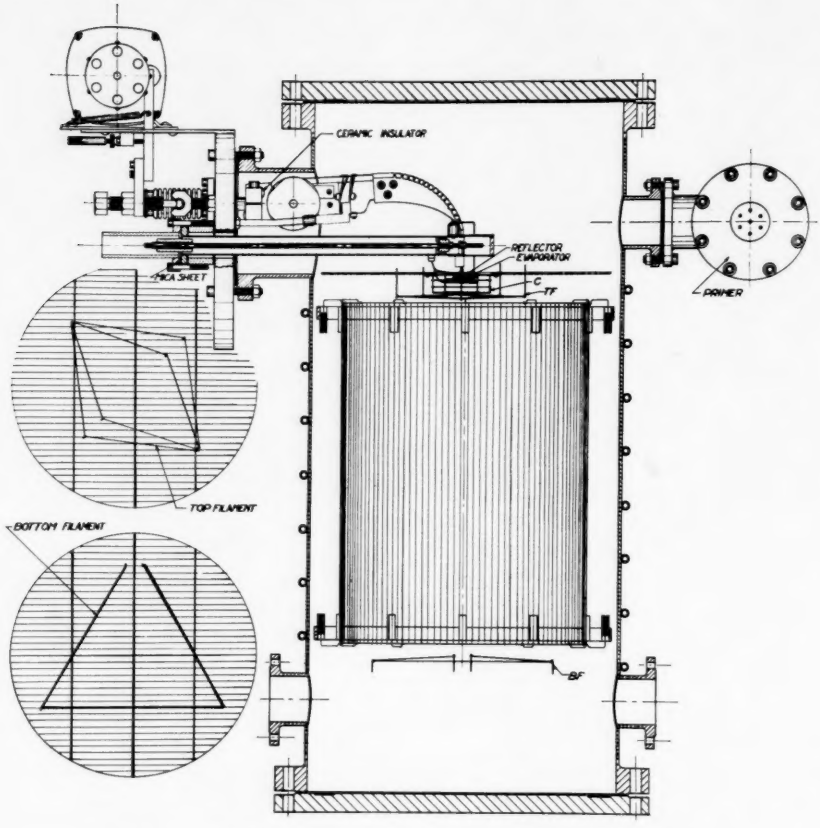

FIG. 4. Twelve-inch pump for study of ion pumping. Grid consists of cylindrical array of tungsten wires of 0.002 in. diameter spaced ¼ in. apart. Top and bottom are closed by disks formed of similarly spaced wire. Electrons for the grid could be supplied from either end.

spaced. This grid, which is similar to the grid described by Alexeff and Peterson[3], gave a pumping speed for argon of about 100 l./s with an electron current of 500 mA and with no magnetic field. Other grid geometries have approached this efficiency but have not surpassed it.

Pumping speed measurements

The pump of Fig. 5 has been used for studying the pumping speeds of a number of gases and vapors. More recently this pump has been used for pump starting experiments. Pumping speed measurements were initiated primarily for the purpose of determining the pumping speed for water vapor. Some earlier experiments had indicated poor performance for this vapor. Values obtained as shown by Table I were surprisingly high for water vapor. At the time of these measurements the diffusion dome shown in Fig. 5 had not been installed and the arrangement of gas inlet and ionization gauge was not satisfactory for accurate determination of high pumping speeds. Additional uncertainties were introduced because of lack of information on ionization gauge sensitivity.

The grid with which this pump was equipped when the data of Table I were taken was one of the most inefficient we have used. It was considered satisfactory, however, for the determination of pumping speed values of one gas relative to another.

TABLE I

Pumping speed data. Pump of Fig. 5 without diffusion dome

Gas	Pumping speed (l./s)	Pressure (mm Hg)
Hydrogen	4200	5×10^{-6}
Oxygen	2100	2×10^{-6}
*Carbon dioxide	3800	5×10^{-6}
*Ammonia	2300	5×10^{-6}
Nitrogen	2300	3×10^{-6}
Air	210	5×10^{-5}
*Water vapor (vapor-pressure method)	6950	1.5×10^{-5}
*Water vapor (mass of liquid method)	6800	5×10^{-6}
The following data were obtained at 200 mA ionization current		
Argon	5.8	2×10^{-5}
*Methane	12.5	7.8×10^{-6}
*Ethane	22.5	4×10^{-6}
*Propane	18.4	1.7×10^{-5}
*Isobutane	81.0	1×10^{-5}
*Sulfur hexafluoride	150.0	6×10^{-6}

* No correction factor used.

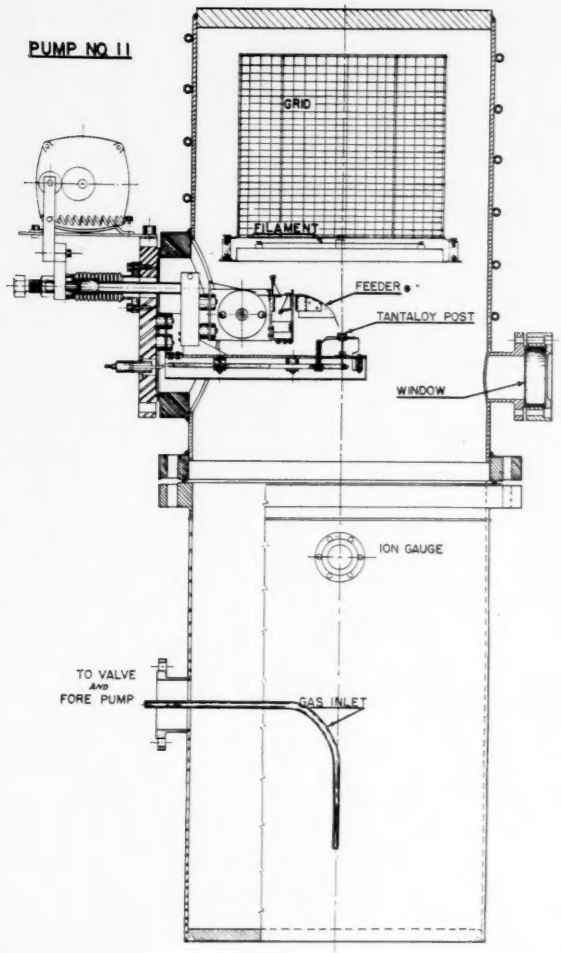

FIG. 5. Twelve-inch pump utilized by H. Lucks, R. Graetzer, G. Westerberg, and I. Sherman for the study of pumping speeds of various gases and vapors and for pump starting experiments. Diffusion dome was not yet available when pumping-speed measurements were made.

Vol. 9 959/60

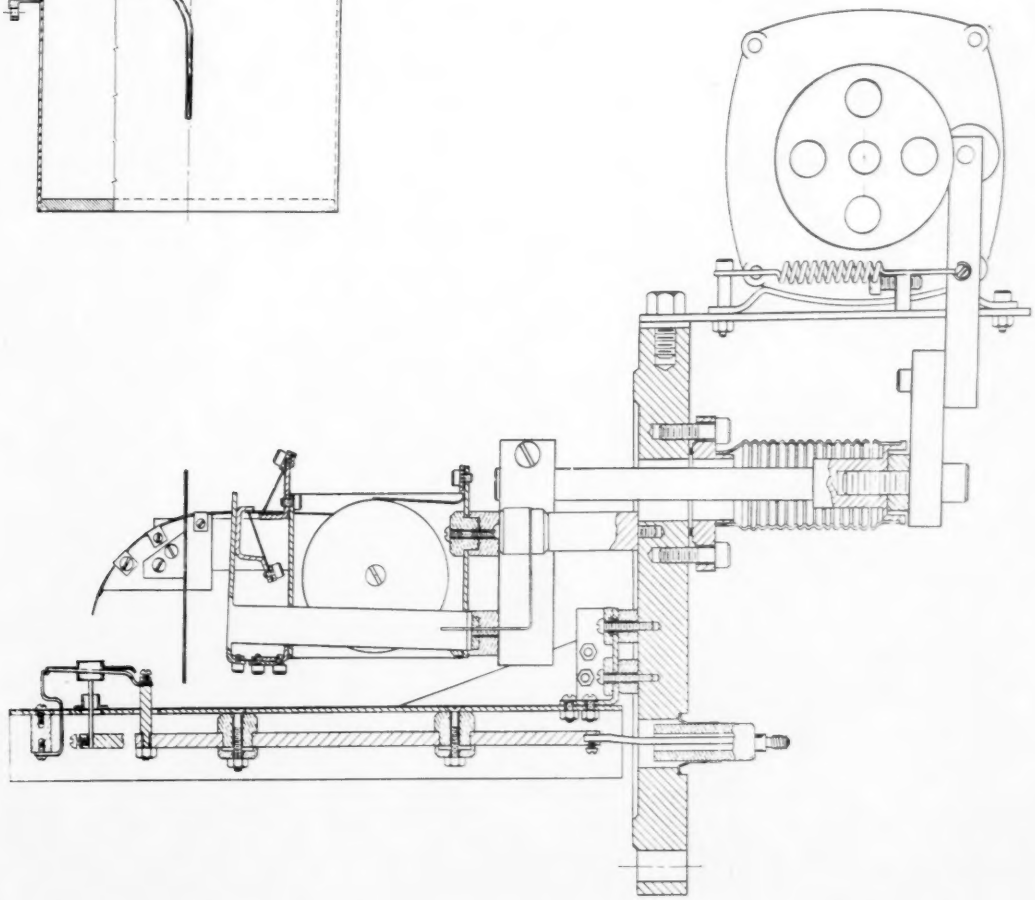

Pump starting measurements

Some interesting experiments at the Argonne National Laboratory in starting a production Evapor-ion pump without the use of primers led to work at our laboratory along similar lines. With the evaporator geometry shown in Fig. 5 electrical circuits were arranged so that the tantaloy post could be grounded and the filament could be at a high negative potential. With this arrangement the tantaloy post can be heated to temperatures required for evaporation with pump pressures as high as 100 μ. Power required increases as pump pressure increases and is about 600 W at a pressure of 100 μ.

Two curves showing pressure as a function of time are shown in Fig. 6. At pressures in the region of 2×10^{-5} mm Hg operation is somewhat more satisfactory with the filament grounded and with the post at high potential. The circuits of our newer pumps are arranged to permit this shift in potentials and primers are not installed.

An extensive series of pumpdown runs was made from atmospheric pressure to a pressure of about 5×10^{-6} mm Hg. Nitrogen, oxygen, argon, and sulfur-hexafluoride pumped down rapidly when they were dry. Pumpdown rates appeared to be almost completely controlled by water-vapor content. Yet water vapor is very rapidly gettered by titanium. The difficulty is probably due to gradual release of water condensed on cold surfaces and poor pumping of water vapor by the forepump. If pump walls are at an elevated temperature when air saturated with water vapor is admitted, pumpdown time is improved. A liquid-air trap in the forepump line also improved pumpdown time by about a factor of two.

Pumps for negative ion sources

In our development program directed toward improvement of electrostatic generators we have put a considerable amount of effort in recent years into production of beams of negative ions. Negative ions can be directed through a generator held at a high positive potential. If electrons are stripped from hydrogen negative ions in the region of high positive potential, they can be again accelerated to a target at ground potential and energy doubling is achieved.

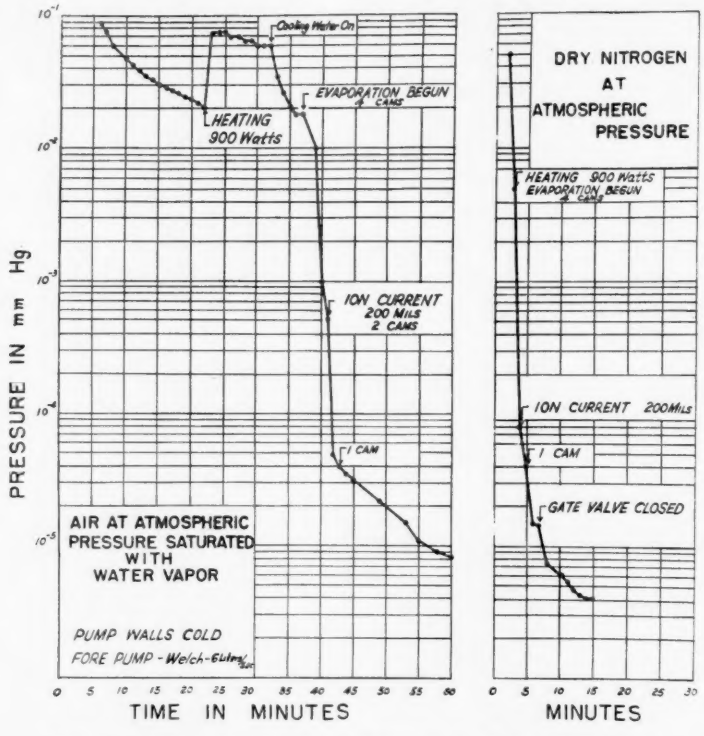

FIG. 6. Showing pressure as a function of time in pump-starting measurements with the pump of Fig. 5. Data were taken by H. Lucks and G. Westerberg. In run with saturated air, pump was outgassed by heating for 10 min. No primer was used. In starting, tantaloy evaporator is grounded and filament is at high negative potential. Polarity is reversed when pressure is in region of 5×10^{-5} mm Hg.

Fig. 7 shows apparatus now being used for production of helium negative ions. The helium positive ion source now being used consumes approximately 80 cm^3 of helium at atmospheric pressure per hour. Even with the best grids so far developed this quantity of helium is difficult to handle with an evapor-ion pump. In this case we have a 6 in. oil diffusion pump in parallel with an evapor-ion pump. No trap is used since the evapor-ion pump serves for this purpose. Nitrogen has been commonly used as the converter gas. A small percentage of the positive ions passing through a stream of nitrogen are converted to negative ions. Nitrogen is pumped rapidly by the Evapor-ion pump.

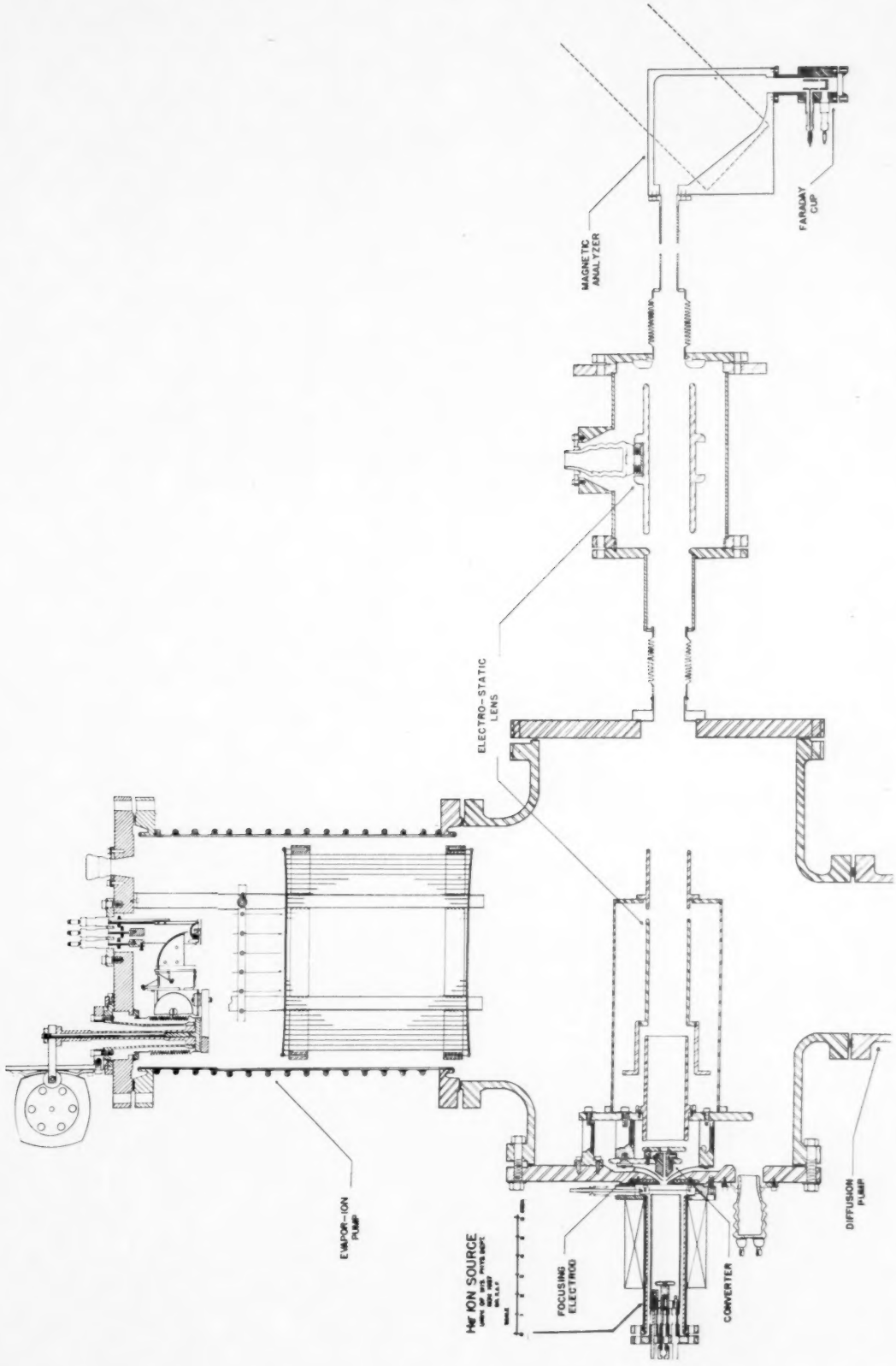

FIG. 7. Helium negative ion source equipped with 6 in. oil diffusion pump and 12 in. Evapor-ion pump operating in parallel.

Vol. 9 959/60

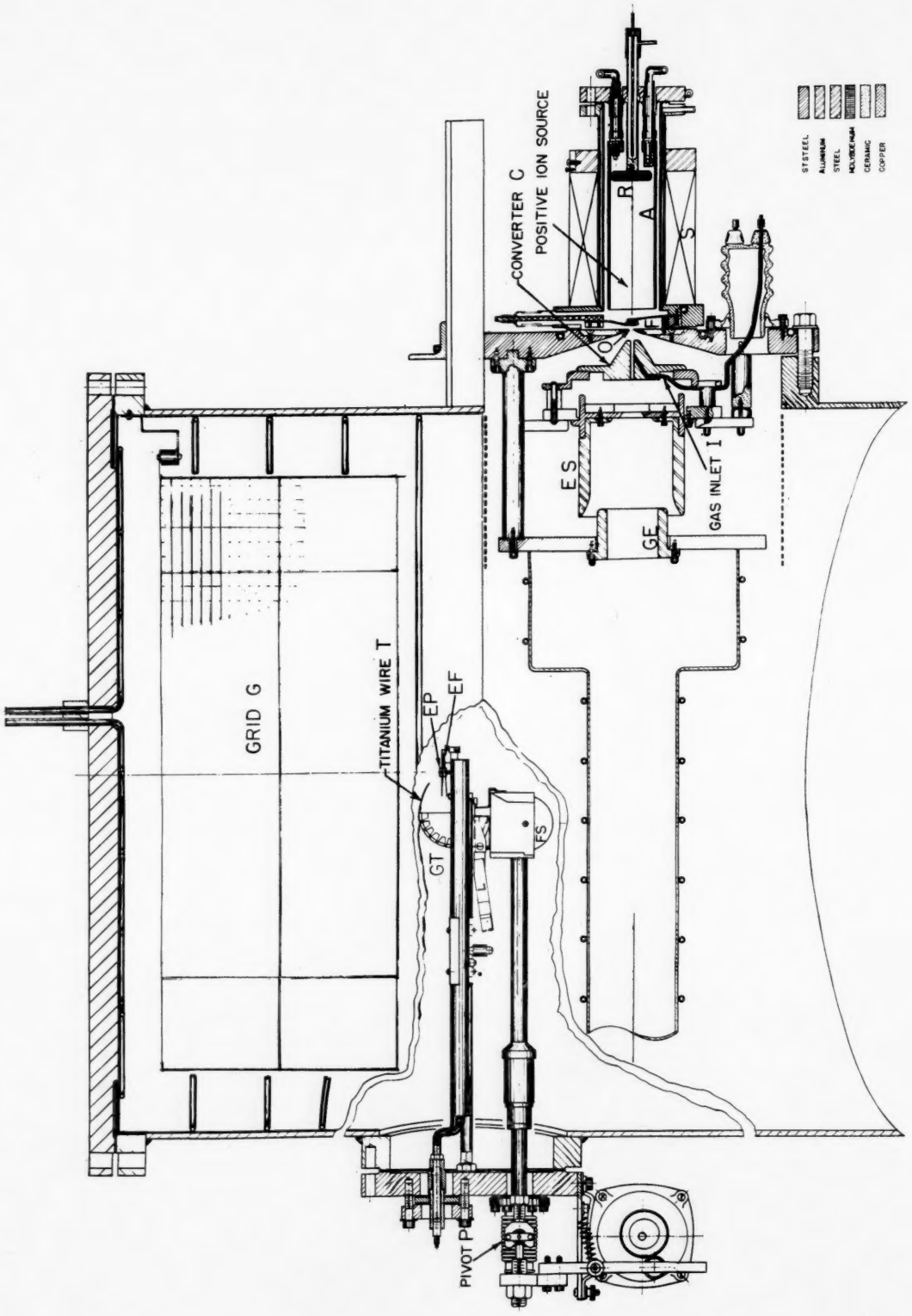

FIG. 8. Hydrogen negative ion source. Container diameter is 24 in. Active pumping surface is very close to source of gas. Hydrogen flow rates from negative ion source have been as high as 500 cm^3/hr. Feeder is arranged to minimize titanium deposition on to tip of guide tube.

VO.
9
1959

The evaporator in this pump is equipped with a " reflector." Pumping speeds provided by an evaporator of this type appear to be somewhat better than are given by evaporators which do not utilize reflectors.

Hydrogen negative ion source

A drawing of the hydrogen negative ion source with its Evapor-ion pump is shown in Fig. 8. The positive ion source in this case requires a hydrogen flow of 50 to 100 cm^3/h at n.t.p. To convert positive hydrogen ions to negative ions hydrogen flow rates of 250 cm^3/h at n.t.p. are commonly used in the conversion capillary. Hydrogen input flows as high as 500 cm^3/h at n.t.p. have been handled satisfactorily by this Evapor-ion pump.

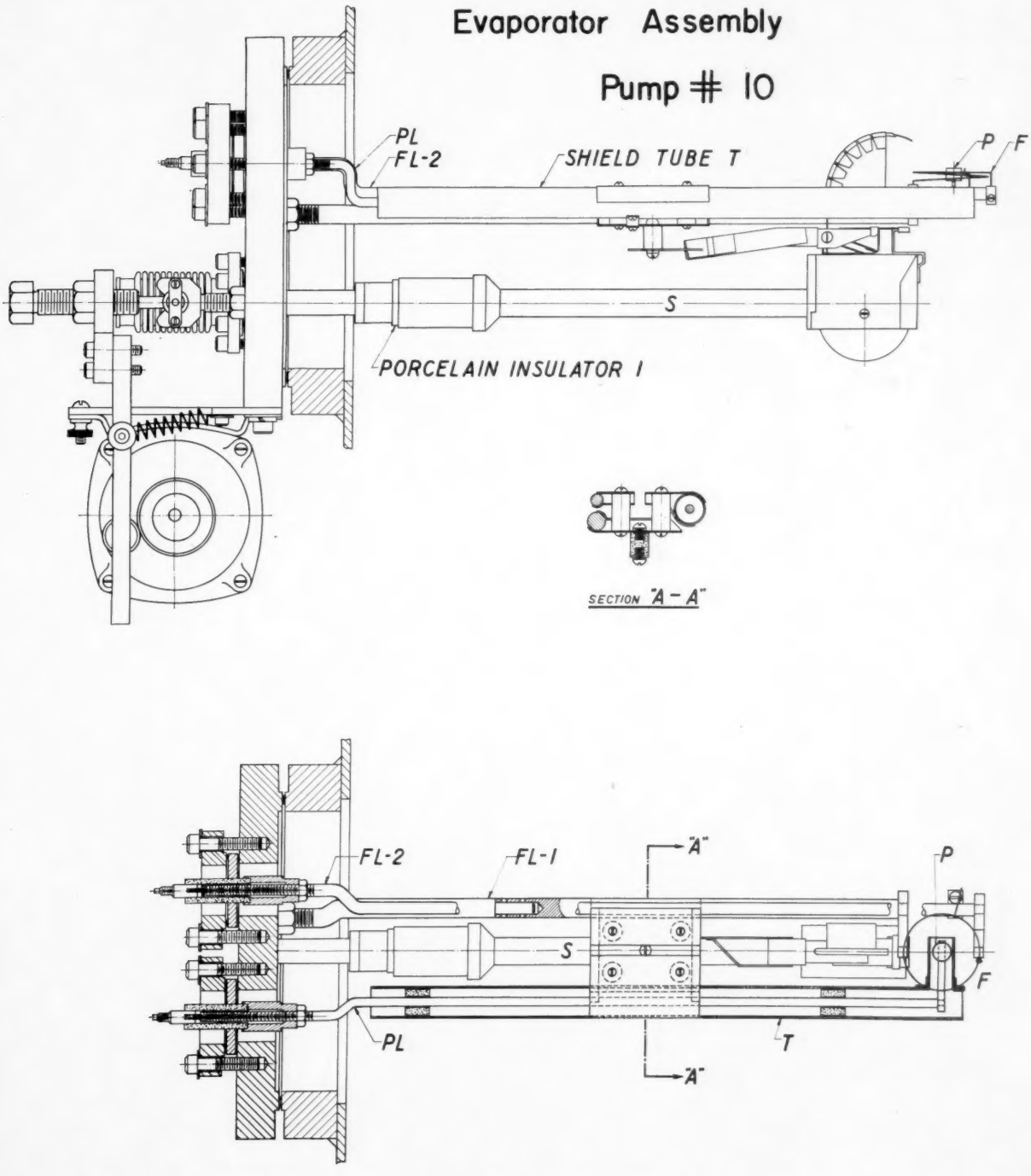

FIG. 9. Showing details of feeder for pump of Fig. 8.

Vol. 9 959/60

Pumping speed measurements gave values of approximately 15,000 l./s when gas was admitted toward the lower part of the container and with the inlet to the pressure gauge located about midway between top and bottom.

The customary definition of pumping speeds does not apply well to this application of the Evapor-ion pump. The source of gas which must be pumped is inside the pump and the usual input impedance is not encountered. The container shown in Fig. 8 has a port toward the lower end for a second evaporator which will be installed if hydrogen input must be increased still further. If this evaporator is suitably arranged, the source of gas will be surrounded by active surface.

Pressures maintained in this pump during operation of the ion source are usually between 1×10^{-6} mm Hg and 5×10^{-6} mm Hg. The feeder used in this pump is arranged to minimize condensation at the open end of the guide tube.

Small pumps

Fig. 10 and 11 show a pump with a 2 in. aperture which is now under development. Two strands of titanium wire

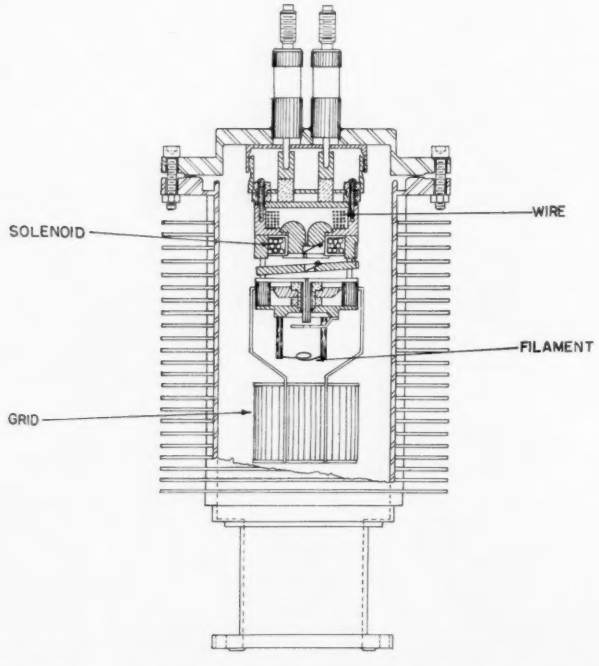

FIG. 10. Two-inch evapor-ion pump utilizing stranded wire. Wire is fed by internal electromagnet. Power consumption is less than 100 W, and pump is air-cooled.

twisted together with two strands of tantalum wire form the stranded wire now being used in this pump. The wire is heated by electron bombardment. The tantalum wire provides the surface from which molten titanium evaporates, and the tantalum wire is evaporated later as it approaches closer to the source of electrons.

Some performance data obtained with this pump are given in Table II. Operational difficulties in the past have been

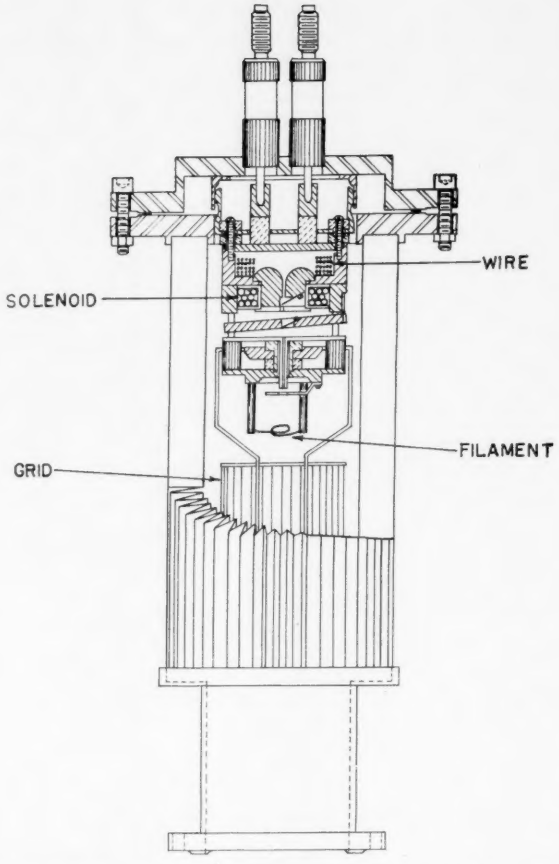

FIG. 11. Two-inch pump with folded metal wall. Folded metal is to increase active pumping surface.

TABLE II

Pumping Speeds of Various Gases (2 in. pump)

Gas	Pumping speed (l./s)
Hydrogen	50–70
Oxygen	60–100
Nitrogen	60–120
Air	20–40
Argon	1–1.5

mainly due to inadequate straightening of the wire before it emerges from the guide tube and build-up of condensed titanium near the tip of the guide tube. These problems appear now to be close to solution.

Discussion

Much work remains before the full potentialities of these pumps can be realized. For many applications they are now advantageous. In each application at our laboratory where an Evapor-ion pump was adopted, research workers involved have become enthusiastic.

Many students in physics and engineering have participated

in this work. The contributions of R. H. Davis* and A. S. Divatia† were most crucial to establishing the basic principles of operation. They have gone on to the Ph.D degree with theses in nuclear physics. Contributions of I. Alexeff and E. C. Peterson have added greatly to our understanding of evaporation problems and factors of importance in ion pumping. D. J. Knecht took much of the responsibility for the design and construction of two pumps. H. Lucks, R. Welton, G. Westerberg and T. Pauly have made extensive contributions to pump-starting problems and to measurements of pumping speeds of inactive gases and vapors. In the development of small pumps W. Dahl and R. Frosch have made major contributions.

This work was supported by the National Science Foundation, by the Graduate School from funds supplied by the Wisconsin Alumni Research Foundation, and by the U.S. Atomic Energy Commission.

References

[1] Ajay S. Divatia and Robert H. Davis ; Construction and performance of Evapor-ion pumps, *Vacuum Symposium Transactions* p. 40, Committee on Vacuum Techniques, Inc. (1954).

[2] Robert H. Davis and Ajay S. Divatia ; *Rev. Sci. Instrum.* **25**, 1193 (1954).

[3] Igor Alexeff and Edward C. Peterson ; Evapor-ion pump performance with noble gases, *Vacuum Symposium Transactions* p. 87, Committee on Vacuum Techniques, Inc. (1955).

* Now at Florida State University, Tallahassee, Florida.

† Now at Tata Institute for Fundamental Research, Bombay, India.

Vol. 9 959/60

Experience in Designing and Manufacturing All-Metal Vacuum Systems*

M. L. LYUBIMOV, K. P. SHAKHOV and YA. A. YUKHVIDIN

Introduction

Late years have seen a clear-cut tendency to replace glass vacuum systems by all-metal systems, for an obvious reason. We have been working in this direction for the last ten years and the main results of our work form the subject of this report.†

As any vacuum system is a composite of individual constructional elements, special attention will be paid to the latter. Accordingly, the subjects to be dealt with are :

(a) the design of demountable, high-vacuum heated joints,
(b) the design of valves,
(c) the design of traps.

1. Demountable heated high-vacuum joints

1. *Types of seals*

We have developed and investigated the following types of seals for various constructional assemblies :

(a) conical seals (Figs. 1, 2) ;
(b) seals with groove-wedge profiles (Figs. 3–5) ;
(c) seals with a rectangular butt projection (Fig. 6) ;
(d) pyramidal seals for rectangular cross-sections (Fig. 7) ;
(e) seals with a double profile (Fig. 8) ;
(f) diffusion seals.

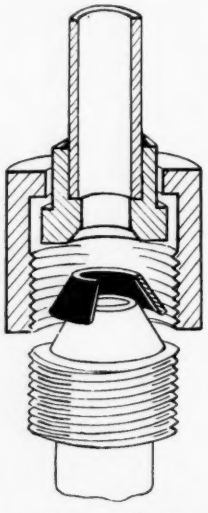

FIG. 1. Conical seal with gasket.

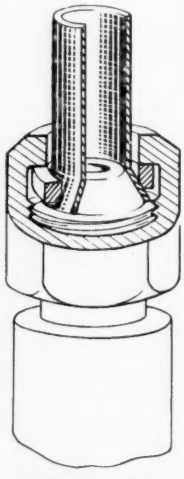

FIG. 2. Conical seal without gasket.

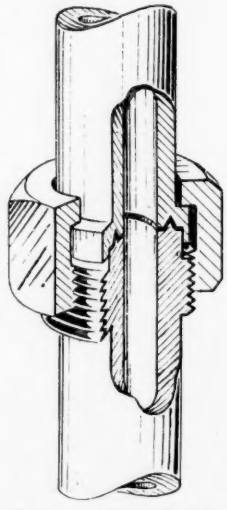

FIG. 3. Groove-wedge seal with union nut.

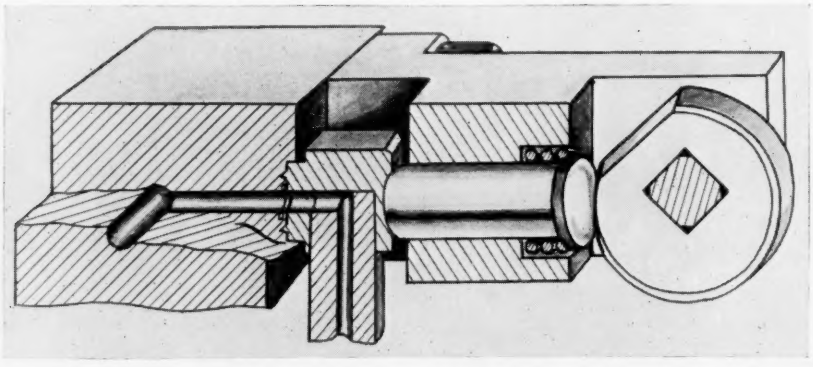

FIG. 4. Groove-wedge seal with cam clamp.

* Paper presented at the First International Congress on Vacuum Techniques, Namur, 10–13 June 1958.

† The report makes use of some of the results of investigations carried out by Candidate of Technical Sciences D. B. Zvorykin.

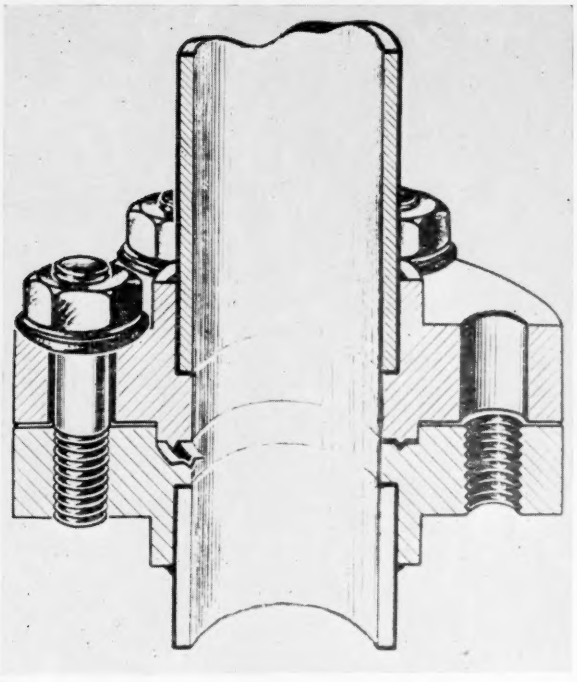

FIG. 5. Groove-wedge seal with bolt connection.

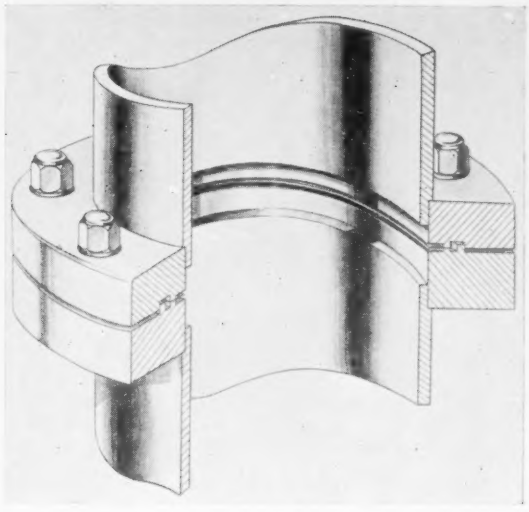

FIG. 6. Seal with butt rectangular projection.

Vol. 9 959/60

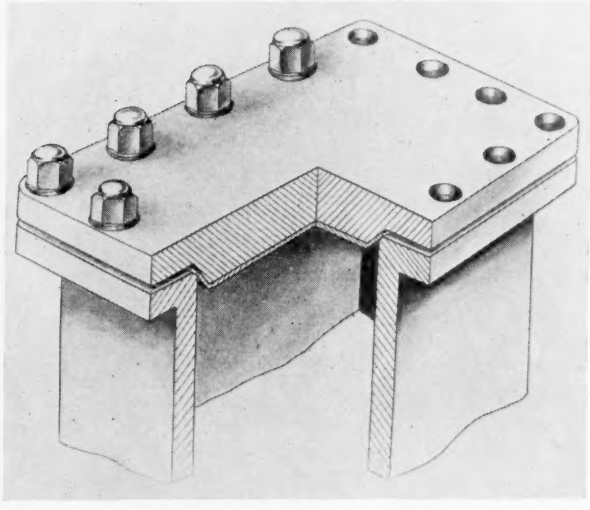

FIG. 7. Pyramidal seal for rectangular sections.

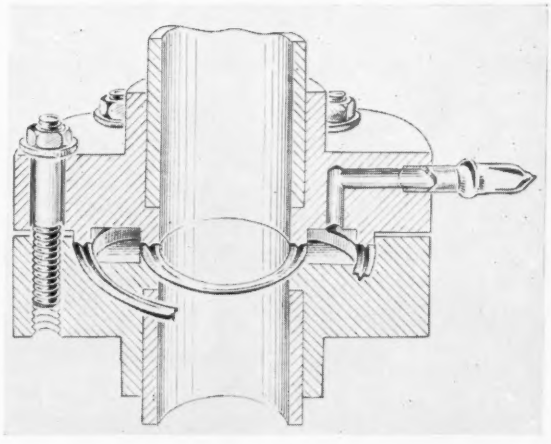

FIG. 8. Groove-wedge seal with two profiles.

2. *Materials used*

The main material used for jointed parts was structural steel, type CT 45–CT 50 ($C = 0.45 + 0.50$ per cent). This steel features sufficient mechanical strength ($\sigma_t = 70$ kg/mm^2) and good technological properties (ease of mechanical processing, soldering and welding).

In those cases when high-vacuum properties, increased strength, non-magnetizability, etc., are required, various types of stainless steel are used. For gasket material use is made of oxygen-free copper annealed in hydrogen, and aluminium. It should be noted that our experience has shown there is no justification in using such materials as gold and silver for gaskets, as such gaskets possess no advantages over copper and aluminium gaskets. The only exception is the case of diffusion seals where gold-plated copper gaskets are used. Hardware (bolts, nuts, etc.) are made of stainless steel.

3. *Main characteristics of seals*

Investigations have shown that the force required for making a joint sufficiently hermetical depends on the type of

seal and the material of the gasket. The mean values of specific pressures are given in Table I, where they are expressed in kilogrammes per millimetre of the average diameter.

Table I

Types of seals	Specific pressure kg/mm of mean diameter		Thermal resistivity	
	Copper	Aluminium	Copper	Aluminium
	—	15÷20	—	400°C
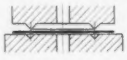	40	20	600°C	400°C
	85÷95	40÷45	600°C	—

The table also gives the maximum temperatures in prolonged use of the seal, for which the value of leakage does not exceed 5×10^{-6} μl./s. At room temperatures all seals are characterized by leakages within the range $1 \times 10^{-6} + 1 \times 10^{-8}$ μl./s (depending on the accuracy and smoothness of surface processing). Investigation of the leakage value was carried out in a number of ways, the most accurate of which must be considered the mass-spectrometric method, which consists in the measurement of the amount of helium leaking through the seal under test during a sufficiently long period of time.

4. *Selection of the type of seal*

One or another type of seal should be preferred, depending on the diameter of the tube to be joined. A tentative division of types of seals according to diameter is given in Table II.

Table II

Type of seal	Diameter range
	3–12
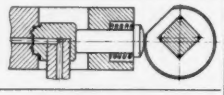	3–12
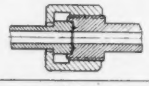	10–20
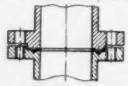	30–100
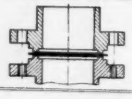	100–300

For sealed demountable devices two types of seals were developed :

(a) with a double profile,

(b) diffusion seals.

In the case of the first type of seal, the space between the profiles is exhausted to a fore-vacuum and in this way the inner seal is isolated from the atmosphere.

Experiments have shown that such seals are hermetical to an extent which allows them to be used in sealed constructions. However, this type of seal is hard to make and consequently expensive.

The second type of seal can be made in any of the constructional shapes listed above, its main feature being that the assembled joint (flanges and gaskets) is placed under such conditions that diffusion of sufficient intensity develops. These conditions consist in heating the joint to a temperature of 450–500 °C and keeping it at this temperature for a certain time. It was found that the best pair of materials for this purpose are steel flanges and gold-plated gaskets (gold plating is 3–5 μ thick).

Diffusion seals are hermetical to such a degree that reliable operation of sealed vacuum devices is ensured for at least one year. Special stress should be made on the importance of selecting the most favourable conditions for making the diffusion seal, because, if the intensity of the diffusion is insufficiently high, vacuum tightness will not obtain. Should the diffusion rate be excessively high, it will become necessary to clean the sealing surfaces after dismantling the seal. Control of the diffusion rate is rendered difficult because of the exceedingly low diffusion depths (of the order of fractions of a micron). For this reason the conditions for making diffusion seals are selected experimentally.

2. Valves

1. *Flexible valve elements*

Membranes and bellows are used as flexible elements designed for the sealing of the moving parts of valves.

(a) *Membranes*—There are two possible ways of joining membranes to the parts of valves : demountable (on the basis of one of the types of seals dealt with above) and non-demountable (soldered or welded). Depending on the method of fastening, various demands are made of the membrane material : high plasticity for demountable constructions or the possibility of obtaining vacuum-tight soldering or welding. A common demand is for high fatigue strength. Demountable constructions were made of copper, nickel, and phosphor bronze, and of these materials nickel should be considered the most preferable, as the one meeting more fully the set requirements.

As membranes in general have a short life, it is necessary to use large-diameter membranes in non-demountable constructions, which allow for sufficient travel at an acceptable period of service.

Therefore, the use of membranes in non-demountable valves is regarded inexpedient. In addition, the use of membranes is limited to valves having orifice diameters of

up to 20 mm, as the use of membranes for valves with larger orifices entails excessively large dimensions.

It should be noted that the theoretical aspect of the problem of selecting the material, the shape of the corrugations, the diameter and thickness of the membrane—which would ensure maximum service life for the given value of travel, is extremely difficult. Therefore, at the present time, these problems are solved experimentally.

The lack of research into these problems makes it possible to suppose that further progress is possible in the field of using membranes as the flexible elements of valves.

(b) *Bellows*—The use of bellows as flexible sealing elements presents considerably greater constructional possibilities, due to the fact that they make it possible to obtain large travel with smaller valve dimensions and greater service life, which, in particular, allows bellows to be used in non-demountable constructions. The use of tombac bellows may be recommended for constructions which do not make high demands of the service life of the bellows. Advantages of tombac bellows are cheapness, ease of soldering, and the possibility of making vacuum seals of one of the above types, with the material of the bellows itself serving as the sealing gasket. Bellows of stainless steel possess a longer service life and allow greater travel to be obtained in comparison with tombac bellows, which allows them to be regarded as the most suitable flexible elements for valves. A shortcoming of stainless-steel bellows is a certain difficulty in obtaining a vacuum-tight joint with parts of a valve. Among such joining methods mention can be made of roller pulse welding and arc welding in a protective atmosphere, and brazing. In spite of the fact that all these methods are well known, the last one should be dealt with in some detail. It is well known that brazing of stainless steel in a furnace with an ordinary protective atmosphere is rendered difficult due to the selective oxidation of the chromium contained in the stainless steel by the admixture of oxygen and water which is always present in such atmospheres. The film of chromium oxide which covers stainless steel does not get wet by the brazing alloys, making brazing impossible. Among the methods used by us for preventing formation of the film of chromium oxide on the surface of the metal are the following :

(a) Brazing in vacuum furnaces,

(b) Brazing in furnaces with sharply dried and cleaned protective gases,

(c) Preliminary galvanic nickel-plating or copper-plating of the stainless steel, after which it becomes possible to braze in furnaces with a protective atmosphere of technical purity. A fourth method of brazing of stainless steel is brazing with the aid of fluxes containing mixtures of fluorine salts with borax and boracic acid. The last two methods are the most convenient and reliable.

2. *Closing elements of valves*

The standard design of valve closing elements is shown in Fig. 9. The mechanism which provides the seal between the flap and the seat of the valve is the same as in the case of the demountable metal joints discussed above.

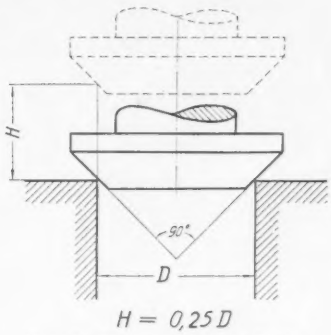

FIG. 9. Closing elements of valve.

Accordingly, the choice of materials for the flap-seat pair is made on the basis of the same considerations as in the choice of materials for demountable vacuum joints with metal gaskets. We use copper and aluminium for making flaps and steel for seats. It is expedient to use soft metal for that element of the pair which is replaceable. Our experience shows that it is simpler to make the flaps replaceable.

The principal geometric considerations for selection of the value of travel are made clear in Fig. 9.

It was found experimentally that it is most expedient to make the seat without beading of the sealing edge. It has been shown, that for vacuum-tight closing of the valve, characterized by a leakage value of not more than 1×10^{-7} μl./s the following forces per mm of the orifice diameter are necessary : copper–steel 40 kg/mm, aluminium–steel 15 kg/mm.

It follows that in designing valves with orifice diameters in excess of 30–40 mm it becomes difficult to develop the necessary closing force. Therefore, it should be regarded expedient to design valves of the type in question with metal-closing elements for orifice diameters of the order of up to 35–40 mm. Further increase in diameter involves complications of the closing mechanism. The design of the closing elements of a valve intended for continuous proportioning of the flow of gas into a vacuum (leakage valve) is shown in Fig. 10. Satisfactory operation of a leakage valve is determined to a large extent by the quality of processing of the surfaces of the needle and seat. Our best results were

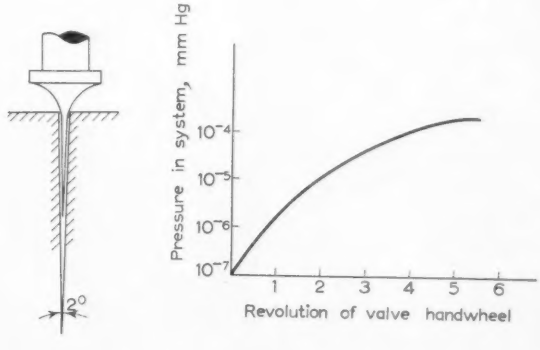

FIG. 10. Closing elements of needle valve.

Vol. 9 959/60

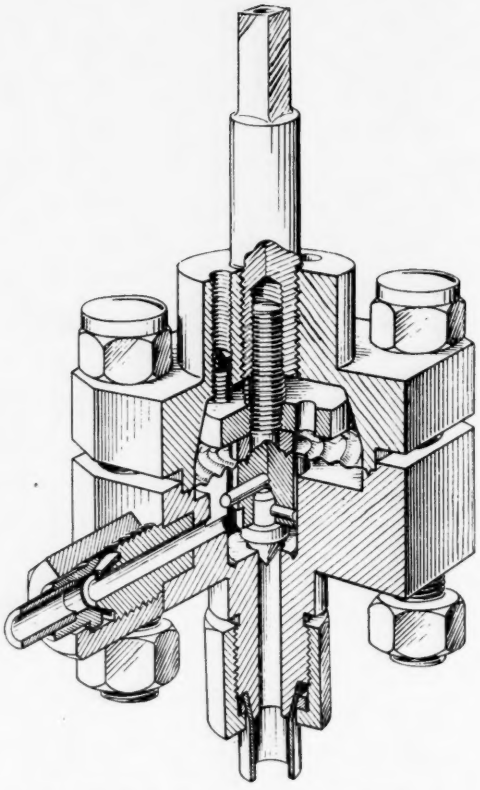

FIG. 11. Shut-off vacuum valve with membrane.

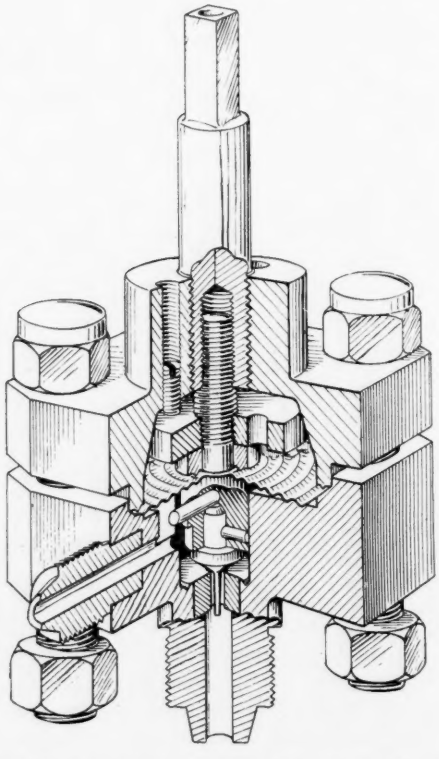

FIG. 12. Proportioning vacuum valve with membrane.

obtained by pressing the seat with a tempered and thoroughly polished steel needle. Subsequently, the same needle serves as the working element of the leakage valve. The operation of the leakage valve is shown diagrammatically in Fig. 10.

Needle-leakage valves do not allow reproducible setting of the gas flow or to determine the amount of gas introduced into the system per unit time. These shortcomings are overcome by the diaphragm leakage valves described below.

3. *Standard valve designs*

Standard design of a vacuum closing valve is shown in Fig. 11. Such valves with orifices of from 3 to 30 mm have found wide use in a large number of vacuum installations. Experience in the assembly of complex vacuum commutations has shown the expedience of having two inlets above the closing element of the valve.

Needle-leakage valves are designed similarly to closing valves and differ from them in the design of the closing pair (Figs. 12, 13). One of the features of the described valves is the possibility of obtaining a molecular flow of the gas. The maximum pressure at which a molecular flow of gas is still possible is determined by the amount of opening of the valve. In order to obtain a molecular flow of gas into a vacuum from low pressure, in cases when it is necessary to reproduce accurately a flow of a given magnitude, diaphragm

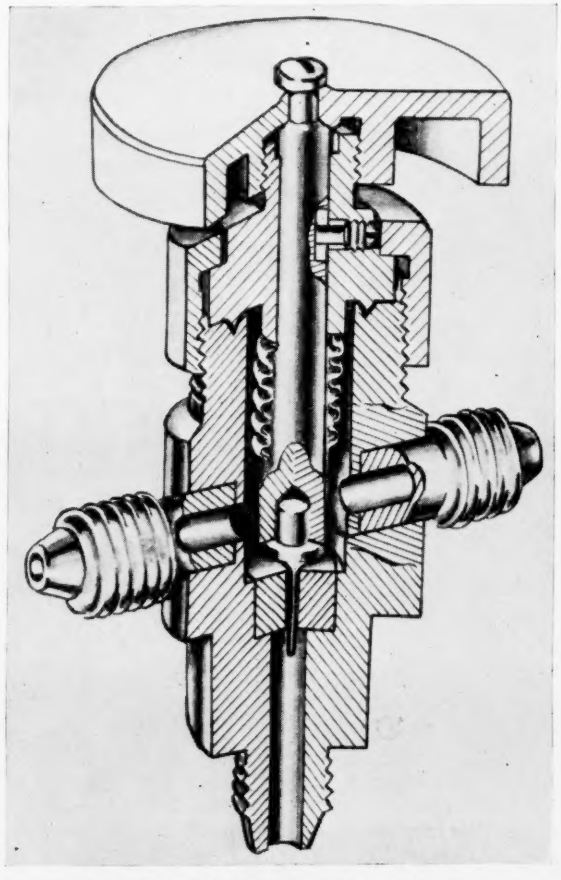

FIG. 13. Proportioning vacuum valve with bellows.

Vo
9
1959

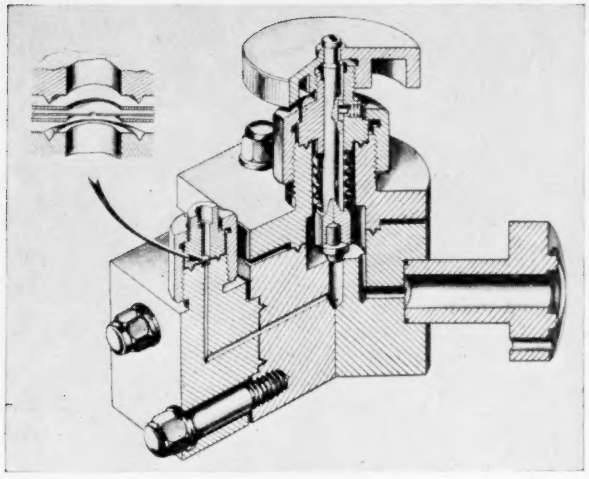

FIG. 14. Diaphragm leakage valve.

leakage valves (Fig. 14) were developed. These leakage valves are made in the shape of closing valves in the body of which is installed a thin replaceable diaphragm with calibrated holes. The diaphragm is made of soft metal foil with one or several holes from 3 to 20 μ in diameter. Vacuum tight joining of the diaphragm to the valve is obtained with the aid of two intermediate gaskets of pliable metal and a groove-wedge seal. Experience has shown that of great advantage in the development of vacuum systems is the combination of several valves in one body. Typical designs of combined valves are shown in Figs. 15–17.

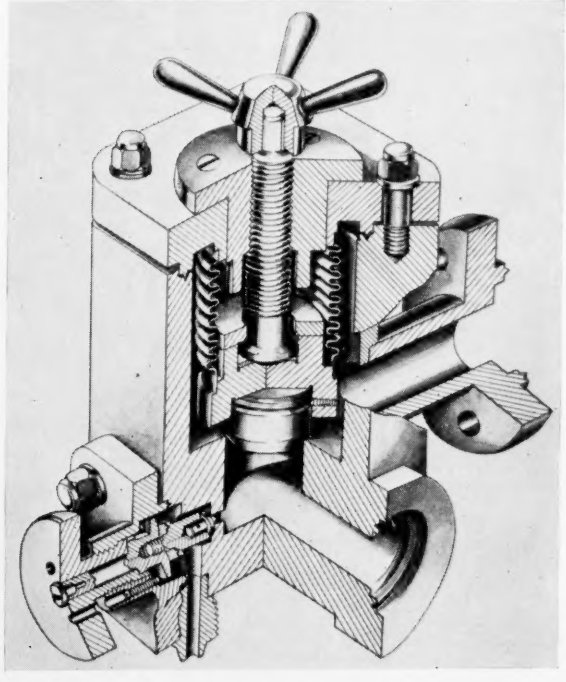

FIG. 15. High-vacuum valve combined with by-pass valve.

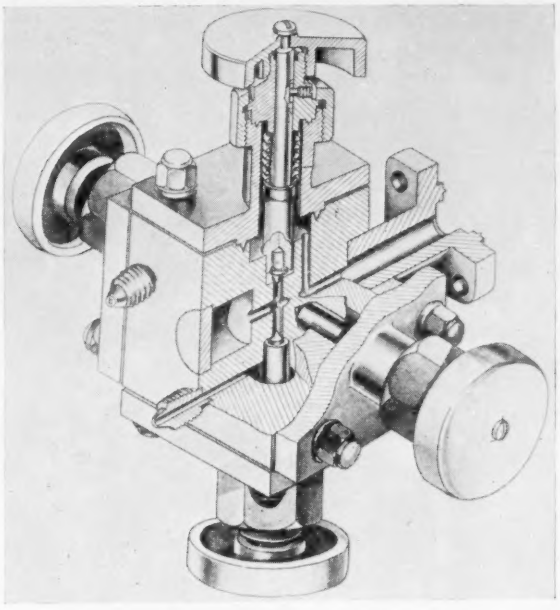

FIG. 16. Four-gang valve.

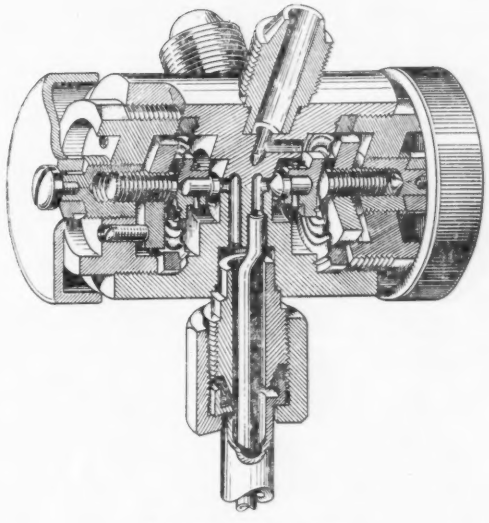

FIG. 17. Double valve.

The high-vacuum valve shown in Fig. 15 is a combination in one body of a main valve with a large diameter orifice and a by-pass valve with a small diameter orifice. Its advantage consists in the elimination from the high-vacuum vessel of the long connecting tube usually used for coupling the high-vacuum vessel to the fore-vacuum main. As a rule such connecting tubes introduce additional contamination into the high-vacuum section of the system. Another example of the happy blending of designing convenience with special physical considerations is the design of the four-gang valve shown in Fig. 16. The valve is designed for the inlet system of a mass-spectrometric gas analyser which requires a small standard vessel included between the closing elements of commutating valves. The development of such a system,

Vol. 9 959/60

using single valves, is complex and entails increasing working surfaces, additional connections, etc.

A logical follow-up of the design principle of combining several assemblies in one unit are combined constructions : trap-valve, ampule-valve, etc. (Figs. 18, 19).

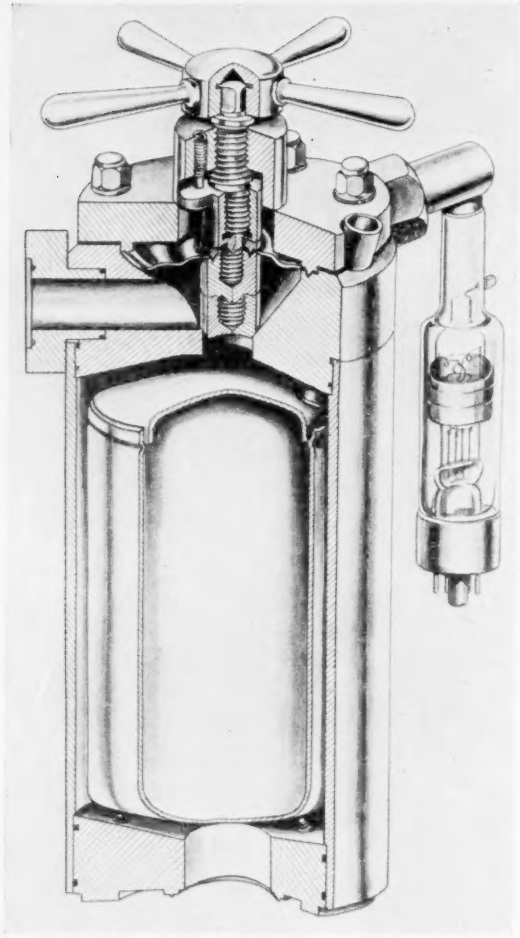

FIG. 18. High-vacuum trap combined with valve.

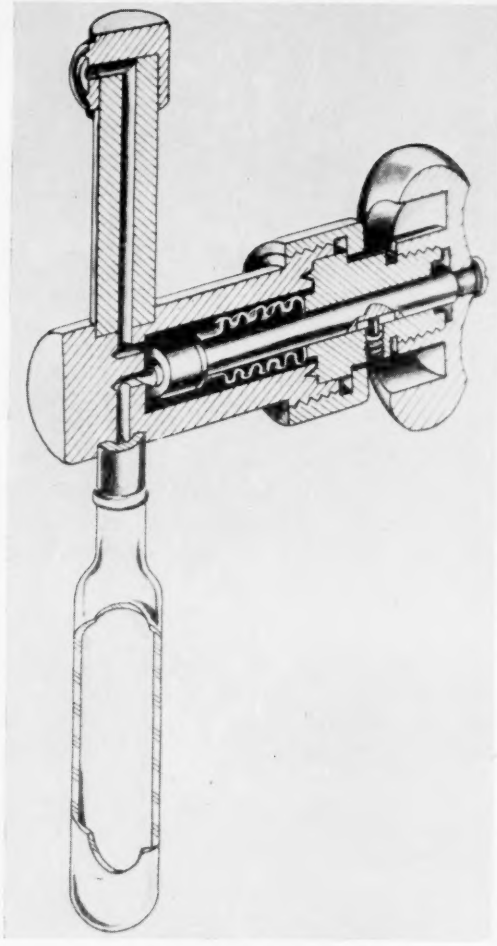

FIG. 19. Ampule with valve.

4. *Traps*

In designing metal traps intended for the freezing out of the pump liquids and condensed vapours always present in vessels being exhausted, it is necessary to consider the following : the design of the trap should ensure minimal heat exchange between the vessel filled with the coolant, and the body. This demand is advanced by economical and operational considerations, since the value of the heat exchange determines the specific consumption of the cooling liquid. With this aim in mind, the reservoir containing the cooling liquid is connected to the body by a long, thin-walled neck made of low-heat conducting material. In order to decrease the dimensions of the neck it is expedient to make it in the shape of two co-axial tubes. A decrease in radiation heat exchange is obtained by using a heat screen arranged between the reservoir with the coolant and the body. Experience has shown the expediency of using demountable constructions which provide for periodic cleaning of the inner surfaces of the trap. In certain cases special demands are made of the design of traps in addition to those mentioned above. For example, traps intended for use in the vacuum systems of mass-spectrometric instruments should possess a minimal " memory ", i.e. the vapours condensed on the cold surfaces of the trap should not evaporate on lowering of the coolant level. Traps should also prevent back diffusion of gases from the pumping system. Non-fulfilment of these demands leads to uncontrollable distortion of measuring results. Traps designed with allowance for the considerations listed above are shown in Figs. 20–22 and 23. These traps are sufficiently economical. For example, the trap shown in Fig. 20 has a liquid-nitrogen consumption of the order of 40 cm^3/hr. These same traps ensure practically complete absence of " memory " (for a lowering of the coolant level of up to 10 per cent of the reservoir volume).

In conclusion it should be mentioned that the experience of many years of operation of various devices designed according to the principles dealt with in this report has shown the high reliability and operational convenience of such devices. All this has brought about a practically complete ousting of glass vacuum systems from laboratories and industry.

Vo
9
1959

Vol.
9
959/60

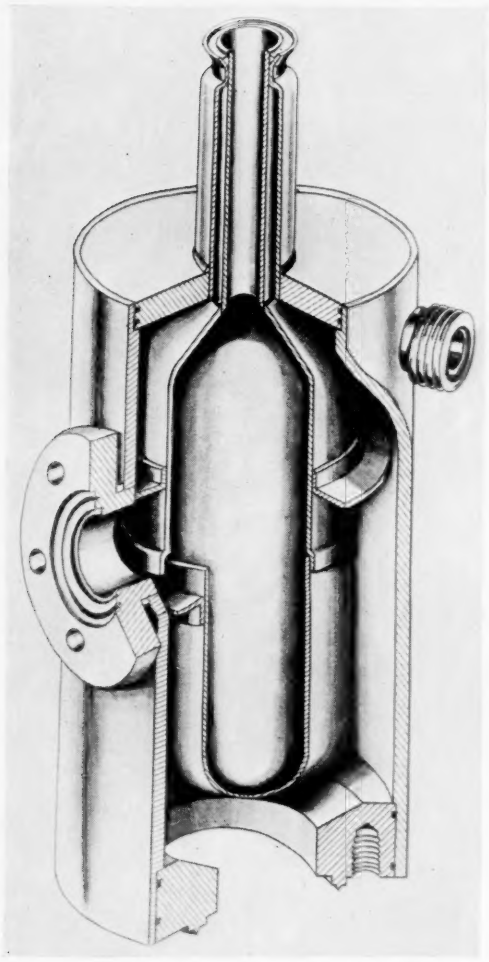

FIG. 20. High-vacuum trap with short " memory ".

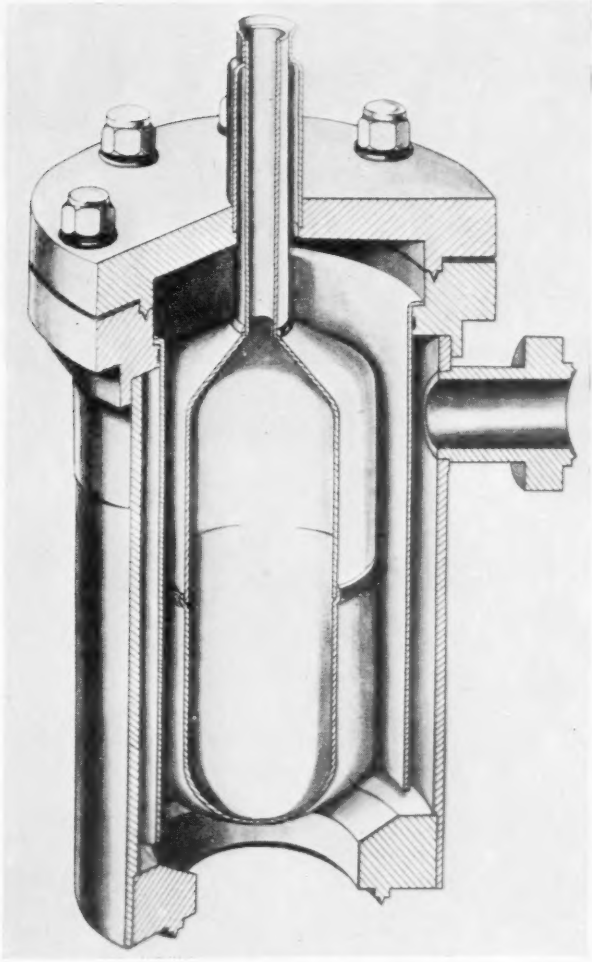

FIG. 21. Economical demountable high-vacuum trap.

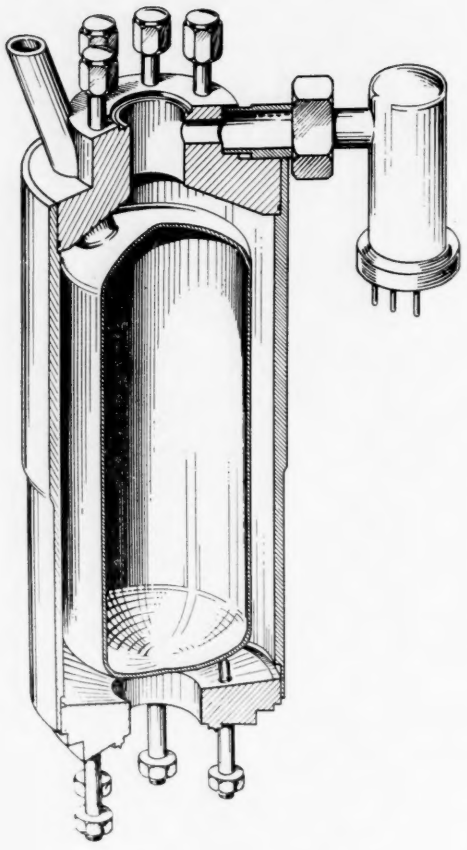

FIG. 22. High-vacuum trap.

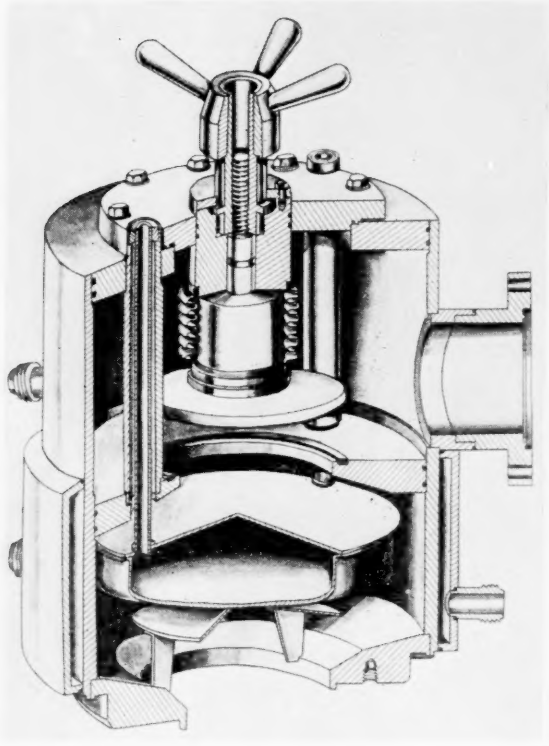

FIG. 23. High-vacuum trap for system with high exhaust rate.

Vo
9
1959

Experience in Using Mass-Spectrometric Methods in Electro-Vacuum Technology*

I. A. KALJABINA and Ya. A. YUKHVIDIN

1. Introduction

The wide use of mass-spectrometric methods of gas analysis in various fields of engineering is well known. In late years, in connexion with certain specific features of these methods, there is an ever-increasing use of them in solving various problems of vacuum technology.

In the main these features boil down to the following :

(1) The high vacuum in the mass-spectrometer itself which allows the gas to be released from the vessels, in which it is contained, at very low pressure (as low as 10^{-6} mmHg), as well as to study processes accompanied by low values of gas evolution (from 1 μl/s to 10^{-5} μl/s) by placing the object under investigation inside the instrument.

(2) The high flow sensitivity of modern mass-spectrometric gas analysers (10^{-4} — 10^{-5} μl/s), which makes it possible to study processes accompanied by gas evolution of the same order, as well as to conduct microanalysis.

During a number of years we have been using mass-spectrometric methods of gas analysis for solving vacuum technological problems arising during the development of electro-vacuum devices. The main results of this work form the subject of this report.

Vol. 9 959/60

2. Fields of application

The greater number of investigations carried out were connected with a study of composition and amount of residual gases in high-vacuum devices, for, to a great degree, it is this that determines the reliability and long life of the devices. These investigations were conducted in the following direction.

(1) The vacuum characteristics of structural materials (the amount and composition of the gases evolved from the materials depending on the temperature and the time of outgassing in the vacuum) was studied.

(2) Those gases were studied which are evolved during forming and activizing of various types of cathodes and the desorption of gases during the electronic bombardment of anodes.

(3) The composition of gases at various stages of exhaustion and training of vacuum devices was determined. Methods were elaborated for studying the conditions of exhaustion and training of both small and powerful devices.

In the development and manufacture of gas discharge electro-vacuum devices, of great significance is the purity of the gases used for filling the devices, and consequently, the possibility of controlling the gas purification processes. In addition, in a number of cases, it is necessary to know the nature of the changes in the composition of the gas in operating gas discharge devices. In solving these problems we also made use of mass-spectrometric methods of analysis.

3. Equipment and methods

Most of the investigations were conducted with mass-spectrometers, type MC-2 (Fig. 1), and mass-spectrometric gas analysers, type MAGC-2 (Fig. 2) which are at present produced. These instruments are ordinary mass-spectrometers with 60° magnetic deflexion. The range of mass numbers of the MC-2 instrument is from 1 to 600 at a resolution of 300 and a flow sensitivity of 10^{-4} — 10^{-5} μl/s. The MAGC gas analyser features a range of mass numbers of from 1 to 90, a resolution of 80 and a flow sensitivity of 10^{-5} — 10^{-6} μl/s. It possesses a gas inlet system which provides molecular leakage and wide-range magnetic scanning of spectra which are recorded on an automatic potentiometer. The block diagram of the gas analyser is shown in Fig. 3. Since the MC-2 mass-spectrometer is an instrument designed for isotope analyses, for conducting the above-mentioned investigations, it was augmented by a gas inlet system and scanning and spectra recording units similar to those used in the MAGC-2 instrument. It should be noted that both the MC-2 and the MAGC-2 are stationary instruments occupying a sufficiently large area, which makes it difficult to use them in shop conditions. At the same time investigations of the conditions of exhausting and training a number of devices, especially powerful ones, in laboratory conditions is rendered difficult by the necessity of installing bulky exhausting and training equipment.

In this connexion, for the purpose of studying exhausting conditions of electro-vacuum devices under shop conditions, a portable mass-spectrometric vacuum analyser was developed The general view of this instrument is shown in Fig. 4. The vacuum analyser is made in the shape of a small mass-spectrometric chamber (the radius of the central trajectory being 50 mm), connected either directly to the electrovacuum device under investigation or to some point of the vacuum system exhausting the device, which is convenient for connexion. Depending on the design of the device under investigation and the exhausting equipment, the chamber is made either of glass or of copper. The 60° deflecting field was developed by a permanent magnet.

The vacuum analyser employs electrostatic scanning of mass-spectra and oscillographic recording of the spectra.

* Paper presented at the First International Congress on Vacuum Techniques, Namur, 10–13 June 1958.

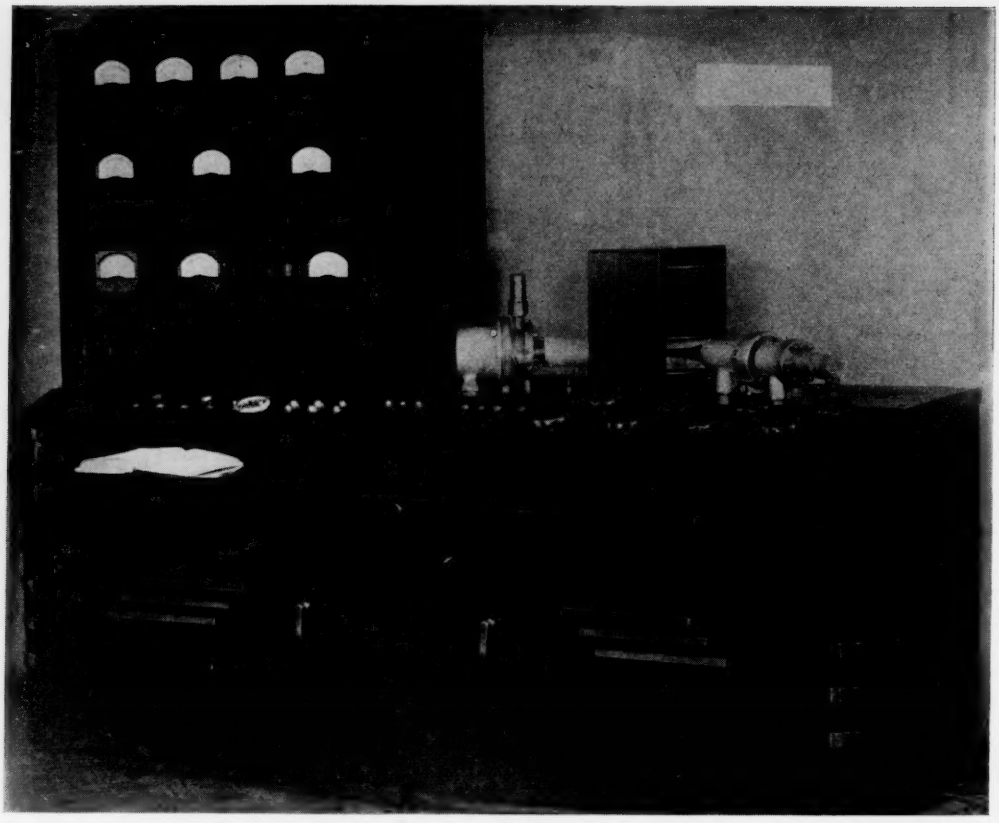

FIG. 1. General view of the MC-2.

All the electronic devices are assembled on a readily mobile rack with dimensions of 300 × 450 × 800 mm. The vacuum analyser has a range of mass numbers from 1 to 45 with a resolution of the order of 30 and a static sensitivity of 10^{-8} mm Hg/mm of the scale. One or the other of the described instruments was used depending on the problem under consideration.

Investigation of the gas evolution of structural materials was carried out on stationary mass-spectrometers. The method which is usually used in studying the gas evolution of materials boils down to the heating of the specimen in a separate vacuum vessel with the aid of an electric heater of a high-frequency inductor. The gas evolved during heating is directed by a communicating system either directly into the mass-spectrometer (when investigating the dynamics of gas evolution) or is gathered in a special container, after which it is analysed by a mass-spectrometer. However, a shortcoming of this method is that there is a danger of the appearance of selective sorption of gas by the walls of the tube connecting the vessel with the specimen to the mass-spectrometer, as a result of which uncontrollable errors may be introduced into the results of the analyses. In this connexion it should be considered expedient to strive for the maximum bringing together of the object under investigation and the region of ionization of a mass-spectrometer.

In particular, this tendency is reflected in a method elaborated for investigating the gas evolution of structural materials, which consists in the introduction of the specimen under investigation directly into the chamber of the mass-spectrometer in the zone adjacent with the region of ionization of the ion source. The ion source used differed from ordinary types of sources in that it had a spiral heater arranged near the ionization chamber and designed for heating the specimens under investigation, as well as a heater designed for outgassing the ionization chamber (Fig. 5). For the purpose of introducing the specimen into the heater zone use was made of a bellows mechanism secured on the chamber of the mass-spectrometer (Fig. 6). The procedure for conducting the analysis was the following. With the specimen removed, the spiral heater was outgassed. Next, the temperature at which gas evolution was investigated was established, the residual mass-spectra of the instrument was recorded, and the specimen was introduced into the heating zone. Throughout the heating process of the specimen, mass-spectra of the evolved gases were recorded.

For investigating the gas evolution of cathodes and the desorption of gases from anodes under the action of electronic bombardment, use was made of experimental diodes connected directly to the input of the ion source of the mass-spectrometric gas analyser. As the amount of evolved gas at the early stages of processing of the cathodes is too great for normal operation of the gas analyser, the pump of the inlet system of the instrument was used for exhausting part of the gas.

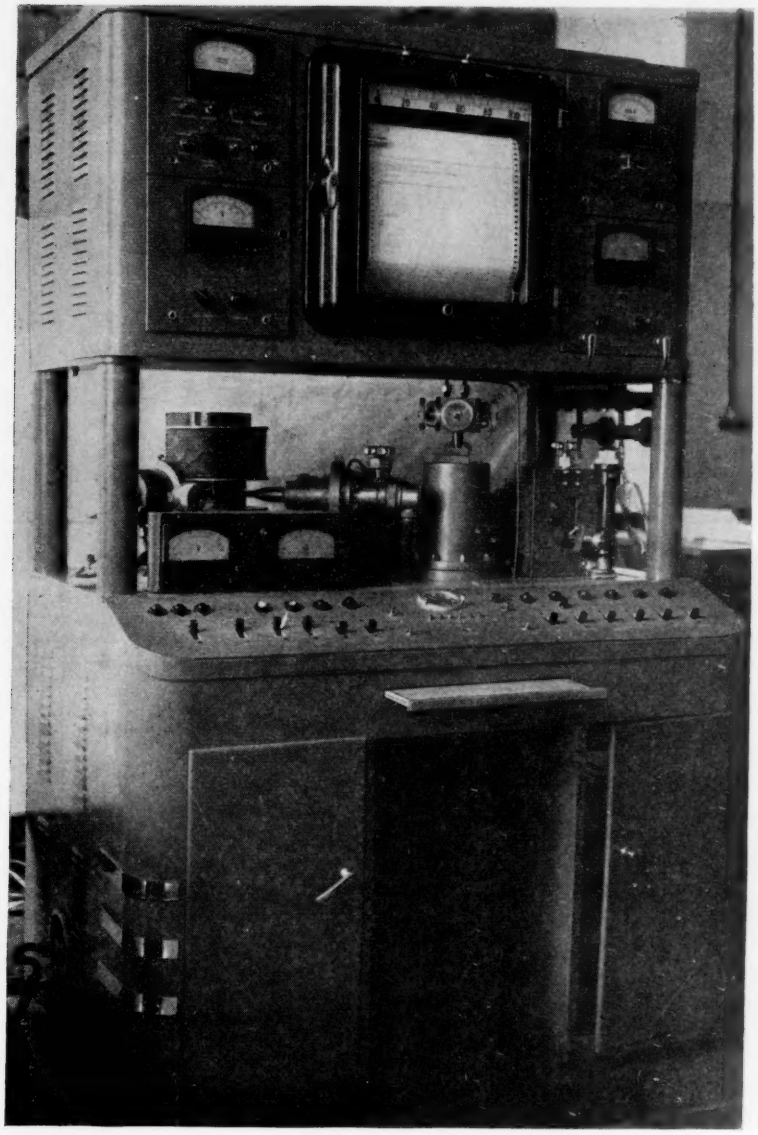

FIG. 2. General view of the MAGC-2.

Vol.
9
959/60

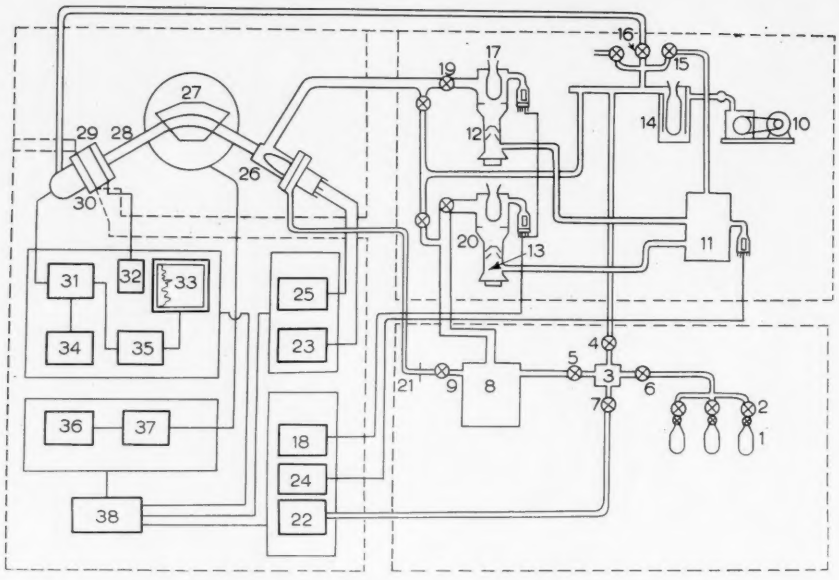

FIG. 3. Block diagram of the gas analyser :
1, ampules with gases to be analysed ; 2, lattice shutter of the inlet system ; 3, standard vessel ; 4, 5, 6, 7, shutters of the four-way valve ; 8, expansion vessel ; 9, inlet valve ; 10, fore-vacuum pump ; 11, fore-vacuum vessel ; 12, 13, mercury diffusion pumps ; 14, fore-vacuum trap ; 15, fore-vacuum exhaust valve ; 16, exhaust valve of electrometer cap ; 17, high-vacuum trap ; 18, ionization manometer ; 19, 20, high-vacuum valves ; 21, inlet diaphragm ; 22, mercury manometer ; 23, thermocouple manometer ; 24, cathode emission stabilizer of ion source ; 25, battery source of accelerating voltage ; 26, ion source ; 27, electromagnet ; 28, chamber ; 29, ion receiver ; 30, electrometer ; 31, d.c. amplifier ; 32, suppressor battery ; 33, self-recording potentiometer ; 34, amplifier supply stabilizer ; 35, manual recording-scale switch ; 36, rectifier for supplying electromagnet ; 37, stabilization and current regulation unit of the electromagnet ; 38, constant voltage transformer.

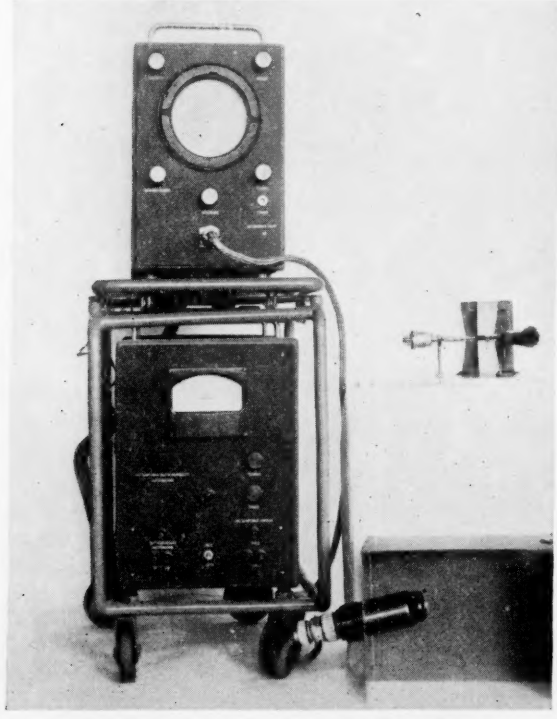

FIG. 4. General view of the vacuum analyser.

Vo
9
1959

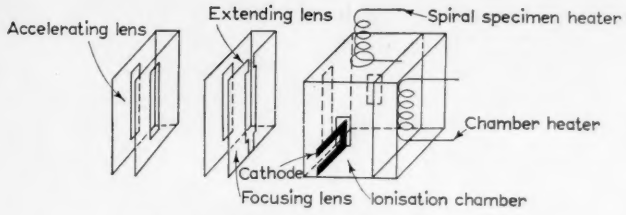

FIG. 5. Diagram of the ion source.

A complete diagram of the connexion of the experimental diode to the gas analyser is shown in Fig. 7. This same method was used in investigation of the gas evolution of small electro-vacuum devices during the process of exhausting and training them.

Investigation of the exhausting and training conditions of such types of electrovacuum devices as cathode-ray tubes,

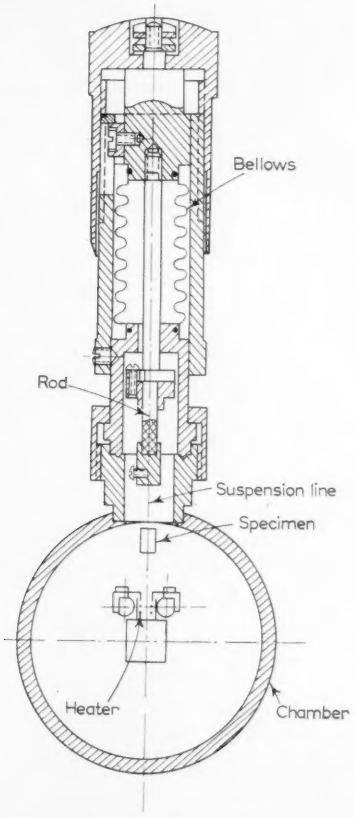

FIG. 6. Specimen feed mechanism.

travelling wave tubes, etc., was conducted by tapping off part of the evolved gases. For this purpose the vacuum system of the exhausting device was connected to the mass-spectrometric gas analysers (Fig. 8). In order to decrease the length of the connecting tube, the exhausting device and the gas analyser were installed side by side. Analysis of the purity of the gases used for filling gas discharge devices was carried out on a mass-spectrometric gas analyser, the ampule system of which was made without the use of ground joints and valves with vacuum lubricants. Rapid manipulation was obtained with the aid of clamp metal seals (Fig. 9).

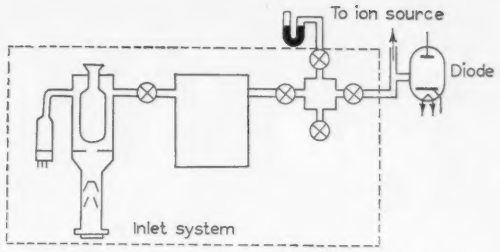

FIG. 7. Diagram for connecting diode to gas analyser.

In order to increase the sensitivity of determining admixtures, use was made of a lattice shutter introduced in front of the receiving slot when measuring peak values of the main gas,

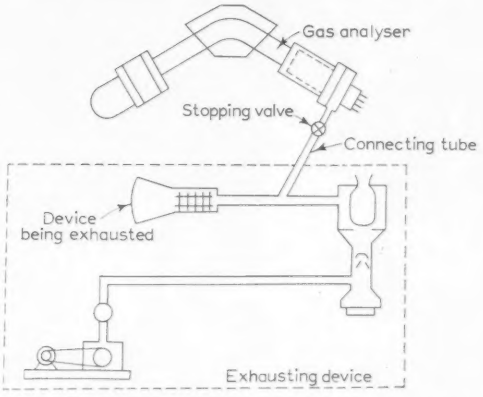

FIG. 8. Diagram for connecting gas analyser to exhausting device.

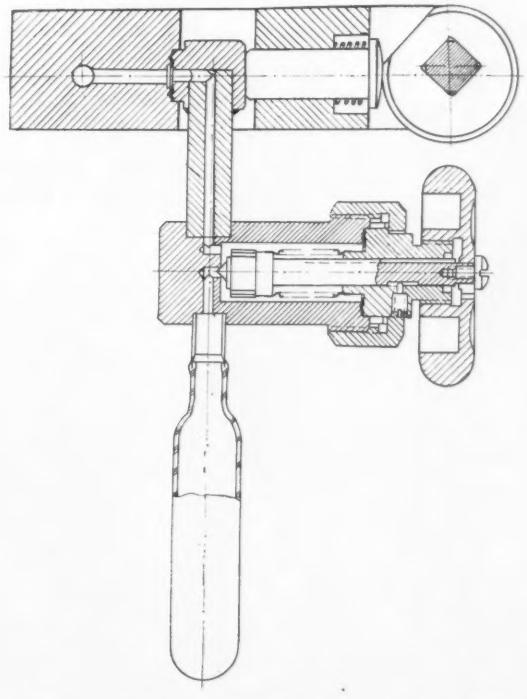

FIG. 9. Connexion of ampule with lattice shutter via metal seal with eccentric clamp.

Vol. 9 959/60

which passed approximately 1/40 of the ion beam. This method of expanding the measuring range of ion currents proved more effective than the use of switched input resistances in the electrometric stage. Since the vacuum conditions in the gas analysers made it possible to increase the inlet, the broadening of the measuring range of ion currents with the aid of the shutter provided a determining sensitivity of up to 10^{-3} — 10^{-4} per cent. In those cases when the gas to be investigated for the presence of impurities was at a pressure of 1 — 10^{-2} mmHg, and it could not be let in by the usual way via the expansion vessel of the inlet system, the gas was let in directly from an ampule via the valve and the inlet diaphragm (Fig. 10). During the working process it appeared that such a two-channel inlet system was also very convenient for the analysis of gas contained in an ampule at a pressure of several tens of mmHg. In this case the main inlet system was used for calibration, while the gas to be analysed was let in with the aid of a needle valve and a diaphragm arranged in series. By decreasing to a minimum the volume between the valve and the diaphragm, it is possible to decrease the inlet time constant to several minutes. The same system made it possible to carry out continuous analysis of the gas in operating gas discharge devices, the envelopes of which were made, for this purpose, with a connecting tube and a break-off seal (Fig. 11). The connecting tube of the device under investigation was fused to the needle valve, the nipple broken in a vacuum and an insignificant amount of the gas was continuously tapped off through the valve and diaphragm from the operating device of the gas analyser. In a number of cases this method proved considerably more convenient than another method used by us in which, for the purpose of analysis, the envelope of a device which had operated for a certain number of hours was broken in a vacuum.

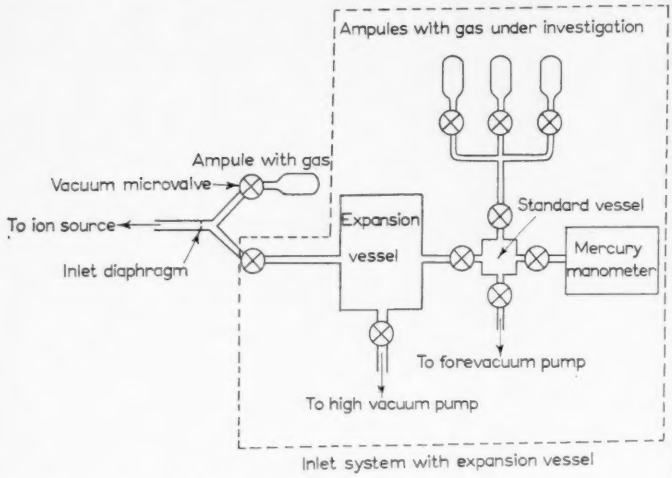

FIG. 10. Two-channel inlet system.

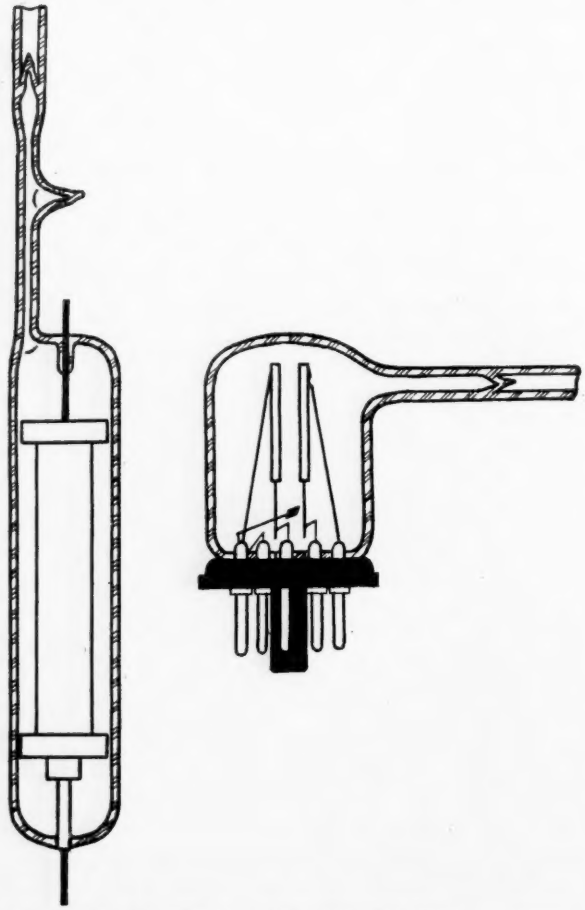

FIG. 11. Design of the envelopes of tubes to be used for the investigation of the composition of the gas filler during operation.

4. Some investigation results

The nature of the information which is usually obtained by mass-spectrometric analysis of the gas evolution of structural materials can be illustrated by the results obtained by investigating ceramics intended for manufacturing internal parts of electronic valves. These results are shown graphically in Fig. 12. It can easily be seen that the main outgassing takes place at a temperature of about 450 °C, at which practically complete evolution of the main poisoning gases (O_2, CO) occurs ; at higher temperatures water vapour and CO_2 continue evolving. Since the evolution of gases is studied in its dependence on temperature and time, the obtained results make it possible to select rational technological conditions of outgassing. Thus in the case under consideration such conditions may be considered outgassing during 1 hr at a temperature of 450 °C. Similar investigations of a number of materials, especially new ones such as ferroxdur, various absorbers of s.h.f. energy, fluorine plastics, etc., have made it possible to determine their suitability for use in high vacuum devices, and the outgassing conditions required for this.

The following can be cited as an example of the possibilities of the mass-spectrometric method in studying the processes obtaining during exhaustment and training of electro-vacuum devices. It was found that during the operation of one type of travelling wave tube when the tube heated up to a temperature of the order of 150 °C, a fall-off of cathode emission occurred. In order to clarify the causes of this phenomenon,

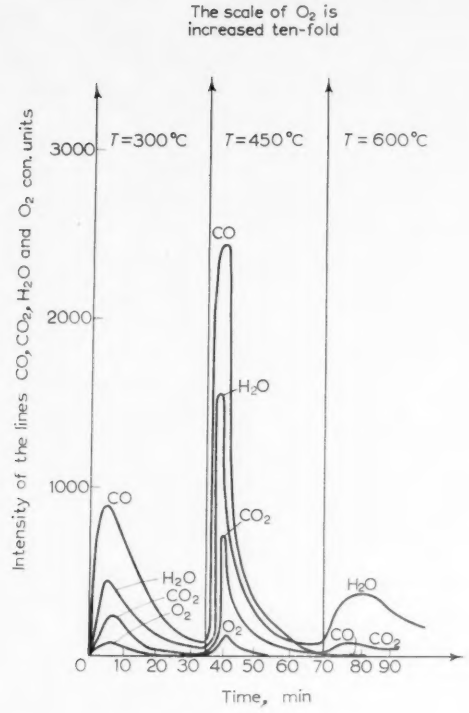

FIG. 12. Gas evolution of ceramics.

mass-spectrometric investigation of the exhausting process was carried out. It was then found that despite two heatings at 400°C during 1 hr (before and after processing of the cathode and all the tube electrodes) and despite the insignificant evolution of poisoning gases during the second heating (Fig. 13), subsequent heating of the tube to 150°C during

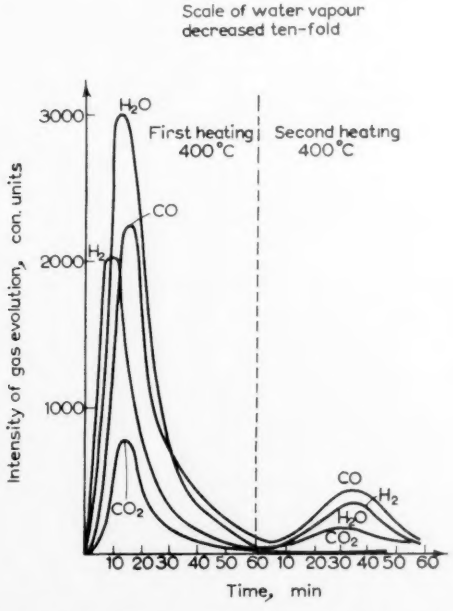

FIG. 13. Evolution of gas during heating of T.W. tubes.

operation still brought about a noticeable evolution of water vapour and carbon monoxide (Fig. 14).

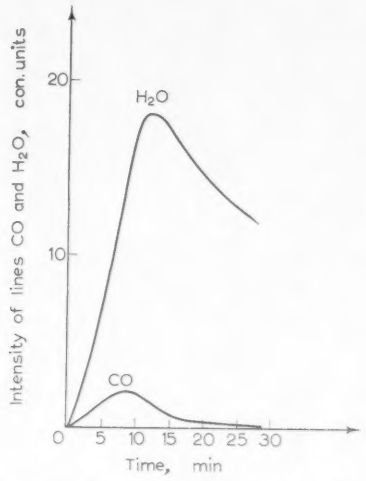

FIG. 14. Evolution of water vapour and CO during operation of T.W. tubes.

Further investigations showed that it was caused by the glass envelope of the tube. Making the tube envelope of another sort of glass eliminated this phenomenon and, it is significant, that the second heating was not accompanied by any substantial gas evolution (Fig. 15). In another case

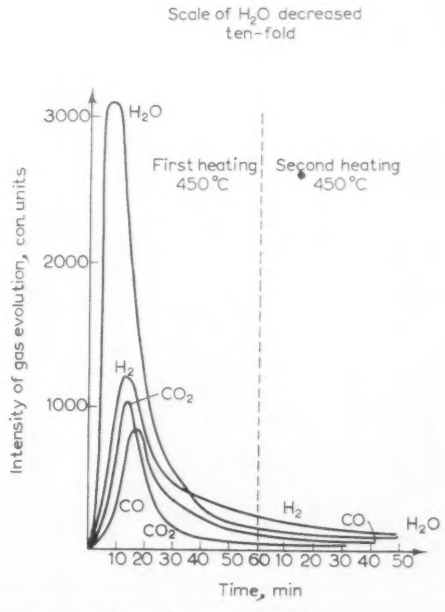

FIG. 15. Evolution of gas during heating of T.W. tubes.

the fall-off in emission of one type of diode was due to admixtures of chlorous compounds in the anodes, which was likewise detected during mass-spectrometric investigations (Fig. 16). The results of investigating the gas evolution of cathodes make it possible, in a number of cases, to come

to definite conclusions concerning the processes obtaining in electro-vacuum devices. Thus, for example, when using an L-cathode with a double carbonate ($BaSrCO_3$), in one of the devices the process of cathode activization proceeded very slowly and not always successfully. It was suggested that this was connected with poisoning of the cathode by gases evolved from the electrodes through the action of electronic bombardment. This supposition was confirmed by mass-spectrometric investigations (Fig. 17). As seen from the graph, the activization of the cathode was accompanied by considerable evolution of carbon monoxide (the graph does not show the evolution in much smaller amounts of hydrogen, carbon dioxide, and water vapour). Mass-spectrometric

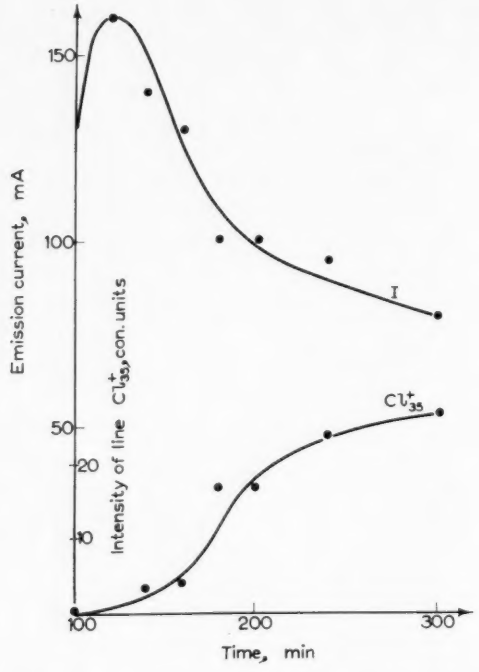

FIG. 16. Poisoning of cathode by chlorine evolved from the anode.

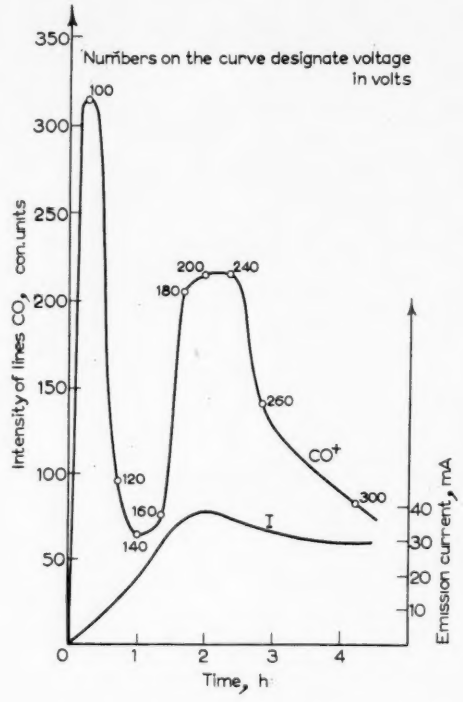

FIG. 17. Evolution of gas during activization of cathode.

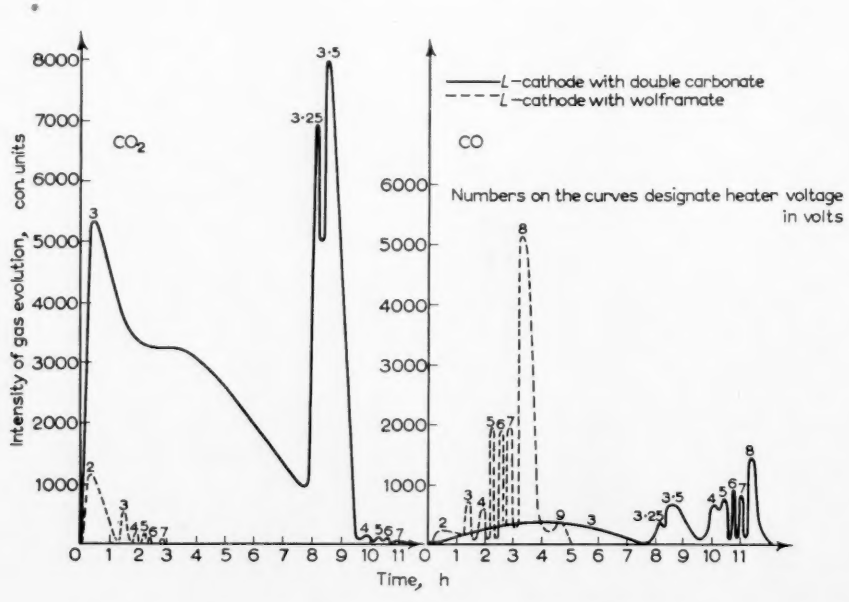

FIG. 18. Evolution of gas during forming of cathodes.

investigation of the gases evolved during forming of this cathode and the gases evolved during forming of an L-cathode made of a mixture of barium wolframate, with a powder of tungsten and aluminium pre-caked at 1900°C, the activization of which was not accompanied by the evolution of cathode poisoning gases, showed that at approximately equal amounts of carbon monoxide evolved in both cases, forming of the L-cathode with the double carbonate was accompanied by considerably greater (approximately two orders) evolution of carbon dioxide (Fig. 18). These results made it possible to come to the conclusion that the evolution of carbon monoxide during electronic bombardment is connected not with a simple desorption of carbon monoxide, sorbed by the electrodes during the forming process, but by the sorption of carbon dioxide. This

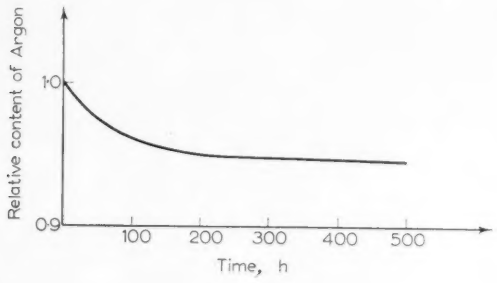

FIG. 19. Sorption of argon in glow discharge.

possibility had been pointed out by Stoll,[1] who proposed that the appearance of carbon monoxide was due to reaction between carbon monoxide and the particles of barium ejected by electronic bombardment :

$$Ba + CO_2 \rightarrow BaO + CO.$$

Mass-spectrometric analysis of gas applied to the investigation of the processes occurring in gas discharge devices made it possible to obtain some interesting data. As an example mention can be made of the results obtained during the investigation of the changes in the composition of the helium-argon filler (98.5 per cent He and 1.5 per cent Ar), with time, in voltage stabilizer with a glow discharge, throughout their operation (Fig. 19). As seen from the graph, obtained as a result of the investigation of a large batch of tubes, desorption of argon in a glow discharge, in the main, occurs during the first 150 hr of operation of the device and in a considerably lesser degree during the subsequent hours of operation. This data is of interest, both for the selection of the composition of the filler and for an understanding of the processes taking place on the cathode during glow discharge. It should be noted that the mass-spectrometric method of investigating the changes in the composition of gases in an electric discharge have proved most useful in the development of ionization-getter pumps.

Conclusions

The experience of using mass-spectrometric methods in electro-vacuum technology has shown that a large number of problems can be successfully solved with their aid. It appears that of special importance is the systematic investigation of the gas evolution of cathodes and structural materials depending on their preliminary processing, method of storage, etc. Wide possibilities are also opened up by the use of portable mass-spectrometric vacuum analysers for controlling exhausting conditions in shops, as well as for investigating the composition of gases in tapped operating electro-vacuum devices.

Reference

[1] S. H. Stoll ; *Brit. J. Appl. Phys.* **7**, No. 3, 94 (1956).

Vol. 9 959/60

The Attainment of Clean Surfaces by Breaking Crystals in Ultra-High Vacuum*

P. C. BANBURY, G. A. BARNES, D. HANEMAN and E. W. J. MITCHELL

Physics Department, University of Reading

Two experiments are described with the object of determining some of the electronic properties of semiconductor surfaces produced by fracture in high vacuum.

In one experiment the photoelectric emission is being measured from freshly broken indium antimonide and gallium arsenide, and from cleaved bismuth telluride. The surfaces are produced and the measurements carried out in sealed-off tubes pumped by ionization gauges. The pressures achieved in these tubes are between 10^{-7} and 10^{-9} mm Hg.

In the other experiment, the transverse mobility of induced surface charge and the photoconductivity are being investigated on germanium surfaces obtained by cleavage in a vacuum of order 10^{-10} mmHg. This vacuum is obtained in a continuously pumped system with a mercury diffusion pump and ionization gauge. Details of the two kinds of tube will be shown.

Two experiments are in progress in these laboratories in which ultra-high vacua are employed in order to study the properties of clean surfaces. In both cases these surfaces are obtained by breaking crystals in the vacuum.

In the first experiment to be described (D.H. and E.W.J.M.), measurements are being made of photo-emission from indium antimonide, gallium arsenide and bismuth telluride. For such measurements a specimen with a surface of approximate dimensions 1 × 0.2 cm was required, located at the centre of a relatively large equipotential (colloidal graphite on glass) sphere with a window for the entry of the light. The method adopted to achieve this involves breaking the specimen in the experimental tube, but outside the equipotential sphere. After breaking, the crystal is moved to the centre of the sphere, and the adjustments for the electrical measurements are made. A vacuum procedure involving sealing off and using an ion pump made it possible to move the tube and to manipulate the parts by magnetic fields and gravity.

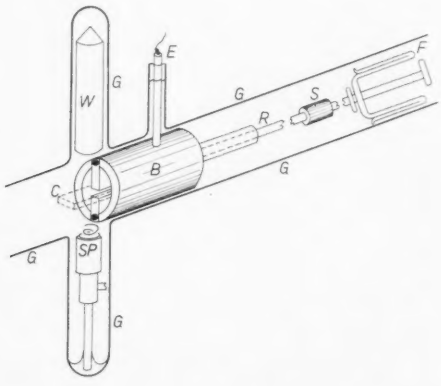

FIG. 1. Diagram illustrating breaking mechanism for measurements of photo-emission. *G*, part of glass envelope of tube ; *C*, crystal in position for breaking ; *B*, Ni barrel ; *W*, breaking hammer having plane face (not shown) to fall flush with end of *B* ; *R*, Ni rod to which crystal is attached and which may be moved along the axis of *B* ; *S*, Ni slider for fine adjustment of translation of *R* ; *F*, Ni framework for fine adjustment of rotation of *R* ; *E*, tungsten electrode providing contact with the crystal ; *SP*, spring and support to stop *W* after breaking.

Specimens of initial size 2.5 × 1.0 × 0.2 cm are mounted on a long tungsten rod. For breaking they are moved into a metal jig and are broken by the impact of a weight falling from a side arm (see Fig. 1), operated, repeatedly if necessary, by rotation of the tube. The rod is then moved forward and adjusted until the specimen is satisfactorily centred in the sphere. The incident ultraviolet radiation enters through a quartz window sealed to the glass envelope with a graded seal.

The method outlined above for exposing fresh surfaces is being used for indium antimonide and gallium arsenide. In the case of tubes containing bismuth telluride—which cleaves easily—the weight is replaced by a steel blade mounted on a suitable guide such that the sharp edge can be lowered from the side arm on to the crystal. By this means good (111) cleavage surfaces are obtained of area 0.5 × 0.5 cm.

The pumping system comprises rotary oil backing pump and mercury diffusion pump, with three liquid air traps. Metal parts are subjected to degassing treatments before assembly, and a pressure approaching 10^{-8} mm Hg is reached after baking for many hours at 400 °C. The system is then sealed off and the pressure reduced to a few times 10^{-9} mm Hg by the use of the Alpert ion pump. During the fracturing and manipulation the pressure rises by about a factor of ten, but is then restored by the switching on of the ion pump again for a period of less than 5 min. The first set of readings is complete within 20 min of the exposure of the surface.

By this means studies have been made of photo emission as a function of wavelength, and of retarding potential. The information obtained includes values of work function on existing and freshly created surfaces on the three materials.

* Paper presented at the First International Congress on Vacuum Techniques, Namur, 10–13 June 1958.

In the second experiment (G.A.B., P.C.B.) surface conductance and surface recombination are being studied on germanium specimens. The measurements involved are of photoconductance, and of the influence of capacitively applied electric fields on surface conductance. The interpretation of these measurements requires that the clean surface shall be plane and of known geometry, and it has been found possible to obtain cleavage on a (111) face by the procedure described below.

It is convenient that the final specimen should be in the form of a rectangular filament (say of length l, width w and thickness t), and for the sake of sensitivity in both studies the thickness (t) of the specimen beneath the freshly exposed surface should be as small as possible. In practice to obtain cleavage it has been necessary to make the thickness (t) somewhat greater than width (w) ; values of $t = 0.2$ cm and $w = 0.1$ cm have been attained.

The system for supporting and cleaving the specimen is illustrated in Fig. 2. An oriented crystal of size about

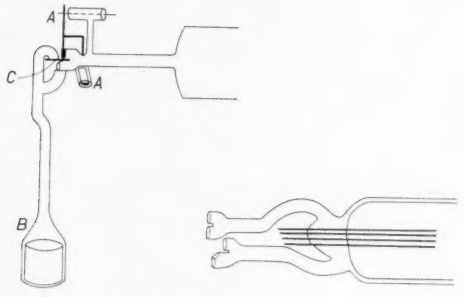

FIG. 2. Diagram of glass jig for cleaving germanium crystals. *A*, Diamond-tipped lever for scratching specimen ; *B*, lever for applying breaking stress ; *C*, specimen.

$2.5 \times 1.0 \times 0.1$ cm, with welded low resistance molybdenum end contacts near one side is mounted by this side in close-fitting jaws of glass. These jaws are built out in solid glass from a pinch which serves to introduce the electric connexions. The jaws are accurately shaped by the use of a diamond saw, after which it is necessary to flame polish and oven anneal for mechanical strength. A magnetically operated lever *A* of carefully adjusted length, carrying a diamond at the tip, is arranged to provide a scratch of length about 2 mm at one end of the specimen, parallel to and about 2 mm from the clamped side. The cleaving stress is applied by a glass lever *B* hung on to the main body of the specimen near the end where the scratch is applied ; this lever hangs freely in a side arm on the envelope, and is again operated by a magnet acting on a glass-enclosed iron pellet. The cleavage thus commences at the scratched end of the specimen, and is allowed to run freely along the length of the crystal, leaving a filament of approximate dimensions $2.5 \times 0.2 \times 0.1$ cm with a freshly exposed surface of 2.5×0.1 cm. As the lever and unwanted section of the crystal fall away, a field electrode of metal with glass bead spacers or of mica with a metal film on the reverse side may be allowed to fall into position near the fresh surface, for the application of electric fields ; alternatively the surface may be illuminated through a nearby slit.

The whole system thus occupies a volume of less than one litre, and contains little metal apart from the specimen itself. By continuous pumping with a mercury diffusion pump with two cold traps, and the use of an Alpert ion pump, pressures in the region of 10^{-10} mmHg are obtained after many hours baking at 420°C. The gauge is not normally operated during the cleavage process, nor while the electrical measurements are being taken. An initial set of measurements of either kind can be completed within a few minutes of cleavage. From measurements of this kind information can be obtained as to the surface potential barrier, and the nature of electronic surface states, on the freshly cleaved surface.

Both types of experiment reported here are continuing ; detailed results and discussions of their significance will be published elsewhere.

Acknowledgements

We are grateful to Prof. R. W. Ditchburn for his interest and for the provision of research facilities, and to the Admiralty for their support.

Vol. 9 959/60

Vacuum Techniques and Components used for a Continuously Pumped Linear Electron Accelerator*

R. C. MARKER

Applied Radiation Corporation, Walnut Creek, Cal., U.S.A.

A vacuum system has been designed to continuously pump a linear electron accelerator having an internal volume of approximately 30 l. and produce vacuums down to 1×10^{-8} or better. The construction avoids all organic materials and is capable of being baked out at 450 °C ; design details of flanges, envelope construction, insulators and valves are discussed. Performance of the diffusion pump traps, which require no refrigeration, and their construction are described. Operating characteristics of the over-all system are discussed in terms of accelerator performance.

THE vacuum systems to be discussed in this paper have been developed for one function alone : to evacuate and maintain a high vacuum in a linear electron accelerator.

Due to the presence of oxide cathodes, high voltage gradients, and the desirability of maintaining a well-collimated beam of electrons, it becomes necessary to operate at vacuums below 5×10^{-7} mm Hg and preferably at pressures in the 10^{-8} mm range.

Increases in pressure above these limits can result from real or " virtual " leaks, release of occluded gases from surfaces, oil vapor from diffusion pumps, or contaminants introduced during manufacture. These gases have the general effect of " poisoning " oxide cathodes and also causing voltage breakdown in the accelerating sections where electrical gradients are 2–3 MV/ft.

Consequently, it was decided early in the development of these accelerators that the vacuum system should have the following characteristics :

1. No materials having high vapor pressures or low melting points inside the vacuum envelope.
2. All metal construction with insulators of alumina ceramic.
3. Bolted joints using metal gaskets only.
4. Flexible bellows-seals on devices having mechanical motion.
5. Dual pumping systems, pumping in parallel.
6. Valves installed to isolate pumps and traps.
7. Interlocks arranged to shut down the pumping system automatically in the event of component failure.
8. Non-refrigerated, active metal traps for diffusion pumps.
9. Bakeout of vacuum envelope at 400–450 °C.

Regarding the first characteristic listed above, it is important to note that the metal used to construct the accelerator vacuum envelope, electrodes and vacuum system include only OFHC copper and 18 per cent Cr 8 per cent Ni stainless steel (type 304). However, nickel, aluminum, Kovar, molybdenum and tungsten are utilized to a minor extent. Specifically avoided are zinc, cadmium, lead and tin because of high vapor pressure and/or low melting point. Also avoided, because of real or unknown effects, are free machining alloys containing sulphur, selenium, bismuth, or tellurium.

All metal construction includes the joining of parts with inert gas arc welding or hydrogen furnace brazing using brazing alloys of copper, silver, gold, nickel, and indium.

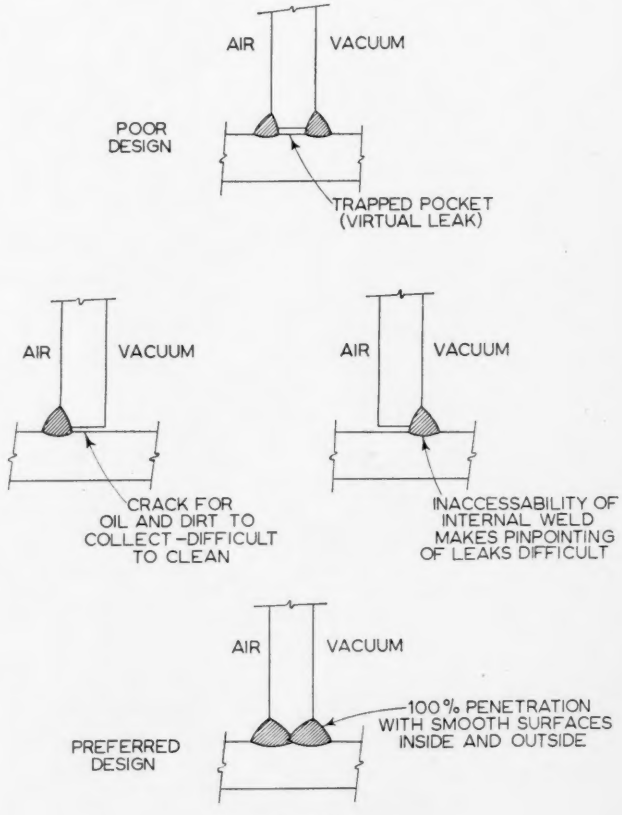

FIG. 1. Weld designs.

* Paper presented at the First International Congress on Vacuum Techniques, Namur, 10–13 June 1958.

Vol. 9 959/60

The alloys have low vapor pressures and are commercially available with a variety of melting points which permit step-brazing of complex assemblies. Chemical fluxes and torch brazing are used only for emergency repairs because of the risk of leaving voids in the brazed joints. Actual joint design is not too critical as long as it provides proper clearances for flow of the brazing alloy and avoids trapped pockets in the joint. The latter consideration is especially important in welded joints. Fig. 1 shows deficient and preferred designs of a common welded joint from the standpoint of good vacuum practice.

The significance of trapped pockets lies in the difficulty of locating leaks inasmuch as a crack on the vacuum side may develop some distance from a crack on the air side. Poor conductance between the cracks results in a long response time when leak hunting. In addition, a crack on the vacuum side will make the pocket a " virtual " leak which continually bleeds gas into the main vacuum envelope until the pocket also is evacuated. Every time the system is evacuated the process repeats itself.

Electric insulators are usually formed from 97 per cent alumina ceramic and joined to the metal parts by high temperature (780°–960°C) brazing to metalized surfaces. The molybdenum-manganese process is generally used to metalize the ceramic. Fig. 2 is a photo of a 150 kV electron gun insulator brazed to stainless steel flanges.

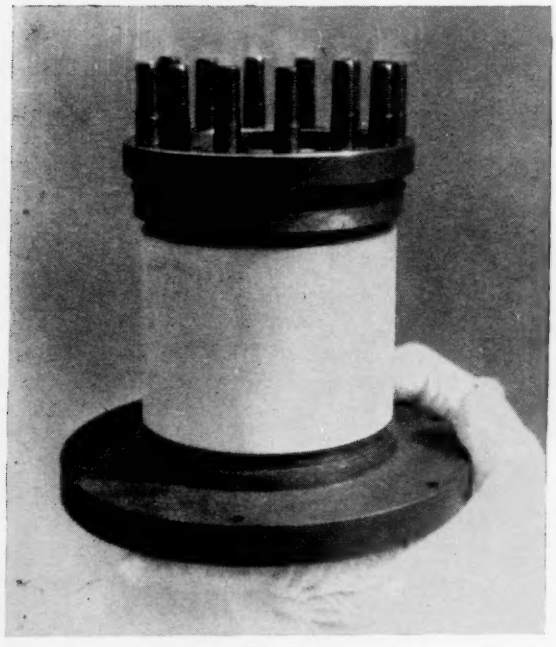

FIG. 2.

For components which must be removed, a standard flange design has been developed using copper gaskets. Fig. 3 illustrates a typical flange. The double ridge has proven successful in preventing continued penetration into the gasket by trapping a volume of copper between the opposing ridges. Where distortion of the flange due to bolting forces would cause difficulties, double ridges are

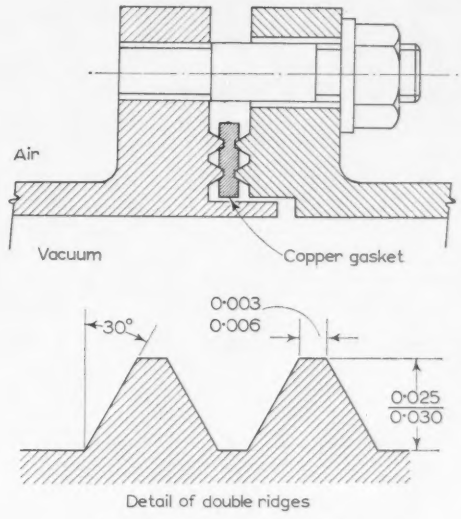

FIG. 3. Details of flange design.

located inside and outside of the bolt circle. Details of the ridges are shown in the second view of Fig. 3. Bolting has been standardized on $\frac{3}{8}$ in.–24 NF studs of 18–8 steel. If double ridges are located inside the bolt circle, studs are spaced $1\frac{7}{8}$ in. O.C. (max.). If ridges are located outside the bolt circle too, studs are spaced $\frac{7}{8}$ in. O.C. Torque is set at 10 ft lb maximum to produce a stress in the studs of approximately 24,000 lb in^2. Studs are lubricated with colloidal graphite to prevent seizure. The gaskets are machined from OFHC copper sheet to finish 0.040–0.060 in. thick. Fig. 4

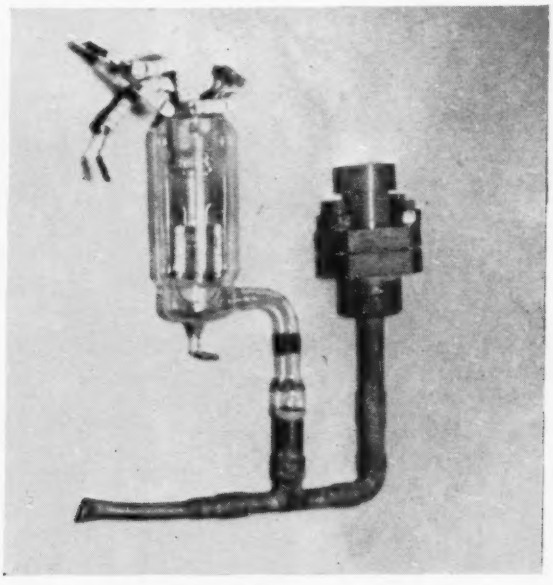

FIG. 4.

is a photo of a test assembly of an ion gage, flange and pinch-off which was evacuated and sealed two years ago after several thermal cycles to 450°C and still shows a vacuum of 10^{-6} mm Hg. This design is expected to be improved in the future by venting the remaining air space between the

ridges to eliminate the possibility of " virtual " leaks. This closure is used to connect ion gages, electron guns, electrical feed-throughs, and vacuum connexions. Specifically avoided are O-ring seals or Teflon gaskets because of vapor pressure limitations as well as adverse performance in high radiation fields.

Devices having mechanical motion inside the vacuum envelope are sealed with stainless steel bellows welded or brazed to the main structure. No rotary seals have been developed yet with sufficient vacuum tightness to permit inclusion in these systems.

The dual-pump vacuum system typically employed on electron linear accelerators is shown in Fig. 5. The forepump

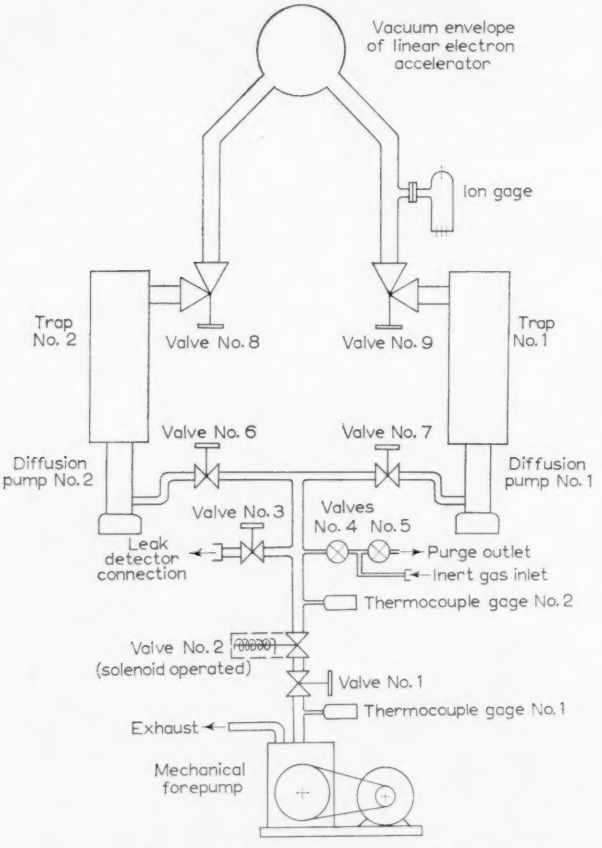

FIG. 5. Dual pump vacuum system.

normally used is a two-stage gas-ballasted rotating vane type having a speed of 30 μl./s at 50 μ pressure. The gas ballasting feature is useful if it is necessary to improve the base vacuum after the pump oil has become contaminated through long use and the pump cannot be stopped to change oil.

The diffusion pumps used to date are water cooled oil pumps having an unbaffled speed of about 2 μl./s at 3×10^{-5} mm Hg.

Isolation valves in the forevacuum system are bellows-sealed, Teflon gasketed globe valves, and are hard soldered into 1 in. copper tubing. Valve No. 1 and thermocouple gage No. 1 are used to isolate and check the base pressure of the mechanical pump. Valve No. 2 is opened automatically only after the mechanical pump has been turned on for two minutes. If electrical power is lost, valve No. 2 closes automatically and thus prevents the hot diffusion pumps from being exposed to the air which leaks back through the stopped mechanical pump. When power is restored, the forepump starts at once, valve No. 2 opens 2 min later and the diffusion pumps start pumping as soon as the forepressure is down to 100 μ.

Valve No. 3 is used to connect a helium mass spectrometer whenever the system must be checked for leaks. For maximum sensitivity, valve No. 1 is closed and the mass spectrometer thus samples all of the throughput of the diffusion pumps. Valves Nos. 4 and 5 are small needle valves used to admit inert gas whenver it becomes necessary to bring the accelerator to atmospheric pressure for repairs or inspection. Dried argon is usually used for this purpose to prevent oxidation of the internal surfaces and prevent possible poisoning of the oxide cathode. This operation has been performed twenty to thirty times without apparent damage to the accelerators. Valves Nos. 6 and 7 are used only if one or the other diffusion pump must be taken out of the system for repair. Valves Nos. 8 and 9 are also employed to isolate the diffusion pumps from the accelerator. They are $1\frac{1}{2}$ in. bellows sealed angle globe type having hard metal seats to make a vacuum tight closure and also withstand bakeout temperatures of 450°C. Whenever the copper traps are reactivated, these valves are closed manually to prevent trapped gases from diffusing back into the accelerator. Interlocks on these valves prevent the trap heaters from being energized unless the valves are closed.

Thermocouple gage No. 2 monitors forepressure on the diffusion pumps and controls power to the diffusion pump heaters via a meter relay set to open the heater circuit at pressures above 100 μ. Thus, even though the switches have been turned on, the diffusion pump heaters will not be energized until the system is pumped down to less than 100 μ pressure. Thermostat switches are strapped to the diffusion pump barrels to prevent overheating due to accidental loss of cooling water. Wattmeters are included in the heater circuit to monitor power input (270 W each). Figure 6 summarizes the interlocks and controls incorporated in the system.

Each diffusion pump has a water cooled baffle immediately above the pump flange, followed by a copper trap which has proven very effective in preventing the migration of pump oil into the accelerator. These traps are an extrapolation of the work done at Westinghouse Corporation laboratories by Dr. Alpert and his staff.[1] Figure 7 shows the physical dimensions and configuration of the trap and baffle. Conductance is 100 l./s through the valve, trap and baffle ; pumping speed is 30 l./s at 5×10^{-6} mm Hg.

The major value of this trap is that no refrigeration is required. The need for liquid nitrogen is therefore eliminated and there are no traps to go dry. We have obtained better vacuums with this trap than with any liquid nitrogen trap of our experience.

The construction which has been described obviously is intended to withstand high temperatures. The entire

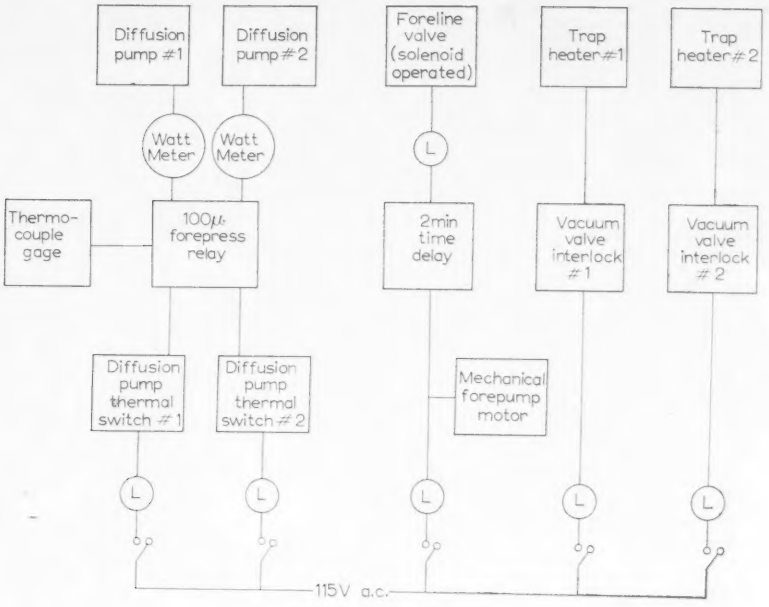

FIG. 6. Interlock diagram.

Vol. 9 959/60

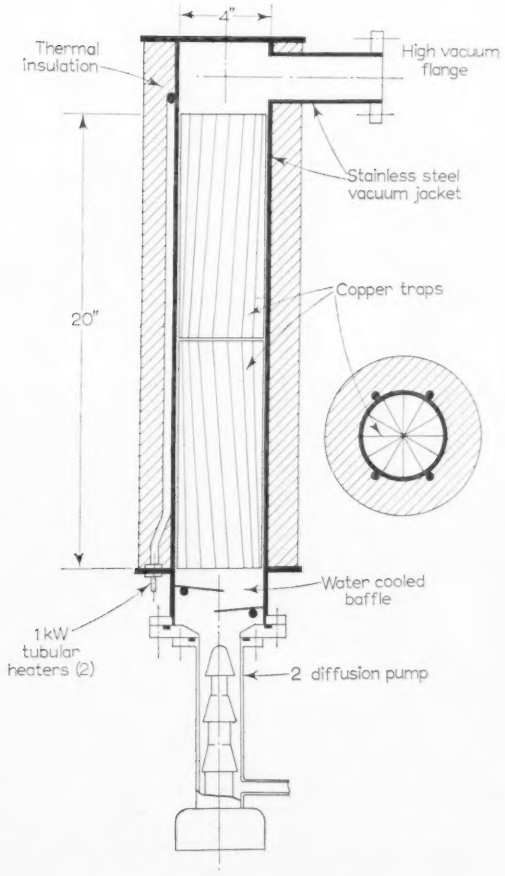

FIG. 7. Copper trap design.

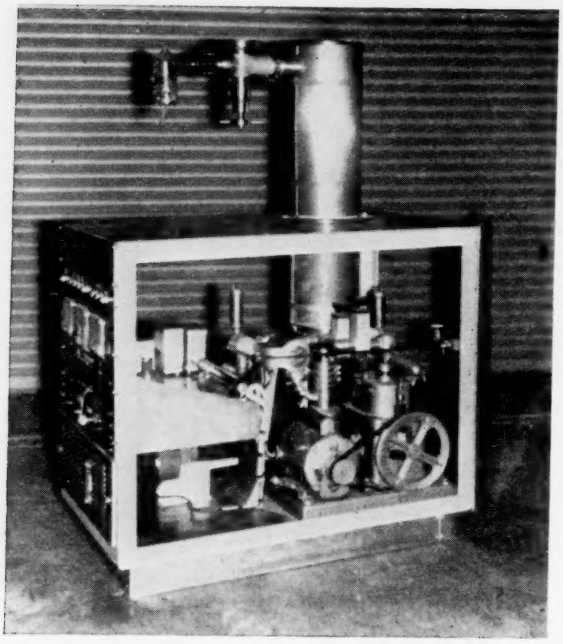

FIG. 8.

VO
9
1959

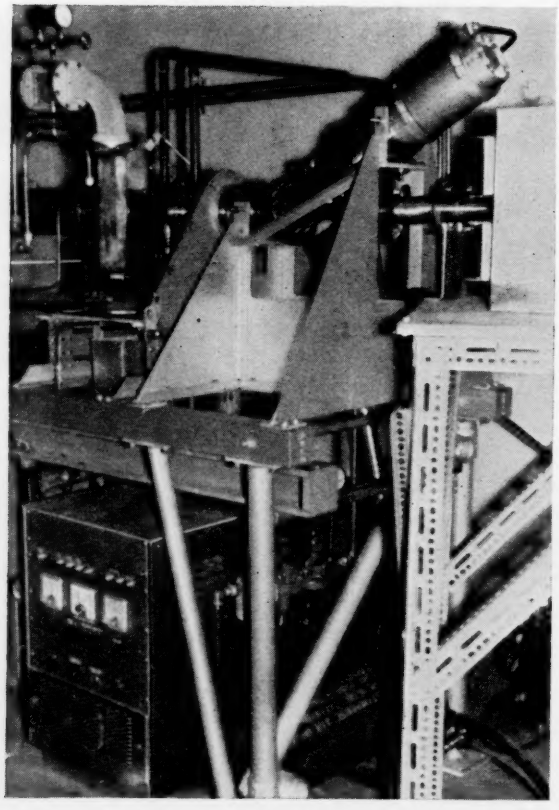

FIG. 9.

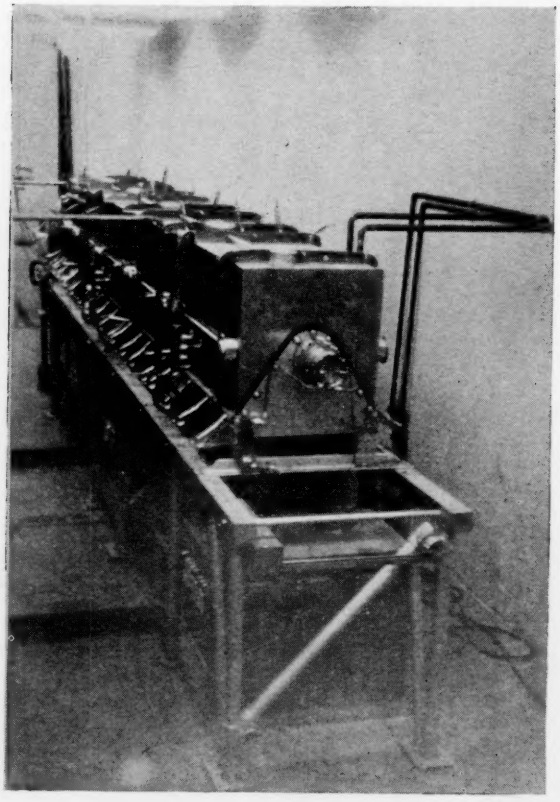

FIG. 10.

accelerator, from the output window to the vacuum traps, is baked out at 400–450 °C upon initial assembly for the purpose of driving off gases from the surfaces which ultimately will experience very high voltage gradients. This operation greatly reduces start-up time for a new accelerator, assures smooth operation, and minimizes chances for cathode poisoning. A typical bakeout cycle lasts 24 h and is usually terminated when the vacuum comes down to 5×10^{-6} mm while the accelerator is hot. Pumping continues all during this process to remove the outgassed vapors. The vacuum improves rapidly as the accelerator is cooled, indicating that considerable " gettering " occurs on the fresh surfaces of the copper envelope. The performance of this system is best illustrated by noting that an accelerator of 30 l volume, containing an activated oxide cathode of 5.5 cm diameter and having a total of 24 flanged joints, will pump down to 100 μ in 15 min, and in 60 min will be down to 10^{-6} mm. Overnight pumping will lower the vacuum to 10^{-7} mm. As the accelerator is operated, clean-up of the internal surfaces occurs and the vacuum continues to improve. Typical operating vacuum while accelerating electrons is 2×10^{-7} mm. With power off but with cathode hot, the vacuum drops on to the 10^{-8} mm scale. These pressures are measured with an ion gage of inverted structure, also developed by Bayard and Alpert at Westinghouse.[2] The lowest vacuum measured on a system of this type was 6×10^{-9} mm.

Figs. 8–10 show views of accelerators on which these vacuum systems are used.

References

[1] D. Alpert ; Copper isolation trap for vacuum systems, *Rev. Sci. Instrum.* **24**, 1004 (1953).

[2] R. T. Bayard and D. Alpert ; Extension of the low pressure range of the ionization gauge, *Rev. Sci. Instrum.* **21**, 571 (1950).

Vol. 9 959/60

Vacuum Treatment of Molten Steel— a New Way of Improving Converter Steel Production*

A. M. SAMARIN and L. M. NOVIK

BESIDES with the rapidly growing industrial application of vacuum induction and arc furnaces used for manufacture of special steel and alloys, various vacuum devices have been introduced recently, designed for processing of molten steel produced in any type of melting furnace.[1, 2, 3]

As a rule these devices are simple, the processing of molten steel goes without interrupting the established practices and the improvement of steel properties is achieved by treating it in a relatively low vacuum. Thus there opens up a possibility of using vacuum to improve the quality of millions of tons steel without any notable increase in its cost. Moreover, in certain cases the application of vacuum even allows to bring down the cost of steel production.

In 1952–53 equipment was built at Ynakiyevo metallurgical plant for processing liquid Bessemer steel in a ladle of 16 tons capacity and in a mould for a 4-ton ingot. The obtained results have been published.[1] The positive results of this plant gave rise to using the method of vacuum treatment of molten steel on other metallurgical plants of the U.S.S.R.

Below is given the data for vacuum treatment of Bessemer rail and rimming steel, obtained at Dzherzhinsky metallurgical plant.

Fig. 1 shows the design of a chamber for vacuum treatment of molten steel in a ladle, built at Dzherzhinsky plant. At present, the evacuating circuit is composed of two mechanical rotary vacuum pumps—RVN 30, of 22 m^3/min capacity, at a pressure of 5 mm Hg. The chamber is designed for processing of 22.5 tons of molten steel in a ladle.

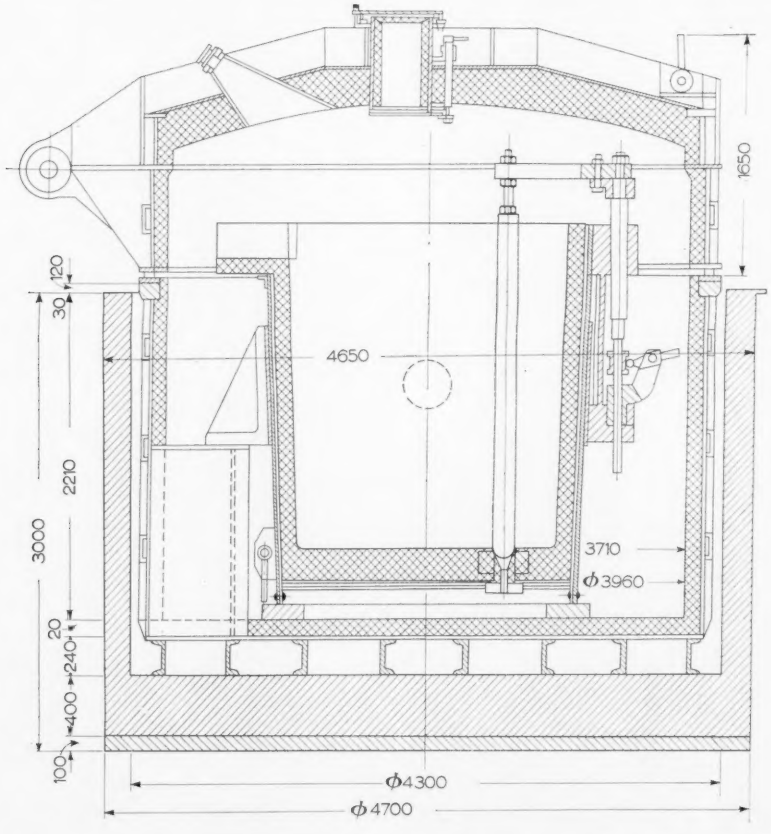

FIG. 1. Scheme of a chamber for vacuum treatment of molten Bessemer steel.

* Paper presented at the First International Congress on Vacuum Techniques, Namur, 10–13 June 1958.

At Dzherzhinsky plant the rail steel is produced in Bessemer converters and the blowing is stopped when a predetermined high level of carbon content in molten metal is reached to avoid the recarburation. The ladle with molten steel is kept in the chamber at a reduced pressure of the order of 5–10 mm Hg for 12–13 min.

Fig. 2 shows diagrams representing data on the change of oxygen content of rail steel as a result of vacuum treatment. The oxygen content of rail steel drops from 0.0057 down to

As a result of vacuum treatment the nitrogen content of rail steel is lowered very little—by 10–20 per cent.

Vacuum treatment considerably improves the properties of Bessemer rail steel.

First, evacuation of hydrogen from the molten steel allows to produce rails without flakes.

Secondly, as follows from the data shown on Fig. 2, the deoxidation of steel during the vacuum treatment is promoted by carbon. Aluminium in the quantities of 300–500 g/ton

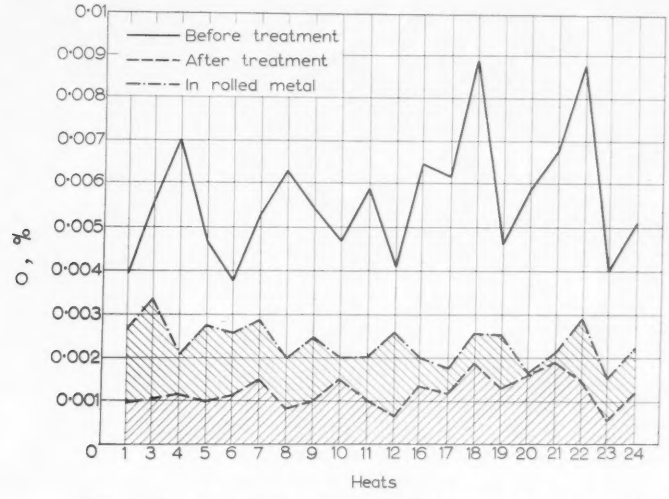

FIG. 2. Change of oxygen content of rail steel during vacuum treatment and pouring.

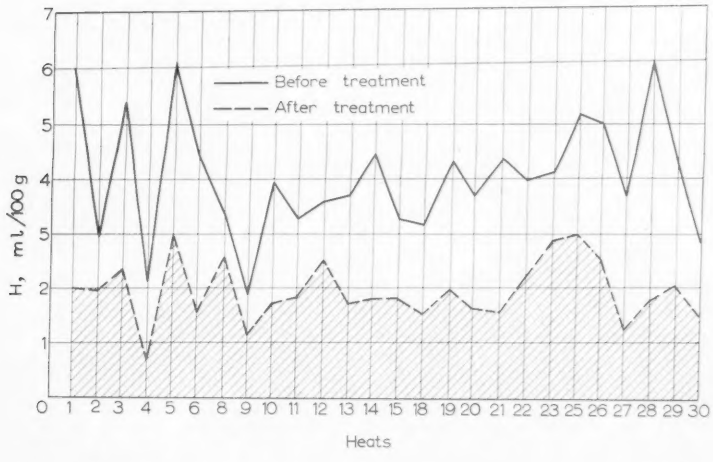

FIG. 3. Change of hydrogen content of rail steel during the vacuum treatment.

0.0012 per cent on the average, i.e. decreases almost five times.

The diagram shows data on oxygen content of rail steel after rolling. The rise of oxygen content is evidently caused by secondary oxidation of steel during pouring which goes on in the air.

Fig. 3 shows change of hydrogen content of molten rail steel during processing of it in vacuum. The hydrogen content is reduced on the average from 4.6 to 2.0 $cm^3/100$ g that is 2.3 times.

is introduced into molten steel mainly for binding the nitrogen.

As is known, the rails from standard Bessemer steel are characterized by an increased strength and decreased plasticity. Such rails are more wear-resistant but brittle. The vacuum treatment almost does not change its ultimate strength and increases its reduction area by 18–30 per cent elongation by 10–20 per cent and impact value by 50–60 per cent.

It has been established that high toughness and plasticity

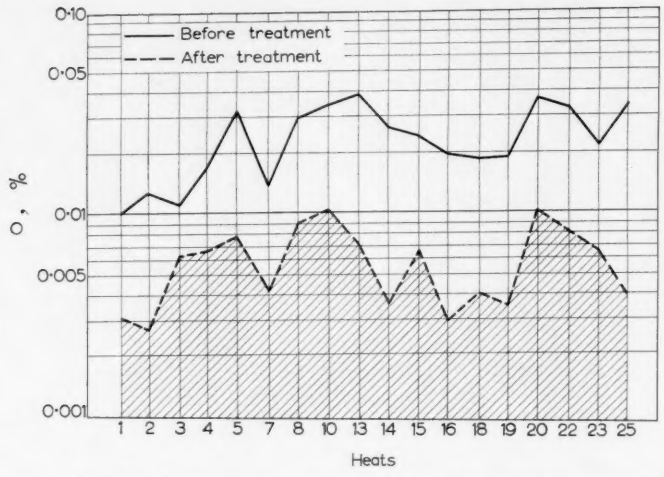

FIG. 4. Change of oxygen content during the vacuum treatment of rimming Bessemer steel.

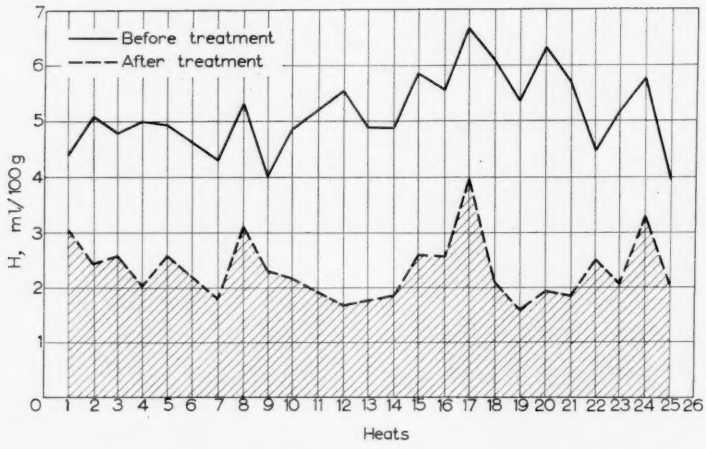

FIG. 5. Change of hydrogen content during the vacuum treatment of rimming Bessemer steel.

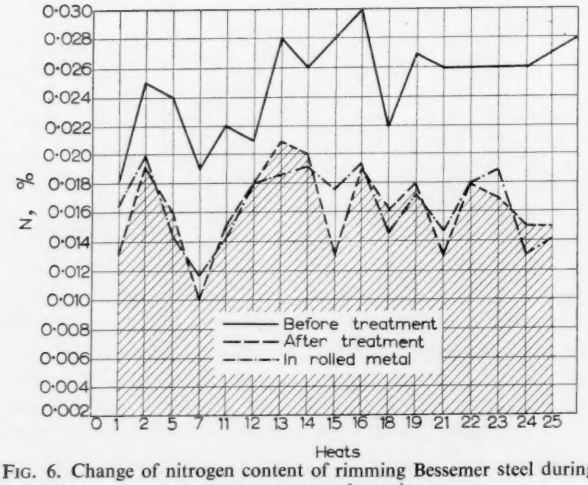

FIG. 6. Change of nitrogen content of rimming Bessemer steel during vacuum treatment and pouring.

of a vacuum-treated Bessemer rail steel can be secured by additional alloying of it. Thus it becomes possible to produce Bessemer steel rails which are not inferior to rails manufactured from open-hearth steel.

While working with rimming Bessemer steel the pressure in the chamber was reduced to 15–20 mm Hg.

Fig. 4 shows the change of oxygen content of rimming steel as a result of vacuum treatment. As you observe the oxygen content went down five times. The hydrogen content, as follows from the data shown on Fig. 5 is decreased two times on the average. As different from the rail steel, a considerable drop of nitrogen content is observed in vacuum treatment of rimming steel. The data presented on Fig. 6 shows that up to 40 per cent of nitrogen can be evacuated from the rimming steel by processing it in vacuum.

A change of composition resulting from the vacuum treatment provided for a tangible improvement of rimming Bessemer steel properties.

First, the ingots cast from this steel are no different from ingots of deoxidized steel by their structure. Fig. 7 shows a cross-section of an ingot cast from vacuum-treated Bessemer rimming steel. An improved structure of this ingot provides for making out of it a higher quality rolled stock. Fig. 8 a shows a sulphur print of a billet produced from an ingot of standard rimming steel, while Fig. 8 b shows a print of a billet produced from the same rimming steel which had been vacuum treated. A presence of a pipe is a drawback, of course. But it is a temporary drawback, considering the rapidly adopted by the industry continuous pouring practices.

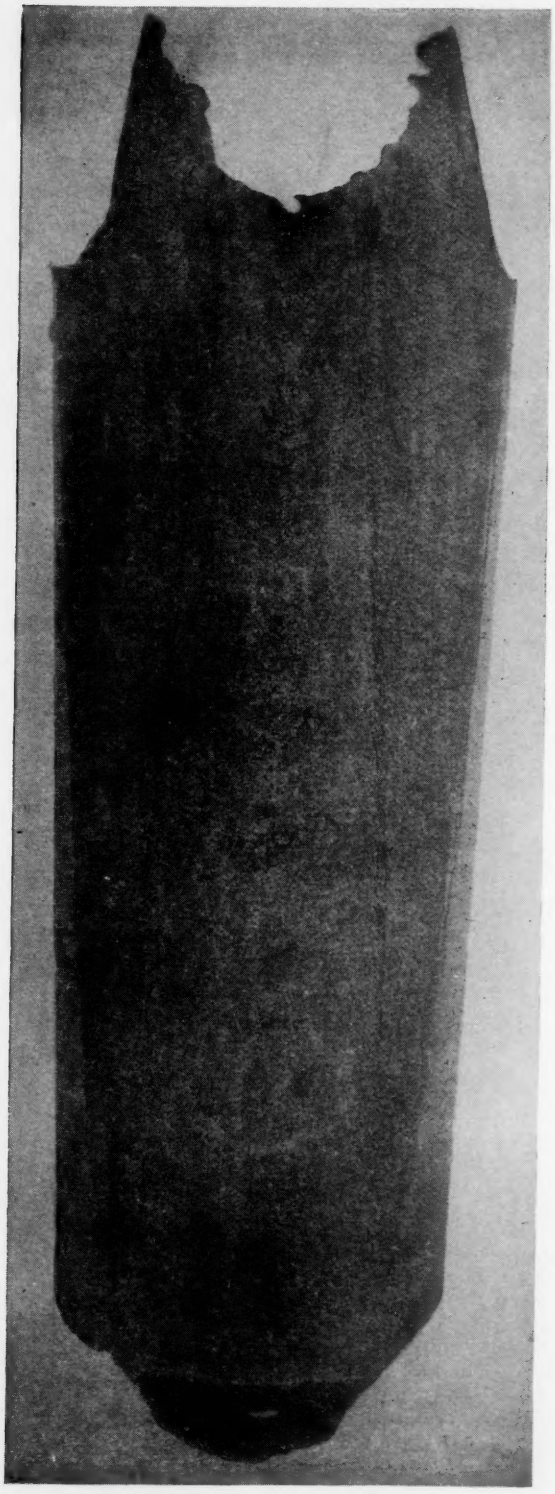

FIG. 7. An ingot cast from vacuum-treated rimming Bessemer steel.

Secondly, a vacuum-treated Bessemer rimming steel possesses excellent mechanical properties at low temperatures. If the transition temperature for standard Bessemer rimming steel is at 0°C the sharp drop of impact strength of vacuum-treated Bessemer rimming steel is observed only at −30° to −40°C.

Thirdly, the zone of welding joint in not subject ageing. In welding joints of standard Bessemer rimming steel the ageing takes place, and while testing samples taken at a distance of 5–10 mm from the welding joint, we observe their brittle destruction.

The previously mentioned results allow us to draw a conclusion that the properties of a vacuum-treated Bessemer steel become as good as those of open-hearth steel.

Among other methods of steel production the converter methods are the best ones and only specific drawbacks of Bessemer and Thomas steels had caused the gradual dying off of these effective methods some time ago. Only during the last few years the utilization of oxygen helped to revive the converter methods of steel production. Now we can already say that the development of converter steel production is possible not only due to use of oxygen, but also due to use of vacuum, which can successfully compete with oxygen.

The investment of oxygen-generating stations is more expensive than making installations for processing molten steel in vacuum. The cost of converter steel production with oxygen blowing is also higher than that involved in vacuum treatment of molten steel. In terms of power consumption the process with oxygen (for instance L–D process) requires about 30 kWh per ton, while vacuum treatment of a ton of molten steel consumes less than 5 kWh.

And finally, a few words on methods of gas evolution from molten steel in vacuum. The most convenient way of vacuum treatment of molten steel is to conduct it while steel is in the ladle. But some specialists say that in this case the hydrostatic pressure and presence of slag on the surface of molten steel prevent the evacuation of gases from the metal and that only surface layers of metal are freed from gases.

Such opinions do not take into consideration the mechanism of gas evacuation from molten metal. The gas bubbles may originate at the contact plane between the molten steel and ladle lining. The observations of gas release in the beginning of the vacuum treatment process also prove this point—the flames appear on the surface around the stopper and at the ladle walls. The gas bubbles which pass through the metal evidently accumulate under the slag, penetrate into it and then break through its surface.

The fact that evacuation of gases is really uniform throughout the entire volume of molten steel is also illustrated by the results of measuring the hydrogen content in steel samples

Vol. 9 959/60

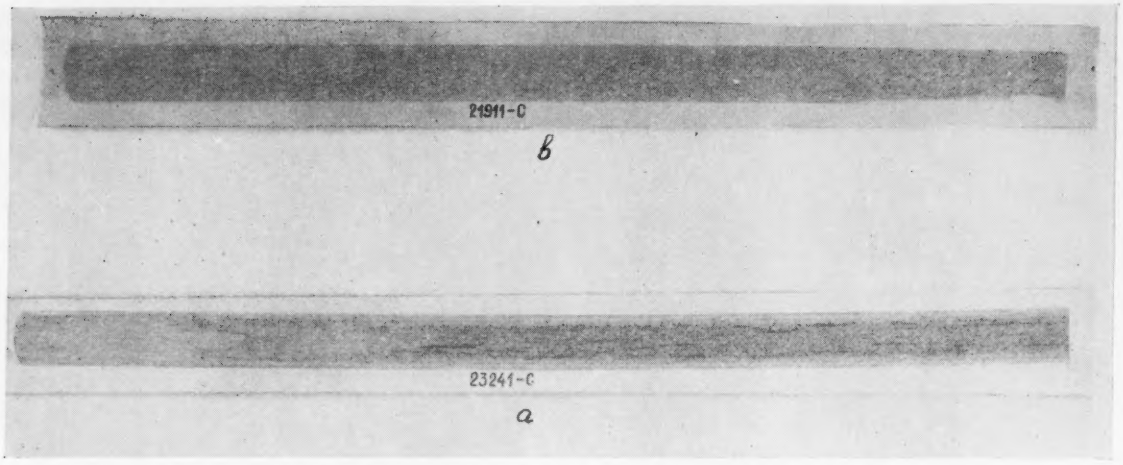

FIG. 8. A sulphur distribution of rolled billets from rimming Bessemer steel.

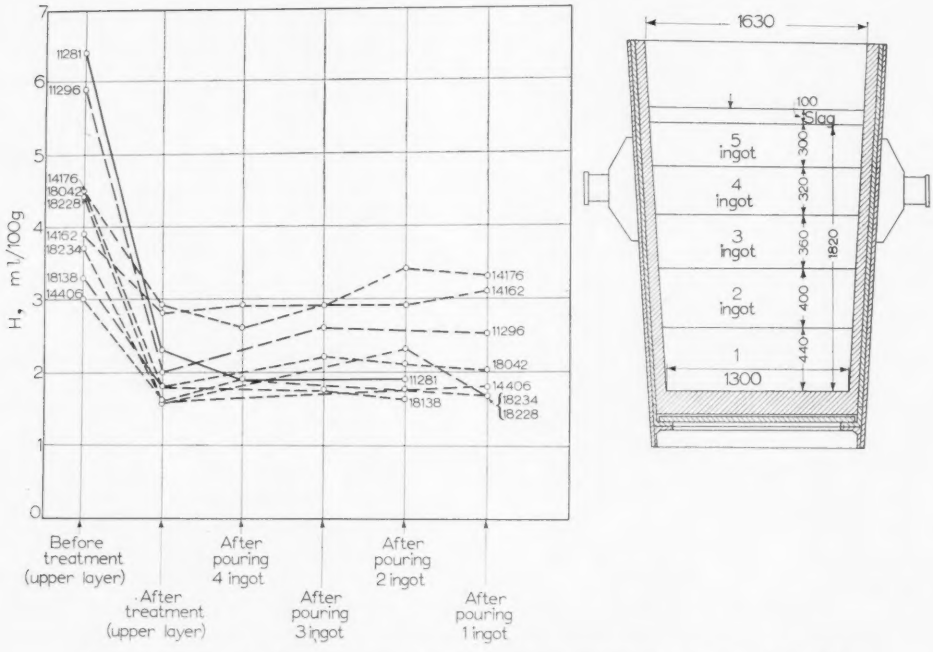

FIG. 9. Change of hydrogen content of steel during the pouring of it into ingot moulds.

taken from the ladle of vacuum-treated steel after pouring from it some of the metal for the first, second, third and fourth ingots.

Actually it is hard to say from what layers comes the steel which goes into this or other ingot moulds, considering the complexity of movements of steel in the ladle, but studying the data presented on Fig. 9, even despite the rather unsuitable shape of the ladle, we can assert that the hydrogen content was uniform throughout the volume of molten steel after its treatment in vacuum.

Conclusion

Vacuum treatment is a reliable and inexpensive means to considerably improve the Bessemer steel properties. The application of vacuum will promote the production of steel in converters.

References

[1] A. M. Samarin, L. M. Novik, N. I. Goncharenko and A. F. Tregubenko ; Treatment of molten metal in vacuum, *Steel* **8**, 700–707 (1956).

[2] A. Tix ; Betriebliche. Anwendung der Stahlentgasung im Vakuum besonders bei grossen Smiedenbloken, *St. Eisen* **76**, no. 3, 61–68 (1956).

[3] F. Garders, H. Knuppel and K. Brotzmann ; Die grosstechnische Behandlung von Stahlchmelzen unter verminderten Druk-, *St. Eizen* **76**, no. 26, 1721–1728 (1956).

Oblique Reflectance and Transmittance Measurements on Aluminium Films

T. TURBADAR

University of Damascus, Syria, U.A.R.

(Received 9 February 1959)

Reflectances and transmittances of thin aluminium films deposited on glass were measured as a function of the angle of incidence and the state of polarization of the incident light. The experimental results were compared with theoretical predictions. The oxide layer which forms on the Al film as this is exposed to air was taken into account and discussed. Experimental results indicate that the refractive index of an Al film thicker than 80Å is independent of thickness.

On a mesuré les coéfficients de réflexion et de transmission de couches minces d'aluminium déposées sur verre, en fonctions de l'angle d'incidence et de l'état de polarisation de la lumière incidente. Une comparaison a été faite entre les résultats expérimentaux et théoriques. Lorsqu'une couche mince d'aluminium est exposée à l'air, elle subit une oxydation superficielle rapide, aussi l'évolution des coéfficients a-t-elle été discutée. Les résultats expérimentaux montrent que l'indice de réfraction d'une couche mince d'aluminium d'épaisseur supérieure à 80 Å est indépendant de l'épaisseur.

Vol. 9 959/60

Introduction

It seems likely that the optical properties of thin films are not always such as to correspond exactly with theory. For example, the effective refractive index of a material may be a function of the film thickness or of the method by which it is measured, or a film may behave as if it had different refractive indices for different angles of incidence. Such effects are particularly to be expected in metal films, which are known to have a granular structure in which the state of aggregation depends on a number of factors. It is therefore desirable to measure the optical properties of films to see how far their behaviour agrees with that predicted by single theory. In this paper some measurements are reported on aluminium, this being a metal of considerable importance in optical instrumentation.

Methods and theory

Thin Al layers were deposited on glass substrates ($n = 1.5$), by the classical evaporation technique in a vacuum of the order of 10^{-5} mm Hg. The glass substrates were cleaned in the usual way with potassium hydroxide solution and dilute nitric acid, then rinsed in water. A further cleaning was made by ionic discharge. The heater was a multi-strand tungsten filament in the shape of a conical basket. The heating current was about 40 A, and the rate of evaporation of the order of 10 Å/s. The source was arranged so that the angle of incidence of the condensing Al molecules was always less than 5°, so that optical effects due to oblique evaporation could not occur.

Reflectances and transmittances for different values of angle of incidence φ were measured with the Wright spectrophotometer, of which a schematic diagram is given in Fig. 1.[1] The experimental results were compared with the theoretical ones computed according to thin film formulae[2].

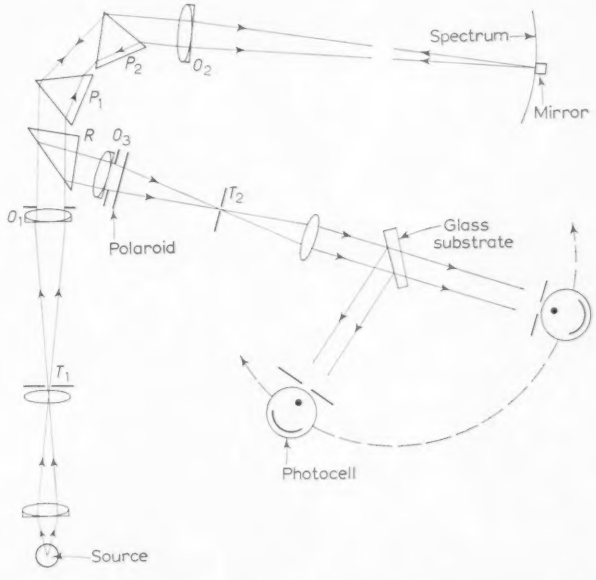

FIG. 1. Optical system of the Wright Spectrophotometer. The 90° prism R, whose height is half that of P_1 and P_2, intercepts only the selected waveband reflected by the mirror back through the lower halves of O_2, P_2 and P_1.

The reflectance R and transmittance T of the single Al layer were expressed in a way which makes computation easier to work out than using the matrix form. The expressions for R and T are the following :

$$R = \left|\frac{(\mu_2-\mu_0)\mu_1 \cos g_1 + i\,(\mu_0\mu_2-\mu_1^2)\sin g_1}{(\mu_2+\mu_0)\mu_1 \cos g_1 + i\,(\mu_0\mu_2+\mu_1^2)\sin g_1}\right|^2, \quad (1)$$

$$T = 4\mu_0\mu_2\left|\frac{\mu_1}{(\mu_2+\mu_0)\mu_1 \cos g_1 + i\,(\mu_0\mu_2+\mu_1^2)\sin g_1}\right|^2, \quad (2)$$

where the suffices 2, 1, 0 refer to the media air, Al, and glass : $\mu = n/\cos\varphi$ or $\mu = n\cos\varphi$, dependent on whether the incident light is polarized with the electric vector in or perpendicular to the plane of incidence ; $g_1 = (2\pi/\lambda)n_1h_1 \cos\varphi_1$, where h_1 is the thickness of the Al film, n_1 its refractive index taken as equal to $(0.79-5.3i)$ at $\lambda = 5500$ Å, the wavelength of light which was used in the present work. The imaginary part of $\cos\varphi_1$ was found to be small compared with the real part, which is very nearly unity. For this reason, $\cos\varphi_1$ was considered as equal to 1 for any angle of incidence.

When the light falls on the Al film from the substrate side instead of from the air side, the same equations (1) and (2) apply, but μ_0 and μ_2 should be interchanged. Since equation (2) is symmetrical for μ_0 and μ_2, the transmittance of the Al film is the same in both cases. This is not the case for equation (1), and therefore the reflectance of the Al film at the substrate side R' is always different from the reflectance at the air side R.[3]

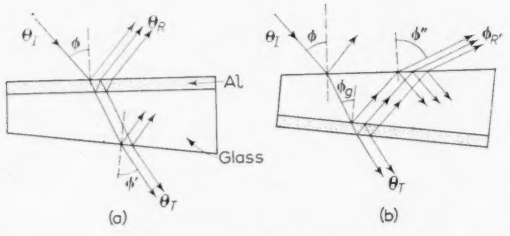

FIG. 2. The wedge-shaped glass substrate showing the path of the reflected and transmitted light when the Al layer is (*a*) at the front surface, (*b*) at the back surface.

The glass substrate ($n = 1.5$) was of a prismatic shape to avoid multiple reflections (Figs. 2a, b).

The reflectances R and R' and the transmittance T were calculated from the following equations which can be deduced from Fig. 2.

$$R = \frac{\theta_R}{\theta_1}, \tag{3}$$

$$T = \frac{\theta_T}{\theta_1}\,\frac{1}{(1-r_{\varphi'})}, \tag{4}$$

$$R' = \frac{\theta_{R'}}{(\theta_1}\,\frac{1}{(1-r_{\varphi})\ (1-r_{\varphi''})}, \tag{5}$$

where θ_1, θ_R, $\theta_{R'}$ and θ_T were measured experimentally with the photocell unit of the spectrophotometer ; and r_φ is the reflectance of the glass substrate at the angle of incidence indexed. The values of φ', φ'' and φ_g (Fig. 2) were calculated for different angles of incidence in the air (φ) ranging between 20° and 80°, and the values of r_φ, $r_{\varphi'}$ and $r_{\varphi''}$ were obtained from the experimental curve (r, φ) for the glass substrate used.

Since the width of the incident beam was 10 mm, and the width of the substrate 40 mm, the upper limit of the angle of incidence φ is such that $\cos\varphi = 10/40 = 0.25$, i.e. $\varphi \cong 75°$. This applies only to the case of reflection at the air side. For transmittance measurements the upper limit of φ was found to be about 65° which corresponds to $\varphi_g \cong 38°$. If a parallel glass plate were used instead, the upper limit of φ_g could extend to about 42° but not further, owing to total reflection in glass. To extend the limit of φ_g still further, a right-angle prism was used, the Al layer being deposited on its hypotenuse. This brought to light a curious reflection anomaly which was reported in a separate paper.[4]

Experimental results

Table I gives the experimental results and (Figs. 3 *a–c*) shows the curves giving R, R' and T as functions of φ, for three different thicknesses of Al films. The thicknesses were obtained from a paper by Walkenhorst,[5] who measured the reflectances and transmittances of Al films at normal incidence as a function of thickness at = 5000 Å.

TABLE I

(*a*) *Al film* ≅ 60 Å *thick*

φ	*Rp*	*Rs*	*Tp*	*Ts*	φg	*R'p*	*R's*
20°	15.2	18.3	59.0	56.5	16°	1.96	2.10
25	14.2	19.0	60.0	55.8	19	1.97	2.20
30	13.1	20.3	61.3	54.7	22	2.01	2.31
35	11.7	21.7	62.0	53.8	25	2.07	2.46
40	10.1	23.4	64.1	51.5	28	2.26	2.64
45	8.6	26.2	66.5	51.0	31	2.60	2.92
50	6.75	29.4	68.0	48.8	33	3.28	3.32
55	4.88	33.0	69.9	45.6	36	4.66	3.90
60	3.33	37.6	71.9	43.0	38	9.08	6.65
65	2.22	43.5	—	—	—	—	—
70	2.57	50.8	—	—	—	—	—

(*b*) *Al film* ≅ 100 Å *thick*

φ	*Rp*	*Rs*	*Tp*	*Ts*	φg	*R'p*	*R's*
20°	54.0	58.0	28.0	25.5	16°	42.5	46.5
25	53.4	59.6	28.4	23.9	19	42.0	47.6
30	51.3	60.4	29.6	23.5	22	41.5	49.3
35	50.5	63.3	30.7	22.4	25	40.9	51.1
40	49.0	65.8	32.2	20.7	28	40.4	53.6
45	47.0	68.4	34.0	19.7	31	39.8	56.7
50	44.0	71.6	35.7	18.0	33	38.8	60.0
55	41.0	74.0	38.2	16.7	36	38.9	63.8
60	37.1	77.5	40.9	15.0	38	40.0	70.2
65	33.2	81.0	43.5	13.3	—	—	—

(*c*) *Al film* ≅ 135 Å *thick*

φ	*Rp*	*Rs*	*Tp*	*Ts*	φg	*R'p*	*R's*
20°	74.2	77.3	11.1	9.65	16°	62.7	64.3
25	73.0	77.6	11.5	9.35	19	61.7	65.5
30	71.3	78.2	12.0	8.55	22	60.6	65.8
35	69.1	78.5	12.6	8.33	25	58.8	65.5
40	67.3	79.2	13.2	7.50	28	58.1	66.9
45	65.6	80.3	14.1	6.98	31	57.0	67.6
50	63.0	81.4	15.3	6.32	33	55.4	68.6
55	60.5	82.9	16.7	5.71	36	54.5	71.8
60	56.3	84.5	18.9	5.25	—	—	—
65	53.4	87.8	21.8	4.95	—	—	—

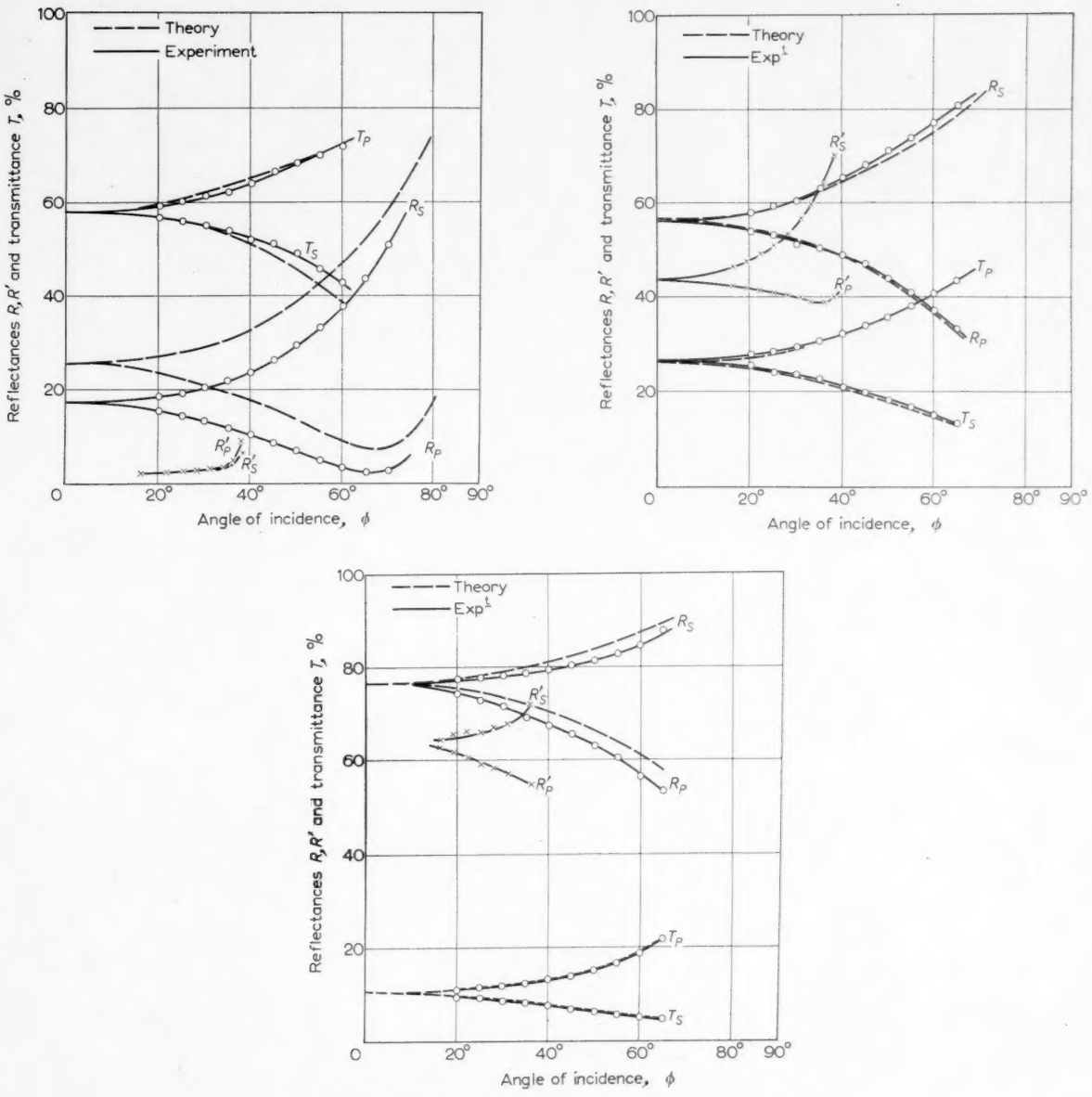

FIG. 3. Comparison of experimental and theoretical curves (R, R' and T as functions of φ) for different thicknesses of Al layer (*a*) 60 Å, (*b*) 100 Å and (*c*) 135 Å.

Theoretical results and discussion

To compute R and T of the deposited Al film one should take into account the oxide layer which forms on the top of the Al film as soon as this film is exposed to air. As a result of the formation of the highly transparent Al_2O_3, the transmission of the Al film increases. This is shown in Fig. 4, which indicates that transmittance increases rapidly at first to about 1.1 of its initial value in less than 1 min, the increase afterwards becoming slow and reaching about 20 per cent after a few hours. A similar curve has been found for the growth of the Al_2O_3 layer. This growth depends on the structure of the deposited Al, i.e. on the rate of evaporation. Hass[6] reported that in the case of a high rate of evaporation, the oxide initially grows rapidly to a thickness of $15 \rightarrow 20$ Å, but further growth only occurs slowly, reaching a limiting thickness of 45 Å after a month.

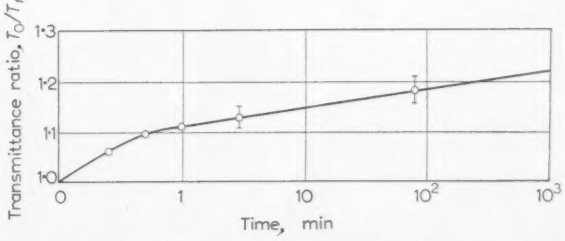

FIG. 4. Proportional increase of transmittance of Al film when exposed to air.

Assuming the oxide layer is 20 Å thick, then the increase in the total thickness of the deposited film is 5.5 Å ; this results from the relation

$$\frac{h_1}{h_2} = \frac{d'}{d}\frac{M}{M'},$$

where d is the density of solid Al = 2.7 ; d' is the density of Al_2O_3 = 3.7 ; M is the weight of Al_2 = 54 ; M' is the molecular wt. of Al_2O_3 = 102 ; h_2 is the thickness of Al_2O_3 = 20 Å ; h_3 is the thickness of the oxidized portion of the Al layer which is given by the above relation as 14.5 Å.

Table II shows the results of computing T and R for $\lambda = 0.55\ \mu$ at normal incidence for the two cases : (*a*) The single unoxidized layer of Al of thickness h ; and (*b*) The two-layer film of Al (thickness $h-14.5$ Å) and Al oxide (thickness 20 Å).

TABLE II

Initial thickness h (Å)		90	110	150
Transmittance T %	(*a*) Al	26.5	20.1	11.76
	(*b*) Al_2O_3	34.3	25.9	14.5
Ratio of (*b*)/(*a*)		1.295	1.29	1.235
Reflectance R %	(*a*) Al	55.0	62.5	72.9
	(*b*) Al_2O_3	48.1	56.3	69.7

Table III shows the experimental data for the transmittance of several Al films with white light for three conditions : (1) Freshly deposited ; (2) aged in the atmosphere for 3 min ; (3) aged in the atmosphere for 80 min.

TABLE III

	Transmittance T(%)						
(1) Fresh deposit (T_f)	9.3	12.95	20.0	28.8	34.5	45.7	54.7
(2) 3 min exposure	10.25	14.25	22.5	31.1	38.7	51.5	61.6
(3) 80 min exposure (T_o)	10.52	14.90	23.1	32.8	40.1	54.3	65.6

These results are shown in Fig. 5 which indicates that T_o/T_f is nearly constant in the range of transmittances considered, as the theory predicts ; and that the thickness of Al_2O_3 formed after 80 min of exposure to air is about 15 Å.

The conclusion which may be drawn from the above results is that an aged Al layer is to a good approximation equivalent to a freshly deposited one whose thickness is smaller by an amount of the order of the thickness of the oxide formed. So, though the Al film is actually composed of two layers one could treat it theoretically as if it were a single layer of Al. This holds for transmittance and reflectance of a single deposition ; in cases where the Al layer forms part of a multilayer, this is not true since phase changes are then involved in the computation. Equations (1) and (2) were used to calculate R and T of Al films for thicknesses ranging between 40 Å and 165 Å, assuming the refractive index of the Al film is constant and equal to $(0.79-5.3i)$. The results are shown in Fig. 6.

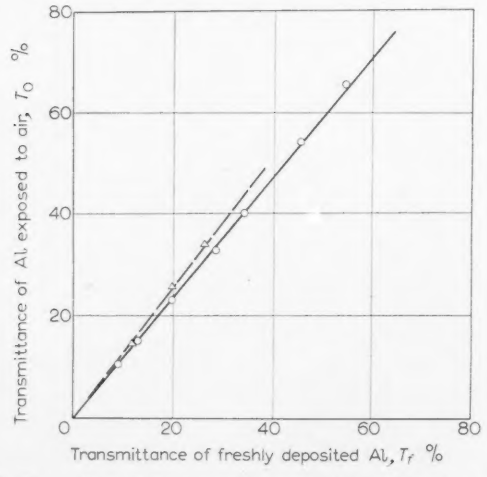

FIG. 5. Comparison of the transmittances of Al films freshly deposited and their transmittances when exposed to air.

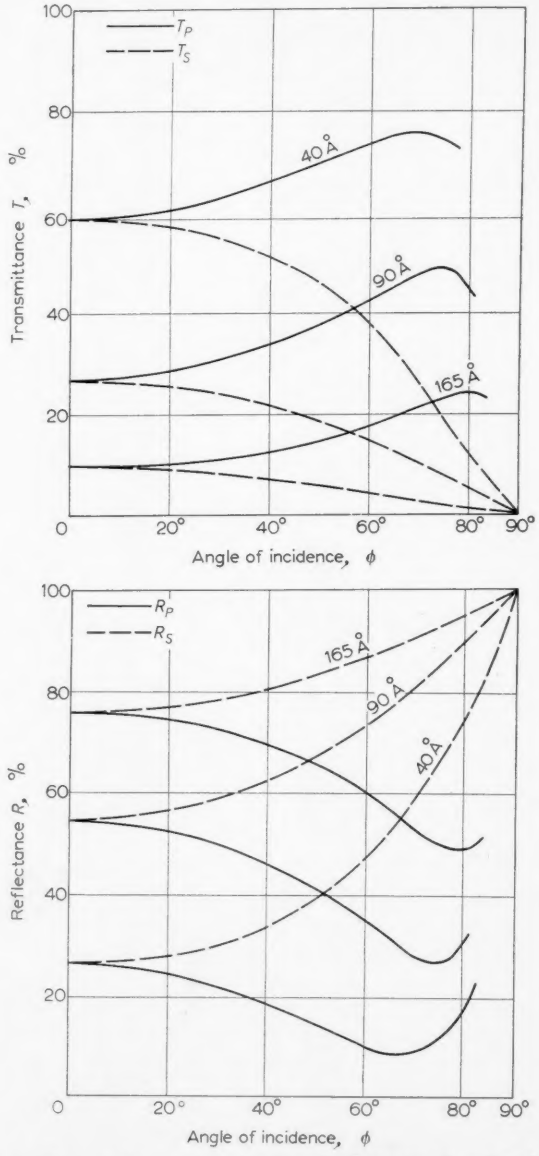

FIG. 6. Theoretical transmittances, T, and reflectances, R, as functions of the angle of incidence φ for the thicknesses indicated on the curves (*a*) transmittances, and (*b*) reflectances.

A comparison between the experimental and theoretical curves, which have the same value of T at normal incidence, shows that the agreement is reasonably good for layers whose thicknesses are more than 90 Å (Fig. 3a–c). For thinner layers, the experimental reflectance curves are shifted towards lower values of R, i.e. higher absorption. The failure in the case of very thin films is certainly due to the fact that below a certain thickness the refractive index is not constant. If the proper refractive index is chosen the experimental and theoretical curves would coincide fairly well. Fig. 7 shows the theoretical curve (R, T) for normal incidence, together with some experimental data. It indicates that the refractive index could be considered constant for films whose thicknesses are over 80 Å, but below that the refractive index assumes values which make the film more and more absorbing.

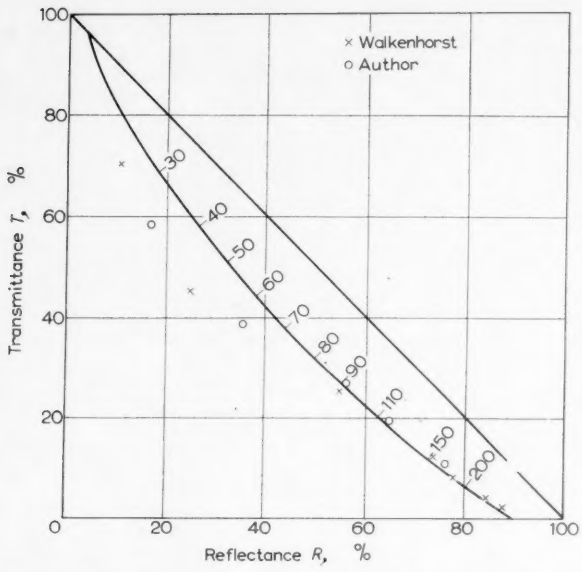

FIG. 7. Theoretical transmittances and reflectances of Al films. The divisions on the curve (R, T) give the thickness of the film. Experimental values are for Al films exposed to air for a day or two.

Acknowledgements

The author is indebted to Professor W. D. Wright for making available the experimental facilities of his laboratories, and to Dr. W. T. Welford for his guidance and invaluable advice. The work described was carried out while the author was a guest worker in the Technical Optics Section, Imperial College of Science and Technology, London.

References

[1] W. D. Wright : A photoelectric spectrophotometer and tristimulus colorimeter designed for teaching and research, *Optica Acta* **1**, 102 (1954).
[2] W. Weinstein ; Computations in thin film optics, *Vacuum* **4**, 3 (1954).
[3] P. Rouard, D. Malé and J. Trompette ; *J. Phys.* **14**, 587 (1953).
[4] T. Turbadar ; Complete Absorption of Light by Thin Metal Films, *Proc. Phys. Soc.* **73**, 40, (1959).
[5] W. Wulkenhorst ; *Z. tech. Phys.* **22**, 14 (1941).
[6] G. Hass ; *Z. anorg. Chem.* **254**, 96 (1947).

Vol. 9 959/60

A Thin Film Resistor for Measuring Strain

G. SIDDALL and G. SMITH

Edwards High Vacuum Ltd., Crawley, Sussex

(Received 9 February 1959)

An investigation has been made into the measurement of mechanical strain in terms of the electrical resistance changes induced in an evaporated metal film on a flexible support cemented to a stressed surface. The results show that a polyester foil coated with a nickel-chromium alloy is suitable for short-term measurement purposes.

Introduction

Films of nickel–chromium alloys[1] and of gold[2, 3] have been deposited on glass by evaporation in a vacuum. These films were shown to possess suitable properties for making stable electrical resistance elements.

The authors[4] have already described the production of resistors on flexible resin bonded glass cloth laminates, some of which have shown good stability whilst under thermal and electrical stress. Work has also been carried out[5] concerning the use of evaporated films for strain gauges, but the results have not been encouraging, due to large irreversible changes in resistance which were observed on applying a stress. We believe that the difficulty has been in choosing the correct film–substrate combination and that a nickel–chromium alloy deposited on a thin flexible support might prove suitable for measuring mechanical strain in terms of change in resistance. The thin film resistor and flexible base would be cemented firmly to the mechanical component in which strain was to be measured. It would be provided with electrodes for resistance measurement and be protected by a suitable lacquer, preferably of the same resin used for cementing the laminate.

Resistance strain gauges using a metal foil or wire resistance element are well known and have been reviewed.[6] In one type the flexible base consisted of an epoxy resin film bonded to a nickel foil. In order to increase the resistance of this foil, the conducting path was increased by printing a pattern in an acid-resisting ink and etching away the unwanted metal.

A thin metal film has the advantage of having a resistance already high enough for reliable measurements to be made without increasing the path length. The problem remaining is that of film stability, since the resistance must follow the strain reversibly. Work on other thin flexible supports[5] has shown that after removal of the strain, the resistance of the foil decreases again but not nearly to its original value.

The aim of our experiments was to make a resistance strain gauge by vacuum deposition using any of the known techniques for making stable resistance elements on flexible bases, and to examine its performance.

Experimental method

Two separate experiments were attempted. In the first series, resistance measurements were made on a strain gauge cemented to a beam. A piece of the nickel–chromium coated plastic material to be tested was sprayed with metal end contacts and then cemented to a beam of mild steel, using a melamine resin lacquer. The resistance film was protected with the same lacquer. The resin was then cured for 30 min at 140°C after which the specimen was found to be firmly fixed to the steel.

The beam was 1 in. wide × $\frac{1}{8}$ in. thick × 3 ft long and the test specimen was fixed to the 1 in. flat side, 2 in. from the supported end. The beam was firmly bolted to a rigid support in the horizontal position. The other end of the beam was drilled to take a weight pan. Bending moment was applied to the beam by loading the pan progressively with 100 g weights. The changes in resistance of a specimen size 2 in. × $\frac{9}{32}$ in. were measured at each loading of the bar using a Wheatstone Bridge capable of an accuracy of 0.1 per cent. The accuracy was not important however, since we were measuring change rather than absolute values.

After loading the pan, the weights were then removed, one at a time, in order to obtain a complete cycle of readings and so reveal any permanent change in resistance of the film due to dislocations or to the relief of strains in the film itself.

In the second series of experiments, the flexible base and films were put under strain by stretching. The strip of coated material was fixed firmly to a rigid support and allowed to hang vertically, with a clamp and weight pan loading it at the bottom. Weights were then added to the pan and the changes in resistance were noted. Measurements of the elongation of the material were also made at the same time using a cathetometer. In this way it was possible to relate resistance value to elongation of the specimen.

Two methods of fixing the material to the support and weight pan were used. The preliminary experiments were carried out by fixing the flexible support to the metal parts using an adhesive, but this method was later replaced by a clamping system which was found to be more reliable.

Results

Samples of a polyester resin bonded glass cloth $\frac{1}{64}$ in. thick were coated with nickel–chromium alloy to give a resistance of about 200 Ω per square. A piece of this material size 2 in. × $\frac{9}{32}$ in. was then fixed to the bending beam in the way already described. Upon loading the beam the

Vo
9
1959

resistance was found to increase irreversibly, and examination of the specimen showed that the film had cracked to make a pattern corresponding to the weave of the glass cloth. This material was therefore considered unsuitable for further tests.

Experiments were then carried out using a 0.001 in. thick film of polyethylene terephthalate manufactured by I.C.I. under the trade name " Melinex ".[7] This was coated with a film of 80 : 20 nickel–chromium alloy to give a resistance about 150 Ω per square and a suitable strip of size 2 in. × $\frac{9}{32}$ in. was cut and sprayed with metal contacts. It was cemented to the beam, and its resistance at no load was found to be 1239.2 Ω. In Fig. 1 the values of resistance are

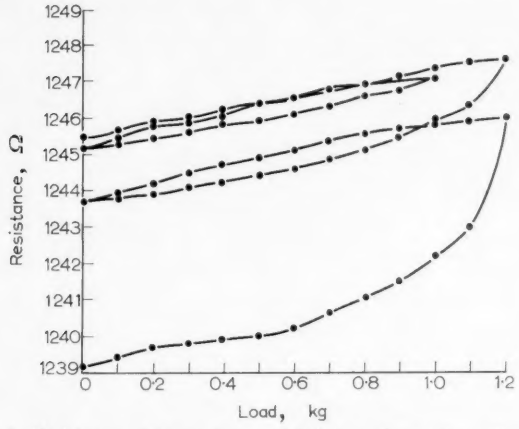

FIG. 1. Resistance changes in a nickel–chromium alloy film on " Melinex " cemented to a beam under stress.

plotted against the loading of the beam over three complete cycles. After the first cycle had been completed the resistance at no load had returned to 1243.7 Ω, corresponding to an increase of 4.5 Ω over the original value. After the second cycle, however, the increase in resistance was only 1.5 Ω over the same loading cycle to 1200 g. This seemed to be an ageing effect, caused either by permanent stretching of the " Melinex " or by permanent changes in the structure of the alloy film. The third cycle was carried out to a loading of 1000 g and the resistance increase was found to be only 0.3 Ω. The same specimen was cycled several times up to a loading of 600 g, after which the permanent changes in resistance could not be measured within the range of accuracy of the bridge. These readings have not been shown in Fig. 1 for the sake of clarity. Flexible resistors on " Melinex " therefore showed promise of effective use as strain gauges after ageing.

Fig. 2 shows the results of a test on a second specimen having a much lower resistance value. This was carried out to discover whether the plastic foil or the metal film were responsible for the ageing effects.

The specimen was first loaded up to 1200 g and kept under strain for 1 h. It was then unloaded and measurement of resistance taken over a period of 3 h at no load. During this time the resistance decreased first rapidly and then slowly, approximately exponentially, to a value midway between the initial and final resistance over the loading cycle. There was no evidence of any further significant changes in resistance after this value had been reached. These results show that the resistance increase in such a film

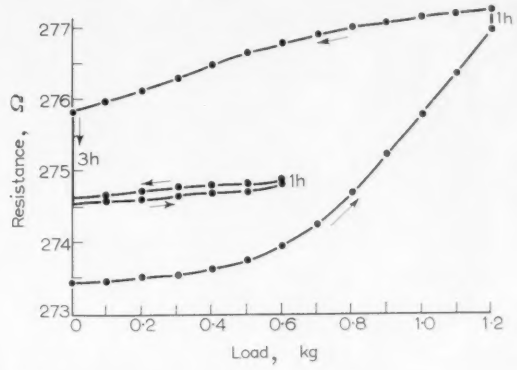

FIG. 2. Resistance changes in a nickel-chromium alloy film on " Melinex " cemented to a beam under stress, showing ageing effects.

is due partly to the elastic properties of the base material, which apparently takes several hours to regain its pre-stressed condition, and partly to dislocations in the film itself which are irreversible.

A second hysteresis was carried out on the same specimen and this is shown in Fig. 2. The load was increased to 600 g and left for 1 h, during which time there was a very small increase in resistance of 0.1 Ω. This change was outside the limit of accuracy of the bridge and could have been due to changes in the room temperature, since the bridge was not compensated. Upon returning to the no load conditions the total change in resistance was found to be only 0.2 Ω.

The second series of experiments was carried out to determine the relationship between the extension of the plastic film under stress and the resistance of the film deposited on it. The measurements on specimens of size 5 cm × 1 cm revealed a surprising result. Upon stretching the plastic support the resistance of the film was decreased for small extensions. After cycling the load, however, a small irreversible increase was observed at no load. This behaviour was observed up to loads at least half as great as those corresponding to the elastic limit of the foil with no exceptions.

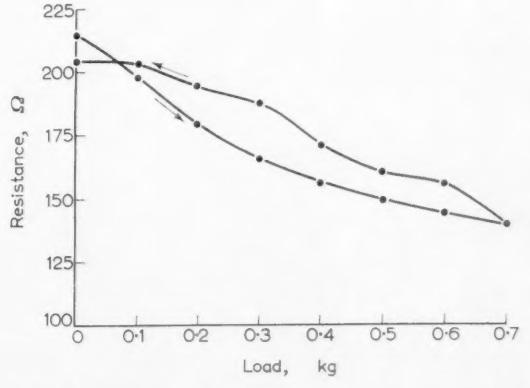

FIG. 3. Resistance changes in a stretched nickel–chromium alloy film on free " Melinex ".

Vol. 9 959/60

Fig. 3 shows the film resistance values obtained when the load was increased up to 1.2 kg on a specimen of foil size 5 cm × 1 cm × .025 mm and then decreased to zero.

The cathetometer measurements showed that within the range considered, the extension was approximately proportional to the load.

The decrease in resistance can only be explained by anisotropy of the plastic foil itself or, by assuming that under tension, there exists a lateral compression across the film which temporarily increases its conductivity by compacting the structure. It is well known that evaporated films, particularly when deposited on plastic substrates, invariably have a density less than that of the bulk material.

The latter series of experiments were not therefore helpful in determining the behaviour of a similar resistance coated plastic foil cemented to a metal surface under strain.

Conclusions

The first series of experiments showed that there is a definite possibility of using nickel–chromium coated polyester foil for measuring strain by resistance change. It would not be used for a direct reading of stress, but for comparative tests over short periods of time, since the absolute stability of the film has not been determined over a long period. The ageing of such a strain gauge will be carried out by loading the gauge for several hours to give a resistance change approximately two times the maximum value to be expected during its period of use.

Acknowledgements

Acknowledgements are made to Mr. A. S. D. Barrett, Technical Director of Edwards High Vacuum Ltd. for permission to publish this work, and to Mr. L. Holland, Head of the Vacuum Coating Research Laboratory, for many helpful discussions.

References

[1] R. H. Alderson and F. Ashworth ; *Brit. J. Appl. Phys.* **8**, 205 (1957).
[2] L. Holland and G. Siddall ; *Vacuum* **3**, 375 (1953).
[3] A. E. Ennos ; *Brit. J. Appl. Phys.* **8**, 113 (1957).
[4] G. Siddall and G. Smith ; *Brit. J. Appl. Phys.* **10** 35 (1959).
[5] W. R. Campbell ; *U.S. Nat. Bur. Stand. Circ.* No. 528, 131.
[6] T. B. Sanson ; *Elect. Rev.* 1 July, 3 (1949).
[7] " Melinex " polyester film for the Electrical Industry, *I.C.I. Tech. Publ.* I.S.408 (1955).

VO
9
1959

Letters to the Editor

A Simple Flexible Vacuum Joint

A SIMPLE design for a vacuum tight joint having a certain degree of flexibility is described. A number of such joints have been constructed for connecting tubes joining pieces of apparatus to an electron accelerator. Beams of high energy electrons pass through these tubes, which together with the accelerator chamber and some subsidiary vessels, are evacuated by continuous pumping. The flanges on the ends of these tubes must be connected in some slightly flexible manner so that their inclination to the tube axis is variable, and also to allow for a small adjustment of the effective length of the tube. These requirements are necessary to facilitate alignment of the whole apparatus; and have previously been realised by having a short length of metal bellows soldered between the tube and flange. As the bellows lacked the necessary mechanical strength for some purposes they had to be supported inside a universal-joint linkage.

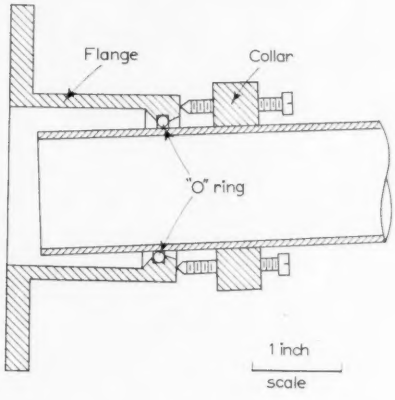

Fig. 1

The new type of vacuum joint which is shown in Fig. 1 appears to have several advantages over the bellows coupling, the principal asset being ease of construction. It can be seen that the joint consists simply of a separate flange of special shape and a cylindrical tube. The vacuum seal between these is accomplished by means of a soft rubber " O " ring which also gives the coupling its flexibility. The " O " ring fits round a polished section of the tube and is kept under compression in a groove which has an outside diameter 0.012 in. smaller than the natural outside diameter of the ring. The width of the groove is 0.005 in. less than the thickness of the ring, and its depth is sufficient to prevent the ring being pushed inwards along the tube by external atmospheric pressure.

In the present design, the tube can be tilted relative to the flange within a cone having a semi-angle of about 10°, which is more than sufficient for our purposes, and it can be kept at the desired angle by adjusting 3 screws in a collar which itself can be located anywhere along the length of the tube. Thus by sliding the tube in or out of the flange and adjusting the collar accordingly, the effective length of the tube can be altered. This design is versatile in so far as different lengths of tube can be used with the same pair of flanges; or interchangeable flanges can be made for fitting various alternative pieces of apparatus to the same tube. The present flanges and tubes are made of brass, but no doubt other metals would also be suitable.

Pressures in our electron accelerator are not very low; a normal working pressure being $\sim 10^{-4}$ mm Hg. Several joints have been in use at this pressure and have not leaked at a detectable rate.

I would like to thank Mr. R. Thornton for constructing several of these joints and Mr. R. J. Fisher for his co-operation.

P. I. P. KALMUS, B.SC., PH.D.

Dept of Physics,
University College London
(*Received* 16 *February* 1959)

A Shutter for Use Between Source and Work During Vacuum Evaporations

DURING the course of developing techniques for evaporation of metals and nonmetals on to plastic for use in alpha-scintillation screens, it was found necessary to prevent unwanted particles from reaching the work. These particles come from dirt on the evaporation source, from impurities within the source, and from residual dirt in the volume and on the surfaces of the bell jar assembly. The latter dirt is driven on to the work through collisions with the atoms or molecules from the evaporating source. Known methods of dealing with the problem, such as iris diaphragms and movable sectors, were found to be difficult to outgas, cumbersome, and unusable owing to space limitations where large area work was being coated.

The shutter arrangement shown schematically in Fig. 1 to a large extent prevents undesirable material from impinging on the work. A sheet of aluminum foil of 0.5 to 2 mil thickness and of ample area to screen the work is folded into accordion pleats, then stretched out nearly flat by moderate hand tension. An edge of the foil is bent over a straight length of 30 to 40 mil piano wire. The ends of the wire, which extend beyond the foil, are placed on the horizontal parts of two ramps. The source is heated to evaporation temperature and allowed to evaporate for a few seconds as convenient. This period serves to remove the particles on the surface of the source, to outgas or otherwise remove most of the impurities from the source, to sweep the ambient volume by gettering, and to prevent premature or excessive heating of the work. The current to the electromagnet is momentarily switched on in order to pull the steel piano wire and attached foil shutter off the ramps. The shutter collapses entirely below the line of sight between source and work if the work is on a short stand. As used, the collapsed shutter neither blocks ports nor shorts electrical leads. Normal evaporation on to the work then proceeds to completion.

Our ramps consist of notches filed in the ring used to support the dome heater. The iron rod of the electromagnet is held

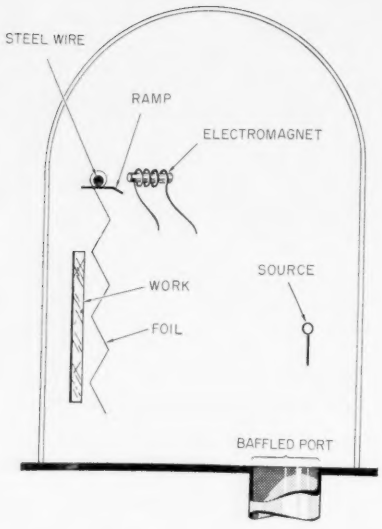

FIG. 1. Schematic cross-section of a shutter arrangement between evaporation source and work to be coated. Scaled to limits of users bell jar.

stationary by the dome mounting. The magnet wires are teflon insulated in order to minimize outgassing.

The system is simple and reusable. No cleaning of the shutter system is required between evaporation runs. Prefusing of the source in an earlier evacuation is eliminated with this as well as other shutter systems. The large number of pinholes usually present in the evaporated aluminum front surface of some plastic work was reduced to a negligible number by using this shutter. Likewise, the adhesion of the aluminum to the plastic was greatly improved. In addition, the horizontal arrangement of source and work has inherent advantages : the usual problems of shadowing of the work by holders when the source is below, and of oxide aggregates falling on to the work when the source is above, are eliminated. The same shutter can also be used when the source–work arrangement is vertical by allowing the shutter to fall over a restraining, stiff wire located on the side of the vertical source-work line opposite to the original wire support.

W. R. LAMB
F. A. RHOADS
P. S. APPLEBAUM

U.S. Naval Radiological Defense Laboratory, San Francisco 24, *Calif., U.S.A.*

(*Received* 23 *January* 1959)

Vo
9
1959

Conferences and Symposia

MILAN

International Symposium on Residual Gases in Electron Tubes and Related High Vacuum Systems

Patronage of Consiglio Nazionale Delle Ricerche (C.N.R.)

THE ITALIAN SOCIETY OF PHYSICS wish to announce that on the 23rd, 24th and 25th of September, 1959, an International Symposium on Residual Gases in Electron Tubes and related High Vacuum Systems will be held at COMO (25 miles from Milan), according to the following program.

MAIN SUBJECTS TO BE TREATED:

1 Residual gases and final vacuum :
   a) in transmitting tubes,
   b) in television tubes,
   c) in receiving tubes,
   d) in other high vacuum systems (accelerators and similars).

2 Method of measuring residual gases during the manufacture and life of tubes.

3 Origin of residual gases. Studies on the condition of internal surfaces of tubes and their gas adsorption and desorption. Effects caused by the surface alterations due to the gas adsorption.

4 Influence of residual gases on tube and cathode life.

5 Removal of gases during the production of electron tubes :
   a) research on pumping systems,
   b) research on the influence of pumping methods on residual gases.

6 Removal of gases during the production and during the life of the tubes :
   a) the getter in transmitting tubes,
   b) the getter in receiving tubes,
   c) the getter in cathode ray tubes,
   d) the non flashing getters,
   e) the getter pumps.

7 Getter activity for various gases and gas mixtures : pertinent parameters.

8 Techniques for measuring getter activity.

COMMUNICATIONS :

Proposals for Symposium communications should be sent in the first place as a summary in English and in French of about 40 typewritten lines and addressed to the Secretariat of the Symposium not later than 31st August, 1959.
In order those attending may hear all communications, it is intended to limit the number of communications so that they can be presented in two sessions a day.
The sessions will be held in the building of the Provincial Administration of Como.

OFFICIAL LANGUAGES :

Communications can be delivered in Italian, German, French or preferably in English.

PUBLICATION OF THE PROCEEDINGS :

The Symposium proceedings will be published in a collected form which will be sold to all participants and to the members of the Societá Italiana di Fisica with a 50 per cent reduction of the general selling price.

VISITS :

Visits to electronic industries of the Milan Province and also a trip on the Lake of Como are planned.

ACCOMMODATION :

The Secretariat of the Symposium, through the touring offices, will book rooms in the hotels according to the requests which will be addressed to the Secretariat not later than 30th June 1959.

PARTICIPATION :

Any one concerned with this Symposium and wishing to participate should apply to the Secretariat, c/o Societá Italiana di Fisica, 50, Via Saldini, Milan, Italy, Tel. 292.178, for a registration card : the Symposium fee is $10.00 or Italian lire 6250.—to be paid to the Symposium Secretariat. Full details of the Symposium will be sent to all those attending in due course.

Vol.
9
959/60

LONDON

Symposium on Current Developments in the Production of High Vacua

On 17 April the INSTITUTE OF PHYSICS held a Symposium on " Current Developments in the Production of High Vacua " at the Royal Society of Tropical Medicine and Hygiene. The great interest shown in the symposium was indicated by the overcrowded hall. This large attendance included many well-known vacuum workers from various countries. The following is a list of the contributions presented :

General principles of chemical and ionic pumping in kinetic vacuum systems. R. N. BLOOMER, *Siemens Edison Swan Ltd., Harlow, Essex.*

The design and use of getter-ion pumps. L. HOLLAND, *Edwards High Vacuum Ltd., Crawley, Sussex.*

The use of getter-ion pumps in the maintenance of high vacua in electron tubes. N. W. ROBINSON, *Mullard Research Laboratories, Salfords, Surrey.*

Some recent results in the development of getter-ion pumps. R. L. JEPSEN, *Varian Associates, Palo Alto, California.*

The dual sorption modes of Bayard-Alpert ionization gauges. G. CARTER, *University of Liverpool.*

The sorption by titanium of oxygen and nitrogen at low pressures. L. G. CARPENTER and W. N. MAIR, *Royal Aircraft Establishment, Farnborough, Hampshire.*

Problems in the production of high vacua in large equipment. J. BLEARS, *Metropolitan-Vickers Electrical Co. Ltd., Urmston, Manchester.*

The vacuum system of the 7 GeV accelerator. S. H. CROSS, *Atomic Energy Research Establishment, Harwell, Berkshire.*

Characteristics of some pumps and experimental results. B. D. POWER, *Edwards High Vacuum Ltd., Crawley, Sussex.*

Some results of vacuum studies relating to large machines. R. S. BARTON, *Atomic Energy Research Establishment, Harwell, Berkshire.*

The role of the omegatron in diffusion pump development. N. T. GALLAGHER, *Leybolds Vacuum Sales Ltd., London.*

The application of miniature mass spectrometers for vacuum leak detection and analysis. A. O. EDMUNDS, *20th Century Electronics Ltd., Croydon, Surrey.*

The study of high vacua with a small mass spectrometer. B. N. GREEN, *Metropolitan-Vickers Electrical Co. Ltd., Trafford Park, Manchester.*

The influence of evaporated metal films on the residual gases in glass envelopes. N. W. ROBINSON, *Mullard Research Laboratories, Salfords, Surrey.*

PARIS

Journées du Vide

The SOCIÉTÉ FRANÇAISE DES INGÉNIEURS ET TECHNICIENS DU VIDE held a most successful conference in Paris on 23rd and 24th April. It was attended by over 200 people including well-known vacuum workers from many countries which indicated the great interest in ultra-high vacuum today. The following is a list of the contributions presented :

Rationalisation et Automatisation de la Lyophilisation des Denrées Alimentaires. K. H. NEUMANN (*Leybold's-Cologne*).

Construction Nouvelle des Pompes à Vide Mécaniques. A. LORENZ (*W. C. Heraeus GmbH, Hanau*).

Mesure de Débit des Pompes. A. VENEMA (*Philips Research Laboratories, Eindhoven*).

Vanne de Sécurité pour les Installations de Vide. R. SERVRANCKX and R. LEYNIERS (*Institut Universitaire des Sciences Nucléaires, Bruxelles*).

Jauge Radiométrique pour Basses Pressions. Mme. J. BAILLEUL-LANGLAIS (*La Radiotechnique, Suresnes*).

Etude d'un Manomètre à Thermistances. D. A. DEGRAS and P. ANDRIEUX (*Compagnie Générale de Radiologie, Paris*).

Mesures de Dégazage des Materiaux. M. R. P. HENRY (*Société de Recherches Techniques & Industrielles, La Corneuve*).

Le Système de Vide du Grand Synchrotron à Protons de Saclay. F. PREVOT and R. LE QUINIO (*Centre d'Etudes Nucléaires de Saclay*).

Les Problèmes de Vide dans la Technique de Séparation Isotopique de l'Uranium. M. R. DORE (*Société de Recherches Techniques & Industrielles, La Courneuve*).

Réflexions sur l'Ultra-Vide. M. J. SCHWEITZER (*Centre d'Etudes Nucléaires de Saclay*).

Applications de l'Ultra-Vide aux Installations de Fusion Thermonucléaire. M. G. MONGODIN (*Laboratoire des Basses Pressions, Argenteuil*).

Pompe Ionique à Adsorption. M. D. A. DEGRAS (*Compagnie Générale de Radiologie, Paris*).

Expériences d'Ultra-Vide sur des Appareils Thermonucléaires. M. Z. SLEDZIEWSI (*Centre d'Etudes Nucléaires de Saclay*).

Un Modèle de Pompe Ionique à Adsorption et ses Applications. R. L. JEPSEN (*Varian Associates, Palo Alto, Calif.*).

Indicateur d'Ultra-Vide et Vide Limite dans les Appareils entièrement Métalliques. K. G. MULLER (*W. C. Heraeus GmbH, Hanau*).

Etude Expérimentale des Joints Métalliques Etuvables pour Ultra-Vide. J. SCHWEITZER and J. BOULLOUD (*Centre d'Etudes Nucléaires de Saclay*).

Pompes Getters and Technique de l'Ultra-Vide. L. HOLLAND (*Société Edwards, Crawley, Sussex*).

Utilisation des Pompes à Huile pour l'Obtention des très Basses Pressions. E. A. TRENDELENBURG (*Geratebau-Anstalt, Balzers*).

Pompage de Tubes Electroniques à l'Aide de Pompes au Titane. H. HUBER, A. SHROFF and Mme. M. WARNECKE (*C.S.F., CEPEC, Corbeville*).

A summary of the proceedings will be published in a future issue of Vacuum.

The full papers presented at this Symposium will appear in Le Vide.

NEW YORK

Vacuum Metallurgy Conference

The NEW YORK UNIVERSITY have announced that a conference on Vacuum Metallurgy is to be held on 1-3 June under the chairmanship of Dr. R. F. BUNSHAH.

The applications of vacuum technology in the extraction, melting, fabrication, and heat treatment of metals are growing at a very rapid pace. The objective of this conference is to present new information based on research on advanced engineering developments in vacuum metallurgy as, for example, the several papers on electron beam melting and welding which are being presented.

The following is a list of the contributions.

VACUUM ARC MELTING AND CASTING

Arc Melting Procedures for Refractory Metals. MAURICE L. TORTI (*National Research Corporation*).

Vo 9 1959

Consolidation and Purification of Tungsten in High Vacuum. R. P. MORGAN and J. C. SCHOTTMILLER (*Union Carbide Metals Company*).

Vacuum Arc-Melting Study on Zircaloy-2. J. H. HART (*Westinghouse Electric Corporation*).

Vacuum Arc Ingot Grain Refinement. D. R. CARNAHAN, J. H. KELLEY and L. M. BIANCHI (*Westinghouse Electric Corporation*).

Segregation in Arc Melting of U-Th and U-Zr Alloys. PHILLIP CORZINE (*Nuclear Metals, Inc.*).

User Experience with Consumable Electrode Vacuum Arc Melting Furnaces in the United Kingdom Titanium Industry. KURT DEUTSCH (*Imperial Chemical Industries*).

The Skull Casting of Refractory Metals. L. M. BIANCHI (*Westinghouse Electric Corporation*).

Vacuum Melting Equipment for the Investment Casting Industry. GEORGE F. BARBER (*NRC Equipment Corporation*).

The Effect of Space Environment of the Properties of Materials. WOLFGANG H. STEURER (*Convair Division of the General Dynamics Corporation*).

VACUUM INDUCTION MELTING, SPECIAL PROCESSES, DEGASSING AND ELECTRON BEAM TECHNIQUES

Deoxidation of Pure Iron by Vacuum Induction Melting. P. P. TURILLON and E. S. MACHLIN (*Kelsey-Hayes Company*).

Development of Melting Procedures for Special Alloys used in Commercial Applications. MARLIN S. WALMER (*Hamilton Watch Company*).

A Continuous Vacuum and Inert Gas Process Apparatus. GEORGE A. PAGONIS, JAMES H. ANDERSON and RALPH PARKMAN (*Light Metals Research Laboratories, Inc.*).

Variations of Vacuum Degassing. K. C. TAYLOR (*F. J. Stokes Corporation*).

Experiences with Ladle Degassing. C. W. FINKL (*A. Finkl & Sons Company*).

New Developments in Electron Beam Melting. HUGH R. SMITH (*Temescal Metallurgical Corporation*).

High-Vacuum Melting of Beryllium by Electron Bombardment. C. O. MATTHEWS (*Lockheed Aircraft Corporation*).

Electron Gun Melting of Titanium and Titanium Alloys. C. B. DITTMAR and S. ABKOWITZ (*Mallory-Sharon Metals Corporation*).

The Purification of Tungsten by Electron Bombardment Floating Zone Melting. WALTER R. WITZKE (*National Aeronautics & Space Administration*).

HEAT TREATMENT, BRAZING, WELDING, EVALUATION AND USES

Vacuum Brazing and Heat Treatment. R. F. GUNOW (*Vac-Hyd Processing Corporation*).

Vacuum : A Must in Refractory Alloys Development. W. A. HENDRICKS and E. G. HUSCHKE, JR. (*General Electric Company*).

Electron Beam Welding. MARSBED HABLANIAN (*NRC Equipment Corporation*).

Design of Electron Beam Welders for Production Service. THEODORE CRANE (*High Vacuum Equipment & Kinetics Corporation*).

Welding of the Active Metals in Vacuum and Inert Gas Chambers. JOHN HUMINIK and PAUL E. RITT (*Melpar, Inc.*).

Quality Aspects and Engineering Properties of Vacuum Melted Steels and Super Alloys. A. M. AKSOY and R. C. BUEHL (*Crucible Steel Company of America*).

The Use of Vacuum Metallurgy and Vacuum Cast Metals in Electron Vacuum Devices. DAVID LICHTMAN (*Sperry Gyroscope Company*).

The Role of Vacuum Metallurgy in Nuclear Fuel Production. J. H. DURANT (*Engelhard Industries, Inc.*).

New Trends in Vacuum Coating. MORTON GILBERT (*F. J. Stokes Corporation*).

A summary of the proceedings of this conference will be included in a future issue of Vacuum.

Vol. 9 959/60

Classified Abstracts

Editorial Note

Because very few libraries subscribe to all publications which occasionally print articles of interest to vacuum scientists and engineers, it is desirable that this journal should provide a classified abstract section which covers as far as possible all articles which have appeared in the literature during the preceding months. It is not intended that the abstracts should replace the need for the individual to go and read the original article. What is required is that the reader be aware of what has appeared and either because of his knowledge of the topic, or the author, be able to decide whether it is worthwhile spending the time and effort to read the original.

The first meeting of the Board of Editors held during the Namur Conference decided that the first essential of an abstracting service was speed in publishing, and with this in mind the first change in the abstracting service, which begins with this issue, is the beginning of an accelerated system by title only. However, following the editorial meeting at Namur when the desirability of including fuller abstracts for more important references was considered, the appointed abstractors have been asked to give two further grades of fuller abstracts ; one giving the author's abstract and the other a specially prepared abstract for a very important reference. It is also the intention of the Editors to publish annually a complete cross-reference index of every abstract that has appeared in the six bi-monthly numbers. The abstracts appearing in Volume 9, No. 1 are all concerned with the First International Congress of Vacuum Techniques held at Namur, June 1958, but the new system is fully established in this issue. This abstracting service has been set up covering most of the important journals of the world, but the editorial groups in each country are co-operating to ensure that the literature of their country is being adequately covered.

In order to improve the abstracting service previously used in *Vacuum*, a change has been made in the classification system, based largely on suggestions from Dr. B. B. Dayton, one of our American editors, and modified as a result of circulating his suggestions to the other editors. The new classification system precedes the abstracts in this issue.

A complete list of the journals abstracted and the appointed abstractors will be included in the final issue of each volume. However, it has been considered desirable to issue these lists in the current number so that readers will know the literature that is being abstracted. Suggestions for additional coverage will be welcomed by the Editors.

VO
9
1959

Classification System

I. General Vacuum Science and Engineering

(Books, review articles, bibliographies, summaries, general techniques, articles on basic vacuum physics)

10. Vacuum Technology

11. Production of Low Pressures

12. Measurement of Low Pressures

13. Vacuum Applications

14. Kinetic Theory of Gases (transport phenomena, diffusion through vapors, molecular flow of gases, etc.)

15. Fluid Dynamics (turbulent and viscous flow of gases, flow through nozzles, boundary layer flow, etc.)

16. Gases and Solids (sorption, diffusion through solids, permeation, etc.)

17. Thermodynamics (compression, temperature, reactions, vaporization, dissociation, vapor pressure, cryogenics, etc.)

18. Gaseous Electronics (ionization, discharges, plasma, emission, etc.)

19. Radiation (light, heat, X-rays, microwave radiation, etc.)

II. Vacuum Apparatus and Auxiliaries

(Design, testing, operation, performance and techniques of using individual apparatus for the production, measurement, and control of low pressures)

20. Pumping Systems (plant)

21. Pumps and Pump Fluids (mechanical pumps, vapor pumps, getter-ion pumps, cryopumps, etc.)

22. Gauges (including mass spectrometer types)

23. Plumbing (joints, pipe, gaskets, fittings, flanges, glass-to-metal seals, shaft seals, etc.)

24. Valves (stopcocks, variable leaks, gas introducing devices, needle valves, etc.)

25. Baffles, Traps, and Refrigeration Equipment

26. Automatic Protective and Control Equipment (cut-offs, switches, liquid level controls, manostats, etc.)

27. Leak Detectors and Leak Detection

28. Heating Equipment (ovens, resistance heating units, induction heating units, etc.)

29. Miscellaneous

III. Vacuum Applications

30. Evaporation and Sputtering (to form solid coatings)

31. Evacuation and Sealing (electronic tubes, switches, lamps, vacuum insulation, gas-filled devices)

32. Nucleonics (particle accelerators, counters, plasma machines, isotope separation, etc.)

33. General Physics and Electronics (electron tube physics, electron microscopy, diffraction camera, field emission microscope, spectroscopes, X-ray tubes, low temperature physics, etc.)

34. High Altitude and Space Technology (test chambers, ion propulsion, etc.)

35. Impregnation and Potting

36. Drying, Degassing and Concentration (including freeze-drying, glass processing, evaporation of solvents, etc.)

37. Metallurgy, Inorganic Chemistry, Analytical Chemistry (production and analysis of metals and inorganic chemicals, melting, casting, annealing, sintering, degassing in molten state, vacuum fusion gas analysis, mass spectrometer analysis of inorganic materials, etc.)

38. Distillation, Organic Chemistry, Isotopic Gas Analysis
39. Miscellaneous Applications (fumigation, etching, forming, surface area measurement, etc.)

IV. Materials and Techniques Used in Vacuum Technology

(Properties, composition, purification and use of materials ; fabrication and processing techniques)

40. Gases and Vapors
41. Metals and Alloys (including mercury)
42. Glass and Ceramics
43. Plastics and Elastomers
44. Waxes, Lubricants, Cements, Lacquers, Paints, Oils
45. Soldering, Welding, Brazing
46. Glass Blowing, Glass-to-metal and Ceramic-to-metal Sealing Techniques
47. Outgassing Data, Vapor Pressure Data Gettering Data
48. Heating, Refrigeration, Ultrasonics, Centrifuging
49. Miscellaneous Materials and Techniques

V. Basic Science and Engineering

(For cross reference purposes)

50. Mathematics
51. Physics, Astronomy, Geophysics
52. Physical Chemistry
53. Metallurgy, Ceramics, Inorganic Chemistry
54. Biology, Biochemistry, Pharmaceutics, Toxicology, Organic Chemistry
55. Chemical Engineering
56. Electrical Engineering, Electronic Circuits
57. Mechanical Engineering
58. Nucleonics
59. Miscellaneous

Vol.
9
959/60

Abstracts

General Vacuum Science and Engineering

10. Vacuum Technology

10 : 27 : 57

1. High Vacuum Practice.
Gt. Britain. Summary of a paper presented to the Institution of Mechanical Engineers dealing mainly with methods of construction of vacuum vessels and leak detection.
Brit. Chem. Engng., **3**, 26–28, 1958.

11. Production of Low Pressures

11 : 21

2. Sur le pompage des tubes à vide.
France. A review of known methods of pumping modern ultra-high frequency valves which, because of their complex structure, are liable to leaks and to gas occlusions. Pt. 1 deals with criteria for pumping against small real or virtual leaks. Pt. 2 deals with the various sources of gas. Pt. 3 deals with the titanium pump for maintaining a satisfactory vacuum in operation. The present article comprises only Pt. 1.
A. H. W. B.
H. Huber and M. Warnecke, *Annales de Radioélectricité*, **13**, No. 53, 230–252, July 1958.

11 : 21

3. Means for Attaining Vacua Without the Use of Pump Fluids.
I. Ames, R. L. Christensen and J. Teale, *Rev. Sci. Instrum.*, **29**, No. 8, 736–737, Aug. 1958.

11 : 21

4. Ionic Vacuum Pumps.
United States. The development of ionic vacuum pumping technique is reviewed. Some new pumps, instead of removing the particles of gas, simply transfer them to the solid phase.
G. M. L.
Lewis D. Hall, *Science*, **128**, 279–285, 1958 (Varian Associates, Palo Alto, Calif., U.S.A.).

13. Vacuum Applications

13 : 54

5. Hypothermia.
Leading article ; a survey with brief bibliography.
Lancet, **I**, 675–676, 1958.

14. Kinetic Theory of Gases

14

6. Kinetic Theory of the Flow of Gas Through a Cylindrical Tube.
O. German, *Soviet Phys. JETP*, **34**, No. 6, 1016–1019, Dec. 1958.

14 : 52

7. Note on Diffusive Separation of Gas Mixtures in Flow Fields.
United States. This paper discusses the effect of pressure-diffusion flux upon the concentration distribution of gas mixtures in flow fields. The equation of concentration is formulated for a binary gas mixture in which the mass ratio is large and the concentration of the lighter gas is very-small. An asymptotic solution to the steady-state equation of concentration is given for an irrotational and incompressible flow. As an illustration, the diffusive separation (i.e. deviation from the original homogeneous state) of a mixture of helium and nitrogen along streamlines at the entrance to a long straight channel is calculated. It is assumed that the pressure inside the channel is 90 per cent of that in the free stream, and that the diffusion coefficient of the mixture corresponds with the atmospheric conditions at 80-km altitude. (Author)
V. C. Liu, *J. Appl. Phys.*, **29**, 1188–1189, Aug., 1958.

15. Fluid Dynamics

15 : 21

8. Mean Gas Flow Velocity and Gas Flow Rate in Jets of High Vacuum Pumps.
M. G. Manov, *Sov. Phys.-Tech. Phys.*, **3**, No. 2, 289–296, Feb. 1958.
Translation of *Journ. of Tech. Phys. of the USSR*, V, 28, No. 2.

15 : 21

9. Velocity and Temperature Discontinuities Near the Walls of a Body Around Which Rarified Gases Flow with Transonic Velocities.
M. F. Shirokov, *Soviet Phys.*, **V**, 34, No. 6, 1029–1032, Dec. 1958.

15

10. The design, instrumentation and operation of the Utia low density wind tunnel.
K. R. Enkenhus, Utia Rpt. No. 44, June 1957, Inst of Aerophysics, University of Toronto, Canada.

16. Gases and Solids

16 : 22

11. Adsorption of Oxygen and Carbon Monoxide on Tungsten.
United States. The adsorption of oxygen, carbon monoxide, and nitrogen on a tungsten ribbon filament at 300°K has been measured by means of the flash filament technique. An omegatron rf mass spectrometer has been used to measure pressure. It is shown that oxygen pressures cannot be measured satistorily with ionization gauges of the hot-tungsten-filament type. The total amounts of gases adsorbed by tungsten are 5.7×10^{14} mol./cm^2 for O_2, 5.8×10^{14} for CO, and 1.8×10^{14} for N_2. The sticking probabilities of these gases on the uncovered surface are 0.65 for O_2, 0.62 for CO, and 0.42 for N_2. All of the CO and N desorb from the heated filament as the gases CO and N_2 ; less than 1 per cent. of the oxygen desorbs as O_2. The filament pumps O at a rate of 9 l./cm^2/sec at temperatures above 2000°K. (Author)
R. E. Schlier, *J. Appl. Phys.*, **29** 1162–1168, Aug. 1958.

16 : 33

12. Work Function and Sorption Properties of Silicon Crystals.
United States. The work functions of silicon single crystals have been obtained by measuring the contact potential differences between the crystals and a gold reference whose work function was measured by the Fowler method. The measurements were carried out in high vacuum ($p < 10^{-9}$ mm Hg). For non-floating-zone silicon, the work function was higher for samples which were radiation quenched from 990 °C than it was for samples which were annealed at 500 °C. This effect was not observed for floating-zone material and was presumably a function of occluded oxygen. The work functions for the different faces after ion-bombardment cleaning were in the sequence (100)> (110)> (111). The values after quenching were : (100), 4.92 ev ; (110), 4.89 ev ; (111), 4.77 ev. The values after annealing were :

Vo 9 1959

(100), 4.82 ev ; (110), 4.70 ev ; (111), 4.67 ev. The work function of the (111) face of a 2000-ohm-cm, *p*-type, floating-zone sample was 4.73 ev after quenching or annealing. Changes in both surface and volume properties were observed when silicon was heated above 1000 °C in contact with quartz. Oxygen exposures of 5×10^{-5} mm Hg min resulted in work function increases which were larger on the annealed surfaces than on the quenched ones. This was observed for both floating-zone and oxygen-doped material and is therefore a property of the silicon itself. Photoelectric evidence indicated a diffusion of oxygen into the silicon (1) when silicon was heated in oxygen, (2) when silicon was heated at 990 °C in high vacuum after O_2 adsorption, and (3) when silicon with residual surface films from chemical etching was heated at 990 °C prior to ion bombardment. Hydrogen exposures of 7.5×10^{-4} mm Hg min resulted in work-function decreases only in the presence of a heated filament. Nitrogen exposures of 4×10^{-6} mm Hg min resulted in no work-function changes. Heating silicon in high vacuum at 990 °C for about 100 hr developed thermal-etch patterns which were rectangular on the (100) face, hexagonal on the (110) face, and triangular on the (111) face. Heating at 1080 °C for 24 hr caused further etching which developed the same triangular patterns on the (111) face but left the (100) and (110) faces with a sandblasted appearance. (Author)

J. A. Dillon, Jr. and H. E. Farnsworth, *J. Appl. Phys.*, **29**, 1195–1202, Aug. 1958.

16 : 18 : 51

13. Ion Induced Re-emission of Noble Gases from a Nickel Surface.

United States. Each of the noble gases, He, Ne, A, and Kr, has been ionically pumped with an energy of about 100 ev into a nickel target and has been subsequently released by a similar bombardment using a different noble gas. A mass spectrometer permitted the measurement of both the re-emission of the trapped atoms and the trapping of the bombarding particles. The re-emission mechanism is described in terms of a simple model which assumes that the trapped atoms are released by the bombarding particles through a mechanism of sputtering of either the target material or the trapped gas or a combination of both. The experimental results are in agreement with the model. A direct replacement of a trapped atom from its trapping site by a bombarding particle is shown to be a relatively unimportant factor in the re-emission process. Measurements of the re-emission rates of the trapped atoms have yielded information concerning the depth distribution of the trapped atoms in the nickel target. In particular, saturation of the depth distribution has been observed for Ne, A, and Kr at concentrations below one equivalent monolayer while He showed no such effects at the highest concentrations used, which corresponded to approximately 15 equivalent monolayers. (Author)

J. H. Carmichael and E. A. Trendelenburg, *J. Appl. Phys.*, **29**, 1570–1577, Nov. 1958.

16 : 33

14. Using Cathode Resistance to Measure Adsorption of Gases on Metals.

Gt. Britain. The adsorption of nitrogen and oxygen on tungsten and molybdenum was studied by measuring the contact resistance between wires of these materials. The wires were cleaned by flashing at high temperatures *in vacuo* and then subjected to the adsorption of the desired gas. The initial period of fast adsorption gave surface resistivities of about 4×10^{-10} Ω-cm² or a layer thickness of circa 1.6 Å. Oxygen, but not nitrogen, could be partially removed by pumping at room temperature. The rate of migration of oxygen into the region between closed contacts is much lower than previously reported in similar experiments. A. H. W. B.

P. Kisliuck, *Bell System Tech. J.*, **37**, No. 4, 925, 1958.

16

15. Adsorption of Water Vapour on Lead Borosilicate Glass in Vacuum.

Japan. The adsorption of water vapour on lead borosilicate glass was studied in the pressure region 10^{-5} to 10^{-6} mm Hg, using the modified flashing technique. The adsorption is composed of at least two parts, physical adsorption and activated adsorption. The amount of the physical adsorption at 1×10^{-6} mm Hg was, for the temperature range 0 to 50 °C, 0.1 to 0.4 per cent of a monolayer, and the heat of adsorption was 11 kcal/mol. The activation energy of adsorption for the activated adsorption was ca. 9 kcal/mol, and the activation energy of desorption was in the range 13 to 40 kcal/mol (in the temperature range 550 to 650 °C). (Author)

Y. Tuzi and H. Okamoto, *J. Phys. Soc. Japan*, **13**, No. 8, 960, 1958.

16 : 30

16. Dissociative Adsorption of Methane and Ethane on Evaporated Metal Films.

P. G. Wright, P. G. Ashmore and C. Kemball, *Trans. Faraday Soc.*, **54**, Part 11, 1692–1702, Nov. 1958.

16 : 51

17. Evidence for Permeability Minima in Low Pressure Gas Flow Through Porous Media.

D. M. Grove and M. G. Ford, *Nature*, **182** (Letter), Issue No. 4641, 999–1000, 11 Oct. 1958.

16 : 17 : 34

18. Theoretical Analysis of Ultra-High Vacuum Condensers.

William R. Mickelsen and J. Howard Childs, *Rev. Sci. Instrum.*, **29**, 871–873, Oct. 1958.

16 : 53

19. Some Observations Regarding the Present Status of Measurements of the Diffusion Coefficients of Hydrogen in Iron and Mild Steel.

United States.

Letter by R. C. Frank, *J. Appl. Phys.*, **29**, 1262–1263, Sept. 1958.

16 : 52

20. Diffusion of Hydrogen in Palladium.

The rate of flow of hydrogen through palladium has been measured in a range of temperatures 200 °C to 600 °C over the pressure range 10 to 76 cm Hg. The flow rate is found insensitive to palladium wall thickness. The data do not seem to be explainable in terms of existing theory. A. G.

P. A. Silberg and C. H. Bachman, *J. Chem. Phys.*, **29**, 777, October, 1958.

16 : 40 : 52

21. Properties of Hydrogen Chemisorbed on Tungsten.

The sticking probability of hydrogen on a single crystal tungsten ribbon was measured as a function of the number of adsorbed atoms. The work function of the same ribbon was measured by a photoelectric technique. The results indicate that during the initial fast chemisorption characterized by an almost constant sticking probability of approximately 0.2 the work function rose from 4.54 ev for the clean surface to a maximum value of 5.0 ev for the covered surface. The maximum coverage at room temperature was $(7.5 \pm 1.0) \times 10^{14}$ cm^{-2}. Evidence for two states of adsorption is presented and the experimental techniques used in these and earlier experiments, are described in some detail. A. G.

Joseph Eisinger, *J. Chem. Phys.* **29**. 1154, November, 1958.

Vol. 9 959/60

16

22. Evidence for Permeability Minima in Low-Pressure Gas Flow through Porous Media.
United Kingdom.
D. M. Grove and M. G. Ford, *Nature*, **182**, No. 4641, 999, 11th Oct. 1958.

17. Thermodynamics

17 : 51

23. A Simple, Automatic, High-temperature Thermal Analysis Apparatus.
Gt. Britain. The sample, in a chamber which may be evacuated to better than 10^{-5} mm Hg at 1000 °C, is heated by a molybdenum element and the thermal arrests are indicated by the differential method. By placing the sample in direct contact with the thermocouple hot-junction, solid state phase changes may be detected in samples as small as 0.3 g. Alternatively, samples of 20–80 g may be contained in crucibles and, using the arrangement, thermal arrests have been detected at temperatures up to 1550 °C. The furnace is surrounded by a stainless steel bell-jar, sealed by a neoprene ring to a base-plate and pumped by a 4 in. oil diffusion pump. M. D. A.

S. J. Lloyd and J. R. Murray, *J. Sci. Instrum.*, **35**, 252–254, July, 1958.

17 : 25 : 26

24. Precision Liquid Nitrogen Trap Level Controller.
George F. Wells, *Rev. Sci. Instrum.*, **29**, 893–895, Oct., 1958.

17 : 52

25. Heat of Formation of BaC_2.
United States. The heat of formation of BaC_2 was determined by measuring the Ba pressure above $BaC_2 + C$ using the Knudsen effusion method. The heat of formation of BaC_2 from the elements is $\Delta Hf^\circ_{298} = -12.1 \pm 4$ kcal/mol. (Author)

Michael Hoch, *J. Appl. Phys.*, **29**, 1588–1589, Nov. 1958.

17 : 16 : 34

Theoretical Analysis of Ultra-High Vacuum Condensers. See Abstr. 18.

18. Gaseous Electronics

18

26. Mechanism of Cataphoretic Segregation in Inert Gas Glow Discharges.
United States. The collection of a minority gas species at the cathode in a glow discharge, termed cataphoresis, appears not to have been completely successfully explained. Observation indicates that in all cases, the minority gas segregated at the cathode, must be capable of being very effectively ionized by the vehicular gas. The recent discovery of the effective creation of ion complexes such as $NeHe^+$ and NeA^+ in pressure dependent reactions above some mm Hg pressure by Oskam, the independent direct observation of these ions and the production of ions such as HeH^+, NeH^+, and AH^+ with 1 per cent H_2 in the inert gas by Weimer, using the effusion mass spectrometer of Pahl, render a basis for the extension of the Druyvesteyn theory developed for metallic ions in inert gas to the general process, aid in the explanation of the Hg–Xe anomaly observed by Kenty, and indicate certain needed corrections which are acting to make the process more efficient. (Author)

L. B. Loeb, *J. Appl. Phys.*, **29**, 1369–1371, Sept. 1958.

18 : 51

27. Formation of Plasma Structure in a Developing Discharge.
A. A. Zaitzev and V. E. Mitsuk, *Soviet Phys. Doklady*, **3**, No. 2, 311. Original Russian Vol. 119, Nos. 1–6, 469.

18 : 51

28. Microwave Investigation of Disintegrating Gaseous Discharge Plasmas.
Gt. Britain. A very detailed account of measurements made on plasmas contained in resonant cavities, the detailed theory of such measurements and results on the afterglow of rare gas mixtures in which the minor constituent has a lower ionization potential than the major constituent. Hypotheses relating to the processes which occur are included. A. H. W. B.

H. J. Oskam, *Philips Res. Rpts.*, **13**, 335–400, 1958; *Philips Res. Rpts.*, **13**, 401–457, 1958.

18 : 56

29. Microwave Method for Measuring the Probability of Elastic Collision of Electrons in a Gas.
United States. A plasma in a d.c. magnetic field has a transverse conductivity component whose reactive part depends, as to both magnitude and sign, on the strength of the magnetic field. By measuring the value of magnetic field that is necessary for bringing this reactive part to zero—and hence removing any resonant-frequency shifts of a TE_{011} mode of cylindrical cavity containing the plasma-determination of the probability of elastic collision of electrons in helium is obtained as a check on the method. The value of $P_m = 20 \pm 1$ cm^{-1} mm Hg^{-1} for the electrons at room temperature thus obtained agrees substantially with the value obtained by previous workers. Sources of error in the measurement are discussed. (Author)

Jay L. Hirshfield and Sanborn C. Brown, *J. Appl. Phys.*, **29**, 1749–1752, Dec. 1958.

18 : 51

30. Impedance and Recovery Time of Glow Discharges in Mixtures of Rare Gases.
United States.
Letter by G. Ahsmann and H. J. Oskam, *J. Appl. Phys.*, **29**, 1768, Dec. 1958.

18 : 51

31. Anode Region in a Low Pressure Gas Discharge.
B. N. Kliarfeld and N. A. Neretina, *Soviet Phys.-Tech. Phys.*, **3**, No. 2, 271, Feb., 1958.
Translation of *Journ. of Tech. Phys. of the USSR*, **28**, No. 2.

18 : 33 : 51

32. The Influence of the Electrode Temperature on the Electrical Breakdown Strength of a Vacuum Gap.
I. N. Slivkov, *Soviet Phys.-Tech. Phys.*, **3**, No. 4, 708, Apr. 1958.
Translation of *Journ. of Tech. Phys. of the USSR*, **28**, No. 4.

18 : 33 : 51

33. Secondary Positive Ion Emission from Metal Surfaces.
United States. Secondary positive ions ejected from surfaces of Mo, Ta, and Pt under bombardment by inert gas ions of low energy (< 1000 ev) have been studied in high vacuum ($\leq 10^{-8}$ mm Hg of background gases) using a 60° sector field mass spectrometer with a 6 in. radius of curvature, the object being to explore this as a technique for investigating solid surfaces in general. Ion species characteristic of the base metal, of surface compounds, and of a few bulk impurities were found. Quantitative analyses based on abundance ratios of the ions are unreliable, however owing to the enormous and essentially unknown differences in ionization efficiencies for the various species. Application of the technique to the investigation of surface kinetics seems highly promising, and as an illustration certain observations on the formation of PtO_3 on a Pt surface and its desorption at high temperatures are presented. Another possible application is to the study of sputtering, although some of the properties of secondary ions are shown to be quite different from those of sputtered particles in general. The secondary ions characteristic of the base metal comprise only a small fraction (0.01 per cent for Pt) of the total sputtering yield, are principally singly charged and monatomic, have a low average

energy (4–5 ev) and energy spread, and may result either from physical sputtering of the base metal or from the dissociation of surface compounds or both. (Author)

Richard C. Bradley, *J. Appl. Phys.*, **30**, 1–8, 1959.

18 : 33 : 51

34. Collisions of Metastable Atoms.
United States. Collision experiments with He 2^3S and Ne^3P metastable atoms are described, giving the total collision cross sections of these atoms with He, Ne, A at thermal energies, also the absorption cross sections of resonance photons from the He, Ne discharges. The secondary electron yields from He metastable atoms and from resonance photons incident upon W, Mo, Pt surfaces flashed to 1700 °C are compared with the yields from an unflashed Au surface, previously determined absolutely. The rate of rise of yield due to gas contamination is examined. The yields from the flashed surfaces are found to be distinctly smaller than Hagstrum's yields for low-energy positive ions. (Author)

J. B. Hasted, *J. Appl. Phys.*, **30**, 22–24, 1959.

18 : 51

35. Inelastic Ion-Atom Collisions.
United States. Ion-atom charge exchange cross sections of incident ion velocity v in the adiabatic region are shown to be proportional to $\exp(-K'a|\Delta E|/v)$ energy defect ΔE. Maximum cross sections of the negative ion-atom detachment collision and certain other inelastic ion-atom collisions are shown to be proportional to the maximum kinetic energy available for internal excitation, $\frac{1}{2}\mu v^2$, where μ is the reduced mass of the system. The semi-empirical prediction of cross-section energy dependence is discussed. (Author)

J. B. Hasted, *J. Appl. Phys.*, **30**, 25–27, 1959.

18 : 51

36. Inelastic Atomic Collision Processes.
United States. At nonrelativistic energies, for arbitrarily complicated collisions of distinguishable or indistinguishable particles, with or without rearrangement, correct formal expressions for the cross sections are known and well established. Nonetheless, all inelastic collision cross sections must be estimated, rather than predicted accurately, because even with present high spread computers there is no three-or-more particle collision for which it is practical to solve the Schroedinger equation exactly. The validity of the customary Born approximation, and of other more elaborate approximate calculations, are discussed, mainly with reference to electron excitation cross sections. The evidence suggests that a " compound ion model " of excitation, which is contrasted with the more usual " direct interaction model ", may prove helpful in understanding the sharp peaks and other anomalous features in some excitation cross sections near threshold. It is argued briefly that (1) there are reasons to think that at high energies Born approximation is not valid for exchange amplitudes, which are the only amplitudes appearing in excitation involving change of spin multiplicity ; (2) there are circumstances when Born approximation becomes increasingly valid as the incident electron energy is decreased. (Author)

E. Gerjuoy, *J. Appl. Phys.*, **30**, 28–33, 1959.

18 : 33 : 51

37. Electron Emission at High Fields Due to Positive Ions.
United States. Two mechanisms have been proposed to account for the observed large yield of secondary electrons in gaseous breakdown at high electric fields. In one of these a single ion in approaching the cathode surface creates a " pass " by decreasing the width of the potential barrier. In the other the increased over-all field due to a large number of ions in the gap is supposed to account for the increased emission. The first effect is re-examined and appears to be effective in the observed breakdowns of extremely small gaps in air. It may also be effective in breakdown at high pressure and in liquid and solid dielectrics. (Author)

P. Kisliuk, *J. Appl. Phys.*, **30**, 51–55, 1959.

18 : 33 : 56

38. Electron Cooling by Heat Exchange.
United States. To obtain an homogeneous electron stream with negligible thermal energy spread the electrons are made to collide with gas molecules in a plasma. Ions and electrons are emitted from a hot tungsten cathode which is bombarded by cesium atoms. The plasma is confined to a beam by an axial magnetic field of a few hundred gauss. This plasma beam extends from the plasma emitter to the electron extractor, passing through the gas-filled cooling region and through a differential pumping system which maintains a pressure difference between the cooling region and the electron extractor. Electron temperatures as low as 400°C have been obtained. The new method is capable of providing electron beams with densities of up to 10^{-3} A/cm^2, currents exceeding 10^{-3} A, and markedly improved homogeneity. B. B. D.

Letter by R. C. Knechtli and W. Knauer, *J. Appl. Phys.*, **29**, 1513–1514, Oct., 1958.

18 : 52

39. Thermionic Ions from Hydrogen Palladium.
United States.
Letter by C. H. Bachman and P. A. Silberg, *J. Appl. Phys.*, **29**, 1266–1267, Aug., 1958.

18 : 16 : 51

Ion Induced Re-emission of Noble Gases from a Nickel Surface.
See Abstr. 13.

19. Radiation

19 : 30 : 52

40. Electroluminescent Thin Films.
Letter by W. A. Thornton, *J. Appl. Phys.*, **30**, 123, Jan., 1959.

19 : 33 : 52

41. Photoconductive Response of Single Crystal Germanium Layers Prepared by the Pyrolytic Decomposition of GeI_2.
United States. Layers of single crystal germanium have been prepared by pyrolytic decomposition of GeI_2 at about 350 °C upon single crystal seeds of germanium by J. C. Marinace. The substrate germanium could be removed and the resultant thin layers ($\sim 5 \times 10^{-3}$ cm) studied. The Hall coefficient and resistivity measured on these layers by Dunlap *et al.* showed that the layers as grown were usually n type and contained about 10^{16} donors/cm^3. These donors are situated at 0.22 ± 0.04 ev below the conduction band. In the work reported here, the photoresponse of such layers at 77° K was found to extend to about 6 μ in substantial agreement with this thermal activation energy. The 0.2-ev donors apparently can be annealed out by prolonged heating at 550° C. The layers could also be intentionally doped with standard acceptors such as Al during formation. It was hoped that it would be possible to obtain the incorporation of Au into the layers. For this purpose, layers for which Au doping was attempted were annealed to remove the 0.2-ev donors. Although some of the layers became p type, a comparison of the photoresponse at 77° K with the photoresponse obtained for a 5×10^{-3} cm thick p-type plate of regularly Au-doped germanium showed no evidence for the 0.15 ev Au level. Likewise, annealed layers for which Ag doping was attempted were examined but yielded no positive identification of the 0.14-ev level of Ag. (Author)

Donald C. Cronemeyer, *J. Appl. Phys.*, **29**, 1730–1735, Dec., 1958.

Vol. 9 959/60

19 : 51

42. Infrared Absorptivities and Emissivities of Gases.

Letter by A. Thompson, W. J. Hooker and S. S. Penner, *J. Appl. Phys.*, **30**, 124, Jan., 1959.

19 : 51

43. Relation between Gas Absorptivities and Emissivities.

Letter by D. Olfe and S. S. Penner, *J. Appl. Phys.*, **30**, 125, Jan., 1959.

19 : 30 : 51

44. A Mechanical Version of the Smith Chart.

Gt. Britain. A modification of the Smith Chart has been devised for the purpose of computing the transmission characteristics of non-absorbing optical or electrical multi-element filters. The conventional printed chart is replaced by a system of mechanical linkages together with a spiral computing element. The computer is more accurate, faster and less laborious to use than the orthodox chart. (Author)

J. E. Knowles, *J. Sci. Instrum.*, **35**, 233–240, July, 1958.

Vo
9
1959

Vacuum Apparatus and Auxiliaries

21. Pumps and Pump Fluids

21

45. Preventing Steam " Slipping " at Ejector Pumps.
Note in *Brit. Chem. Engng.*, **3**, 158, 1958.

21 : 24 : 26

46. Vapour Cut-Off for Vacuum Plant.
A. Mohr and Siemens & Halske A.G., *German Pat. Appl.*, DAS 1037644.

21

47. Interior Component of Vapour Pumps.
W. Baechler, H. G. Noeller and E. Leybold's Nachfolger, *German Pat. Appl.*, BAS 1037061.

21

48. A New Type of Titanium Getter Pump.
L. Holland, L. Laurenson and J. T. Holden, *Nature*, **182**, 1958. (Letter) Issue No. 4639, 851, 27 September.

21 : 11

Sur le Pompage des Tubes à Vide. See Abstr. 2.

21 : 11

Means for Attaining Vacua Without the Use of Pump Fluids. See Abstr. 3.

21 : 11

Ionic Vacuum Pumps. See Abstr. 4.

21 : 15

Mean Gas Flow Velocity and Gas Flow Rate in Jets of High Vacuum Pumps. See Abstr. 8.

21 : 15

Velocity and Temperature Discontinuities Near the Walls of a Body Around Which Rarified Gases Flow with Transonic Velocities. See Abstr. 9.

22. Gauges

22

49. A High-Precision Differential Manometer.
Gt. Britain. When using conventional mercury manometers, difficulties in sighting on the meniscus with a cathetometer and due to capillarity limit the available precision to about 0.01 mm. The apparatus described uses the observation of contact between tungsten points and the Hg surfaces in the two arms of the manometer, and a change in Hg level of about 2×10^{-4} mm can be detected. Each tungsten point is accurately centred in a glass bulb of diameter 34 mm (considered the minimum to avoid errors due to variations in capillary depression), the two bulbs being connected by a U-tube. The dead-spaces at the two sides of the manometer can be varied in volume by forcing Hg into and out of weighed bottles, fine control being given by Hg micrometer pipettes. To use the apparatus, it is first rinsed with dry nitrogen, evacuated with a diffusion pump for some hours and levelled. Dry nitrogen is then admitted to one side as a reference gas and its pressure adjusted to balance that of a similar sample in the other side of the apparatus, whose pressure is measured as accurately as possible with a conventional manometer. When balance is obtained, the volume of the reference gas is measured (to better than 1 in 10^5) by means of the weighed Hg bottles and calibrations of the connecting tubes. By keeping the same reference sample of gas, unknown pressures can be measured (relative to the initial measurement of pressure made during calibration) by readjusting the volume of the reference gas to give a new balance. It was observed that volume changes of up to 50 parts in 10^5 would occur after manipulation and it might be necessary to wait as long as 18 hr for steady conditions to be obtained. The optical set-up for viewing the contact between tungsten point and Hg surface is described ; it resembles the Foucault knife-edge test of a mirror for irregularities. The whole apparatus is rigidly mounted in a thermostat on a concrete floor. There is a sketch showing the dead-space assembly and a note on forming the tungsten points from 1 mm rod. An interesting comment is that glass points were found unsuitable because of static electricity generated by the movement of Hg inside the extremely dry apparatus distorted the Hg meniscus.
M. D. A.
G. A. Bottomley, *J. Sci. Instrum.*, **35**, 254–257, July, 1958.

22 : 16

Adsorption of Oxygen and Carbon Monoxide on Tungsten. See Abstr. 11.

23. Plumbing

23 : 43 : 57

50. Vacuum Limitations of Rubber O-Ring Joints.
J. R. Young, *Rev. Sci. Instrum.*, **29**, No. 9, 795–796, 1958.

23 : 57

51. Simple Vacuum Coupling.
John T. Heinrich, *Rev. Sci. Instrum.*, **29**, 1053. Nov., 1958.

23 : 57

52. Demountable Vacuum Seal for Attaching an End-Plate to a Glass Tube.
Horace R. Moore, *Rev. Sci. Instrum.*, **29**, No. 8, 737, Aug., 1958.

23 : 57

53. Electrical Lead for Vacuum Systems.
H. Wieder and A. W. Smith, *Rev. Sci. Instrum.*, **29**, No. 9, 794, Sept., 1958.

23 : 43 : 57

54. A Note on the Use of P.T.F.E. in Vacuum Seals.
Note by A. J. Davies, *J. Sci. Instrum.*, **35**, 378, Oct., 1958.

23 : 57

55. A Neoprene Vacuum Gasket for Wires.
Note by A. C. Prior, *J. Sci. Instrum.*, **35**, 382, Oct., 1958.

23 : 57

56. A Metal Through Glass Seal.
Note by E. J. Davis, *J. Sci. Instrum.*, **35**, 308, Aug., 1958.

24. Valves

24 : 27 : 57

57. The Construction of Small Vacuum Leaks of Constant Value.
Note by R. O. Jenkins, *J. Sci. Instrum.*, **35**, 428, Nov., 1958.

24 : 57

58. Valve for the Grease-Free Manipulation of Mercury.
Letter from J. A. Frost, *J. Sci. Instrum.*, **35**, 268, July, 1958.

24 : 40 : 52

59. Kinetic Theory of Nonspherical Molecules. III.
Charles Muckenfuss and C. F. Curtiss, *J. Chem. Phys.*, **29**, 1257, December, 1958.

24 : 21 : 26

Vapour Cut-Off for Vacuum Plant. See Abstr. 46.

25. Baffles, Traps and Refrigeration Equipment

25 : 33 : 51

60. Helium Dewar with Incorporated Magnet Pole Tips.
David F. Edwards, Robert W. Terhune and Vito J. Lazazzera, *Rev. Sci. Instrum.*, **29**, 1049. Nov., 1958.

25 : 17 : 26

Precision Liquid Nitrogen Trap Level Controller. See Abstr. 24.

Vol. 9 959/60

26. Automatic Protective and Control Equipment

26 : 57

61. Corrosion Proof Vacuum Controller for Pressures under 1 mm Hg.

Note by I. Amariglio and M. M. Benarie, *J. Sci. Instrum.*, **35**, 385, Oct., 1958.

26 : 17 : 25

Precision Liquid Nitrogen Trap Level Controller. See Abstr. 24.

26 : 21 : 24

Vapour Cut-Off for Vacuum Plant. See Abstr. 46.

27. Leak Detectors and Leak Detection

27 : 10 : 57

High Vacuum Practice. See Abstr. 1.

27 : 24 : 57

The Construction of Small Vacuum Leaks of Constant Value. See Abstr. 57.

Vo
9
1959

Vacuum Applications

30. Evaporation and Sputtering

30 : 41

62. On P. A. Kurov's Letter on the Structure and Properties of Layers Obtained on Evaporation of InSb in Vacuum.
I. D. Konozenko and R. M. Kaikina, *Sov. Phys.-Tech. Phys.*, **3**, No. 4, 738, Apr., 1958.
Translation of *Journ. of Tech. Phys. of the USSR*, **28**, No. 4.

30 : 51

63. Structure of Thin Films of Sb_2S_3 Obtained by Sublimation at Pressures of Nitrogen Below 4 mm Hg.
A. M. Reshetnikov, *Soviet Phys. Doklady*, **3**, No. 2.

30 : 51

64. Stability of Evaporated Films.
Letter by M. Wyn Roberts, *Nature*, **182**, Issue No. 4643, 1151–1152, 25 October, 1958.

30 : 56

65. Electrodes for Thin Metal Films.
Note by S. Chandra and G. D. Scott, *J. Sci. Instrum.*, **35**, 349–350, Sept., 1958.

30 : 33 : 51

66. Thin Film Magnetization Reversal by Coherent Rotation.
United States. Several theoretical analyses of the process of magnetization reversal in thin films by coherent rotation of the magnetization vector have been published. However, these analyses suffer from the use of questionable assumptions and from a lack of generality. This paper presents results obtained by employing an electronic digital computer to solve differential equations of greater accuracy and generality than those previously used. These results show how the optimum damping factor (which, as defined herein, differs slightly from the critical damping factor), the peak output voltage, and the reversal time vary with the magnitude and direction of a field applied to a thin ferromagnetic film with uniaxial anisotropy. The results for a particular reversal time decreases with increasing magnitude of the field ; and that a plot of reciprocal reversal time versus field magnitude is a parabola if the damping factor is always equal to its optimum value, but a hyperbola if the damping factor is a constant. (Author)

P. R. Gillette and K. Oshima, *J. Appl. Phys.*, **29**, 1465–1470, Oct., 1958.

30 : 51

67. Crystal Growth on Cathode Sputtered Copper Films by Pairs of Double Spiral Mechanisms Analogous to Frank-Read Sources.
United States. Unique crystal growth patterns with closed loops, partly concentric and partly eccentric, with very large step heights between the ledges were observed on microblisters of copper films sputtered on to glass substrate. While the primary cause for the generation of the blisters is explained as due to diffusion-oil deposits present on the glass substrate and to heat from secondary electrons released by the target producing a high vapor pressure underneath the sputtered film, the generation of the loop patterns on the flat circular surface of the blisters is considered to be caused by alternative slips induced by the inside pressure which affect a triangular part of the 111 surface with two sides of 111 slip planes, one in radial 110 direction and the other in a 110 direction along the rim of the blister. Two alternately generated monatomic radial steps on the flat part of the blister produce two superposing spirals of opposite sense each due to one-half of two Frank-Read sources and create by repetition of this process the observed patterns with very large step heights of the ledges. (Author)

Erich B. Henschke, *J. Appl. Phys.*, **29**, 1495–1502, Oct., 1958.

30 : 51

68. Selective Delineation of Screw Dislocations by Cathodic Sputtering.
United States. A method of revealing screw component dislocations involving low-energy cathodic sputtering with argon ions is presented. It is observed that hillocks having the shape of truncated cones with a spiral pattern on their tops form at the sites of intersection of screw dislocations with the surface. The hillocks probably form by mobile surface atoms attaching themselves to the step provided at the intersection of a screw dislocation with the surface. It is shown that the density of screw dislocations on a given plane depends on the orientation of the plane with respect to the crystal growth axis. (Author)

B. B. Meckel and R. A. Swalin, *J. Appl. Phys.*, **30**, 89–93, 1959.

30 : 52

69. Production of Cadmium Sulfide Crystals by Coevaporation in a Vacuum.
United States. Apparatus was developed by which beams of cadmium and of sulfur were simultaneously directed to a common point on a temperature controlled substrate in a demountable vacuum apparatus. Cadmium sulfide crystals were obtained. The various types of crystals : spiroidals, globules, ribbons, and needles are described together with the conditions tending to produce each type. Crystal size can be increased by repeated exposure to the beams. (Author)

R. J. Miller and C. H. Bachman, *J. Appl. Phys.*, **29**, 1277–1285, Sept., 1958.

30 : 33 : 52

70. n-Type and p-Type Conduction in Alkali-Antimonide Photoemitters.
United States. Conductivity measurements were made during the formation of alkali antimonides to deduce whether these materials are *p*-type or *n*-type conductors. Reproducible results were obtained, indicating that K_3Sb and Na_3Sb are *n*-type while Cs_3Sb and the multialkali antimonides are *p*-type. A correlation between high-quantum efficiency of photoemission and *p*-type conduction is suggested. (Author)

A. H. Sommer, *J. Appl. Phys.*, **29**, 1568–1569, Nov., 1958.

30 : 33 : 56

71. Magnetic Writing with an Electron Beam.
United States. Experimental evidence is presented that magnetic writing with an electron beam is possible. The method is based on Curie-point writing which permits local reversal of the direction of magnetization in suitable, premagnetized magnetic films by temporarily elevating the temperature above the Curie point. By utilizing the dissipation energy of a focused electron beam for this purpose, quite well-defined traces of reversed magnetization could be recorded on MnBi films. The traces were erasable magnetically. Writing speeds corresponding to 3.10^4 bits/sec and information densities corresponding to 10^5 bits/cm^2 could be achieved in these first experiments. Considerably higher writing speeds and some increase in information density should be feasible. By means of an electron mirror micrograph of the electronically recorded magnetic trace, evidence is presented which shows that, in addition to read-in with an electron beam, electronic read-out of the magnetically stored information is also possible. Electronic writing of magnetic half-tone images by controlling the size of the spots of reversed magnetization appears to be feasible also. (Author)

Ludwig Mayer, *J. Appl. Phys.*, **29**, 1454–1456, Oct., 1958.

30 : 33 : 51

72. Variation in the Temperature Derivative of Resistivity.
United States. Measurements of the temperature derivative of electrical resistivity of evaporated nickel and palladium films

Vol. 9 59/60

show a decrease to a minimum about 10 per cent below the bulk value as the film thickness decreases to a few hundred Angstroms thickness. No decrease is found for films of copper or silver. The temperature derivative increases rapidly as the film thickness falls below 100 Å. This is attributed to the anomalously high resistivity of the very thin films which are ultimately transformed into isolated clumps of metal during the annealing process used. B. B. D.

Letter by T. G. Knorr and R. W. Hoffman, *J. Appl. Phys.*, **29**, 1512–1513, Oct., 1958.

30 : 16

Dissociative Adsorption of Methane and Ethane on Evaporated Metal Films. See Abstr. 16.

30 : 19 : 51

A Mechanical Version of the Smith Chart. See Abstr. 44.

30 : 19 : 52

Electroluminescent Thin Films. See Abstr. 40.

32. Nucleonics

32 : 51

73. Neutron Generation from Straight Pinches.
United States. Experiments on the neutrons produced in deuterium gas during a high-current pulsed discharge are described. With 15 kV applied to a straight discharge tube 30 cm long, neutrons are produced during a 0.1 μsec pulse 1.4 μsec after gas breakdown. The yield of 10^7 to 10^8 neutrons per discharge depends on gas purity and the discharge tube wall material. The axial asymmetry in neutron energy indicates that the neutrons are produced in reactions whose center of mass moves preferentially towards the cathode. (Author)

R. E. Dunway and J. A. Phillips, *J. Appl. Phys.*, **29**, 1137–1143, Aug., 1958.

32 : 58

74. A High Voltage Electron Injector Gun for Synchrotrons.
Gt. Britain. An improved demountable electron injector gun designed primarily for use in 140 and 30 MeV synchrotrons is described. The maximum energy of injection is 100 keV : facilities for the exploration of synchrotron injection parameters are provided by micrometer control of both the radius and the injection angle of the beam. Both the cathode assembly and the anode are easily detachable for replacement and experimental purposes. Details of the gun design, its electrical characteristics, and the test apparatus are given. There is a photograph of the gun and two sectional drawings. M. D. A.

E. W. V. Acton and K. T. W. Milne, *J. Sci. Instrum.*, **35**, 245–247, July, 1958.

32 : 58

75. A Nuclear Plate Camera for Angular Distribution Measurements with Gaseous or Solid Targets over a Wide Range of Angles.
W. M. Jones and D. G. Waters, *J. Sci. Instrum.*, **35**, 286–288, Aug., 1958.

32 : 33 : 58

76. A Cryostat for Reactor Irradiations in Liquid Nitrogen.
M. W. Thompson and D. W. Jefferson-Loveday, *J. Sci. Instrum.*, **35**, 397–399, Nov., 1958.

32 : 58

77. Research on Controlled Thermonuclear Reactions at the Atomic Energy Institute of the USSR Academy of Sciences.
Russia. The vacuum chamber and pumping system of " Ogra ", one of the Soviet thermonuclear devices, is described. The chamber and system have been designed and fabricated by the Vacuum Institute of the Soviet Union. The internal diameter of the device is given as 1.4 m, and the vacuum chamber is constructed of stainless steel. The entire chamber is capable of being baked at 450° C. In order to achieve the very low ultimates required in plasma machines, two types of pumping systems are used. First, mercury diffusion pumps evacuate the vessel to 1×10^{-6} mm Hg at which pressure getter-ion pumps are employed to bring the pressure to 1×10^{-8} mm Hg. These getter-ion pumps are not entities themselves but are an integral part of the chamber. Titanium is therefore evaporated directly onto the walls of " Ogra " and the entire chamber surface becomes an adsorptive getter surface, continuously and regeneratively. C. L. G.

I. V. Kurchatov, *Atomnaya Energiya*, **5**, No. 2, 168–175.
Included in *Journal of Nuclear Energy*, **8**, Nos. 1–3, Nov., 1958.

32 : 56

78. 150 kV Cockcroft-Walton Type Particle Accelerator.
India. The design and operation of a 150 kV Cockcroft-Walton Generator is discussed in some detail in the article. The vacuum system consists of an MCF-700 oil diffusion pump with a speed of 650 l./sec. This is backed by a Duo-Seal mechanical pump with a speed of 380 l./min. The diffusion pump is fitted with a freon baffle and when this is chilled the pressure in the accelerating column is 1×10^{-6} mm Hg. Even though the machine is relatively leak tight, a high pumping speed must be maintained since the constant flow of ions from the ion source is necessarily accompanied by a considerable flow of neutral gas. C. L. G.

C. S. Khurana and H. S. Hans, *Indian J. Phys.*, **32**, No. 10, 468–472, Oct., 1958.

32 : 58

79. New Proportional Counters for Gases and Vapors.
United States. New proportional-counter designs simplify the inherently sensitive tool for assay of C^{14} and H^3 and extend its use to gas-flow applications. Comparison is made with the sensitivity and convenience of ther systems. (Author)

Richard Wolfgang and C. F. MacKay, *Nucleonics*, **16**, 69–73, Oct. 1958.

32 : 58

80. Evacuated Pinhole Camera Maps Beta-Active Deposits.
L. E. Preuss and G. Jenkins, *Nucleonics*, **16**, 98–99, Oct., 1958.

33. General Physics and Electronics

33 : 56

81. Electrically Driven Shock Tube.
Letter by D. Bloxsom, Jr., *J. Appl. Phys.*, **29**, 1128–1129, July 1958.

33 : 51

82. Contact Potential Measurements on Graphite.
Letter by A. Fowler, *J. Appl. Phys.*, **29**, 1132, July 1958.

33 : 56

83. Beam Noise in Crossed Electric and Magnetic Fields.
United States.
Letter to the Editor by R. P. Little, H. M. Ruppel and S. T. Smith, *J. Appl. Phys.*, **29**, 1376, Sept. 1958.

33 : 56

84. Vacuum Arcs on Tungsten Cathodes.
Letter by H. Wroe, *Nature*, **182**, Issue No. 4631, 338, 1958.

33 : 51

85. Production of High Concentrations of Hydrogen Atoms.
Letter by K. R. Jennings and J. W. Linnett, *Nature*, **182**, Issue No. 4635, 597, 30 August, 1958.

33 : 51

86. The Recombination of Oxygen Atoms at Surfaces.
J. C. Greaves and J. W. Linnett, *Trans. Faraday Soc.*, **54**, 1323. Sept., 1598.

Vo 9 1959

33 : 51

87. Grating Vacuum Monochromator for the Spectral Range 1000-6500 A.
Th. J. M. Sluyters and E. de Haas, *Rev. Sci. Instrum.*, **29**, 597–600, July, 1958.

33 : 51

88. A Broadband Oscilloscope Tube.
Gt. Britain. Describes a broadband oscilloscope tube in which the deflexion is obtained by passing the beam through a slow-wave structure. The structure consists of a tape helix with a centre conductor, the beam passing between conductor and helix. The response is flat up to 600 mcs/sec.
A. H. W. B.
D. J. Brangaccio, A. F. Dietrich and J. W. Sullivan, *Bell System Tech. J.*, **37**, 447, 1958.

33 : 52

89. A Mass Spectrometer Mass Marker.
J. H. Beynon and S. Clough, *J. Sci. Instrum.*, **35**, 289–291, Aug., 1958.

33 : 56

90. Soft X-Ray Spectroscopy Using an Electron Multiplier.
J. A. Catterall, L. F. Wilson and J. Trotter, *J. Sci. Instrum.*, **35**, 393–395, Nov., 1958.

33 : 56

91. An X-Ray Tube Target Current Stabilizer.
Note by R. S. Crisp, *J. Sci. Instrum.*, **35**, 470, Dec., 1958.

33 : 51

92. Properties of a Thermoelectric Cell.
United States. A diode is evacuated and then filled with cesium vapor maintained at pressures from 10^{-6} mm Hg to 1 mm Hg depending on the temperature of a thermostatically controlled silicone oil bath. The vapor-filled diode acts as a thermoelectric cell for the direct conversion of heat energy into electrical energy.
B. B. D.
Letter by G. M. Grover, D. J. Roehling, E. W. Salmi and R. W. Pidd, *J. Appl. Phys.*, **29**, 1611–1612, Nov., 1958.

33 : 51

93. Noise in Oxide Cathode Coatings.
United States. Noise measurements have been performed on oxide-coated cathodes at frequencies of 8 Mc and 30 c. At 8 Mc, where thermal noise and shot noise predominate, the measurements show thermal noise at high cathode temperatures (pore conduction region) and at low cathode temperatures (grain conduction region) with a pronounced noise peak caused by shot noise in the temperature range where pore conduction switches over to grain conduction. Noise measurements at 30 c where flicker noise (with a 1/f noise spectrum) predominates, indicate that the pore noise corresponds to the flicker noise expected for a semiconductor with a voltage-independent conductivity, whereas the grain noise corresponds to the flicker noise expected for a semi-conductor with voltage-dependent conductivity. The measurements also show that the pores are inherently noisier than the grains at low frequencies. The results agree with a qualitative theoretical analysis. (Author)
H. J. Hannam and A. Van Der Ziel, *J. Appl. Phys.*, **29**, 1702–1705, Dec., 1958.

33 : 51

94. Thermometric Study of the Frozen Products from the Nitrogen Microwave Discharge.
United States. Thermometric observations have been made of the phenomena accompanying the stabilization and the recombination of free nitrogen atoms in a solid molecular nitrogen matrix at liquid helium temperatures. Condensation from the gas phase may occur at temperatures considerably above the 4.2 °K coolant temperature as the result of the normal change in heat content and the heat of atom recombination. Estimates, made from the latter effects, of the free atom concentration in the gas phase were as high as 4 atom per cent. Qualitative confirmation of the presence of an energetic species stabilized in the solid phase was made by detection of heat release upon warmup. From the latter effect a minimum nitrogen atom concentration in the solid of 0.03 atom per cent was estimated. For the conditions used the initiation of atom recombination occurs at a temperature of about 9 °K. The upper limit of about 36 °K for stabilization coincides with the known thermal transition in solid nitrogen. The data suggest that at least about 9 °K diffusion of nitrogen atoms occurs throughout the solid matrix during deposition from the gas phase. If recombination during warmup is diffusion-controlled, unusual dependence upon temperature is indicated. (Author)
B. J. Fontana, *J. Appl. Phys.*, **29**, 1668–1673, Dec., 1958.

33 : 37 : 52

95. High Vacuum Studies of Surface Recombination Velocity of Germanium.
H. H. Madden and H. E Farnsworth, *Phys. Rev.*, **112**, 793–800, 1958.

33 : 39 : 51

96. Application of the Ion Bombardment Cleaning Method to Titanium, Germanium, Silicon, and Nickel as Determined by Low-Energy Electron Diffraction.
United States. The ion-bombardment cleaning method has been successfully applied to the (100) faces of germanium, silicon, and nickel, and to the (0001) face of titanium. Conditions and precautions necessary for the production of clean surfaces are described. Tests have been made for contamination from the ambient during the cleaning procedure for germanium. It has been shown that contamination approximating one-half monolayer does not occur under the conditions which were obtained, and that the method is capable of producing surfaces which are atomically clean. Results for clean (100), (111), and (110) germanium faces and the (100) silicon face indicate that the atomic positions in the surface planes are not the same as the corresponding positions in the bulk structure. For (100) nickel and (0001) titanium, the positions of the atoms in the surface planes are in agreement with X-ray data. In the case of titanium, an unidentified surface structure was present until after several cycles of alternate heating and ion bombardment. In the case of nickel, a double-spaced surface monolayer and in some cases a single-spaced, simple-square structure, attributed to carbon, was present until after several cycles of alternate heating and ion bombardment. (Author)
H. E. Farnsworth, R. E. Schlier, T. H. George and R. M. Burger, *J. Appl. Phys.*, **29**, 1150–1161 Aug., 1958.

33 : 39 : 51

97. Preparation and Regeneration of Clean Germanium Surfaces.
Letter by S. Wolsky, *J. Appl. Phys.*, **29**, 1132–1133, July, 1958.

33 : 51

98. Measured Thermal Efficiencies of a Diode Configuration of a Thermo Electron Engine.
Letter by G. Hatsopoulos and J. Kaye, *J. Appl. Phys.*, **29**, 1124–1125, July, 1958.

33 : 51

99. Liberation of Electrons by Fast Neutral Helium Atoms from a Tungsten Target.
United States. The electron emission from tungtsen by bombarding helium atoms of energy ranging from 300 to 3500 ev has been measured for a surface with less than a monolayer and with multilayers of adsorbed gas. The yield expressed in electrons per particle rises almost linearly from about zero at 300 ev to 0.42 electrons/particle at 3500 ev for a monolayer of adsorbed

Vol. 9 959/60

gas. Further adsorption of gas gives a much increased yield. These yields are compared with the ion under like conditions. The distribution of the normal velocity and a component of the tangential velocity are compared for the ion and neutral atom on hot and cold targets. (Author)

H. W. Berry, *J. Appl. Phys.*, **29**, 1219–1225, Aug., 1958.

33 : 16

Work Function and Sorption Properties of Silicon Crystals. See Abstr. 12.

33 : 16

Using Cathode Resistance to Measure Adsorption of Gases on Metals. See Abstr. 14.

33 : 18 : 51

The Influence of the Electrode Temperature on the Electrical Breakdown Strength of a Vacuum Gap. See Abstr. 32.

33 : 18 : 51

Secondary Positive Ion Emission from Metal Surfaces. See Abstr. 33.

33 : 18 : 51

Collisions of Metastable Atoms. See Abstr. 34.

33 : 18 : 51

Electron Emission at High Fields Due to Positive Ions. See Abstr. 37.

33 : 18 : 56

Electron Cooling by Heat Exchange. See Abstr. 38.

33 : 19 : 52

Photoconductive Response of Single Crystal Germanium Layers Prepared by the Pyrolytic Decomposition of GeI_2. See Abstr. 41.

33 : 25 : 51

Helium Dewar with Incorporated Magnet Pole Tips. See Abstr. 60.

33 : 30 : 51

Thin Film Magnetization Reversal by Coherent Rotation. See Abstr. 66.

33 : 30 : 51

Variation in the Temperature Derivative of Resistivity. See Abstr. 72.

33 : 30 : 52

n-Type and p-Type Conduction in Alkali-Antimonide Photoemitters. See Abstr. 70.

33 : 30 : 56

Magnetic Writing with an Electron Beam. See Abstr. 71.

33 : 32 : 58

A Cryostat for Reactor Irradiations in Liquid Nitrogen. See Abstr. 76.

34. High Altitude and Space Technology

34 : 16 : 17

Theoretical Analysis of Ultra-High Vacuum Condensers. See Abstr. 18.

36. Drying, Degassing and Concentration

36 : 55

100. Low Temperature Evaporation Plus Energy Economy.
J. A. Cross, *Chem. Eng. Prog.*, **54**, 132–134, 1958.

36 : 52

101. Method of Freeze Drying Sensitive Material.
K. Neumann and Leybold-Hochvakuumanlangen G.m.b.H., *German Pat.* 1028741.

36 : 54

102. A Machine for Freeze-Drying and Storing Tissues Under Aseptic Conditions.
Gt. Britain. The machine was designed to carry out the entire process of freeze-drying and rehydration in a single tube. The tube and its cap form a wide base tap ; one turn leaves the orifice open for the freeze-drying process, another turn seals the tube. It is then given a sterile over-cap. For rehydration, the second cap is removed, the tap turned, and the fluid added. A vacuum pump is connected to a condenser, joined to a manifold with 8 ports for the artery tubes. These fit into the manifold by ground glass sockets ; the various articulations of the machine are of the spherical joint type. At the other end of the manifold is a brass closure connecting it to a P_2O_5 desiccator. The low temperature vacuum drying lasts for 12 hr and the drying by the desiccator 4 days. The artery tubes are then sealed. Fruit jars and other larger vessels can be adapted to the apparatus by the appropriate taps and plugs, for bulky tissues. Sterilization of the apparatus is by formaldehyde tablets in the port glass stoppers. The procedure is bacteriologically sound ; and the tissues so prepared have proved satisfactory in use. M. B.

A. M. N. Gardner and A. Leemans, *Lancet*, **1**, 247–248, 1958.

36 : 54

103. Continuous Freeze-Drying of Serratia Marcescens.
United States. An investigation was undertaken of the effects of various conditions on the ability of Serratia Marcescens strain 8UK to survive continuous freeze-drying and storage. A rather unusual freeze-dryer was used. Factors affecting the drying of S. Marcescens in the continuous freeze-dryer and the storage of the dried product are discussed. The material was dried successfully to a moisture content of 1 per cent, a suitable level for good storage stability, with a recovery of viable cells of 80 per cent or higher. A production rate of 50 to 55 g of dried material/hr could be maintained in continuous operation. (Author)

H. G. Maister, E. N. Heger and W. M. Bogart in *Ind. Eng. Chem.*, **50**, 623–626, 1958.

36 : 54

104. Pilot-Plant Production of Ground Serratia Marcescens.
United States. The development of a process for preparing relatively large amounts of fine powder containing high concentrations of Serratia Marcescens was investigated. Powdered concentrates of S. Marcescens were produced by suitable combinations of fermentation, centrifugation, pelleting, freeze-drying and grinding. The complete process incorporated pH control throughout fermentation, the use of a continuous controlled solids-discharge centrifuge, a continuous freeze-dryer, and a high speed centrifugal grinding mill. The powder contained about 21 per cent of the viable cells present in the fermented liquor, exhibited good storage stability, and had a viable cell count of about 1400×10^9/g. (Author)

V. F. Pfeifer, C. Vojnovich, H. G. Maister, V. E. Sohns, E. N. Heger and W. M. Bogart, *Ind. Eng. Chem.*, **50**, 1143–1148, 1958.

36 : 51

105. Freezing and Drying (p. 849). A brief report of the second international symposium of freezing and drying, held under the auspices of the Institute of Biology, London, on April 1–2.

37. Metallurgy, Inorganic Chemistry and Analytical Chemistry

37 : 55

106. Sampling from a Vessel Under Vacuum.
Note in *Brit. Chem. Engng*, **3**, 335, 1958.

37 : 52

107. Factors Determining the Oxygen Content of Liquid Silicon at its Melting Point.
United States. The oxygen content of liquid silicon increases

proportionally to the oxygen content of the ambient helium-oxygen mixture for oxygen partial pressure pO_2° 8 mm Hg. This observation is explained by the proportionality between the oxygen partial pressure pO_2° in the ambient gas and the SiO partial pressure on the surface of liquid silicon. For pO_2° 8 mm Hg the silicon melt is covered by a film of silica and a saturation value of about 2×10^{18} oxygen atoms/cm^3 is observed in the crystallized sample. (Author)

W. Kaiser and J. Breslin, *J. Appl. Phys.*, **29**, 1292–1294, Sept. 1958.

37 : 55

108. Sampling System for High-Vacuum Furnace Atmosphere.
Note in *Brit. Chem. Engng.*, **3**, 99, 1958.

37 : 51

109. The Preparation of Single-Crystal Ingots of Silicon by the Pulling Technique.
Gt. Britain. The construction and operation of a laboratory furnace for preparing monocrystals of silicon by the pulling technique are described. The design, based on a standard vacuum evaporation plant, allows for close observation of the growth front of the ingot during its preparation. It has been found possible to assess the quality of high-grade silicon and also to obtain an indication of the concentration of dominant impurities responsible for the measured resistivity by comparison with computed distribution curves. M. D. A.

E. Billig and D. B. Gasson, *J. Sci. Instrum.*, **35**, 360–365, Oct., 1958.

37 : 53

110. Vacuum Degassing at Bethlehem.
Metal Progress, **74**, 146–148, August, 1958.

37 : 53

111. Vacuum Degassing.
Metal Progress, **74**, 142–146, August, 1958.

37 : 52

112. Preparation of Indium Arsenide.
Letter by Roy H. Harada and Alan J. Strauss, *J. Appl. Phys.*, **30**, 121, January, 1959.

37 : 53

113. Whisker Growth from Iodide Titanium Wire.
Letter by A. Russell and R. Abbott, *J. Appl. Phys.*, **29**, 1130–1131, July, 1958.

37 : 56

114. Resolution of Electron Probe Microanalyzers.
United States. In microanalysis using X-ray emission excited on the surface of a thick specimen by an electron probe, the minimum volume element which can be analyzed is limited by the size of the electron probe, by fluorescence excitation, and by the penetration and diffusion of the electrons in the specimen. With an electron accelerating voltage of about 30 kV the electrons have an energy of the order of 3 times the critical excitation energy of the K or L X-ray levels of the target and the minimum volume which can be analyzed (in the absence of strong fluorescence effects) is of the order of 8 cu.μ for a copper target, and is considerably larger than this for targets of low atomic number or density. It is shown that the resolution in this method of analysis can be improved without loss of statistical accuracy or increase in the time of measurement by (1) improving the quality of the electron optics and by (2) selecting the accelerating voltage and electron probe size. The minimum volume element for practical quantitative analysis can thereby be made as small as about 0.2 cu.μ in a copper target. This is obtained by using slightly larger electron probes and lower accelerating voltages than those representative of current practice. (Author)

David B. Wittry, *J. Appl. Phys.*, **29**, 1543–1548, Nov., 1958.

37 : 53

115. Production of Discaloy by Vacuum Arc Melting.
United States. Consumable-arc remelting was developed for melting titanium and zirconium which are highly reactive metals and are easily contaminated by atmospheres and refractory. This process has been adapted to refine known inactive metals and their alloys. This article considers the problems of melting in vacuum one of the super-alloys, namely, " Discaloy " (registered trade name, Westinghouse Electric Corp.). The pilot run discussed was made with a vacuum arc furnace with pumping accessories which could be operated between 2 and 10 μHg. The power supply could provide up to 15,000 amp at 35 V. A 12-in. mold with a removable bottom attached to a hydraulic ram was used so that the ingot could be lowered to floor level. The problem of processing electrodes is discussed. It was found necessary to thoroughly condition air-melted electrodes. Those used in the pilot plant run were assemblies of 7-in. round machined billets known to be internally sound. The melting rates were determined by the requirements for progressive solidification and acceptable surfaces. Various currents and voltages were tried. Large pipe cavities were reduced by reducing the power input during the hot top period and increasing the time of hot topping. In the pilot plant run the electrodes were 17 ft long, made by melting two 7-in. diameter machined " Discaloy " billets. The vacuum was maintained at 4 μHg under a steady current of 7000 amp. At 22–24 V melting took about 3 hr for each ingot including the 20 min hot topping schedule. Twenty-one ingots were produced, each 12-in. in diameter and 48–50 in. long weighing about 1500 lb. Typical properties of these vacuum re-melted ingots as compared with air-melted ingots is as follows :

	Rupture Life	Elongation
Air-melted	10–75 hr	3–14 per cent
Vacuum Arc Re-melted	18–94 hr	14–38 per cent

A. G.

D. R. Carnahan, *Metal Progress*, **74**, 100–102, August, 1958.

37 : 53

116. Removal of Gases in High Vacuum Systems by Metal Abrasion.
Letter by M. E. Haine, E. W. R. Francis and R. N. Bloomer, *Nature*, **182**, Issue No. 4640, 931–932, 1958.

37 : 38 : 55

117. The Achema Meeting 1958. Chemical Plant Exhibition. New developments in vacuum apparatus as exhibited at the XIIth Achema Meeting which took place in Frankfurt from 31 May to 8 June, 1958.

Review by G. Müschenborn *Chem.-Ing.-Tech.*, **30**, 796–798, 1958.

37 : 51

118. Report on U.S. Reactor Fuel Technology.
United States. The editorial staff of *Nucleonics* presents a summary of reactor fuel technology. The fabricating capabilities of U.S. companies are presented in a table which includes vacuum melting and annealing facilities. B. B. D.

Staff article in *Nucleonics*, 77–104, 16 August, 1958.

37 : 33 : 52

High Vacuum Studies of Surface Recombination Velocity of Germanium. See Abstr. 95.

38. Distillation, Organic Chemistry and Isotopic Gas Analysis

38 : 58

119. Low Temperature Distillation of Hydrogen Isotopes.
United States. Description of the pilot plant at Boulder giving details of the new column and discussing special problems involved in insulating low temperature columns. These were

Vol. 9 959/60

solved by enclosing the cold parts in a high vacuum of the order of 10^{-5} to 10^{-7} mm Hg and maintaining the vacuum by continuous pumping of the cold box. (Author)

K. D. Timmerhans, D. H. Weitzel and T. M. Flynn, *Chem. Eng. Prog.*, **54** (6), 35–39, 1958.

38 : 55

120. Removal of Some Volatile Impurities from Uranium Hexafluoride.

United States. Experimental data reported can be used to design a distillation column capable of refining crude uranium hexafluoride to high purity. Vacuum apparatus used for determination of vapour-liquid equilibrium data is described.

W. H. Mears, R. V. Townend, R. D. Broadley, A. D. Turissini and R. F. Stahl, *Ind. Eng. Chem.*, **50**, 1771–1773, 1958.

38 : 55

121. A Fraction Collector (with Drop Counter).

A. Snow, F. A. E. Porter and A. W. Tomalin, *J. Sci. Instrum.*, **35**, 243–244, July, 1958.

38 : 37 : 55

The Achema Meeting 1958. Chemical Plant Exhibition. See Abstr. 117.

39. Miscellaneous Applications

39 : 54

122. Cooling Cannula for Use in the Treatment of Cerebral Neoplasms.

Gt. Britain. Cerebral gliomata are among the commonest groups of tumour, and there is no entirely satisfactory treatment. General hypothermia and local cooling of the brain by means of a blanket have not proven to be great advances. The authors constructed a device of a cannula attached to a vacuum pump and cooled by means of a cardice-acetone freezing mixture. The brain tissue's low thermal conductivity (12.00×10^{-4} cal. cm^{-1} sec^{-1} $°C^{-1}$) and its circulation made it possible to freeze a core of brain to $-20°C$ in 35 min, whereas 5 cm from the cannula there was a fall of only 7° in temperature. The core of frozen diseased tissue is removed. Two hopeless cases were treated ; one case of a highly malignant glioma of the right frontal region has improved, which is also due to the release of brain pressure. The object was to see if malignant cells are killed by some degrees of differential cooling and the neurones left alive. This has not been shown yet. M. B.

G. F. Rowbotham, A. L. Haigh and W. G. Leslie, *Lancet*, **I**, 12–15, 1959.

39 : 54

123. Effect of Hypothermia on the Adrenocortical Response to Operation.

Gt. Britain. An index of trauma response is measurable by secretion of adreno-cortical steroids. Using animals, the authors measured, (a) the AC response to operation during a 72 hr post-operative hypothermic (26–30°C) period, (b) the AC response to operation before hypothermia, (c) and the response after recovery from hypothermia. The measurements were of the urinary cortical steroid production. None of the animals recovered after the procedure, due to broncho-pulmonary trouble. There was a slight alteration in the blood coagulation factors of two of the four dogs. The effect of hypothermia appears not to depress the cortical function but the response to injury. The hypothermia insulates the cortex from the demands made on it during the trauma stage only ; recovery from hypothermia after operation is associated with an increased excretion of AC steroids which is greater than after operation alone. During the hypothermic post-operative stage there was no normal post-operative rise in cortical steroid production. M. B.

I. W. MacPhee, T. C. Gray and S. Davies, *Lancet*, **II**, 1196–1199, 1958.

39 : 54

124. Hyperpyrexia in Encephalitis Treated by Hypothermia.

Gt. Britain. A case history. The patient had marked neurological symptons, and respiratory difficulties made a tracheotomy necessary. Cooling was external, with eventual aid of chloropromazine and pethidine. The difficulty of controlling the skin cooling systems of hypothermy favours the intragastric method. Reduction of cerebral metabolism is greatest at temperatures of 82°F ; shivering increases cerebral metabolism. M. B.

A. W. Johnston, A. C. M. McLean, R. V. Morris and E. J. Ross, *Lancet*, **II**, 670–671, 1958.

39 : 54

125. Accidental Hypothermia.

Gt. Britain. The electrocardiogram is pathognomonic. The RR, PR, QRS, and QTC intervals were lengthened. The characteristic *J* deflection of hypothermia was present in leads related to the left ventricle ; when it was conspicuous, *T* was sometimes inverted. In other leads the base of QRS was widened. The changes were identical with human induced and animal experimental hypothermia.

D. Emslie-Smith, *Lancet*, **II**, 492–495, 1958.

39 : 54

126. Accidental Hypothermia.

Gt. Britain. Four case histories are presented. The ECGs did not show the " hypothermic " pattern ; in two of the patients their appearance was suggestive but the condition was not immediately diagnosed due to the use of a rectal thermometer which did not have a sufficiently low reading. Moderate warming up procedures are contraindicated as the heart may be chilled by cold blood, in accidental and acute hypothermia. In chronic hypothermia, rapid warming may lead to hypotension. In hypothermia there is evidence of adrenal damage, and depletion of hepatic and cardiac glycogen. Accidental hypothermia may protect against shock, which process is evidenced if the patient begins to deteriorate on rewarming. M. B.

J. R. Rees, *Lancet*, **1**, 556, 1958.

39 : 54

127. Hypothermia by Internal Cooling in Man.

Gt. Britain. The apparatus consists of a water tank with heating and cooling coils immersed in it ; the fluid is driven to and from the intragastric double condom balloon by means of pumps. Air traps are included to prevent air from entering the balloon or the hermetically sealed pump. Cooling and warming the body can be immediately controlled by adjusting the volume and temperature of the fluid in the balloon. Two cases for neurosurgery were successfully treated ; in one cardiac arrythymia developed but was arrested by the rewarming process described above. Neither case suffered gastric symptoms. M. B.

H. H. Khalil, *Lancet*, **1**, 1092–1094, 1958.

39 : 57

128. An Apparatus, Capable of Being Heated, for High Vacuum Grinding of Solids.

Note describing an all-glass apparatus, with totally-enclosed rotor carrying a 10 mm rotary file. The rotor is driven from outside by the rotating magnetic field obtained by spinning a ferrite ring magnet at speeds up to 2000 rev/min. The brass or copper ring forming part of the rotor reaches speeds up to 600 rev/min.

Note by E. Baronetzky, *J. Sci. Instrum.*, **35**, 427, Nov., 1958.

39 : 33 : 51

Application of the Ion Bombardment Cleaning Method to Titanium, Germanium, Silicon, and Nickel as Determined by Low-Energy Electron Diffraction. See Abstr. 96.

39 : 33 : 51

Preparation and Regeneration of Clean Germanium Surfaces. See Abstr. 97.

Vo 9 1959

Materials and Techniques used in Vacuum Technology

40. Gases and Vapors

40 : 52

129. Effect of Pressure on Ion Formation in Propane-Air Flames.
I. R. King, *J. Chem. Phys.*, **29**, 681–683, September, 1958.

40 : 51

130. Gas or Vapour Filled Discharge Vessel Fitted with a Hollow Cathode and a Starting Electrode Located Outside the Main Discharge Path.
H. Gawehn and Siemens & Halske A.G., *German Pat. Appl.* DAS 1041602.

40 : 16 : 52

Properties of Hydrogen Chemisorbed on Tungsten. See Abstr. 21.

40 : 24 : 52

Kinetic Theory of Non spherical Molecules. III. See Abstr. 59.

41. Metals and Alloys

41 : 53

131. Cleanliness of Vacuum-Melted Alloys.
Donald E. Nulk, *Metal Prog.*, **74**, 103–109, August, 1958.

41 : 51

132. Comments on a Theory of Double Block Walls in Thin Films.
United States.
Letter to the Editor by R. E. Behringer, *J. Appl. Phys.*, **29**, 1380, Sept., 1958.

41 : 30

On P. A. Kurov's Letter on the Structure and Properties of Layers Obtained on Evaporation of InSb in Vacuum. See Abstr. 62.

43. Plastics and Elastomers

43 : 23 : 57

Vacuum Limitations of Rubber O-Ring Joints. See Abstr. 50.

43 : 23 : 57

A Note on the Use of P.T.F.E. in Vacuum Seals. See Abstr. 54.

49. Miscellaneous Materials and Techniques

49 : 55

133. Size Reduction in Ball Mills.
Germany. As a result of movements of grinding elements air currents are created which carry the fine material out of the grinding zones. This process can be eliminated by application of vacuum and it results in doubling the size reduction performance.

W. Batel, *Chem.-Ing.-Tech.*, **30**, 567–572, 1958.

Vol.
9
959/60

Journals Abstracted for Vacuum

Acta Metallurgica
Acta physica Austriaca
American Journal of Physics
Analytical Chemistry
Analyst
Annalen der Physik
Annales de Physique
Annales de Radioéléctricité
Applied Scientific Research
Archiv für technisches Messen
Archiv für das Eisenhuttenwesen
Australian Journal of Applied Science
Australian Journal of Physics
Bell Laboratory Record
Bell System Technical Journal
British Chemical Engineering
British Communications and Electronics
British Journal of Applied Physics
Bulletin de la Classe des sciences de l'Académie R. de Belgique
Canadian Journal of Physics
Chemical Engineering
Chemical Engineering Progress
Chemie-Ingenieur-Technik
Chemische Technik
Chemistry and Industry
Chimie & Industrie
Comptes rendus hebdomadaires des Séances de l'Académie des Sciences
Czechoslovak Journal of Physics
Discovery
Electrical Communication
Electronics
Electronic Engineering
Electronisches Messen
Elektronische Zeitschrift
Elektrotechnische Zeitschrift Ausgabe A
Elektrotechnische Zeitschrift Ausgabe B
Endeavour
Engineer
Experimental Cell Research
Food Engineering
Foundry Trade Journal
Glastechnische Berichte
General Electric Review
Geochimica et Cosmochimica Acta
Helvetica Physica Acta
Huttenzeitung
Inco (International Nickel Co.)
Industrial and Engineering Chemistry
Industrial Finishing
Industrial Laboratories
Instruments and Automation
Instrument Practice
Instrument Review
Iron Age
Investigationae Physicae
IBM Journal of Research and Development
Journal of the American Ceramics Society
Journal of Applied Chemistry
Journal of Applied Physics
Journal of Applied Physics (Japan)
Journal of Chemical Physics
Journal de chimie physique
Journal of the Electrochemical Society
Journal of Electronics and Control
Journal of the Electrodepositors' Technical Society
Journal of the Franklin Institute
Journal of the Institute of Metals
Journal of the Institution of Electrical Engineers
Journal of the Iron and Steel Institute
Journal of the Japan Institute of Metals
Journal of Nuclear Energy
Journal of the Optical Society of America
Journal of the Physical Society of Japan
Journal de Physique et le Radium
Journal of Research of the National Bureau of Standards
Journal des Recherches du Centre National de la Recherche Scientifique
Journal of Scientific Instruments
Journal of the Scientific Research Institute (Tokyo)
Journal of the Society of Glass Technology
Journal of Physical Chemistry
Lancet
Light Metals
Manufacturing Chemist
Materials and Methods
Mechanical Engineering
Mededelingen van de Koninklijke Vlaamse Academie voor Wetenschappen van Belgie
Mémoires de l'Académie Royale de Belgique. Classe des Sciences
Metal Finishing
Metal Progress
Metallurgical Review
Metallurgia
Metalloberfläche
Microtechnic
M.I.T. Quarterly Progress Reports
National Bureau of Standards Reports
Nature
die Naturwissenschaften
Nederlandsch tidjdschrift voor Natuurkunde
Nuclear Engineering
Nucleonics
Nuclear Power
Optik
Product Engineering
Philosophical Magazine
Philips Research Reports
Philips Technical Review
Physica
Physics of Fluids
Physical Review
Plansee Proceedings
Planseeberichte für Pulvermetallurgie
Proceedings of the Institution of Electrical Engineers
Proceedings of the Institution of Radio Engineers
Proceedings of the Physical Electronics Conference (M.I.T.) (Annual)
Proceedings of the Royal Society
Proceedings of the Physical Society
Proceedings of the American Society for testing Materials
Pribori i Teknika Eksperimenta
R.C.A. Review
Refrigeration Engineering
Reports on the Progress of Chemistry
Reports on Progress in Physics
Research

VO
9
1959

Review of Scientific Instruments
Revue de la Société Royale des Ingénieurs et des Industriels
Science
Science Abstracts
Services Electronics Research Laboratory Technical Journal
Sprechsaal für Keramik Glas Email
Stahl und Eisen
Sylvania Technologist
Scientific Publications of the Osram Concern (Germany)
Times Science Supplement
Transactions of the Faraday Society
Transactions of the Institution of Chemical Engineers
Verhandelingen van de Koninklijke Vlaamse Academie voor Wetenschappen van Belgie
Vacuum Chemistry (Japan)
Vacuum Engineering (Japan)
Vakuum Technik
Le Vide
Welding Journal
Welding and Metal Fabrications
Westinghouse Engineer
World Science Review
Zavodskaja Laboratoria
Zeitschrift für angewandte Physikalische Chemie
Zeitschrift für Physikalische
Zeitschrift für anorganische und allegemeine Chemie
Zeitschrift für Instrumentenkunde
Zeitschrift für Metallkunde
Zeitschrift für physikalische Chemie
Zeitschrift des Vereines deutscher Ingenieure
Zeitschrift für angewandte Physik
Zeitschrift für Naturforschung
Zhurnal Tekhnicheskoi Fizki
Zeitschrift für Physik

Appointed Abstractors

M. D. Armitage
A. S. D. Barrett
A. H. Beck
K. H. Behrndt
R. N. Bloomer
M. Burns
J. H. Carmichael
D. Cosutta
D. J. Crawley
B. B. Dayton
J. M. Dunoyer
H. Ebert
A. J. Gale
A. Gordon-Foster
C. L. Gould
A. Guthrie
R. Jaeckel
H. Klumb
W. H. Kohl
J. H. Leck
A. Lorenz
W. G. Matheson
C. R. Meissner
K. H. Mirgel
G. L. Munday
H. Nakagawa
J. Newton
L. E. Preuss
W. Pupp
P. A. Redhead
D. J. Santeler
H. Sawistowski
K. Schaefer
G. Siddall
E. Thomas
A. H. Turnbull
O. Winkler
E. Wyatt
A. Venema
J. Yarwood

Vol. 9 959/60

VACUUM

Papers to be published in future issues

C. G. J. Jansen and A. Venema. A McLeod manometer with prescribed volumes for use as a standard instrument.

R. Jaeckel. Die diffusionspumpe ihre physik und technik.

S. A. Vekshinsky, M. I. Menshikov and I. S. Rabinovich. High-vacuum pumps and units for accelerators.

S. Veis. The measurement of the pressures of various gases by means of a Pirani gauge.

E. Thomas, R. Servranckx and R. Leyniers. On the choice of units of pressure and of flow in vacuum technique.

W. Steckelmacher, J. M. Parisot, L. Holland and T. Putner. Apparatus for the controlled deposition of optical film systems.

D. J. Santefer. Vacuum process evaluation.

H. Batey. Carbon contamination of glassware used for vacuum purposes.

D. S. Stark. Measurements on the properties of a simple omegatron.

Vo
9
1959

VACUUM

Apparatus for the Controlled Deposition of Optical Film Systems

W. STECKELMACHER, J. M. PARISOT, L. HOLLAND, T. PUTNER

Research Laboratories, Edwards High Vacuum Ltd., Crawley, Sussex

(Received 2 February 1959)

Some of the problems of producing multi-layer interference systems are discussed in relation to the design of the deposition plant and film thickness control apparatus. A vacuum plant is described in which multi-layer films of evaporated or sputtered layers can be deposited in sequence on a rotating plane surface. The thickness of the individual films is controlled by measuring their reflectance or transmittance during deposition with a modulated-beam photometer of high sensitivity and stability. The monitoring light is chopped at frequency of 33 c/s and the output from the photocell amplified by a tuned low frequency amplifier. The conditions for obtaining minimum light scattering in the instrument are discussed. The design of the low frequency amplifier is considered in relation to noise level and filter design. In conclusion the use of the combined apparatus is described for producing a variety of optical systems such as TiO_2 beam-splitters, $Bi_2O_3/Au/Bi_2O_3$ heat reflecting mirrors, two-layer anti-reflection coatings of Bi_2O_3/MgF_2 and all-dielectric broad-band filters of MgF_2/ZnS.

Vol. 9 959/60

1. Introduction

Ever since the last war a new field of applied optics dealing with the design of interference film systems has been steadily growing. This development stems from the early successful use of thin films for anti-reflection coating and single layer beam-splitters and has given rise to novel multi-layer systems used in narrow band-pass filters, cold mirrors and heat-reflecting filters, etc. Undoubtedly the growth of the new technology has been intimately linked with the development of techniques for depositing thin films by evaporation and cathodic sputtering at reduced pressures. However, in spite of the attention given to optical film systems, only limited production of such combinations has been undertaken in industry, i.e., apart from anti-reflection coating which is widely used. The writers believe that the reasons why many of the novel films systems are not extensively produced arises from the technical problems associated with their preparation.

There are at least three major technical requirements which must be fulfilled before optical film systems can be easily produced on a large scale. These are :—

1. The provision of metal or dielectric films in sequence on large surface areas with a thickness distribution following a specified pattern.
2. The deposition of metal and dielectric films to specified thicknesses.
3. The deposition of durable coatings possessing stable optical properties.

For single layer anti-reflectance coatings none of the foregoing requirements are difficult to fulfil. The film thickness does not have to be controlled within close tolerances. The required optical thickness can be obtained by visual control, and magnesium fluoride can be deposited to produce durable anti-reflection films. A similar situation exists for single layer films used in beam-splitters. However, to prepare for example, dichroic mirrors requires much greater control during the deposition, and it is apparent that the complex film systems would be produced more widely if suitable apparatus was available. This report is concerned with the design and uses of a deposition apparatus which has been developed to meet as simply as possible the requirements itemised above.

2. General purpose deposition plant

The vacuum plant to be described is shown in Fig. 1. It consists of a metal jar of 19 in. diameter in which is mounted the deposition apparatus. The plant is exhausted by a fractionating oil diffusion pump charged with Silicone 703 and fitted with a water cooled baffle valve giving a baffled speed of 1000 l/s. The elements of the deposition apparatus will now be discussed separately, their general assembly is shown in Figs. 2 and 3.

Work Holder. The work to be coated is mounted at the top of the chamber on a rotary holder of 14 in. diameter, which is supported by three ball races and rotates at 120 rev/min. Lateral play is prevented by three bearings one of which is spring loaded permitting the ring to expand if the work is heated. The holder is driven at the top of the chamber by a motor connected to a hollow shaft. The rotary shaft is sealed with a glass plate and the transmittance of the glass being coated can be measured with the monitoring beam passing at normal incidence through the centre of the work holder as shown in Fig. 2. The reflectance of the glass can also be measured at the centre of the plate as shown in Fig. 2,

FIG. 1. General view of vacuum deposition plant and photometric apparatus.

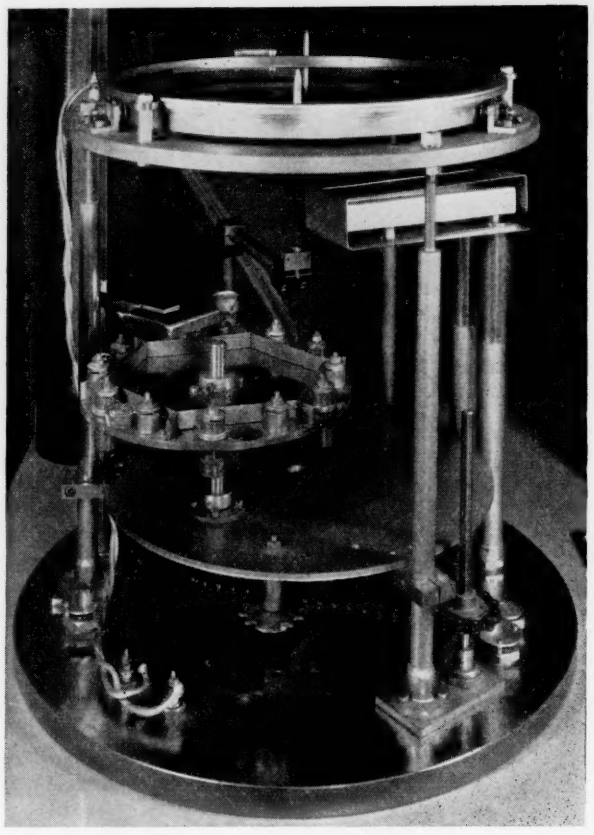

FIG. 2. Interior view of vacuum coating chamber showing rotary work-holder, vapour source turret head and high tension cleaning electrodes. The collimating tubes of the photometer are arranged for projecting the monitoring beam at normal incidence on to the centre of the work-holder.

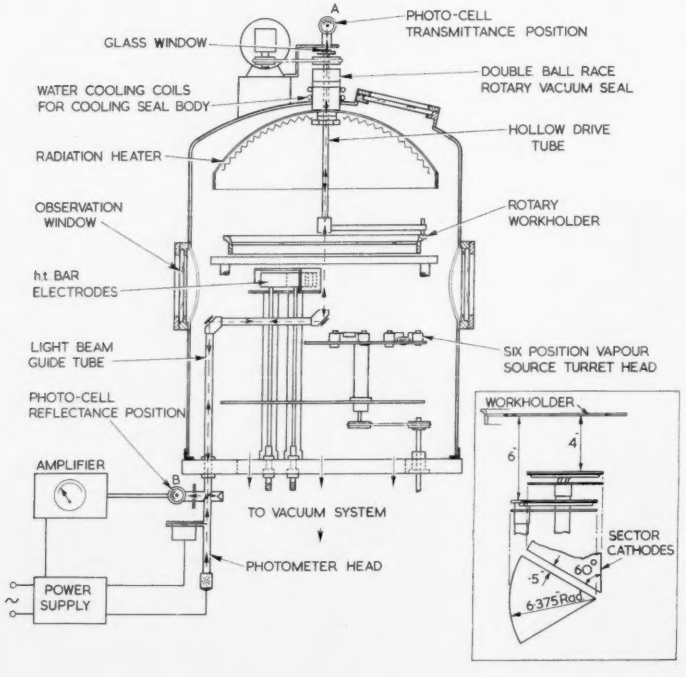

FIG. 3. Schematic drawing of the vacuum deposition apparatus showing the arrangement of chamber components illustrated in Fig. 2. When sputtered films are to be prepared the h.t. cleaning electrodes are replaced by the sector shaped electrodes as in the inset.

with the monitoring beam reflected back over the incidence path until it strikes a 45° beam-splitter in the photometer body which deflects it on to the photo-cell. The design of the photometer is dealt with in Section 3.

A radiant heater is mounted at the top of the vessel for heat treating the deposited coatings when required.

H.T. Cleaning System. The glow discharge cleaning system is that described by Holland[1, 24] for avoiding electron induced contamination of the work support and for obtaining maximum ion bombardment of the glass. It consists of a pair of aluminium bars mounted radially under the work holder and connected to an a.c. high tension supply as shown in Fig. 2. Shields are mounted above and below the bars so that the electrons traversing the twin cathode dark spaces are accelerated parallel to the glass which is bombarded by positive ions and electrons of low velocity. With such a system highly clean glass can be obtained in a few minutes at a power input of 5 kV and 160 mA. The bombardment at this rating is very intense and after 10 min a sheet of $\frac{1}{4}$ in. thick plate glass rises in temperature to 150°C, which prevents readsorption of contaminants before subsequent deposition. The gas pressure is controlled during bombardment by the system described in reference 2a.

Evaporation Sources. The conditions for obtaining uniform evaporated films on rotary plane holders when using vapour sources with approximately *point* or *surface* emission characteristics have been discussed by Holland Steckelmacher[3]. More recently Ring and Lissberger[4] have reported the degree of uniformity obtained when producing narrow band-pass filters of the Fabry–Perot type on a rotary work holder. Calculations show that a *point* vapour source should be placed under the edge of the holder at a normal distance (h) equal to the radius (r) of the holder, whereas for a surface source the optimum ratio of h/r is about 1.2 to 1.3. In our work using an open molybdenum boat closely approximating to a surface source, the optimum measured ratio is $h/r = 1.3$. whereas Ring and Lissberger found an optimum ratio in their experimental work of 1.7. Calculations show that the deposit should be very uniform for h/r values above 2 when using a point source. Obviously a greater h/r value will be required if the vapour atoms tend to be beamed in the vertical direction when leaving the source, as, for example, occurs when vapour is emitted from a deep narrow necked crucible.

In the plant described here six vapour sources are mounted on a turret head which can be rotated via a vacuum sealed shaft so that each source is brought in turn into the optimum position. This is preferable to arranging the vapour sources in circular array under the holder circumference because it permits the fitting of adjacent services such as the high tension electrodes, without obstruction of the vapour beam. Generally two kinds of vapour source have been used, namely, a metal foil boat and a wide necked alumina crucible with a tungsten spiral heater mounted internally which radiates heat on to the material to be evaporated.

A shutter is mounted over the vapour source for rapid termination of the evaporation.

Cathodic Sputtering. The range of materials which can be evaporated for high refractive index ($n \geqslant 2$) layers in interference filters is limited either because most of the high index materials dissociate during evaporation or have a low volatility. Zinc sulphide is widely used for high index layers because it evaporates without marked reduction. However, this material is unsatisfactory because it contaminates the vacuum system and the coatings are soft. For this reason ZnS is mainly used in filters which are protected with a cemented cover glass. It has been claimed[5, 6] that the rare earth oxides such as cerium oxide, evaporate without chemical reduction at low gas pressures, but exceptionally high temperatures and electrical energies are required for their evaporation and the evaporation rate is not easily controlled.

Dielectric films of high refractive index may be prepared by reactive sputtering of metals in an oxygen atmosphere, however they cannot be easily deposited in sequence for use in multi-layers with the normal cathode sputtering system. To overcome this problem Holland[7] has devised a sputtering system consisting of a pair of sector shaped cathodes mounted under the rotary holder as shown in Fig. 3. Each of the sector electrodes is connected to an a.c. high tension supply and sputters alternately on to the work holder. More than one material may be sputtered in sequence by fitting additional sets of cathodes, also evaporated films may be deposited on to the work holder during the same deposition cycle.

3. Modulated beam photometer

(1) *Choice of Photometer*

Various types of apparatus have been developed for controlling the thickness of dielectric films showing interference maxima and minima in their reflectance or transmittance factors. Dufour[8] determined the reflectance and transmittance maxima and minima with a photocell. Similar apparatus has been described by Turnbull and Belk.[9] Giacomo and Jacquinot[10] devised a more elaborate apparatus in which the rate of change of the reflectance or transmittance with wavelength ($dR/d\lambda$ or $dT/d\lambda$) could be determined at a given wavelength as the film grew ; the maxima or minima of the interference order occurring when the $dR/d\lambda$ or $dT/d\lambda$ become zero. A similar apparatus has also been developed by Ring and Lissberger.[4]

The foregoing apparatus can be used in the preparation of many kinds of interference film combinations but it is not suitable for the production of Fabry–Perot type filters using metal reflecting layers on either side of a spacer-layer. With this type of filter the principal wavelength of the pass-band can only be determined when the outer metal film is deposited. This is because the pass-band of the filter is not determined by the optical thickness of the spacer-layer alone. A phase change occurs in the light reflected at each of the spacer-to-metal layers which does not correspond exactly to π radians. Greenland and Billington[11] have invented a simple system for determining the pass-band during deposition of the spacer-layer but their apparatus is only suitable for use with a stationary receiver. Hermansen[12] has developed a polarimetric method of thickness control which can be used when Fabry–Perot filters with metal reflecting layers are deposited on a plane rotary work holder.

It would appear that control apparatus most useful for

Vol. 9 959/60

general work would be one which could be used in the preparation of all types of filters excluding those based upon the metal/dielectric/metal systems. For general production purposes the instrument should also be capable of controlling the thickness of transparent metal films and should not be limited to producing dielectric films of different interference orders. For these reasons it was decided to produce a photometer in which the monitoring light beam was modulated by a rotating shutter permitting the output from a photo-cell to be amplified by an a.c. amplifier. The apparatus has been termed a " modulated beam photometer ". This method of monitoring was chosen because the photometer is insensitive to both the daylight and the light from the vapour source reaching the photo-cell during the evaporation. Such an instrument has also been used on a sputtering plant without interference from the light of the glow discharge.

The modulated beam photometer consists of two principal parts, namely, the photometer head containing the optical unit and the electrical unit containing the amplifier and power supply. These are discussed in detail below.

(2) *The Photometer Head*

Introduction. The light source in the photometer head is an incandescent electric lamp. Two lenses and limiting apertures serve to focus the light from the lamp filament to a narrow beam which is modulated by a shutter in the form of a rotating disc, having 10 holes around its periphery (see Fig. 4). The disc is driven by a synchronous induction type clock motor at 200 rev/min directly from the 50 c/s a.c. mains so that the light beam is chopped at a frequency of 33 c/s. The modulated light passes through a beam-splitter arranged at an angle of 45°. The reflected light is lost in a side tube making a cavity in the wall and the transmitted light passes through a vacuum tight glass plug in the chamber baseplate. In order to make use of standard drillings in the baseplate of the evaporation plant it is necessary to have at least two reflectors arranged at about 45° to direct the light on to the surface film undergoing monitoring. The reflectors are protected against coating by evaporation and heating by the glow discharge used for sputtering or cleaning purposes by enclosing them in collimating tubes inside the vacuum chamber. The 45° mirrors are adjusted so that the beam passes down the centre of the collimating tubes and the surface to be monitored is adjusted to ensure normal incidence of the light beam.

For reflectance measurements the modulated light beam is reflected normally from the surface undergoing coating and passes back along its path through the glass plug to the beam splitter. The beam-splitter is made from a single $\lambda/4$-film of TiO_2 with a reflectance of about 45 per cent and almost no absorption. The light transmitted through the beam-splitter is lost while the reflected part passes through a suitable filter on to the cathode of a vacuum photo-electric cell.

For transmittance measurements the modulated light beam is transmitted through the coated glass and passes through a second glass plug mounted in a hollow shaft drive at the top of the vessel. The filter and photocell unit fitted to the main photometer head is detached and fixed above the hollow shaft drive for measurements of transmittance. Due to the loss of light at the beam-splitter there is about twice as much light available at the photocell cathode in transmission compared with that available in reflection.

Problems encountered in the design and construction of the photometer head can be summarized as follows :—

(a) The intensity of the incident light must be as high as possible when measuring very small transmittance and reflectance factors, but the intensity of the light reaching the photocell must not exceed a critical value above which saturation of the instrument occurs.

(b) Light must be prevented from reaching the photocell which has been reflected internally in the photometer head and did not come from the surface under investigation. Such spurious light signals will be called scattered light. Scattered light gives rise to a background reading on the photometer amplifier.

(c) The photocell and light source are outside the vacuum chamber so that the light has to pass through and out of the vacuum chamber. For reflection measurements on a large evaporation plant this means that light has to travel a distance of about 150 cm from the light source to the photocell.

(d) The light must pass through a standard vacuum seal in the chamber base plate which limits the width of the light beam on its return path to an aperture of about $\frac{1}{2}$ in. diameter.

(e) There must be no optical surfaces which produce normal reflections in the path of the monitoring beam because these would increase the amount of scattered light reaching the photocell.

Bearing in mind these problems and limitations the photometer construction shown in Fig. 4 was evolved.

The Light Source. The sensitivity of the instrument is governed by the quantity of light reaching the photocell. The problem was therefore to be able to gather as much light as possible from the source and getting it to the cell with the minimum of loss from stops, lenses, mirrors and scattering. The size of the light beam which can be used is limited by the dimensions of the photometer tubes and base plate drilling. The intensity of the light beam depends on the amount of light collected from the source bulb which ultimately depends on the temperature of the tungsten filament and the area of the lamp filament employed. Using the same condensing lens in turn in front of lamps of different wattage, namely 1/3, 6 and 32 W, the light transmitted to the photocell remained constant in intensity. This was because the lens gathered light from the same length of filament in each case, and all of the three bulbs gave a similar light output per unit length of filament. It was finally decided to use a 1/3 W lamp in which the condensing lens formed part of the bulb envelope. With these bulbs one has to rely on the filament being accurately mounted in the centre of the lens and a certain amount of selection is necessary to ensure a good central light beam. Tests on a batch of " Osram " lens flash lamp bulbs (2.2 V 0.2 A) have shown that a large percentage are usable even under the most stringent conditions.

We were rather surprised to find in early tests with 6 W car type bulbs that the light output from the bulb dropped considerably after only a few days continual use. In some

cases the glass surface of the lamps was considerably blackened. The short life was partly due to insufficient ventilation of the bulb and slightly increased filament voltages. However, when used under the conditions specified by the manufacturers these bulbs still had a short life. Similarly the 32 W projection lamp which requires fan cooling has a guaranteed life of only 100 h. The small wattage lamp now in use generally has a life of from 8–12 h, but is very inexpensive to replace. The lamp housing and the adjustments on the photometer for lining up the light beam are designed so that the lamp can be easily renewed.

The Lens System. Referring to Fig. 4 the lens L_1 in front of the lamp produces an image of the filament at a distance of about 1 cm behind it. For minimum scattering of light it is best to place a limiting aperture A_1 at this point the size of which is such that the light beam throughout the photometer head is less than $\frac{1}{2}$ in. (i.e. the limiting aperture of the transmission system). A second lens L_2 with a focal length at 10.16 cm is placed as near as possible to the modulator and this produces an image of the filament approximately at the photocell cathode. As the first image was approximately 10 cm away from this lens and the focused image is required at distances varying between 100–150 cm away (depending on the application) the effect of this lens is to produce an image magnified by about 10–15 times. As the apertures at the photocell are about 1 cm diameter it follows that the useful size of the limiting aperture A_1 can only be about 1 mm diameter and this in turn determines the portion of the emitting filament which is used. To allow for different distances between the surface to be tested and the photometer, the position of the light source and its aperture has to be adjusted relative to the lens L_2.

When considering the amount of light available it is clear that this is not determined by the solid angle subtended at A_1 but the very much smaller solid angle subtended at the lens L_2. This can only be increased by increasing the diameter of L_2, the distance between A_1 and L_2 being fixed by the distance between the photometer (L_2 in this case) and the surface being tested. The size of the aperture A_1 is determined by the size of the final image which can be usefully employed. In a photometer designed for maximum sensitivity, the light transmission system to the photocell would have to be at least as large as the photocell cathode and the size of the aperture A_1 could be increased accordingly. With the photometer here this modification would result in about four times as much light arriving on the active photocathode.

The Modulator. This consists of a disc rotated by a synchronous motor. In the early photometers the disc was connected to the motor by a small gear but some irregularity in rotation was introduced unless the bearings were accurately adjusted. Due to the sharp frequency characteristics of the amplifier any irregularity in light modulation causes unsteady meter readings. Small irregularities in rotation have no effect on the meter if the meter is sufficiently damped and additional damping was introduced by inserting a 2000 μF capacity in the output circuit. Also the modulator disc was mounted directly on the motor shaft.

The frequency of modulation depends on the speed of rotation of the motor and the number of holes in the disk. Circular holes were spaced to provide approximately equal open and shut periods. The waveform produced by the shutter is unimportant as the tuned amplifier will shape any signal to a nearly perfect sine-wave. Slotted holes could be used in the rotary disc but to get maximum light transmission it would be necessary to line up the lamp filament parallel to the length of the slots.

The early model of the modulated beam photometer was made to work at a frequency of 66 c/s but it was found that the amplifier could not be made sufficiently selective of the frequency to cut out all unwanted 100 c/s light signals. Light is modulated at 100 c/s chiefly by fluorescent discharge lamps and to a lesser extent by the filament in the evaporation plant. An amplifier tuned to 66 c/s could be made to cut a 100 c/s signal to less than 30 per cent. If the amplifiers were tuned to 33 c/s then the 100 c/s signal would be cut to less than 10 per cent. Consequently it was decided to use a 33 c/s modulation frequency.

Beam Splitter. The beam splitter is necessary when making reflection measurements at normal incidence but it creates two serious problems :

1. The amount of light available at the photocell is reduced by a factor of 4 as 50 per cent of the light is lost every time the beam splitter is traversed ;
2. It reflects and transmits a large amount of light on to the photometer walls which may by scattering reach the photocell.

The effect of light scattering is greater when either the amplifier sensitivity or light source intensity is raised to aid the measurement of low values of transmittance or reflectance. With the early instruments an intolerably high level of light scattering was present. In the first photometers the back of the beam-splitter was bounded by the inside of the main photometer tube which was painted with various black paints to reduce the reflection of scattered light. The best paint surface proved to be a base coating of black poster paint (water soluble) treated when dry with a coating of Johnson's Camera Black. With this coating the " zero " photometer reading as normally used (i.e. with a green absorption type filter in front of the photocell) comprised about equal scale readings due to scattering and amplifier noise.

However these precautions were still insufficient when the photometer was operated at maximum sensitivity without the absorption filter in front of the photocell, because the effect of scattered light increased the residual " zero " by a factor of 150–200. Thus in tests without an optical filter more than full scale deflection was obtained in the least sensitive amplifier range because of the high degree of light scattering.

Experiments were carried out by cutting a hole into the tube at the place where all the light was reflected. When the beam of light was let out into the dark room through this hole, this source of scattered light could be made negligibly small even without the filter in the photometer. Due to space limitations in the coating plant a light trap surface had to be placed within 2 in. of the beam splitter. Experiments were therefore carried out to determine the best inclination of such a surface. With a plane surface at about $1\frac{1}{2}$ in. from

Vol. 9 959/60

the beam splitter and inclined at 60° to the reflected beam as in Fig. 4 a " zero " reading of about ½ F.S.D. on the most sensitive photometer range could be obtained with the light beam not reduced by a filter.

Light was also prevented from reaching the photocell by reflection from the faces of the vacuum sealed glass plug in the baseplate by mounting it so that the light beam did not impinge on the glass at normal incidence.

Measurements without an optical filter are not foreseen at the moment and the residual light scattered in the instrument under the foregoing conditions is not excessive. Thus if the light scattering and amplifier noise are taken as a

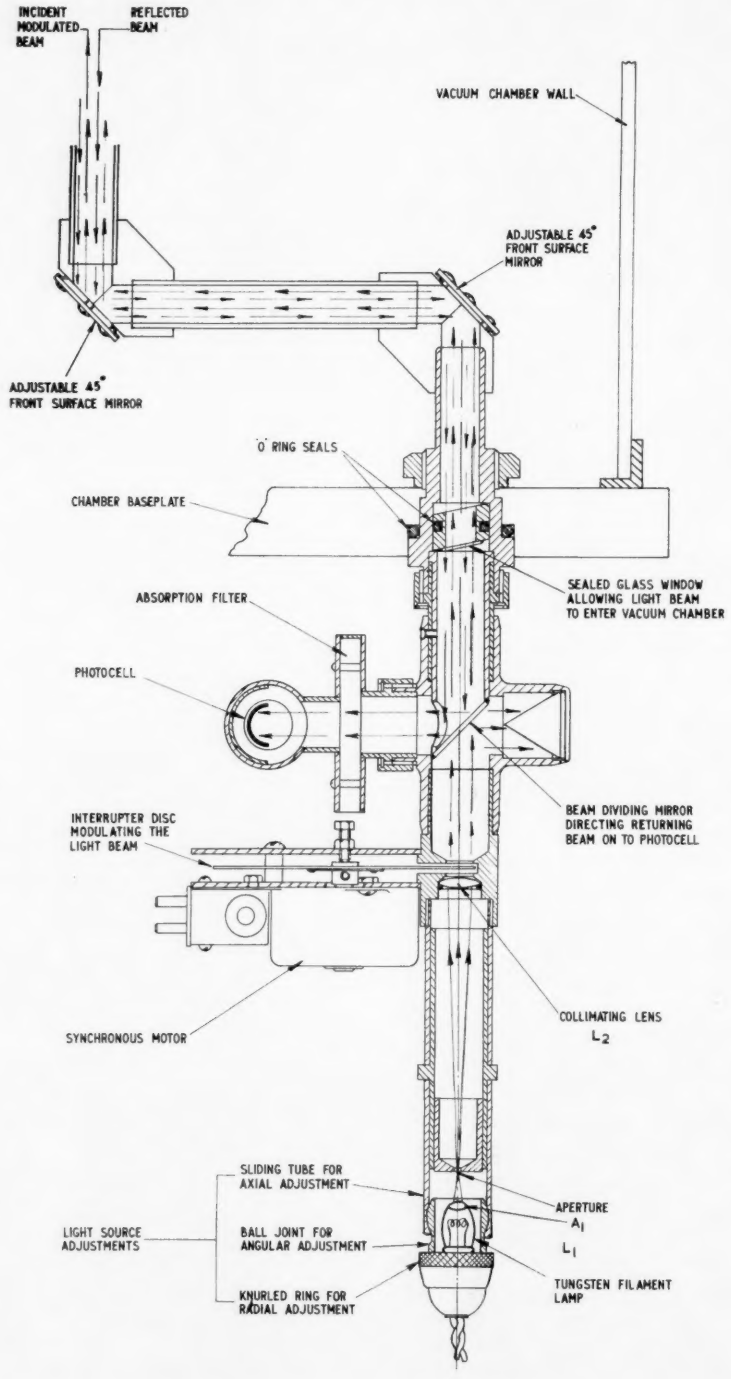

FIG. 4. Modulated beam photometer.

fraction of the reading obtained when measuring the total reflectance of parallel glass blank (R = 8 per cent) then both residual effects amount to less than 1.6 parts per thousand.

(3) *The Photometer Amplifier*

Introduction. The photometer amplifier converts the weak 33 c/s signal received at the photocell into a reading on a robust mA meter. Signals at other frequencies particularly 0–10 c/s due to steady or slowly varying background illumination and 100 c/s due to illumination from filaments, lamps and discharge devices operating from the 50 c/s a.c. mains are effectively rejected while the unit is also insensitive to 50 c/s a.c. mains pickup. This has been achieved by a conventional R–C coupled 4 stage a.c. amplifier having a twin–T–R–C filter network arranged in negative voltage feedback across the second stage. This filter is tuned to give maximum attenuation to the 33 c/s signal. The negative feedback stage incorporating this filter will pass the 33 c/s signal (minimum feedback) while signals at all other frequencies will be much attenuated (maximum feedback). The other stages of the amplifier have been designed to give a fall off in frequency characteristics for both high and low frequencies so that an amplifier with very sharp frequency selectivity is obtained.

Design considerations. The input stage and degree of amplifications required need to be specially considered. The amount of light received at the photocell will vary from one extreme of very sparse illumination, e.g. when measuring the reflection from a single surface to the other extreme of considerable light intensities, e.g. in measurements involving the transmission of light through uncoated glass plates or lenses. It was estimated that a variation in amplifier gain covering a range of 10,000/1 would be required. Also it may be required to make comparative measurements in which for any given light intensity (at any level between the two extremes) the amplifier should be adjusted to give full scale deflection at the output meter.

These requirements were met by fitting a switch on the input stage which would alter the photocell load resistance and in addition to this by fitting a gain control at the input to the third stage. The effect of the load resistance change also serves the purpose of preventing undue voltage drop at the photocell for large light intensities, i.e. large photoelectric currents. At the beginning of this work it was clear that very little light would be available under certain conditions of use.

Under extreme conditions of light intensities, i.e. when measuring the light reflected from a glass surface using a " Wratten " type absorption filter, the amplifier was still required to have sufficient gain to give more than full scale deflection with switch and gain control turned to maximum sensitivity. Preliminary tests were therefore carried out using an unmodulated light source and straight amplifier to indicate the maximum amplification which would ultimately be required. It was found that the minimum input signal to the amplifier would be of the order of 60–100 μV and consequently an amplifier which would give full scale deflection for a signal less than 50 μV was aimed at.

There is a definite limit for the minimum signal which any amplifier is capable of differentiating from a background of random signals appearing in the amplifier. Because such signals are in fact usually at quite random frequencies this background is termed " noise ", i.e. the signal-to-noise ratio has to be sufficiently high. The various theoretical sources of noise were analysed and may be expressed in terms of an equivalent noise voltage appearing at the amplifier input. It was shown that the total noise voltage would be at most of the order of 2 μV, i.e. a 4 per cent reading when the amplifier is operating at maximum gain (assuming a sensitivity of 50 μV F.S.D.).

In addition to these random noise voltages there are two other main causes of signals other than true input signals which may appear in the output amplifier. These are, (i) signals picked up by stray electrical or magnetic fields varying at some frequency accepted by the amplifier and (ii) the effect of mechanical vibration on components and valves. Both these mainly act on the input stage and special precautions had to be taken to guard against them.

Pick up can be considerably reduced by adopting certain principles in wiring, earthing and screening of the amplifier and by providing sufficient attention to 100 c/s hum from the rectified d.c. supplies. Electromagnetic pickup at the input can be much reduced by having the shortest possible current loops in the grid circuit of the input valve. Pickup within the input valve and the effect of vibration on the valve can be much reduced by choosing a valve specially designed for low noise and microphony. We have therefore used 6BR7 valves (Brimar) throughout the amplifier. An EF86 valve (Mullard-Philips) was also tried and gives a similar performance but these two types are not interchangeable. A new development in valves to withstand vibration and giving generally a more reliable service is the new range of so called " trustworthy " valves. There is some indication that the " trustworthy " equivalent of the 6BR7 (type G6059) gives a slightly improved performance with regard to vibration. Mechanical vibration is generally more erratic than other forms of interference and its effect on the amplifier is consequently more difficult to measure. Experiments with the early experimental photometer amplifier showed that mechanical vibrations could seriously effect the readings of the amplifier and under the worst condition could represent 50–100 μV input. The ideal solution would be to mount the amplifier in such a way that no vibrations are picked up. This is hardly practical, however, since the photometer is used on a coating plant and even if it was mounted on a separate shelf, vibrations could still be transmitted through the photometer head coaxial cable. Experiments were therefore carried out to devise special anti-vibration mountings of the input stage. We found that one rough and ready test of the effectiveness of any design was to place the amplifier on a wooden laboratory bench with a rotary pump running only about 12 in. away.

While the present anti-vibration mounting does not entirely eliminate vibration pickup, it much reduces the effect and must be regarded as a compromise between simplicity and perfect anti-vibration mounting. The chief difficulty is the low working frequency of the amplifier.

Vol. 9 959/60

In early experimental work there was a considerable microphonic effect due to vibration and flexing of the coaxial input cable (connecting the photocell to the input stage of the amplifiers). This effect was shown to be due to the generation of local electrical charges on the polythene insulation of the coaxial cable due to rubbing of the metal braiding. We now use a special cable (type PTIIMS) made by " Telcon " which has a conducting coating on the surface of the polythene.

All pickup and noise effects are best measured by the residual output reading obtained on the meter when there is no input. This measurement is best carried out by shutting the photocell against any light. If the measurement is attempted with the input lead disconnected the coaxial input socket on the amplifier has to be screened with an earthed dummy plug to prevent ordinary a.c. pickup.

Tests of residual noise voltages in the latest design have shown that the theoretical figure of about 2 μV is approached. A sensitivity of about 30 μV F.S.D. has been achieved with the switch and gain control at maximum. Hence, the unavoidable noise voltage accounts for a reading of about 6 per cent maximum gain and this clearly shows that no further increase in sensitivity of the amplifier is justified. The complete circuit of the photometer is shown in Fig. 5a and discussed in detail below.

Input Stage. The signal comes from the photocell. This is a blue sensitive vacuum cell on a B7G base (Cinema Television type V.A. 50 or Mullard type 90 A.V.). The photocell cathode is at earth potential, the anode being connected to the conductor of the coaxial socket. The photocell is connected to the amplifier by an approximately 10 ft length of coaxial lead using coaxial plugs at either end.

The anode voltage is obtained through the load resistances R1 or R2 connected to a potential divider across the h.t. supply. The signal appearing on these load resistances is fed through C_2 to the grid of the input valve. The long length of coaxial input cable has a considerable capacitative shunting effect, even at this low frequency, so that load resistance R_2 and R_1 have to be 100 MΩ and 1 MΩ respectively to get a range factor of 10. The cable capacity is approximately 120 pF which corresponds to an impedance of about 40 MΩ at 33 c/s. To get the exact range factor R_3 may have to be adjusted or an additional shunting capacity may be inserted across R_3.

The input valve, together with the following components of the first stage : R3, R6, R7, R8, C2, C4, C5, are all mounted on a block of brass or steel weighing about 3 lb. This is suspended by " Silentbloc " bonded rubber instrument suspensions to suppress the effect of vibration on the input valve. Suitable stops have to be fitted to this suspension to limit its travel when subjected to strong impacts. The connections of the circuit to the components on the anti-vibration suspension have to be made carefully so that no additional restraints are imposed. Short lengths of bare 30 S.W.G. tinned copper wires have been found suitable. Three other conditions have to be watched :

1. The wire connecting to the input must be kept away from the h.t. carrying conductors because of capacitative pickup when the input lead is vibrating.
2. The input wire must be kept short to prevent inductive pickup from stray a.c. fields (from nearby transformers, etc.).
3. It must also be remembered that the rubber mounting acts as an insulation and therefore the whole block has to be separately earthed to the chassis.

Noise and Vibration Sensitivity. The theory of anti-vibration mountings is discussed in Ref. 13. It is shown there that a successful low frequency anti-vibration mounting has to be very massive or very complex. Previous methods of resilient mountings tried by us were much less effective than the present design.

In sensitive amplifiers special attention has to be given to the wiring layout especially in the first stages of amplification. The greatest source of trouble can arise in the wiring of the earth returns of decoupling circuits in each stage. If the chassis is used as the earth and different points of the chassis are used to connect components to earth it is possible to obtain chassis currents which can inject unwanted signals into the input stage. A single wire earth lead was therefore adopted in this amplifier one end of which is connected to the negative of the supply and the other end, near the input, is connected to the chassis. All decoupling condensers and earth leads were connected to this line in the order shown on the circuit diagram and no trouble due to interaction between stages was experienced.

To reduce hum from imperfect smoothing of the d.c. h.t. supply this is progressively decoupled by R–C-filters towards the input stage. High R.C. products could be obtained with small capacitors and this method is more economical than perfect smoothing of the whole d.c. h.t. supply. Hum from the heater was prevented by using a rectified heater supply. The heaters of all the valves were connected in series and therefore a smoothed d.c. supply of 150 mA, 25.2 V was required.

Of the various possible sources of noise in an amplifier working with a high value of input resistance, the predominant source is due to the thermal agitation of electrons in the input resistance (see Ref. 14–15). Nyquist has shown that the RMS input voltage equivalent to this noise is given by the expression

$$(4KTRB)^{\frac{1}{2}} \text{ Volts}$$

where K = Boltzmann's const
T = absolute temperature
R = input resistance
B = bandwidth of amplifier

The noise voltages to be expected under various conditions are given in the table below :—

R	B		
	1 c/s	10 c/s	100 c/s
1 MΩ	0.25 μV	0.76 μV	2.5 μV
10 MΩ	0.76 μV	2.5 μV	7.6 μV
100 MΩ	2.5 μV	7.6 μV	25.0 μV

These voltages have to be compared with the figure of 50 μV

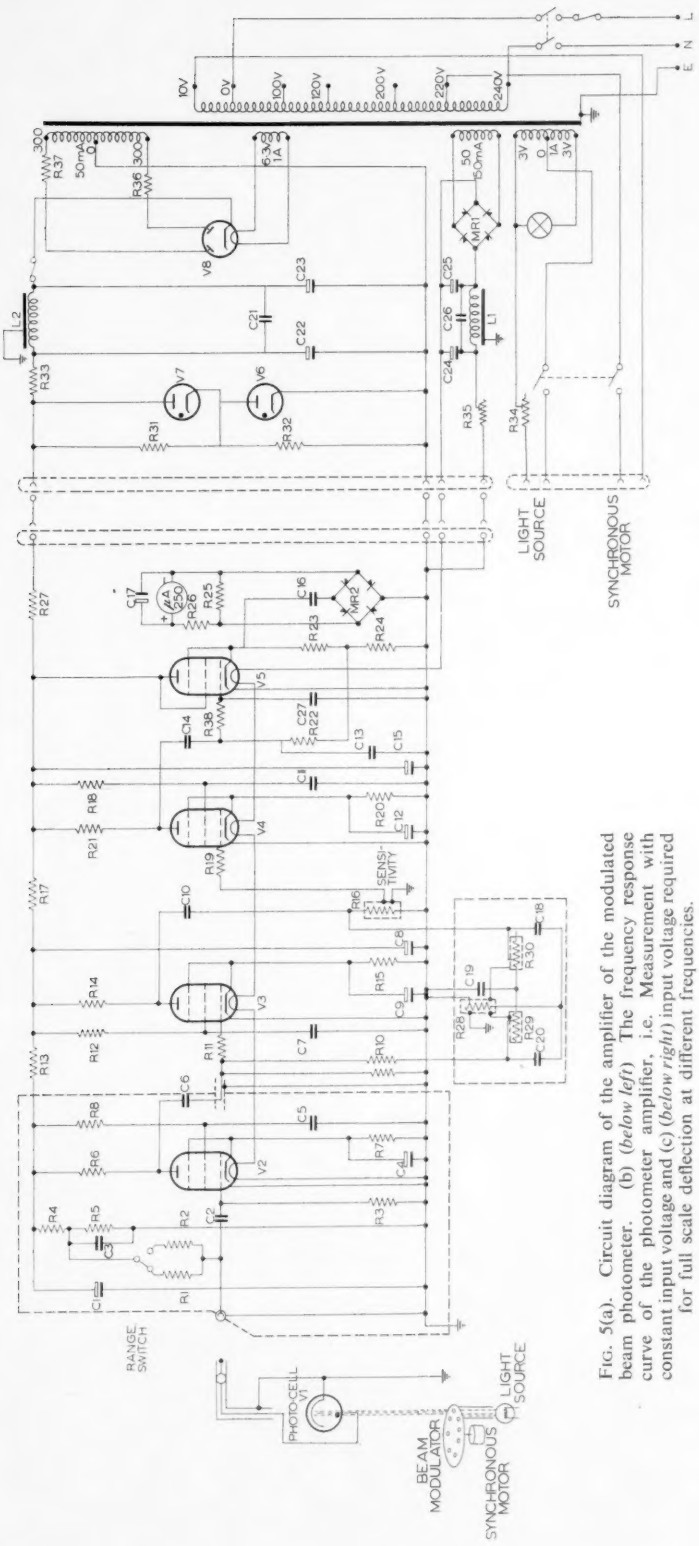

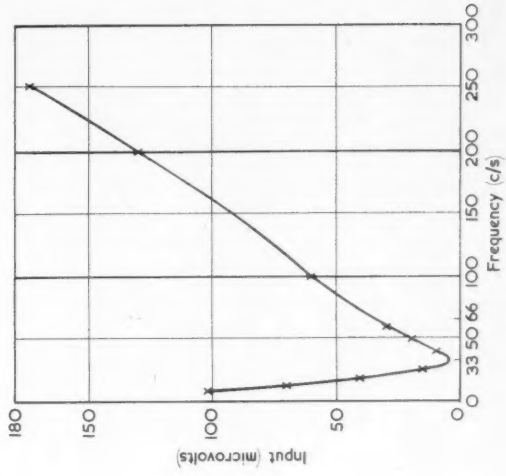

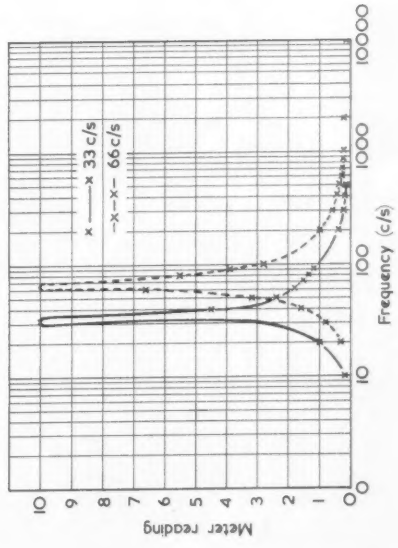

FIG. 5(a). Circuit diagram of the amplifier of the modulated beam photometer. (b) (*below left*) The frequency response curve of the photometer amplifier, i.e. Measurement with constant input voltage and (c) (*below right*) input voltage required for full scale deflection at different frequencies.

Vol. 9 959/60

which was the sensitivity (full scale deflection) aimed at. It is clear from this that the bandwidth should preferably be less than 10 c/s and the input resistance not more than 10 MΩ. The maximum R.M.S. noise voltage would then be 2.5 μV, i.e. 5 per cent of the reading at maximum sensitivity. In practice a noise voltage of this order was observed.

Frequency response and filter circuits. The second stage in the amplifier has a twin-T filter circuit arranged in degenerative feedback. The frequency selective properties of such a network are well known. The twin-T network can be pictured as a super-position of a low-pass and high-pass filter. At higher frequencies a frequency selective amplifier is usually best designed using a parallel tuned circuit of an inductance and capacitance. At low frequencies the inductance would have to be large and elaborate screening of the coils would be required to reduce the 50 c/s voltages induced by stray fields in the inductance elements. The twin-T network has the advantages of only using resistance and capacitance elements and tuning is achieved by using 3 variable resistances. The sharpness of tuning which can be achieved by a twin-T network in a feedback amplifier is limited and no cut-off is achieved at frequencies far removed from the tuned frequency. The equivalent Q-factor of a selective feedback amplifier of this type is approximately one-half the amplifier gain (without feedback) between the ends of the filter. The selectivity may be considerably improved by incorporating additional low-pass and high-pass filter elements into the amplifier which in effect cut off the unwanted high and low frequency signals.

Good low frequency cut-off in a R.C. coupled A.C. amplifier can be easily achieved by proportioning the interstage coupling condensers. Together with the anode load and input resistance they form a high-pass R.C. filter network. If the capacitance values are chosen to give a slight attenuation at the working frequency, then considerable attenuation of the signal will occur at much lower frequencies.

Good high frequency cut-off is achieved by inserting a low-pass R.C. filter. The effect of a low-pass filter element in which $\omega CR = 1$ at the working frequency f ($\omega = 2\pi f$) is to reduce the voltage at this frequency by about 30 per cent actually the voltage ratio is $1/\sqrt{2}$. The rejection factor at the second and third harmonic (i.e. at 66 c/s and 99 c/s) of such a filter can be defined as the ratio of the output voltages at these frequencies to the output voltage at the fundamental. The rejection factors of a single π section low-pass filter element for the second and third harmonic is 0.63 and 0.45. Lower rejection factors are obtained if more low-pass filter elements are put in series, but we found that with a single filter section between the third stage and the output valve sufficient attenuation of higher frequencies (particularly 100 c/s) was obtained.

The frequency characteristics of the whole amplifier is shown in the two graphs given in Fig. 5b. In Fig. 5b a constant voltage of 20 μV is applied to the input of the amplifier and the output current as seen on the meter is shown plotted against frequency. It is seen that full scale deflection is obtained at 33 c/s while readings at 25 c/s and 50 c/s drop to 1/4. At 100 c/s output currents for the same input voltage drop to less than 1/10th of full scale deflections. The residual noise of this particular amplifier with all controls at maximum sensitivity corresponded to about 5 per cent of full scale deflection (i.e. 1 μV).

These results can be compared with the best obtainable with an amplifier made for 66 c/s (see dotted curve in Fig. 5b). In that case the reading at 100 c/s dropped to only 28 per cent and at 50 c/s to 32 per cent.

In Fig. 5c an input sufficient to obtain 20 per cent of full scale deflection over a range of frequencies from 10 to 250 c/s is applied to the amplifier. The graph shows a plot of the required input signal against frequency. It is seen that at 100 c/s a signal of 58 μV is required, i.e. to obtain the same output as at 33 c/s a signal 14.5 times as strong is required at 100 c/s.

Output stage and meter circuits. The voltage obtained after the third stage of amplification is quite sufficient but if this is used to drive a 1 mA meter the loading is too high resulting in poor sensitivity and linearity. The fourth stage is therefore a cathode follower valve whose output is fed to the 1 mA rectifier and meter through a 0.2 μF condenser.

(4) *Supply Unit*

Normally in equipment of this type in which the amplifier is not very bulky, the power unit and amplifier would be accommodated in the same box. In this case with an amplifier tuned to 33 c/s which is very near the mains frequency (50 c/s), there is a great risk of electrical pickup in the amplifier. It was therefore decided from the start to separate all 50 c/s a.c. voltages from the amplifier by using separate boxes for amplifier and power supply. To prevent pickup from the heater current supply to the amplifier valves this current was also rectified so that only the residual 100 c/s ripple from the full wave rectified d.c. supplies appear in the amplifier box.

The power unit then contains a mains transformer supplying all h.t. and heater voltages as well as the supply to the light source and synchronous motor. Conventional full wave rectification is followed by π smoothing filters. The h.t. is stabilized against mains voltage fluctuations by two 150 V gas filled stabilizing valves to give a total of 300 V d.c. output. Tests were carried out to show the necessity of the precaution to prevent any a.c. reaching the amplifier although this might have been achieved by suitable electrical screening.

The voltage supply to the light source is obtained from a winding on the mains transformer and the output voltage is adjusted to the correct rating of the lamp by a series resistance. It was established that with normal mains voltage fluctuations there was no need to stablilze this voltage during the short periods in which measurements are carried out with the photometer. If stabilization of the lamp supply should prove desirable a small constant voltage transformer would probably give sufficient stability.

4. Uses of the vacuum deposition plant

The deposition apparatus described earlier has been used for the preparation of optical film systems involving single and multi-layers, and the results of this work are discussed below after a brief account of the manner in which the modulated beam photometer is arranged for monitoring.

Vo
9
1959

(1) *Setting Up the Photometer*

Monitoring Wavelength. It is usually necessary to use filters in combination with the photometer to obtain a response within a desired wavelength interval. When depositing broad-band filters such as beam-splitters or neutral density filters, Wratten type absorption filters may be used with the photometer. The response curves of a group of such filters has been plotted in Fig. 6, together with that of the photocell and tungsten lamp used in the photometer. The combined response curves for the complete measuring system when used with the different filters is given in Fig. 7 and the normalized response curves in Fig. 8. Also, given in Fig. 8 is the half-width of each filter combination, $\Delta\lambda_{\frac{1}{2}}$, i.e. the bandwidth at half peak transmission. The bandwidths cover several hundred angstrom units and thus could not be used for accurately setting the maximum transmission

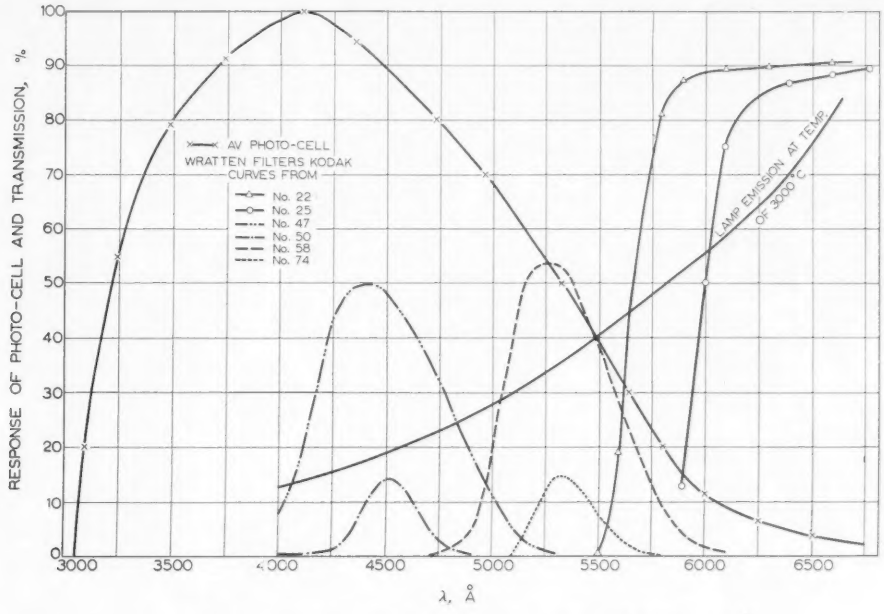

FIG. 6. Transmittance and response curves as a function of wavelength of a range of Wratten filters, tungsten filament lamp and photocell used in the modulated beam photometer.

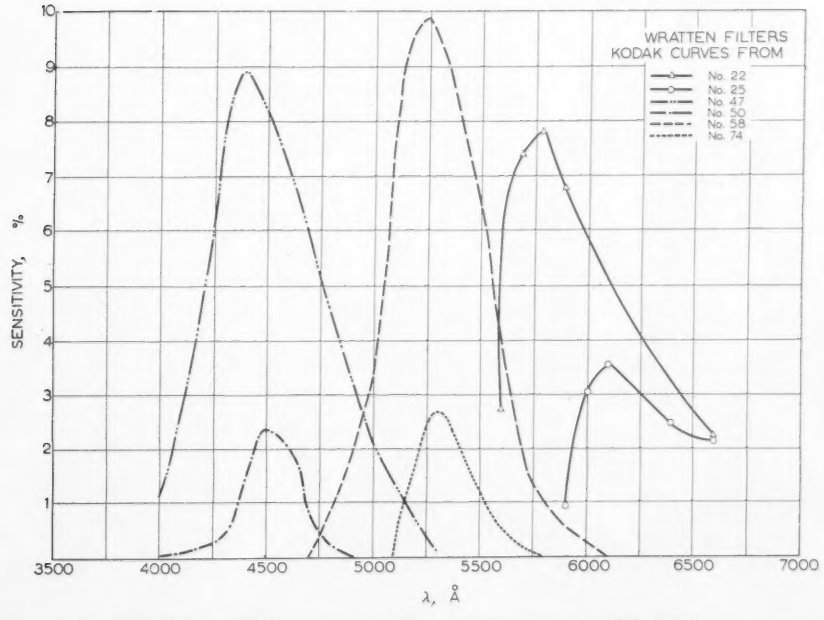

FIG. 7. Combined response as a function of wavelength of the modulated beam photometer when used with separate Wratten filters.

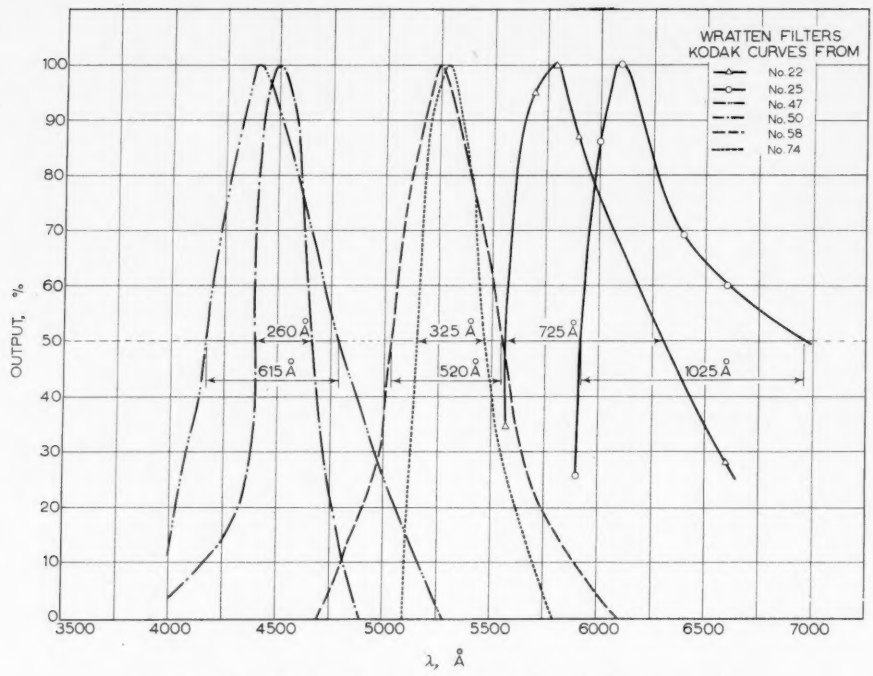

FIG. 8. Normalized version of the curves shown in Fig. 6. together with values of the wavelength band-width $\Delta\lambda_{\frac{1}{2}}$ of the filter system measured at half peak response.

wavelength of narrow band-pass filters. For the latter work a source of monochromatic light is essential (e.g. a monochromator or calibrated interference filter). However when the light beam falling on the photocell is of a high intensity, as for reflectance or transmittance values approaching 100 per cent then two or more Wratten filters may be used in series which sharpens up the peak response curve and prevents the light saturating the photocell.

Calibration of the Photometer. The photometer reading is initially adjusted using a glass or coating of known reflectance or transmittance so that all other measurements read from the meter are in terms of the initial setting. Thus, when the receiver is a parallel sided glass blank with a refractive index of 1.5 the total reflection from both surfaces is approximately 8 per cent at normal incidence and the meter reading is set accordingly. The reflection from the uncoated side of a glass blank can be reduced to zero by blackening the surface to make it absorbing (a solvent suspension of graphite known as " Dag " is suitable for this purpose). Thus, when one of the surfaces of a glass blank is being anti-reflection coated the change in the reflectance can be made to occupy the full scale of the photometer meter, i.e. the initial meter reading can be set to read full-scale (R = 4 per cent) which falls nearly to zero and not half-scale reading when the lens coating is complete.

When the instrument is used for measuring transmittance the meter is initially set to read 100 per cent which falls to 92 per cent when the glass blank is inserted. If the photometer is saturated when measuring high values of transmittance then the light beam must be attenuated as already discussed above. When the coating being prepared is a neutral density filter then a similar filter can be used for reducing the light intensity. The response of the instrument may then be raised by a known amount during the coating of evaporated filters of low transmittance by removing the attenuating filter which has a calibrated optical density.

(2) *Single Layer Beam-Splitters*

Titanium Dioxide. The deposition apparatus can be used for preparing metal films with a specified transmittance as described above. Thus, a typical use of the apparatus is controlling the thickness of evaporated titanium films which are subsequently heat oxidized in air to form titanium dioxide beam-splitters[16, 17].

When the completed beam-splitter is to have an optical thickness of $\lambda/4$ for green light the Ti-film is deposited until the transmittance (measured with Wratten Filter No. 74 $\lambda = 5300$Å) has fallen to 8–10 per cent (Hass[16] gives a value of 5 per cent measured at $\lambda = 5500$Å). Holland *et al.*[18] have found that the Ti-films used for beam-splitters may react with the glass base when oxidized at 400°C but this can be prevented by depositing a base layer which is chemically inert to the titanium at high temperature, for example, MgF_2, Al_2O_3 or SiO. When a $\lambda/4$ film of MgF_2 is used for the base layer the resulting beam-splitter has almost equal transmittance and reflectance for white light which is effective over a large range of incidence angles. With this system the glass support is first coated with a $\lambda/4$-film of MgF_2 which on a glass with a refractive index of 1.5 reduces the reflectivity of a single surface from 4 per cent to 1.5 per cent. The titanium is then evaporated until the transmittance is 8–10 per cent and the film combination baked at 400°C in air.

Sputtered Bismuth Oxide. As discussed in Section 2 metal oxide films may be prepared by reactive sputtering using the sector shaped cathodes shown in Fig. 3. In the apparatus described here the cathodes are arranged at a height which will not impede the vapour stream should the sputtered film be coated with an evaporated layer. The sector electrodes are set at different heights as shown in Fig. 3, so that the cathode dark space and the uniformity of the glow discharge above each cathode is not affected by the neighbouring sector. It has been shown elsewhere that a cathode electrode may have dead zones at the edges if it is in close proximity to an anode electrode as discussed in reference 2(b).

The Bi_2O_3 is sputtered in a stream of pure oxygen at 2.5 kV and 500 mA using an a.c. 50 c/s supply. The light from the unrectified glow discharge does not affect the modulated beam photometer and the growth of the sputtered film can be determined by measuring its transmittance. The refractive index of Bi_2O_3 is about 2.45 so that the reflectance of a $\lambda/4$-film on glass is about 38 per cent. The sputtering is ceased when the transmittance has fallen to 62 per cent which takes about 8 min. Rapidly sputtered films have been found to have the least optical absorption (A $\simeq$ 2 per cent). The uniformity of the sputtered oxide layer obtained with the sector cathodes has been shown in Fig. 9 in terms of the transmittance at $\lambda = 5300$Å of a $\lambda/4$ thick film measured across the diameter of the rotary work holder.

(3) *Heat Reflecting Gold Mirrors*

Thin gold films with low optical absorption may be prepared if they are sandwiched between two Bi_2O_3 films, because the oxide coatings prevent the metal film from developing a granular texture[19]. Holland and Siddall[20] have investigated the use of this film combination as heat reflecting mirrors on observation windows where the yellowish tinted transmission colour of the metal film can be tolerated. Heat reflecting coatings of 450Å Bi_2O_3/100Å Au/450Å Bi_2O_3 can be produced with a transmittance of 73 per cent at $\lambda = 4500$Å and an integrated reflectance of 74 per cent over the wavelength interval 0.9–2 μ. Such film

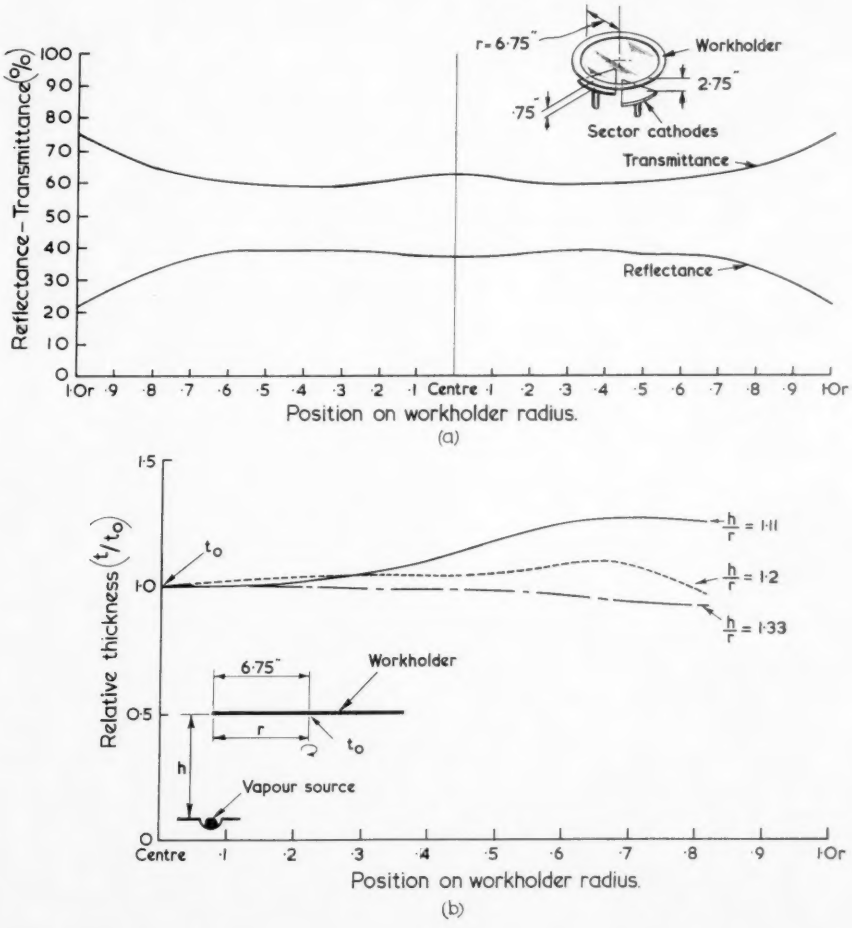

FIG. 9. (a) Reflectance and transmittance of a $\lambda/4$-film of sputtered bismuth oxide measured across the diameter of the rotary work-holder to illustrate the distribution of the deposit, (b) relative thickness of MgF_2-films evaporated from a molybdenum strip with a dimple holding the MgF_2. Film thickness measured by multiple beam interferometry[26].

Vol. 9 959/60

combinations may be prepared by first sputtering Bi_2O_3 from the sector cathodes so that the transmittance, measured at $\lambda = 4500$Å, falls to 62 per cent. Gold is then evaporated from a molybdenum boat and the outer layer of Bi_2O_3 is then deposited until the transmittance rises to 75 per cent. The Bi_2O_3 films form anti-reflection coatings on either side of the gold layer.

(4) *Two Layer Anti-Reflection Coating*

Glasses of low refractive index ($n = 1.5$) cannot be efficiently anti-reflection coated because the index of the currently used film material (MgF_2) is too high to satisfy the relation $n_{film} = \sqrt{n_{glass}}$, which must be fulfilled to reduce the reflectance to zero. Various multi-layer interference systems have been proposed to overcome this difficulty, but the most simple is that in which the glass reflectivity is augmented by application of a thin high index film before deposition of the low index layer. Such a system has been fully analysed by Sawaki and Kubota[21] and for a given pair of materials the approximate optical thickness of each layer can be easily determined from a vector formed by the three boundary amplitude coefficients. The greatest obstacle to the production of two layer anti-reflection coatings is the provision of a durable high index layer. Holland and Putner[22] have solved this problem by using Bi_2O_3 sputtered from sector cathodes with MgF_2 evaporated from an offset source under a rotary work table. The uniformity of sputtered Bi_2O_3 films produced from sector cathodes has been discussed in an earlier section and the uniformity of evaporated MgF_2-films deposited on a rotary table is shown in Fig. 9b.

At commencement of deposition of the two-layer film the photometer is set to read 8 per cent (reflectance of both glass surfaces) and the Bi_2O_3 sputtered until the reflectivity of the exposed surface is raised to 8 per cent, i.e. 12 per cent including the reflection from the uncoated side. The total enhanced reflection may be made to read nearly full scale and the MgF_2 then evaporated until the reflectivity, after passing through a small maxima, falls to minimum value, i.e. a residual reflection of less than 0.05 per cent from the coated surface.

The reflectance of the two-layer coating is not symmetrical on either side of the wavelength minima but rises steeply on the short wavelength side. This has the effect of making the transmission colour strongly yellow when the anti-reflection coating has a minima in the green, because less blue light is transmitted than red. Almost untinted coatings can be prepared for use in visible light by making the reflectance minima occur in the near green ($\lambda = 5000$Å). This cannot be achieved by measuring the reflectance using a green filter because the reflectance changes slowly in the region of the minima, which prevents accurate setting of the wavelength at which the minima occurs. The problem has been solved by measuring the reflectance with a blue filter (Wratten No. 50 $\lambda = 4550$Å) and ceasing the evaporation of the second layer when its reflectance rises by a known amount above the minimum for the blue. With this method the Bi_2O_3 is deposited until the reflectance of one surface has risen to 9 per cent, the MgF_2 is evaporated until the minima has been passed and the reflectance has risen to 0.5 per cent. Both coatings are then arranged to be effective at $\lambda = 5000$Å. Shown in Fig. 10 is the reflectance of a two-layer anti-reflection coating measured across the diameter of the work holder which demonstrates the uniformity of the coating and the low value of reflectance obtained.

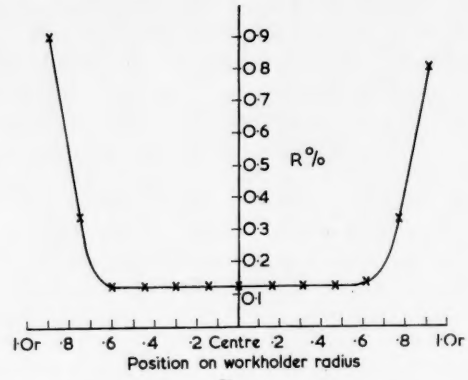

FIG. 10. Reflectance of two-layer anti-reflection coating measured across the diameter of the rotary work-holder.

(5) *Dichroic Mirrors*

The novel properties of multi-layer coatings of high and low refractive index materials have been well discussed. Banning[23] in an early report described the preparation of multi-layer interference films for beam-splitters and polarizing filters. Such optical systems are currently prepared by evaporating ZnS and cryolite. These two materials are preferred because of their large difference in refractive index and relative optical stability when protected with a cemented glass. The sputtered Bi_2O_3 coatings discussed in the earlier section may be used in combination with evaporated low index films. However, the uniformity obtainable at present

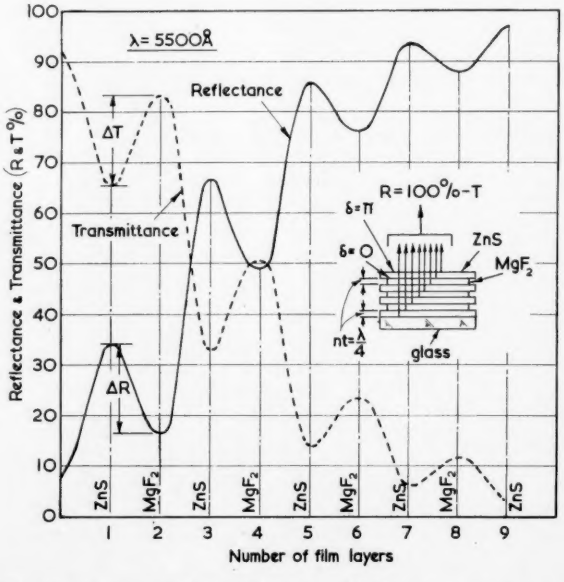

FIG. 11. Curve showing continuous reduction in R and T with increasing number of dielectric layers in a interference type filter.

with the sector cathode system limits the maximum number of films for most purposes to five layers, whereas it has been reported that as many as 31 layers have been deposited using evaporated high and low index films of ZnS and cryolite.

Uniform films of ZnS and cryolite (or MgF_2) may be prepared by evaporation using the filament turret head in the plant described here.

When a high-low index stack is being deposited the difference in the reflectance or transmittance (ΔR or ΔT) between the interference maximum and minima progressively decreases as the number of layers is increased. Fig. 11 shows that, when monitoring in reflection, the value of ΔR becomes quite small after nine layers have been deposited.

Lindberg and Ireland[25] have overcome this difficulty using a photo-electric device in which two photo-cells were connected in series opposition. One photocell was illuminated by monochromatic light reflected from the specimen, the other cell was illuminated by an ordinary incandescent light source with a variable control. By adjustment of the illumination on the second cell and of a shunt on the meter, which was in series with the two cells, each quarter wavelength film deposited could be made to produce full scale deflection on the meter. Such a system becomes complex when applied to the modulated beam photometer described here. However, the exceptional high gain of the photometer amplifier can be used to increase the indicated scale change between maximum and minimum if the films are monitored in transmission and T and ΔT are measured. If the gain of the amplifier is increased so as to obtain full scale deflection each time T decreases to a low value, then the scale range occupied by ΔT can be maintained at a measurable quantity for coatings up to 21-layers. An example of a filter made in this way is shown in Fig. 12.

Our thanks are due to Mr. K. Hacking, formerly of these laboratories, for his valued assistance in the development of the early models of the photometer described here, and to Mr. A. S. D. Barrett, Technical Director of Edwards High Vacuum Ltd., for permission to publish this account.

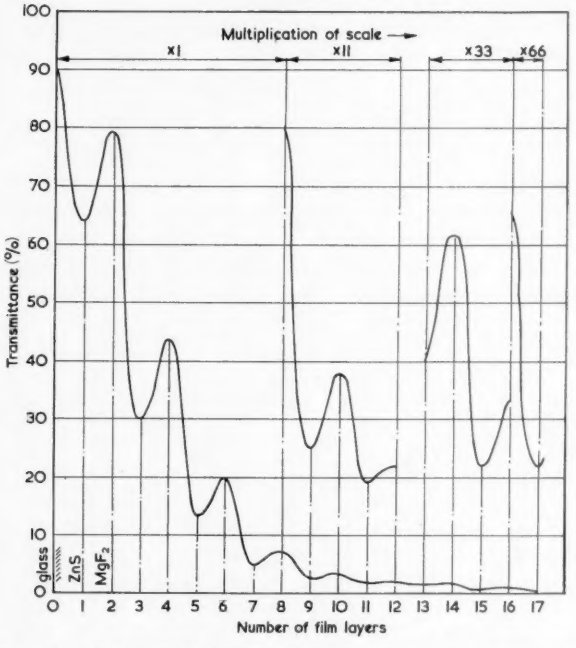

FIG. 12. Curve showing how the photometer scale can be expanded to increase changes between interference maximum and minimum when working in transmission.

References

1 L. Holland ; *Nature*, **181**, 1451 (1958).
2 L. Holland ; *The Vacuum Deposition of Thin Films*, Chapman & Hall Ltd., (a) p. 87 : (b) p. 426 (London 1956).
3 L. Holland and W. Steckelmacher; *Vacuum*, **2**, 346 (1952)
4 J. Ring and P. H. Lissberger ; *Optica Acta*, **2**, 42 (1955)
5 G. Hass and J. B. Ramsey ; *J. Opt. Soc. Amer.*, **45**, 408 (1955).
6 A. Vogt; *Brit. Pat.* 697,403 (April 1950) Patent.
7 L. Holland; *Nature*, **177**, 1229 (1956).
8 C. L. Dufour; *Le Vide*, No. 16–17, 480 (1948).
9 D. T. Turnbull and J. A. Belk ; *Laboratory Practice*, **1**, 403 (1952).
10 P. Giacomo and P. Jacquinot ; *J. Phys., Radium*, **13**, 59A (1952).
11 K. M. Greenland and C. Billington, *J. Phys., Radium*, **11**, 418 (1950).
12 A. Hermansen ; *Nature*, **167**, 104 (1951).
13 J. A. Harings ; *Phil. Res. Rep.*, **3** (1948), **4** (1949).
14 R. Wilson ; *Rev. Sci. Instrum.*, **23**, p. 217–223 (May 1952).
15 Valve and circuit noise, D.S.I.R. Radio Research Special Report No. 20.
16 G. Hass ; *Vacuum*, **2**, 331 (1952).
17 L. Holland, K. Hacking and T. Putner ; *Vacuum*, **3**, 159 (1953).
18 L. Holland, T. Putner and S. Bateman ; *J. Opt. Soc. Amer.*, **47**, 668 (1597).
19 E. J. Gillham and J. S. Preston ; *Proc. Phys. Soc. Lond. B*, **65**, 649 (1952).
20 L. Holland and G. Siddall ; *Brit. J. Appl. Phys.*, **9**, 359 (1958).
21 T. Sawaki and Kubota, H. ; *Science of Light*, **2**, 128 (1953).
22 L. Holland and T. Putner ; *Brit. J. Sci. Instrum.*, **36**, 81, 1959.
23 M. Banning ; *J. Opt. Soc. Amer.*, **37**, 792 (1947).
24 L. Holland ; *Brit. J. Appl. Phys.*, **9**, 410, 1958.
25 V. L. Lindberg and M. J. Irland ; *J. Opt. Soc. Amer.*, **45**, 328 (1955).
26 S. Tolansky ; *Multiple-Beam Interferometry*, Oxford Press (1948).

Vol. 9 959/60

The Measurement of the Pressures of Various Gases by means of a Pirani Gauge

S. VEIS

Department of Physics, Faculty of Natural Sciences, Komensky University, Bratislava

(Received 1 March 1959)

The relation between the gas pressure and the potential difference existing across the diagonal of the Wheatstone bridge, E_{12}, which is a function of pressure, has been determined for a Pirani gauge. Using this relation, calibration curves for various gases may be calculated from Pirani gauge calibration curves for a given gas.

1. Introduction

A disadvantage of the Pirani gauge (and of the thermocouple gauge) as compared with the McLeod manometer is the varying response to various gases[2–5]. It is necessary, therefore, to calibrate these gauges for each gas separately, which is a rather inconvenient and time-consuming procedure.

The aim of this work is to develop a theoretical relationship between the pressure and the quantity used to measure pressure. Usually, pressure is determined by the current flowing through a microammeter across the diagonal of the Wheatstone bridge. It is, however, preferable to use a voltmeter with a very high internal resistance such as a valve voltmeter[6]. The gas pressure is then recorded in terms of the potential difference, E_{12}, existing across the diagonal of the Wheatstone bridge.

For the thermocouple gauge, the problem of obtaining the appropriate theoretical relationship was successfully solved by Rubinshteyn[7] and Khavkin[8].

2. Calculation of the calibration curve for a Pirani gauge

E_{12} is given by the simple formula

$$E_{12} = E\left(\frac{R_3}{R_1+R_3} - \frac{R_4}{R+R_4}\right) \tag{1}$$

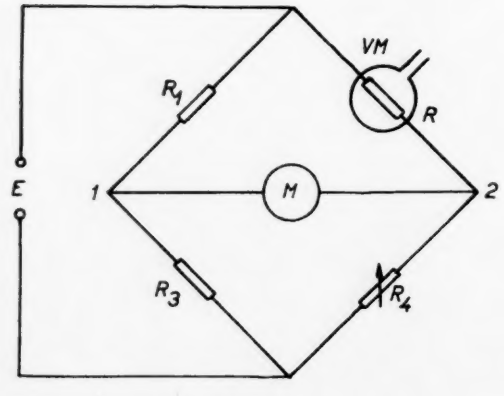

FIG. 1.

where R is the resistance of the Pirani gauge element, R_1, R_3, and R_4 are the resistances of the remaining three arms of the Wheatstone bridge, and E is the supply voltage across the bridge (fig. 1).

If the Pirani element is a thin metallic wire, then its resistance at a given pressure p may be estimated using the equation

$$R = R_a(1 + \alpha_0.\Delta T) \tag{2}$$

where R_a is the resistance of the metallic wire measured at atmospheric pressure, α_0 is the resistance temperature coefficient, and ΔT the temperature difference corresponding to the decrease of pressure from atmospheric to the value p. If we further take into consideration that, if the bridge is balanced at atmospheric pressure, the equation

$$\frac{R_1}{R_3} = \frac{R_a}{R_4} = k \tag{3}$$

must necessarily hold true, equation (1) may be transformed to give

$$E_{12} = E\left[\frac{1}{1+k} - \frac{1}{1+k(1+\alpha_0.\Delta T)}\right] \tag{4}$$

This equation for E_{12} clearly demonstrates the importance of the appropriate selection of the resistance ratios given by equation (3) in the Wheatstone bridge. In a previous paper[6] it was shown that, for a metallic wire used as the Pirani element, the resistance ratio k must be necessarily less than unity.

This formula makes it possible to determine the relation between the pressure p and E_{12}, because the temperature difference ΔT corresponding to the pressure reduction from atmospheric to the value p may be determined by using the equation for the energy transfer W/unit time from unit area of the wire to the gas :

$$\mathrm{W} = \frac{\alpha}{4}\left(\frac{\gamma+1}{\gamma-1}\right)\left(\frac{2R'}{\pi T_0 M}\right)^{\frac{1}{2}} p(T-T_0') \tag{5}$$

where α is the accommodation coefficient, γ the ratio of the specific heats, R' the gas constant, M the molecular weight, p the pressure, T is the temperature of the heated wire and T_0 the ambient temperature.

The temperature T_0' in equation (5) is unknown. It is

however, a function of the mean free path of the gas molecules, λ, and thus also a function of the pressure p. If $\lambda \gg D$, where D is the diameter of the cylinder containing the metallic wire, even if $D > \lambda \gg d$, where d is the diameter of the wire, T_0' is equal to T_0. If it is, however, not true that $\lambda \gg d$, then $T_0' > T_0$. The difference $(T_0' - T_0)$ increases with the increase of pressure, in other words, this difference is inversely proportional to the mean free path of the gas molecules λ.

For lower pressures, for which the inequality $\lambda \gg d$ holds true, T_0' may be replaced by the ambient temperature T_0. For these pressures, the temperature difference may be calculated from equation (5)

$$T - T_0 = \frac{C}{a}\left(\frac{\gamma - 1}{\gamma + 1}\right)\frac{\sqrt{M}}{p} \tag{6}$$

where

$$C = 4aW\left(\frac{\pi T_0}{2R'}\right)^{\frac{1}{2}} \tag{7}$$

and a is a constant dependent on the dimensions of the wire.

The temperature difference ΔT appearing in equation (4) may be calculated by means of $(T - T_0)$ given by equation (6)

$$\Delta T = T - T_a = (T - T_0) - (T_a - T_0) \tag{8}$$

where T_a is the temperature of the wire at atmospheric pressure. The difference $(T_a - T_0)$ may be then calculated from the equation

$$R_a = R_0[1 + \alpha_0(T_a - T_0)]$$

where R_0 is the resistance of the wire at the temperature T_0, whence for $(T_a - T_0)$ it holds that

$$T_a - T_0 = \frac{R_a - R_0}{\alpha_0 R_0} \tag{9}$$

From equation (8) after performing a substitution for ΔT from equation (4), and for $(T_a - T_0)$ from equation (9), we get for $(T - T_0)$

$$T - T_0 = \frac{1}{\alpha_0}\left[\frac{R_a - R_0}{R_0} + \frac{(1+k)^2}{k}\frac{E_{12}}{E - (1+k)E_{12}}\right] \tag{10}$$

Comparing equation (10) with equation (6), we get for the pressure, p :

$$p = \frac{C}{a}\left(\frac{\gamma - 1}{\gamma + 1}\right)\sqrt{M}\frac{\alpha_0}{\frac{R_a - R_0}{R_0} + \frac{(1+k)^2}{k}\frac{E_{12}}{E-(1+k)E_{12}}} \tag{11}$$

From this equation, the pressure p for any gas could be determined, if the dependence of C on pressure were known for different gases. If, however, the calibration curve of a certain gas is known, it is possible to calculate the calibration curve from equation (11) for any gas by determining the pressure ratio for the two gases in question under the same conditions.

Under the same conditions, i.e. with the same potential difference, E_{12}, the pressure is a function of the molecular weight, M, the accommodation coefficient α, and of the ratio of the specific heats γ. This means that, for the same E_{12}, the pressure p of various gases will be different but C will be the same. This statement follows from equation (5) applied to the case of low pressures, if the condition $D > \lambda \gg d$ holds true. In this case, the expression $W/(T - T_0)$ at a constant $(T - T_0)$ for a given pressure of one gas remains the same. Using another gas instead of the gas in question under unchanged conditions, that is for the same value of E_{12}, this expression will remain constant. This means that W remains constant, and so does the value of C given by equation (7).

If values characteristic for the gas number 1 are marked with suffix 1, whereas values characteristic for gas number 2 are marked with suffix 2, we get for the pressure ratio

$$\frac{p_2}{p_1} = \frac{\alpha_1}{\alpha_2}\frac{(\gamma_2 - 1)(\gamma_1 + 1)}{(\gamma_2 + 1)(\gamma_1 - 1)}\sqrt{\frac{M_2}{M_1}} \tag{12}$$

Hence p_2/p_1, for the same E_{12}, is constant for two different given gases. Therefore, if p_1 for various values of E_{12} is known, that is if we know the course of the Pirani gauge calibration curve for the one gas, p_2 for the second gas can be calculated using equation (12), and thus the whole calibration curve for any gas may be determined, provided of course that the accommodation coefficient α for this gas is known. In Fig. 2, the calibration curves for the inert gases He, Ne, Ar, Kr, and Xe are given. The full lines are the experimentally determined calibration curves, while the dashed lines are the calibration curves calculated from equation (12), the values of the factors in this equation being given in Table 1.

TABLE 1

Gas	He	Ne	Ar	Kr	Xe
Molecular weight M	4,003	20,183	39,944	83,7	131,3
Ratio of the specific heats γ	1,66	1,64	1,67	1,68	1,66
Accommodation coefficient α	0,5	0,74	0,80	0,93	0,92
Ratio of the pressures p/p_{He}	1	1,49	2,00	2,55	3,11

Equation (12) may be also used to determine the accommodation coefficient α, when the accommodation coefficient for one gas, the material of the wire, and the calibration curves of the Pirani gauge for both gases are known. The calibration curves are necessary, if the pressure ratio p_2/p_1 has to be determined in a pressure range where $\lambda \gg d$. According to Khavkin[8], the accommodation coefficient α may be given as a function of the molecular weight M of the gas

$$\alpha = 1 - e^{-\beta\sqrt{M}}$$

where β is a constant which may be determined for the material in question.

For want of data on values of the accommodation coefficient for the tungsten wire and the inert gases in the literature, the accommodation coefficients for the inert gases given in Table 1 were obtained as averages computed from [8, 9], from values calculated using the above-mentioned equation as well as from equation (12) with the pressure ratio p_2/p_1 determined from the calibration curves of the tungsten

Vol. 9 959/60

wire Pirani gauge. This Pirani gauge was not identical with that for which the inert gas calibration curves of which are shown on Fig. 2.

From Fig. 2, it follows, moreover, that the theoretical calibration curve coincides with the experimentally determined calibration curve for lower pressures, for the range

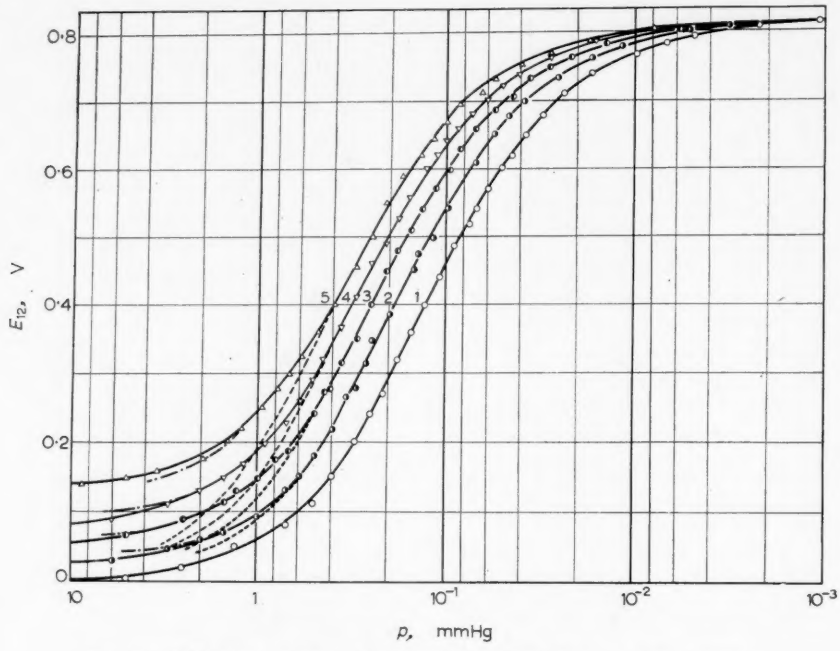

FIG. 2. Calibration curve of the Pirani gauge for the inert gases: 1–He, 2–Ne, 3–Ar, 4–Kr, and 5–Xe.

where the difference between T_0' and T_0 may be neglected. For higher pressures, rather considerable deviations are noted. The He calibration curve has been taken as a basis in our case. From Fig. 2, it is obvious that the deviation of the theoretical calibration curve as compared with the experimentally found calibration curve increases with increasing molecular weight, and, for this reason, it would be better to take as the basis the curve for a gas with a mean molecular weight. The relationship (12) may be applied to any gas, not only to the inert gases.

3. More accurate calculation of the calibration curve of the Pirani gauge

The calibration curves calculated using equation (12) for pressures higher than about 5.10^{-1} mm Hg show a deviation from the experimentally determined calibration curves. This deviation is due to the fact that, for these pressures, the condition $\lambda \gg d$ does not hold true, and thus $T_0' > T_0$. For this reason, equation (12) is not valid in a pressure range where T_0' is not equal to T_0. The difference $(T_0' - T_0)$ is, however, inversely proportional to the mean free path of the molecules λ, and this is, again, inversely proportional to the pressure, p, and to the square of the effective diameter of the molecules d_1^2. Owing to this, it may be written that

$$T_0' - T_0 = bpd_1^2$$

where b is the proportionality constant. Between the effective diameter and the molecular weight, a simple relationship exists, namely

$$d_1^2 = M^{\frac{2}{3}}$$

resulting from Table 2[10]. Only the effective diameter for He is too large. This relationship is verified for the other inert gases.

TABLE 2

Gas	He	Ne	Ar	Kr	Xe
Molecular weight M	4,003	20,183	39,944	83,7	131,3
Effective diameter of the molecule 10^8 d_1	2,26	2,7	3,4	4,3	5
10^{16} $d_1^2/M^{2/3}$	2,02	0,98	0,99	0,97	0,97

Using this relationship, T_0' may be written as follows

$$T_0' = T_0 + ApM^{\frac{2}{3}} \tag{13}$$

where A is the proportionality constant. When T_0' is substituted for in equation (5), we get for the reduced energy transfer W from unit area of the wire to the gas per unit time an equation with a higher degree of accuracy and valid also for higher pressures, namely

$$W = \frac{\alpha}{4}\left(\frac{\gamma+1}{\gamma-1}\right)\left(\frac{2R'}{\pi T_0 M}\right)^{\frac{1}{2}} p(T - T_0 - ApM^{\frac{2}{3}}) \tag{14}$$

This equation, when C from equation (7) is introduced, may be rewritten in the form

$$p = \frac{C}{\alpha}\left(\frac{\gamma-1}{\gamma+1}\right)\frac{\sqrt{M}}{T - T_0}\,\frac{1}{1 - AM^{\frac{2}{3}}\dfrac{p}{T - T_0}} \tag{15}$$

After performing a substitution for $(T - T_0)$ from equation (10), equation (15) assumes the form

$$p = \frac{C}{a}\left(\frac{\gamma-1}{\gamma+1}\right)\sqrt{M}\frac{\dfrac{a_0}{\dfrac{R_a-R_0}{R_0}+\dfrac{(1+k)^2}{k}\dfrac{E_{12}}{E-(1+k)E_{12}}}}{1-\dfrac{a_0AM^{\frac{2}{3}}p}{\dfrac{R_a-R_0}{R_0}+\dfrac{(1+k)^2}{k}\dfrac{E_{12}}{E-(1+k)E_{12}}}} \tag{16}$$

When this equation is compared with equation (11), it can be seen that the pressure p as determined from equation (16) is higher, for the right-hand part of equation (16) is divided by a factor less than unity.

For the pressure ratio of two different gases, provided that E_{12} is the same, we get a relation with a higher degree of accuracy, namely

$$\frac{p_2}{p_1} = \frac{a_1}{a_2}\frac{(\gamma_2-1)(\gamma_1+1)}{(\gamma_2+1)(\gamma_1-1)}\sqrt{\frac{M_2}{M_1}}\left(\frac{\dfrac{R_a-R_0}{R_0}+\dfrac{(1+k)^2}{k}\dfrac{E_{12}}{E-(1+k)E_{12}}-a_0AM_1^{\frac{2}{3}}p_1}{\dfrac{R_a-R_0}{R_0}+\dfrac{(1+k)^2}{k}\dfrac{E_{12}}{E-(1+k)E_{12}}-a_0AM_2^{\frac{2}{3}}p_2}\right) \tag{17}$$

The pressure p_2 appearing on the right side of this equation may be replaced by the pressure p_2' which is lower, and may be calculated from equation (12) as follows

$$p_2' = \frac{a_1}{a_2}\frac{(\gamma_2-1)(\gamma_1+1)}{(\gamma_2+1)(\gamma_1-1)}\sqrt{\frac{M_2}{M_1}}p_1$$

After an appropriate substitution, equation (17) assumes the form

$$\frac{p_2}{p_1} = \frac{a_1}{a_2}\frac{(\gamma_2-1)(\gamma_1+1)}{(\gamma_2+1)(\gamma_1-1)}\sqrt{\frac{M_2}{M_1}}\left(\frac{\dfrac{R_a-R_0}{R_0}+\dfrac{(1+k)^2}{k}\dfrac{E_{12}}{E-(1+k)E_{12}}-a_0AM_1^{\frac{2}{3}}p_1}{\dfrac{R_a-R_0}{R_0}+\dfrac{(1+k)^2}{k}\dfrac{E_{12}}{E-(1+k)E_{12}}-a_0A\dfrac{a_1}{a_2}\dfrac{(\gamma_2-1)(\gamma_1+1)}{(\gamma_2+1)(\gamma_1-1)}\sqrt{\dfrac{M_2}{M_1}}M_2^{\frac{2}{3}}p_1}\right) \tag{18}$$

For lower pressures, this equation assumes the form of equation (12), while for higher pressures, where the condition $\lambda \gg d$ is not satisfied, the agreement with the experimentally determined calibration curves of the Pirani gauge for the individual gases is better, as can be seen also from Fig. 2. The calibration curves calculated from equation (18) are drawn with a dot-and-dashed line on Fig. 2. From this diagram it is obvious that it is possible to calculate the calibration curve for any gas by using this equation, if the experimental calibration curve of the manometer for one gas is known. The calculated calibration curves coincide with the experimental calibration curves determined for the inert gases in a pressure range up to 2 mm Hg.

Conclusion

In this work, the mathematical dependence of the pressure p on the measured value of E_{12} was ascertained by determining the pressure under appropriately selected Pirani gauge performance conditions. Using this dependence, the calibration curves of the Pirani gauge for various gases can be calculated, if the calibration curve for one gas has been determined.

By means of this dependence, it is not possible to determine the course of the portion of the calibration curve which corresponds to higher pressures, where the condition $\lambda \gg d$ is not satisfied, i.e. if T_0' is not equal to T_0.

In the course of this work, it becomes evident that T_0' may be given by the equation

$$T_0' = T_0 + ApM^{\frac{2}{3}}$$

which is used to derive the relation with a higher degree of accuracy between the pressure p and the measured value E_{12} given by equation (16). Using this equation, the calibration curves for various gases may be calculated with a sufficient degree of accuracy, including the pressure range where the condition $\lambda \gg d$ is not satisfied.

In addition to the calculation of the calibration curves for various gases, equations (11) and (16), respectively, make it possible to calculate the calibration curves for the same gas, but using various supply voltages E, provided, of course, the calibration curve for a given supply voltage is known. When deriving the accurate dependence in such cases, heat carried off from the surface of the heated wire by radiation has to be considered, chiefly at lower pressures, because the radiation intensity increases rapidly because it is proportional to $(T^4 - T_0^4)$.

Analogous equations for the dependence of pressure on the measured value E_{12} could be derived also for the case of the Wheatstone bridge balanced under high-vacuum conditions.

References

[1] S. Dushman ; *Scientific Foundations of Vacuum Technique*, John Wiley & Sons, New York (1949).

[2] R. Jaeckel ; *Kleinste Drücke, ihre Messung und Erzeugung*, Springer Verlag, Berlin-Göttingen-Heidelberg (1950).

[3] H. Laporte ; *Vakuummessungen*, VEB Verlag Technik, Berlin (1955).

[4] Ya. Groskowskiy ; *Tekhnologiya vysokogo vakuuma*, translation from Polish, Izdatelstvo inostrannoy literatury, Moscow (1957).

[5] J. H. Leck ; *Pressure Measurement in Vacuum Systems*, The Institute of Physics, London (1957).

[6] Š. Veis ; *Mat. fyz. časopis SAV.* In press.

[7] R. N. Rubinshteyn and V. J. Fistul ; *Zavodskaya Laboratoriya*, **22**, 241 (1956).

[8] L. P. Khavkin ; *Zhurnal tekhnicheskoy fiziki*, **25**, 726 (1955).

[9] E. H. Kennard ; *Kinetic Theory of Gases*, McGraw-Hill Book Company, New York (1938).

[10] M. von Ardenne ; *Tabellen der Elektronenphysik, Ionenphysik und Übermikroskopie*, VEB Deutscher Verlag der Wissenschaften, Berlin (1956).

Vol. 9 959/60

Electrical Clean-up of Gases in Hot Cathode Discharge Tubes

G. CARTER

Department of Electrical Engineering, University of Liverpool

(Received 21 May 1959)

1. Introduction

When, in 1858, Plücker[1] noted a continuous reduction in pressure if a current was passed in a low pressure gaseous discharge tube, he was making the first recorded observations on the phenomenon of the electrical clean-up of gases, i.e. the removal of molecules from the gaseous phase under the influence of an electrical discharge. In Plücker's experiments the reduction in pressure was shown by the continuous increase in voltage required to pass a current through the gas, and subsequently, when the phenomenon was observed in Roentgen tubes it became known as hardening, since the emitted X-rays became more penetrating with increase in tube operating voltage.

Pietsch[2] reviewed the earlier research that had been carried out on gas clean-up until 1926 and it is clear that a large number of workers had investigated this phenomenon with a consequent wide variety of explanations to account for their observations. Generally it was found that one or both of two distinct types of clean-up were operative in the removal of gas molecules. The first type, known as chemical clean-up, was found to depend upon the presence of some chemical reagent, specially inserted in the discharge tube, which removed the gas molecules as a result of their interaction, and formed stable compounds. The first recorded application of such a reagent was by Malignani[3] in 1894, who used a viscous suspension of red phosphorus within a carbon filament incandescent lamp to remove residual gases from the tube, this material was the first of many which later came to be known as " getters " since they received and held the gas.

Where an electronic discharge is operating under apparently getter free conditions, chemical combination may still be an active mechanism in the clean-up process since activated gas molecules may react with the materials used in the construction of the tube. Langmuir[4] has designated this type of clean-up as " electro-chemical ".

When the disappearance of gas cannot be accounted for by any chemical processes however (e.g. with rare gases) then the second type of clean-up is said to be operating : Langmuir[4] designates this type as " electrical " or " electro-mechanical ".

This contribution will be concerned chiefly with the latter type of clean-up process, and more especially the case of gas removal from hot cathode discharge tubes in the presence of electron accelerating fields. Our attention will be confined largely to the clean-up into the walls of the discharge tube, since it has been found that this contribution is of major importance, but it must be remembered that sorption at the electrodes does occur ; this sorption has been the subject of a great deal of research but is beyond the scope of this paper.

Since Dushman[5] published an excellent review of the general phenomenon in 1947 the need has become apparent for experiments to be conducted under carefully planned conditions in order to clarify the physical mechanisms involved. As a consequence of a desire for a more detailed knowledge of the phenomenon, and because of its increased application in the achievement of ultra-high vacuum, notably by Alpert[6] and his co-workers, a number of interesting investigations have since been reported which lend themselves to a readier analysis. These investigations in which certain disagreements appear will be described in this paper, and it is the intention of the author, whilst attempting to summarise the present knowledge on the clean-up process, to resolve, with some reference to the author's own work at Liverpool, some of these disparities.

2. The experimental work

Much of the earlier work on the subject of clean-up was performed under conditions in which the fundamental processes involved could be obscured by secondary effects ; e.g. relatively high gas pressures were used with accompanying space charge effects, distortion of the discharge conditions and electrode sputtering occurred, etc. It was often impossible to distinguish between the electrical and chemical factors which influenced the clean-up and so much of this work could not be interpreted easily. Nevertheless, it would be an incomplete review if this earlier work was neglected and a brief résumé will be given, noting that Dushman has published an exhaustive synopsis of this work. It will be convenient to subdivide this chapter into the discussion of two topics, electrical clean-up in hot cathode tubes at higher pressures ($>1\mu$) under which conditions the earlier research was conducted, and the electrical clean-up in hot cathode tubes at much reduced pressures ($<0.1\mu$). The content of this second section will be concerned with the work of Von Meyeren[7] and Schwarz[8], who pioneered the low pressure techniques and from whose principles the more recent work has developed (these investigations were the latest reviewed by Dushman) and the post 1950 research which forms the major part of this paper.

3. Electrical clean-up at pressures higher than 1μ.

Campbell[9] investigated the relationships between the " blue glow " onset potential (a phenomenon in which a blue glow is observed in hot cathode discharge tubes at potentials greater than the ionisation potential), the gas pressure and

the clean-up of various gases, and found that the chemically active gases such as hydrogen, carbon monoxide, mercury and nitrogen were sorbed at more rapid rates than the inert argon. Chemical reaction or molecular dissociation explained the disappearance of CO_2 and H_2 but could not account for the sorption of A. Campbell concluded that the clean-up he observed was not primarily chemical, but that there was a dependency upon the nature of the gas and the cleanliness of the glass walls of the tubes.

Mrs Andrews[10] investigated the relation between the glow onset potential and such parameters as the electrode configuration, electron emission, gas pressure and anode potential ; her investigations are of interest since at higher pressures clean-up usually takes place only in the presence of the blue glow. Subsequently Andrews, Huthsteiner and Dushman[11] investigated the disappearance of N_2 and A at pressures in the region of 1μ, where blue glow is absent, and found that the clean-up rate varied almost linearly with gas pressure and electron current (at values of this below 1mA.). They found also that below anode potentials of 25V there was no sorption but above this and up to 250 V, the rate was practically voltage independent. Again it was observed that A cleaned up at a rate appreciably less than that of N_2.

Hughes[12] investigated the disappearance of N_2 and H_2 in a hot cathode tube, the walls of which were generally held at liquid nitrogen temperature, and concluded that clean-up was a result of molecular dissociation at the hot filament and the subsequent physical adsorption of atoms on the walls of the tube. Campbell and New[13], using sealed off triode type discharge tubes investigated the sorption of N_2, CO_2, O_2, H_2 and A. H_2, N_2 and CO_2 were found to clean-up at a faster rate than A, but the investigations on O_2 produced many inexplicable results. The freedom of the walls from occluded gas was observed to exert a profound effect upon the sorption, but evaporation of many different materials on to the walls had little effect. Campbell and New found that an equilibrium between disappearance of gas and evolution from the walls was established as a result of the release of occluded gas from the walls under the impact of the sorbing gas molecules, and they investigated the relationship between this equilibrium and the thermal history of the tube.

Finally, Huthsteiner and Dushman[14] made observations on sorption in vacuum incandescent filament lamps, and concluded that residual gases were removed as a result of the interaction of electrons, emitted from the low voltage end of the filament and accelerated to the high voltage end, and gas atoms.

The conclusions that can be drawn from this work seem to be that all gases clean up to some extent in the presence of an electronic discharge, the mechanism of reaction being dependent upon the nature of the gas and the condition of the walls of the discharge tubes, to which it seems fairly well established the sorbed gas adheres. It also seems to be established that the sorbing gases simultaneously release occluded gas from the walls and an apparent limit is set to the quantity of gas which can be sorbed.

There is disagreement however between the investigators as to the mechanism of clean-up. Dushman and his associates produced evidence to show that ions were the sorbing entities whilst Campbell & New and Hughes refuted this, but could not advance a satisfactory alternative.

This is a convenient point to conclude our survey of the earlier work, since the succeeding research has been conducted at lower pressures, and much of the earlier uncertainty of interpretation removed. It is hoped, that by collecting the results together some elucidation of any conflicting evidence may result.

4. Electrical clean-up at lower pressures

When the gas pressure in the discharge tube is reduced, the rate of formation of ions is also reduced, consequently it would appear that the rate of clean-up (at constant electron current) would decrease. Von Meyeren[15] compensated in part for the reduction in ion formation, caused by lowering the gas pressure, by increasing the path length of the ionising electrons before their collection. To achieve this he constructed his discharge tube with a tungsten filament cathode and a ring shaped anode, so that ionising electrons were not immediately captured by the anode but oscillated about the ring many times before collection. Von Meyeren also enclosed the tube within a solenoid to produce a magnetic field of up to 300 G. The electrons then followed helical trajectories in travelling to the anode, with a consequent increase in ionisation. In his initial investigations, with tubes sealed off from the pumps at initial pressures of 0.1 μ, Von Meyeren found that with a magnetic field of 280 G the rates of clean-up of H_2 and air were approximately equal and fell to zero in about 3 min (i.e. an equilibrium pressure was reached) but in the absence of a field H_2 cleaned up at roughly twice the rate of air (clean-up ceasing at much higher pressures but after about 10 min operation of the tube). In thees experiments the initial electron current was 1.5 mA and the electron accelerating voltages were 820 and 900 V for H_2 and air respectively. Von Meyeren observed in these experiments that when the discharge was stopped the pressure in the tube rose gradually to one-sixth its initial value, the full gas pressure could be easily restored by heating the tube to 200 °C. If, in the experiments using the magnetic field, when the pressure had reached an equilibrium value, the field was removed but the electron current left on, gas was re-evolved and the pressure rose. Von Meyeren found that the total quantity of gas cleaned up was never more than a fraction of that required to form a monolayer upon the walls of the tubes, and concluded that an equilibrium between the rate of clean-up and the rate of re-evolution from the walls was established.

Von Meyeren[16] subsequently extended his studies of clean-up under the influence of high anode voltages and magnetic fields to He, N_2 and A at pressures between 0.05 μ and 10^{-4} μ. He used similar discharge tubes to those previously employed and before each clean-up experiment rigorously baked the tubes in order to degass the walls thoroughly. A, he found, cleaned up in accordance with the law $-dP/dt = k(P - Pe)$, where P is the instantaneous pressure, Pe the equilibrium pressure finally established and k a constant depending upon the magnetic field strength and the anode voltage. The equilibrium pressure attained was observed to depend on the inverse exponential of the anode

voltage from 400 V to about 700 V, above which an increase in the accelerating voltage caused no further reduction in the equilibrium pressure, and similarly upon the inverse exponential of the magnetic field strength from 0–220 G, above which any increase had little effect upon the equilibrium pressure.

Helium cleaned up only in the presence of a magnetic field (240 G) but A and N_2 cleaned up regardless of the presence of such a field but at a reduced rate in its absence of course, the rate for N_2 was somewhat greater than for A. The quantity of gas sorbed in these experiments was observed to be in direct proportion to the pressure of gas at the start of an experiment and simultaneously the final equilibrium pressure was found to increase with increased starting pressure. Once again an evolution of gas took place when a discharge was allowed to continue after removing the magnetic field.

In 1940 Schwarz[17] published details of observations he had made in tubes similar to those used by Von Meyeren but including a second electrode, an electron repeller, beyond the anode. This electrode prevented electrons from striking the tube walls beyond the anode, and so outgassing them during an experiment. Schwarz employed anode voltages of up to 5000 V, and magnetic field strengths up to 2400 G and investigated the clean-up of air when both these parameters, and the initial gas pressure, were varied. Schwarz proposed that under the influence of electron and ion bombardment and the diffusion of occluded gases from within the glass walls of the tube to the surface, the interior surface of the glass walls of the discharge tube could stabilise at either of two potentials. One, such that the net surface charge was negative, the other such that the surface charge was positive. Under the former conditions the anode current could not be increased to more than a fraction of a mA but clean-up was observed both in the absence and presence of a magnetic field. Under the latter conditions, however, no clean-up whatsoever was evident but the anode current was generally in the region of 30 mA and appreciably more ionization must have been occurring. Capacitance methods enabled Schwarz to show that the wall charges were indeed as he had postulated, and by the insertion of a cylindrical metal screen covering the walls found that he could reproduce the observed current changes in the tube. Under no circumstances however would the metal clean up gas from the discharge. In this work Schwarz observed that no saturation of the walls occurred, as much gas as that required to form 1.7 monomolecular layers on the surface being sorbed without evidence of fatigue occurring, but he also observed that the state of the walls determined whether clean-up occurred or not, since the freedom of the walls from gas determined at which potential the walls would be stabilised.

In later work Schwarz[18] studied the clean-up at low pressures of H_2, N_2 and A in a conventional triode type of ionization gauge. The central tungsten filament in this tube produced thermionic electrons at currents of 1–2 mA, which were accelerated to a nickel wire electron collector spiral which surrounded the filament and was maintained at +110 V with respect to the filament.

The electrons oscillated many times about the spiral before collection and any ions formed by collision with the gas molecules were drawn to a cylindrical nickel ion collector whose axis was coincident with the central filament. By constraining the electrons to travel long distances before eventual collection Schwarz was able to maintain a relatively high rate of ion production at reduced pressures. The sorption rate was therefore maintained at a readily measured value, for example, H_2 cleaned up, by molecular dissociation at the heated filament, from 1.55 μ to 1.5×10^{-2} μ in 3 min. A and N_2 however were found to disappear only when ionization was produced. An interesting fact reported by Schwarz is that if one gas was cleaned up by the discharge and the discharge subsequently operated in a second gas, molecules of the first gas re-entered the gaseous phase, i.e. they were released from the walls, at which Schwarz showed they were held, by bombardment of ions of the second gas. Furthermore, continued running of the discharge resulted in clean-up of most of the second gas, whilst the first was re-evolved. It was also found that if a discharge was operated in these same two gases but in the reverse order, substitution of one molecular species for the other once again took place. In one experiment N_2 was cleaned up until the walls became saturated and when A was admitted to the discharge, a gradual replacement of N_2 by A on the walls was observed. Conversely if A was initially sorbed, a subsequent discharge in N_2 resulted in a substitution of N_2 for A at the walls. As a result of these observations, Schwarz concluded that the ionization gauge was unreliable as a pressure measuring device, since it not only lowered the pressure by its own operation, but any sample of gas introduced to it would be contaminated as a result of the substitution effects.

Before reviewing the data which has been accumulated since 1950 it is necessary to discuss at greater length the physical manifestation of the clean-up phenomenon. If, for example, an ionization gauge is sealed off at a known pressure and an electronic discharge is activated, providing that ionization occurs, gas molecules will be removed from the volume of the gauge by electrical and possibly chemical clean-up. Since the gauge is sealed off, a continuous reduction of pressure will take place. The gauge is therefore operating as a pump and possesses by definition a pumping speed equal to the slope of the curve relating the instantaneous rate of removal of gaseous molecules, i.e. the rate of clean-up, to the corresponding pressure. It should be possible therefore to describe a clean-up experiment in terms of a characteristic pumping speed and, as we shall see later, in some circumstances this description is possible. Generally speaking, however, the pumping speed of the gauge varies over the period of the experimental observations, usually decreasing as an experiment progresses as a result of saturation of the available pumping surface by sorbed gas, evolution of gas from the surfaces of the gauge by bombardment, etc. A more complete description of the clean-up process is therefore obtained by examining not only an instantaneous evaluation of the pumping speed, but the variation of this parameter with the duration of the experiment and other relevant factors, and also the quantities of gas which may be accommodated by the surface of the gauge.

Bearing these points in mind we will describe the experimental techniques used in the succeeding work, discuss the

results in terms of the pumping speeds and saturation quantities observed and indicate the theoretical attempts which have been made to describe the clean-up process.

In 1953 Alpert[19] published a work describing the advances made at the Westinghouse Research Laboratories in the achievement of ultra-high vacua, which contained a report on the use of an ionization gauge as a means of continuously evacuating a vacuum system by the pumping action associated with clean-up. The ionization gauge used by Alpert in this work was of a design developed to reduce the limit to the measurement of low pressures and was described by Bayard and Alpert[20] in 1950. In the conventional ionization gauge a lower limit is set to pressure measurement by inherent soft X-rays which liberate a large number of photo-electrons from the ion collector, and constitute, virtually a standing pressure. Bayard and Alpert reduced the X-ray limitation by reducing the ion collector surface area whilst maintaining a high pressure sensitivity with a favourable field configuration, using the now well known "inverted" electrode disposition.

Alpert measured the pumping speed of such an ionization gauge for N_2 by observing the time required for reduction of the pressure, in a gauge sealed off from the pumps, to $1/e$ of the initial value, assuming that the pumping action of the gauge could be described by a constant pumping speed and a constant rate of evolution of gas from the gauge surfaces (which is probably true for the initial period of the experiment at pressures of 10^{-4}–10^{-5} mm Hg which Alpert used). This pumping speed was found to be about 0.05 l./sec for an electron emission current of 10 mA which agreed reasonably well with data taken from Schwarz's earlier publication. Alpert also found that if the pressure was maintained at about 10^{-4} mm Hg by a continuous introduction of gas, the pumping action of the gauge ceased after about 1 h, saturation being evident at what approximated to monolayer coverage of the internal glass surface of the gauge by the sorbed gas. Furthermore, as predicted by this experiment, if the gas pressure was maintained at 10^{-9} mm Hg, the gauge would continue to pump for at least three months without any sign of saturation. Alpert found that both the pumping speed and ultimate pressure attained depended on the previous outgassing history of the gauge and the geometric design of the gauge. Comparison of the measured value of pumping speed with a theoretically predicted value (assuming that clean-up was due to the removal of gaseous ions at the ion collector only) showed order of magnitude agreement. As suggested by Alpert the probable reason for no better agreement than this is that in the Bayard–Alpert design of gauge the glass walls generally assume approximately cathode potential (demonstrated experimentally by Alpert) and consequently a large number of ions strike the walls and are removed there, calculated speeds cannot include this contribution and will be too low. Alpert recognised that the pumping action of the gauge was a disadvantage when it was used as a pressure measuring device, but showed that by using low electron emission and short intermittent periods of operation only this drawback could largely be overcome.

Bloomer and Haine[21] published details of a comprehensive study of the clean-up of residual gases in several different types of ionization gauge. They employed the same technique of measurement as Alpert, sealing off the ionization gauge from the pumps at a known residual gas pressure and observing the resulting decrease in pressure (using the gauge itself as the pressure manometer) when an electronic discharge was operated. Experiments were performed using three different designs of ionization gauge, namely the conventional cylindrical sheet ion collector type; a modification of this in which the ion collector was replaced by a continuously wound wire spiral and a Bayard–Alpert type of gauge. The pre-run treatment (i.e. the method of baking, radio frequency or conductive, the use of Hg or oil diffusion pumps and refrigerated traps) was varied but for all combinations of gauge and treatment the resulting clean-up curve was of the form illustrated in Fig. 1, where a semi-

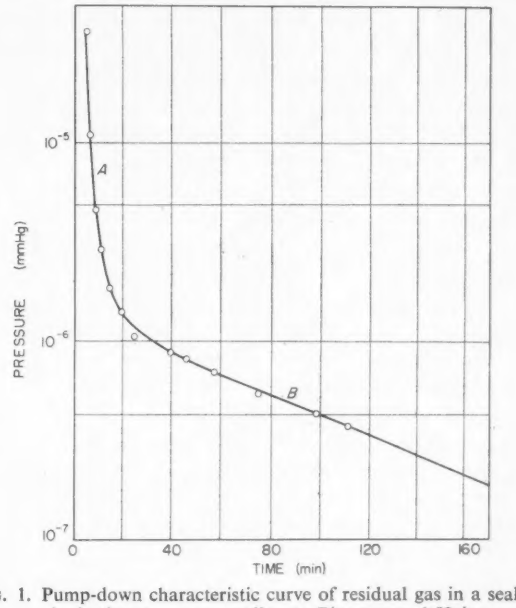

FIG. 1. Pump-down characteristic curve of residual gas in a sealed-off ionisation gauge, according to Bloomer and Haine.

logarithmic plot is made of the pressure versus the time after initiating the discharge. On consideration of this curve it is apparent that the speed of pumping of the gauge which conventionally would be proportional to the slope of the log pressure/time curve is not constant, in fact Bloomer and Haine subdivided the curve into an initial '*A*' region and a subsequent '*B*' region in which the pumping speeds were approximately constant but different. They found that the pumping speed in region '*A*' (about 0.004 l./sec at an emission current of 1.25 mA) was generally about 20 times that in region '*B*' and after some time the clean-up rate in region '*B*' decreased to zero when an equilibrium pressure was established. The pressure at which the gauge was sealed off had no marked effect upon the fraction of the initial pressure at which the knee between regions '*A*' and '*B*' occurred.

Since it was generally assumed that clean-up was related to the formation of ions, experiments performed by Bloomer and Haine to verify this assumption would appear to be of vital interest. By varying the electron emission current

Vol. 9 959/60

it was possible to relate the rate of clean-up to the rate of production of ions. In region '*A*' of the clean-up curve, a linear dependence of pumping speed upon emission current was found, as expected if the sorption of ions is the operative mechanism, but in region '*B*' the speed was proportional to emission only below a value of the latter of 50 μa, above this, up to 10 mA, the rate was independent of the electron emission. These results led Bloomer and Haine to study the efficiency of removal of ions from the gauge by calculating the ratio of the rate of removal (from the observed pressure drop) to the rate of formation of ions (measured by the collected current). A correction was applied from experimental observations to the second of these quantities to take into account the ions which do not strike the ion collector but strike the walls of the gauge. In the Bayard–Alpert design it was found that 80 per cent of the ions formed struck the walls, but even in this case the removal efficiency was only 6.5 per cent in region '*A*' and 0.34 per cent in region '*B*'. A strong dependence of the tube temperature on the rate of evolution was observed leading Bloomer and Haine to believe that the inefficiency of clean-up could be accounted for by a simultaneous evolution of sorbed gas, particularly in region '*A*' of the curve. After the clean-up experiments, exploration of the surface of the gauge with a fine flame showed, by observations of the instantaneous pressure rise which occurred, that in a conventional sheet ion collector type of gauge the cleaned up gas was located on the inner glass surface in the region near the ends of the ion collector, while in the other two types the region of clean-up extended along the length of glass opposite the electrode structure. Bloomer and Haine found further that if the glass walls of one of the spiral ion collector tubes was coated with aquadag, no sorption occurred, but if the tube was cracked open and a 2 cm wide gap, around the circumference of the gauge made in the aquadag, pumping occurred at the '*B*' rate. Experiments to test Schwarz's belief that sorption depended on the state of charge of the walls, by application of suitable potentials to judiciously placed electrodes inside and outside the gauge showed no such dependence. Finally if the electron collector was heated to different temperatures by a conduction current, no change in the sorption rate was observed, this vitiated a tentative theory advanced by Bloomer and Haine in which active molecules desorbed from the electron collector under electron bombardment were sorbed at the walls.

Bloomer and Haine concluded from their observations that clean-up was not primarily due to removal of ions from the discharge, since the pumping speed in region '*B*' was virtually independent of electron emission, but constant in each of the two regions. No other explanation that was advanced could adequately explain all their observations but they held the view that the part played by excited molecules was significant.

Varnerin and Carmichael[22] in 1955, investigated the effect of deposited metallic films on the inner surfaces of Bayard–Alpert gauges on the clean-up of He. The method used was similar to those described previously, but the initial electrode outgassing was minimised to prevent evaporation of metal on to the walls. The gauge was sealed off from the pumps at a low background pressure, filled to approximately 10^{-4} mm Hg pressure of He, the discharge activated and the subsequent pressure drop observed. After some time the discharge was stopped and the electron and ion collectors heated for 10 min at 700°C by electron bombardment from the filament. The discharge was then re-activated and the clean-up characteristic observed. The heating cycle was repeated twice, once for 20 min at 700°C and once at 1000°C, followed by pumping cycles. The four pumping curves obtained are shown in Fig. 2, where the instantaneous

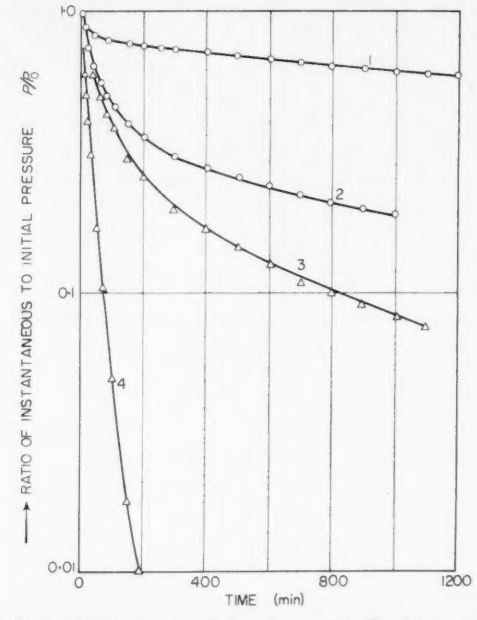

FIG. 2. Pump-down characteristic curves of He in a sealed-off Bayard–Alpert gauge, according to Varnerin and Carmichael. Curves 1 through 4 indicate increasing evaporated metallic deposits on the gauge walls.

pressure is normalised by dividing by the starting pressure. Curve 1, which was obtained after no outgassing had been performed, shows that the initial pumping speed was approximately 0.0001 l./sec at 10 mA emission and saturation effects appear to occur after about $1\frac{1}{2}$ h. An invisible deposit after the first outgassing appears to increase the initial pumping speed considerably, while further outgassings (after which the deposited film became clearly visible and was estimated to be about 50 Å thick) resulted in further increases in speed. A further experiment, after washing the contaminated glass in acid, showed a considerable reduction in pumping speed.

Varnerin and Carmichael concluded that these experiments demonstrated that a metallic layer upon the glass surface was necessary before clean-up became appreciable. This layer acted as a barrier to He atoms (which had been driven in under their kinetic energy) diffusing out from the glass. A final experiment in which the filament posts were shielded by glass tubes showed that the gas clean-up in the first experiment (curve 1) was largely at the filament posts (and to a lesser extent the ion collector) which lent added weight to their conclusions.

In a description of an ultra-high vacuum valve Bills and

Allen[23] quoted research performed on the measurement of the pumping speed of a Bayard–Alpert gauge. They gave a figure of 0.3 l./sec for N_2 for the initial pumping speed but did not quote the corresponding emission current or the conditions under which the measurements were made. Subsequently however details of their experimental technique[24] and a theoretical interpretation of the results by Bills and Carleton[25] were delivered to an American Physical Society congress. The work presented at this congress was published later by Bills and Carleton[26] and we shall describe this shortly.

Varnerin and Carmichael[27] extended their studies of the pumping action of a Bayard–Alpert gauge, in which an evaporated layer of tungsten was deposited upon the walls, by observing not only the pump down curves as in Fig. 2, but also the manner in which gas was re-evolved from the surfaces of the gauge. This was accomplished by recording the initial portion of a pump down run in He, quickly removing the test gas from the tube with the aid of fast diffusion pumps and, after isolating the gauge from the pumps at a low pressure, observing the increase in pressure as gas evolved from the experimental gauge walls, on an auxiliary ionization gauge.

It was found that the rate at which gas re-evolved after clean-up was proportional to the quantity which had cleaned up and to the time at which the rate was measured after the cessation of pumping, raised to the power -1.15, if the gauge had been operating at room temperature, but in experiments in which the gauge was immersed in liquid nitrogen the evolution rate was not simply related to the time after sorption was ceased.

The minimum time between the cessation of clean-up and the commencement of evolution observations in this work was 0.3 min dictated by the time required for pumping, closing taps, etc. but for times as short as this, and up to 250 min the evolution function was found to obey the relation quoted.

Varnerin and Carmichael were unable to draw any final conclusions as to the mechanism responsible for the observed evolution rate. A phenomenological analysis of the pumping characteristic, in which the observed sorption rate was assumed to be the resultant of a constant real sorption rate and an evolution rate, which depended upon the quantity sorbed and the time of sorption according to the experimental relation they obtained, showed that at liquid nitrogen temperatures the reduction in pumping speed of the gauge for He could be accounted for by a spontaneous evolution of gas, but at room temperature some other factor, such as the depletion of available pumping sites, must be introduced to account for discrepancies between their observations and theory.

The above work was later extended to include the pumping of He ions into molybdenum[28] electrodes in a specially designed gauge, and later[29] the pumping of several other noble gases into nickel and molybdenum. We will not discuss this work here, since in general in an electronic discharge in the tubes with which we are concerned, the sorption into metal parts is of minor importance, and furthermore the study of the sorption of gas atoms by metals is an exhaustive topic in itself. It is sufficient to state that under a wide range of experimental variables a somewhat similar form for the evolution rate as observed for glass was found and in these cases agreement between theory and experiment was excellent.

In 1956 Young[30] substantiated Varnerin and Carmichael's observations on the clean-up of He in a Bayard–Alpert gauge using a somewhat different technique. The test procedure was similar to that of these other authors in that the experiments were performed on a sealed off gauge, but, included within the envelope of the gauge was a cylindrical glass sheath which could be positioned opposite the electrode structure, so shielding the walls from the discharge, or lowered so that the walls were exposed. After thoroughly degassing the electrodes, the shield so positioned as to prevent the walls becoming metallised, the filaments were activated in the absence of any accelerating fields in order to remove O_2 and H_2 by dissociative gettering[4], then, with the glass shield lowered from the electrodes, the discharge was initiated. A reduction in pressure was observed, the rate of which gradually decreased until, after about $1\frac{1}{2}$ h, the shield, which had been contaminated during degassing, was raised magnetically so that it was presented to the discharge. An immediate increase in the pumping rate occurred, but after a further $1\frac{1}{2}$ h saturation effects became apparent. Fig. 3

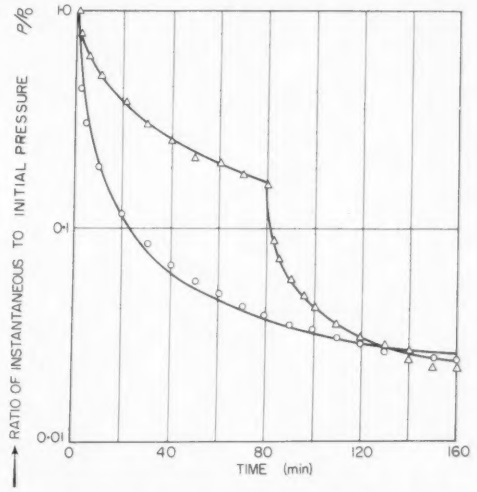

FIG. 3. Pump-down characteristic curves of He in a sealed-off Bayard–Alpert gauge, according to Young. Curve (1) obtained with a gauge incorporating a glass shield : the discontinuity indicates the instant at which the contaminated shield was presented to the discharge. Curve (2) obtained with a gauge not incorporating the glass shield.

demonstrates this effect and includes, for comparison, a pumping characteristic of a gauge, processed as above, but without the glass shield, in which the initial pumping rate is more rapid but saturation occurs when roughly the same quantity had been sorbed. Young infers that these results indicate the necessity of a slight metal deposit to ensure a maximum pumping rate for He.

Whilst the maximum pumping speed observed for He was 0.0004 l./sec at an emission current of 10 mA, Young found that N_2 and air cleaned up at a maximum speed of 0.1 l./sec and that shielding of the glass walls in the case

of these latter gases had no detectable effect on their clean-up.

In order to decide whether ion bombardment of the walls was sufficient to account for the observed pumping speeds, Young coated the inner glass surface with aquadag to which an electrical connection was made, and found that between five and eleven times as many ions struck the walls as the ion collector, a large enough proportion to account for the observed speeds. Furthermore, contradictory to Bloomer and Haine's results, the pumping action of an aquadag coated gauge was practically identical with that of an untreated gauge, and the direction of a fine flame to the coated regions released large amounts of gas. A gauge in which the electrode structure was surrounded by a tantalum can exhibited similar characteristics to these, once again at variance with Bloomer and Haine's results. Young accounts for these discrepancies by assuming them to be due to differences in outgassing techniques but what, in the author's opinion, is felt to be a more satisfactory explanation will be given in the discussion. One further interesting observation made by Young was that if the aquadag coating was maintained at electron collector potential, a situation in which positive ions could hardly be expected to strike the walls, the clean-up rate was reduced to a value which could be readily accounted for by pumping into the ion collector alone.

Young also treated the problem semi-quantitatively and by assuming that a limited area of the walls was available for sorption, that bombarding ions had only a certain probability of capture and that during clean-up there was simultaneous evolution of gas from the walls, succeeded in deriving equations which gave a good approximation to the curves in Fig. 3. He therefore concluded that the observed clean-up could adequately be explained by the capture of gaseous ions at the walls of the gauge.

Chronologically the next contributions were two papers by Comsa and Musa[31, 32] on the pumping action of a modified form of ionization gauge. In 1957, these authors described an " ionization pump " in which electrons were accelerated from a tungsten filament located at the centre of the tube to a helical electron collector, the ions formed were collected by the glass walls themselves since these became stabilized at approximately cathode potential under the influence of primary electron bombardment. The electrode configuration was, therefore, essentially that of the original Buckley–Dushman[33] gauge. It was found necessary to stringently outgass the electron collector and filament so that bombardment of these during operation did not impair the pumping action by releasing occluded gases. Since, with this form of tube, pressures could not be measured, it was necessary to employ an auxiliary Bayard–Alpert gauge in order to measure the pumping speed of the modified gauge. This was achieved by sealing the connected pumping tube and measuring gauge from the diffusion pumps and upon activating both simultaneously, observing the temporal change of pressure. After some time the pumping tube was shut off and the Bayard–Alpert gauge continued to pump alone, and assuming a simple pumping action the speed of the gauge was measured by the slope of the rate of removal versus the pressure curve. Since, in the initial stage, the two gauges operated as pumps in parallel it was possible from the two sets of observations to evaluate the pumping speed of the modified gauge. The pumping speed of such a tube for residual gases was found to be approximately 0.19 l./sec for an applied electron accelerating voltage of 200 V and 0.26 l./sec for a voltage of 300 V, at an emission current of 10 mA. These speeds, which were practically constant over a pressure range from 10^{-5} mm Hg to 10^{-8} mm Hg, are of course higher than those reported by Alpert but of a comparable magnitude to those measured by Young, the increase was explained by the larger ion production volume of the modified gauge.

In their second paper (in Rumanian) Comsa and Musa[32] enlarged upon the problems of the stabilization potential of the gauge walls and the methods of measurement of the gauge pumping speed, but the essential details of the work are outlined in the first paper.

A fuller description of investigations on the clean-up of N_2 and O_2 in Bayard–Alpert gauges was published by Bills and Carleton[34] in 1958.

Whereas previous investigators had sealed off the experimental gauge at a known pressure and observed the subsequent reduction in pressure as a result of clean-up from the discharge, Bills and Carleton maintained the test gas pressure in the gauge constant throughout an experiment, continuously leaking fresh gas into the tube from a reservoir by a manually controlled vacuum valve. These authors claim the above method enables more straightforward analysis of the results, while the effect of evolution of gas is minimised since the gas pressure is maintained relatively large. In much of the previous work the cessation of pumping action could have been accounted for by a lack of gas to pump and a further advantage of this work appears to be that true saturation of the walls was possible without using a prohibitively high gas pressure.

In these experiments the pumping speed of the gauge was evaluated by measuring the rate of fall of pressure in the reservoir, using a Pirani gauge, and the quantities of gas cleaned up could be evaluated using the same data.

In Table 1 part of a list of experimental observations on

TABLE I

Initial pumping speed in l./sec (10 mA emission	Maximum quantity of gas cleaned up in μl.	Condition of surface
0.065	25	(a) Well baked glass surface with minimum amount of evaporated metal on surface.
0.50	14	(b) Same as (a) but with slight amount of evaporated tungsten on surface.
0.50	19	(c) Well baked glass surface with visible deposit of freshly evaporated tungsten on surface.
0.34	22	(d) Glass surface covered with very thick layer of freshly evaporated tungsten.

the clean-up of N_2 given by Bills and Carleton is reproduced. This table shows how the initial pumping speed of the gauge and the quantity of gas which could be accommodated by the gauge depended upon various surface conditions of the glass. Generally it was found that the initial pumping speed tended to be low with a gauge in which the glass surface was clean, and high when the surface was covered with a layer of evaporated tungsten, varying from 0.065 l./sec to 0.5 l./sec. These speeds agree with those of Young as regards orders of magnitude, but not in their dependence on surface condition. They do agree in this respect however with most of the observations on the clean-up of He.

Bills and Carleton derived a theoretical expression in which the speed of pumping was related hyperbolically to the quantity of gas cleaned-up. This agreed well with their experimental data. By assuming that clean-up was a result of the bombardment of a limited number of surface sorption sites by particles activated in the discharge, introducing a number of factors to represent the probabilities of reflection, the removal of excitation energy of incident particles at the walls, etc., and neglecting simultaneous evolution from the walls, they were able to conclude from their data that the clean-up of N_2 resulted from the removal of molecular ions rather than dissociated atoms. They concluded further that de-activation of a bombarding particle at a surface was an important process in the clean-up. We will not discuss the data on O_2 which these workers presented since it is possible that a dissociative mechanism (Ref. Langmuir[35]) played a part in the clean-up, although these workers claim that this mechanism is unimportant, and a discussion of such is outside the scope of this paper.

Finally a brief discussion will be given of the work carried out at Liverpool by Leck and Carter[36, 37] on the clean-up of several rare gases in a Bayard–Alpert gauge. The technique employed in this work differed from that previously described in that (1) a continuous flow system was used, in which the gas under investigation was pumped at constant pressure through the gauge from a reservoir, and (2) the quantity of gas cleaned up was estimated after the discharge was terminated by heating the experimental gauge to about 400 °C, recording the pressure transient on either an auxiliary ionization gauge or a mass spectrometer situated elsewhere in the pumping line, and integrating the response over the period of desorption.

From this method it is possible to plot a curve of the quantity of gas cleaned up versus a parameter representing the total ionization produced in the previous discharge. Plots of this type are made in Fig. 4 for A, where the abscissae are in units of electron current × gas pressure × the period for which the discharge operated (a factor which can be simply related to the total charge passing to the collector and hence to the total ionization produced). The speed of pumping can be readily deduced from such a curve and the saturation quantity of gas is self evident. In Fig. 4 two clean-up curves for A are shown, the experimental conditions were identical in the measurement of each curve, and it is immediately obvious that for any one value of the ionization produced, two distinct quantities of gas may be sorbed. This effect has been ascribed[36] to different states

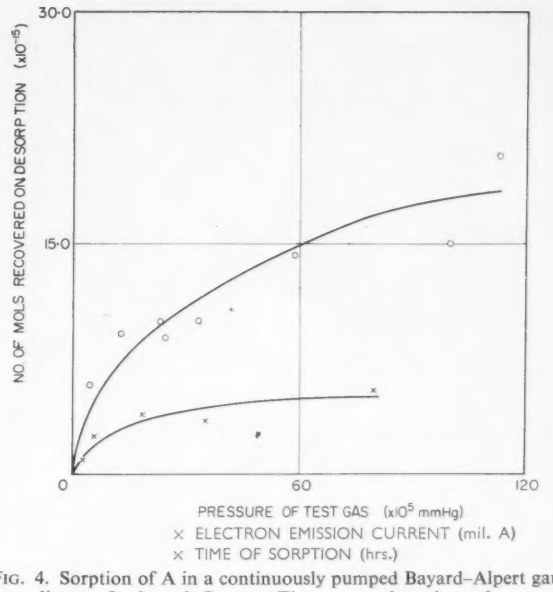

FIG. 4. Sorption of A in a continuously pumped Bayard–Alpert gauge, according to Leck and Carter. The curves show how the quantity of gas cleaned up varies with the ionisation produced in the gauge and demonstrates the dual mode of sorption.

of charge of the glass walls resulting from secondary emission processes, such that in one state ions are able to strike the walls with a greater density than in the other. Measurements have been made in a metal screened gauge which confirm this hypothesis. No control could be exercised over the mode of operation of the gauge, i.e. the quantity which cleaned up for a certain ionization, but it was always possible to infer which mode had operated before desorption was performed since it was found that the pressure sensitivity of the gauge also assumed one of two values, the higher one operated when the larger quantity of gas was cleaned up. A complete report on the observations of this change of sensitivity is given elsewhere[37] where the reasons for the variation are shown to be the same as those which govern which clean-up mode shall operate, namely the surface charging effect.

The maximum pumping speed for A is seen from curve *B* of Fig. 4 to be 0.004 l./sec at 1.0 mA emission and the maximum quantity cleaned up approximately sufficient to form 15 per cent of a monolayer coverage on the glass surface. Experiments were performed on krypton and neon also, using the mass spectrometer as the evolution detector. The pumping speed of these gases was approximately the same as for A, whilst the double mode of operation was also noted with krypton.

No attempt was made in this work to ensure that the walls were free from a metallic deposit except that no electrodes, apart from the filaments, were ever heated, vacua better than 10^{-9} mm Hg being achieved without recourse to this operation. Tungsten from the filament may have distilled to the walls during the course of the work, but results obtained at the commencement of observations (with glass rigorously outgassed to 400 °C) were different to no more than the limits of experimental error to the results obtained after many hours operation of the tube and it

Vol. 9 959/60

seems unlikely, therefore, that even if a deposit had formed it would have had any perceptible effect. It should be realized that this work was performed on the heavier rare gases, not He, and therefore in no way contradicts the observations of Varnerin and Carmichael on this latter gas.

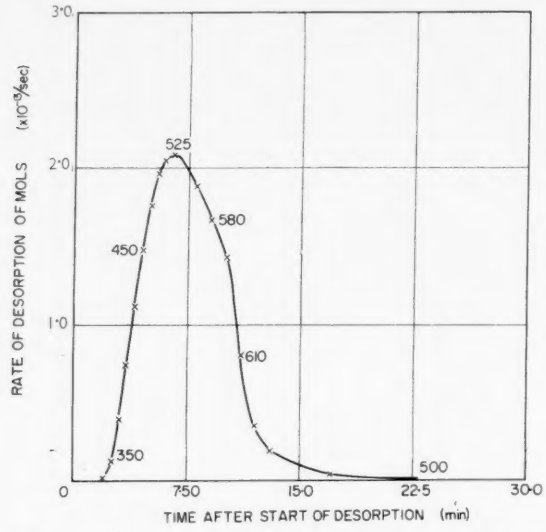

FIG. 5. Desorption of A from the walls of a Bayard–Alpert gauge. The graph indicates how the desorption rate varies with the gauge temperature.

Further information is derived from this work by observing the temperature dependence of the desorption rate on heating the gauge. A typical desorption transient for A is shown in Fig. 5 in which the desorption rate, i.e. the number of desorbed atoms/second is plotted as a function of the time after commencing desorption (a plot convenient for the measurement of the quantities sorbed) and on which the corresponding degassing temperatures are shown. A study of this transient reveals that the cleaned up gas atoms are probably driven into the walls by virtue of their high energy from where they are released by heating, simple surface binding mechanisms appear to be out of the question. An analysis of the desorption is at present being undertaken and it is hoped to learn more of the physical mechanisms responsible for clean-up by correlating this analysis with varying experimental conditions.

The first conclusion, about the kinetics of the sorption process, that can be drawn from all these experiments is that a simple clean-up mechanism of the continuous capture of bombarding particles cannot account for the observations since the constancy of speed and lack of saturation which this mechanism predicts are never observed. Alpert's introduction of a constant rate of evolution term certainly explains the saturation, but usually gives an inconsistent pump-down curve. (Von Meyeren's data is an exception

TABLE II

Investigators	Gases investigated	Max. pumping speed observed in l./sec/mA Emission	Quantity cleaned up in μl.	Conclusions reached about mechanism of clean-up
Alpert and co-workers	Residual gas	0.005 l./sec/mA	Approx. sufficient to form monolayer coverage (approx. 3 μl).	Gas ions captured at ion collector and walls of gauge. Probably penetrating these to some depth.
Bloomer and Haine	Residual gas	0.0032 l./sec./mA	Approx. 0.02 μl	No definite conclusions but thought likely that clean-up due to removal of excited molecules.
Varnerin and Carmichael	He	0.00001 l./sec/mA on clean surface. 0.000056 l./sec/mA when evaporated metal on surface.	Approx. 0.1 μl	Gas ions penetrate into glass walls and their re-diffusion back to the gas phase is impeded by evaporated metallic layers on the glass. The re-emission of sorbed gas causes a reduction in the pumping speed and an apparent saturation.
Bills and Allen	N_2	0.03 l./sec		
Young	He N_2 and Air	0.00004 l./sec/mA on contaminated surface. 0.01 l./sec/mA	Approx. 0.06 μl	Ions adsorbed at surface capture sites, with a certain probability of capture. The reduction of pumping speed is a result of the gradual occupation of capture sites.
Comsa and Musa	Residual gas	0.026 l./sec/mA		
Bills and Carleton	N_2	0.0065 l./sec/mA on clean surface. 0.050 l./sec/mA when metal evaporated on to surface.	25 μl	As Young, but also show existence of probabilities of reflection and de-excitation of active molecules at capture sites.
Leck and Carter	A Ne Kr	0.0038 l./sec/mA	0.59 μl	Gas ions penetrate glass walls by virtue of their high energy, but two separate rates of clean-up occur due to differences in the electrical potential of the glass.

It should be noted that, in the experiments of Bloomer and Haine, Varnerin and Carmichael and Young, the amount of gas contained within the tube was never sufficient to lead to monolayer coverage of the tube walls. The quantities quoted in column 3 are, in fact, almost equal to the initial quantity of gas present.

Vo
9
1959

to this.) In the case of N_2 it seems possible to describe the clean-up, as did Young and Bills and Carleton, by assuming a limited number of capture sites and their gradual filling leads to saturation. The omission of spontaneous or induced evolution seems to be an over-simplification however; Schwarz's early work revealed the importance of bombardment induced re-emission and the rediffusion, of small molecules particularly, to the surface is inevitable.

The clean-up of He can, according to Varnerin and Carmichael, be described not necessarily by a depletion of capture sites, but by a time dependent evolution function. Young, on the other hand, was able to account for similar results for He by the former clean-up process. The solution to this disparity seems to be that either description finally requires a curve fitting technique to determine the constants involved (some of which are theoretically indeterminate) and with the data available either solution can be made to agree by a suitable choice of these constants.

One would finally conclude that as far as He is concerned, Varnerin and Carmichael's approach is probably the more correct where the evolution rate is large, whilst for N_2 Bills and Carleton's solution seems appropriate.

In concluding this chapter it is useful to recapitulate the results in tabular form, showing the pumping speed and saturation quantities for various gases with different surface conditions, reported by the authors quoted. Their conclusions as to the operative mechanisms are also given, the validity of which were discussed above. These are given in Table 2, which is similar in part to a table given by Alpert in a recent review of the production of high vacua in the Handbuch der Physik[38].

Vol. 9 959/60

5. The physical mechanisms involved in clean-up

It appears to be well established that the clean-up of gases in a hot cathode discharge tube is largely a result of the production of activated gaseous particles by electron-gas molecule collisions and the interaction of these particles with the glass walls of the containing vessel. It is less well established, but extremely probable, that the activated particles are in fact gaseous ions, molecular or atomic, although Bloomer and Haine prefer to invoke only excited states, and these ions can be accelerated by electric fields. In most discharge tubes used in this work, it has been demonstrated that the glass walls acquire a potential close to that of the cathode since then only a very few electrons can reach the walls and charge it negatively, and these can be readily neutralised by ion bombardment. Since the largest positive voltage in the tube may be of the order of 200–300 V, the singly charged ions formed in the discharge may acquire energies of up to 300 eV, whilst multiply charged ions will have considerably larger energies, and will bombard the low potential glass with these high energies. At the normal operating temperatures of the gauge the constituent atoms of the glass envelope vibrate with thermal energies of only some tenths of an electron volt at most, and interaction between the bombarding ions and the glass would thus appear likely. The nature of this interaction is, of course, the crux of the problem.

The forces associated with physical adsorption can give rise to interaction energies of about 1/3 eV and at room temperature this leads to the time which an adsorbed atom or molecule spends at the adsorbent surface of less than a microsecond. Most clean-up experiments reveal that a particle spends a much longer time at the surface, those performed at Liverpool, for instance, show that the particles remain in contact with the glass for times of the order of hours and temperatures of 375 °K are required before the particles evolve to any appreciable extent. This evidence strongly suggests that simple physical adsorption is not the important mechanism in producing clean-up.

The next possibilities are chemisorption processes and chemical reactions. Undoubtedly, in gettered tubes, these processes are of great importance but it is difficult to understand why, if these mechanisms also operate in the non-gettered tubes, rare gases are also cleaned up. It must be admitted that the equivalent temperature of the bombarding ions is 10^6 °K and that under such conditions the rare gases may become active. Loeb[39] has, for example, reported observations of short-lived ionic combinations of rare gases in arc discharges. A long term combination between the bombarding ions and the glass walls seems very unlikely however.

The most likely explanation is that the gas ions bombarding the glass walls with high kinetic energy are able to penetrate between the atoms of the glass lattice. The assignation of a lattice structure to glass is acceptable in the light of a recent theory of the structure of glass proposed by Tilton[40]. The distance of penetration will be dependent upon their incident energy, and angular distribution, their size, and the atomic structure of the glass, but it will be at least a few atom diameters. Young[41] has observed, for example, that 250 eV He ions should penetrate to a depth of about 10 atom layers in aluminium. Once the initial energy of the particles has been dissipated by collision processes they will come to rest and then constitute large (except in the case of He) impurity molecules in the glass lattice, since the molecular diameters of the gases involved in clean-up are generally appreciably larger than the majority of the glass interatomic distances (e.g. the A atom has a dia. = 3.2 Å while the S_i–O distance in the simple silica glass is 1.6 Å). The probabilities of spontaneous evolution of one of these particles is now extremely small since, using a crude picture, the large cleaned up particle cannot squeeze between the glass atoms at normal temperatures and, thus, cannot reach the surface. Confirmation of this picture can be obtained by examining the diffusion coefficients of the rare gases in various glasses[42] from which we learn that only He and, to a much reduced extent, neon diffuse at measureable rates through borosilicate glass at room temperature. Bombardment induced evolution is possible in this model since a bombarding ion may remove a captured particle from the lattice by " opening up " the lattice for a sufficient time to allow a particle to escape (by thermal transfer of its energy and local heating) or if the captured particle is close to the surface, collision of the bombarding ion may impart sufficient energy to the particle to allow escape. Other processes are of course conceivable but the statement of these two is sufficient to show that bombardment induced evolution is feasible.

Evidence to support the mechanism of gaseous occlusion is found in a comparison of the clean-up characteristics of He and any other gas. It is always found that a comparatively much larger spontaneous evolution occurs when He is cleaned up, consistent with the higher diffusion rate for He than of other gases in glass, where bombarding particles brought to rest in the glass can readily diffuse back to the surface and re-enter the gas phase. Furthermore the apparent clean-up rate for He is always increased if the glass surface is covered with, for example, a tungsten deposit, the layer of close packed tungsten atoms probably has little effect on high energy ions bombarding the glass, but can inhibit the evolution by acting as a barrier to the particles in the sorbed state. The evidence obtained in the work at Liverpool also supports the penetration hypothesis in that the post clean-up evolution of atoms of argon, neon and krypton does not occur rapidly until the glass temperature has been raised to about 375°K.

An apparent contradiction in the published work also lends weight to the theory that the ions are driven into the glass by virtue of their acquired kinetic energy. Bloomer and Haine reported that completely coating the inner surface of an ionization gauge with an aquadag layer inhibited clean-up, but removing a small area of the coating caused clean-up to re-appear, while on the other hand Young found that on coating a gauge with aquadag the clean-up proceeded unimpaired, but that applying electron collector potential to the aquadag caused clean-up to cease. It is well known that under electron bombardment an isolated conducting or insulating body can acquire either of two stable potentials, one close to that of the cathode delivering the primary electrons, when no charging electrons can reach the body, or a second, close to that of the anode accelerating the electrons (providing that the anode potential is close to that at which the secondary emission coefficient of the material of the body is unity) when the primary electron current is balanced by the current flowing from the body due to secondary electron emission.

It seems likely that in Bloomer and Haine's experiments the completely aquadag coated glass acquired a large positive potential so that ions would not strike the walls with energy sufficient to cause sorption, as confirmed by Young when the aquadag was deliberately held at electron collector potential, but that baring areas of the glass caused a reduction in the mean secondary emission of the walls so that they became stabilised at the lower potential and sorption could take place. Young probably did not observe such inhibition of sorption because his experimental technique involved the initial activation of the filament before applying any accelerating field, the wall would stabilise initially at close to cathode potential and sorption could proceed. The author's own observations on the dual mode of sorption has also been ascribed to the wall potential duality.

An alternative mechanism to that of particle penetration into the bulk of the glass is one in which the cleaned-up particles enter, again by virtue of their high energies, deep narrow superficial cracks or dislocations, the arguments applying to evolution, outlined above, being similar in this case. An attraction of this mechanism is that one would expect to find a limited number of such cracks on a surface, so that an upper limit is set to the number of particles which may be accommodated, this limit may well be less than the number of particles required to give monolayer coverage of the surface which, since the number of particles cleaned up generally falls below this value, would tend to support the "clean-up into cracks" hypothesis. The introduction of the concept of a limited site density required by most of the authors of the theory of the sorption kinetics is not incompatible with either of the above mechanisms since only inter-atomic surface spaces can be considered as being available for penetration, but the assumption that any "site" can accommodate only one particle may require revision in the light of future work. At present it is not possible to decide which of these mechanisms is operative or whether a combination of both takes place, but the evidence strongly supports the contention that processes such as these are important in the clean-up phenomenon.

Until it became possible to reach a decision on the physical phenomena involved in the electrical clean-up of gases it is probably most convenient to interpret the experimental data in terms of the sorption kinetics which, as we have seen, to a great extent explain the observations if applied judiciously.

References

1 J. Plücker ; *Pogg. Ann.* **105**, 84 (1858).
2 E. Pietsch ; *Ergebn. exakt. Naturw.* **5**, 213 (1926).
3 A. Malignani ; (See J. W. Howell and H. Schoeder), *History of the Incandescent Lamp*. The Maqua Co., Schenectady, N.Y. p. 126 1927).
4 I. Langmuir ; *J. Amer. chem. Soc.* **35**, 931 (1913).
5 S. Dushman ; *Scientific Foundations of Vacuum Technique*, John Wiley & Sons Inc., New York (1949).
6 D. Alpert ; *J. appl. Phys.* **24**, 860 (1953) and subsequent papers.
7 W. Von Meyeren. (See Refs. 15 and 16.)
8 H. Schwarz. (See Refs. 17 and 18.)
9 N. R. Campbell ; *Phil. Mag.* **41**, 685 (1921).
10 M. R. Andrews. (See Ref. 5.)
11 S. Dushman, H. Huthsteiner, and M. R. Andrews. (See Ref. 5.)
12 A. L. Hughes ; *Phil. Mag.* **41**, 778 (1921).
13 N. R. Campbell and E. G. New ; *Phil. Mag.* **48**, 553 (1924).
14 H. Huthsteiner and S. Dushman. (See Ref. 5).
15 W. Von Meyeren ; *Z. Phys.* **84**, 531 (1933).
16 W. Von Meyeren ; *Z. Phys.* **91**, 727 (1934).
17 H. Schwarz ; *Z. Phys.* **117**, 23 (1940).
18 H. Schwarz ; *Z. Phys.* **122**, 437 (1944).
19 D. Alpert ; *loc. cit.*
20 R. T. Bayard and D. Alpert ; *Rev. sci. Instrum.* **21**, 571 (1950).
21 R. N. Bloomer and M. E Haine ; *Vacuum* **3**, 128 (1953).
22 L. J. Varnerin and J. H. Carmichael ; *J. appl. Phys.* **26**, 782 (1955).
23 D. G. Bills and F. G. Allen ; *Rev. sci. Instrum.* **26**, 654 (1955).
24 D. G. Bills, N. P. Carleton, and F. G. Allen ; *Bul. Amer. phys. Soc.* **30**, 36 (1955).
25 N. P. Carleton and D. G. Bills ; *Bul. Amer. phys. Soc.*, **30**, 36 (1955).
26 D. G. Bills and N. P. Carleton ; *J. appl. Phys.* **29** 692 (1958).
27 L. J. Varnerin and J. H. Carmichael ; *Bul. Amer. phys. Soc.* **30** 36 (1955).
28 L. J. Varnerin and J. H. Carmichael ; *J. appl. Phys.* **28**, 913 (1957).
29 J. H. Carmichael and J. S. Knoll ; *Westinghouse Scientific Paper*, No. 6–94436–1–Pl.
30 J. R. Young ; *J. appl. Phys.* **27**, 926 (1956).
31 G. Comsa and G. Musa ; *J. Sci. Instrum.* **34**, 291 (1957).
32 C. Gomsa and G. Musa ; *Stud. Cercet. de Fizica*, **2** (1957).
33 O. E. Buckley and S. Dushman ; *Proc. nat. Acad. Sci. Wash.* **2**, 683 (1916).
34 D. G. Bills and N. P. Carleton ; *loc. cit.*
35 I. Langmuir ; *J. Amer. chem. Soc.* **37**, 1139 (1915).
36 J. H. Leck and G. Carter ; *First International Vacuum Symposium, Namur* 1958. (To be published by the Pergamon Press, London.)
37 G. Carter and J. H. Leck. To be published.
38 D. Alpert ; *Handbuch der Physik.* **12**, (1958).
39 L. B. Loeb ; *J. appl. Phys.* **29**, 1369 (1958).
40 L. W. Tilton ; *Res. Nat. Bur. Standards*, **59**, 139 (1957).
41 J. R. Young ; *J. appl. Phys.* **27**, 1 (1956).
42 F. J. Norton ; *J. Amer. ceram. Soc.* **36**, 90 (1953).

High-Vacuum Pumps and Units for Accelerators*

S. A. VEKSHINSKY, M. I. MENSHIKOV and I. S. RABINOVICH

HIGH-VACUUM PUMPS for accelerators should be provided with some special devices to prevent the vapour migration of the operating fluid (oil or mercury) from the pumps into the vacuum chambers. These special devices should function without cutting down the pumping speed in the range of the order of 10^{-6} mmHg.

The following report gives the description of the specific characteristics of the devices which are used in the high-vacuum pumps for the accelerators designed in the U.S.S.R.

Among the routine oil-vapour pumps the pump with a diameter of 380 mm and a pumping speed of 5000 l./s is the most common. The construction of this pump closely resembles the pump used for the 10 BeV synchrophasotron (Fig. 1).

There are two high-vacuum stages and a final jet stage in this pump. The latter being able to withstand the back

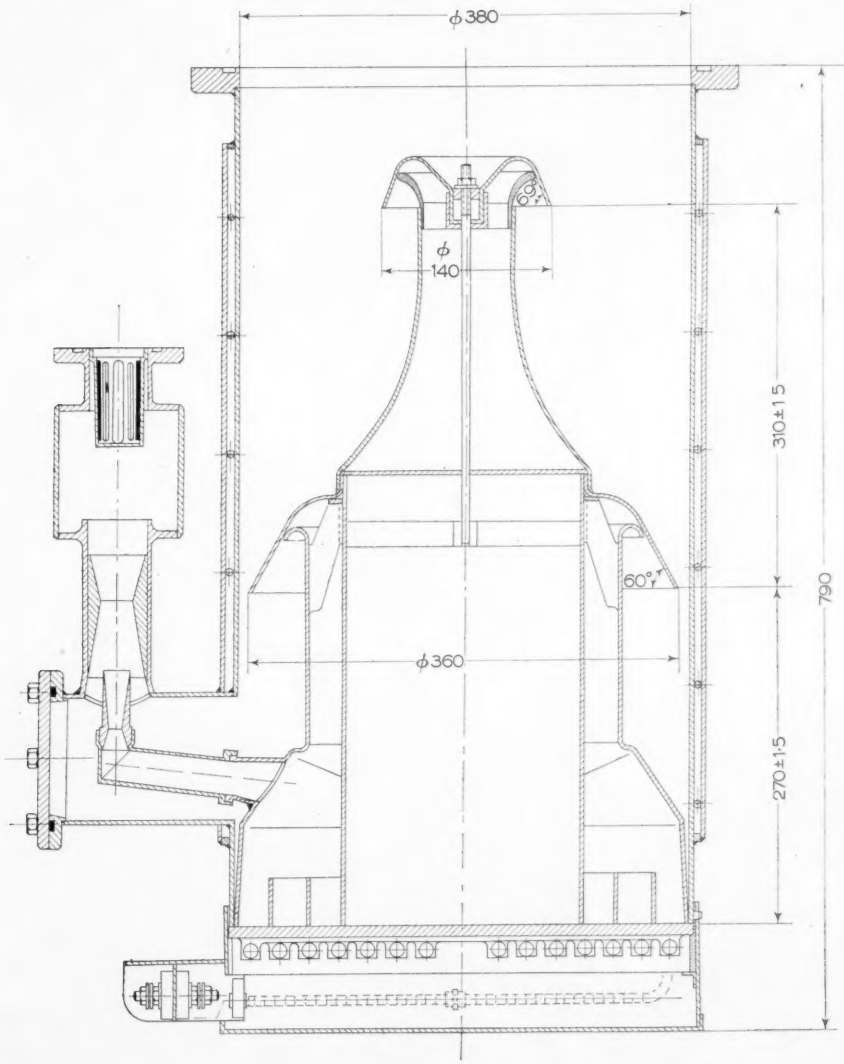

FIG. 1. Sketch of the high-vacuum oil-vapour pump with a pumping speed of 5000 l./s.

* Paper presented at the First International Congress on Vacuum Techniques, Namur, 10–13 June 1958.

Vol. 9 959/60

pressure of more than 100 μ Hg, the high-vacuum pump can be directly connected to the fore-vacuum.

In the pumps of a like design there always exists a certain fractionating of the operating oil during the working process. It occurs because the steam-oil flow gets on to the cooled walls of the housing and condenses. Then the condensate at first flows down to the periferal zone of the boiler and only from there penetrates into the central zone which feeds the upper high-vacuum nozzle with vapour. In the given pump the fractionating is intensified.

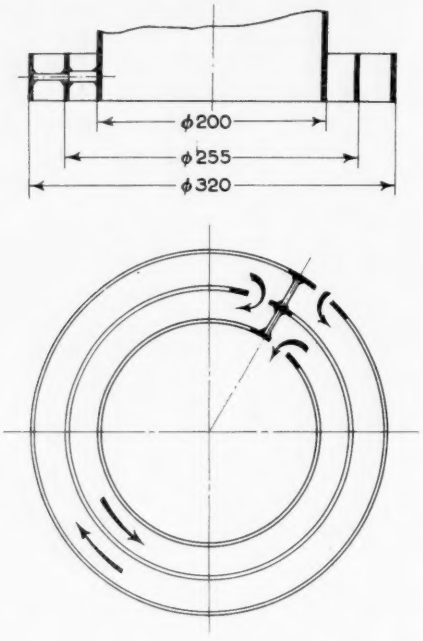

FIG. 2. Sketch of the fractionating ring device of the 5000 l./s pump.

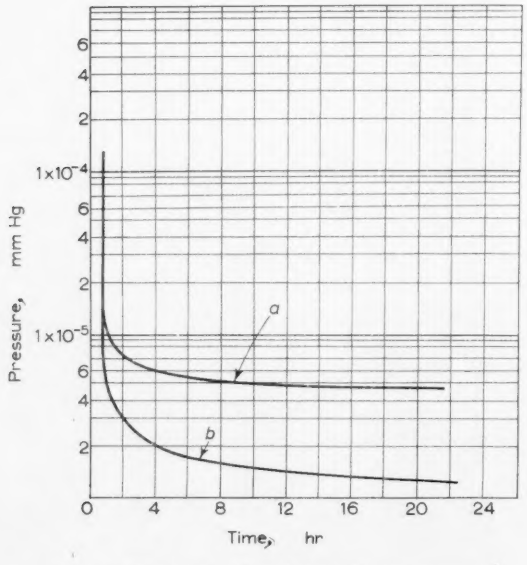

FIG. 3. The curve of reaching ultimate vacuum.

At the bottom of the vapour tube there is a ring device (Fig. 2) intended to speed up the process of the oil fractionating.

The intensification of the above process improves the ultimate vacuum and reaches it in a shorter time (Fig. 3). It is experimentally found that the intensification of the oil fractioning leads to the decrease of the oil vapour flow from the pump to the evacuated vessel. For example, a big pump having a speed of 25,000 l./s with the ring-fractionating device has an oil migration amounting to 2 cm^3/h and without such device 10 cm^3/h.

The oil-catching device shown in Fig. 4 is a cone cap with a water-cooling pipe soldered from the outside. The cap is

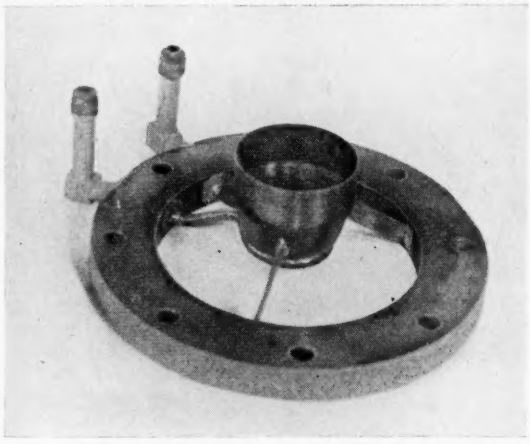

FIG. 4. A model of oil-catching device to be placed above the pump upper nozzle.

fixed on the steel flange having two nipples outside for connecting it to the cooling system. When assembled with the pump the cap covers the upper nozzle (Fig. 5).

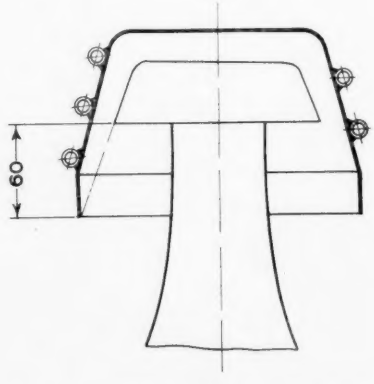

FIG. 5. The mounting sketch of the oil-catching device.

The functioning of the oil-catching device is based on the following principle : V, the velosity of the vapour flow behind the nozzle, has components perpendicular to the nozzle axis. Therefore, a part of the vapour flow contains some lines of vapour current $\psi_i - \psi_n$ directed to the side

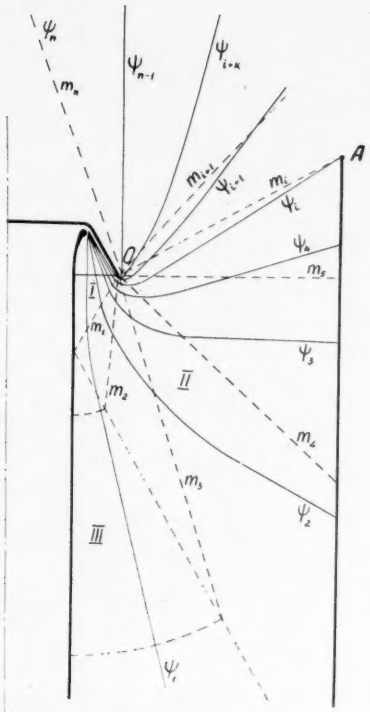

FIG. 6. Diagrammatic representation of the vapour flow from the nozzle of the high-vacuum diffusion pump.

opposite to the gas flow. This portion of the vapour flow (almost without disturbing the pumping) is the main source of the back-streaming.

The cooled cone cap of the vapour-catching device is immersed into the flow so as to intersect the back-streaming current lines. The part of the inlet section of the pump, additionally shadowed with the cap, is so small that it does not cause any considerable decrease of the pump speed (10–15 per cent). This, together with the simplicity of the design and making, shows the advantages of this device as compared to the known ones. Model oil-catching devices from 10^2 to 10^3 times decrease the oil flow from the pump.

The ultimate vacuum reaches approximately 2×10^{-6} mm Hg. At this pressure the effective pumping speed equals zero. However, sometimes it is necessary to have a better vacuum than 2.10^{-6} mm Hg. Then a cold trap is added to the pumping unit. The ultimate vacuum reached, with the addition of the cold trap which is cooled with liquid nitrogen ($t = -192°C$), improves respectively and reaches 10^{-7} mm Hg.

The trap (Fig. 7) represents a set of baffle plates overlapping the pump inlet section and answers the demands of an optical barrier. Shown in Fig. 7 is a relative displacement of two rows of the baffle-plates with a simultaneous enlargement of the space between them as compared to the usual, allows to increase the trap conduction up to 25–30 per cent, depending on the area of the overlapped channel and at the same time to maintain the optical barrier.

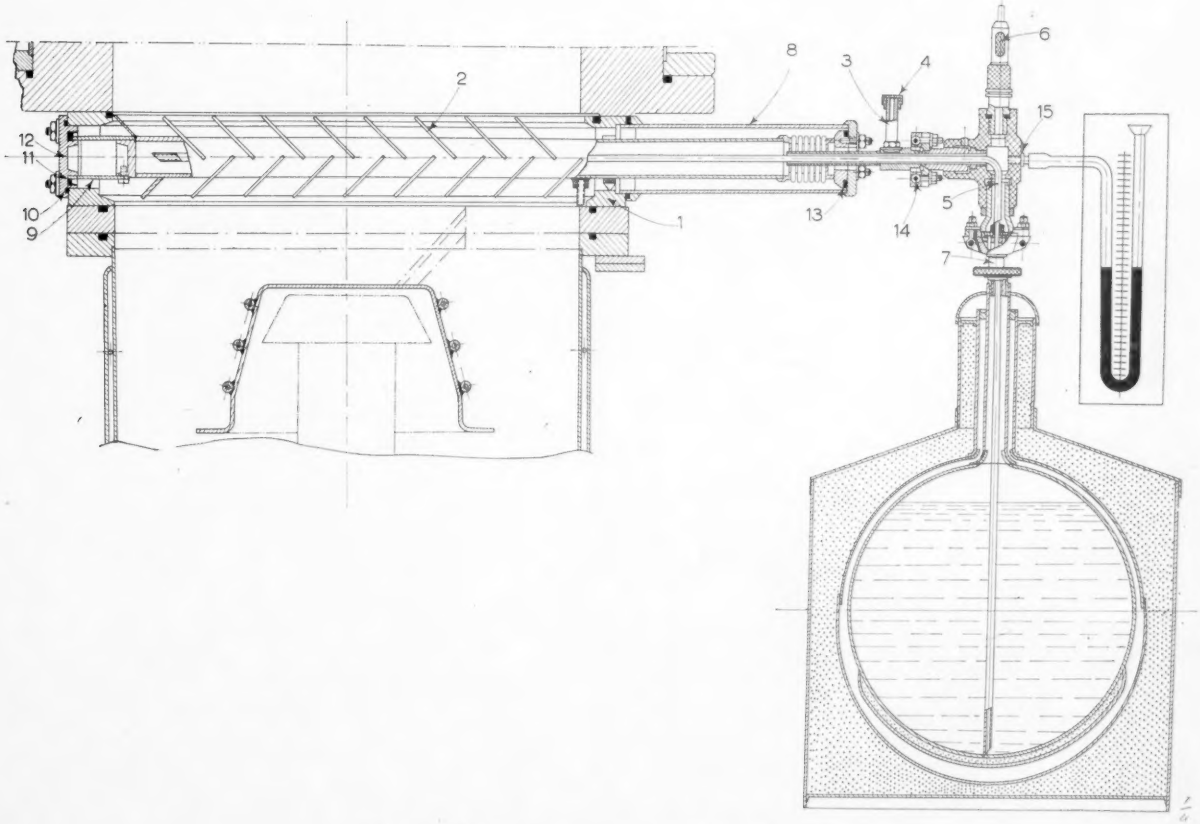

FIG. 7. The cold trap cooled with liquid nitrogen.

Vol. 9 959/60

The sketch of constructing such baffles with increased conduction is given in Fig. 8.

Nitrogen is supplied to the central tube of the trap (Fig. 7) by means of the bent feeding pipe (5). The vertical part of it passes through the plug into the vessel with nitrogen. Under the influence of the overpressure produced in the vessel by nitrogen evaporation, the nitrogen through the bent pipe comes into the central pipe and evaporates. Then its vapour, through the adjusted aperture (4), volatilizes into the atmosphere.

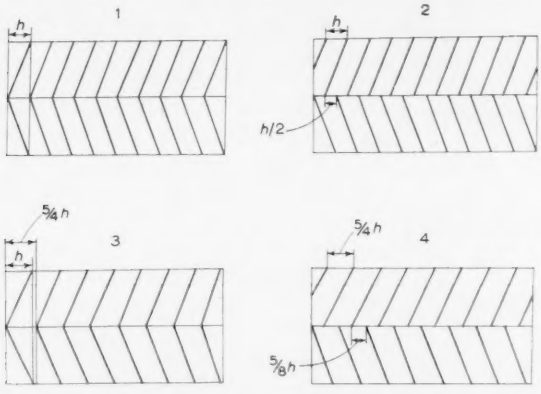

FIG. 8. The sketch of constructing the baffles of the increased conduction : (1) Commonly used baffle plates without optical paths. (2) Displaced baffle plates without optical paths with the same space between the plates. (3) Baffle plates with optical paths and an enlarged space as compared with the usual. (4) Displaced baffle plates with no optical paths and an enlarged space.

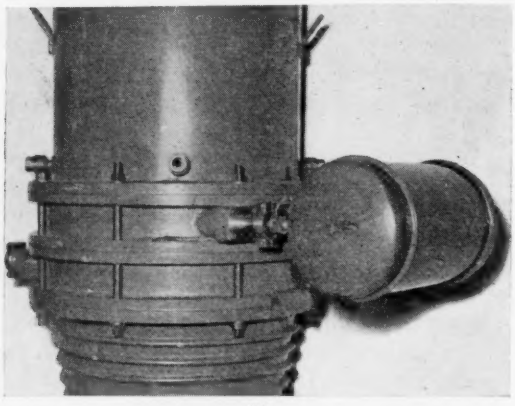

(a)

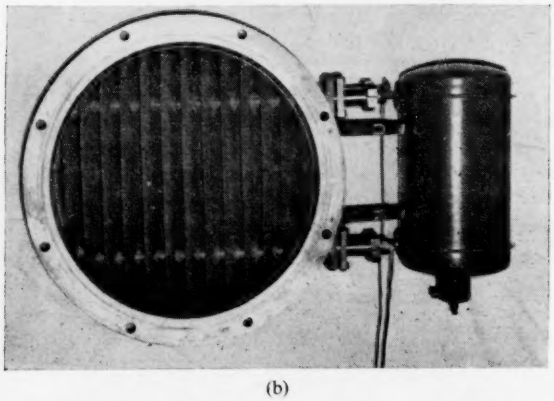

(b)

FIG. 9. Small-size liquefier : (a) mounted on a pumping unit, (b) assembled with a trap.

The safety valve (6) of the feeder, and adjusting outlet aperture (4), allow to maintain the vessel pressure and nitrogen consumption constant. The outlet throttle and safety valve being correctly adjusted, the liquid-nitrogen sputtering is eliminated and nitrogen consumption becomes rather low.

The trap, together with the feeder, allows a supply of liquid nitrogen to the trap directly from standard Dewar vessels, or tanks used for its transportation.

If a centralized liquid-nitrogen feeding of a considerable number of cold traps is necessary as, for example, in the pumping units of accelerators of great extension, each trap can be provided with a separate small-size liquefier (Fig. 9). The latter is fed from a common compressor with gaseous nitrogen (air) compressed up to 200 atm. Liquid nitrogen formed at the liquefier nozzle goes directly to the central part of the trap where it evaporates. The place of the liquid nitrogen formation and consumption being the same, the liquid nitrogen loss becomes negligible.

The distribution of the gaseous compressed nitrogen among the pumping units, by means of small diameter pipes, is much easier and more economical than the liquid-nitrogen distribution ; the loss of which in intermediate tanks and volumes is very great. For example, the loss of nitrogen in 100 m isolated vacuum piping amounts to about 50 per cent.

The external view of a model pumping unit is shown in Fig. 10 a. It consists of a high-vacuum pump with a hydrorelay, associated with the heater, an oil-catching device, a high-vacuum gate, an intermediate head to be connected to the chamber and a wheeled frame.

A mercury-vapour pumping unit is mounted in the same way. In the mercury-vapour units usually in front of the cold trap ($t = -192{\cdot}6\,^{\circ}C$), the second trap ($t = -38{\cdot}6\,^{\circ}C$) is placed. (See, for example, Hugh R. Smith ; The technology of large mercury-pumped vacuum systems, *Vacuum Symposium Transactions*, 1954.) However, using the above described water-cooling vapour-catching cone cap makes this second trap unnecessary.

The vapour-catching cone cap, mounted in the mouth of the mercury-vapour pump, with a speed of 5000 l./s is shown in Fig. 11. On the inner surface of the pump housing one can clearly see a layer of mercury, the upper boundary of which is on the level of the cap-cut.

Oil- and mercury-pumping units with different pumping speed (from 100 to 25,000 l./s) are being used. Their design is like the one described above.

Figure 12 demonstrates a series of high-vacuum oil-vapour pumps with a pumping speed from 100 to 8000 l./s, and Fig. 13 a shows the vacuum gates used in the units with these pumps. The gates can have both manual and remote control.

The main technical data of oil-vapour pumps are given in literature (see Savinsky, K. A. ; in *Zavodskaya Laboratoria*, no. 5 (1955) ; High vacuum equipment, *Vacuum* **4**, no. 3, 326 (1954).

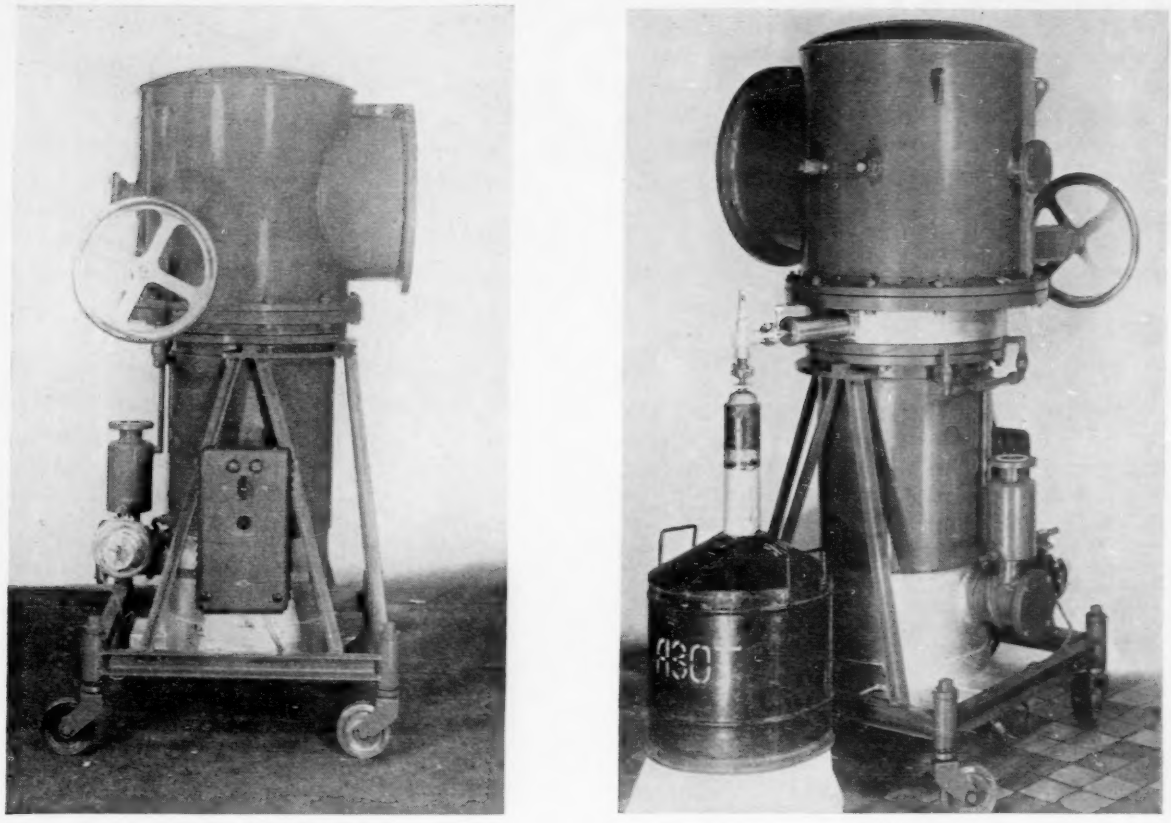

(a) (b)

FIG. 10. A model pumping unit based on the 5000 l./s high-vacuum pump : (a) without a cold trap, (b) with a cold trap fed by liquid nitrogen from a standard Dewar vessel.

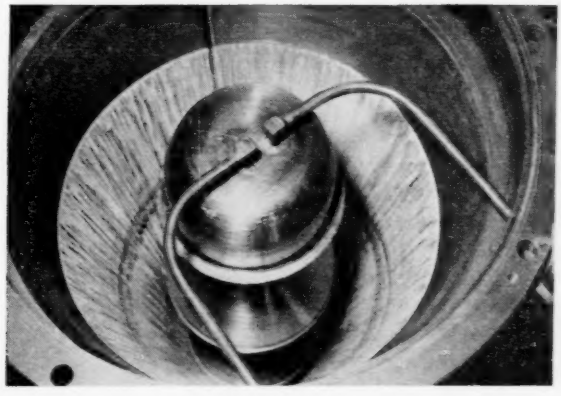

FIG. 11. The vapour-catching cap in the mouth of a mercury-vapour pump.

Vol.
9
959/60

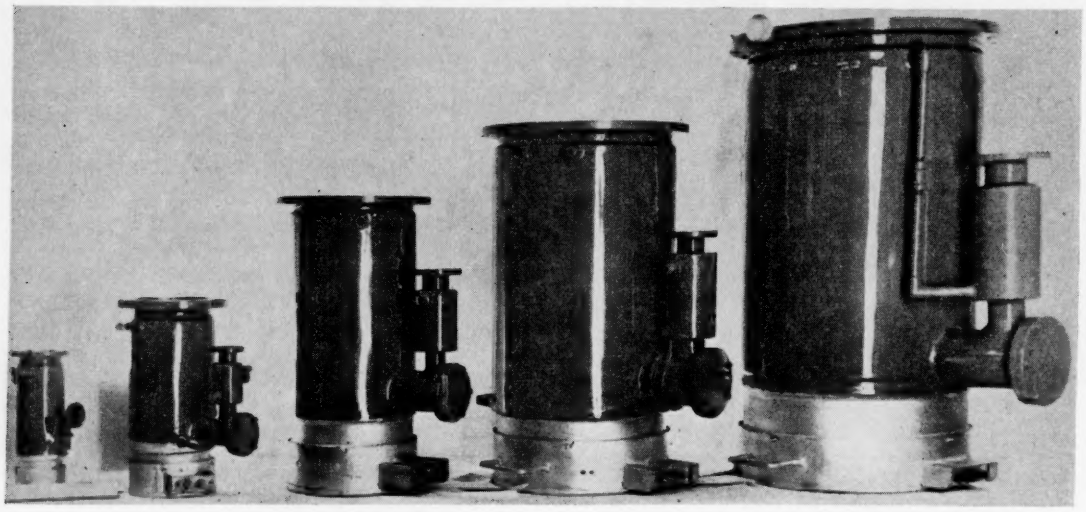

FIG. 12. A series of high-vacuum oil-vapour pumps with a pumping speed of 100, 500, 2000, 5000 and 8000 l./s.

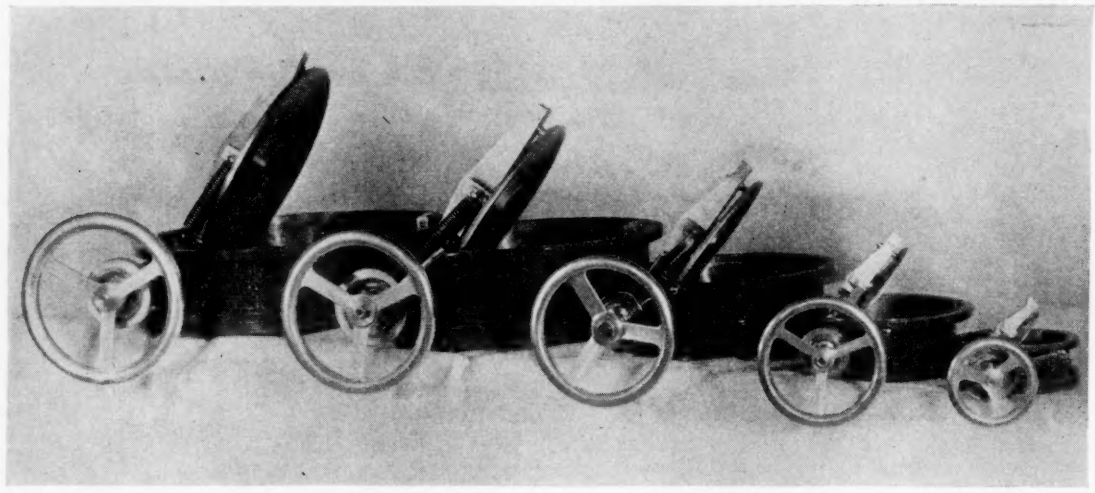

(a)

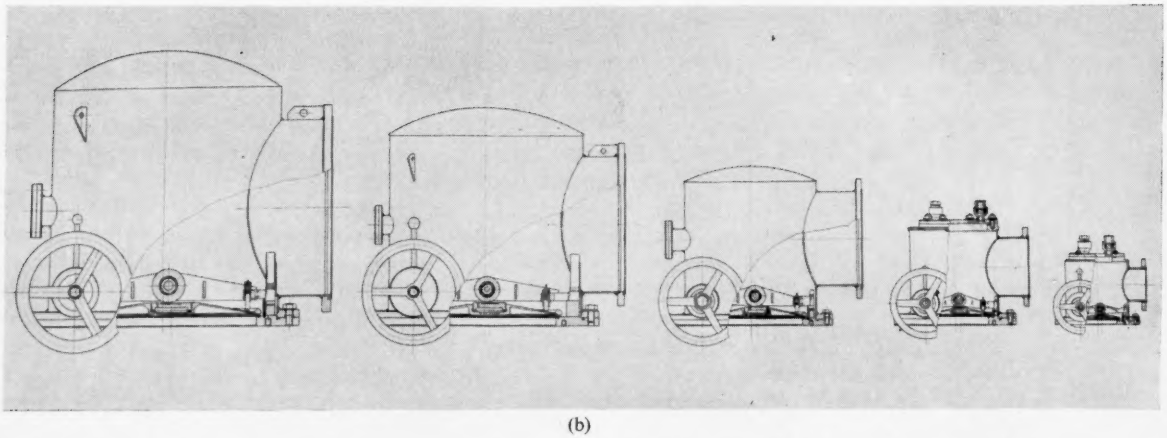

(b)

FIG. 13. High-vacuum gates for a series of the pumps with a speed of 100, 500, 2000, 5000 and 8000 l./s : (a) direct, (b) with an intermediate elbow socket.

On the Choice of Units of Pressure and of Flow in Vacuum Technique*

E. THOMAS, R. SERVRANCKX and R. LEYNIERS

Institut Interuniversitaire des Sciences Nucléaires (Centre de l'Ecole Royale Militaire), Belgium

The various units of pressure and flow used in vacuum technique are examined. The use of a more adequate unit of pressure, related in a simple way to existing units, is proposed.

Vol. 9 59/60

1. Units of pressure

According to the formula which defines them, units of pressure used in vacuum technique belong to two groups.

The first group comprises the units defined by the formula

$$p = F/S \qquad (1)$$

which gives the pressure as the quotient of force and surface area.

The units of this group used in vacuum technique are

(a) in the MKSA system, the newton per square metre (N/m^2), which it is proposed to call the pascal,

(b) in the CGS system, the dyne per square centimetre or microbar or barye

$$1 \text{ dyn/cm}^2 = 1 \ \mu\text{bar} = 1 \text{ barye}$$

also

$$1 \text{ N/m}^2 = 10 \text{ dyn/cm}^2.$$

For measuring low pressures, units such as kilogramme-force per square metre, kilogramme-force per square centimetre, pound-force per square foot, pound-force per square inch, are not used in practice ; however these units are used at the present time to measure pressures greater than atmospheric pressure.

Concerning the units of the second group they are defined by applying the general theorem of the statics of perfect fluids to the equilibrium of a liquid column, used in Torricelli's experiment.

Therefore

$$p = h\varrho g \qquad (2)$$

where p is the pressure, h is the height of the liquid column used, ϱ the density of this liquid and g the acceleration of free fall at the location of the experiment.

It can be seen, therefore, that a unit of the second group depends on the liquid used and on the location of the experiment. Let us choose mercury and assume that the experiment is made at 0 °C and at a location where the acceleration of free fall is 9.806 65 m/s².

A millimetre of mercury is defined thus

$$1 \text{ mmHg} = 1 \text{ mm} \times 13.595\,1 \text{ g/cm}^3 \times 980.665 \text{ cm/s}^2 = 1.333\,22 \times 10^3 \text{ dyn/cm}^2 = 133.322 \text{ N/m}^2.$$

In practice the following is often taken

$$1 \text{ N/m}^2 = 0.75 \times 10^{-2} \text{ mmHg}.$$

It has been suggested that the millimetre of mercury should be called torr and that it should be represented by the symbolic abbreviation Torr, but this symbolic abbreviation has not been accepted internationally.

Let us remember that up to 1954 the normal atmosphere (atm) was defined as being the pressure exerted by a column of mercury of height 760 mm, at 0 °C, at a location where acceleration of free fall was 980.665 cm/s².

It could therefore be written

$$1 \text{ atm} = 760 \text{ mmHg} = 760 \text{ Torr} = 1\,013\,250.144\,354 \text{ dyn/cm}^2 \qquad (3)$$

and

$$1 \text{ mmHg} = \frac{1\,013\,250.144\,354}{760} \text{ dyn/cm}^2. \qquad (4)$$

In 1954, the 10th General Conference on Weights and Measures adopted

$$1 \text{ atm} = 1\,013\,250 \text{ dyn/cm}^2 = 101\,325 \text{ N/m}^2 \text{ (exactly)}.$$

Since then, from equation (4) and from

$$1 \text{ Torr} = \frac{1 \text{ atm}}{760} = \frac{1\,013\,250}{760} \text{ dyn/cm}^2,$$

one finds

$$1 \text{ mmHg} = \frac{1\,013\,250.144\,354}{760} \times \frac{760}{1\,013\,250} \text{Torr} = 1.000\,000\,14 \text{ Torr}.$$

The millimetre of mercury and the torr are no longer equal. In practice, the small difference between these units is disregarded.

In vacuum technique, decimal submultiples of the millimetre of mercury are used ; pressures can therefore be expressed in millitorrs (1 mTorr = 10^{-3} Torr), in microtorrs (1 μTorr = 10^{-6} Torr), in nanotorrs (1 nTorr = 10^{-9} Torr), in picotorrs (1 pTorr = 10^{-12} Torr).

2. Units of mass flow

Logically, the unit of mass flow is the quotient of the unit of mass and the unit of time. In vacuum technique, it is accepted, by applying the law of perfect gases that the mass flow is expressed by the product of unit of pressure and the unit of volume divided by the unit of time.

Hence the torr-litre per second is used (Torr.l.s^{-1}).

Sometimes " lusec " and " clusec " are used. These units, which seem to be going out of use, are equal respectively to the litre-micron of mercury per second and to the centilitre-micron of mercury per second. Hence

$$1 \text{ Torr.l.s}^{-1} = 10^3 \text{ lusec} = 10^5 \text{ clusec}.$$

If an attempt has been made to justify the introduction of the lusec and the clusec because the Torr.l.s^{-1} is a unit which

*Paper presented in French at the *First International Congress on Vacuum Techniques*, Namur, 10–13 June, 1958.

is too large for measuring small mass flows, it can be seen that this can be overcome if the pressure is expressed in millitorrs or in another decimal submultiple of the torr.

3. Suggestion for a more adequate unit of pressure

The question can be asked whether the millimetre of mercury (or the torr) is suitable for measuring low pressures which can actually be obtained.

It would appear not to be so since the smallest submultiple of the torr which has a name is the picotorr and since pressures of this order of magnitude are almost possible in practice.

It is required therefore to suggest a more adequate unit of pressure which shall be related in a simple way to existing units.

We shall choose this unit from the MKSA system. Let us, moreover, point out that in meteorological barometry the millimetre of mercury is being used less and less whilst the millibar which is a multiple of the MKSA unit of pressure is being used more and more ; it is equal to one hundred newtons per square metre

$$1 \text{ mbar} = 10^2 \text{ N/m}^2.$$

Let us first see whether the newton per square metre is

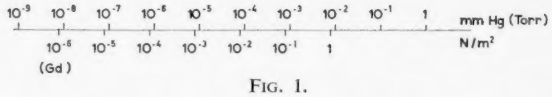

FIG. 1.

suitable and let us plot on a logarithmic scale (see Fig. 1) the millimetre of mercury (or torr) and its submultiples as well as the newton per square metre.

It can be seen immediately that the advantage gained by using the newton per square metre is not sufficient.

We therefore propose to take as the unit for the measurement of low pressures a decimal submultiple of the newton per square metre for example the micronewton per square metre, and to call this unit the *gaede*, in honour of Gaede, and to represent this unit by the symbolic abbreviation "Gd".

Die Diffusionspumpe ihre Physik und Technik*

R. JAECKEL

Universität Bonn, Deutschland

Die Wechselwirkung von physikalischer Forschung und technischer Entwicklung wird am Beispiel der Diffusionspumpe besprochen. Die Erfindung Gaede's und ihre Ausgestaltung durch Gaede selbst und zahlreiche andere Forscher gibt der Technik neuartige Mittel an die Hand, die von der Fabrikation von Vakuumröhren bis zum Bau moderner Vakuumgrossapparaturen reichen. Die sich hierbei ergebenden Anforderungen wirken zurück auf die Ausgestaltung der Pumpen.

Aber nicht nur der Technik, sondern auch der physikalischen Grundlagenforschung insbesondere der Atomphysik lieferte die Diffusionspumpe grundsätzlich neue Möglichkeiten. Die dadurch stets wachsenden Anforderungen an die Leistungen der Pumpen gaben wiederum Anlass zu weiteren Untersuchungen über die physikalischen Vorgänge in den Diffusionspumpen selbst. Diese förderten schliesslich ihrerseits neuere Untersuchungen und Erkenntnisse über rein physikalische Probleme wie die Strömung in verdünnten Gasen beispielsweise bei hohen Mach'zahlen (Düsenströmungen).

Vol. 9 959/60

Vor etwa 45 Jahren am 25 September 1913 meldete der damalige Privatdozent Dr. Wolfgang Gaede eine Vorrichtung zum Evakuieren beim Deutschen Patentamt an. Sie trägt die Nummer DRP 286 404. Dies war die Geburtsstunde der Diffusionspumpe. Hierdurch wurde eine ausserordentlich fruchtbare technische Entwicklung ausgelöst. Betrachten wir hierzu nur die Glühlampe, Verstärkerröhren, Senderöhren, das Fernsehen, die Funkortung und die Quecksilberdampfgleichrichter. Aber auch weite Gebiete der reinen physikalischen Forschung wurden durch sie erst ermöglicht. Genannt seien nur Atomphysik, Kernphysik und die Ausnutzung der Kernenergien. Es lohnt sich daher wohl heute rückblickend den historischen Ablauf der Entwicklung der Diffusionspumpe etwas näher zu verfolgen. Ausserdem ist diese Entwicklung typisch für die ganz allgemeine Wechselwirkung zwischen Physik und Technik.

Am Anfang steht im allgemeinen eine technische Aufgabe, die durch ein physikalisches Prinzip gelöst wird. Im ersten Stadium der Entwicklung erfolgt dann die technische Ausgestaltung des physikalischen Prinzips. Die so gefundenen technischen Lösungen geben aber dann ihrerseits der physikalischen Experimentierkunst neue Möglichkeit. Im zweiten Entwicklungsstadium erfolgt die physikalisch wissenschaftliche Durchdringung der technischen Konstruktion um diese zu verbessern und zu rationalisieren. Auch dieses zweite Stadium hat seine Rückwirkungen auf die reine Physik einerseits dadurch, dass es Impulse gibt zu physikalischen Untersuchungen über die Vorgänge in den technischen Konstruktionen und darüberhinaus geben diese verbesserten technischen Konstruktionen auch der physikalischen Experimentiertechnik neue Möglichkeiten.

Betrachten wir nun im einzelnen die historische Entwicklung der Diffusionspumpe. Am Anfang stand die Aufgabe, Gefässe zu evakuieren und zwar mit einfacheren Mitteln, als sie bisher bekannt waren, und bis zu niedrigeren Drucken als dies bisher möglich war. Gaede fand nun, dass man durch Anwendung der physikalischen Gesetze der Diffusion in Gasen diese Aufgabe lösen könnte. Die Lösung besteht darin, dass Gase von Orten höherer Konzentration zu Stellen niedrigerer Konzentration durch Diffusion gelangen und zwar selbst dann, wenn ausser dem diffundierenden Gas der gesamte Raum noch mit einem zweiten Gas erfüllt ist, dessen Teildruck sogar wesentlich höher sein kann, als der Teildruck des diffundierenden Gases. Handelt es sich bei dem zweiten Gas z. B. um einen strömenden Dampf, so führt dieser das durch Diffusion in ihn eingedrungene Gas fort. Dieser Vorgang kann also dazu ausgenutzt werden, das erste Gas an dem Ort ursprünglich höheren Teildruckes zu verarmen, d. h. zu evakuieren. Dieses ist der Gaede'sche Grundgedanke, dessen physikalische Richtigkeit nicht bestritten werden kann. Trotzdem hat es in späterer Zeit vielfach zu Polemiken geführt, obgleich alle späteren Konstruktionen von Duffusionspumpen von diesem Gaede'schen Grundgedanken Gebrauch machen. Hinzu kommt nur noch die Gaede'sche Forderung eines Diffusionsspaltes. Ein enger Spalt war notwendig, da die ersten Gaede'schen Pumpen mit kleinen Dampfgeschwindigkeiten arbeiteten. Bei den modernen Pumpen mit grossen Dampfgeschwindigkeiten können die ursprünglich engen Spalte sehr weit (bis zu mehreren dcm) dimensioniert werden. Ausserdem ist diese Bedingung bei grossen Dampfgeschwindigkeiten nicht unbedingt notwendig, sondern im wesentlichen eine Ökonomiebedingung. Abb. 1 zeigt das Schema der ersten Gaede'schen Diffusionspumpe, die, wie bereits erwähnt, noch mit kleinen Geschwindigkeiten des strömenden Quecksilberdampfes betrieben wurde. Demgegenüber bedeutete die Diffusionspumpe von Langmuir (Abb. 2) schon einen Fortschritt, da sie mit grösseren Dampfgeschwindigkeiten arbeitete und daher einen weiteren

* Paper presented at the First International Congress on Vacuum Techniques, Namur, 10–13 June 1958.

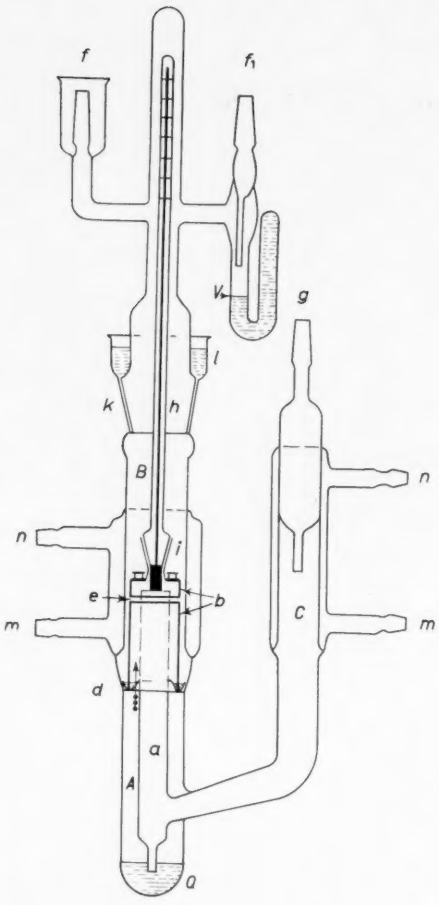

ABB. 1. Erste Quecksilberdiffusionspumpe von Gaede.

Der in dem Siedegefäss *Q* entwickelte Quecksilberdampf gelangt zunächst in den Dampfraum *A* und strömt dann zwischen den Rohren *a* und *b* nach oben. Beim Vorbeistreichen an dem Diffusionsspalt *e* nimmt er das durch *f* angesaugte Gas durch Diffusion auf und in den Vorvakuumraum mit. Das Vorvakuum ist bei *C* angeschlossen. Der durch die Wasserkühlung *m n* kondensierte Quecksilberdampf läuft als flüssiges Quecksilber durch das Innere des Rohres *a* nach *Q* zurück.

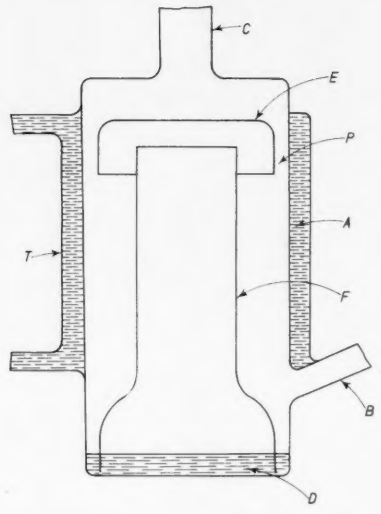

ABB. 2. Diffusionspumpe nach Langmuir.

D Quecksilbersiedegefäss, *F* Dampfsteigrohr, *E* Umkehrdüse, *P* Diffusionsspalt (Diffusionsfläche), *A* Kondensationsfläche, *B* Vorvakuumanschluss, *C* Ansaugstutzen.

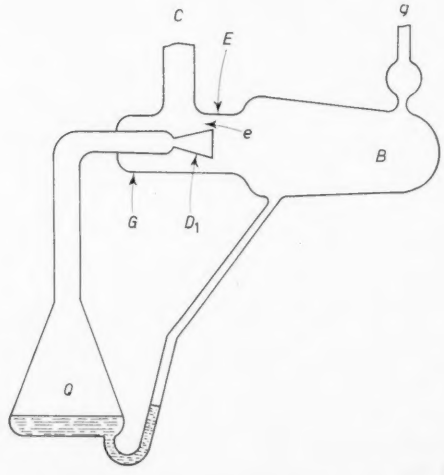

ABB. 3. Diffusionspumpe nach Crawford.

Q Quecksilbersiedegefäss, D_1 Lavaldüse für den Treibdampf, *e* Diffusionsspalt (Diffusionsfläche), *C* Ansaugstutzen, *g* Vorvakuumanschluss.

Diffusionsspalt zuliess und somit grössere Sauggeschwindigkeiten erzielte. Sie zeigt ausserdem schon die auch heute noch vielfach gebräuchliche Form der Diffusionsdüse als Umkehrdüse. Einen weiteren Schritt in Richtung auf hohe Strömungsgeschwindigkeiten des Quecksilberdampfes stellte die Diffusionspumpe von Crawford (Abb. 3) dar, die als Treibdüse für den Quecksilberdampf eine Lavaldüse verwendet. Damit ist nun aber auch die Entwicklung der Quecksilberdiffusionspumpe im Prinzip abgeschlossen.

Die Quecksilberdiffusionspumpe hat noch den Nachteil, dass sie zur Erzielung von Totaldrucken unter 10^{-3} Torr Kühlfallen benötigt. Es bedeutete daher einen Fortschritt, als von Burch im Jahre 1929 statt Quecksilber neue Treibmittel angegeben wurden, die bei der Temperatur des Kühlmantels der Diffusionspumpen Dampfdrucke von 10^{-6} Torr und darunter hatten, und die es also ermöglichten, entsprechend niedrige Drucke ohne Verwendung von Kühlfallen zu erzielen. Durch verwendete als Treibmittel hochsiedende Mineralölfraktionen, die durch Destillationen im Hochvakuum gewonnen wurden, sogenannte Apiezonöle. Alsbald wurden dann von Hickmann chemisch einheitliche Substanzen angegeben, die ebenfalls bei Raumtemperatur Dampfdrucke unter 10^{-6} Torr hatten. Diese neuen Treibmittel besassen aber noch den Nachteil, dass sie im Betrieb durch thermischen Zerfall und Oxydation Zerfallsprodukte bildeten, die höhere Dampfdrucke besassen und damit das erzielbare Vakuum verschlechterten. Technisch brauchbar wurden daher die Öldiffusionspumpen erst durch die Einführung der fraktionierenden Öldiffusionspumpen (Abb. 4),

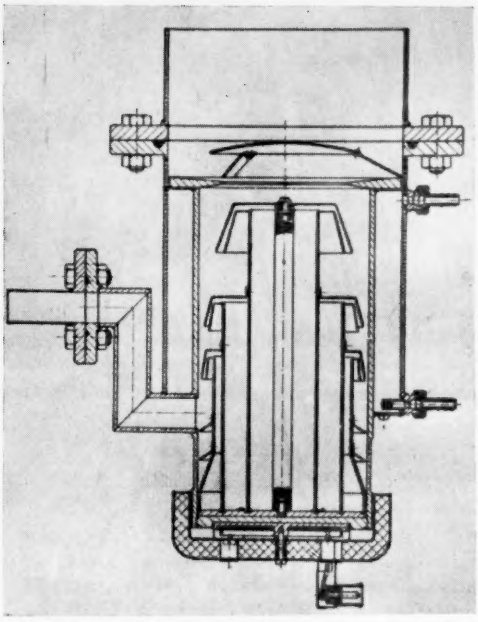

Abb. 4. Dreistufige Ölfraktionsdiffusionspumpe aus Metall.

Sauggeschwindigkeit 250 l/s, Vorvakuum 0,3 Torr. Der an der wassergekühlten Kondensationsfläche niedergeschlagene Öldampf läuft in flüssiger Form in das Siedegefäss zurück. Die drei übereinander befindlichen Pumpstufen stehen im Flüssigkeitsraum des Siedegefässes miteinander in Verbindung, haben aber getrennte Dampfsteigrohre. In dem äussersten der drei konzentrischen Ringe steigt zunächst der leichtest verdampfbare Anteil des Treibmittels in Dampfform auf und dient zum Betrieb der Düse, die dem Vorvakuum am nächsten gelegen ist. Schwerer siedende Anteile verdampfen in dem mittleren der drei konzentrischen Ringe. In den innersten gelangen so schliesslich nur noch die am schwersten verdampfbaren Anteile mit dem niedrigsten Dampfdruck.

Vol. 9 959/60

bei denen die Zerfallsprodukte durch Destillationsprozesse in der Pumpe in kurzer Zeit von der Hochvakuumseite auf die Vorvakuumseite gebracht und dadurch unschädlich gemacht werden. Um die Weiterführung der fraktionierenden Öldiffusionspumpen hat sich insbesondere Hickmann bemüht. Ihr Betriebsverhalten wurde insbesondere von Hickmann, Jaeckel, Dayton und in neuerer Zeit von Latham, Power und Dennis untersucht. Dies ist etwa die Entwicklung der Diffusionspumpe bis zum Jahre 1935. Damit war auch das erste Stadium ihrer technischen Ausgestaltung abgeschlossen. Durch dieses erste Entwicklungsstadium wurde vor allen Dingen die Technik der Röhren (Elektronik) und die Atomphysik befruchtet.

Zu Beginn des zweiten Entwicklungsstadiums zeichnete sich die Möglichkeit zum Bau grosser Leistungsfähiger Diffusionspumpen ohne Kühlfalle schon ab. Damit setzte die Anwendung des Hochvakuums für grosstechnische Anlagen ein. Von den hierbei ausgeübten Verfahren seien genannt Molekulardestillation, die Vakuum-Metall-Bedampfung grosser Spiegel, die Vakuum-Aufdampfung von optischen Antireflex-Belegungen, die Teilchenbeschleuniger für die Kernphysik, die Gefriertrocknung, die Vakuummetallurgie sowie Vakuum-Imprägnieranlagen. Als neues Element kam der Dampfstrahlsauger als abgewandelte Form der Diffusionspumpe hinzu.

Um die Diffusionspumpe für diese grosstechnischen Aufgaben in rationeller Weise leistungsfähig zu machen, war es notwendig, die in ihr ablaufenden physikalischen Vorgänge theoretisch zu durchdringen und zu diesem Zweck im einzelnen experimentell zu durchforschen. Hierum haben sich besonders bemüht, in älterer Zeit Gaede selbst, dann Langmuir, Molthan und Matricon, in neuerer Zeit Jaeckel, Dayton, Witty, Alexander, Blears, Nöller, Kutscher, Reich sowie auch Florescu.

Da es schwierig ist, die physikalischen Vorgänge in den Diffusionspumpen in voller Strenge zu berechnen, geht man zweckmässiger Weise so vor, dass man sie durch vereinfachte Modellstellungen annähert. Die Vorgänge in den vereinfachten Modellen können dann durchgerechnet werden. Die sich hieraus ergebenden Konsequenzen für das Betriebsverhalten der Diffusionspumpen lassen sich dann schliesslich mit den Werten vergleichen, die bei den Diffusionspumpen im technischen Betrieb beobachtet wurden. Die einfachste Form einer solchen Modellvorstellung wurde von Matricon angegeben (Abb. 5). Die rechte Hälfte der Abbildung zeigt

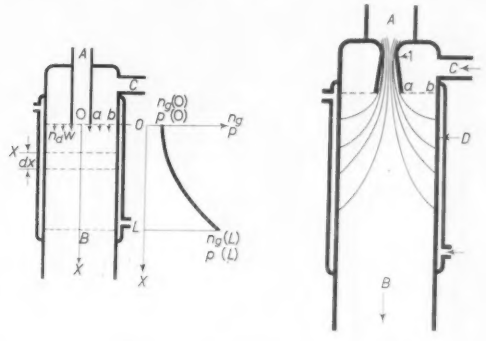

Abb. 5. *Rechts* : Schema der Vorgänge in einer Diffusionspumpe.

A Eintritt des Treibdampfes in die Düse 1, *ab* Trennfläche zwischen Treibdampf und dem bei *C* eintretenden angesaugten Gas, *D* wassergekühlte Kondensationsfläche für den Treibdampf, *B* Vorvakuum.

Links : Modellanordnung hierfür, daneben Diagramm für den Verlauf des Gasdruckes p von $x = 0$ bis $x = L$ und der Verlauf der Gasdichte n_g.

das vereinfachte Schema einer Diffusionspumpe. Ein von *A* kommender Dampfstrom wird in der Lavaldüse 1 beschleunigt und tritt bei *a* kegelförmig aus der Düse aus. Er trifft auf die wassergekühlte Wand *D* und wird dort kondensiert. Die Fläche *a...b* ist Trennfläche zwischen dem Dampfstrom und dem bei *C* angesaugten Gas. Dieses tritt durch die Fläche *a...b* durch Diffusion in den Dampfstrom ein und wird von diesem in das Vorvakuum bei *B* gefördert.

Abb. 5 linke Hälfte zeigt die ersatzweise behandelte Modellanordnung. Hiernach wird angenommen, dass alle Dampfmoleküle von der Fläche *a...b* starten und mit gleicher Geschwindigkeit w nach abwärts laufen und dass sie hier nach Erreichen der Fläche L kondensiert werden. Der Dampfstrom hat dabei auf der ganzen Strecke zwischen $x = 0$ und $x = L$ die konstante Dampfdirchte n_d. Die bei *C* angesaugten Gasmoleküle treten durch Diffusion durch die Fläche *a...b* in den Dampfstrom ein und werden von diesem nach abwärts gefördert bis sie schliesslich nachdem der Dampf selber hinter der Stelle $x = L$ kondensiert ist,

in das Vorvakuum bei B abgegeben werden. Die Gasmoleküle mögen oberhalb der Fläche $a...b$ die Dichte v und unmittelbar unterhalb der Fläche $a...b$ im Dampfstrom die Dichte n_g^s (O) haben. Damit ergibt sich für die Anzahl der Gasmoleküle N die pro Zeiteinheit durch die Diffusionsfläche F mehr von oben nach unten in den Gastrom hinein als von unten nach oben aus demselben austreten, die Beziehung

$$N = \tfrac{1}{4} F \bar{c} (v - n_g^s(\mathrm{O})) \tag{1}$$

$\bar{c}$ = mittlere thermische Geschwindigkeit der Gasmoleküle. Ganz allgemein wird angenommen, dass die Dampfdichte n_d stets grösser ist als die Gasdichte n_g

$$n_d \gg n_g \tag{2}$$

Für irgendeine Stelle x ergibt sich für die Mitnahme des abgepumpten Gases aus dem Hochvakuumraum in den Vorvakuumraum der Wert $w n_g^s(x)$ und die Rückdiffusion aus dem Vorvakuumraum in den Ansaugraum entgegen den strömenden Dampf (und zwar infolge des im Vorvakuumraum höheren Gaspartialdruckes) zu $D\, dn_g^s(x)/dx$. Als Differenz dieser beiden Grössen hat der Gastransport infolge der Saugwirkung S der Pumpe den wert vs

$$vs = w\, n_g^s(x) - D\, dn_g^s(x)/dx$$
$$\text{mit } s = \mathrm{S/F} \tag{3}$$

Die Lösung dieser Differentialgleichung unter Berücksichtigung der Randbedingung 1 liefert für den Fall des Enddruckes, d. h. $vs = 0$

$$\text{mit } D_0 = D/n_d$$
$$\ln\ p(L)/p(O) = L n_d w / D_0 \tag{4}$$

Hieraus folgt also, das Verhältnis vom Druck auf der Vorvakuumseite $p(L)$ zum Druck auf der Saugseite $p(0)$ (Enddruck) bzw. der Verlauf von Druck p und Gasdichte n_g im Dampfstrom zwischen $x = 0$ und $x = L$ (siehe das Diagramm auf der linken Seite der Abb. 5). Für das Verhalten der Pumpe bei geöffnetem Ansaugstutzen bei C, (d. h. also bei Sauggeschwindigkeit) gilt $vs \neq 0$. Dann folgt aus der Gleichung 3

$$s = \frac{\bar{c}}{4} \cdot \frac{1}{1 + \bar{c}/4w} \tag{5}$$

Wie die Prüfung von technischen Pumpen gezeigt hat, gibt die Gleichung 5 die Abhängigkeit der Sauggeschwindigkeit von der Gasart ($\bar{c}$) und von der Strömungsgeschwindigkeit des Dampfes (w) richtig wieder. Dagegen sollten nach diesem einfachen Modell die spezifische Sauggeschwindigkeit s unabhängig von der Grösse der Diffusionsfläche F und auch unabhängig von der Heizleistung sein, was beides in Widerspruch mit der Erfahrung steht. Um dieses Verhalten zu erklären ist daher ein verbessertes Modell notwendig. Dies erhält man durch Berücksichtigung des sogenannten Dampfsaumes, siehe Abbildung 6, rechte Hälfte. Danach wird ein kegelförmig aus einer Lavaldüse austretender Dampfstrom (mit etwa der kegeligen Begrenzungsfläche $a...b$) von einem Dampfsaum (schraffierte Fläche in Abb. 6 rechts) umgeben, der daher rührt, dass in dem Dampfstrom, der aus der Düse austritt, immer einige Moleküle eine so grosse nach rückwärts gerichtete Komponente der thermischen Geschwindigkeit haben, dass sie den Dampfstrom durch die Fläche $a...b$ nach rückwärts verlassen können und dort den Dampfsaum

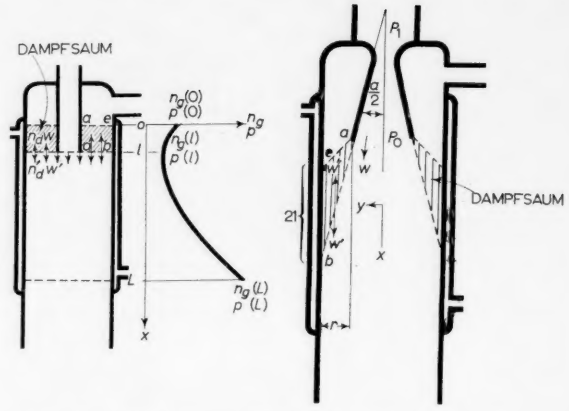

ABB. 6. *Rechte Seite* : Schema der Vorgänge in einer Diffusionspumpe (zweite Näherung, Dampfsaum).

Links : Modellanordnung hierzu, das Diagramm zeigt wieder den Verlauf von Gasdruck p und Gasdichte n_g zwischen $x = 0$ und $x = L$.

zwischen der Fläche $a...b$ und $a...e$ bilden. Dieser Sachverhalt wird durch das verbesserte Modell (Abbildung 6, links) berücksichtigt. Hierin wird angenommen, das von der Fläche $a...b$ nach abwärts Dampfmoleküle mit der Geschwindigkeit w' und der Zahl pro cm³ n'_d fliegen und dass eine kleinere Anzahl von Dampfmolekülen von derselben Fläche mit der Geschwindigkeit w'' und der Zahl pro cm³ n''_d nach aufwärts bis zur Begrenzungsfläche $a...e$ fliegen. Durch analoge Betrachtungen wie bei Abb. 5 kann man jetzt zeigen, dass die Dichteverteilung der angesaugten Gasmoleküle im Dampfstrom $n_g^s(x)$ und ebenso der Gang des Partialdruckes p_g durch das in Abb. 6 gezeigte Diagramm gegeben ist, wonach also die Dichte von $x = 0$ bis $x = 1$ zunächst abnimmt und dann bis $x = L$ wieder ansteigt. Die angesaugten Gasmoleküle müssen also zunächst entgegen einer Dampfströmung $n''_d.w''$ (im Dampfsaum) bis zur Fläche $a...b$ diffundieren. Dort gelangen sie in einen Dampfstrom, der sie in Richtung auf das Vorvakuum mitnimmt. Die Existenz des Dampfsaumes führt damit zu einer Verschlechterung des Druckverhältnisses $p(L)/p(0)$ zwischen Vorvakuumdruck und Enddruck und gleichfalls zu einer Herabsetzung der spezifischen Sauggeschwindigkeit s. Der Einfluss des Dampfsaumes wächst mit seiner Tiefe. Andererseits nimmt die Breite des Dampfsaumes (2 1, siehe Abb. 6, rechts) mit der Breite der Diffusionsfläche $a...b$ zu. Im Hinblick auf die Ökonomie der Diffusionspumpen sollte daher die Breite des Dampfsaumes und damit die Breite der Diffusionsfläche ein gewisses Mass nicht überschreiten. Diese Grenzbedingung ergibt sich daraus, dass die schädliche Wirkung des Dampfsaumes entfällt, wenn die mittlere freie Weglänge der Gasmoleküle im Dampfsaum grösser ist als die Breite 2 1 des Dampfsaumes. Es ist damit gleichzeitig eine Grenzbedingung für die Breite der Diffusionsfläche. Sie entspricht der Gaede'schen Forderung nach einem Diffusionsspalt für Diffusionspumpen mit kleinen Dampfgeschwindigkeiten.

Aus dem Modell der zweiten Näherung folgt ausserdem, dass die spezifische Sauggeschwindigkeit s mit zunehmender Heizleistung, d.h. mit zunehmenden Strömungsgeschwindigkeit des Dampfes zunächst anwächst (siehe Abb. 7). Nach

Erreichung eines Optimalwertes fällt die spezifische Sauggeschwindigkeit dann bei weiter zunehmender Heizleistung wieder ab, weil nunmehr die Dichte der Dampfmoleküle n''_d im Dampfsaum so grosse Werte annimmt, dass die angesauten Dampfmoleküle den Dampfsaum nicht mehr ohne Stösse durchfliegen können.

Zur Erlangung noch weitergehender Kenntnisse über die Vorgänge in Diffusions und Dampfstrahlpumpen kommt man nicht mehr mit Modellvorstellungen aus, sondern man muss nunmehr experimentelle Untersuchungen über die wirklichen physikalischen Vorgänge in den Pumpen durchführen (siehe hierzu Abb. 8). Die Diffusions- und Dampfstrahl-pumpen unterscheiden sich in ihrem Aufbau dadurch, dass bei den Dampfstrahlpumpen eine voll ausgebildete Staudüse vorhanden ist. Diese können daher auch gegen höhere Vorvakuumdrucke arbeiten als die Diffusionspumpen. Charakteristische Unterschiede zeigen auch die Kurven für

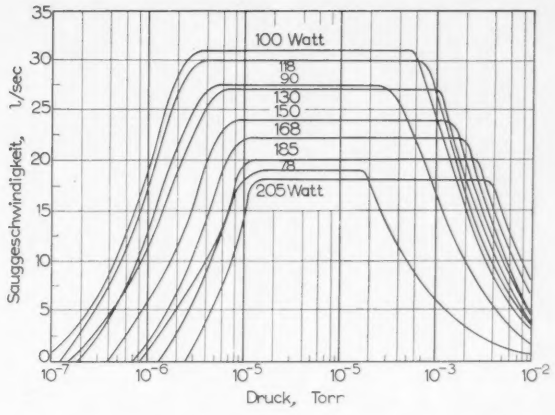

Abb. 7. Sauggeschwindigkeit einer Öldiffusionspumpe in Abhängigkeit vom Ansaugdruck für verschiedene Heizleistungen.

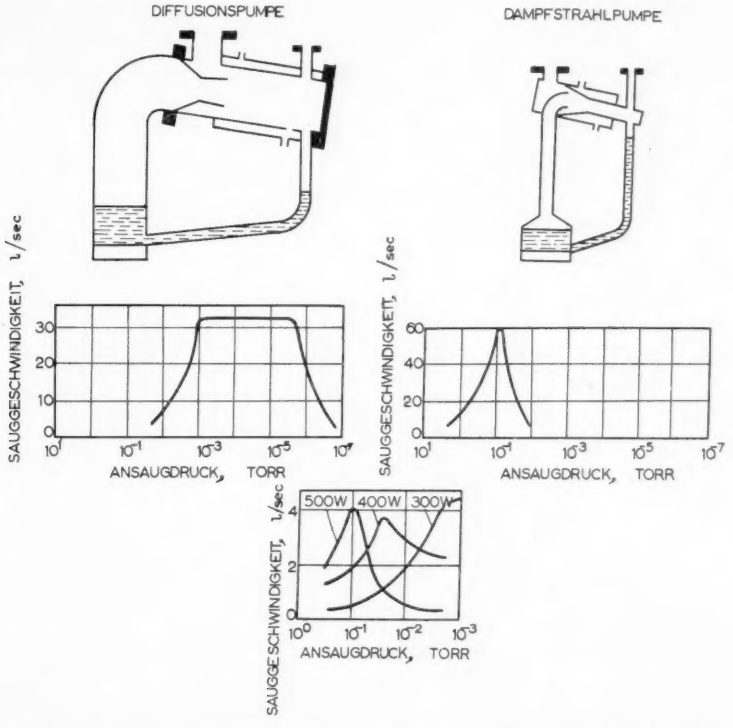

Abb. 8. Schema des Aufbaues einer *Diffusionspumpe links* und einer *Dampfstrahlpumpe rechts*. Darunter die Kurven für die zugehörigen Sauggeschwindigkeiten in Abhängigkeit vom Ansaugdruck.

die Sauggeschwindigkeit in Abhängigkeit vom Ansaugdruck. Durch Erhöhung der Heizleistung lässt sich bei der Diffusionspumpe die Kurve für die Sauggeschwindigkeit in Abhängigkeit vom Ansaugdruck in die für Dampfstrahlpumpen charakteristische Form überführen (siehe Abb. 8, das untere Diagramm).

Für die Untersuchung der physikalischen Vorgänge in den Pumpen sind 3 wesentliche Teile zu unterscheiden, der Treibstrahl, die Durchmischung und die Vorgänge in der Staudüse.

Abb. 9 zeigt einen Quecksilberdampfstrahl, der mit Überschallgeschwindigkeit aus einer Lavaldüse austritt. Man sieht, wie die Weite des Öffnungskegels mit zunehmendem Dampfdruck am Eintritt in die Lavaldüse (Kesseldruck p_0) zunimmt und gleichzeitig auch die Abhängigkeit vom Gasdruck p in der Umgebung der Düsenmündung. Durch höhere Gasdrucke wird der Öffnungskegel zusammengedrückt.

Abb. 10 zeigt die verschiedene Form der Durchmischung zwischen angesaugtem Gas und dem Dampfstrom (nach Nöller) : bei Diffusionspumpen, d. h. bei niedrigen Dampfdrucken gilt die linke Hälfte der Abb. 10 und bei Dampfstrahlpumpen, d. h. bei hohen Dampfdrucken in der

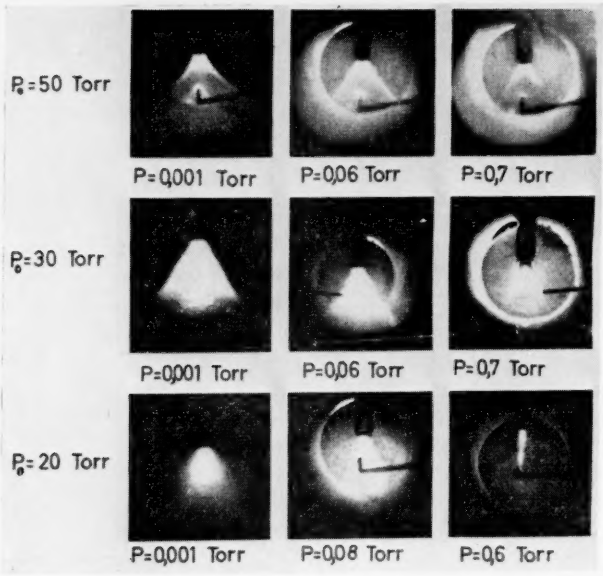

ABB. 9. Strömungsbilder für den aus einer Düsenmündung austretenden Quecksilberdampf in Abhängigkeit vom Druck am Eintritt in die Düse p_0 und vom Druck p in der Umgebung der Düsenmündung (nach Nöller).

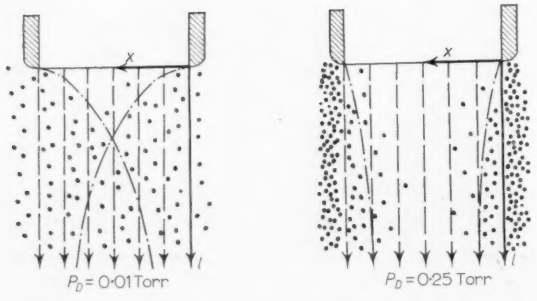

ABB. 10. Schema für die Eindringtiefe von Luft durch Diffusion in den Treibdampfstrahl (nach Nöller).
Links für niedrige Dampfdrucke (Diffusionspumpe); rechts für höhrer Dampfdrucke (Dampfstrahlpumpe).

Dampfströmung, die rechte Hälfte in der Abb. 10. Bei niedrigen Dampfdrucken kann das Gas durch Diffusion gleichförmig den ganzen Dampfstrom durchdringen, während es bei hohen Dampfdrucken nur in die Randpartien der Dampfströmung durch Diffusion eindringen kann. Dies erklärt die verschiedenen Formen der Sauggeschwindigkeitskurven in Abhängigkeit vom Ansaugdruck bei den beiden Pumpenarten (siehe Abb. 17).

Die Abb. 11, 13 und 15 zeigen das Verhalten von Überschallöldampfströmungen in Staudüsen nach Kutscher und insbesondere das Auftreten von schrägen und geraden Verdichtungsstössen in diesen Staudüsen. Bei niedrigen Gasdrucken in der Umgebung der Düsenmündung (Abb. 11) breitet sich der Öffnungskegel von der Düsenaustrittsöffnung

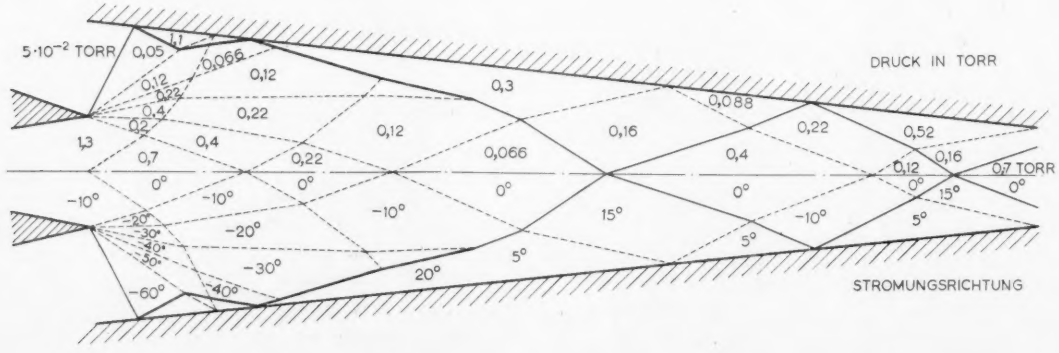

ABB. 11. Gasdynamische Konstruktion des Strömunsverlaufes beim Austritt einer Öldampfströmung aus einer Lavaldüse bei niedrigem Aussendruck. Ansaugdruck 5×10^{-2} Torr; Vorvakuumdruck 0,7 Torr.

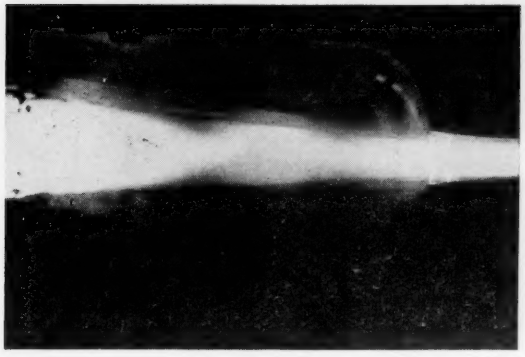

Abb. 12. Photographische Aufnahme eines Strömungsbildes entsprechend Abb. 11.

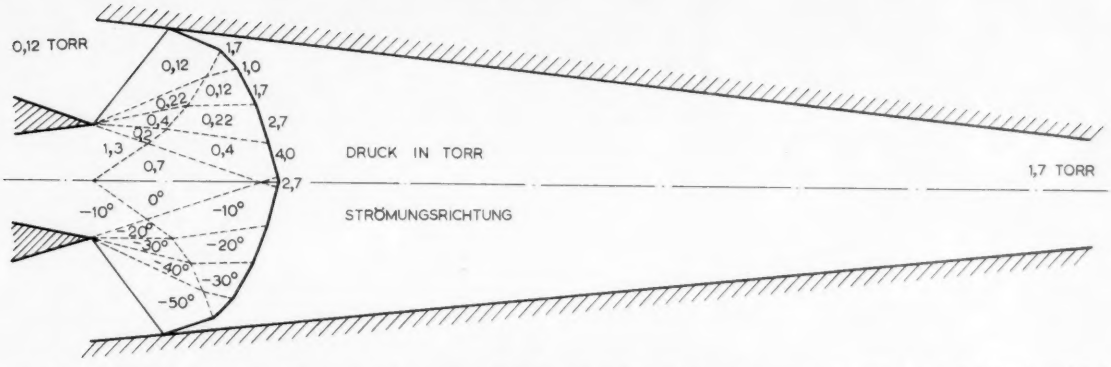

Abb. 13. Gasdynamische Konstruktion des Strömungsverlaufes für den Fall erhöhten äusseren Gegendruckes (0,1 Torr) und bei hohem Vorvakuumdruck (1,7 Torr).

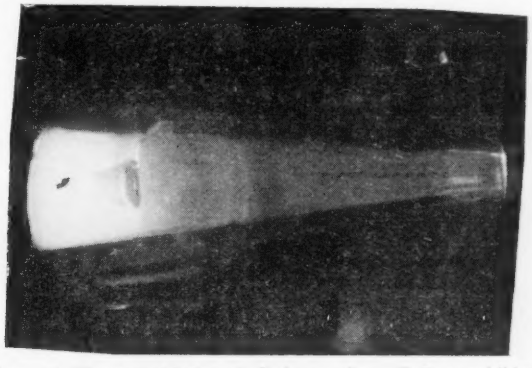

Abb. 14. Photographische Aufnahme eines Strömungsbildes entsprechend Abb. 13.

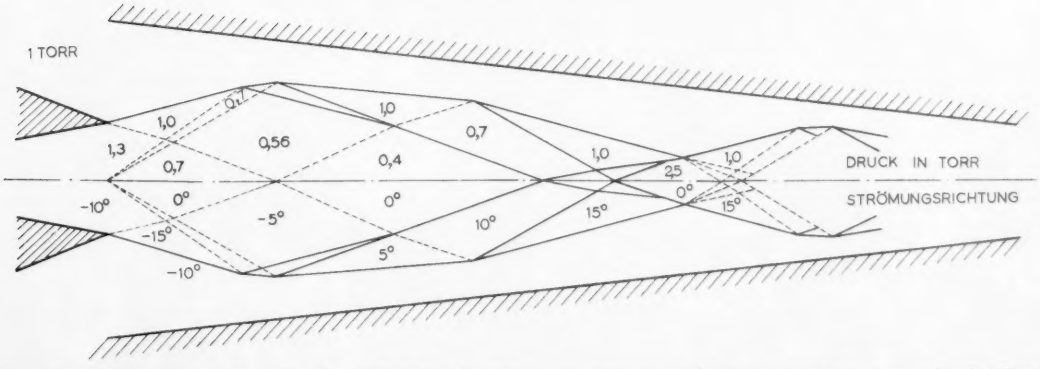

Abb. 15. Strömungskonstruktion für den Fall hoher Drucke in der Umgebung der Dösenmündung, Ansaugdruck 1 Torr.

Vol. 9 59/60

ABB. 16. Photographische Strömungsaufnahme zu Abb. 15.

bis zur Staudüsenwand aus und löst dort schräge Verdichtungsstösse aus. Bei höheren Gasdrucken (Abb. 13) kommt es zu einem geraden Verdichtungsstoss. Abb. 15 zeigt wie bei einem hohen Ansaugdruck der Austrittskegel der Dampfströmung aus der Treibdüse soweit zusammengedrückt wird, dass der Dampfstrom die Staudüsenwand nicht mehr erreicht. Die Abb. 12, 14, 16 zeigen jeweils photographische Aufnahmen von experimentellen beobachteten Strömungen zum Vergleich mit den zugehörigen Konstruktion en des Strömungsverlaufes aufgrund gasdynamischer Berechnungen (Abb. 11, 13 u. 15).

Aus diesen Beobachtungen ergibt sich die Erklärung für das verschiedenartige Verhalten von Diffusions- und Dampfstrahlpumpen in Bezug auf die Form der Sauggeschwindigkeitskurve in Abhängigkeit vom Ansaugdruck (siehe Abb. 17). Bei der Diffusionspumpe (links) ist der Gasdruck in der Umgebung der Düsenmündung stets so klein, dass er ohne Einfluss auf die Weite des Öffnungskegels bleibt. Die Sauggeschwindigkeit ist daher im gesamten Arbeitsbereich nahezu konstant, anders bei den Dampfstrahlpumpen (siehe Abb. 17, rechte Hälfte). Bei niedrigen Ansaugdrucken ist die Weite des Öffnungskegels so gross, dass die Randschichten in die das Gas nur durch Diffusion eindringen konnte, garnicht bis in die Staudüse gelangen. Die resultierende Sauggeschwindigkeit der Pumpe ist sehr gering. Bei wachsenden Ansaugdrucken wird der Öffnungskegel schliesslich soweit zusammengedrückt, dass die mit Gas beladenen Randpartien der Dampfströmung in die Staudüse hineinkommen. Die Sauggeschwindigkeit erreicht ihren Maximalwert (siehe das darunter stehende Diagramm). Bei noch weiter anwachsenden Ansaugdrucken wird schliesslich der

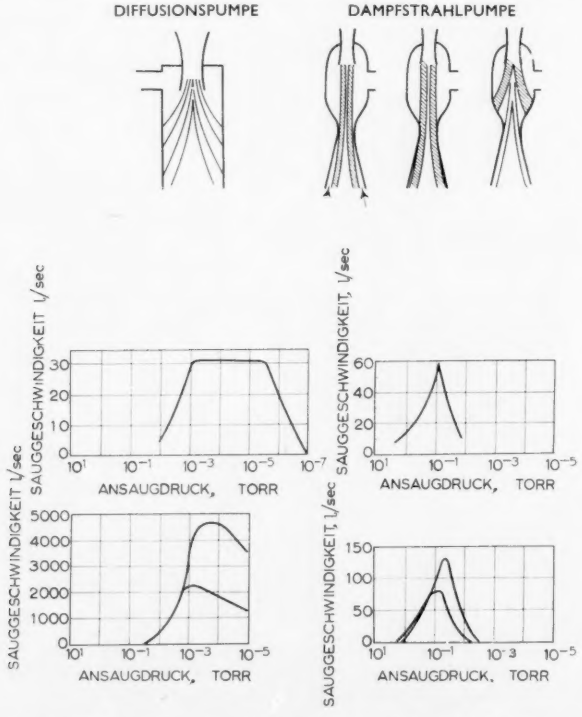

ABB. 17. Schema für den Verlauf der Treibdampfströmung nach Austritt aus der Treibdüse.

Links : bei niedrigen Drucken (Diffusionspumpe).

Rechts : bei höheren Drucken (Dampfstrahlpumpe).

Darunter Diagramme für die Sauggeschwindigkeit in Abhängigkeit vom Ansaugdruck in allen darunter Sauggeschwindigkeitskurven für verschiedene Gase (obere Kurve : H_2; untere Kurve : Luft).

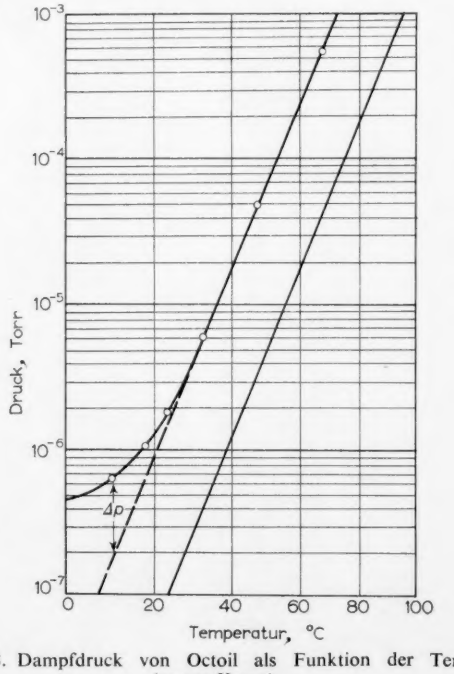

ABB. 18. Dampfdruck von Octoil als Funktion der Temperatur (untere Kurve).

Obere Kurve Ionisierung des Restdampfes einer mit Octoil betriebenen Pumpe (nach Reich).

Öffnungskegel der Dampfströmung soweit zusammengerückt, dass die Dampfströmung die Staudüse nicht mehr vollständig abschliesst. Demzufolge kann jetzt Gas aus dem Vorvakuumraum durch den Randteil der Staudüse, der von der Dampfströmung nicht erfüllt wird, zur Ansaugseite zurückströmen und damit die wirksame Saugwirkung der Pumpe wieder herabsetzen (siehe das darunter stehende Diagramm). Auch die Abhängigkeit der Sauggeschwindigkeit von der angesaugten Gasart ergibt sich aus den obigen Beobachtungen in Übereinstimmung mit der Erfahrung (siehe die Diagramme in der untersten Reihe der Abb. 17).

Misst man bei Öldiffusionspumpen den erreichbaren Enddruck, so findet man in vielen Fällen Werte, die höher liegen als dar Dampfdruck des Treibmittels bei der Kühlwassertemperatur. Zur Untersuchung dieser Frage hat Reich auf der Saugseite einer Diffusionspumpe ein Ionisationsmanometer angebracht, wobei gleichzeitig die Möglichkeit bestand, den Messraum mit dem Ionisationsmanometer und die Kondensationsfläche der angeschlossenen Öldiffusionspumpe mittels eines Thermostaten auf gleiche Temperatur zu bringen. Die auf diese Weise von Reich gemessene Ionisation in Abhängigkeit von der Temperatur zeigt Abb. 18, obere Kurve. Zum Vergleich ist die unabhängig davon mit anderen Methoden gemessene Dampfdruckkurve (Abb. 18, untere Kurve) mit eingetragen. Man sieht, dass beide Kurven bei höheren Temperaturwerten mit konstantem Abstand zueinander parallel verlaufen, d. h. also, dass bei hohen Drucken die Ionisation dem Dampfdruck des reinen Treibmittels proportional ist, d. h. also, dass im wesentlichen der reine Treibmitteldampf für den Enddruck massgebend ist. Anders sieht der Verlauf der gemessenen Ionisationskurve bei niedrigen Temperaturen aus. Man sieht, dass bei niedrigen Temperaturen die Ionisationskurve nicht mehr zur Dampfdruckkurve parallel verläuft, sondern nach oben gegenüber der verlängerten Gerade abbiegt und zwar in einem von der Temperatur unabhängigen Absolutbetrag Δp.

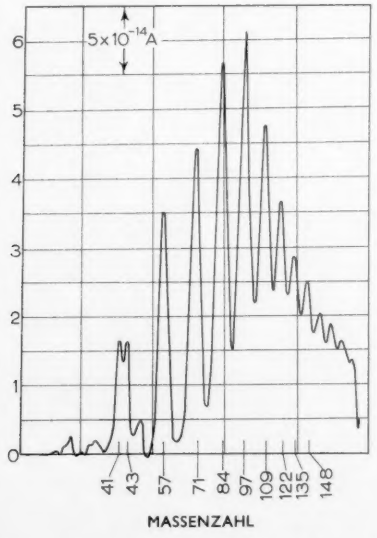

Abb. 19. Massenspektrum in einer mit Öldampf betriebenen Diffusionspumpe, aufgenommen mittels eines Omegatrons (Reich und Nöller).

Diese Messung legt die Deutung nahe, dass bei niedrigen Temperaturen und Drucken nicht kondensierbare Zersetzungsprodukte des ursprünglich reinen Treibmittels einen merklichen Anteil an dem vorhandenen totalen Restdruck ausmachen.

Dies steht im Einklang mit massenspektrometrischen Messungen von Reich und Nöller unter Verwendung eines Omegatrons (siehe Abb. 19).

Als Ursache für den erhöhten Enddruck der Öldiffusionspumpen wurde ausser dem Vorhandensein der oben genannten Zersetzungsprodukte von verschiedenen Autoren ein zurückfliegen der Treibmittelmoleküle unmittelbar aus der Dampf-

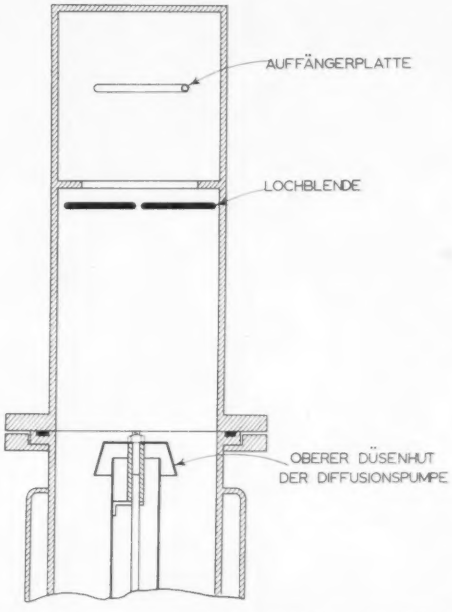

Abb. 20. Lochkameraanordnung zur Aufnahme der Rückströmung von Ölmolekülen aus dem Treibdampfstrahl nach rückwärts in den evakuierten Rezipienten (nach Ruf und Winkler).

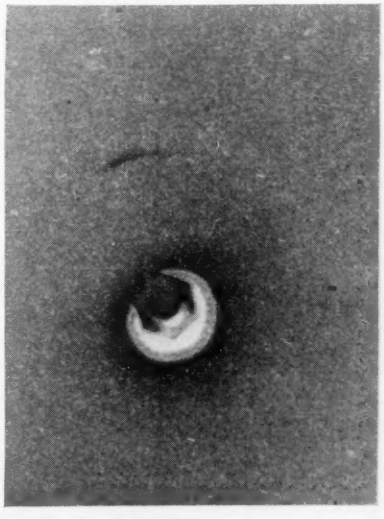

Abb. 21. Aufnahme der Öldampfrückströmung aus einer Diffusionspumpe mit der Lochkameramethode (Bild der Auffängerplatte).

Vol. 9 959/60

strömung in den Vakuumraum (d. h. also ohne Berührung einer gekühlten Kondensationsfläche), vermutet. Besonders eindrucksvoll zeigen diesen Vorgang Ruf und Winkler mit der an sich bekannten Lochkamaramethode (Abb. 20). Abb. 21 zeight ein solches Rückströmungsbild. Darin gehen die zurückgeflogenen Öldampfmoleküle zum Teil von einer Undichtigkeit an der Befestigungsschraube des Düsenhutes aus und zum andern Teil vom Düsenrand. Abb. 22 zeigt eine analoge Aufnahme bei der die Beteiligung des Düsenrandes an der Öldampfrückströmung noch stärker in Erscheinung tritt.

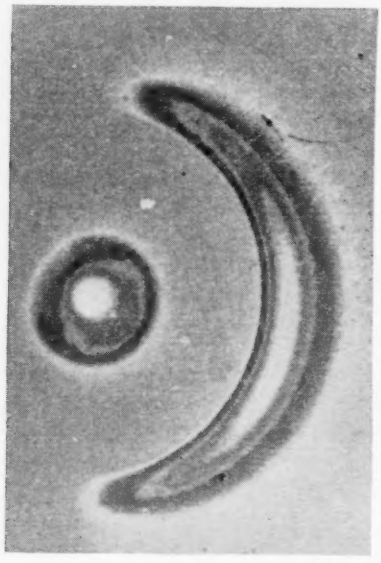

ABB. 22. Aufnahme der Öldampfrückströmung aus einer Öldiffusionspumpe mit der Lochkameramethode (Bild der Auffängerplatte).

Nach dem hiermit dargelegten Stand der Untersuchungen über die Vorgänge in den Diffusions- und Dampfstrahlpumpen dürfte die Arbeit der Physiker hieran in der Hauptsache abgeschlossen sein und die weitere technische Entwicklung dieser Pumpen vorzugsweise in den Händen der Ingenieure liegen.

Literatur

[1] P. Alexander ; *J. Sci. Instrum.* **23**, 11 (1946).
[2] J. Blears ; *Proc. Roy. Soc.* A **188**, 62 (1946).
[3] C. R. Burch ; *Proc. Roy. Soc.* **123**, 271 (1929).
[4] W. W. Crawford ; *Phys. Rev.* **10**, 557 (1917).
[5] B. B. Dayton ; *Ind. Eng. Chem.* **40**, 795 (1948).
[6] B. B. Dayton ; *Rev. Sci. Instrum.* **19**, 793 (1948).
[7] N. A. Florescu ; *Investigationes Physicae*, 1952, Nr. 1 u. 2 ; 1953, Nr. 1 u. 2 ; 1954, Nr. 1 ; 1955, Nr. 2.
[8] W. Gaede ; *Ann. Phys.* **41**, 289 (1913).
[9] K. C. D. Hickmann und C. R. Sanford ; *Rev. Sci. Instrum.* **1**, 140 (1930).
[10] K. C. D. Hickmann ; *J. Phys. Chem.* **34**, 637 (1930).
[11] K. C. D. Hickmann ; *J. Franklin Inst.* **221**, 215, 383 (1936).
[12] K. C. D. Hickmann ; *Rev. Sci. Instrum.* **22**, 141 (1951).
[13] R. Jaeckel ; *Z. tech. Phys.* **23**, 177 (1942).
[14] R. Jaeckel ; *Z. Naturf.* **2a**, 666 (1947).
[15] H. Kutscher ; *Z. angew. Phys.* **7**, 229, 234 (1955).
[16] J. Langmuir ; *Phys. Rev.* VI, **8**, 48 (1916) ; *Gen. Elect. Rev.* XIX **10**, 1060 (1916) ; *Electrican*, **79**, 13, 579 (1917).
[17] D. Latham, B. Power und N. T. M. Dennis ; *Vacuum* **1**, 97 (1951) ; **2**, 33 (1952).
[18] M. Matricon ; *J. Phys. Radium* (7) **2**, 86 (1931) ; **3**, 127 (1932).
[19] W. Molthan ; *Phys. Z.* **26**, 712 (1955) ; *Z. tech. Phys.* **7**, 377, 452 (1926) ; **8**, 80 (1927).
[20] H. G. Noeller *Z. angew. Phys.* **7**, 218, 225 (1955).
[21] H. G. Noeller und G. Reich ; *Z. angew. Phys.* **9**, 617 (1957).
[22] G. Reich ; *Z. angew. Phys.* **9**, 23 (1957).
[23] J. Ruf und O. Winkler ; *Ergebnisse d. Hochvakuumtechnik* v. M. Auwärter, Wissensch. Verl. Ges., Stuttgart (1957).
[24] R. Witty ; *J. Sci. Instrum.* **22**, 201 (1945) ; *Brit. J. Appl. Phys.* **1**, 232 (1950).

VO 9 1959

A McLeod Manometer with Prescribed Volumes for Use as a Standard Instrument

C. G. J. JANSEN and A. VENEMA

Philips' Research Laboratories, Eindhoven

(Received 31 January 1959)

The McLeod manometer is one of the few instruments with which it is possible to measure the actual values of low gas pressures (5—10^{-5} mm Hg) without changing the composition of the gas. The McLeod gauge is therefore indispensable for calibrating the faster indicating instruments which only register relative pressure units, e.g. ionization gauges, heat-conductivity manometers, etc.

Since it is very cumbersome to make and calibrate a McLeod gauge that can be used as a standard, it is worthwhile to improve the construction in such a way that a calibration can be omitted. In connexion with this problem a critical study was made of the formulae used to calculate the gas pressure from the readings of the McLeod manometer, which lead to expressions for the relative systematic and accidental errors limiting the measuring accuracy.

By using a very accurate set of jigs in making the capillaries and the transition volumes at the connexion between capillaries of different diameters and by addition of a small correction volume to the compression bulb it was possible to construct a McLeod gauge indicating the actual gas pressures in the range of 3.5—10^{-5} mm Hg on one convenient set of scales. The volume of the compression bulb and the volume and diameters of the capillaries were calculated in such a way that full centimetres on the various scales correspond to 10^{-3}, 10^{-2} and 10^{-1} mm Hg respectively. The zero lines of the different sub-ranges of the instrument lie at whole centimetres from each other and at multiples of half-centimetres from the top of the compression capillary.

Vol. 9 959/60

1. Introduction

The classical instrument for measuring low gas pressures ranging from 1 to 10^{-5} mm Hg is the McLeod manometer[1]. Since McLeod published his invention in 1874 many research workers have contributed to improving the instrument and the readers of this journal may well ask themselves what is so new about the experiments of the present authors as to justify this article.

The McLeod manometer is a slow instrument in that it only registers the pressure existing in a given system (i.e. the space the pressure of which is to be measured) after a number of manipulations have been carried out. The need for finding *instantaneous* values of pressure has led to the construction of manometers operating on different principles. The drawback of these instruments, however, is the fact that the gas pressure can only be derived from their physical and geometrical properties with great difficulty, or not at all, so that they must be calibrated by means of an instrument which measures absolute values. The McLeod manometer has been found to constitute the best possible calibration standard for the simple reason that the only parameters which must be known for the purpose of establishing the relation between its reading and the wanted pressure, are the volumes of its bulb and capillaries and these can be determined with great accuracy.

The present authors have occupied themselves mainly with the problem of the measuring accuracy of the McLeod manometer used as a calibration standard. By having the glass components in question made to very accurate specifications they have moreover been able to eliminate the time-consuming process of measuring the volumes.

Making secondary standards by calibration against the primary standard is now no longer necessary. It is also quite feasible to choose the volumes of a McLeod manometer with a wide measuring range—obtained by the use of a number of capillaries having different diameters—in such a way that the pressures in the various sub-ranges can be read on *one* standardized scale, graduated, for example, in centimetres and millimetres, on which the zero lines are multiples of centimetres apart and full centimetres correspond with decades of mm Hg. This enhances the simplicity of the construction, the ease of reading and the measuring accuracy.

2. Arrangement of the McLeod Manometer

In principle one is not restricted to mercury in the choice of the compression liquid for the McLeod manometer but it has many evident advantages for use in a standard ; it can be introduced into the manometer in a very pure form ; it does not release decomposition products ; it does not absorb the gases, the pressure of which is to be determined. Of course the use of mercury excludes those gases from a calibration procedure which react chemically with it.

About 5×10^{-1} cm Hg* is usually taken as the upper

* Instead of the commonly used unit of gas pressure (mm Hg), the " cm Hg " will be used henceforth in this article so as to simplify calculations.

limit of the measuring range of the McLeod manometer, since higher pressures can be measured by other and easier procedures. Due to gas release by the glass walls the lower limit of the measuring range can hardly be taken below 10^{-6} cm Hg. Between these limits the whole range can be covered by variation of the compression ratio, V_s/V_c, where V_s is the gas volume in the compression capillary and V_c the total compression volume (see Fig. 1). Experiments

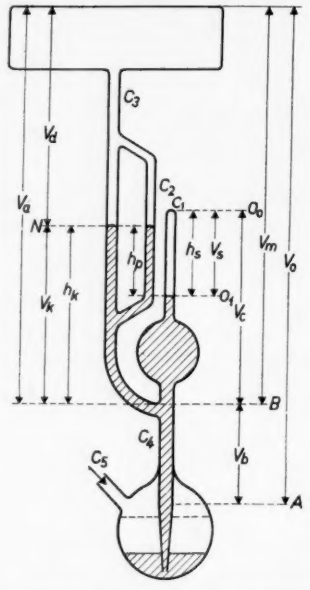

FIG. 1. Principle of the McLeod manometer.

V_0 = gas volume in cm³ of the McLeod gauge plus the system in which the pressure is to be measured at the lowest level of the mercury (level *A*).
V_s = gas volume in compression capillary C_1, in cm³.
V_c = total compression volume in cm³.
V_a = gas volume, in cm³, of the system plus McLeod gauge minus the compression volume V_c, at the moment that the mercury shuts off V_c (level *B*).
V_b = adjusting volume in cm³.
V_d = gas volume, in cm³, of the system with the mercury at level *N*.
h_p = difference in height between the mercury levels in compression capillary C_1 and comparison capillary C_2 in cm.

have shown that capillary diameters smaller than 0.05 cm cannot be used as a result of the capillary forces occurring[2–5]. The mercury in the compression capillary should never be allowed to rise to within 0.5 cm of the top, because otherwise the reading accuracy will deteriorate as a result of the different curvatures of the capillary top and the mercury meniscus. This fact makes the minimum value of gas volume V_s : $V_{s\,\min} = 0.00098$ cm³. If a gas pressure of 10^{-6} cm Hg is to be measured with this gas volume, V_c must be 490 cm³. The highest pressure which can be reached in the compression capillary when the rise of the mercury column is brought about by atmospheric air, $p_{s\,\max}$, is about 40 cm Hg. Together with the maximum value of the pressure which has to be measured (4×10^{-1} cm Hg), the value of $p_{s\,\max}$ determines the maximum compression volume, $V_{s\,\max} = 4.90$ cm³. When, in accordance with the principle of Dunoyer[6], the compression volume is divided over three capillaries with different diameters, the whole pressure range between $4 \times 10^{-1} - 10^{-6}$ cm Hg can be covered.

3. Systematic errors arising from the construction of the McLeod manometer

The errors made during a calibration are partly due to the standard used and partly to misreadings of the instrument which is to be calibrated. The former category may again be divided into those made during reading and those inherent to the standard. The latter, the systematic errors, have a fixed value and will be described below.

The systematic errors inherent to the McLeod manometer are the result of :

(I) The application of Boyle's law.

(II) The use of a simplified relation between the pressure read off and the original pressure, involving the assumptions that the volume of the system is infinitely large, and the original pressure negligibly small with respect to that read off in the compression capillary.

(III) Inaccuracies of manufacture.

(I) One of the best approximations for indicating the relations between the pressure, the volume and the temperature of a gas is van der Waals' equation which reads :

$$(p + a/V^2) \,.\, (V - b) = RT, \tag{1}$$

where p = pressure, to be expressed in cm Hg ; V = volume in cm³/mole ; T = temperature in °K ; a = a constant, expressed in cm Hg.cm⁶ per mole² ; b = a constant, expressed in cm³ per mole ; $R = 6236.4$ cm Hg.cm³ per mole degree. a and b depend on the nature of the gas.

The McLeod manometer gives reliable results only when used in the region of the p–V characteristics where only gas is present. This is the case for :

(a) All gases with a critical temperature T_c lower than the temperature T_k at which the gas pressure is measured

$$T_c < T_k \tag{2}$$

(b) All other gases with a critical temperature higher than T_k, but whose saturated vapour pressure p_d in the compression capillary at temperature T_k is higher than the pressure, p_0, in volume V_d plus the pressure corresponding to the difference in height, h_p, between the mercury levels in the compression and comparison capillaries (see Fig. 1).

$$p_d > p_0 + h_p \text{ cm Hg if } T_c > T_k \tag{3}$$

In Table I a certain number of gases and vapours are listed with the values of T_c, p_c (critical pressure), a, b and p_d which are of interest in the present case. T_k is taken as 288 °K (15 °C). The largest value of h_p is 40 cm.

The table shows that, if mercury is left out of consideration, only the vapours of benzene and water do not always obey relation (3) ; all other gases, listed in Table I, satisfy the conditions of (2) or (3) at room temperature and may, therefore, be subjected to pressure measurements with the McLeod manometer.

When van der Waals' equation (1) is simplified to the ideal gas formula

$$p_0 V_0 = RT, \tag{4}$$

the relative systematic error introduced in the measurement of p_0 is :

$$\left(\frac{\Delta p_0}{p_0}\right)_{S_1} = \frac{p - p_0}{p_0} \sim -\frac{p_0}{RT}\left(\frac{a}{RT} - b\right) \qquad (5)$$

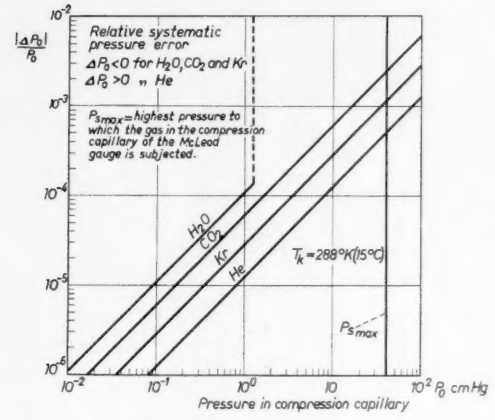

FIG. 2. Values of the relative systematic error $\Delta p_0/p_0$ for He, Kr, CO_2 and H_2O introduced in the measurement of the pressure p_0 when van der Waals' equation is simplified to the ideal gas formula.

TABLE I

Gas Properties

Derived from tables in *Handbook of Chemistry and Physics* (32nd Ed., Editor-in-Chief C. D. Hodgman)

Gas	T_c (°K)	P_c (cm Hg)	a (cm Hg.cm^6/mole^2)	b (cm^3/mole)	
		$T_c < T_k$; $T_k = 288$ °K			
A	151.	3.65×10^3	1.02×10^8	3.22×10^1	
CO	134.	2.66×10^3	1.13×10^8	3.99×10^1	
He	5.1	1.72×10^2	2.58×10^6	2.37×10^1	
H_2	33.1	9.73×10^2	1.85×10^7	2.66×10^1	
Kr	210.	4.11×10^3	1.76×10^8	3.98×10^1	
CH_4	190.5	3.48×10^3	1.71×10^8	4.28×10^1	
Ne	44.3	1.97×10^3	1.60×10^7	1.71×10^1	
NO	179.	4.94×10^3	1.02×10^8	2.80×10^1	
N_2	125.9	2.54×10^3	1.05×10^8	3.92×10^1	
O_2	154.2	3.78×10^3	1.03×10^8	3.20×10^1	
		$T_c > T_k$; $T_k = 288$ °K			$P_d(T_k)$ (cm Hg)
NH_3	405.4	8.47×10^3	3.17×10^8	3.71×10^1	5.3×10^2
C_2H_2	309.	4.71×10^3	3.33×10^8	5.13×10^1	2.9×10^3
C_6H_6	561.5	3.63×10^3	1.36×10^9	1.16×10^2	6×10^0
CO_2	304.1	5.55×10^3	2.72×10^8	4.27×10^1	3.8×10^3
Hg	>1823.	$>1.52\times10^4$	6.12×10^8	1.70×10^1	7.76×10^{-5}
NO_2	431.	7.52×10^3	4.01×10^8	4.43×10^1	5.65×10^1
SO_2	430.2	5.91×10^3	5.08×10^8	5.65×10^1	2.1×10^2
H_2O	647.	1.64×10^4	4.14×10^8	3.06×10^1	1.28×10^0
Xe	289.6	4.42×10^3	3.10×10^8	5.10×10^1	4.4×10^3

T_c = critical temperature.
T_k = measuring temperature.
p_c = critical pressure.
$p_d(T_k)$ = saturated vapour pressure at T_k °K.

In Fig. 2 the value of $\Delta p_0/p_0$ is plotted as a function of p_0 in the compression capillary for some extreme cases :

(i) for He, which satisfies the condition $T_c < T_k$ and has small values of a and b ; for Kr, which also satisfies the condition $T_c < T_k$ but has large values of a and b ;

(ii) for CO_2, for which $T_c > T_k$ and which has small a and b values ; for H_2O, for which $T_c > T_k$ but which has large a and b values.

It is evident from these graphs that the simplification from the van der Waals' equation to the Boyle–Gay Lussac equation introduces an error into the pressure value of less than 0.5 per cent. As will be shown later the errors introduced by other causes are much larger, so when the temperature is kept constant, Boyle's Law

$$pV = \text{constant} \qquad (6)$$

may be applied in the case of all gases mentioned in Table I provided the conditions of (2) or (3) are satisfied.

It is obvious that the gas should not react appreciably with the mercury or the glass walls[2].

(II) Assuming that Boyle's Law (6) is a sufficiently accurate approximation for indicating the relation between pressure and volume of a gas, the following formula can easily be derived with reference to Fig. 1 :

$$p_0 = \frac{V_s}{V_c} \cdot \frac{h_p}{(1 - V_s/V_c \,.\, V_a/V_d)} \cdot (1 - V_b/V_0)\ \text{cm Hg}, \qquad (7)$$

where p_0 = pressure of the gas present in starting volume V_0, in cm Hg ; V_0 = gas volume in cm^3 of the McLeod gauge plus the system in which the pressure is to be measured at the lowest level of the mercury (level A) ; V_s = gas volume in compression capillary C_1 in cm^3 ; V_c = total compression volume in cm^3 ; V_a = gas volume in cm^3 of the system plus McLeod gauge minus the compression volume V_c, at the moment that the mercury shuts off V_c (level B) ; V_b = adjusting volume in cm^3 ; V_d = gas volume in cm^3 of the system with the mercury at level N ; h_p = difference in height between the mercury levels in compression capillary C_1 and comparison capillary C_2 in cm.

In this expression only the quantities h_p, V_c and V_s are as a rule accurately known. For this reason a simpler formula will be used instead of (7), viz. :

$$p_0 = \frac{V_s}{V_c}\, h_p \ \text{cm Hg}. \qquad (8)$$

This formula is exactly valid if volume V_d of the system may be regarded as infinitely large, and if the pressure p_0 is negligibly small with respect to the pressure in the comparison capillary, indicated by h_p. This means, however, that certain requirements must be imposed on the dimensions of the McLeod gauge and of the system, the gas pressure of which is to be measured. The requirements are such that the absolute value of the relative systematic error

$$\left(\frac{\Delta p_0}{p_0}\right)_{S_2} = \frac{1 - V_b/V_0}{1 - V_s/V_c \cdot V_a/V_d} - 1 \qquad (9)$$

remains smaller than a fixed permissible value.

It may become clear from (8) that the great advantage of the McLeod gauge is the simple law governing the relation

between the scale readings, h_p, and the units in which the actual gas pressure is to be measured.

(III) The constructional errors are :

(a) Deviations of the total compression volume, V_c, and the gas volume V_s, from the specified values. From (8) the relative pressure errors can be found :

$$\left(\frac{\Delta p_0}{p_0}\right)_{C_1} = \frac{-\Delta V_c}{V_c}, \tag{10}$$

$$\left(\frac{\Delta p_0}{p_0}\right)_{C_2} = \frac{\Delta V_s}{V_s}. \tag{11}$$

(b) Differences in the diameters of the compression and comparison capillaries and in the boundary angles between the mercury surface and the wall of the capillary, both causing a change in the capillary depression and thus giving rise to a systematic error in h_p (height difference between mercury levels in cm), which results in a relative pressure error :

$$\left(\frac{\Delta p_0}{p_0}\right)_{C_3} = \frac{2\alpha \cos \varphi_s}{\varrho g r h_p} (\Delta r/r + \tan \varphi_s \Delta \varphi_s) = \frac{\Delta h_{\varphi_s}}{h_p}, \tag{12}$$

where α = surface tension of mercury, about 465 dyn/cm at 15°C ; ϱ = density of mercury, 13.56 g/cm³ at 15°C ; φ_s = boundary angle glass-mercury, about π radians ; r = radius of the capillary in cm ; g = gravitational acceleration, 981 cm per sec.² ; Δh_{φ_s} = difference in capillary depression between the mercury levels in the compression and the comparison capillaries.

The systematic error in the radii of the capillaries, Δr, can be measured, but the error in the boundary angle, $\Delta \varphi_s$, is difficult to establish. The best results are still obtained by directly determining Δh_{φ_s}, the method being to let the mercury rise in the capillaries under high vacuum and to measure differences in levels from point to point with the mercury level in the widest comparison capillary as a reference. This should be done regularly to check the compression and comparison capillaries of a McLeod gauge in frequent use, since the physical state of the capillary-wall surface may change owing to absorption or release of gases or deposition of mercury compounds.

4. Design of the standard McLeod Manometer

Capillaries, as used in the McLeod manometer, having great lengths and any diameter between 0.05 and 1 cm can now be manufactured with a high degree of accuracy by drawing them over a core. Special accurately made jigs permit the transitions between capillaries of different diameters to be made according to specification.

With these techniques the capillaries of the McLeod manometer can be made to have pre-calculated dimensions within known tolerances. The advantage is that it is no longer necessary to calibrate the instrument and to adapt the scale to each calibration which, in the past, resulted in the scales for the subranges becoming different for each manometer and, moreover, the distances between the zero lines and between the pressure-unit graduations deviating from the convenient full centimetre and millimetre values. In designing the improved McLeod manometer, therefore, the aim has been to provide it with one simple and standardized scale suitable for all the subranges of each instrument. This was possible by using the above mentioned technique for the compression capillary and by calibrating the compression bulb to the calculated value with the aid of a special correction volume. The inaccuracy of the manometer readings due to constructional variations in the volumes can now be kept between known limits.

The new design is schematically shown in Fig. 3 and the chief components will be described below.

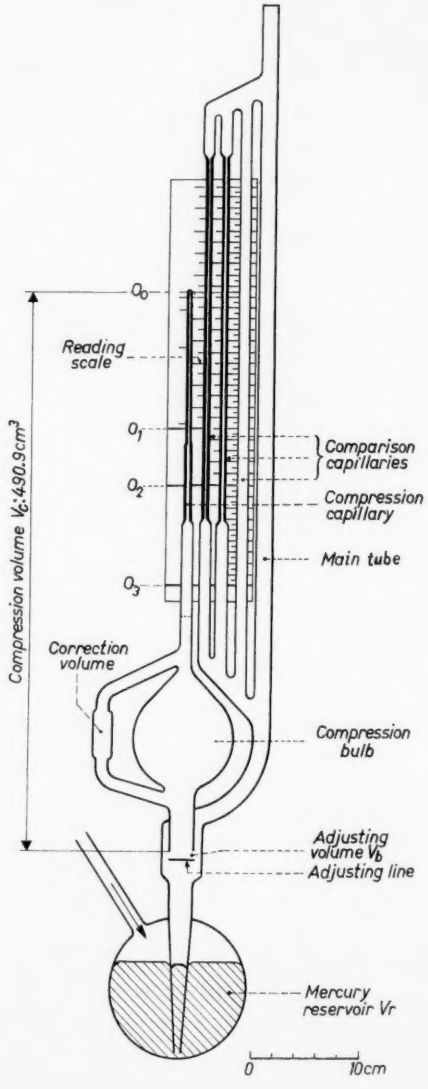

FIG. 3. Design of the McLeod manometer with prescribed volumes and standardized reading scale indicating gas pressures in the range of 0.35–10^{-6} cm Hg.

(a) *The Compression Capillary*—Starting from the conditions that the narrowest capillary should have a diameter of 0.0500 cm, that the height difference between the mercury levels when using the quadratic scale should be $h_p = 0.500$ cm at a pressure $p_0 = 10^{-6}$ cm Hg, and using formula (8), a McLeod manometer was calculated and manufactured having a total measuring range of 3.5×10^{-1}–10^{-6} cm Hg, a total

compression volume $V_c = 490.9\ cm^3$ and three compression capillaries with different diameters. The exact diameters and lengths of the compression capillaries are shown in Fig. 4. Table II indicates that the following results were obtained :

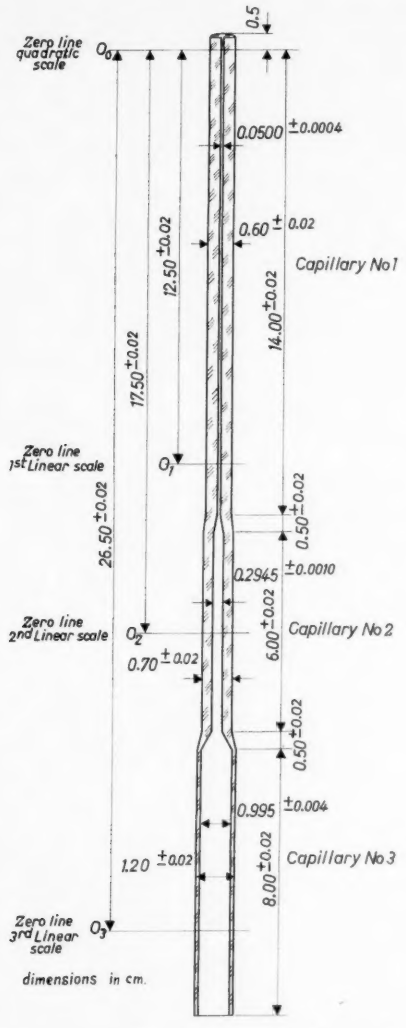

FIG. 4. Construction of the compression capillary.

(i) The three sub-ranges overlap due to the fact that the maximum pressure in the compression capillary, $p_{s\,max}$, can rise to 40 cm Hg with the mercury level on the third zero line.

(ii) The zero lines of the three linear scales pertaining to the three capillaries are full centimetres apart and they are situated multiples of half-centimetres from the top of the compression capillary.

(iii) On the first and second linear scale a pressure of 10^n cm Hg corresponds to 2 cm of height difference between the mercury levels (n being an integer, in the present case -4, -3 respectively), on the third linear scale a pressure of 10^{-2} cm Hg corresponds to 1 cm of height difference between the mercury levels.

When a half-centimetre graduation of the relevant scale is made to coincide with the top of the compression capillary, the zero lines of the other scales automatically coincide with full-centimetre graduations.

Proper alignment of the scales in the fashion outlined above is only possible if the compression capillary remains purely cylindrical up to the very top, which must be provided with a flat cover. This condition was met in the way indicated by Barr and Anhorn[5] by fusing a piece of glass rod, ground flat and accurately fitting, into the capillary at the correct position determined with the aid of a jig.

(b) *Compression Volume* V_c—Compression volume V_c (see Fig. 3) is composed of the volume of the compression capillaries plus that of the compression bulb, which has an inner diameter of 9.4 cm. The bottom opening of the bulb is provided with a short cylindrical piece of tubing, in accordance with the method of Barr and Anhorn[5]. The dimensions of this tube are : length 5.5 cm, diameter 2.0 cm ; its lower rim is accurately flat and horizontal so that the amount of gas shut off in V_c by the rising mercury is reproducible.

The total compression volume, V_c, must approach the calculated value, 490.9 cm³, as closely as possible. Since this would be a very difficult job for the glass-blower, the bulb is underdimensioned to wide limits (0.2 cm in diameter) and later brought to the required volume by addition of a small correction bulb. This procedure enables the volume, V_c, to be guaranteed to within 0.3 cm³ at a fixed temperature. The shape of the correction bulb and the connecting tubes was chosen in such a manner that no gas can be trapped by the rising mercury.

(c) *The Comparison Capillaries*—The three parallel-connected comparison capillaries are spaced 1 cm apart and run parallel to the compression capillaries ; each of them has the same diameter as the associated compression capillary. They were made so long that they can be used for measuring

TABLE II

Sensitivity and Measuring Range of the McLeod Gauge

Scale	Diameters of the compression and comparison capillaries (cm)	Distances of the scales from the top of the compression capillary (cm)	Sensitivity (10^{-6} cm Hg/cm)	Measuring range ($\times 10^{-6}$ cm Hg)
Quadratic	0.0500 ± 0.0004	0.00	($P_0 = 4 \times 10^{-6} h_p^2$)	1–6.25 × 10²
1st linear	0.0500 ± 0.0004	12.50 ± 0.02	5 × 10¹	5 × 10¹–1.0 × 10³
2nd linear	0.2945 ± 0.0010	17.50 ± 0.02	5 × 10²	5 × 10²–1.25 × 10⁴
3rd linear	0.9950 ± 0.0040	26.50 ± 0.02	10⁴	10⁴–3.5 × 10⁵

purposes over the full height to which the mercury can rise, this being about 40 cm in the widest comparison capillary, reckoned from the zero level of the associated compression. capillary.

The main tube which also runs parallel to the other tubes has a diameter of 1.5 cm and serves to keep the adjusting time of the McLeod manometer as low as possible.

(d) *Adjusting Volume V_b and System Volume V_d*—If the relative error in the pressure indication, resulting from the use of the simple formula (8), is to be as small as possible, then the adjusting volume must be minimum and the system volume, V_d, has to exceed a certain minimum value, see formula (9). This was achieved by fixing the " rest " level of the mercury (at 0.5 cm below the lower rim of the piece of tubing fitted to the compression bulb) with the aid of a marking line written on the glass wall. Thus V_b is reduced to 4.5 cm^3. When, at the same time, for the system volume, V_d, 2000 cm^3 is maintained as the lower limit, the relative systematic pressure error due to the use of formula (8) is less than 0.3 per cent, except in the case of the third linear scale for which the error remains 1 per cent.*

(e) *Mercury Reservoir V_r*—The diameter of the mercury reservoir, V_r, is 12.5 cm ; its dimensions are not critical. The only conditions which must be fulfilled are that the required amount of mercury should fill it to about three-quarters and that the distance to the piece of tubing fitted to the compression bulb should be as short as possible (6 cm). The last condition must be met because otherwise the rising mercury cannot reach the maximum height of 40 cm in the third compression capillary, if atmospheric pressure is attained on the mercury in V_r. The air introduced for raising the mercury is chemically dried.

5. The relative systematic errors in reading the pressure on a McLeod Manometer with prescribed volumes

Since all essential dimensions of the components of the McLeod manometer and also their tolerances, are now known, the absolute measuring accuracy can be calculated with the aid of formulae (5), (9), (10), (11) and (12) for the relative systematic errors in the pressure : $\Delta p_0/p_0$. The results of these calculations are given in Table III.

In Fig. 5 the overall relative systematic error $\Delta p_0/p_0$ is plotted for the quadratic scale as a function of the pressure p_0, using Table III and the assumptions that all systematic errors due to the applied formulae and to constructional deviations have *the same sign* (*the most unfavourable case*), and that the systematic error in the capillary depression of the narrowest capillary (diameter 0.0500 cm) : $\Delta h_{\varphi_s} = 0.0$ and 0.1 cm respectively.

From these maximum relative systematic pressure errors to be expected it may be concluded that :

(a) The measuring accuracy is strongly influenced by systematic capillary depression errors. It is therefore necessary to check the capillaries regularly for these errors especially the narrowest one ; if necessary, the errors should be incorporated in the measuring results.

(b) The described McLeod manometer can only be regarded as a reliable measuring instrument for pressures above 10^{-5} cm Hg.

TABLE III

Relative Systematic Pressure Errors

	Quadratic scale	1st linear scale	2nd linear scale	3rd linear scale	Remarks
(1) Errors caused by the simplification of the formulae					
$\left\lvert\frac{\Delta p_0}{p_0}\right\rvert_{S_1} = \left\lvert\frac{p_0}{RT}\left(\frac{a}{RT} - b\right)\right\rvert$	$<0.2\%$	$<0.2\%$	$<0.2\%$	$<0.2\%$	For almost all gases
$\left\lvert\frac{\Delta p_0}{p_0}\right\rvert_{S_2} = \left\lvert\frac{1 - V_b/V_0}{1 - V_a/V_c \cdot V_a/V_d} - 1\right\rvert$	$\leqslant 0.2\%$	$\leqslant 0.2\%$	$\leqslant 0.3\%$	$= 1\%$	On condition that the measured gas-volume $V_d \geqslant 2000$ cm^3
(2) Constructional errors					
$\left\lvert\frac{\Delta p_0}{p_0}\right\rvert_{C_1} = \left\lvert\frac{\Delta V_c}{V_c}\right\rvert$	$<0.1\%$	$<0.1\%$	$<0.1\%$	$<0.1\%$	
$\left\lvert\frac{\Delta p_0}{p_0}\right\rvert_{C_2} = \left\lvert\frac{\Delta V_s}{V_s}\right\rvert$	$\leqslant (1.5 + \frac{2}{h_p})\%$	$\leqslant 1.5\%$	$\leqslant 2.0\%$	$\leqslant 2.0\%$	
$\left\lvert\frac{\Delta p_0}{p_0}\right\rvert_{C_3} = \left\lvert\frac{2a\cos\varphi_s}{\rho \cdot g r h_p}\cdot\left(\frac{\Delta r}{r} + \tan\varphi_s \Delta\varphi_s\right)\right\rvert$	$\frac{100\Delta h_{\phi_s}\%}{h_p}$	$\frac{100\Delta h_{\phi_s}\%}{h_p}$	$\frac{15\Delta h_{\phi_s}\%}{h_p}$	$\frac{5\Delta h_{\phi_s}\%}{h_p}$	

Δh_{φ_s} = systematic capillary depression difference in the compression and comparison capillaries.

* If the system volume V_d is kept so big that the ratio V_a/V_d (see Fig. 1) remains $\leqslant 1.001$ it is even possible to construct a McLeod gauge with the same easy standardized scale for which the relative systematic pressure error caused by using the simplified formula (8) is kept below 0.3 per cent for the three measuring ranges.

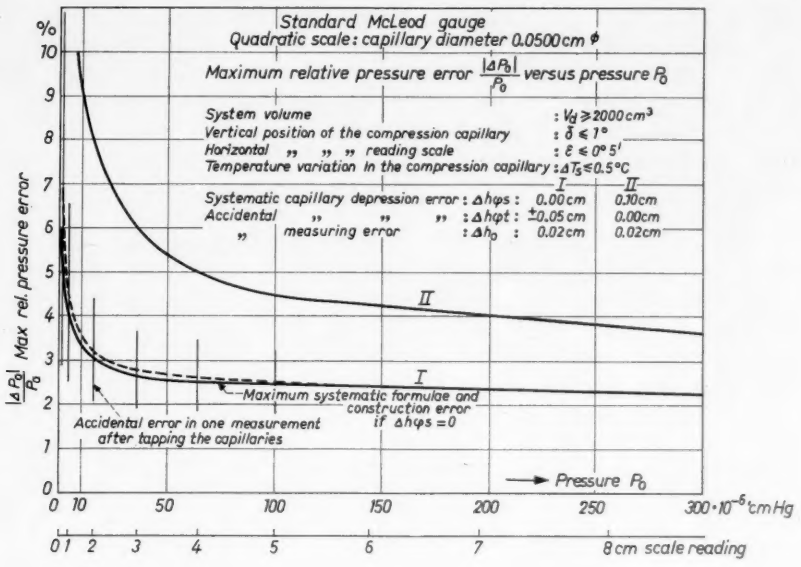
Standard McLeod gauge
Quadratic scale: capillary diameter 0.0500 cm ϕ
Maximum relative pressure error |Δp0|/p0 versus pressure p0
System volume : Vg ≥ 2000 cm³
Vertical position of the compression capillary : δ ≤ 1°
Horizontal " " " reading scale : ε ≤ 0° 5'
Temperature variation in the compression capillary : ΔTs ≤ 0.5 °C
I II
Systematic capillary depression error : Δhφs : 0.00 cm 0.30 cm
Accidental " " " : Δhφt : ±0.05 cm 0.00 cm
" measuring error : Δh0 : 0.02 cm 0.02 cm
II
I
Maximum systematic formulae and construction error if Δhφs = 0
Accidental error in one measurement after tapping the capillaries
Pressure p0
% Max rel. pressure error |Δp0|/p0
0 10 50 100 150 200 250 300 · 10⁻⁶ cm Hg
0 1 2 3 4 5 6 7 8 cm scale reading

FIG. 5. Overall relative systematic and accidental errors Δ_{p_0}/p_0 for the quadratic scale as a function of the gas pressure p_0 using Table III.

6. Accidental errors made during gas pressure measurements

The accidental errors arise when a measurement is performed with the manometer. They may result from :

(a) An incorrect position of the manometer tubes and/or the scales.

(b) The use of liquid-air (carbon dioxide) traps during the calibration.

(c) A chancy position due to irregular flow of the mercury caused by local differences in the capillary depression.

(d) Temperature fluctuations which may arise during the compression of the gas.

(e) Inaccurate reading of the mercury levels.

(a) To obtain an accurate reading of the height difference, h_p, between the mercury levels, the axis of the compression capillary should be accurately vertical and the zero lines on the calibrated scale horizontal. If these requirements are not satisfied the relative pressure errors will be :

(i) if the axis of the compression capillary makes an angle δ (radians) with the vertical :

$$\left(\frac{\Delta p_0}{p_0}\right)_{m_1} = \delta^2 \text{ for small values of } \delta. \tag{13}$$

(ii) if the zero lines of the scale are not horizontal :

$$\left(\frac{\Delta p_0}{p_0}\right)_{m_2} = \frac{\eta z \varepsilon}{h_p} \tag{14}$$

where z = distance between the axes of the compression and comparison capillaries in cm ; ε = angle between the zero line of the scale and the horizontal in radians ; $\eta = 1$ on the linear scales, $= 2$ on the quadratic scale.

The influence of these mounting errors on the relative pressure error is summarized in Table IV.

(b) When the McLeod gauge is used for the calibration of another manometer in the pressure range of about 2×10^{-2} cm Hg and lower, traps must be used and in that case errors will be introduced as a result of the pressure difference between the warm and cold parts of the set-up. Rusch and Bunge[7] have paid attention to this problem. At low pressures

TABLE IV

Influence of Mounting Errors

Nature \ Mounting error value	Quadratic scale	1st linear scale	2nd linear scale	3rd linear scale	Remarks
$\left\|\frac{\Delta p_0}{p_0}\right\|_{m_1} = \delta^2$	$\leqslant 0.05\,\%$	$\leqslant 0.05\,\%$	$\leqslant 0.05\,\%$	$\leqslant 0.05\,\%$	δ = angle between the axis of the compression capillary and the vertical = 1° = 0.017 rad.
$\left\|\frac{\Delta p_0}{p_0}\right\|_{m_2} = \left\|\frac{\eta z \epsilon}{h_p}\right\|$	$\leqslant \frac{0.4\,\%}{h_p}$	$\leqslant \frac{0.2\,\%}{h_p}$	$\leqslant \frac{0.4\,\%}{h_p}$	$\leqslant \frac{0.5\,\%}{h_p}$	ϵ = angle between the zero line of the scale and the horizontal = 0° 5' = 0.0015 rad.

when the mean free path of the gas molecules is large in relation to the dimensions of the tubes, there will be a difference in pressure between areas having different temperatures whereas areas with the same temperature will have the same pressure. At high pressures, when the mean free path is small with respect to the tube dimensions, the gas pressure will be the same everywhere, irrespective of local temperature differences. Between these two cases there are those where the pressures are moderately high and in these cases there will be pressure differences between warm and cold places which depend on the tube dimensions, especially those of the traps. The two research workers mentioned above have proved that the errors introduced with the application of a liquid-air trap may rise to 10 per cent. Proper dimensioning of the trap or the use of a symmetrical one (U-tube)* can reduce the error considerably. Moreover it is, however, not necessary to cool to the liquid-air temperature for it is always possible, e.g. with freezing mixtures, to select the trap temperature in such a fashion, taking into account the pressure of the gas, that the error caused by this effect and by the presence of mercury vapour in the manometer, which is to be calibrated, is negligibly small.

Use of a trap always results in a flow of mercury from the McLeod manometer to the cooled spot. A supposed pressure difference due to this effect[8] could not be detected by the present authors. Theoretical considerations also hardly point in this direction, the mean free path of the mercury atoms at room temperature (about 3 cm) not being small with respect to the dimensions of the manometer tubes.

(c) to (e) Taking the local capillary depression and the temperature into consideration, the pressure p_0 is given by :

$$p_0 = \frac{V_s}{V_c} \cdot \frac{T_0}{T_s} \cdot (h_p \pm \Delta h_\varphi), \qquad (15)$$

where h_p = the measured height difference between the mercury levels ; Δh_φ = difference in height caused by the differences of the capillary depression in the compression and comparison capillaries ; T_0 = temperature of the gas

TABLE V

Average Observation Errors With and Without Tapping against the Capillaries

Well evacuated McLeod gauge ($p_0 < 10^{-6}$ cm Hg)

Capillary diameter

(a) *Measurements without tapping against the capillaries*

Position 1				Position 2			
Level of the mercury in		Difference in height : Δ_h	$\lvert \Delta h_{mean} - \Delta h \rvert^2$	Level of the mercury in		Difference in height : Δ_h	$\lvert \Delta h_{mean} - \Delta h \rvert^2$
Compression capillary h_c (cm)	Comparison capillary h_v (cm)			Compression capillary h_c (cm)	Comparison capillary h_v (cm)		
5.08	5.12	−0.04	0.000137	16.52	16.40	0.12	0.00044
4.80	4.92	−0.12	185	16.58	16.40	0.18	152
4.95	5.00	−0.05	073	16.04	15.90	0.14	000
5.30	5.35	−0.05	073	16.44	16.32	0.12	044
5.03	5.12	−0.09	017	16.21	16.04	0.17	084
4.80	4.86	−0.06	029	16.68	16.50	0.18	152
4.72	4.85	−0.13	280	16.58	16.50	0.08	372
		$\Delta h_{mean} = -0.077$	$\Sigma = 0.000794$			$\Delta h_{mean} = 0.141$	$\Sigma = 0.00848$
Average error for one observation : $m = \pm\sqrt{\frac{\Sigma}{n-1}} = \pm 0.036$				Average error for one observation : $m = \pm\sqrt{\frac{\Sigma}{n-1}} = \pm 0.037$			

(b) *Measurements with tapping against the capillaries*

Position 1				Position 2			
4.99	5.06	−0.07	0.00029	16.10	15.92	0.18	0.00040
4.92	5.00	−0.08	005	16.40	16.25	0.15	010
5.01	5.11	−0.10	017	16.13	15.98	0.15	010
5.22	5.30	−0.08	005	16.34	16.18	0.16	000
4.80	4.90	−0.10	017	16.38	16.23	0.15	010
4.98	5.08	−0.10	017	16.67	16.52	0.15	010
5.05	5.13	−0.08	005	16.60	16.42	0.18	040
		$\Delta h_{mean} = -0.087$	$\Sigma = 0.00095$			$\Delta h_{mean} = 0.160$	$\Sigma = 0.00120$
Average error for one observation : $m = \pm\sqrt{\frac{\Sigma}{n-1}} = \pm 0.012$				Average error for one observation : $m = \pm\sqrt{\frac{\Sigma}{n-1}} = \pm 0.014$			

* Private communication of Mr. J. J. Opstelten from these laboratories.

before compression ; T_s = temperature of the gas after compression.

In this formula V_s, h_p, Δh_φ, and T_s are independent variables subject to incidental errors ; the other quantities may be regarded as constants. Since the average error ΔV_s in the gas volume of the compression capillary may be written as :

$$\Delta V_s = q_s \left(\Delta h_s + 2h_s \frac{\Delta r_s}{r_s} \right), \tag{16}$$

where q_s = cross-sectional area of the comparison capillary ; h_s = height of the gas column in the compression capillary ; r_s = radius of the compression capillary, the following relation can be found from (15) and (16) (also see Mielenz[9]) :

$$\left(\frac{\Delta p_0}{p_0} \right)_i = \pm \sqrt{\left(\frac{\Delta h_s}{h_s} + \frac{2\Delta r_s}{r_s} \right)^2 + \frac{\Delta h_0^2 + \Delta h_{\varphi t}^2}{h_p^2} + \frac{\Delta T_s^2}{T_s^2}}. \tag{17}$$

The average error Δh_s in the height of the gas column in the compression capillary is governed by the accuracy with which it is possible to measure the mean distance between the mercury level and the top of the compression capillary ; the radius error Δr is governed by the accuracy with which the capillaries are manufactured.

The average error Δh_0 in the height of the mercury levels is a function of the accuracy with which the positions of the menisci can be read from the McLeod scale (± 0.01 cm).

The average capillary depression error $\Delta h_{\varphi t}$ is partly caused by local errors in the diameters of the compression and comparison capillaries, but mainly by local variations in the boundary angle between mercury and glass. It is this error which, in the case of narrow capillaries (diameter less than 0.1 cm), mainly determines the measuring accuracy of the McLeod manometer. It has been found by experiment that the capillary depression errors are generally about a factor 10 higher than is to be expected from the tolerances in the capillary diameters. These deviations can be substantially reduced if :

(i) the mercury is allowed to reach its final position only by rising ;

(ii) the operator is instructed to tap against the capillaries with a finger or an automatic device is used for the purpose.

When the condition mentioned first is fulfilled, the boundary angle between glass and mercury changes least, and the final position of the mercury meniscus is not affected by the electrostatic charge of the glass wall. This charge is caused by the friction between the glass and the falling mercury and can give rise to serious misreadings in narrow capillaries.

Tapping against the capillary tubes enables the mercury meniscus to reach its most stable position, corresponding to the average position of a large number of positions found during experiments without tapping. To illustrate the effect of tapping more clearly, several values of the position of the mercury meniscus in the smallest compression and comparison capillaries (h_c and h_v) of a well evacuated McLeod manometer (capillary diameter 0.05 cm, $p_0 < 10^{-6}$ cm Hg) are set out in Table V, showing the height variations with and without tapping.

The results clearly show that, although the average difference in height, Δh_{mean} is almost the same with and without tapping, the average error in one observation *with* tapping is much smaller than without.

The average temperature error, ΔT_s, is negligible with normal use of the manometer because of the small amounts of gas involved.*

Table VI gives the values of the average errors for the different scales.

The average accidental errors for the quadratic scale are set out in Fig. 5.

7. Setting up the McLeod Manometer

In the preceding sections the requirements which have to

TABLE VI

Values of the Different Average Accidental Errors

Nature of average accidental error	Quadratic scale	1st linear scale	2nd linear scale	3rd linear scale	Remarks
$\left\lvert \frac{\Delta h_s}{h_s} \right\rvert$	$\leqslant \frac{2}{h_p}\,\%$	$\leqslant 0.2\,\%$	$\leqslant 0.6\,\%$	$\leqslant 0.4\,\%$	
$\left\lvert \frac{2\Delta r_s}{r_s} \right\rvert$	$\leqslant 1.5\,\%$	$\leqslant 1.5\,\%$	$\leqslant 0.7\,\%$	$\leqslant 0.8\,\%$	
$\left\lvert \frac{\Delta h_p}{h_p} \right\rvert$	$\leqslant \frac{2}{h_p}\,\%$	$\leqslant \frac{2}{h_p}\,\%$	$\leqslant \frac{2}{h_p}\,\%$	$\leqslant \frac{2}{h_p}\,\%$	If the reading accuracy at the top of the mercury menisci $= \pm 0.01$ cm.
$\left\lvert \frac{\Delta h_{\varphi t}}{h_p} \right\rvert$	$\leqslant \frac{5}{h_p}\,\%$	$\leqslant \frac{5}{h_p}\,\%$	$\leqslant \frac{0.8}{h_p}\,\%$	$\leqslant \frac{0.25}{h_p}\,\%$	If the local capillary depression differences are ± 0.05 cm.
$\left\lvert \frac{\Delta T_s}{T_s} \right\rvert$	$\leqslant 0.15\,\%$	$\leqslant 0.15\,\%$	$\leqslant 0.15\,\%$	$\leqslant 0.15\,\%$	If the temperature changes not more than 0.5 °C.

* If the compression is performed too rapidly the position of the mercury levels may change at first. This is caused by pressure variations of the gas in the volume V_r (fig. 3) due to temperature change during air inlet.

Vol. 9 959/60

be met by the glass components and the scale of the McLeod manometer have been discussed. Tables III, IV and VI show that, for a good measuring accuracy to be obtained, the setting up of the instrument must be done with great care. This fact, coupled to the other features of the improved manometer, viz. the standardized dimensions and scale, gave rise to the need for a frame in which the glass components and the scale could be aligned and set up. Moreover before placing the manometer in the frame it is filled with mercury by vacuum distillation. Fig. 6 shows the complete instrument. A plumb-line assembly which can be moved up and down around the narrowest compression capillary is used for bringing the manometer proper in the required vertical position.

Next the scale is aligned to the top of the compression capillary and the zero lines of the scale are put horizontally. This is done in high vacuum by letting the mercury rise to the third zero level, and aligning the third zero line on the mercury menisci in the widest compression and comparison capillary. At this stage the compression capillary and the scale will have the correct position.

To facilitate reading, the scale is chromium-plated and a sliding indicator "knife" can move up and down in the space between the capillaries and the scale. The knife edge is exactly parallel with the zero lines on the scale. Parallax-free reading of the position of the mercury meniscus is achieved when the top of the meniscus, its image in the mirror surface of the scale and the knife edge are seen on one line.

Accidental differences in the capillary depression are averaged out as a result of the action of small motor-driven rubber hammers which tap against the capillary tubes while the mercury is rising.

It is obvious that a pressure measurement only gives the right value if it is carried out at that fixed temperature at which the critical volumes of the manometer are guaranteed.

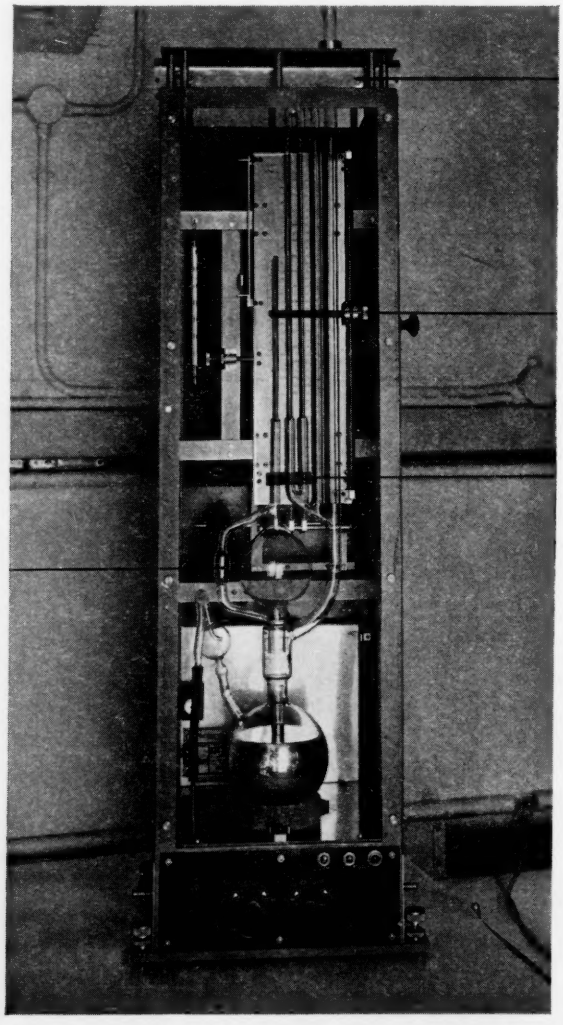

FIG. 6. Complete McLeod manometer with prescribed volumes.

Vo
9
1959

8. Experimental results

Four McLeod manometers manufactured to specified inside dimensions and tolerances as discussed in Section 4 were compared mutually and also with an instrument (McLeod No. S) which did not have prescribed volumes and was calibrated in the conventional way. The results are shown in Table VII (on page 230).

Every pressure value in this Table was obtained from one reading of the height difference between the mercury levels ; capillary-depression differences were averaged out by tapping against the tubes and a correction was introduced to account for systematic capillary-depression deviations as measured in high vacuum. The mean pressure values calculated from the readings of the four McLeod gauges with prescribed volumes most probably represent more accurate absolute pressure values than those obtained from the calibrated McLeod gauge No. S formerly used as a standard. We may, therefore, conclude that it is possible to manufacture McLeod manometers with a standard scale, which need not be calibrated, their pressure readings showing maximum variations about 2 per cent around the mean measured pressure values.

9. Acknowledgement

The authors wish to thank Mr. M. Bandringa for valuable advice given during these experiments and Messrs. J. C. Schepers and J. C. Hendriks for manufacturing the instruments.

References

[1] H. McLeod ; *Phil. Mag.* **48**, 110 (1874).
[2] S. Dushman ; *Scientific Foundations of Vacuum Technique*, John Wiley, New York pp. 267–270 (1949).
[3] P. Rosenberg ; *Rev. Sci. Instrum.* **10**, 131 (1939).
[4] G. Haase ; *Z. tech. Phys.* **24**, 27 (1943).
[5] W. E. Barr and V. J. Anhorn ; *Instruments* **19**, 666 (1946).
[6] L. Dunoyer ; *Bull. Soc. Fr. Phys.* 246 (1923).
[7] M. Rusch and O. Bunge ; *Z. tech. Phys.* **13**, 77 (1932).
[8] F. Bergter ; *Lehrbuch der Technischen Physik* (G. Gehlhoff) 2ter Band, p. 1026 (1926).
[9] K. D. Mielenz ; *Glas Hochvak. Tech.* **7**, 139 (1952).

Vol.
9
959/60

TABLE VII

Experimental Results with Four McLeod Manometers with Prescribed Volumes

Compression volume	McLeod No. 1				McLeod No. 2				McLeod No. 3				McLeod No. 4				McLeod's No. 1 t/m 4		Calibrated McLeod No. S used as standard	
	490.9 ± 0.3 cm³				490.9 ± 0.3 cm³				490.9 ± 0.3 cm³				490.9 ± 0.3 cm³							
Scale	Mean capillary diameter (cm)	Difference in height of the mercury levels (cm)	Capillary depression correction (cm)	Pressure *(10^{-6} cm Hg)	Mean capillary diameter (cm)	Difference in height of the mercury levels (cm)	Capillary depression correction (cm)	Pressure *(10^{-6} cm Hg)	Mean capillary diameter (cm)	Difference in height of the mercury levels (cm)	Capillary depression correction (cm)	Pressure *(10^{-6} cm Hg)	Mean capillary diameter (cm)	Difference in height of the mercury levels (cm)	Capillary depression correction (cm)	Pressure *(10^{-6} cm Hg)	Mean pressure value *(10^{-6} cm Hg)	Max. variation around the mean pressure value	Pressure *(10^{-6} cm Hg)	Variation in the mean pressure value McLeod's No. 1 t/m 4 and the standard No. S
Quadratic	0.0497	8.90	0.00	3.16×10^{2}	0.0495	9.00	−0.10	3.16×10^{2}	0.0499	9.10	−0.15	3.20×10^{2}	0.0495	9.12	−0.10	3.25×10^{2}	3.19×10^{2}	2%	3.10×10^{2}	3%
1st linear	0.0497	6.31	0.00	3.16×10^{2}	0.0495	6.51	−0.10	3.21×10^{2}	0.0499	6.55	−0.15	3.20×10^{2}	0.0495	6.60	−0.07	3.27×10^{2}	3.21×10^{2}	2%	3.13×10^{2}	3%
2nd linear	0.294	13.95	−0.05	6.95×10^{3}	0.294	13.90	0.00	6.95×10^{3}	0.294	13.77	−0.10	6.84×10^{3}	0.297	13.80	0.00	6.90×10^{3}	6.91×10^{3}	1%	7.10×10^{3}	3%
3rd linear	0.995	7.47	0.00	7.47×10^{4}	0.995	7.50	0.00	7.50×10^{4}	0.995	7.50	0.00	7.50×10^{4}	0.995	7.50	0.00	7.50×10^{4}	7.49×10^{4}	0.3%	7.50×10^{4}	0.15%

*The pressure values are corrected for the systematic capillary depression errors.

Vol. 9 1959

Letters to the Editor

Application of the Air Pump.

Dear Sir,

THE following extract is probably one of the very first accounts of vacuum technology ever printed :

From " *The Annals of Philosophy* " [2] **2**, 395 (1821). Scientific Intelligence and Notices of Subjects connected with Science.

Till within the last 10 years, the use of the air-pump had been exclusively confined to the service of the pneumatic chemist and philosophical experimentalist. Now, however, this valuable instrument is very generally employed in many of our manufactures. We believe that the sugar refiners working under Messrs. Howard and Hodgson's patent were the first who employed it in a large way. It is a fact very generally known that fluids boil at a lower temperature beneath the exhausted receiver of an air-pump than when exposed to the ordinary pressure of the atmosphere, and the sugar refiner, taking advantage of this principle, very readily prevents the charring incident to the old process. To accomplish this, it is merely necessary to enclose the pan containing the saccharine fluid in a close vessel, and by the continued action of an air-pump, the air is so rarified as to produce ebullition at a temperature seldom exceeding 100° of Fahrenheit's thermometer.

This simple instrument has also been employed in the sizing and wetting of paper. In the former case, the paper is piled up evenly in a vessel capable of being rendered air-tight, and a vacuum being first formed, the size is introduced, which is afterwards pressed in by the force of the atmosphere ; passing through the pores of the paper without injury to its fabric. In the process of dyeing, also, the air-pump has been found highly efficacious. In the ordinary way, the cloth is merely immersed in the dye, so that the internal part is of a lighter hue ; but, in this case, the colouring matter passes through the entire fabric.

E. MENDOZA.

The University,
Manchester.

N.B.—" *Annals of Philosophy* " was absorbed in *Phil. Mag.* a few years later.

Vol.
9
959/60

Automatic Level Control for Liquid Nitrogen Trap

IN connection with the development of a thin aluminum coating for a scintillation screen, the occurrence of pinholes was believed to be partly due to the backstreaming of diffusion pump oil in the system. To eliminate oil, a mercury diffusion pump was installed.

Using a mercury diffusion pump requires a liquid nitrogen trap between the pump and the coating chamber in order to obtain coating pressures of 10^{-5} mm and lower. Because of the small volume of the cooling thimble and the continual evaporation of the liquid nitrogen, it was necessary to check and fill the cooling trap periodically. The coater could not conveniently be left running overnight without someone in attendance.

It was realized that an automatic filling device was needed. A search of the literature revealed many systems of varying degrees of complexity. It was felt, however, that a less complex unit could be developed and constructed. Many types of commercial units are available to control the flow of the liquid nitrogen from the storage Dewar*, but no simple and reliable device apparently is available for sensing the liquid level.

After a number of trials, it was found that a component that changes its internal resistance with temperature would be suitable. The component could be used to close a relay which would operate the solenoid to control the flow of liquid nitrogen. Because of the possibility of using liquid oxygen, it was necessary to use a completely enclosed sensing unit so as not to generate a spark, which might cause an explosion. For continuous operation, a unit with no make and break contact was desirable. A number of germanium diodes, glass enclosed type, were found to fill the above requirements. One type in particular had the greatest change in its forward resistance for the smallest difference in temperature, giving the greatest sensitivity, Ω/°C.

TABLE I

Diode No.	Temp. °C	Forward Resistance† Ω
1N96	− 78°	1400
	−195°	8200
1N191	− 78°	1700
	−195°	6900

†Average Resistance (ten samples each)

A schematic drawing of the control circuit is shown in Fig. 1. At temperatures above that of liquid nitrogen, the forward resistance of the sensing diode is approximately 1000 Ω ; for this resistance, sufficient current passes through the relay 8 to close the control solenoid to pass the liquid nitrogen. When the diode 7 is placed in the liquid nitrogen, its resistance increases (to approximately 10,000 Ω), so that the relay opens, which shuts the control solenoid stopping the flow of liquid nitrogen. As the level of the liquid falls, the resistance of the diode again falls, closing the relay and starting the flow of the liquid nitrogen into the cold trap. The rheostat 6 can be used to control the current through the relay, thus allowing an adjustment of the time lag between the dropping of the liquid nitrogen level and the opening of the control solenoid. Measurements made on a number of diodes of the same type indicated that the greatest deviation in forward resistance can be compensated for by the

*Hoffman Container Discharge Equipment, Blair Martin, Inc., 1010 Fair Oaks, So. Pasadena, California.

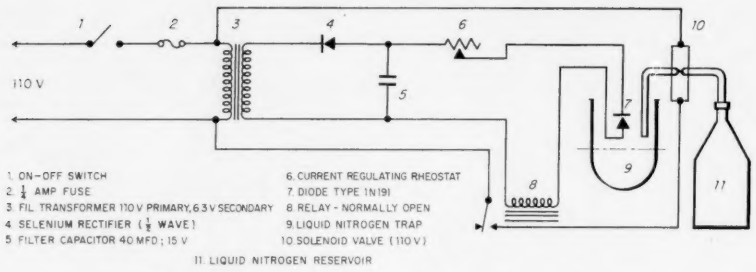

FIG. 1. Control circuit for liquid nitrogen trap.

rheostat adjustment, 6. With this unit, the liquid nitrogen level can be kept constant within ¼ in. or less variation.

Normally sufficient pressure is generated inside the storage Dewar from the evaporation of the liquid nitrogen. However, when initially filling the cold trap, or when a large quantity of liquid nitrogen is needed, auxiliary pressure can be introduced into the Dewar by means of a laboratory air line. Pressures of from 1 to 2 p.s.i. have been used.

After one month of continuous operation, the diode is still in operating condition; thus it appears that the cooling and heating cycles do not adversely affect the diode properties.

LEWIS D. MILLER
PAUL N. PETERSEN

U.S. Naval Radiological Defense Laboratory,
San Francisco 24, *Calif., U.S.A.*

On the Production of Silver Apertures by the Vacuum Evaporation Technique

A method is described for the production of small apertures of silver metal. The technique consists of the vacuum evaporation of a metallic silver charge from a tungsten filament. The silver is condensed at room temperatures on the masked surface of a platinum aperture which serves as the template. Evaporation takes place at short range and the silver film with the duplicate aperture is teased from the surface of the platinum template. Aperture diameters are roughly duplicated.

Very thin duplicate films of silver with a small aperture have been produced by the vacuum evaporation technique. The system may be repeated *ad infinitum* using a single platinum aperture as a template. The method is of note because of the rapid facility with which duplicate apertures may be made.

Fig. 1 schematically illustrates (in cross section) the technique used for this. A platinum aperture *P* is mounted directly behind a 2 mil stainless steel mask *M*. Spacing between the two is between 1 and 10 mil. The silver *S* is evaporated from a helical tungsten source which is 1 or 2 cm from the platinum aperture and the filament is oriented so that, in the region of the aperture, the evaporant impinges normal to the platinum surface. The evaporation is carried on at a temperature just above the melting point of the silver and completed in less than 2 min. Filament temperature has been observed (above the silver melting point) but no attempt has been made to hold it to a single value. It is apparently not critical. Some heating of the condensing surfaces undoubtedly takes place in the sequence and may play an important role. The silver condensate *S* on the platinum surface replicates both the template surface and the aperture. At the conclusion of the distillation the silver aperture may be teased from the surface, starting at point *T*, with the aid of a jeweller's tweezers.

This may be done on a repetitive basis with one aperture being made after another. The platinum template surface is not given any special preparation. Presumably some contaminant on the platinum aperture tends to provide for easier stripping of the silver.

Apertures of 100 μ diameter have been duplicated with this method. It may be that smaller diameters may also be made by the system. This has not been attempted here. While the authors have not attempted to use metals other than silver, presumably any strippable metal may be used as the condensate. Aperture disks have been made as small as 3.2 mm in diameter and weighing 0.5 mg. Larger diameters, up to 25 mm maximum are also possible.

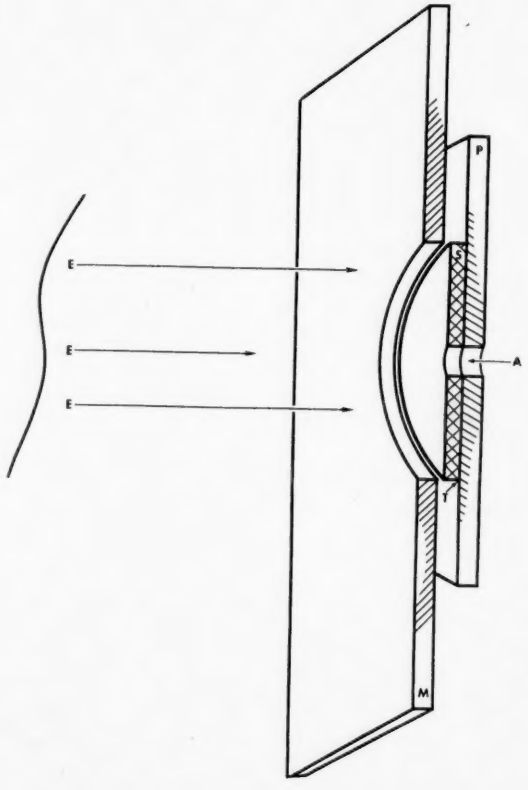

FIG. 1. Silver evaporant *E* condenses on the platinum aperture *P*. The aperture *A* is replicated by the condensate *S*.

C. E. ANTHONY
L. E. PREUSS

Physics Department,
Edsel B. Ford Institute for Medical Research,
Detroit 2, *Michigan, U.S.A.*

VO
9
1959

Vacuum Distillation Source Image Formation by Surface Sensitization

IMAGE formation of the vacuum distillation source has been carried out by the use of a radioactive charge and autoradiography[1]. This method has considerably greater sensitivity than the simple use of the distillation camera[2], but it suffers from certain disadvantages[3]. The major problem is the need for high specific activities, of the radioactive agent. In addition, only a few metals are available with an appropriate tagging for high resolution work. A new method has been developed which utilizes the sensitization technique and which, on preliminary investigation, appears to have a greater experimental reach than the radioactive method. Additionally, the sensitization method encompasses a greater gamut of metals and results in better quality and more informative images.

The steps in the technique are schematized in Fig. 1. A sensitizer metal at the evaporation source, a substrate *T*, and a

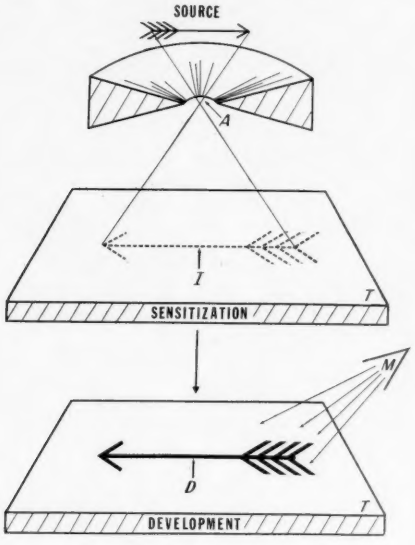

FIG. 1

developer metal *D* are selected. The sensitizer metal *I* is distilled from the vacuum source (arrow at top of Fig. 1) and an integrated image of the process is made with a distillation camera (aperture at *A* and focal plane at *T*). This first step results in an invisible image of the distillation source being condensed on *T* (shown as the broken arrow). The metal *I* is chosen for its high accommodation coefficient on *T*. Following this first step the camera is removed and a second vacuum distillation takes place using the developer metal *D*, (from the crucible *M*), the evaporant of which is allowed to condense on *T*. Now, *D* is chosen for its very low sticking coefficient for substrate surface *T*. However, in the area of the image *I* the sticking coefficient of *D* for *T* has been raised to near unity (for certain conditions) by the nuclei of metal *I* which make up the ' latent image ' of the source on *T*. In this area, the metal *D* is readily condensed, whereas the remainder of the substrate is free of the developer.

Only a few of the many combinations of *I*, *T*, and *D* have been tested here. Heavy, high melting point metals for *I* and low melting point metals for *D* have been used thus far.

Substrates which have been tested are coated condenser paper, glass, mylar, and some plastic surfaces. A fine surface structure which interferes with image quality is a problem with some of these substrates. Presumably other surfaces are also applicable.

Fig. 2 is an example of the successful image produced by the sensitization process. The sensitizer is gold and the developer cadmium. This is the image of a side view of a tungsten helix, from which the sensitizer (gold) has been distilled at a temperature

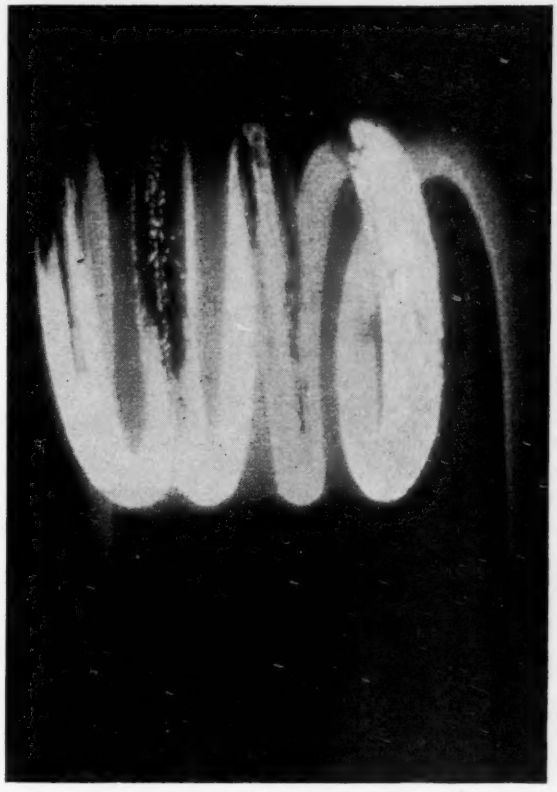

FIG. 2

well above the melting point of the metal. The camera aperture is 50 μ radius and the magnification is 4 X. Developer is cadmium metal done at $5 \cdot 10^{-4}$ mm Hg. The substrate is cellulose acetate butyrate singly coated Schweitzer Kraft capacitor paper.

Note the fine detail of the distillation image and the definition of the ' mottled ' areas which represents regions of alloying from an earlier evaporation.

It should be pointed out that the development process allows for a good deal of control of the image (much as in the case of the photographic development). The development process (at this stage of development of the technique) is a delicate one and demands considerable practice before it can be done well. Distillation rate and pressure have been observed to influence the efficacy of development.

Initial work here indicates that the sensitization process will supplement the radioactive technique by making a wider spectrum of metals available for imaging studies. Resolution and image quality appears to be superior to the tracer method. The method should prove very useful in investigation of the vacuum distillation process.

[1] L. E. Preuss ; *International Journal of Applied Radiation and Isotopes*, **3**, 143–155 (1958).

[2] E. Odeblad ; *Acta Radiologica*, **43**, 2 (1955).

[3] L. E. Preuss ; *Transactions of The Exploding Wires Conference* (1959), sponsored by the Geophysics Research Directorate, Air Research and Development Command, Plenum Press, N.Y., (1959).

LUTHER E. PREUSS

Department of Physics,
Edsel B. Ford Institute for Medical Research,
Detroit 2, *Michigan, U.S.A.*

(*Received* 11 *May* 1959)

Vol. 9 959/60

Abstracts

General Vacuum Science and Engineering

11. Production of Low Pressures

11 : 17 : 51

134. Cryopumping.
This is a new, unconventional and also economical technique for producing a high vacuum at a low temperature on a large scale. It has been used to simulate flight conditions of missiles at high altitudes and at hypersonic speeds. In a windtunnel supplied with dry, gaseous nitrogen at a controlled rate of flow, the model or object under test is located at one end in the throat of the main nozzle. At the far end of the windtunnel large cooling plates are maintained at a temperature of −420°F. Freezing of the gaseous nitrogen to a solid on these plates causes a high speed flow of the remaining gaseous nitrogen toward the cold end to fill the void caused by that fixation. Gas velocities of the order of 20 times the speed of sound have been obtained for 10 hr at a stretch. The low temperature is obtained with a He refrigerator driven by a 50 h.p. motor. These constitute the only moving parts. Pressures of the order of 10^{-4} Torr have been achieved representing the air density at perhaps sixty miles above the earth. C. R. M.

Franklin Inst. **267**, 97–98, Jan. 1959. (Current Topics).

12. Measurement of Low Pressures

12

135. The Speed of Evacuation of High Vacuum Plant.
This is an attempt to predict the speed of evacuation of vacuum plant down to the order of 10^{-6} Torr taking into account the evolution of gas.

Th. Kraus, *Vakuum-Technik* **8**, 39–43, 1959.

12

136. Two Methods for the Measurement of Low Vapour Pressures.
(a) Radiometer method using a thermal molecular manometer. A well evacuated system is isolated with the gauge and the equilibrium vapour pressure measured. This method is useable in the pressure range 10^{-3}–10^{-6} Torr (and lower).
(b) Molecular beam method.
Vapour molecules streaming from an evaporation chamber into a space evacuated to a low pressure are detected by a molecular flow meter. The indication is directly proportional to vapour pressure. This method is best suited for the pressure range 10^{-1}–10^{-4} Torr.

H. Klumb und J. Lückert, *Vakuum-Technik* **8**, 62–66, 1959.

12 : 34

137. Density Determinations based on the Explorer and Vanguard Satellites.
I. Harris and R. Jastrow, *Science* **128**, No. 3321, 420–421, 22 August, 1958.

12

138. Partial Pressure of Ammonia in Alveolar Air.
John A. Jacquez, J. William Poppell and Rudolph Jeltsch, *Science* **129**, No. 3344, 269–270, 30 January, 1959.

15. Fluid Dynamics

15 : 51

139. Polyhedral Satellite for more accurate Measurement of Orbit Data of Earth Satellites.
Donald R. Herriott, *Opt. Soc. Amer.* **48**, No. 9, 667–668, Sept. 1958.

15 : 58

140. Stabilized Pinch and Controlled Fusion Power.
S. A. Colgate and H. P. Furth, *Science* **128**, No. 3320, 337–343, 15 August, 1958.

15

141. Flow through Capillary Tubing with Eccentric Annular Sections.
C. H. Bachman and H. G. Hottentrot, *Rev. Sci. Instrum.* **30**, No. 2.

16. Gases and Solids

16

142. The Influence of the Gas Atmosphere on the Pulverisation Process in Vibratory and Rotary Mills.
Among other things the influence absorbed layers and the effect of residual atmospheres on pulverization in a high vacuum are investigated. The milling processes are partly carried out at a pressure of 10^{-5} Torr. It is shown that the surface conditions affect the processes of fracture during milling as well as the formation of agglomerates.

W. Batel, *Chemie-Ingenieur-Technik* **30**, 651–660, 1958.

16

143. First Adsorbed Layer of He at 4.2°K.
J. P. Hobson, *Canad. J. Phys.* **37**, 300, March, 1959.

17. Thermodynamics

17

144. Simple Continuous He^3 Refrigeration System.
United States. A simple continuous He^3 refrigerator which uses a minimal amount of gas (80 cc S.T.P.) has been built. Temperatures below 0.5°K may be attained for as long as He^4 remains in the cryostat. Commercial components are used throughout. (Author)

H. A. Reich and R. L. Garwin, *Rev. Sci. Instrum.* **30**, 7, Jan. 1959.

17

145. Extremely Low Temperatures.
This review article covers methods of attaining cryogenic temperatures, applications of low temperatures and the types of equipments used. Included are the physical properties of various liquid gases and of metals at room and liquid nitrogen temperatures, the thermal conductivities of fine powders as a function of pressure and the absorbing capacities of molecular sieves as functions of temperature and pressure. A. G.

O. Arnold Hansen, *Chem. Eng.* **66**, 123–138, Feb. 1959.

17

146. Cryostat for Electron Bombardment and Electron Diffraction Work.
United States. A cryostat was constructed for the production

Vo 9 1959

of free radicals by electron bombardment of condensed gases at liquid He and liquid H_2 temperature. Provisions were made for simultaneous investigations of the bombardment products by electron diffraction and optical spectroscopy.

E. M. Horl and L. Morton, *Rev. Sci. Instrum.* **29**, 859, Oct. 1958.

17

147. Use of Neon in Cryogenics.
J. F. Dillon and V. Jaccarino, *Rev. Sci. Instrum.* **30**, No. 2.

17 : 41

148. The Selection of Stainless Steels for Use in Liquid Hydrogen Bubble Chambers.
Pierre Amiot, *Nuclear Instr. and Methods* **4**, No. 2.

17 : 25

149. Hydrogen Liquefaction.
United Kingdom. This is a report of a one-day symposium on hydrogen liquefaction and associated techniques, organised by the Low Temperature Group of the Physical Society, and held on March 12th, 1959 at the Institute of Physics in London. It was evident from the attendance at the meeting that interest in the large scale liquefaction of hydrogen is developing in Great Britain.

D. H. Bowen, *Nature* **183**, No. 4674, 1504, 30 May 1959.

17

150. Resistance Thermometer Bridge for Measurement of Temperatures in the Liquid Helium Range.
United States. A 33-cps resistance thermometer bridge, suitable for precise temperature measurements in the liquid He range, has been designed as a completely self-contained unit. The amplifier has a gain of 120 db, band width of 0.3 cps, and input impedance of 10 Ω. With a power dissipation of 2×10^{-8} W in the thermometer, resistance changes of 0.1 Ω can be detected. For a typical resistance thermometer this corresponds to a temperature change of 4×10^{-6}°K at 2°K. Other features include high rejection of line-frequency pickup, short recovery time after saturation, and a combination gain band-width control which shortens the response time during preliminary balancing operations. (Author)

C. Blake, C. E. Chase and E. Maxwell, *Rev. Sci. Instrum.* **29**, 715–716, Aug. 1958.

17 : 51

151. Growth and Properties of " Whiskers ".
S. S. Brenner, *Science*, **128**, No. 3324, 569–575, 2 Sept. 1958.

17 : 51

152. Ultrahigh-Pressure Research.
H. Tracy Hall, *Science* **128**, No. 3322, 445–449, 29 August 1958.

17 : 34

153. Atmospheres of other Planets.
Seymour L. Hess, *Science* **128**, No. 3328, 809–814, 10 October 1958.

17

154. Air Conservation.
A. J. Haagen-Smit, *Science* **128**, No. 3329, 869–878, 17 October 1958.

17

155. On Evaporation from Wind-swept Surfaces.
Karol J. Mysels, *Reports, Science* **129**, No. 3340, 38–39, 2 January 1959.

17

156. How Does a Raindrop Grow ?
Roscoe R. Braham, Jr., *Science* **129**, No. 3342, 123–129, 16 January, 1959.

17 : 11 : 51

Cryopumping. Abstr. No. 134.

18. Gaseous Electronics

18

157. Effect of Humidity on the Spark Breakdown Voltage.
United Kingdom. Letter by K. R. Allen and K. Phillips, *Nature* **183**, No. 4655, 174, 17 Jan. 1959.

18

158. Alfven Waves in a Gas Discharge.
United Kingdom. D. F. Jephcott, *Nature* **183**, No. 4676, 1652, 13 June 1959.

18

159. Some Experiments with an Electrodeless Discharge.
United Kingdom. Letter by J. K. Wright, W. T. Ecles and J. D. Herbert, *Nature* **183**, No. 4676, 1665, 13 June 1959.

18

160. Townsend's First Ionization Coefficient in Pure Nitrogen.
United Kingdom. Letter by A. E. D. Heylen, *Nature* **183**, No. 4674, 1545, 30 May 1959.

18

161. Production of High Concentrations of Hydrogen Atoms.
United Kingdom. Letter by K. R. Jennings and J. W. Linnett, *Nature* **182**, No. 4635, 597, 30 August 1958.

18

162. Vacuum Arcs on Tungsten Cathodes.
United Kingdom. In the course of a programme of work on d.c. arc discharges at low gas pressure an interesting phenomenon was observed. Photomicrographs of tungsten cathode surfaces were taken before and after an arc of 150 amp. had operated for 30 msec in air at 1 μ Hg. Small areas of tungsten were melted and the craters were distributed along fine cracks which were present before arcing.

Letter by H. Wroe, *Nature* **182**, No. 4631, 338, 2 August 1958.

18

163. High Power Vacuum Spark Gap.
D. C. Hagerman and A. H. Williams, *Rev. Sci. Instrum.* **30**, No. 3.

18 : 42 : 43

164. Investigation of Breakdown in Vacuum.
The authors of this paper have done a very thorough investigation into two separate problems. First they have experimented with the surface dielectric strength of insulators and second they have performed many tests with metallic electrode breakdown in vacuum. The pumping system used for these experiments was a hydrogen condensation cryogenic pump capable of producing pressures of 10^{-9} mm. Tables of the results illustrate the most promising dielectrics and also the preferred metals for both anode and cathode use. C. L. G.

E. S. Borovik and B. P. Batrakov, *Soviet Tech. Phys., Eng. Trans.* **3**, No. 9.

18 : 56

165. New Developments of Air Cooled Condensers for the Processing Industry.
One of the subjects under review is also air cooled condensers for the pressure range 2–5 Torr.

W. Rose, *Chemie-Ingenieur-Technik* **31**, 101–105, 1959.

19. Radiation

19 : 51

166. Electroluminescence of Zinc Sulfide Phosphors as an Equilibrium Process.
The intensity of the time-average output of the steady-state electroluminescence of powdered zinc sulfide phosphors in an intense alternating electric field is characterized by a dynamic equilibrium between the monomolecular collision excitation

Vol. 9 959/60

process and the bimolecular recombination process. This equilibrium condition permits predictions of the dependence of the emission intensity, the efficiency, and other properties on several parameters such as the voltage, the temperature, and the concentrations of electron traps and activator centers. These predictions are compared with experimental results. (Author)

Willi Lehmann, *J. Opt. Soc. Amer.* **48**, No. 9, 647–653, Sept. 1958.

19 : 30 : 51

167. Reflexion Coefficient of Optically Inhomogeneous Layers.

The reflexion coefficient is calculated for radiation incident normally on a non-absorbing, optically inhomogeneous, plane parallel layer bounded on either side by non-absorbing semi-infinite media. The theory is applied to determine the reflectance of a layer in which the index of refraction varies nearly linearly with the thickness. (Author)

Joseph F. Hall, Jr., *J. Opt. Soc. Amer.* **48**, No. 9, 654–657, Sept. 1958.

19 : 30

168. Optical Transmission of Evaporated IN, SN, and BI Films in the Vacuum Ultraviolet.

W. C. Walker, O. P. Rustgi and G. L. Weissler, *J. Opt. Soc. Amer.* **48**, No. 12, 1017, Dec. 1958.

19 : 30

169. Optical Constants of Evaporated Se Films by Successive Approximations.

Experimental values of the refractive index μ and the absorption constant k in the wavelength range 0.24 to 2.5 microns are reported for evaporated films of Se. Methods of successive approximation were used to obtain an average precision of ± 0.003 in the non-absorbing region and ± 0.005 in the absorbing region. Electron microscope and electron diffraction techniques indicate that the Se films were amorphous and non-porous. (Author)

W. F. Koehler, F. K. Odencrantz and W. C. White, *J. Opt. Soc. Amer.* **49**, No. 2, 109–115, Feb. 1959.

19 : 30

170. Optical Properties of Various Evaporated Rare Earth Oxides and Fluorides.*

To furnish a greater choice of film materials for application in optical multilayer coatings, the optical properties of evaporated rare earth compounds such as Y_2O_3, La_6O_{11}, Pr_2O_3, Nd_2O_3, Sm_2O_3, LaF_3, NdF_3, and CF_3 were studied in the wavelength region from 0.22 μ to 2 μ. The materials were evaporated from tungsten boats and condensed on glass and fused quartz substrates at various temperatures. The optical constants n and k were determined mainly from reflectance, transmittance, and true thickness measurements. The following oxides were found to be useful because of their low absorption in the visible : La_2O_3 with n ranging from 1.85 to 1.95 with increasing thickness, Pr_6O_{11} with n ranging from 1.92 to 2.05, also with increasing thickness and Nd_2O_3 with $n = 2.05$ for films of sufficiently low absorption. LaF_3 ($n = 1.60$) and NdF_3 ($n = 1.61$) showed no appreciable absorption in the whole wavelength region studied ; CeF_3 ($n = 1.63$), however, exhibited two weak absorption bands at 0.234 and 0.248 μ. All n values are given at a wavelength of 0.5 μ and for unbaked films deposited at 300°C substrate temperature. The oxides condensed as almost amorphous films, whereas the fluorides developed fairly large grains as indicated by their sharp electron diffraction rings. All films were hard and showed excellent chemical and mechanical durability. (Author)

G. Hass, J. B. Ramsey and R. Thun, *J. Opt. Soc. Amer.* **49**, No. 2, 116–120, Feb. 1959.

*Presented at the Meeting of the Optical Society of America, Columbus, Ohio, October 17–19, 1957.

19 : 30 : 51

171. Transmittance and Reflectance of Cesium Iodide in the Far Infrared Region.

Earle K. Plyler and Nicolo Acquista, *J. Opt. Soc. Amer.* **48**, No. 9, 668–669, Sept. 1958.

19

172. Infrared Spectra of Monolayers on Metal Mirrors.

A double-beam infrared spectrophotometer has been modified so that spectra of films as thin as one or a few-monolayers in thickness on metal mirrors can be obtained. It is theoretically predicted and experimentally confirmed that, at the mirror surface, the electric intensity is predominantly perpendicular to the surface. Vibrational modes for which the matrix element of dipole moment is parallel to the surface appear abnormally weak in the spectra. The spectra, therefore, provide information about the orientation as well as the composition of sample films. Spectra of Blodgett films of metal stearates show differences in band positions and band intensities between films one molecular layer in thickness and thicker films. The shifts in band positions are attributed to interactions between carboxylate ions in films thicker than a molecular layer and the absence of such interactions in the first layer. The intensity differences are not explained. (Author)

S. A. Francis and A. H. Ellison, *J. Opt. Soc. Amer.* **49**, No. 2, 131–138, Feb. 1959.

19 : 30 : 51

173. Luminescent Phases in Willemite Films.

Red-, yellow-, and green-luminescent films have been formed by evaporation of powdered Zn_2SiO_4 (Mn). The yellow-emitting form was formed by firing the evaporated film plus additive in air at relatively low temperatures (750 °C). The red form was produced on Vycor substrates at higher temperatures (1100 °C). Infrared reflexion studies and x-ray diffraction analyses of these films indicate that the red-emitting form is SiO_2(Mn) and that the yellow form is amorphous Zn_2SiO_4(Mn). The luminescence of both of these phosphors is probably due to interstitial manganese ions. The strong chemical reaction between the luminescent film and the glass substrate is brought out. (Author)

Charles Feldman and Margaret O'Hara, *J. Opt. Soc. Amer.* **48**, No. 11, 816–820, Nov. 1958.

19 : 30

174. Stokes' Equations and Their Application to the Refractivity of Thin Films.

A solution to the problem of determining the refractivity of n identical planar arrays from the properties of a single array is obtained by first extending Stokes' equations to a form appropriate to a microscopic situation and then appropriately modifying Crook's results for thin films. The results of such development are found to be in agreement with data taken at microwave frequencies. (Author)

A. F. Wickersham, Jr., *J. Opt. Soc. Amer.* **48**, No. 12, 958–964, Dec. 1958.

19 : 29 : 30

175. Obtaining Low Orders of Interference in Measuring Film Thicknesses by Multiple Beam Interferometry.

G. David Scott, *J. Opt. Soc. Amer.* **48**, No. 11, 858, Nov. 1958.

19 : 29 : 51

176. Ultraviolet Transmission Properties of Conducting Coatings on Glass.

D. W. Juenker and E. W. Parsons, *J. Opt. Soc. Amer.* **48**, No. 11, 857, Nov. 1958.

19 : 51

177. Pressure Modulation of Infrared Absorption. I. Entire Vibration-Rotation Bands.

The effects of pressure modulation on the total absorption SA (v)dv of rotation-vibration bands of carbon monoxide,

nitrous oxide, methane, and propane have been investigated. Although the ultimate limitations of pressure modulation as a detection technique have not yet been completely established, the present results are in qualitative agreement with predictions based on the earlier studies of Howard, Burch, and Williams. Modulation is of use in distinguishing weak absorption bands from background absorption in the atmosphere. In strong absorption bands, the wings are enhanced in the modulated spectrum ; in weak bands, the modulated spectrum approximates that obtained by conventional methods. Possible applications of pressure modulation are suggested. (Author)

James C. Gilfert and Dudley Williams, *J. Opt. Soc. Amer.* **48**, No. 11, 765–769, Nov. 1958.

19 : 30 : 51

178. Antireflexion Coatings for Ge and Si in the Infrared.
Very hard and durable single layer antireflexion coatings for Ge and Si have been made which result in a peak transmittance of better than 98 per cent at any desired wavelength in the infrared up to about 15 μ. Silicon monoxide makes an excellent antireflexion coating for Si and Ge in the near infrared, but cannot be used in the 10-μ region where it becomes strongly absorbing. Zinc sulfide has been found to be the most suitable antireflecting material at the longer wavelengths. Under proper conditions zinc sulfide films, which in the past have frequently exhibited unsatisfactory durability, can be prepared as very hard and adherent antireflexion coatings for Ge and Si. The best zinc sulfide films are obtained when the substrate is heated to about 150 °C and cleaned with a d.c. glow discharge just before the evaporation is made. The coatings can stand several hours boiling and several days immersion in water without damage and have been used for periods up to one year without showing any deterioration. (Author)

J. T. Cox and G. Hass, *J. Opt. Soc. Amer.* **48**, No. 10, 677, Oct. 1958.

19 : 51

179. Index of Refraction of Ge.
Calvin D. Salzberg and John J. Villa, *J. Opt. Soc. Amer.* **48**, No. 8, 579, Aug. 1958.

19

180. Spectral Effects in Interferometry.
The influence on the fringe intensities of sources with known spectral energy density functions is analysed both theoretically and experimentally for double beam interferometers of the Mach-Zehnder type. Simple relations between the spectrum and the fringe intensity and extent of the fringe field are presented. Special attention is given to energy sources consisting of a primary source used with a monochromator. Experimental confirmation is demonstrated. (Author)

G. D. Kahl and D. B. Sleator, *J. Opt. Soc. Amer.* **48**, No. 8, 525–530, Aug. 1958.

19

181. Light Guide Radiation Pyrometry.
A method of calculating and describing transmission characteristics of light guides is developed and applied to rods of synthetic sapphire. The total transmission is shown to be an inadequate measure of the extent to which a calibration curve relating relative signal to temperature is possible for a light guide radiation pyrometer. The angular field of view of synthetic sapphire rod is presented in terms of fractional emergent power per five degree angular increment. It is concluded that the transmission properties presented here, in combination with data for a single point, permit the simple, individual calibration of commercially available light guide radiation pyrometers. (Author)

J. Vollmer, G. C. Rein and J. A. Duke, *J. Opt. Soc. Amer.* **49**, No. 1, 75–77, Jan. 1959.

19 : 30

182. Design of Multilayer Filters by Successive Approximations.
A relaxation method is used to adjust the thicknesses of the film of a multilayer in order to alter its transmission characteristics in a limited spectral region. This region is used to modify the spectral transmission of a short-wavelength pass multilayer and a broad-band dielectric mirror. The computations also furnish information useful in controlling the thicknesses of the layers in the fabrication of a multilayer. (Author)

Philip Baumeister, *J. Opt. Soc. Amer.* **48**, No. 12, 955–958, Dec. 1958.

19 : 32

183. Primary Frequency Standard Using Resonant Caesium.
United States. Caesium atoms in a sealed beam tube comprise the heart of a primary frequency standard. New techniques of evacuating the tube, 6 ft long, have made possible a practical and reproducible frequency standard. The complete system generates 9,192.6318 Mc/s (the resonance frequency) from a 5 Mc/s crystal oscillator, whose frequency is automatically corrected by a control loop. Outputs, accurate to 1 in 10^9 are available at 100 kc/s, and 1, 5, 10 and 100 Mc/s. M. D. A.

W. A. Mainberger, *Electronics* **31**, 80–85, 1958.

19

184. Semiconductor P-N Junction Radiation Counter.
Letter from B. Salzberg and K. Siegel, *Proc. Inst. Rad. Engrs.* **46**, 1536. Aug. 1958.

Vol. 9 959/60

Vacuum Apparatus and Auxiliaries

20. Pumping Systems

20

185. Measurement of Partial Pressures of HCl and H_2O in the $MgCl_2$–H_2O–HCl System.
E. Mirsch, *Chemische Technik* **10**, 539–541, 1958.

20

186. The Attainment of High Pumping Speeds Using Ionization Pumps.
Discussion concerning the variation in pumping speed of the Bayard–Alpert tube observed by different workers.

G. Comsa, *Vakuum-Technik* **8**, 76–77, 1959.

20

187. The Pumping Speed of an Ion and Absorption Pump of the Comsa–Musa Type.
Contribution to the discussion on the same subject as above under " Comsa ".

F. A. Baker and J. Yarwood, *Vakuum-Technik* **8**, 77–78, 1959.

20

188. Application of New Vacuum Pump Combinations.
A review of the use of pump combinations consisting of water ring pumps and roots pumps in large scale vacuum metallurgical plants. A combination consisting of 2 roots pumps in series followed by a water ring pump gives a pumping speed of up to 30,000 m^3/h in the pressure range 10 Torr–10^{-1} Torr.

W. Armbruster, *Chemie-Ingenieur-Technik* **31**, 338–342, 1959.

21. Pumps and Pump Fluids

21

189. Annular Jet Pump.
Werner Haak and Frederick Vratny, *Rev. Sci. Instrum.* **30**, No. 4.

21

190. Dual Pumping Speeds of Some Ionization Pumps.
United Kingdom. The phenomenon of ion pumping in ionization gauges has received much attention during the past few years. In an ionization gauge activated gas molecules interact with the glass walls of the tube and are removed from the gas phase at a rate depending principally on the vacuum history of the gauge. In the Bayard–Alpert type of gauge the glass assumes a potential negative with respect to the cathode, and the pumping action is dependent on ions which are accelerated and are driven into the walls. The author has made measurements of pumping speeds in gauges of this type over the past few years, and has shown that such gauges possess two speeds for argon, one about five times that of the other. The speed is dependent upon the electrical potential of the inner surface of the glass wall. Measurements showed that when the potential of the glass wall approximated to that of the cathode, the gauge pumped relatively quickly, but when the potential was high (about 200 V) there was only a slight pumping action. These two separate charged conditions of the inner glass wall arise in the following way. The walls become stabilized at cathode potential when the primary electron and ion currents balance, but it is believed that a second stabilization potential occurs at which the primary electron current is balanced by a current of secondary electrons emitted from the glass. When the glass is new, and contains occluded gas, the second stabilized condition can be obtained because the yield of secondaries is greater than unity. When the glass is well outgassed this condition cannot be obtained. In this work a dynamic vacuum system maintained at 10^{-5} Torr of A was used. Subsequent release of the adsorbed gas by heating enabled the pumping speeds to be measured. When the glass was at -5 V the speed was 0.0003 l/s/mA, but when the potential of the glass was about 200 V the speed was reduced to 0.00005 l/s/mA.

Letter by G. Carter, *Nature* **183**, No. 4675, 1619, 6 June 1959.

21

191. Étude d'une Pompe à Évaporation et Ionisation. Study of an Evapor-ion Pump.
A vacuum pump working on the principle of the ion pumping of gases and of the gettering by titanium which evaporates continuously and condenses on the inner wall of the pump is described. The mechanism for the feeding of titanium is also described. The pump is now under trial. (Author)

E. Thomas, *Bull. Acad. Roy. Belg. Sc.* **42**, 778, 1956.

21

192. Theory and Design of Getter-Ion Pumps.
Gt. Britain. Attention has been given recently to the use of absorbing devices to supplement rotary and vapour types of high-vacuum pump, in cases where ultra-high vacua are required or where the vapour of pump fluids might be harmful. Films of certain metals have long been used in thermionic valves as " getters " : pumps have now been developed in which the metal films are evaporated continuously, or are renewed by cathodic sputtering, and are given the general name " getter-ion " pumps in this review. The various mechanisms of gas sorption in electrical discharges are considered briefly, as follows :—

(1) the electrodeless discharge,
(2) the cold-cathode discharge (the importance of sputtering is emphasised),
(3) the hot-cathode discharge (e.g. in an ionization gauge), the action of evaporated films (" getters "), which may take place during deposition or after,
(4) the action of a metal film when the gas is ionized by an electrical discharge. (Some workers suggest that atoms, or metastable molecules, are formed in the discharge and that these, rather than ions, are responsible for the increased rate of sorption).

The properties of different getter materials are discussed, an extensive table giving data on the sorptive capacity and adsorption rates of various metal-gas combinations, and stating the effect of ionization on the process. It is noted that some metals, notably the transition elements of the fourth to sixth groups, usually operated at high temperatures, are good getters in the solid state and are therefore used in thermionic valves. The alkaline earth metals are generally used for thin film getters, and titanium is also useful. The effect of the structure of a thin film on its gettering properties is discussed, the importance of the effective surface area being emphasized. The relative effectiveness of getters for different gases is discussed and an order of affinity given which is relevant to chemisorption. It is pointed out that the metal to be used should be free from impurities which may evolve gas on heating. There is some discussion of the different designs of getter-ion pump which have been used and data on their performance is tabulated. These include the Evapor-ion pump, in which titanium wire is fed downwards on to a graphite post which is heated by electron bombardment, ionization pumping occurring as well to deal with inert gases. Data is given on the effect of the temperature of the gettering surface and on the residual gases found in the pump. Three other arrangements for evaporating titanium are described : in one, the wire is fed upwards into an electron beam, in a second it is fed downwards on to a copper anode so that a 5 mm droplet forms which is heated by electron bombardment from a nearby cathode filament, in the third the wire is fed upwards on to the molten tip of a molybdenum rod. Evaporation rates as high as 100 mg/min are mentioned. In another type of pump, the titanium wire is wound on to a tungsten grid, which is heated by electron bombardment, a third (negative) electrode acting as

Vo
9
1959

a positive ion collector. Other types make use of the Penning gauge principle to sputter titanium from the cathode(s), and provide heavy ionization. In yet another pump, barium is evaporated on to an extensive water-cooled surface, with a Penning gauge adjoining. In discussing the future of these pumps, the author points out that none have the high and constant pumping speed of oil diffusion pumps of comparable size. Ultimates of the order 10^{-10} mm have been obtained, but usually with systems designed for low degassing rates. There is an advantage in the absence of oil vapours, and small pumps may be permanently connected to sealed-off devices such as magnetrons and X-ray tubes. It is concluded that these new pumps will be used increasingly in research and in the electron industry, but not in applications where very large gas throughputs have to be handled. An appendix discusses definitions of speed and sorptive capacity as applied to gettering agents. There are 63 references. M. D. A.

L. Holland, *J. Sci. Instrum.* **36**, 105–116, March 1959.

21

193. A New Molecular Pump.

A new molecular pump constructed like a turbine is described. An axis rotating inside a cylindrical housing has bearings at both extremities of the housing. To the axis are fixed 19 rotors from the centre towards each bearing mounted so as to interlock with 21 stators fixed to the housing. It follows from this that gas is transported axially from the centre of the rotor to the two ends. The pumping action is achieved by a series of slanting slits cut into the outer perimeter of both rotors and stators.

Some technical data :

Thickness of rotor and stator disks : some mm
Radial gap between rotor and housing : 1 mm
Axial distance between rotors and stators : 1 mm
Rotor diameter 170 mm, revolutions : 16,000 rev/min
Power required 0.3 KW
Overall length of pump : 670 mm
Speed for air : 500 m^3/h for pressures below 10^{-2} Torr.

The compression ratio is very dependent on the molecular weight of the gases to be pumped. For hydrogen it is 1 : 250 for air $1 : 5 \times 10^7$. Speed curves are reported showing a region of constant speed of 500 m^3/h between 10^{-2} and 10^{-9} Torr. It is further reported that the ultimate vacuum of the pump is determined largely by hydrogen coming from the steel walls by diffusion or degassing.

In the use of the pump in a high vacuum installation the use of high vacuum and roughing valves can be dispensed with. Both the primary and the molecular pumps may be started simultaneously as it may be assumed that the full number of revolutions of the molecular pump is only obtained when the primary pump has evacuated the vessel to about 10^{-1} Torr and that the final evacuation of the vessel down to the desired ultimate is then taken over by the molecular pump. A sliding coupling prevents overloading of the motor. When pumping at more than 10 Torr the rotational speed is automatically reduced. Below this pressure the pump will attain the full rotational speed.

The following fields of applications for this type of pump are suggested :—

Manufacture of large transmitting valves for VHF.
Accelerators for nuclear physics.
Vacuum systems for mass spectrometers.
Melting installations for the highest degree of purity.

Furthermore it is thought that the pump may be employed in the separation of light isotopes because the compression ratio for normal hydrogen is only 1 : 250 rising to 1 : 2400 for heavy hydrogen (separation factor 9.6).

W. Becker, *Vakuum-Technik* **7**, 149–152, 1958.

21

194. Removal of Gases in High Vacuum Systems by Metal Abrasion.

United Kingdom. Gettering is a well-known process for the removal of free gas in vacuum devices, but removal can cease once a thin protective layer of reaction product has been formed. A method had been devised for removing the protective film from a reactive metal such as titanium by abrading the surface, so that a continuous take-up of gas is obtained.

Letter by M. E. Haine, E. W. R. Francis and R. N. Bloomer, *Nature* **182**, No. 4640, 931, 4 Oct. 1958.

22. Gauges

22

195. Liquid Manometer with Electromagnetic Balance Indicator.

S. Africa. The paper describes the construction and operation of a null-reading type of liquid manometer, which utilizes an electromagnetic device for balance indication, and a set of analytical weights for indirect "weighing" of the unknown differential pressure. The apparatus was designed specially for measurements in the range of differential pressures below 5 mm water gauge. The probable error under laboratory conditions was found to vary from less than 0.01 mm water gauge at maximum range, to about 0.0005 mm water gauge at a differential pressure of 0.01 mm water gauge. Apart from its normal applications as a manometer, the apparatus can be used as an indicator of the flow dynamic head in low-speed wind tunnels. (Author)

J. F. Kemp, *J. Sci. Instrum.* **36**, 77–81, Feb. 1959.

22

196. Construction of a Mcleod Type Vacuum Gauge having a Linear Scale.

G. Haase, *Chemische Technik* (Beiblatt Glas-Apparate-Technik) **10**, 37–39, 1959.

22

197. Pressure Gauge for Corrosive Gases in the Micron and Submicron Region.

Australia. For use with corrosive gases in the range 10^{-2} to 10^{-5} Torr a gauge is described in which the pressure is indicated by the rate of damping of a hinged silica fibre pendulum, the amplitude of which is measured photoelectrically. The gauge exposes only glass and silica to the gas, may be baked 450 °C, and gives an accuracy of pressure measurement of better than 5 per cent. (Author)

J. R. Anderson, *Rev. Sci. Instrum.* **29**, No. 12, 1073, Dec. 1958.

22

198. Investigations of Radiometer Forces in the Pressure Range 10^{-3} to 3 Torr.

Experiments are described with the thermal-molecular vacuum gauge of Klumb.

H. Klumb und D. Fuchs, *Vakuum-Technik* **7**, 131–135, 1958.

22

199. Vacuum Gauges in Glass.

A discussion of pressure units and pressure ranges below 760 Torr is followed by an historical survey of the different groups of gauges. A detailed treatment is given on : U-tube, membrane, capsule, bourdon-tube, micro-manometer, further : compression —(e.g. McLeod, rotary) vacuum gauges, as well as barometers. The details of construction and design of these instruments are dealt with.

H. Wilhelm, *Sprechsaal* **91**, 233–236, 267–270, 285–288 and 308–311, 1957.

22

200. Thermocouple for Vapor Pressure Measurement in Biological and Soil Systems at High Humidity.

L. A. Richards and Gen Ogata, *Science* **128**, No. 3331, 1089–1090, 31 Oct. 1958.

Vol. 9 959/60

23. Plumbing

23

201. Vacuum Seals at Liquid Nitrogen Temperatures.
J. R. Hearst, S. H. Ahn and E. N. Strait, *Rev. Sci. Instrum.* **30**, No. 3.

23

202. Coolable Vacuum-tight Window Seals for Optical Use.
Note by V. Roberts, *J. Sci. Instrum.* **36**, 99, Feb. 1959.

23

203. O-Ring Seals for Pressures of 10 Kilobars.
Note by E. Whalley and A. Lavergne, *J. Sci. Instrum.* **36**, 47–48, Jan. 1959.

23

204. Cleaning Techniques for Rubber O-Rings Used in Vacuum Systems.
United States. It was previously reported that demountable joints using Neoprene rubber O-rings gave off butane and therefore could limit the vacuum under some circumstances. Recently the quantity of gases evolved from rubber O-rings has been found to depend markedly upon the O-ring cleaning technique. When an O-ring was cleaned in acetone, alcohol, or trichloroethylene, dried in air at room temperature and then mounted in an O-ring joint of a vacuum system, a low-pressure limit between 10^{-5} and 10^{-6} Torr was obtained. This O-ring was $1\frac{1}{8}$ in. dia. and was pumped at about 1 l/sec. Mass spectrometer analysis of the gases present indicated large quantities of hydrocarbons, and for the trichloroethylene cleaning large HCl peaks. It was found possible to reduce these contaminants to a negligible value by baking the O-rings in air at 100 °C for several hours. Also no contaminants were observed when an O-ring was used which had not been cleaned after unpacking. In some cases it was found necessary to lubricate the O-rings with Apiezon N stopcock grease in order to prevent small air leaks. This lubrication did not contribute a measurable contaminant to the vacuum system. When a $1\frac{1}{8}$ in. dia. O-ring joint having a cleaned and air baked Neoprene or silicone rubber O-ring was pumped at about 1 l/sec. a pressure of 1×10^{-7} Torr was obtained after about 24 hr of pumping. A mass spectrometer analysis of the residual gases in this vacuum is shown. The major gases are H_2O, CO, N_2 and CO_2, the hydrocarbon partial pressure being about 5×10^{-9} Torr. It is therefore believed that rubber O-rings which are properly cleaned, or, if carefully handled, not cleaned at all, do not limit the vacua obtainable under many conditions. (Author)

Note by J. R. Young, *Rev. Sci. Instrum.* **30**, No. 4, 291, April 1959.

23

205. Valve for Pressures of 10 Kilobars.
Note by E. Whalley and A. Lavergne, *J. Sci. Instrum.* **36**, 46–47, Jan. 1959.

23 : 42

206. Glass Problems in Electron Tube Technology.
The influence of glass on vacuum conditions is surveyed (permeability and degassing, absorption of radiation, heating by dielectric loss, impact by ions and electrons, electrolysis). The survey continues with a discussion on the effect of temperature and mechanical stress on the dimensional stability of glass and finally with a discussion on glass to metal seals (copper seals, molybdenum and tungsten seals).

A. Zincke, *Vakuum-Technik* **7**, 93–100, 1958.

23 : 33

207. Transmission Specimen Holder for Electron Diffraction.
Australia. A specimen stage for electron diffraction and electron shadow microscopy has been constructed, to enable a holder containing two transmission specimens to be inserted into, or withdrawn from, the specimen chamber without breaking the vacuum in the system. The time required to change specimens is less than 1 min. Controls are provided to give specimens two independent translations in a plane normal to the electron beam and a rotation about the axis of the holder. (Authors)

R. I. Garrod and R. K. Hart, *J. Sci. Instrum.* **36**, 44–45, Jan. 1959.

24. Valves

24

208. O-Ring Vacuum Valve for use with a Visible Flow Industrial Glass Apparatus.
Note by G. S. Martin and A. Lench, *J. Sci. Instrum.* **36**, 141, March 1959.

24

209. Vacuum Type Gas Flow Calibrator.
United States. A vacuum-type gas-flow calibrator was designed and constructed for making accurate calibration of flowmeters needed for the investigation of high-pressure flames. This calibrator operates by automatically measuring the time required to pressurize a known volume from a near vacuum to 1 atmosphere pressure. The gas volume flow rate is obtained by dividing the calibration volume by the pressurization time and applying corrections from PVT data. This apparatus has been successfully used to calibrate flowmeters for use with hydrogen, oxygen, nitrogen, air, methane, nitric oxide, carbon monoxide, and various homogeneous nonexplosive gas mixtures. (Author)

W. A. Strauss and R. Edse, *Rev. Sci. Instrum.* **30**, No. 4, 258, April 1959.

24

210. Small Valves for Instrumentation.
Donald Salmon, *Instrum. and Control Systems* **32**, 1026–1027, July 1959.

24

211. Mercury Glass Check Valves.
H. A. Smith, J. C. Posey and C. O. Thomas, *Rev. Sci. Instrum.* **30**, No. 3.

25. Baffles, Traps and Refrigeration Equipment

25

212. Liquid-Air Level Controller for Cold Traps.
Note by K. H. Purser and J. R. Richards, *J. Sci. Instrum.* **36**, 142, March 1959.

25 : 17

Hydrogen Liquefaction. Abstr. No. 149.

26. Automatic Protective and Control Equipment

26

213. Vacuum Valve Indicator Light.
Note by D. H. Cooper, *J. Sci. Instrum.* **36**, 141, March 1959.

26

214. Bellows-operated Water Switch.
Note by J. Preston, *J. Sci. Instrum.* **36**, 98, Feb. 1959.

26 : 37

215. Two Emission Stabilizers for Electron-Bombardment Furnaces.
Gt. Britain. Stabilization requirements and techniques for electron-bombardment heating are considered, and basic design formulae are presented for a flexible control system applicable to temperature-limited emission furnaces. Power handling capacity, loop stability and speed of response are discussed, and full circuit details of practical stabilization systems for a 250 W and a 6 kW furnace are given. It is concluded that emission

Vo 9 1959

stabilization is always beneficial and sometimes essential, and that emission stabilities of better than 0.5 per cent at powers up to 20 kW are practicable. (Author)

D. Allenden, *J. Sci. Instrum.* **36**, 66–70, Feb. 1959.

27. Leak Detectors and Leak Detection

27

216. Thermal Conductivity Leak Detector.
United States. Note by Clarke C. Minter, *Rev. Sci. Instrum.* **29**, No. 9, 793, Sept. 1958.

27 : 40

217. Experiments on flow of gases through leaks.
As in 1956 National Vacuum Symposium on Vacuum Technology Transactions (Pergamon Press, London 1957), p. 1–7.

A. Nerken, *Vakuum-Technik* **7**, 111–116, 1958.

27 : 37

218. Application of Mass Spectrometry to Vacuum Technique.
Survey of different types of mass spectrometers, their applications and limitations as manometers (for measuring partial pressures and vapour pressures). The use of mass spectrometers for the analysis of residual gases in vacuum systems is discussed. Experimental results from many publications including curves and tables are cited and discussed. Finally the survey concludes with a discussion of the application of mass spectrometers to leak detection, the sensitivity obtainable, the working principle and the selection of detector gases.

H. Hintenberger and E. Dörnenburg, *Vakuum-Technik* **7**, 121–130, 159–171, 1958.

28. Heating Equipment

28 : 30

219. Electron Bombardment Apparatus for Vacuum Evaporation.
Gt. Britain. Certain metals are difficult to evaporate by conventional means because they are of very high melting point, or react with convenient crucible or filament materials. The method described here uses the specimen in the form of a wire, held vertically, the lower end being heated by electron bombardment until a molten drop is formed from which evaporation takes place at a useful rate in favourable cases. (In this connexion, see also Abstract no. 241.) The cathode used here is a single loop of 0.5 mm tungsten wire, supported in a horizontal plane between two shields at cathode potential. These prevent evaporated metal from contaminating the filament : the upper one is pierced by a small hole to allow the emission current to pass. The work to be coated is mounted a little to one side, and the filament is shielded from this as well. The anode wire is mounted from a bellows with three screw adjustments. It is reported that if overheated, the pendant drop may oscillate in shape, with danger of touching the cathode shield plate when longest. The power supply to the system was controlled only by a hand-operated Variac, and it is mentioned that for a 3 mm zirconium rod 10 mA at 2.2 kV was needed ; for a 2.5 mm tantalum rod, 80 mA at 2.2 kV. M. D. A.

J. C. Kelly, *J. Sci. Instrum.* **36**, 89–90, Feb. 1959.

28

220. Concerning a Large Capacity Uranium Melting Furnace.
H. Hardung-Hardung, *Vakuum-Technik* **7**, 135–137, 1958.

28

221. High Temperature Laboratory Vacuum Furnace.
Canada. This note describes a small resistance heated furnace of simple design which has proved very satisfactory for the vacuum degassing of small ultra-high vacuum system components. It can achieve a temperature of 1600 °C using 2 kW of power at a pressure of 2×10^{-5} Torr.

Note by E. V. Kornelson and J. O. Weeks, *Rev. Sci. Instrum.* **30**, 290, April 1959.

29. Miscellaneous

29 : 59

222. Molybdenum Disilicide for High Temperature Sliding.
An investigation into the use of molybdenum disulphide as a lubricant at temperatures up to 700–800 °C in vacua or in air is reported. J. N.

G. W. Rowe, *Engineer 206*, 5357, 497, Sept. 1958.

29

223. Method for Breaking Open Sealed Electronic Devices in Vacuum.
Note by M. G. Charlton and G. M. C. Perkin, *J. Sci. Instrum.* **36**, 49–50, Jan. 1959.

29

224. Five Ways to Automatically Control Pressure for Ejector Vacuum Systems.
Graham B. Knight, *Chem. Eng.* **66**, 171–174, March 1959.

29 : 42

225. Use of Borosilicate Glass in Ozonizer Tubes.
Richard F. Grossman, Allen C. Bluestein, *Science* **128**, No. 3338, 1578, 19 December 1958.

29

226. Le spectromètre à rayons β du centre de physique nucléaire Liège. β Spectrometer of the Nuclear Physics Center of Liège (Belgium).
The principles of the β spectrometer are recalled. The vacuum installation is described in great detail. The vessel, for secondary emission reasons, is made of aluminium and was manufactured with great care by the " London Aluminium Company." Each end of the tube is linked to side chambers by a slide valve. These chambers are mounted to insure the quick introduction of the β sources and of the scintillation crystal. Detailed description of the construction and operation of the valves is given as well as that of the vacuum accessories to insure a very speedy operation needed for the study of low lifetime β radioactive elements. The problem set by the vapour pressure of the average scintillation crystal is examined thoroughly and the simplest solution found was the use of a plastic phosphor with a vapour pressure of 10^{-6} Torr. The vacuum pumping set is a 1S50 Edwards rotary pump backing a 203 oil diffusion pump. The pressure in the vessel is lower than 5×10^{-5} Torr. A Penning gauge indicates the pressure and security measures have been taken to prevent damage due to current failure, heating element of the oil diffusion pump failure, or cooling water failure.

M. Gueben, M. Legros and, *Rev. Soc. Roy. Belge Ingrs. et Indus.* 27–35, 1957.

29 : 19 : 30

Obtaining Low Orders of Interference in Measuring Film Thicknesses by Multiple Beam Interferometry. Abstr. No. 175.

29 : 19 : 51

Ultraviolet Transmission Properties of Conducting Coatings on Glass. Abstr. No. 176.

Vol. 9 959/60

Vacuum Applications

30. Evaporation and Sputtering

30

227. Optically Active Fluorite Films.
United Kingdom. Letter by Niels O. Young and Jakym Kowal, *Nature* **183**, No. 4654, 104, 10 Jan. 1959.

30

228. The Production of Thin Films by Thermal Evaporation of Inorganic Materials in High Vacuum.
Survey of present day techniques and evaporation plant design. Discussion concerning the measurement of thickness of coating during deposition and the selection of materials to be evaporated and evaporation sources.

Albert Ross, *Vakuum-Technik* **8**, 1–11, 1959.

30

229. Thin Magnetic Films.
United Kingdom. The preparation by vacuum deposition of thin films of magnetic alloys with specific characteristics is complicated by the large number of parameters involved. The relation between film thickness and coercivity has already been studied by other workers for film thicknesses in excess of domain wall thickness. Small variations in thickness were shown to give rise to energy changes as domain walls were moved such that the relation $H_c \propto t^{-4/3}$ is obtained where H_c is the coercivity and t the average thickness. This dependence has been investigated more fully in this report. An apparatus was built which enabled the low frequency hysteresis loop to be monitored both during deposition of the film and afterwards. A diagram of the apparatus is shown. Various nickel iron alloys were evaporated from an induction heated source on to glass substrates held at temperatures in the region 250–400 °C. An alternating (50 c/s) aligning field in the plane of the substrate was used. The measuring apparatus was sensitive enough to give a recognisable hysteresis loop for films only 150Å thick. In most evaporations the coercivity changed only slightly as the thickness increased from 150 to 1500Å. Up to about 10,000Å a steady decrease of coercivity from 2 oersteds to about 0.5 oersteds is seen. A sudden increase to about 20 oersteds may occur at a thickness of about 2000Å and this is attributed to atomic arrangements within the layer. On other substrates the behaviour of the coercivity may be different. If the glass is coated with a layer of heat-oxidized aluminium a few hundred angstrom units thick, an initial coercivity of 10–20 oersteds may be obtained, which steadily decreases to 1–5 oersteds as the thickness increased to 1500Å. In general these results show that the variation of coercivity with thickness is not a simple relation but is influenced strongly by the substrate. Certainly it is possible to make magnetic specimens with a well defined magnetic axis and relaxation time less than 200 mμ in an applied field of twice the coercivity. G. S.

Letter by R. S. Webley, *Nature* **183**, No. 4666, 999, 4 April 1959.

30

230. Calculation of Absorption Peaks in Thin Metal Films.
United Kingdom. Letter by R. M. Hill, *Nature* **182**, No. 4643, 1150, 25 Oct. 1958.

30

231. Errors in the Measurement of Film Thickness by Multiple-Beam Interferometry.
United Kingdom. When making measurements of film thickness by multiple-beam interferometry it is necessary to produce a sharp step in the film. This can be done by scribing a line with a pointed instrument, across the film surface. The authors show that serious errors may arise in this method due to marring of the substrate surface. G. S.

Letter by C. Weaver and P. Benjamin, *Nature* **182**, No. 4643, 1149, 20 Oct. 1958.

30

232. Mechanical Properties of Whiskers and Thin Films.
United Kingdom. This is a review of the nineteen papers which were presented at a convention on 17–19 March 1958 held at the Cavendish Laboratory, Cambridge and Tube Investments Research Laboratories. The main purpose of the meeting was to review the present state of knowledge on the high mechanical strength observed when one or two dimensions of a test specimen are reduced to a low value. Papers were invited from universities and from industrial research laboratories in Great Britain and the United States of America.

Review by J. E. Gordon and J. W. Menter, *Nature* **182**, No. 4631, 296, 2 August 1958.

30

233. Measurement of the Optical Constants of Thin Dielectric Films by Means of Frustrated Total Reflexion.
New Zealand. It is shown that the transmission of light through a thin dielectric film under conditions of frustrated total reflexion can be used to measure the refractive index and thickness of the film. The refractive index and thickness have been measured for each of several magnesium fluoride films. The thickness was checked in each case by multiple beam interference and the refractive index compared with the results obtained by other authors for similar films. It appears that many present concepts on which the theory of the optical properties of thermally evaporated films is based are inadequate for the problems involved. (Author)

B. P. Sanford, *J. Opt. Soc. Amer.* **48**, 482–486, July 1958.

30

234. Use of Fe^{55} for Measuring Titanium Coating Thickness.
United States. Note by P. D. Zemany, *Rev. Sci. Instrum.* **30**, 292, April 1959.

30

235. Two-layer Anti-reflexion Coating for Low Refractive Index Glass.
Gt. Britain. A single-layer anti-reflexion coating on glass of index about 1.5 would require a coating material of index about 1.23, but available materials which form durable coatings all have indices greater than 1.3. Various multi-layer coatings have been proposed, but have met difficulty with absorption, and lack of durability, in the high-index layer needed. The authors propose the use of Bi_2O_3 as the high-index material in a two-layer coating, the layer being obtained by sputtering Bi in O_2. The oxide film has a refractive index of about 2.45 and is used with MgF_2 (1.38), the high-index layer being made 0.049 λ thick and the low-index 0.33 λ. The apparatus is described in some detail, with a sectional drawing. The evaporation source and sputtering electrodes are mounted in the same vacuum chamber. The electrodes are 60°, $6\frac{3}{8}$ in. r sector plates, made from $\frac{1}{8}$ in. Cu, with Cu cooling pipes brazed to the underside. Each is mounted, on a vertical pillar (which encloses pipes for the cooling water), in a horizontal plane with the apex near the centre of the chamber. One is 4 in. below the surface of the glass to be coated, which is mounted in a rotary holde, the other 6 in. below. The electrodes are connected to the secondary of an h.t. transformer (not earthed) so that each becomes the cathode in turn. Each plate is coated with Bi and earthed shields are arranged to prevent sputtering of the Cu fittings. A photometer system projects a beam of light on to the underside of the glass plate being coated and receives the reflected light, to allow the reflectance to be monitored during coating. To obtain Bi_2O_3 films with low light absorption, it was found necessary to sputter at a high current density (10 mA/cm^2) and to allow O_2 to flow continuously through the chamber. The film of oxide was deposited at 1 A/sec. The Bi_2O_3 is deposited until the reflectance has increased from 4 per cent (clear glass) to 8 per cent : the MgF_2 is then evaporated until the combined reflectance

falls to zero at a particular wavelength (5300Å is suggested). To avoid the difficulty of stopping the evaporation when the reflectance reaches a minimum, the authors describe a method in which a lower wavelength (4550Å) is used for the monitoring system, the deposition then being allowed to proceed until the minimum is passed by a calibrated amount. A calibration graph for this procedure is given. Data is given of the wear-resistance of the films. The tests were made by a rubbing machine in which a $\frac{1}{4}$ in. dia. rubber, loaded to 112 lb/in.^{2} was arranged to trace out a series of flat spirals on the film. A figure of merit given is the ratio of the area of coating removed to the total area abraded. The two-layer films compare favourably with single MgF_2 films, in spite of not having been discharged cleaned prior to sputtering. This is attributed to the cleaning effect of the sputtering discharge itself. M. D. A.

L. Holland and T. Putner, *J. Sci. Instrum.* **36**, 81–84, Feb. 1959.

30

236. Ultraviolet Normal Incidence Grating Vacuum Spectrograph.
France. Note by J. Romand and B. Vodar, *Rev. Sci. Instrum.* **29**, 732–733, August 1958.

30

237. Interfacial Phenomena.
United Kingdom. This is a report of the biennial conference of the Physical Society on solid state physics which was held in December 1958 at Cambridge. The papers presented could be divided into three major groups, consisting of effects associated with vacuum deposited films, electrodeposited films and the nature of solid/liquid interfaces.

Report by J. Nutting, *Nature* **183**, No. 4668, 1097, 18 April 1959.

30

238. Ionization Potential and Absorption Coefficients of Nitrogen Dioxide.
Toshio Nakayoma, M. Y. Kitamura and K. Watanabe, *J. Chem. Phys.* **30**, 1180–1186, May 1959.

30

239. Thermal Conductivity and Euckin Correction for Diatomic Gases and Mixtures.
The thermal conductivity of pure oxygen, nitrogen and hydrogen gases and of the binary gas mixtures O_2–A, N_2–A, and H_2–A at several concentrations have been measured by using a thick-wire conductivity cell at 38 °C. Observations at different pressures between 3 and 20 cm of Hg showed that above 6 cm of Hg the thermal conductivity is independent of pressure. Theory and experimental results are compared. A. G.

B. N. Srivastava and R. C. Srivastava, *J. Chem. Phys.* **30**, 1200–1205, May 1959.

30

240. Control Vacuum Evaporation by Temperature.
Note by Paul W. Kilpatrick, *Chem. Engineering* **66**, 132, Feb. 1959.

30

241. Evaporation of Metals by Electron Bombardment.
Great Britain. This article discusses the evaporation of metals from a pendant drop heated by making it the anode of a diode and drawing current from a cathode in the vacuum chamber. For the method to work, the surface tension at the melting point has to be sufficient for the drop to hold together and the vapour pressure sufficient to give a useful rate of evaporation. The rate of deposition of condensed metal on a given surface is related to the radius (r) of the drop and its distance from the surface, and the rate of evaporation/unit area, which in turn depends on the molecular weight (M) of the metal and its vapour pressure (p) and melting point (T). The analysis indicates that the quantity $(mT^{\frac{1}{2}}/r^2pM^{\frac{1}{2}})$ should be constant, where m is the mass condensing/unit area/sec at a given distance from the drop. The results of measurements on Fe, Ni, Mo, Ag, Ta, W and Pt are reported, the value of the quantity being reasonably close to 1.8×10^{-5} for all the metals, except tungsten. (The condensed deposits are assumed to have the same density as the bulk metal). The result is used to predict deposition rates for Ti, Cu, Zr and Au : the predicted very low rate for Au has been confirmed, as has a moderate rate for Zr. The method should work very well for titanium. M. D. A.

O. S. Heavens, *J. Sci. Instrum.* **36**, 95, Feb. 1959.

30

242. Evaporated Layers formed from Semi-conducting III-V combinations.
Vacuum evaporation from two evaporation sources (boats) at temperature T_1 and T_2 with a suitably chosen temperature T_3 of the receiving condensing surface.

K. G. Günther, *Naturwiss.* **45**, 415, 1958.

30

243. Electrical Breakdown of Id-S Evaporated Layers.
Evaporation takes place in high vacuum.
K. W. Boer, U. Kummel and W. Misselwitz, *Naturwiss.* **45**, 331, 1958.

30 : 19 : 51

Reflexion Coefficient of Optically Inhomogeneous Layers. Abstr. No. 167.

30 : 19

Optical Transmission of Evaporated In, Sn, and Bi Films in the Vacuum Ultraviolet. Abstr. No. 168.

30 : 19

Optical Constants of Evaporated Se Films by Successive Approximations. Abstr. No. 169.

30 : 19

The Optical Properties of Various Evaporated Rare Earth Oxides and Fluorides. Abstr. No. 170.

30 : 19 : 51

Transmittance and Reflectance of Cesium Iodide in the Far Infrared Region. Abstr. No. 171.

30 : 19 : 51

Luminescent Phases in Willemite Films. Abstr. No. 173.

30 : 19

Stokes' Equations and their Application to the Refractivity of Thin Films. Abstr.. No. 174.

30 : 19 : 29

Obtaining Low Orders of Interference in Measuring Film Thicknesses by Multiple Beam Interferometry. Abstr. No. 175.

30 : 19 : 51

Antireflexion Coatings for Ge and Si in the Infrared. Abstr. No. 178.

30 : 19

Design of Multilayer Filters by Successive Approximations. Abstr. No. 182.

30 : 28

Electron Bombardment Apparatus for Vacuum Evaporation. Abstr. No. 219.

32. Nucleonics

32

244. Isotopic Analysis of Lithium by Mass Spectrometry.
Great Britain. This instrument allows rapid and automatic measurement of the isotope ratio of lithium samples by using two ion sources and two beams, each of which can be focussed

Vol. 9 959/60

for one isotope. The direction of current in the focus magnet decides which beam falls on the collector. Each ion source is mounted at the end of one of three side arms, and can be sealed from the main chamber by a vacuum lock consisting of a neoprene-seated gate valve operated through a Wilson seal. This allows rapid changing of the sources. The triple-filament surface ionization sources use solid material (e.g. lithium nitrate) and work at 500 V. Beam currents of 2×10^{-10} A can be obtained from microgram quantities. The spectrometer is constructed from welded stainless steel sheet, either source and the collector forming a 60 °, 10 cm system. The unit is pumped by a Hg diffusion pump with liquid nitrogen trap to give a limiting pressure of about 10^{-6} mm. After changing a source, the pump reduces the pressure to 5×10^{-6} mm in about 15 min. The currents to the collector from the two beams are compared by being amplified and then used to charge " memory capacitors " ; the amplifier gain is varied automatically for one beam until the two give equal voltages on the capacitors. A change in isotope ratio of 0.2 per cent can be detected in the concentration range 1–99 per cent Li. The electrical circuits are not described in detail. Some data is given on the likely errors due to fractionation of the isotope mixture. It is believed that an absolute accuracy of not worse than 2 per cent is obtained. M. D. A.

P. G. Bentley, J. Bishop, D. F. Davidson and P. B. F. Evans, *J. Sci. Instrum.* **36**, 32–34, Jan. 1959.

32

245. Surface Ionization Source for Mass Spectrometry.
Great Britain. The source described is based on the principle of replacement of the usual " source slit " by a demagnified image of the ionizing filament. Using a 0.030 in. wide filament and 0.040 in. wide slits an effective source width of 0.003 in. has been obtained. (Author)

R. D. Craig, *J. Sci. Instrum.* **36**, 38–39, Jan. 1959.

32 : 56

246. The Resnatron as a 200 Mc/s Power Amplifier.
U.S.A. The *resnatron* is the name given to U.H.F. valves in which the valve proper and the resonant circuits are all contained within the same evacuated envelope, to overcome difficulties at U.H.F. due to the finite transit time of the electrons within the valve. The tubes described in this article were developed for the Minnesota Linear Proton Accelerator. They operate at about 200 Mc/s under pulsed conditions : the output power rises to a peak of 8 MW during the first 50 μ of the pulse, falling to an average of 4 MW during the remaining 250 μ. They are used as amplifiers, with a power gain of about 10, and in the complete equipment one resnatron is used to drive three others. Each tube weighs 2.5 tons, with an overall height of 15 ft and is evacuated by a 1400 ft³/min oil diffusion pump, with a freon-cooled baffle. The tube can be isolated automatically by air-operated valves in case of vacuum trouble. A pressure of 5×10^{-7} Torr can be obtained at the manifold with the tube cold, after several weeks pumping, but conditions within the tube with the filaments hot are believed to be much worse. The tetrode valve portion itself is described in some detail. The cathode structure consists of a central vertical cylinder with 36 slots machined in it axially, a pure tungsten filament bar being positioned centrally in each slot. The control grid and screen grid each consist of 36 nickel tubes (roughly rectangular in section) mounted between two coaxial cylinders. The grids are aligned, with the members parallel to the cathode structure so that each filament bar lies on a radial line passing midway between a pair of grid members. The anode is a copper cylinder with deep internal fins, one on each radial line containing a grid member. There are effectively 36 separate tetrode structures connected in parallel, each having a focussed beam of electrons from one filament wire, between the members of both grids, into the space between a pair of fins on the anode. The fins are designed to trap secondary electrons emitted from the anode. The anode is cooled by water circulating in external copper tubes, the grids by water circulating in the hollow supporting cylinders and along the grid members themselves. Each filament bar is rectangular in section, thinner near the ends to reduce temperature variation along the length, which is 5 in. The bars have a fixed clamp at their upper ends and a spring-loaded flexible clamp (detail sketch given) of chrome copper and high-temperature tool steel, at their lower ends. The filaments operate at about 2700 °C, to give an emission of 3A/cm². The valve operates at about 70 kV, and the vacuum conditions have not been considered good enough to try more efficient types of emitter. Filament lives have varied from a few hours to more than 1000 ; failures seem to have been due to crystal growth and breakage rather than to evaporation. Sectional drawings show the arrangement of the whole tube, consisting of valve, resonant cavities, input and output lines, etc. M. D. A.

E. B. Tucker, H. J. Schulte, E. A. Day and E. E. Lampi, *Proc. Inst. Rad. Engrs.* **46**, 1483–1492, Aug. 1958.

32

247. Low Background Gas-flow Counter.
Canada. A low-background flow counter of comparatively simple construction, operating in the Geiger region, is described. The sample counter is shielded by Hg and surrounded by an anti-coincidence ring of 18 overlapping counters, a top counter, and Pb and Hg shields. The counting efficiency with 1 in. dia. steel planchets is 62 per cent for low-energy particles such as ^{14}C ; the background is 1.040 ± 0.005 counts/min ; and the limit of sensitivity is 0.025 counts/min. (Author)

G. H. Bergold and G. R. Haney, *J. Sci. Instrum.* **36**, 39–44, Jan. 1959.

32

248. Simple Pulsed Neutron Source Based on Crossed-Field Trapping.
United States. A simple pulsed neutron source has been constructed which consists of an anode formed by a cylindrical-shell permanent magnet and of two disk cathodes. One of the cathodes forms the neutron-producing target and the device is exhausted adjacent to the other. In operation, the anode is pulsed positive at 140 Kv for 1 μsec at up to 200 pulses/sec. Continuous operation has also been achieved in a slightly different configuration. Ions are produced adjacent to the anode in a toroidal trapping region which exists as a result of the crossed electric and magnetic fields. The ionization is enhanced by the action of electrons reflecting through the inside of the magnetic shell. As a consequence of this trapping, large fluxes of soft X-rays are created which may be injurious to personnel. (Author)

J. D. Gow and L. Ruby, *Rev. Sci. Instrum.* **30**, 315, May 1959.

32

249. He³ Recirculation and Purification System for a Cyclotron Ion Source.
United States. A He³ circulation system for a cyclotron has been built which will recover the gas and purify it continuously. This is accomplished by modifying a mechanical vacuum pump to meet the following special requirements ; intake and exhaust sealed for both pressure and vacuum : small volume on the exhaust side ; minimum oil volume. This pump, which is used instead of the cyclotron forevac pump during He³ operation, recovers the gas and forces it through a liquid nitrogen-cooled charcoal trap and on to the ion source. The system is completely interlocked to ensure He³ safety in the event of operator or electrical failure. With a flow rate of 6 cc/min, the normal He³ loss over a period of 200 hr operation was less than 3 cc/hr after an initial charge of 1000 cc NTP. With trap reactivation periods of 50 hr, no change in ion yield was observed. External beams of approximately 100 μa of doubly charged particles were obtained. (Author)

H. E. Wegner and W. S. Hall, *Rev. Sci. Instrum.* **29**, 1100, Dec. 1958.

Vo
9
1959

32

250. Possibility of Ion Runaway in ZETA.
United Kingdom. Letter by A. Gibson, *Nature* **183**, No. 4654, 101, 10 Jan. 1959.

32

251. Development of an Occluded-Gas Ion Source.
United States. An ion source for pulsed operation has been developed which is based on producing a spark discharge between electrodes of a transition metal in which ordinary hydrogen or deuterium has been occluded. The beam consists principally of ions of hydrogen and of the electrode material. No neutral gas is evolved between pulses. High beam current densities have been obtained, both with axial and with radical extraction. Various methods have been devised for filtering out the heavy-mass components of the beam. (Author)

K. W. Ehlers, J. D. Gow, L. Ruby and J. M. Wilcox, *Rev. Sci. Instrum.* **29**, 614–619, July 1958.

32

252. A 22-Mev Electron Linear Accelerator.
N. A. Austin and S. C. Fult, *Rev. Sci. Instrum.* **30**, No. 4, 1959.

32

253. Gas Scattering in a Strong Focusing Synchrotron.
Morton D. Kostin, *Nuclear Instr. & Meth.* **4**, No. 2, 1959.

32

254. Catalytic Activity and Surface Structure after Ion Bombardment.
Australia. Single crystals of silver have been prepared with surfaces having an orientation within 2 ° of the (111) plane. After bombardment with low-energy argon ions the surfaces have been studied by :
(1) measurements of the rate of the catalytic decomposition of formic acid (zero-order reaction) ;
(2) electron diffraction in transmission and reflexion. The results of these experiments suggest that the catalytic decomposition of formic acid on silver occurs at points on the surface where dislocation lines emerge. G. S.

Letter by H. M. C. Sosnovsky, G. J. Ogilvie and E. Gillam, *Nature* **182**, No. 4634, 523, 23 Aug. 1958.

32

255. The Electron Temperature in Sceptre III.
United Kingdom. S. Kaufman and R. V. Williams, *Nature* **182**, No. 4635, 557, 30 August 1958.

32

256. New Investigations with Sceptre III.
United Kingdom. T. P. Hughes and Dr. S. Kaufman and Dr. A. A. Ware, *Nature* **183**, No. 4653, 7, 3 Jan. 1959.

32 : 19

Primary Frequency Standard Using Resonant Caesium. Abstr. No. 183.

33. General Physics and Electronics

33

257. Effect of Cathode Inclusions on Electrical Discharges.
United Kingdom. Letter by P. C. L. Pfeil and L. B. Griffiths, *Nature* **183**, No. 4673, 1481, 23 May 1959.

33

258. Electron Microscope Study of Finback Whale Myoglobin Crystals.
United Kingdom. The dimensions of such large molecules as the protein myoglobin are well within the limit of resolution of the modern electron microscope. Replicas of crystals of myoglobin were shadowed with a platinum/iridium/carbon mixture by deposition from a resistance heated contact in vacuum. Electron micrographs of three crystal faces were obtained, and a periodic structure which could be measured was observed. G. S.

D. E. Bradley, *Nature* **183**, No. 4666, 941, 4 April 1959.

33

259. Microscopy with X-rays.
United Kingdom. V. E. Cosslett, *Nature* **183**, No. 4673, 1423, 23 May 1959.

33

260. High-Current Ion Source.
United States. A high-current ion source is described that is of simple design and construction. It is capable of producing an ion beam of 1/2 amp. The energy spread of the ions is large. (Author)

R. G. Meyerand, Jr., and S. C. Brown, *Rev. Sci. Instrum.* **30**, 110, Feb. 1959.

33

261. Mass Spectrometer Ion Source for Solid Samples.
Western Australia. R. F. Kendall, *Rev. Sci. Instrum.* **29**, 1089. Dec. 1958.

33

262. An Effect of Oxide Layers on the Behaviour of Vacuum Arc Cathode Spots.
United Kingdom. Letter by H. Wroe and R. H. Alderson, *Nature* **183**, No. 4674, 1544, 30 May 1959.

33

263. Emission of Slow Secondary Electrons.
Canada. Letter by J. M. Anderson, *Nature* **183**, No. 4656, 241, 24 Jan. 1959.

33

264. Helium Temperatures from Vapour Pressure Measurements.
United Kingdom. It is found that the temperature at any point below the surface of a He bath, as deduced from pressure measurements over the surface corrected for hydrostatic head, does not agree with the temperature obtained using a vapour pressure bulb, the He bath pressure invariably indicating a lower temperature, except below the λ point. The discrepancy can be reduced but not eliminated by employing a heater at the bottom of the bath to provide a copious supply of vapour bubbles throughout the bath. A sharp temperature gradient at the surface of the bath is indicated. Below the λ point no discrepancy is observed. (Author)

F. E. Hoare and J. E. Zimmerman, *Rev. Sci. Instrum.* **30**, 184, March 1959.

33

265. Simple Attachment to the Sucksmith Ring Balance for use at Low Temperatures.
Letter from J. Crangle and M. J. C. Martin, *J. Sci. Instrum.* **36**, 100, Feb. 1959.

33

266. Calorimeter with Automatic Control.
Great Britain. The temperature difference between the specimen and its surrounding reference shield in a Smith's calorimeter, modified to operate in a vacuum so as to eliminate variations in thermal transfer and reduce thermal capacity of the insulation. Specific heat-temperature curves smooth to within ± 0.5 per cent and reproducible within 3 per cent have been obtained between 50–250 °C. M. D. A.

G. Bullock, *J. Sci. Instrum.* **36**, 20–23, Jan. 1959.

33 : 56

267. Space-charge Grid High-transconductance Electron Gun.
Letter from P. H. Gleichauf, *Proc. Inst. Rad. Engrs.* **46**, 1542, Aug. 1958.

Vol. 9 959/60

33

268. Microscopic Examination of Interior of Highly Curved Surfaces by Means of Replicas.

United States. Replicas of cellulose acetate film have been taken for surface studies of inaccessible places or highly curved surfaces. In order to increase the contrast for electron microscopy, a carbon replica was made from the cellulose acetate replica, and shadowed with platinum. In order to increase the contrast for optical microscopy, the cellulose replicas were coated with gold by evaporation. G. S.

Note by A. P. Young, *Rev. Sci. Instrum.* **29**, 661, July 1958.

33

269. Photoconductivity and the Visual Receptor Process.

United States. Measurements were made using B-carotene melted and cooled between two conductive glass plates in a vacuum. It was shown that B-carotene glass qualifies as a highly photoconductive organic material. Some of the properties were determined.

Letter by H. Steffen Peiser, *J. Opt. Soc. Amer.* **48**, 581–582 Aug. 1958.

33

270. Improved, Single Flash, Continuum Source for use below 2000 Å.

United States. A high intensity low energy flash lamp for use below 2000 Å is described. The radiation from a single flash at 4000 V and 15 mfd produces an emission continuum to 1500 Å which is of sufficient intensity to be used with either photographic or photomultiplier techniques. A densitometer trace of the Schumann-Range O_2 absorption band system is shown. Also, oscilloscope traces are presented which were taken at 1700 Å. These show attenuation of the signal as a function of oxygen concentration. The associated vacuum technique is described. (Author)

Joseph A. Golden and Albert L. Myerson, *J. Opt. Soc. Amer.* **48**, 548–552, Aug. 1958.

33

271. High-Sensitivity Crystal Infrared Detectors.

United States. The intrinsic photosensitivity of germanium and indium antimonide disappears at wavelengths greater than 1.8 and 7μ respectively. In Ge this upper limit can be extended by doping the crystals with impurities, the activation energies of the impurity centre then become the determining factor for the maximum infra-red wavelength that can be absorbed. In this work Ge infrared detectors are cut from a large zone levelled crystal. Compensation with antimony donors is used to obtain *n*-type material. The gold-antimony doped detectors have a long wavelength cutoff at 6μ and a photoconductive time constant which is dependent on the wavelength of the incident radiation. A table is given which shows the sensitivity characteristics of a number of these detectors. Indium antimonide detectors have been made with sensitivities comparable to those of the gold-doped Ge. The indium antimonide detector is made either by alloying or diffusing a thin layer of impurities into the surface layer of a single crystal of material. Cadmium is now being used, giving a thin *p*-type surface on *n*-type indium antimonide. If light is allowed to fall on the front surface of the alloyed material, a photo-voltage may be measured between the *n* and *p* parts of the detector. The cutoff wavelength for this type of detector when cooled to liquid nitrogen temperature also is of the order of 6μ. A comparison is made between the characteristics of the two types of cells and a description is given of a multiple contact cell which can locate a target as well as detect it. A section is included on the standard measuring techniques used in evaluating infrared detectors. G. S.

M. E. Lasser, P. Cholet and E. C. Wurst, Jr., *J. Opt. Soc. Amer.* **48**, 468–473, July 1958.

33

272. High-temperature X-ray Diffractometer.

Great Britain. A vacuum furnace designed for use with a commercial diffractometer is described. It uses a high-current heater made from tantalum foil, and allows the full Bragg spectrum to be recorded whilst satisfying the Bragg-Brentano focusing condition. The specimen temperature is uniform and can be measured accurately; the furnace has been operated successfully at temperatures up to 1100 °C, and it is believed that considerably higher temperatures can be achieved. (Author)

J. Spreadborough and J. W. Christian, *J. Sci. Instrum.* **36**, 116–118, March 1959.

33

273. Electron Microscope and Electron Diffraction Study of Optically Transparent Electrically Conducting Coating on Glass and Acrylic Plastics.

United States. An abstract of the above unpublished Finishing Report is given. The report is issued by the U.S. Air Force under No. P.B.118266.

Note by Anon, *Product Finishing* **11**, 73, August 1958.

33

274. Some Properties of Thin Barium-Strontium-Titanate Single Crystal Layers Evaporated in the Presence of an Electrical Field.

In this paper an attempt is made to achieve the growth of single crystals of the ferro electrical Barium-strontium-titanate from the gas phase where this has as yet not been technically possible to carry out from the melt. After developing two evaporation devices for barium-strontium-titanate evaporation is carried out mainly in the presence of an electric field. The oriented single crystals formed at an adjustable condensation temperature of around 200 °C are investigated in detail. The dependance of dielectric constant on thickness of layer is notable and approaches the limit $\epsilon \to 9000$ in the frequency range 1000 to 2000 Mc/s as the thickness is reduced. A discontinuous ageing process was observed only in the thicker deposits and is explained by the increase in the number of lattice errors and the resulting displacement of the domain boundaries. The breakdown strength of the layers achieved a maximum value of 5×10^5 V/cm. (Authors)

A. Moll, *ZS. f. angew. Phys.* **10**, 410–416, 1958.

33

275. Investigations on Ion Absorption and Corrosion using Radioactive Indicators.

K. Schwabe, *Chemische Technik* **10**, 469–474, 1958.

33

276. Investigations of a High Frequency Ion Source.

The optimal operating conditions for an ion-beam apparatus consisting of a high frequency ion source, ion accelerator and mass separator were determined. Under certain conditions an anomalous differential ionization of the in hydrogen was observed (probably due to metastable ions).

R. Holz u. H. Löb, *ZS. f. Naturforschung* **13**, 602–608, 1958.

33

277. Vacuum Sampling Device.

Devices designed to take liquid samples in vacuum from an evacuated reaction vessel.

S. Lesek and M. Sytar, *Chemische Technik* **10**, 421, 1958.

33

278. Note on the Observation of Molecules by Field Emission Microscopy.

Note by R. J. Hill and P. W. M. Jacobs, *J. Chem. Phys.* **30**, 853–854, March 1959.

Vo
9
1959

33

279. Thermal Contact at Low Temperatures.
United Kingdom. Mechanical heat switches are becoming of increasing importance in low-temperature calorimetry. An apparatus has been made to study thermal contact for practical application to a heat switch and also to study the mechanism of heat transfer. The contact pressure is applied by a screw and measured by a strain gauge attached to a cantilever assembly. The thermal conductance of gold-gold, copper-copper, copper-diamond, and sapphire-sapphire contacts have been measured with this apparatus and are shown at various temperatures in the range up to 20 °K. G. S.

Letter by R. Berman and C. F. Mate, *Nature* **182**, No. 4650, 1662, 13 Dec. 1958.

33

280. Automatic Recording Vacuum Microbalance.
United States. An automatic control and recording system for the null-type vacuum microbalance of Czanderna and Honig [*Anal. Chem.* **29**, 1206 (1957)] has been assembled from commercial components. A variable permeance transducer is employed to detect beam movement and to control a force to restore the beam to the null position. This force is recorded in a selection of ranges extending from 0–20,000 μg to 0–5 μg with accuracies ranging from 0.1 per cent to 2 per cent of full scale. On the most sensitive settings the balance can detect weight changes as small as 0.01 μg in loads up to 1 g. Stabilities of 0.1 μg have been observed for periods of many hours on the most sensitive ranges. The balance is undamped, and no corrections are made to the restoring force if beam oscillation is centered about the null point. (Author)

C. N. Cochran, *Rev. Sci. Instrum.* **29**, 1135, Dec. 1958.

33

281. Electron-permeable Window for Cathode Ray Tubes.
United States. J. Seehof, S. Smithberg and M. Armstrong, *Rev. Sci. Instrum.* **29**, 776, Sept. 1958.

33

282. Low-temperature Optical Window Seal used at 80 °K.
United States. Note by J. Willis, *Rev. Sci. Instrum. 29*, 1053. Nov. 1958.

33

283. Vacuum Plant for Crystal Pulling.
In order to satisfy the purity requirement in the production of semi conducting devices based on Ge or Si material apparatus was developed to grow single crystals of these materials in a high vacuum by a number of different methods.

H. Bumm, *Vakuum-Technik* **8**, 12–15, 1959.

33 : 46

284. Mica as Constructional Material for use in High Vacuum.
The author discusses all technological questions related to this topic with the usual thoroughness covering : origin, composition, fabrication, physical and chemical properties, degassing, surface treatment, seals of mica with glass or metal, special applications. The production and properties of synthetic mica is also dealt with.

W. Espe, *Vakuum-Technik* **8**, 15–19, 1959 ; **8**, 29–38, 1959 ; **8**, 67–76, 1959.

33 : 23

Transmission Specimen Holder for Electron Diffraction. Abstr. No. 207.

34. High Altitude and Space Technology

34 : 51

285. Stratospheric Fallout of Strontium-89 and Barium-140.
Lois Fry and P. K. Kwroda, *Science* **129**, 1742–1743, 26 June 1959.

34 : 58

286. Concentrations of Radioactive Materials in the Air during 1957.
Luther B. Lockhart, Jr., *Science*, **128**, 1139, 7 Nov. 1958.

34 : 51

287. Mass of the Moon from Satellite Observations.
W. J. Gallagher, *Science* **128**, 1207, 14 Nov. 1958.

34

288. Ground Rules for Space Research.
J. T., *Science* **128**, 1479, 12 Dec. 1958.

34

289. Radar Echoes from Venus.
R. Price, P. E. Green, Jr., T. J. Goblick, Jr., R. H. Kingston, L. G. Kraft, Jr., G. H. Pettengill, R. Silver, and W. B. Smith, *Science* **129**, 751–753, 20 Mar. 1959.

34

290. Effect of Transverse Atmospheric Drag on Satellite Orbits.
W. A. Wildhack, *Science* **128**, 309–310, 8 Aug. 1958.

34

291. Optical Tracking of Artificial Earth Satellites.
Fred L. Whipple, *Science* **128**, 124–129, 18 July 1958.

34

292. Cloud Physics.
Henry G. Houghton, *Science* **129**, 307–313, 6 Feb. 1959.

34

293. Earth Oblateness in Terms of Satellite Orbital Periods.
Leon Blitzer, *Science* **129**, 329–330, 6 Feb. 1959.

34

294. Frontal Cloud System Pictures obtained by Rocket.
Science **129**, 198–200, 23 Jan. 1959.

34

295. "IGY" Conference in Moscow.
Homer E. Newell, Jr., and J. W. Townsend, Jr., *Science* **129**, 79–84, 9 Jan. 1959.

34

296. International Geophysical Year.
Hugh Odishaw, *Science* **128**, 1599–1609, 26 Dec. 1958.

34

297. International Geophysical Year.
Hugh Odishaw, *Science* **129**, 14–25, 2 Jan. 1959.

34

298. Modifying Weather on a large Scale.
H. Wexler, *Science* **128**, 1059–1063, 31 Oct. 1958.

34 : 12

Density Determinations Based on the Explorer and Vanguard Satellites. Abstr. No. 137.

34 : 17

Atmospheres of other Planets. Abstr. No. 153.

35. Impregnation and Potting

35 : 56

299. Vacuum Drying.
Short account of the use of vapour booster pumps in plant intended for the drying and impregnation of electrical components. J. N.

Engineer **206**, 5361, 660, Oct. 1958.

36. Drying, Degassing and Concentration

36

300. Large Scale Laboratory Freeze-drying Apparatus.
Great Britain. An apparatus is described which will freeze-dry a total of 6 l. of solution distribution in 20 flasks each 24 hr, with a minimum of attention and at a low operating cost. The plant uses a two-stage gas-ballasted pump, a Pirani gauge with magnetic valves. M. D. A.

P. M. Grant and R. B. Ward, *J. Sci. Instrum.* **36**, 133–134, Mar. 1959.

37. Metallurgy, Inorganic Chemistry and Analytical Chemistry

37 : 53

301. General Purpose Vacuum Furnace.
Description of a small furnace which can be used for a wide range of vacuum heating processes, including sintering and outgassing. J. N.

Engineer **207**, 5390, 779, May 1959.

37 : 53

302. Vacuum Arc Furnace for Laboratory Operation.
Description of a commercial versatile vacuum arc furnace which may be used for button, consumable electrode cold mould, and non-consumable electrode cold mould melting. J. N.

Engineer **207**, 5371, 39, Jan. 1959.

37

303. Vacuum Levitation Melting.
United States. Letter by R. T. Begley, G. Comenetz, P. A. Flinn and J. W. Salatka, *Rev. Sci. Instrum.* **30**, 38, Jan. 1959.

37

304. Vacuum Melting Stainless Steels and Superalloys.
Digest of " Quality Improvements in Stainless Steels and Superalloys by Vacuum Melting," by W. W. Dyracz, *Metal Progress* **75**, 138–144, May 1959.

37 : 53

305. Vacuum-melting of Metals.
The arc-melting and induction-melting furnaces in operation at the Sheffield works of Jessop-Saville Ltd., constitute the largest plant outside America for melting *in vacuo*. The former is of the consumable electrode type and has a capacity for producing ingots of 2½ tons weight. The electrode is fed from underneath by two motors coupled to the ram through a differential gearbox, thus eliminating the disadvantage of inertia associated with a reversing motor. The pressure can be held below 1 μ by two pumps having capacities of 4000 l/sec. Ti ingots produced range from 9 in *dia.*, 120 lb to 420 lb, to 24 in *dia*, exceeding 2½ tons in weight. Similar Zr and steel ingots can be produced. The 600 lb high-frequency induction furnace is designed for the semi-continuous vacuum-melting of steel and other alloys, thus enabling the oxygen content to be reduced to below five parts per million. J. N.

Engineer **207**, 5386, 607, April 1959.

37 : 53

306. Vacuum Furnaces.
Description of a vacuum furnace for heat treatment processes.

Engineer **206**, 5369, 980, Dec. 1958.

37 : 53

307. Vacuum Flow Steel Degassing.
Short description of a method of removing gas from steel contained in ladles.

Engineer **206**, 5366, 845, Nov. 1958.

37

308. Vacuum Furnace for Continuous Strip.
This article describes an experimental vacuum furnace for heat treating strip or wire continuously. Operating conditions and metals which have been treated are discussed. Comparative costs are given for bright-annealing with gas-fired muffle furnaces and electrically heated strip vacuum furnaces. A proposed design of vertical furnace is discussed briefly. A. G.

Anon, *Metal Progress* **76**, 111–113, July 1959.

37

309. Vacuum Furnace Features Quick Changeover.
This note discusses a rapid method of replacing consumable electrodes in a vacuum furnace. The pumping system has a speed of 4500 cu. ft/min and a blank-off pressure of 5 μ Hg. The furnace can be used to cast ingots of 20 in. *dia.* and 8500 lbs in weight with an annual capacity of 3000 tons. A. G.

Anon, *Metal Progress* **75**, 118–119, June 1959.

37

310. Hydrogen in Heavy Forgings.
This article discusses problems in reducing hydrogen in heavy forgings. It is shown that lengthy heat treatments are not reliable. Some reduction in H_2 content is possible through careful melting but the best results are achieved by vacuum casting techniques. The unit which was used could vacuum cast ingots up to 110 in. *dia.* Ingots were obtained with a H_2 content of about 1 ppm. A. G.

J. E. Steiner, *Metal Progress* **76**, 72–75, July 1959.

37

311. Welding with an Electron Beam.
Briefly describes an electron beam welding piece of equipment. Includes principle of operation and advantages over other methods. A. G.

Anon, *Metal Progress* **75**, 119–120, June 1959.

37

312. Pattern for Better Alloys.
Briefly describes a consumable electrode vacuum furnace operating at lower pressures than usual. A. G.

Anon, *Metal Progress* **75**, 123, June 1959.

37 : 53

313. Spectrographic Analysis of Oxygen in Titanium.
Description of a method using normal spectrographic equipment and a special arc chamber with appropriate gas-vacuum apparatus. J. N.

Engineer **206**, 5366, 845, Nov. 1958.

37 : 53

314. Beryllium—Present and Potential Uses.
The properties, production methods and fabrication techniques are briefly described. J. N.

Engineer **206**, 5362, 688, Oct. 1958.

37

315. The Effect of Oxygen, Hydrogen and Water Vapour on the Electrical Conductivity of Barium Oxide and Barium-strontium Dioxide.
The conductivity of sintered test bodies is measured at different temperatures (above and below 1000 °K) and different gas pressures in the range 10^{-5} and 500 Torr.

J. Rudolph, *Z. f. Naturforsch.* **13a**, 757–767, 1958.

37

316. Préparation du fluorure de Zirconium anhydre pur. Preparation of Pure Anhydrous Zirconium Fluoride.
C. Decroly, D. Tytgat, J. Gerard, Rapport B 6 du Centre d'Etudes pour les applications de l'Energie Nucléaire, Bruxelles, Aug. 1956.

VO. 9 1959

37

317. Contribution à l'étude de l'élimination par vaporisation du zinc contenu dans les alliages Zirconium-zinc.
Contribution to the Study of the Elimination by Vaporization of Zinc contained in Zirconium-Zinc Alloys.
C. Decroly, D. Tytgat, Rapport Blg 10 du Centre d'Etudes pour les applications de l'Energie Nuclëaire, Bruxelles, Feb. 1957.

37

318. Contribution à l'étude de la préparation du Zirconium et de certains de ses alliages par réduction métallothermique.
Contribution to the study of the Preparation of Zirconium and certain Alloys by Metallothermic Reduction.
C. Decroly, J. Gerard, D. Tytgat, Rapport Blg 18 du Centre d'Etudes pour les applications de l'Energie Nuclëaire, Bruxelles, May 1958.

37

319. Aluminium Nitride Precipitates in α-Iron.
United Kingdom. Electron micrographs show that aluminium nitride is precipitated as rod-like particles in an α-iron matrix. A vacuum melted alloy containing 1 per cent aluminium alloy was used for the investigation. It was nitrided in dry ammonia gas for 5 hr at 640 °C and cooled in the furnace. This rod-like form is also likely to be the characteristic form of aluminium nitride in steels. G. S.

Letter by G. R. Booker and J. Norbury, *Nature* **182**, No. 4630, 255, 26 July 1958.

37

320. Vacuum as a Furnace " Atmosphere".
L. W. Johnson, *Metal Progress* **75**, 71–72, Feb. 1959.

37

321. Vacuum Metallurgy in Europe.
A. K. Aksoy, *Metal Progress* **75**, 87–89, Feb. 1959.

37 : 26

Two Emission Stabilizers for Electron-Bombardment Furnaces.
Abstr. No. 215.

Vol. 9 959/60

Materials and Techniques used in Vacuum Technology

40. Gases and Vapours

40

322. Pressure Induced Shifts of HCl Absorption Lines in the Infrared.
S. Kimel, M. A. Hirschfeld and J. H. Jaffe, *J. Chem. Phys.* **31**, 81–84, July 1959.

40

323. Paramagnetic Line Widths in Gaseous Atomic Hydrogen.
Note by A. F. Hildebrandt, F. B. Booth and C. A. Barth, *J. Chem. Phys.* **31**, 273, July 1959.

40

324. Multiple Ionization of Sodium Vapor by Electron Impact.
Note by Vernon H. Dibeler and Robert M. Reese, *J. Chem. Phys.* **31**, 282–283, July 1959.

40

325. Dissociation Energies of Some Gaseous Alkali Halide Complex Ions and the Hydrated Ion $K(H_2O)^+$.
William A. Chupka, *J. Chem. Phys.* **30**, 458–465, Feb. 1959.

40

326. Interaction of Rare Gases with Metal Surfaces I. A, Kr, and Xe on Tungsten.
Gert Ehrlich and F. G. Hudda, *J. Chem. Phys.* **30**, 493–512, Feb. 1959.

40

327. Production of Atoms by a Glow Discharge in Dry Hydrogen.
Note by Frances Dunkle Coffin, *J. Chem. Phys.* **30**, 593–594, Feb. 1959.

40

328. Adsorption of Oxygen on Silicon.
J. Eisinger and J. T. Law, *J. Chem. Phys.* **30**, 410–412, Feb. 1959.

40

329. Adsorption of Oxygen on Tungsten.
Article by Joseph Eisinger, *J. Chem. Phys.* **30**, 412–416, Feb. 1959.

40

330. Electrical Properties of Hydrogen Adsorbed on Silicon.
The photoemission from a silicon surface has been studied as a function of the number of hydrogen atoms adsorbed on it. The electric dipole moment of an adsorbed H atom is found to be 0.5×10^{-18} e.s.u. approximately. (Author)
Joseph Eisinger, *J. Chem. Phys.* **30**, 927–993, April 1959.

40

331. Mutual Diffusion of Pairs of Rare Gases at Different Temperatures.
Diffusion is allowed to take place through a precision capillary tube from one diffusion bulb at a pressure of 10 cm Hg to a second diffusion bulb, from which samples of gas can be withdrawn for analysis by a differential conductivity analyzer. The coefficient of mutual diffusion of the binary gas mixtures Ne–A, A–Kr, and Ne–Kr has been determined at 0 °, 15 °, 30 ° and 45 °. A. G.
B. N. Srivastova and K. P. Srivastova, *J. Chem. Phys.* **30**, 984–990, April 1959.

40

332. Kinetics of Nitrogen Atom Recombination.
The rate of recombination of nitrogen atoms in the nitrogen afterglow has been measured in a flow system using NO as a titrant and determining the NO content continuously by mass spectrometer. Above about 3 mm Hg the reaction is predominantly homogeneous and third order. The rate constant, 5.7×10^{15} cc^2 mole^{-2} sec^{-1}, is independent of temperature in the interval studied (195–450 °K). The rate is reduced by substituting helium or argon for N_2 as the third body, the ratios of the third order constants with these third bodies being about the same as those for recombination of iodine and bromine atoms. Below about 3 mm Hg a pseudo-first-order wall recombination becomes important. The recombination coefficient was found to be 1.6×10^{-5} on a glass wall that undoubtedly was partly poisoned by water. (Author)
John T. Herron, J. L. Franklin, Paul Bradt and Vernon H. Dibeler, *J. Chem. Phys.* **30**, 879–885, April 1959.

40 : 27

Experiments on Flow of Gases through Leaks. Abstr. No. 217.

41. Metals and Alloys

41 : 17

The Selection of Stainless Steels for use in Liquid Hydrogen Bubble Chambers. Abstr. No. 148.

42. Glass and Ceramics

42

333. Quartz Glass, Fused Quartz and Quartzlike Glasses as Constructional Materials in High Vacuum Technique.
An extensive survey covering the production, fabrication physical and chemical properties as well as applications. The literature survey comprises 63 notable contributions to this subject.
W. Espe, *Vakuum-Technik* **7**, 65–77, 101–110, 1958.

42

334. A Contribution to the Technology of Large Ceramic Bodies.
The manufacture by machine in one piece by means of the vacuum press is described. A discussion of sources of errors and creep in the press follows. Further subjects treated deal with the theoretical basis for drying and its effect on the production of large bodies ; the firing of massive porcelain ; techniques which determine the chemical and physical behaviour.
H. Schubert, *Sprechsaal fur Keramik-Glass-Email* **91**, 533–535 und 556–564, 1958.

42 : 18 : 43

Investigation of Breakdown in Vaccuum. Abstr. No. 164.

42 : 23

Glass Problems in Electron Tube Technology. Abstr. No. 206.

43. Plastics and Elastomers

43

335. Electron Spin Resonance Studies of Irradiated Teflon : Effects of Various Gases.
The radical produced by x- or γ irradiation of polyfluoroethylene (Teflon) in a high vacuum is shown to have five *F* atoms with nuclear coupling to the electron spin, four with equivalent coupling of 33 G each and a fifth with coupling of 92 G. The radical is probably of the form XCF_2CFCF_2Y, where *X* and *Y* represent the continuing Teflon chains with no significant electron spin density. Molecular oxygen was found to combine with undetectable radicals or ions in the irradiated Teflon to produce a new resonance. Carbon monoxide alters the latter resonance to a different one while H_2, NO, and ionized air destroy it. The resonance of the fluorocarbon radical is also nullified by H_2 and NO. When Teflon is irradiated under an atmosphere of NO gas, a triplet resonance structure apparently arising from N^{14} nuclear interaction is produced. The triplet can also be produced by admission of NO to a sample of Teflon previously irradiated in vacuum. (Author)
Harvey N. Rexroad and Walter Gordy, *J. Chem. Phys.* **30**, 399–403, Feb. 1959.

43 : 18 : 42

Investigation of Breakdown in Vaccuum. Abstr. No. 164.

45. Soldering, Welding and Brazing

45

336. The Technique of Soldering in Vacuum.
The technology and selection of suitable solders and soldering alloys including detailed description of a vacuum soldering plant.
Bernhard F. und H. Bumm, *Vakuum-Technik* **7**, 153–158, 1958.

46. Glass Blowing, Glass-to-metal and Ceramic-to-metal Sealing Techniques

46

337. Precision Ends for Fused Silica Tubes.
Note by J. Conaboy, *J. Sci. Instrum.* **36**, 148, March 1959.

46

338. Contribution to the Question of Electrolysis of Glass in Electronic Valves.
F. Engel, *Vakuum-Technik* **8**, 44–47, 1959.

46

339. Vacuum Tight Seals between Molybdenum and Glass.
Methods for the production of glass seals to molybdenum rods up to 10 mm *dia.* and ring seals up to 75 mm *dia.* without the need for a special protective hydrogen atmosphere are discussed.
H. Adam, *Vakuum-Technik* **8**, 59–62, 1959.

46 : 33

Mica as Constructional Material for use in High Vacuum. Abstr. No. 284.

47. Outgassing data, Vapour Pressure data and Gettering data

47

339. Vapor Pressure, Mass and Infrared Spectra of Hexaborane.
Sidney G. Gibbins and I. Shapiro, *J. Chem. Phys.* **30**, 1483–1485, June 1959.

49. Miscellaneous Meterials and Techniques

49

340. Vaporization of Beryllium Oxide and its Reaction with Tungsten.
W. A. Chupka, Joseph Berkowitz and Clayton F. Giese, *J. Chem. Phys.* **30**, 827–834, March 1959.

49

341. Free Evaporation of Alkali Halide Crystals.
G. M. Rothberg, M. Eisenstadt and P. Kush, *J. Chem. Phys.* **30**, 517–527, Feb. 1959.

49

342. Structure and Adsorption Characteristics of Clean Surfaces of Germanium and Silicon.
A vacuum system designed for minimum contamination is briefly described. It has been found that the rate of absorption of oxygen on silicon and germanium surfaces is proportional to the pressure, at least for pressures below 10^{-6} Torr. Methods of regenerating the clean surfaces are described. A. G.
R. E. Schlier and H. E. Farnsworth, *J. Chem. Phys.* **30**, 917–926, April 1959.

49

343. Adsorption of Hydrogen on Silicon.
The adsorption of both atomic and molecular hydrogen on silicon films and single crystals has been studied. The kinetics of the processes as a function of coverage and gas pressures are discussed, and it is shown that in the case of adsorption of atoms, two types of adsorbed species exist. Data obtained for the areas of silicon films as a function of the number of silicon atoms evaporated are in good agreement with previous work. (Author)
J. T. Law, *J. Chem. Phys.* **30**, 1568–1576, June 1959.

49

344. Adsorption of Carbon Dioxide on Tungsten,
Note by D. O. Hayward and R. Gomer, *J. Chem. Phys.* **30**, 1617, June 1959.

49

345. Evaporation of Aluminium Oxide.
Note by Gerold W. Sears and Louis Nuvias, *J. Chem. Phys.* **30**, 1111–1112, April 1959.

Vol. 9 959/60

Basic Science and Engineering

51. Physics, Astronomy and Geophysics

51

346. Formation of Elements in the Stars.
Margaret and Geoffrey Burbidge, *Science* **128**, No. 3321, 387–399, 22 August 1958.

51 : 11 : 17

Cryopumping. Abstr. No. 134.

51 : 15

Polyhedral Satellite for more Accurate Measurement of Orbit Data of Earth Satellites. Abstr. No. 139.

51 : 17

Growth and Properties of " Whiskers." Abstr. No. 151.

51 : 17

Ultrahigh-pressure Research. Abstr. No. 152.

51 : 19

Electroluminescence of Zinc Sulfide Phosphors as an Equilibrium Process. Abstr. No. 166.

51 : 19 : 30

Reflexion Coefficient of Optically Inhomogeneous Layers. Abstr. No. 167.

51 : 19 : 30

Transmittance and Reflectance of Cesium Iodide in the Far Infrared Region. Abstr. No. 171.

51 : 19 : 30

Luminescent Phases in Willemite Films. Abstr. No. 173.

51 : 19 : 29

Ultraviolet Transmission Properties of Conducting Coatings on Glass. Abstr. No. 176.

51 : 19

Pressure Modulation of Infrared Absorption. I. Entire Vibration-rotation Bands. Abstr. No. 177.

51 : 19 : 30

Antireflexion Coatings for Ge and Si in the Infrared. Abstr. No. 178.

51 : 19

Index of Refraction of Ge. Abstr. No. 179.

51 : 34

Stratospheric Fallout of Strontium-89 and Barium-140. Abstr. No. 285.

51 : 34

Mass of the Moon from Satellite Observations. Abstr. No. 287.

53. Metallurgy, Ceramics and Inorganic Chemistry

53 : 37

General Purpose Vacuum Furnace. Abstr. No. 301.

53 : 37

Vacuum Arc Furnace for Laboratory Operation. Abstr. No. 302.

53 : 37

Vacuum-melting of Metals. Abstr. No. 305.

53 : 37

Vacuum Furnaces. Abstr. No. 306.

53 : 37

Vacuum Flow Steel Degassing. Abstr. No. 307.

53 : 37

Spectrographic Analysis of Oxygen in Titanium. Abstr. No. 313.

53 : 37

Beryllium—Present and Potential Uses. Abstr. No. 314.

56. Electrical Engineering, Electronic Circuits

56 : 18

New Developments of Air Cooled Condensers for the Processing Industry. Abstr. No. 165.

56 : 32

The Resnatron as a 200 mc/s Power Amplifier. Abstr. No. 246.

56 : 33

Space-charge Grid High-transconductance Electron Gun. Abstr. No. 267.

56 : 35

Vacuum Drying. Abstr. No. 299.

58. Nucleonics

58 : 15

Stabilized Pinch and Controlled Fusion Power. Abstr. No. 140.

58 : 34

Concentrations of Radioactive Materials in the Air during 1957. Abstr. No. 286.

59. Miscellaneous

59 : 29

Molybdenum Disilicide for High Temperature Sliding. Abstr. No. 222.

Vo
9
1959

VACUUM

Papers to be published in future issues

D. J. Santeler. Vacuum process evaluation.

H. Batey. Carbon contamination of glassware used for vacuum purposes.

D. S. Stark. Measurements on the properties of a simple omegatron.

P. T. Stroud. Cathodic etching in a Penning cold cathode discharge.

D. J. Pacey. A piezoelectric oscillator manometer.

N. C. Balchin and B. L. Mordike. Semi-automatic control of vacuum pumping systems.

E. Thomas. The International Organization for Vacuum Science and Technology.

G. Siddall. Vacuum deposition of dielectric films for capacitors.

R. Hawley. Vacuum as an insulator.

J. D. Mellor and D. F. Ohye. An ampoule freeze-dryer for microbiological research.

N. A. Florescu. Theoretical developments of the vapour vacuum pump.

Vol.
9
959/60

Vo
9
1959

Vol.
9
959/60

VACUUM

Biographical Notes

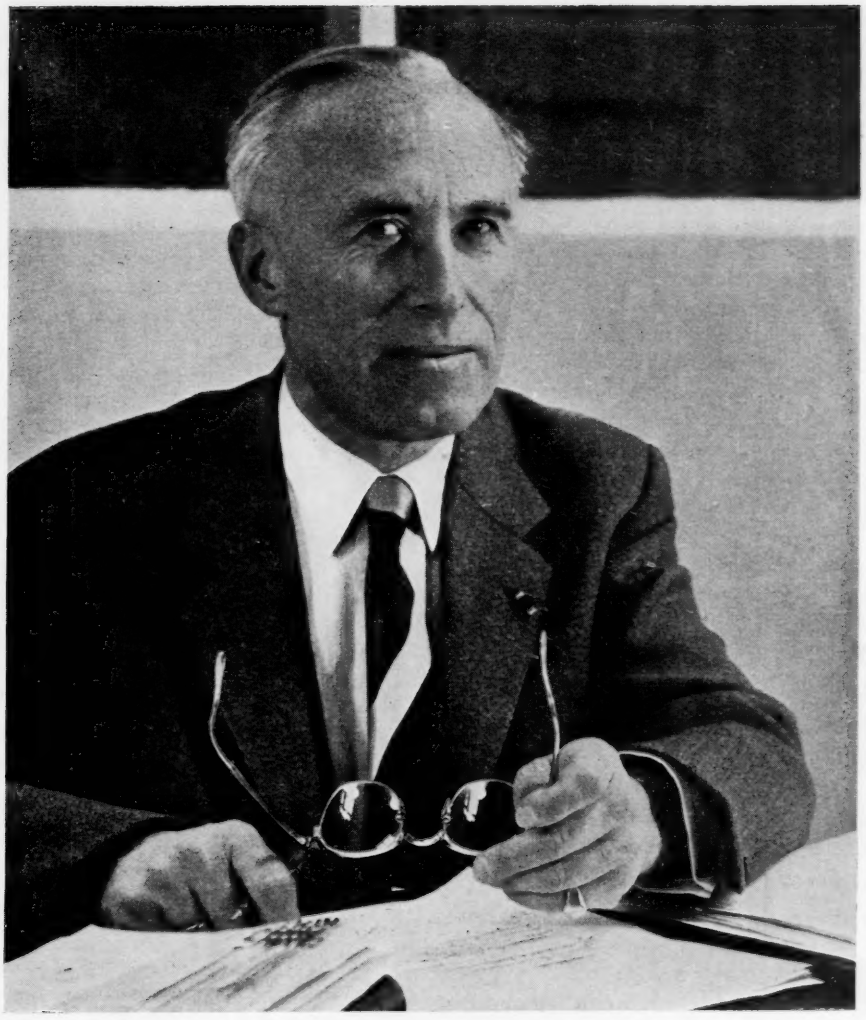

Emile THOMAS

Professor of Physics, Royal Military School, Brussels, Belgium

PROFESSOR E. THOMAS was born in Brussels, Belgium, in 1907. He was awarded the degree of ' Ingénieur Civil ' (Royal Military School) and of Doctor of Sciences (Free University of Brussels).

He is a member of the professorial staff (Chair of Physics) of the Royal Military School since 1936. When in 1947 the Center of Nuclear Sciences was created in that establishment, he was named Assistant-Director and, consequently, Director thereof since January, 1959. He is a member of the Scientific Commission of the ' Institut Interuniversitaire des Sciences Nucléaires '.

Before the second world war, he made researches in solid state physics. Since 1946, when he resumed his scientific activity, he made and directed researches, in nuclear physics (more especially particle accelerators and ion sources) as well as in vacuum science and technology (particularly : ultrahigh vacuum).

Professor Thomas is the author of various books and papers concerning the thermodynamics, metrology, nuclear physics, vacuum science and technology.

He takes an active part in the work of the Belgian Standards Institute and the International Organization for Standardization, in the field of quantities, units, symbols, conversion factors and conversion tables. He also contributes to the work of the Belgian scientific groups dealing with vacuum science and technology.

He presided over the First International Congress on Vacuum Techniques which was held at Namur (Belgium) in June, 1958, and he is now presiding the International Organization for Vacuum Science and Technology which was created by the Congress.

The International Organization for Vacuum Science and Technology

E. THOMAS

Professor at the Royal Military School (Belgium), Director of the Center for Nuclear Sciences in this School, President of the IOVST

Origin of the International Organization

The International Organization for Vacuum Science and Technology (IOVST) was created in Namur (Belgium) on 13 June 1958 by the 520 participants (from 26 countries) attending the First International Congress on Vacuum Techniques*, and arose out of the general appreciation of the value of an international gathering such as that held at Namur.

In his friendly message delivered at the Closing Session of the Namur Congress, Mr. M. W. WELCH, the then President of the American Vacuum Society, recommended the creation of an international committee that would continue the action borne by the organizers of that congress. He also suggested that the seat of such a committee be established in Belgium and that the future congresses should take place in different countries†.

These suggestions were favorably greeted by all and were later reproduced in a draft resolution submitted to the participants by Messrs. J. YARWOOD (U.K.), R. CHAMPEIX (France), G. OETJEN (Germany) and which was unanimously adopted.

This resolution† recommended an Organizing Committee composed of Messrs. A. S. D. BARRETT (U.K.), K. DIELS (Germany), J. M. DUNOYER (France), E. THOMAS (Belgium, President) and Mr. M. W. WELCH (U.S.A.) with the following duties :

(1) to establish an international organization for vacuum science and technology, whose aims would be :

  (*a*) to hold and organize in various countries once every three years an international congress on vacuum science and technology ;

  (*b*) to promote the dissemination of information and the advancement of and the education in vacuum science and technology ;

  (*c*) to affiliate with such other national and international bodies to achieve these objects ;

(2) to organize and call the Second International Congress on Vacuum Science and Technology ;

(3) to submit to the participants of the Namur Congress a Draft Constitution and Bylaws, by mail vote.

The resolution indicates that the seat of the new Organization will be in Brussels‡.

Structure—Constitution

An international secretariat was immediately set up in Brussels to ensure the daily life of the Organization and to co-operate with the Executive Committee (name given to the organizing committee created by the Congress).

Considering as a charter the resolution approved at Namur, the Executive Committee established firstly a draft constitution and the draft bylaws, which documents were submitted to the participants of the First Congress, as agreed. At the same time, it was also deemed advisable to submit these drafts to many societies and persons interested in vacuum science and technology although they did not all attend the congress, in order that they may furnish their competent remarks and suggestions, as the case may be ; also, to induce them to participate to the work of the International Organization for Vacuum Science and Technology.

The drafts were thereafter adopted by the Executive Committee with a few minor amendments resulting from such observations as were received from competent personalities consulted in that respect.

The Constitution outlines the legal form, the seat, the aims, the composition, the financial means, the organs and the languages agreed upon by the Organization.

Legal form and location of the Organization Headquarters

The International Organization for Vacuum Science and Technology is constituted in conformity with the Belgian law respecting the international organizations having scientific aims, and whose seat is in Belgium.

It is a fact that international associations established in other countries very often benefit by analogous legal rights, in conformity with the law set up in these countries.

The civil rights were granted to the Organization's Constitution and approved by a Belgian Royal Decree on 7 August 1959, published in the Moniteur Belge on 20 August 1959§.

* See appendix for details of the origin, aims and organization of the 1958 International Conference at Namur.

† The address of the President of the American Vacuum Society and the resolution adopted by the 1958 Congress are reproduced in extenso with the Proceedings of the First International Congress on Vacuum Techniques (Pergamon Press, London, New York, Paris, Los Angeles).

‡ The International Headquarters of the International Organization for Vacuum Science and Technology are in Brussels 4, Belgium, 30 Avenue de la Renaissance.

§ Furthermore, the Constitution is published in French, English and German, as an appendix to the Moniteur Belge of 17 September 1959, in accordance with the law. It also appears in a booklet.

Vo
9
1959

Object

The Organization's aims are detailed in the Namur resolution (see reference † on p. 256).

Membership

The Organization is composed of :

(*a*) individual members : persons ;

(*b*) associate members : corporate bodies such as national vacuum societies, non-profitable institutions and scientific organizations, firms, commercial and industrial corporations, etc. ;

(*c*) honorary members.

The Executive Committee gave considerable thought and attention at the meeting held in Brussels to the most desirable structure for the International Organization. It was firstly decided that the best way to resolve certain initiation difficulties, bearing in mind the different conditions in many countries, was to admit individual and associate members at the beginning.

The final goal is obviously a Federation of the National Vacuum Societies, and the reasons for this have been strongly presented by many people. But to begin with, one must be realistic. Up to the present time, there are but a few such national societies. The Executive Committee, nevertheless, is making every effort to encourage their creation in the different countries, and there is already in some of them a tendency to bring this idea into focus. But of course some patience is required until the members from each country are able to group themselves and work together.

On the other hand, a strictly federative structure would not have allowed the co-operation of specialists and firms in the countries where no national vacuum society exists. The Constitution of the International Organization for Vacuum Science and Technology does permit their affiliation and this structure contributes notably to the advancement of vacuum science and technology.

Finance

The financial means of the Organization are derived from : regular subscription dues of its members, grants from public and private institutions, any other emoluments deriving from any other source whatsoever.

Administration

The International Organization for Vacuum Science and Technology is administered by the General Meeting, the Executive Committee and the Secretariat at the Headquarters in Brussels.

The General Meeting represents the whole of the members. It is invested with the widest powers to take or ratify all decisions which concern the Organization, which is administered by the Executive Committee to be made up of twelve members.

The Executive Committee will be assisted by an Advisory Committee having international representation. The members of these two committees will ensure a proportional representation of all the countries taking part in the aims and objects of the Organization.

Languages

All communications and discussions are accepted in English, French and German. The Executive Committee may decide to use other languages for certain publications and communications as may prove desirable or necessary.

Activities

The Executive Committee and the Secretariat have not only been engaged upon the establishment of the Constitution and Bylaws.

As stated above, the Organization is encouraging the establishment of national vacuum societies in the countries where they do not yet exist. When such national societies have been developed, the International Organization for Vacuum Science and Technology will then be able to form a " Federation "—this being its most important task for the future. (Reference is made to the resolution adopted by the Executive Committee on 21 February 1959)*.

Furthermore, the Advisory Committee and Technical Standing Committees are being established : a Congress Committee, a Committee for the formation of specialists and a Standardization Committee. Progressively, the Organization proceeds with the aims of meeting the further needs for the advancement of vacuum science and technology. The various committees envisaged will help to achieve the Organization's aims.

A News Bulletin is regularly published in order to furnish all members with the latest information concerning vacuum science and technology (announcement of meetings, letters to the editor, abstracts of scientific reports, abstracts of articles submitted to vacuum and other scientific reviews).

By rapid diffusion of such information, the International Organization for Vacuum Science and Technology has in mind (*a*) to create bonds of friendship between its members and (*b*) to complement and aid the work of the existing vacuum reviews.

Naturally, the Organization exists through and for its members and is striving to increase the membership. On 30 November 1959, there were 32 Associate Founder Members and 418 individual Founder Members (24 countries).

Conclusion

The creation of the International Organization for Vacuum Science and Technology fulfilled a need and, in consequence, a large number of persons and organized groups interested in vacuum science and technology have already had the opportunity to express their desire towards a closer international co-operation in this field.

The Organization is and will remain a bond between its

* See News Bulletin No. 3 of the International Organization for Vacuum Science and Technology.

Vol. 9 959/60

members. They are not controlled in any way. The present structure, it is believed, is the one that best meets the conditions now prevailing in some countries, and which allows the rapid realization of its objective. It is hoped too, that the national societies and groups will be able, through the International Organization for Vacuum Science and Technology, to co-ordinate their respective activities on an international scale and in the most concrete manner.

The affiliation of an increasing number of members will permit the International Organization for Vacuum Science and Technology to contribute effectively to the advancement of vacuum science and its applications.

APPENDIX

The First International Congress on Vacuum Techniques held at Namur

Origin and aims of the congress

After the second world war, some groups of specialists in the field of vacuum science and technology were constituted in various countries (France, U.S.A., Japan, Germany, Belgium, . . .) and they contributed to the development of such technique and its applications.

The activity of these groups merit a more detailed account, but, unfortunately, space prevents it from being given here. However, it may be useful to give an outline of the work done by the Belgian group, which was formed in 1954 under the name of Vacuum Techniques Section, in the framework of the Research Committee within the Société Royale Belge des Ingénieurs et des Industriels (SRBII). This Section was responsible for the idea of the 1958 First International Congress on Vacuum Techniques.

The first activity of this Section was the study of the industrial applications of vacuum.*

It should also be recalled that in 1954 the Institut Interuniversitaire des Sciences Nucléaires de Belgique (IISN) formed working groups, each commissioned to organize discussions on a specified subject, and one of which should include research workers who, within the six Institute's centers, are more particularly interested in the use of vacuum technique in nuclear sciences.†

The working group and the section above mentioned organized meetings either separately or jointly, and they contacted the vacuum specialists of various countries as well as scientific societies whose activity include this technology.

In 1956, when the question of the organization of international congresses was raised, in the framework of the 1958 Universal and International Exhibition of Brussels, members of the above mentioned Section proposed to organize an international congress in the field of vacuum techniques.

Of course, several conferences and meetings dealing with these techniques have been held in various countries in the past, but they were not organized as real international events—the participation of specialists, foreign to the organizing country, was rather small. The Brussels exhibition seemed to provide an excellent opportunity to hold for the first time an international congress including all the vacuum specialists of most countries ; these specialists would then be in a position to advise their colleagues of their latest researches concerning production, vacuum measurement as well as vacuum applications in the laboratory and in industry. At the same time, the opportunity would afford for initiating a closer co-operation between the delegates in their respective fields.

Organization of the congress

In January 1957, following the first steps taken by the provisionally appointed committee, an Organizing Committee (whose members belonged to the research and industrial bodies) decided to hold the congress in Namur (Belgium). They prepared the program of work and agreed that the communications and discussions should take place in French, English and German.

With the co-operation of several scientific societies and reviews in and outside Belgium, the organizers publicly announced the congress, and sought the co-operation of authors and attendees. A Papers Committee examined and selected the program of papers, and a Publications Committee prepared the publication of the congress' proceedings.

All this work was only made possible with the moral and material help supplied by the Organizing Committee.

His Majesty Leopold III, President of the National Commission for Sciences, honoured the congress with His High Patronage.

The Commissariat General of the Belgian Government for the 1958 Universal and International Exhibition of Brussels, officially recognized the congress, thus giving vacuum techniques an important place in the international gathering provided by the Brussels Exhibition.

The necessary funds were generously provided by industrial organizations including 58 Belgian, 3 Luxembourg and one Swiss.

Work of the congress

Participants

Three categories of participants were foreseen : (*a*) industrial and commercial business concerns officially represented by one or more delegates, (*b*) persons not representing officially such business concerns, (*c*) students.

The Table I hereunder shows the attendance by country and of the lectures and communications delivered.

* For more details on the subject, see Bulletin de la SBRII : 5 (1954), p. 192, Revue de la SRBII : 4 (1955), p. 283 and p. 309 ; 7/8 (1956), p. 294 and p. 325 ; 6 (1957), p. 254 and p. 282 ; 5 (1958), p. 263 and p. 288 ; 5 (1959), p. 234, p. 270 and p. 292.

† The activity of this committee is outlined in the Reports of the working groups of the IISN.

Vo
9
1959

TABLE I

Countries	Firms officially represented	Participators (delegates, private persons, students)	Accompanying persons	Number of lectures and communications delivered			
				Total	French	English	German
Europe (CERN)* ..		4		3	1	2	
Argentine		1		1	1		
Australia		1		1		1	
Austria		3					
Belgium	32	138	8	8	8		
Canada		1		2		2	
Czecho-Slovakia	1	5					
Denmark		2					
France	16	80	25	27	27		
Germany :							
Democratic Republic ..	1	12	1				
Federal Republic ..	22	88	19	35			35
Hungary	1	7					
India		1	1				
Italy	5	9	2	5	3	1	1
Japan	3	10		21		21	
Liechtenstein	1	4	1	6			6
Netherlands	2	21		6	2	4	
Norway	1	1		1			1
Poland	1	4		1	1		
Spain	1	3	2	1	1		
Sweden	1	4					
Switzerland	8	21	2	5	1		4
Turkey		1					
United Kingdom ..	26	60	9	18		18	
U.S.A.	7	27	12	15		15	
U.S.S.R.		8		6		6	
Yugoslavia		6		2	1		1
Total	129	522	82	164	46	70	48

Vol. 9 959/60

TABLE II

		Lectures given during the Opening Session			Lectures given during the Plenary Sessions			Communications given during the Sections' Sessions			
		F	E	D	F	E	D	Total	F	E	D
Fundamental problems in vacuum techniques (62 lectures and communications)	1.—Generalities (units, standards, etc.)	2	1			1		12	2	5	5
	2.—Mechanical pumps							5		2	3
	3.—Diffusion pumps and ejectors			1				6	1	4	1
	4.—Problems arising in vacuum systems ..							3		2	1
	5.—Leak detection							8	5	3	
	6.—Vacuum measurement							13	6	5	2
	7.—Pumping speed measurement							4	3	1	
	8.—Leads and connections							6	5		1
Ultra-high vacuum (25 lectures and communications)	9.—Generalities		1					6	1	4	1
	10.—Measurement							6		3	3
	11.—Getter pumps and ionization pumps ..					1		9	3	3	3
	12.—Applications							2		2	
Vacuum systems applications in various sciences and techniques (77 lectures and communications)	13.—Nuclear sciences					1	1	16	6	7	3
	14.—Metallurgy							13	3	3	7
	15.—Electron tube industry and related problems ..							18	2	10	6
	16.—Chemistry							3		3	
	17.—Biology, pharmacy and food industry ..							6	2	2	2
	18.—Vacuum evaporation							7	1	3	3
	19.—Vacuum concrete							4	2	1	1
	20.—Miscellaneous subjects							8	2	2	4
F : in French E : in English D : in German	Total	5			4			155			
		164									

*CERN. European Organization for Nuclear Research.

Lectures and communications

With the co-operation of 208 speakers from 18 countries and of a European Institute (CERN), the organizers of the congress were able to prepare the program of lectures and communications covering to a large extent the field of vacuum science and technology.

This program included :

5 lectures given during the Opening Session (10 June 1958)

4 lectures given during the plenary sesssion of 11, 12 and 13 June,

155 communications delivered 11, 12 and 13 June, divided up into 20 sections (see Table II hereunder),

the total of which being 164 lectures and communications : 46 delivered in French, 70 in English and 48 in German.

A. Opening Session

M. GUILMIN, President of the permanent Deputation of the Province of Namur, representing the Governor M. GRUSLIN, opened the congress.

Professor E. THOMAS, President of the congress, thanked all those who brought their help to the organization of the congress, welcomed the attendees and outlined the program of work ; he hoped that with the co-operation of all the attendees, the aim of the organizers' efforts would be plainly realised.

Thereafter, the following lectures were delivered :

1.—*Bases expérimentales de la théorie cinétique des gaz*, by L. DUNOYER, Dr., ancien Professeur à la Sorbonne, Membre du Bureau des Longitudes, Président d'Honneur de la Société Française des Ingénieurs et Techniciens du Vide, Paris (France). This lecture was read by J. M. DUNOYER, Dr., Professor at the Faculté des Sciences de Rennes (France).

2.—*History of the vacuum-pump*, by E. N. da C. ANDRADE, D.Sc., Ph.D., LL.D., F.R.S., Professor at the Imperial College of Science and Technology, London (U.K.).

3.—*Die Diffusionspumpe—Ihre Physik und Technik*, by R. JAECKEL, Dr., Professor an der Universität Bonn, Vorsitzender der Arbeitsgemeinschaft Vakuum des VDI, des Verb. Dtsch. Phys. Ges. u. d. DECHEMA (Deutschland).

4.—*Recent Advances in Ultra-high Vacuum Technology*, by D. ALPERT, Dr., Professor at the University of Illinois, Urbana (U.S.A.).

5.—*L'apport de la technique du vide à la science et à l'industrie*, by R. CHAMPEIX, Ing.-Dr., Ingénieur en Chef aux Laboratoires d'Electronique et de Physique appliquées, Paris (France),

they threw a light on the important aspects of vacuum sciences and techniques and constituted an excellent introduction for the exposés to be delivered the next day.

B. Plenary Sessions (11, 12, 13 June 1958)

The following conferences were delivered during these sessions :

— on 11 June : *Evapor-ion pump development at the University of Wisconsin*, by R. G. HERB, Dr., Professor at the Department of Physics, University of Wisconsin, Madison (U.S.A.).

— on 12 June : *Die Anwendung der Vakuumtechnik bei der Herstellung von Reaktor-Baustoffen*, by H. HARDUNG-HARDUNG, Dr., Degussa, Frankfurt am Main (Deutschland).

— on 12 June : *High vacuum pumps and units for accelerators*, by S. A. VEKSHINSKY, M. I. MENSHIKOV and I. S. RABINOVICH, Academy of Sciences, Moscow (U.S.S.R.).

— on 13 June : *Education in Vacuum Technology*, by J. YARWOOD, M.Sc., F.Inst.P., Head of Department of Mathematics and Physics, The Polytechnic, London (U.K.).

C. Sections' Sessions (11, 12, 13 June)

We only mention the dividing up of the 155 communications delivered during these sessions (Table II overleaf). Most of these were followed by a discussion.

Results

We may reasonably affirm that the two aims of the organizers of the congress were fulfilled.

The congress had planned and achieved the exchange of views between specialists in the field of vacuum science and its applications. The basis of a greater co-operation between these specialists have been assured by the creation of the International Organization for Vacuum Science and Technology.

VO
9
1959

A Piezoelectric Oscillator Manometer

D. J. PACEY

Brunel College of Technology, London

(Received 17 June 1959)

This paper describes a simple manometer for the measurement of pressures of gases and vapours within the range 760 torr to 10^{-1} torr, with a linear scale. It uses the damping effect of the gas or vapour upon the sustained vibrations of a commercially available piezoelectric quartz crystal. The damping effect is examined theoretically and the behaviour of the gauge is shown to be generally in accordance with calculation.

Vol. 9 959/60

1. Introduction

The decrement gauge suggested by Langmuir[1] and developed by Haber and Kerschbaum[2], Scott[3] and Wetterer[4] makes use of the variation of gas viscosity with pressure which occurs when the mean free path is of the same order of magnitude as the dimensions of the apparatus. These devices are simple in construction and do not interact chemically with gases or vapours in the system to which they are attached, but the readings are time consuming and subject to serious errors due to external vibrations. In an attempt to produce a continuously sensitive viscosity gauge free from the above defects, the piezoelectric oscillator manometer was developed, and was found to have sensitivity in the range of pressures within which the viscosity of the gas is found to be constant. Schwartz[5] has described a similar manometer in which the damping effect of the gas upon the maintained vibrations of an iron membrane are used, and since the frequency of vibration is in the audible range it is described as an acoustic gauge. Other types of gauge based upon the transmission of sound waves through the gas are known, notably those of Millar[6] and Antal and Konig[7]. The piezoelectric gauge described here aims at the greatest simplicity combined with effective zero stability and sensitivity.

2. Description of the gauge

The circuit of the gauge is shown in Fig. 1. The quartz crystal Q is mounted in the gas or vapour whose pressure is to be measured, and is maintained in oscillation by coupling to one half of a double triode V_1 connected as a Pierce-Miller[8] oscillator. The average value of the anode current of V_1 increases when the amplitude of the crystal oscillations is reduced by the presence of gas or vapour. The other half of the double triode V_2 is used in a potential divider circuit to balance the steady anode potential of V_1. This enables the use of a sensitive meter to indicate small changes in the anode current of V_1, and minimizes drift due to fluctuations of the mains supply voltage.

Stability is further improved by the use of gas filled voltage regulator tubes connected across the H.T. supply. Three ranges are provided by the resistors R_3 and R_4 selected by the switch S. A 200 kc/sec crystal type $Q6B$ supplied by the Brush crystal company is used. This is a D.T. cut crystal which vibrates in the face shear mode at its fundamental frequency[9], and is of the evacuated glass enclosed type. It is connected to the vacuum system by means of a compression joint, after carefully breaking off the exhaust tubulation. To keep the high frequency leads short and avoid the effect of stray capacitances, the oscillator components are contained in an earthed metal box 3 in. × 3 in. × 1 in., which is attached to the compression joint so that the base of the crystal envelope projects into the box. This box

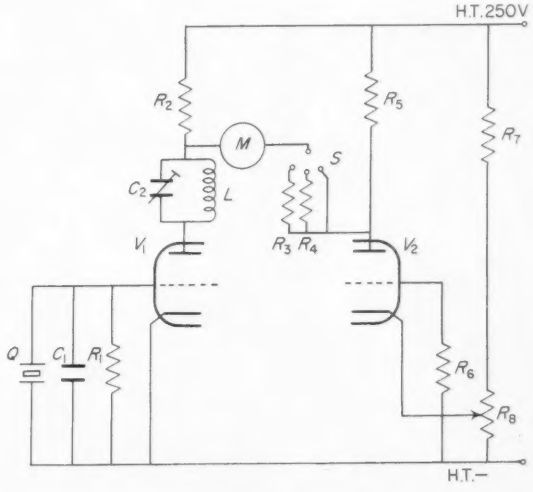

$C_1 = 40\ pF$ — $R_7 = R_8 = 20\ K\Omega$

$C_2 = 250\ pF$ trimmer — $R_4 = 1\ M\Omega$

$R_1 = R_6 = 1\ M\Omega$ — $L = 2200\ \mu H$

$R_2 = R_5 = 47\ K\Omega$ — $M = 50\ \mu A\ FSD$

$R_3 = 10\ K\Omega$ — $V_{12} =$ ECC 83

FIG. 1.

constitutes the head unit, which is connected by a convenient length of 5 core cable to the meter unit, which also houses the power supplies.

3. Setting up and operation

After evacuation of the system to a pressure below 10^{-2} torr, the power supply is switched on, and after a short warm-up period the trimmer capacitor C_2 is adjusted from maximum to the point F in Fig. 2, at which the anode current

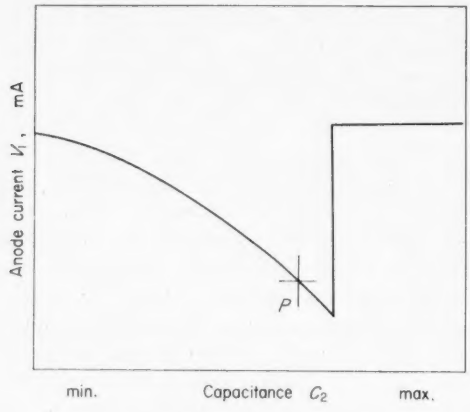

A Calibration for Argon
B Calibration for Air
C Calibration for Hydrogen

FIG. 2.

falls suddenly when crystal oscillations commence. C_2 is finally adjusted to bring the anode current of V_1 to the working point P. This setting is not critical. The meter is

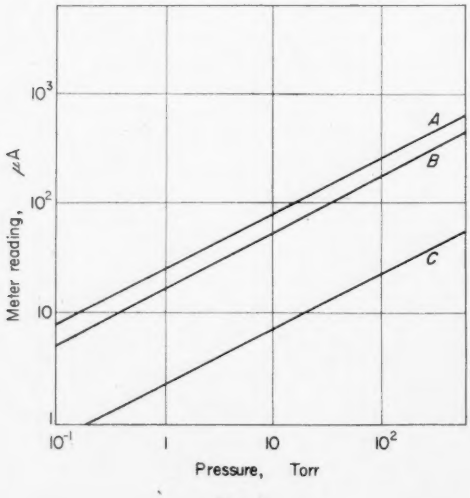

FIG. 3.

then set to zero by adjustment of the bias resistor R_8, after which the gauge will respond to pressure variations according to the calibration graphs shown in Fig. 3.

4. Theory of the damping effect

This consists of two parts, firstly internal, due to hysteresis effects in the quartz, which is small, and is independent of the pressure, and secondly due to the supply of kinetic energy to the gas or vapour molecules by the vibrations of the crystal, at a rate determined by the pressure. The kinetic energy supplied to the molecules striking the crystal will be distributed through the gas by intermolecular collisions, and possibly by the formation of eddies and vortices, resulting in a small increase in the temperature of the contents of the gauge. A calculation of the power supplied to the gas is carried out below, neglecting the effects of internal damping.

If N is the number of gas molecules/cm^3, having an average velocity $\bar{c}$, the number of molecules striking unit area of the crystal in time dt is given by $\frac{1}{4} N \bar{c}\, dt$. If the instantaneous velocity of the crystal is v, the energy dW supplied in time dt to the molecules is $\frac{1}{2} . \frac{1}{4} Nm\bar{c}\, dt\, [(\bar{c} + v)^2 - \bar{c}^2]$

where m is the mass of a molecule

Hence $$dW = \tfrac{1}{8} Nm\bar{c}\,(2\bar{c}\, v + v^2)\, dt$$

and the total energy W supplied in unit time to the molecules is given by $$W = \tfrac{1}{8} Nm\bar{c} \int_0^1 (2\bar{c}\, v + v^2)\, dt$$

Assuming the vibrations of the crystal to be sinusoidal

$v = V \sin 2\pi ft$ where f is the frequency of vibration

And $$W = \tfrac{1}{8} Nm\bar{c} \int_0^1 (2\bar{c}\, V \sin 2\pi ft + V^2 \sin^2 2\pi ft)\, dt$$

The first term of the integral is zero

Hence $$W = \tfrac{1}{8} Nm\bar{c}\, V^2 \int_0^1 \sin^2 2\pi ft\, dt$$

$$W = \tfrac{1}{8} \varrho\bar{c}\, \frac{V^2}{2}$$ since $Nm = \varrho$ the density of the gas

Substituting $$\varrho = \varrho \frac{M}{RT} \text{ and } \bar{c} = \sqrt{\frac{8}{\pi} \frac{RT}{M}}$$

$$W = \tfrac{1}{8} pV^2 \sqrt{\frac{2M}{\pi RT}}$$ where M is the molecular weight of the gas.

This shows that the rate of supply of energy to the gas and hence the damping effect will be greater for substances of high molecular weight, as shown in the calibration graphs in Fig. 3. The damping effect is seen to be proportional to the pressure, this also is shown in the calibration graphs which have the same slope of approximately $\frac{1}{2}$. This follows from the fact that changes in the anode potential of V_1 are proportional to changes in the grid potential of V_1, and the power supplied to the crystal is proportional to the square of this potential. Further measurements are being carried out to observe whether the changes in anode potential of V_1 are in fact related to $M^{\frac{1}{2}}$.

5. Conclusions

The gauge described above provides a simple means of measuring pressures in the range 760 Torr to 10^{-1} Torr, with a linear scale. Extension of the pressure range down to 10^{-2} Torr is possible provided sufficient regulation of the power supplies is provided. A constant voltage transformer used to supply the power unit is found to be satisfactory. The gauge exerts no pumping action, and it is unaffected by reasonable temperature variations, vibration, and external magnetic fields.

References

[1] I. Langmuir ; *J. Amer. Chem. Soc.* **35**, 105 (1913).
[2] F. Haber and F. Kerschbaum ; *Z. Electrochem.* **20**, 296 (1914).
[3] D. H. Scott ; *Phil. Mag.* **47**, 32 (1924).
[4] G. Wetterer ; *Z. tech. Physik* **20**, 281 (1939).
[5] H. J. Schwartz ; *Vacuum Symposium Transactions*, Pergamon Press, Ltd., 1956.
[6] W. Millar ; *A.E.R.E. Harwell Memo No.* : GP/M 190 (1956).
[7] J. Antal and A. Konig ; *Periodica Polytech. Elec. Eng.* **3**, 279 (1957).
[8] W. G. Cady ; *Piezoelectricity*, p. 495, McGraw Hill Book Co. (1946).
[9] D. Fairweather and R. C. Richards ; *Quartz crystals as oscillators and resonators*, p. 2, Marconi's Wireless Telegraph Co. Ltd. (1957).

Vol.
9
59/60

Semi-Automatic Control of Vacuum Pumping Systems

N. C. BALCHIN and B. L. MORDIKE*

Physics and Chemistry of Solids, Cavendish Laboratory, Cambridge.

(*Received 15 July 1959*)

1. Introduction

High Vacuum techniques are becoming increasingly important both in research and industry. The precise selection of equipment will depend upon the exact application but the same principles apply. In the high vacuum pumping systems now generally adopted the required pressure is obtained by using a diffusion pump and a mechanical pump (rotary vane or piston) arranged in tandem.

Since the vacuum system is only a part of the complete equipment it ought to be installed so that it requires a minimum of effort both in operation and in maintenance : while it should not dictate the method of working. The diffusion pump must be cooled or isolated before air can be admitted to the work chamber. If handvalves are used operation is tedious, time consuming and liable to mistakes, and in addition no protection is provided against mains failure and consequent suck back of the rotary pump oil.

2. Semi-automatic system

For a large enough system a completely automatic system may be set up using magnetic valves and relays operated by vacuum gauges.[1]

In a smaller system of the type usually used in research, such a control system would exceed the actual pumping system in complexity and cost, and so something simpler must be used. We describe below a method of achieving a considerable simplification in operation without any unduly complex control gear. Our systems are based on the following points :—

1. The system relies on the operator to take action if the pressure is abnormal, as it is not connected to any gauges.

2. Protection against failure of the mains supply flooding the system with oil from the rotary pump is provided.

3. Controls are simplified to the minimum required : we use,

   One switch for the rotary pump

   One switch for the diffusion pump

   Flap-valve—(according to its position this selects :— (a) Closed—rough pumping, (b) Open—fine pumping.) One switch to allow air to be admitted to work-chamber —functioning only when the flap-valve is closed.

4. Magnetic valves are used for all the other requirements.[2]

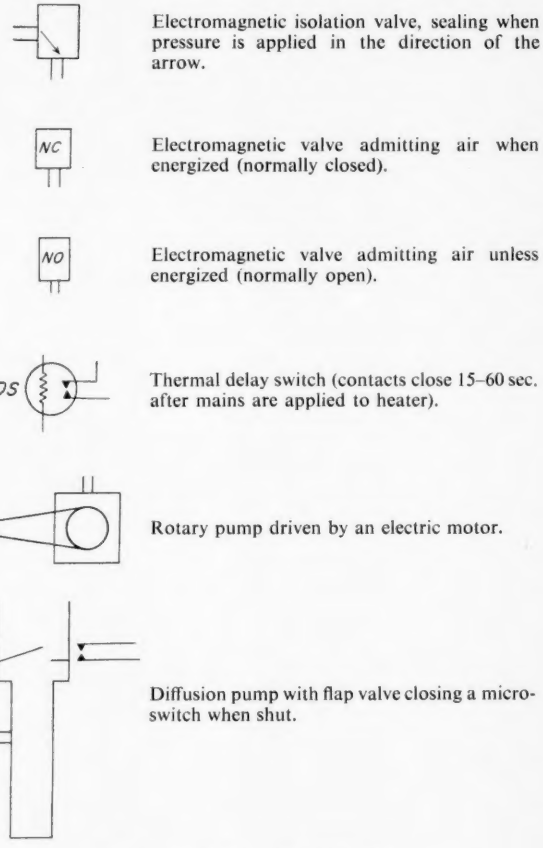

Electromagnetic isolation valve, sealing when pressure is applied in the direction of the arrow.

Electromagnetic valve admitting air when energized (normally closed).

Electromagnetic valve admitting air unless energized (normally open).

Thermal delay switch (contacts close 15–60 sec. after mains are applied to heater).

Rotary pump driven by an electric motor.

Diffusion pump with flap valve closing a micro-switch when shut.

FIG. 1. Symbols used in this article.

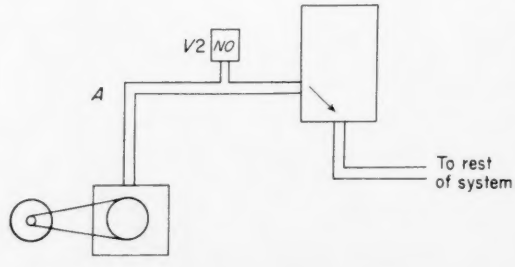

FIG. 2. Schematic drawing of vacuum system.

*Now at the University of Göttingen (Institut für Metallphysik)

A suitable control circuit to achieve the above requirements was developed. For mains supply failure protection a standard arrangement, as shown in Figs. 2 and 3, was used in a slightly modified form (Fig. 4). To signal the position of the flap-valve a microswitch was fitted, to make contact when the flap-valve was fully closed. The vacuum system

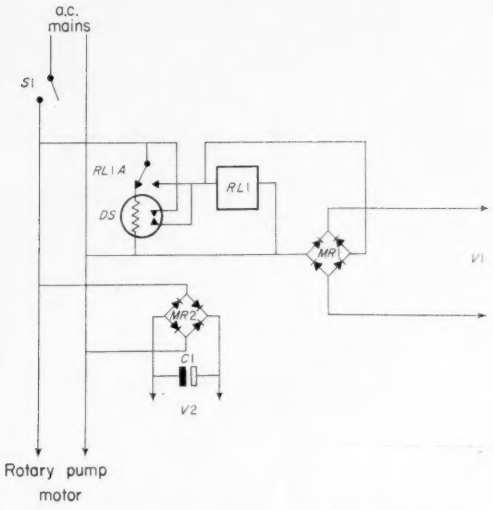

FIG. 3. Basic circuit for mains failure protection, used with vacuum system of Fig. 2.

Start : *S*1 closed, motor starts, *MR*2 energises *V*2, which closes : part *A* of system is pumped down, while *DS* warms up : then *DS* contacts close, energizing *RL*1 : *RL*1*A* holds on *RL*1 and deenergizes *DS* heater : *MR*1 operates *V*1, connecting pump to rest of system.

Stop : If either *S*1 is opened, or mains fail, *V*1 is deenergized, isolating *A* from rest of system : *C*2 keeps *V*2 energized for several seconds until after *V*1 has closed, then *V*2 opens admitting air to the pump.

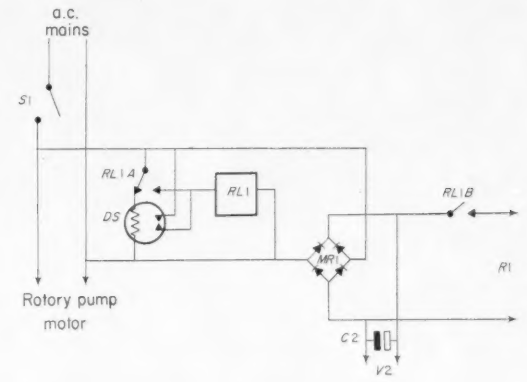

FIG. 4. This circuit improves on Fig. 3, by using only one rectifier.

Operation : Start : *S*1 on, motor starts. *MR*1 energizes *V*2, which closes, then (as in Fig. 3) *DS* warms up and *RL*1 operates, when *RL*1*B* energizes *V*1 from *MR*1.

Stop : *RL*1 deenergized, *RL*1*B* disconnects *V*1, which closes : *C*2 keeps *V*2 energized, as in Fig. 3.

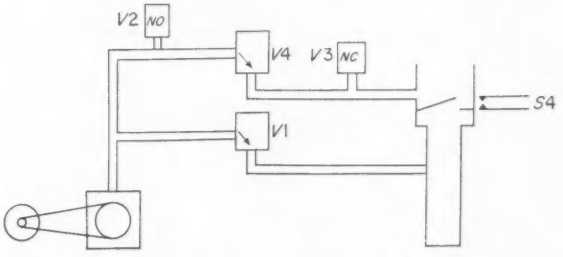

FIG. 5. Schematic vacuum system as used on carbon tube furnace.

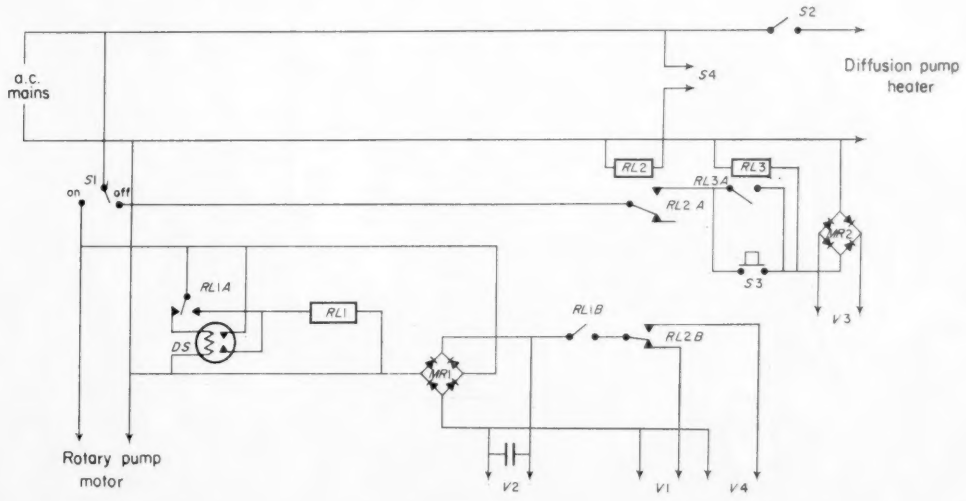

FIG. 6.

Operation : Start : *S*1 on, action as in Fig. 4, except that *MR*1 now opens *V*1 or *V*4, via *RL*2*B* as appropriate to the position of the flap-valve and *RL*2. *S*2 controls the diffusion pump independently.

Stop : *S*1 off, or mains failure, action as in Fig. 3. Admit air to work-chamber—*S*3 operated : if *S*1 has switched off the rotary pump, and *RL*2*A* closed (Flap-valve and *S*4 closed, and *RL*2 energized), *RL*3 is energized, and holds on via *RL*3*A* : *MR*3 energizes *V*3 to admit air : *V*3 is released when *S*1 is switched to " on " (*S*3 and *RL*3 are used to prevent air being admitted when the rotary pump is next switched off, as might happen if a normal switch were used).

Vol. 9 959/60

with which this was to work is shown schematically in Fig. 5 : the fact that *V*4 will seal in only one direction imposes the limitation that the rotary pump must be stopped before the work-chamber is let down to atmosphere.

These features are provided by the circuit of Fig. 6 : the flap-valve itself provides one desirable feature in that it cannot easily be opened against atmospheric pressure, that is, if the work-chamber is open, and the diffusion pump is under vacuum.

The success of this circuit, as applied to the pumping system of a vacuum furnace, encouraged us to develop and improve it for use in a pumping system for leak testing. The limitation mentioned above means that the rotary pump cannot be used to back the diffusion pump when the work-chamber is open. This can be overcome by adding an extra magnetic valve to the system : two alternatives are available, illustrated in Fig. 7, of which we chose that of Fig. 7(a), as there is only one valve in the backing line to restrict pumping speed. The work-chamber can be isolated for determination of leak rate from pressure rise measurements.

Fig. 8 shows the complete schematic circuit for the system of Fig. 7(a) : Fig. 9 shows the addition of indicator lamps and other practical details for the circuit as used.

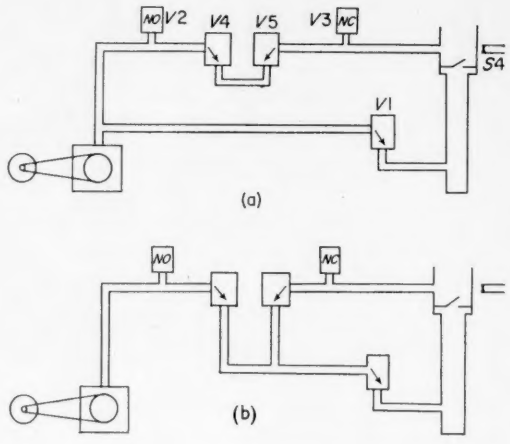

FIG. 7. Alternative three-valve arrangements.

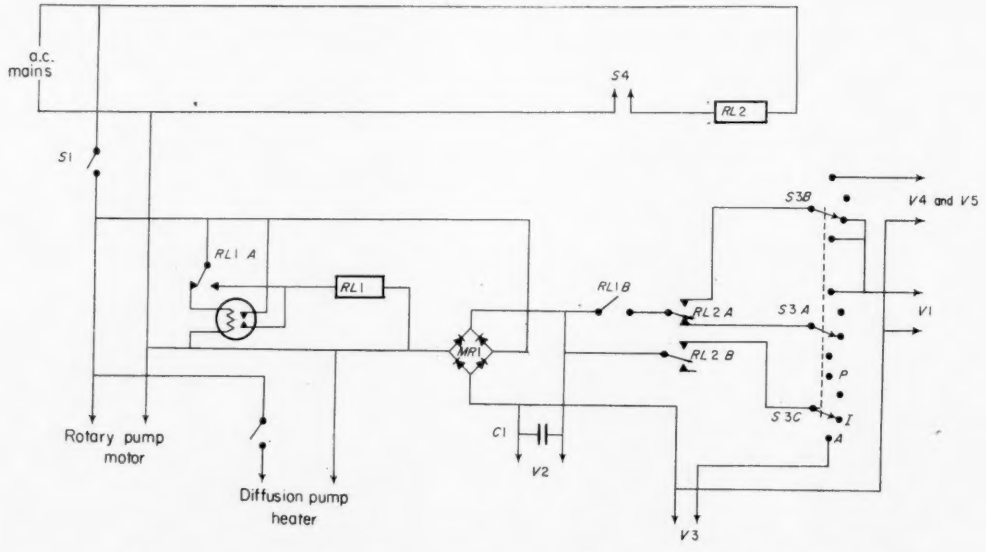

FIG. 8. Control circuit for system shown in Fig. 7(a) : Procedure. Start : *S*1, *RL*1, *MR*1, and *V*2 operate as in Fig. 6.

Position of *S*3.

	P-Pump	Blank	I-Isolation	A-Air Admittance
Flap valve open *S*4 open, *RL*2 deenergized	Fine pump *V*1 energised via *RL*1*B*, *RL*2B, *S*3*A*		*V*1, *V*4, *V*5 closed	*V*1, *V*4, *V*5 closed
Flap valve closed *S*4 closed, *RL*2 energized	Rough pump *V*4 and *V*5 energized via *RL*1*B*, *RL*2*A*, *S*3*B*	On switching to *P* for rough pump permits *V*1 to close before *V*4, *V*5 open	*V*1 energized via *RL*1*B*, *RL*2*A*, *S*3*B* to evacuate diffusion pump	*V*3 energized via *RL*2*B*, *S*3*C* to admit air. As under " Isolation " *V*1 is open

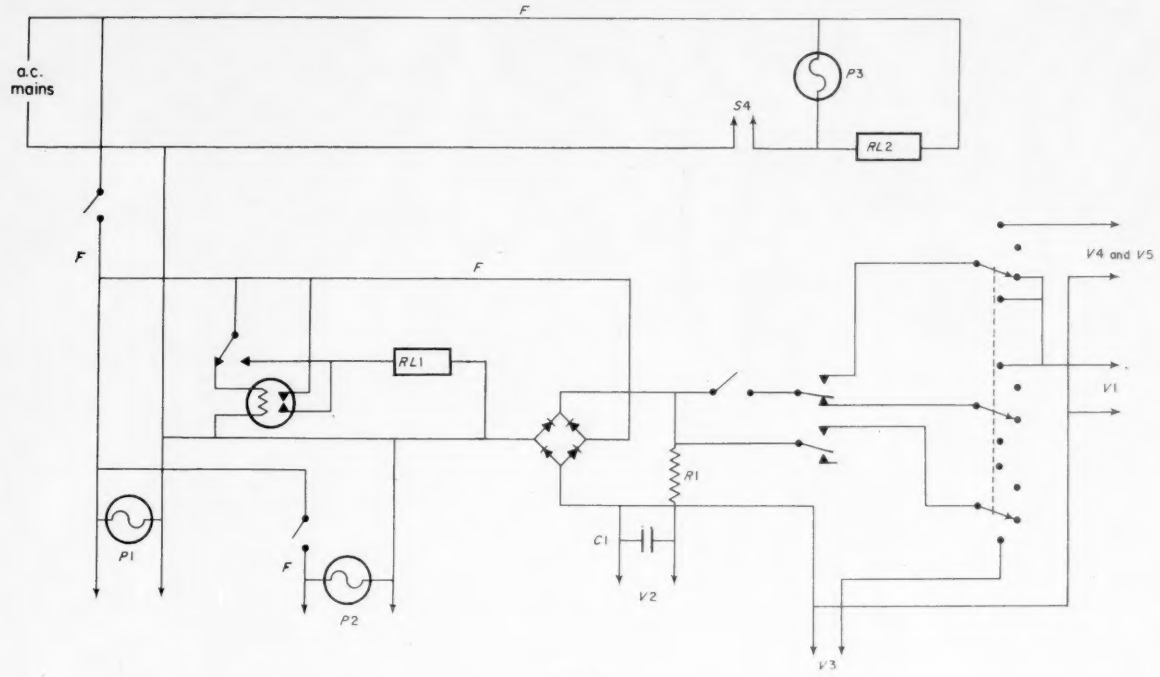

FIG. 9.

*P*1–3 are pilot lamps (Switchboard Indicator).
*P*1–Rotary Pump.
*P*2–Diffusion Pump.
*P*3–Flap-valve closed.

F Fuses (positions chosen to maintain interlocks as far as possible in the event of failure).

*R*1 (2 k Ω) is included to prevent *C*1 (32 μF electrolytic) acting as reservoir capacitor for *MR*1.

DS is a Sunvic TYE M/1.

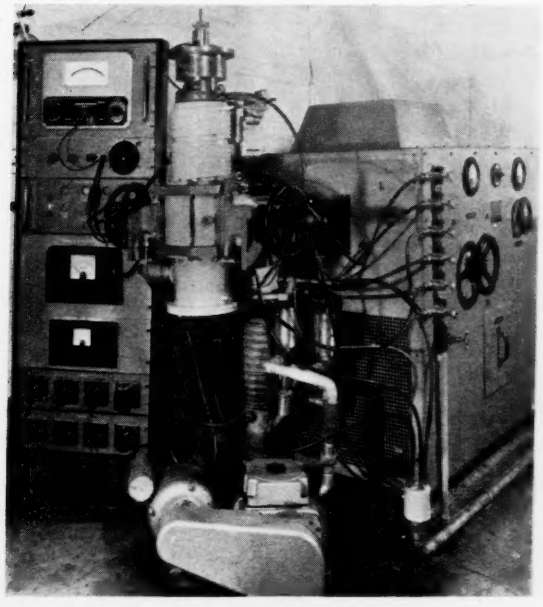

FIG. 10(a).

Vol. 9 59/60

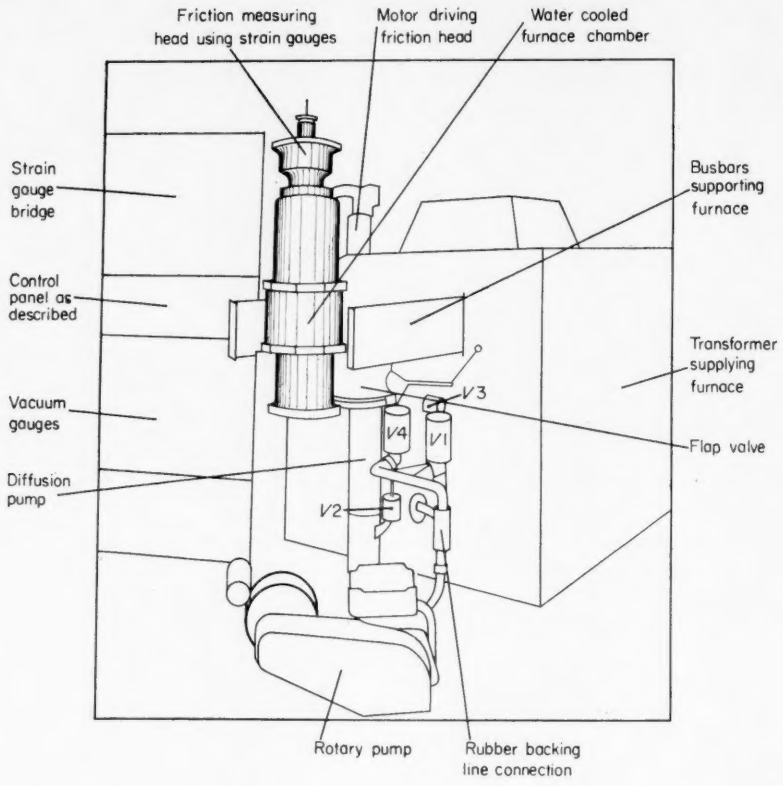

FIG. 10(b).

This arrangement too has been very successful and easy to operate, well repaying the effort involved in its construction : it provides a much more versatile and easily operated system than the use of valve blocks, which are in any case available in only a very limited range.

Figs. 10(a) and 10(b) show how the system system was applied to the furnace mentioned above : this is a carbon-tube resistance furnace used for heating specimens to temperatures up to 2500°C for tensile tests and measurements of the coefficient of friction. The pumping system employs a 4 in. oil diffusion pump and 6 l/sec. rotary piston pump, and in conjunction with the control arrangements allows the specimens to be changed and the furnace to be heated up again with the minimum of trouble and loss of time.

Acknowledgements

We would like to express our appreciation to our respective supervisors Drs. D. Tabor and F. P. Bowden for their encouragement.

References

[1] A. H. Turnbull ; *Applications of vacuum technique in Atomic Energy Research, Vacuum* **5**, 131 (1955).
[2] J. Yarwood ; *Isolation valves for vacuum systems, Vacuum* **3**, 398 (1953).

Vol 9 1959

Cathodic Etching in a Penning Cold Cathode Discharge

P. T. STROUD

Research Laboratories, Edwards High Vacuum Ltd.

(*Received 18 July 1959*)

An apparatus for cathodic etching using a Penning cold cathode discharge is described. One of the twin cathodes is the specimen to be etched whilst the other is made of aluminium. The cathodes are water cooled so that metals of either low melting point or low sputtering rate will not overheat during the cathodic etching. The Penning system is used because the glow discharge can be maintained at a sufficiently low pressure ($\leqslant 1\mu$ Hg) for most of the sputtered atoms to escape from the specimen surface and not be returned by collision with gas molecules. The higher sputtering rate attained at low pressure permits etch patterns to be obtained speedily. Several metals viz. phosphor bronze, copper, pure iron, mild steel, bismuth, cadmium and Telcoseal 5 (an alloy consisting of 25 per cent chromium in iron with additions of manganese and silicon) have been cathodically etched satisfactorily and photomicrographs of some of the etched surfaces prepared. Generally the cathodically etched surfaces were similar to those obtained by chemical etching, but only cathodic etching truly exposed the crystalline structure of Telcoseal 5.

Vol. 9 59/60

1. Introduction

The etching of metallurgical specimens by positive ion bombardment in a glow discharge has been investigated by McCutcheon[1] and others. In this laboratory Holland and Sutherland[2] have etched a number of specimens with a a simple cathode–anode arrangement and confirmed that metals difficult to etch chemically such as certain Al:Mg alloys, could be satisfactorily cathodically etched. Also the writers' colleague G. Siddall etched uranium in a similar apparatus. Popenova[3], Grivet[4] and others have reported using cathodic etching for preparation of metallurgical specimens for the electron microscope. Generally workers in electron microscopy have investigated the vacuum etching process to a greater degree than have metallurgists using optical microscopy. The electron microscopist is more familiar with high vacuum technique, which he is often using when preparing specimens by shadow casting and this has helped him to apply cathodic etching techniques. Apart from this the fine control afforded by cathodic etching is important to the electron microscopist.

The experiments described here were all carried out using conventional metallurgical techniques and it is hoped that the optical metallographist will find the results interesting and instructive.

When cathodic etching is carried out in a glow discharge at pressures between 0.01 and 0.1 Torr the mean free path of the sputtered atoms in the residual gas is sufficiently small for most of them to be returned to the specimen by collision with gas molecules. This back diffusion of atoms lowers the speed at which etch patterns can be obtained, Holland[5] has described a method of using a Penning cold cathode discharge in which the bombardment of the specimen occurred at a lower pressure ($\leqslant 1\ \mu$ Hg) than that of the usual glow discharge ($\simeq 0.1$ Torr). At $1\ \mu$ Hg the mean free path of the metal atoms in the gas is about 5 cm so that most of the sputtered metal escapes from the cathode. The present experiments at low pressure were carried out with apparatus based on Holland's design. Wehner[6] has etched germanium crystal specimens at a low gas pressure by bombarding their surfaces with positive ions extracted from a mercury vapour plasma.

2. Cathodic etching apparatus

A photograph of the apparatus is shown in plate 1(*a*). Where *A* is a yoke shaped cathode attached to a water cooled electrode *B* (see Fig. 1). This cathode has two small studs

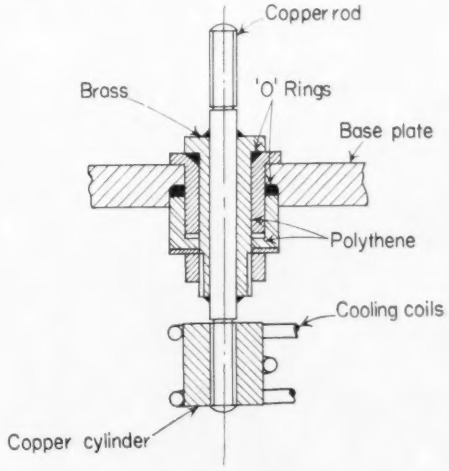

FIG. 1.

to which may be screwed the specimen *C* and a pure aluminium counter electrode *D*. The anode *E* is a ring made of copper because due to its good conductivity it is the only metal that does not overheat under the electron bombardment. The anode ring, counter electrode, specimen, and magnet pole pieces *F* are concentric. The bar magnet *G* produces a field of 200–300 G between the poles. The anode, magnet and poles are all earthed to the base plate of the vacuum chamber.

The apparatus was mounted in a 12 in. dia. Pyrex bell jar. The d.c. power supply used had an open circuit voltage of 5 kV and a short circuit current of 60 mA. The power supply anode terminal was earthed to the plant. Dry argon was admitted through a needle valve on the chamber.

3. Experimental procedure

Preparation of specimens

For convenience specimens were mainly produced from cylindrical bars as shown in Fig. 2. The face to be etched

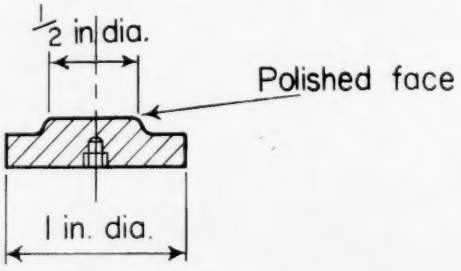

FIG. 2.

was first filed level and then smoothed with various grades of abrasive paper. The finest grade used was of 600 grit size. After smoothing, the surfaces were polished first with metal polish (Bluebell) on a Selvyt covered wheel and then by hand using alumina suspended in water on a Selvyt cloth.

Cathode etching

After mounting the specimen on the cathode electrode the chamber was pumped down to 0.1 μ Hg and argon was admitted to flush the system. The pressure in the chamber was then adjusted to obtain the desired H.T. current and voltage and the specimen was bombarded for a set time. After a few experiments the best operating conditions were found for etching given materials and the specimens were then examined and some were photographed on a Vickers Projection Microscope.

The following metals were etched successfully :—phosphor bronze, copper, cast bismuth, mild steel, vacuum melted iron, cadmium and Telcoseal 5 (an alloy of 25 per cent chromium in iron with small additions of silicon and manganese). Given in Table 1 are suitable cathodic etching conditions for each metal.

TABLE I

Suitable cathodic etching conditions for various metals

Metal	Pressure	Current	Voltage	Etching Time	Remarks
(1) Phosphor bronze	0.5 μ Hg	5 mA	2.5 kV	20 min	See plate 1(b)
(2) Copper	0.6 μ Hg	4 mA	2.0 kV	25 min	See plate 2(*a*)
(3) Pure Iron (vacuum melted)	0.7 μ Hg	5 mA	3.2 kV	30 min	See plate 2(*b*)
(4) Mild Steel	0.4 μ Hg	4 mA	2.5 kV	20 min	See plate 3(*a*)
(5) Bismuth (cast)	1.0 μ Hg	10 mA	500 V	15 min	See plate 3(*b*)
(6) Bismuth (cast)	0.5 μ Hg	4 mA	2.5 kV	8 min	Structure revealed as in plate 3(*b*)
(7) Cadmium	0.5 μ Hg	4 mA	2.5 kV	2 min	A little over-etched, shorter time may be needed
(8) Telcoseal 5	0.6 μ Hg	5 mA	3.2 kV	60 min	See plate 4(*a*)

No. 8 specimen (Telcoseal 5) proved difficult to etch chemically but with cathodic etching little experience was required to achieve the good results shown. No. 5 specimen (bismuth) was etched at 10 mA and 500 V and required 15 min to achieve a depth of etch similar to No. 6 specimen. The difference in etching time could be explained by the different ion energy. In general a potential difference of 2–3 kV

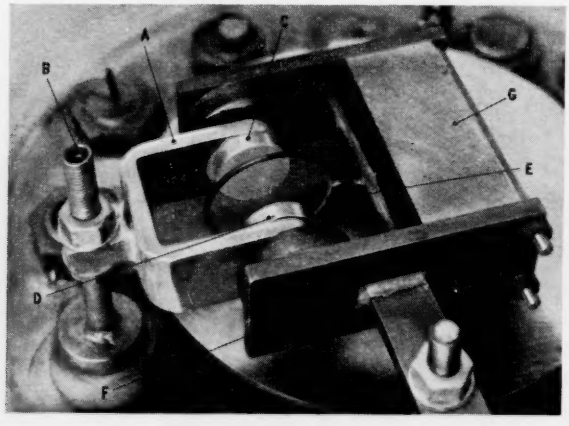

PLATE 1(*a*). Penning cold cathode discharge apparatus used for cathodic etching.

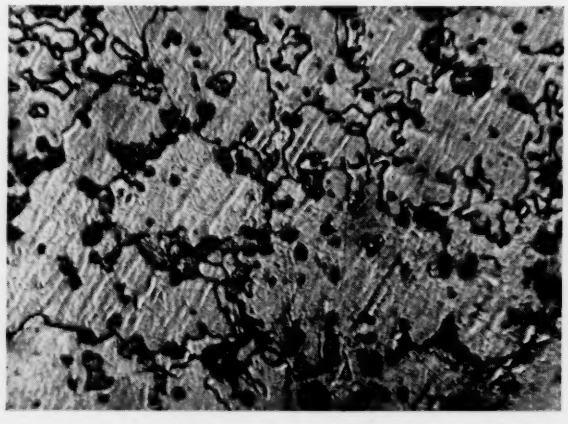

PLATE 1(*b*). Phosphor bronze X 500 cathodically etched for 20 min at 0.5 μ Hg in argon at 5 mA 2.5 kV.

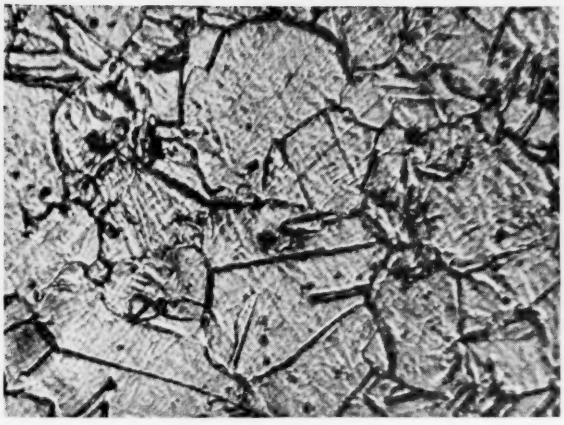

PLATE 2(*a*). Copper X 500 cathodically etched for 25 min at 0.6 μ Hg in argon at 4 mA 3.0 kV.

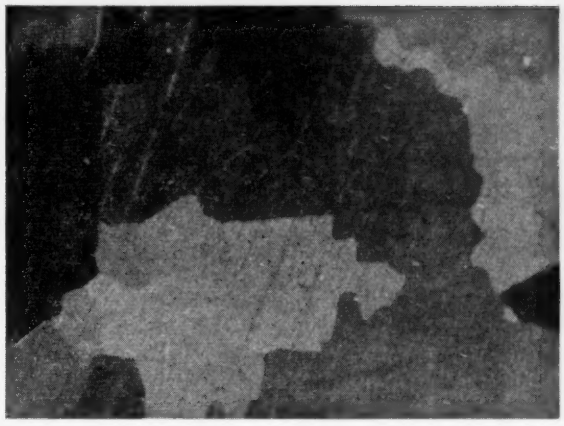

PLATE 3(*b*). Bismuth (cast) X 50 cathodically etched for 15 min at 1.0 μ Hg in argon at 10 mA 500 V.

PLATE 2(*b*). Pure Iron X 300 cathodically etched for 30 min at 0.7 μ Hg in argon at 5 mA 3.2 kV.

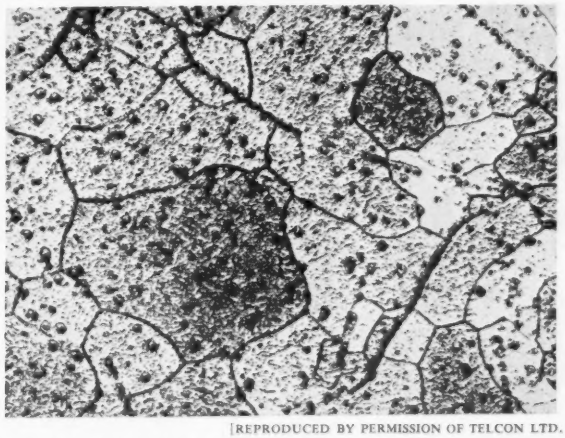

[REPRODUCED BY PERMISSION OF TELCON LTD.

PLATE 4(*a*). Telcoseal 5 X 165 cathodically etched for 60 min at 0.6 μ Hg in argon at 5 mA 3.2 kV.

PLATE 3(*a*). Mild Steel X 500 cathodically etched for 20 min at 0.4 μ Hg in argon at 4 mA 2.5 kV.

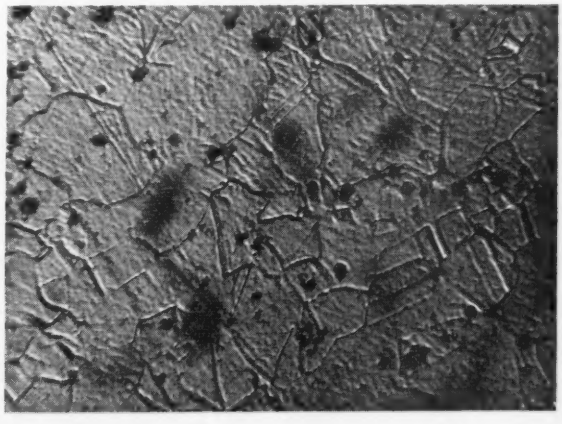

PLATE 4(*b*). Copper X 500 cathodically etched at high pressure (500–100 μ Hg) in argon at 5 mA 3.0 kV in apparatus shown in Fig. 3.

Vol.
9
959/60

was satisfactory with a current of 5 mA for specimens of about 2.5 cm dia. Under these conditions the quality of etch pattern depended only upon the duration of bombardment.

Etching at high current density is not recommended for metals of low melting point and low thermal conductivity, even with water cooled supports, because of the risk of melting the specimen. An example of such a metal is bismuth.

Unpolished specimens were also bombarded in the apparatus. Copper which had been smoothed with 600 grit size abrasive paper but left unpolished was bombarded for 35 min with H.T. conditions of 10–30 mA, 500–1500 V. Although the scratches were not removed they were greatly reduced. The polishing effect of bombardment thus helped to diminish slight scratches left on the surface by mechanical polishing.

Etching at high pressure

An experiment was made to compare the etch patterns obtained at low pressure (0.5–1.0 μ Hg) with those at high pressure (50–100 μ Hg). Specimens of copper, phosphor bronze, mild steel and Telcoseal 5 were etched at a high gas pressure with the electrode system shown in Fig. 3.

The copper, phosphor bronze and mild steel specimens were etched for 30 min in an argon discharge operating at 5 mA and 2.5–3 kV. Examination under a low power microscope after bombardment indicated a less depth of etching than was obtained with the Penning cold cathode discharge. The difference could be seen with the naked eye ; Telcoseal 5 was bombarded in the same apparatus at 3.2 kV 5 mA for 1 hour but no etching was apparent after the treatment.

Comparison may be made between the etching efficiency of the two kinds of apparatus by deriving a figure proportional to the number of ions that fall on each square centimetre of the specimen when etched at low and high pressures. Such a figure may be approximately estimated from the simple expression :—

$$N \alpha \frac{i}{A} t,$$

where i is the total current (ion and electron), A the surface area etched and t the etching time in min. The expression assumes a constant current density over the etched surface and although the Penning system tends to concentrate the bombarding ions, the effect is small enough to be neglected

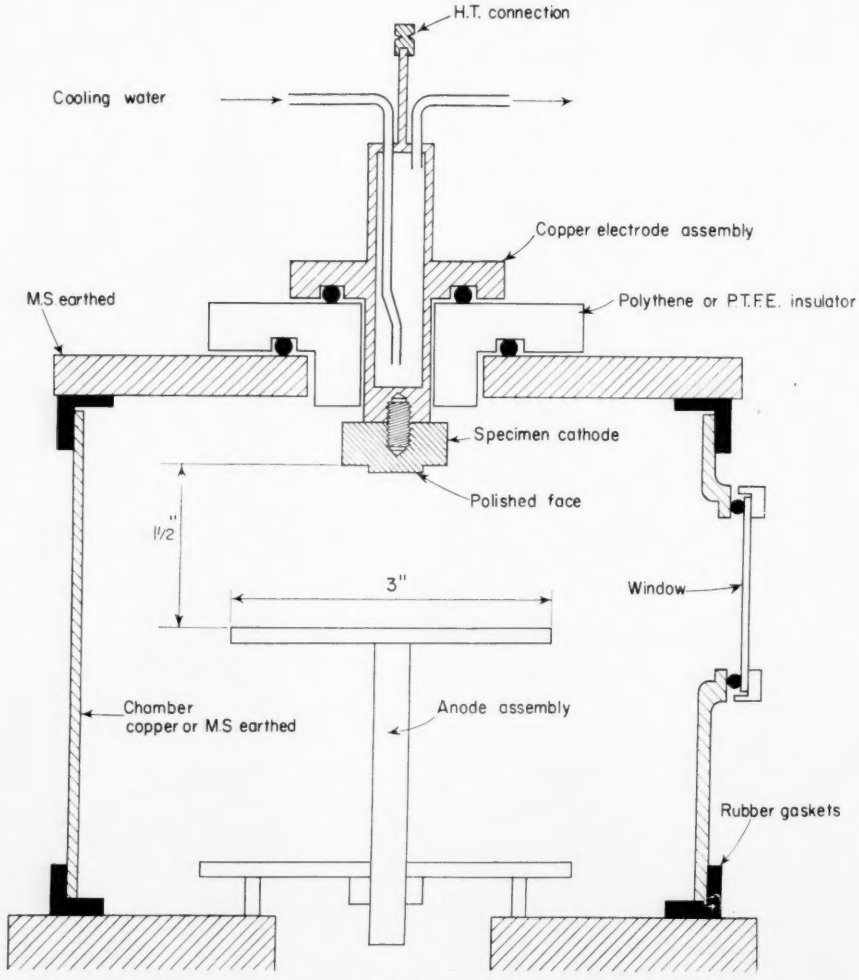

FIG. 3.

in practice. It is also assumed that the ratio of ions to electrons are the same for both discharges.

The copper specimen was etched under the same applied voltage in both sets of apparatus, therefore values for N in both cases can be compared. (One must not discount the possibility that positive ions strike the cathode with greater energy at low pressure because in the Penning system the ions are not scattered by collision with gas molecules to the same degree as occurs at high pressure.)

For copper bombarded at high pressure $i = 5$ mA, $A = 11.2$ cm^2, $t = 30$ min, $N = 13.4$ and in the low pressure experiment $i = 2$ mA, $A = 4.9$ cm^2, $t = 25$ min, $N = 10.2$. It should be noted that the total current used at low pressure was really 4 mA which was shared between the specimen and counter cathode. The larger value of A in the high pressure case was due to sputtering extending over the sides of the specimen.

Although N was slightly greater for the high pressure experiments, comparison of plates 2(*a*) and 4(*b*) shows that more metal was sputtered in the low pressure case. If the number of atoms sputtered per impacting ion was the same at high and low pressure working, then the difference in the rate of etching can be attributed to metal atoms sputtered from the surface in the high pressure discharge being returned to the cathode by collisions with gas molecules. Thus Holland's claim that the Penning system produces a higher effective sputtering rate, because less material is returned to the specimen, would appear to be confirmed by these experiments.

4. Conclusions

The photomicrographs show that the results obtained by cathodic etching compare in all cases with those given by chemical etching. However a suitable chemical etch could not be found for Telcoseal 5, but cathodic etching clearly revealed the crystalline structure. The writer found that the correct conditions for satisfactory etching in all cases could be obtained with the minimum of experiment and it is thought that in the development of new alloys this is an advantage because chemical methods often require a great deal of trial and error work prior to the final etch. When using the apparatus described here a power rating of 2–3 kV at 5 mA is probably satisfactory for most metals and only the duration of bombardment need vary from metal to metal.

The ability of the Penning system to produce etch patterns faster than the conventional discharge is an advantage especially when large numbers of specimens are to be etched, as in routine metallurgical testing.

Another advantage of the Penning system is its ability to limit the bombardment to the front face of the specimen for applied voltages above 1.5 kV. Therefore the specimen support is not bombarded and there is no need for screening to avoid extraneous sputtering. The focusing effect can be readily observed by the configuration of the plasma, a sketch of this can be seen in Fig. 4.

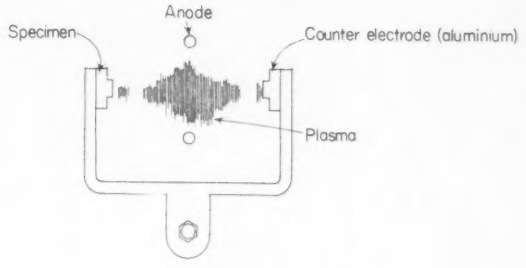

FIG. 4.

Acknowledgement

The writer wishes to thank Mr. L. Holland, head of the Vacuum Coating Research Laboratory at Edwards High Vacuum Ltd., for his guidance throughout the work, Mr. G. Siddall for producing the photomicrographs and Telecon Ltd., for the loan of their Vickers Projection Microscope. Also the writer thanks Mr. A. S. D. Barrett, Technical Director, for permission to publish this paper.

References

[1] D. M. J. McCutcheon ; *J. Appl. Phys.* **20**, 414 (1949).
[2] L. Holland and N. Sutherland ; *Edwards High Vacuum Research Report No.* 117.
[3] I. Popenova and A. Frimer ; *Zavodskava Laboratoriya* **21**, 432–436, (1955).
[4] P. Grivet ; *Symposium on Metallurgical Applications of the Electron Microscope, Inst. of Metals, London*, 30 (1949).
[5] L. Holland, ; *Brit. Patent No.* 779, 347.
[6] G. K. Wehner ; *Amer. J. Appl. Phys.* **29**, 217 (1958).

Vol. 9 959/60

Vacuum Deposition of Dielectric Films for Capacitors

G. SIDDALL

Research Laboratories, Edwards High Vacuum Ltd., Crawley, Sussex
(Received 17 November 1959)

The first part of this work deals with the evaporation of inorganic materials suitable for making thin dielectric layers for capacitors. The evaporation of a mixture of oxides, for example a glass, is also discussed, and the electrical properties of some glasses are given. The stability of metal oxide compounds at high temperatures is considered in relation to their free energies of formation. The reported vapour pressures of the components of the more commonly used glasses show that their evaporation is not possible from a single vapour source without separation of the components by fractional distillation. The second part of the report describes an experimental investigation into the preparation and properties of dielectric films of silicon oxide in the thickness range 0.14 to 1.7μ produced by the evaporation of silicon monoxide at varying rates. Capacitors of 0.001–0.01μF/cm² have been deposited on 'Pyrex' glass using evaporated aluminium films for the conducting-plates, and measurements of the electrical properties of the silicon oxide films have been made. The working voltage of capacitors in this range lies between about 12 and 60 V depending upon the thickness of the dielectric and upon the working temperature. At temperatures above 200°C the values of loss angle and leakage current are generally unacceptable. It is established that the rate of deposition of the oxide layer has a marked effect on the loss angle, dielectric constant and leakage current. Generally the lowest values of leakage current and loss angle are obtained with rates of deposition below 5Å/s. The dielectric constant of slowly deposited silicon oxide films is less than that of bulk silica, which is attributed partly to their lower density. The work carried out with silicon oxide shows that satisfactory dielectric films for capacitors can be made by the evaporation technique.

Vo
9
1959

Introduction

There is an increasing demand for small capacitators having a working temperature of 200°C. At this temperature, organic dielectrics are generally unstable and electrically unsuitable. Many inorganic dielectrics can be used at high temperature but thin layers must be used to obtain high values of capacitance per unit area of dielectric. Thin dielectric films can be prepared by evaporating inorganic substances in vacuum and by condensing the vapour on a suitable supporting base. The advantages of vacuum deposited metal films on organic dielectric foils are already well known[1] but high values of capacitance per unit area are difficult to obtain, because the thickness of the dielectric must be at least 10–12μ to enable the material to be handled and rolled and also to absorb the latent heat of condensation of the deposited film without melting or decomposing the base.

Thus in addition to the advantage of a higher working temperature, the capacitor made by evaporation of the dielectric also has the advantage of smaller size. However, the use of a very thin dielectric implies a lower safe working voltage, but now that transistor circuitry is established a need for lower working voltage components has arisen.

Many papers dealing with the evaporation of dielectric films have already been published, but they have been concerned principally with the optical properties rather than the electrical properties of dielectrics. Although the optical and electrical properties of dielectrics are analogous and are related by the Electromagnetic Theory the relationship is not simple over the complete spectrum of frequencies because of the dispersion. However, it is of interest to review some of the more important results of the work on optical films, because the physical requirements of an insulating dielectric are similar. One important difference does exist. An insulating layer must be free from structural defects which might cause repeated breakdown, or existing defects must be rendered ineffective.

The following properties are desirable in a dielectric layer suitable for making capacitors :—

(*a*) It must have stable physical and electrical properties over the working temperature range of the capacitor.

(*b*) The value of dielectric constant should be as high as possible, but this will necessarily be a compromise with the values of loss angle and dielectric strength. Materials having a high value of dielectric constant usually possess a lower dielectric strength or greater loss angle, both of which are undesirable properties.

(*c*) Finally, the material must be easy to deposit by evaporation, and ideally must have a uniform and homogeneous structure reasonably free from pinholes.

Much of the required information on deposited techniques

and film structure is available from electron and optical microscope studies of thin inorganic films. The first part of the report is a review of the relevant work that has been carried out on the evaporation of dielectrics. Some of the electrical properties of glasses have also been summarized.

The second part of the report gives the method of preparation and the results of tests on experimental capacitors using evaporated silicon oxides, deposited on " Pyrex " glass, with evaporated aluminium films for the conducting electrodes. This work has been carried out in order to reveal and solve some of the basic problems which will be met in the production of capacitors by vacuum deposition.

Part I. Evaporation Characteristics and Properties of Dielectric Materials

1. Elementary metal oxides

A complete account of the work carried out on the preparation and properties of vacuum deposited dielectric films up to 1956 has already been given by Holland[2], but those papers of direct interest to the deposition of insulating films will be referred to here. The optical properties of some materials have also been given by Heavens and Smith[12].

Titanium dioxide seems an obvious choice for making a thin dielectric for a capacitor, because it is already used in bulk and its electrical properties are well known, but the preparation of TiO_2 films by evaporation is made difficult because of the dissociation and reaction with the source which occur when the dioxide is raised to its melting point in vacuum. The deposited films are light-absorbing, and probably consist of a mixture of lower oxides of titanium. Holland has found that the optical absorption of evaporated films of the black oxide (TiO) is decreased by evaporating slowly. The degree of oxidation can also be increased by raising the oxygen pressure in the chamber to 0.1μHg.

Films having a rutile structure are obtained by heat—oxidation at 450 °C in air of titanium metal films deposited rapidly at a low gas pressure. This method could be used for making oxide films on metal foil, but Hass[3] found that the rate of oxidation of thick titanium films (greater than 1000Å) is as low as 20Å/h at 450 °C. Hiesinger and Koenig[4] have made films of TiO_2 by reactive sputtering in pure oxygen and have shown that they possessed a rutile structure after heating to 450 °C.

Apart from the difficulty of preparing TiO_2 and titanate films in suitable form, both the evaporation and sputtering techniques require very large power supplies. The evaporation source must be maintained at above 2000 °C and very heavy tungsten heating elements are needed. The current density for sputtering must be of the order 10 mA/cm² of cathode surface, so that the cathode or the work may be melted in the intense glow discharge.

Many other oxides which would otherwise be suitable, are also difficult to evaporate because of their very high melting points and low volatilities. It is fairly easy to deposit thin films of such oxides about 200Å thick, but thick films above 2000Å are much more difficult to deposit. Thus Hass was able to deposit $\lambda/4$-films of cerium dioxide (m.p. 1950 °C) using heavy tungsten heaters and very large power supplies. He found that the refractive index of CeO_2 films depended upon the temperature of the substrate. An increase of substrate temperature from 25 °C to 300 °C increased the index from 2.2 to 2.4 at $\lambda = 5500$Å. Evaporated CeO_2 films showed the same cubic structure as the bulk, and crystallized in no preferred orientation on amorphous substrates. The crystal size in the deposited film increased with increasing substrate temperature.

Alumium oxide, thorium oxide, tantalum oxide, and chromium oxide also have very high melting points but their preparation in thin film form might be made less difficult by reactive sputtering from the metal cathodes in an oxygen glow discharge.

The oxides of indium, iron, tin and cadmium, have a fairly high electrical conductivity[6] which could not be tolerated in a capacitor. The effective value of the loss angle would be increased by the presence of conduction current. Many other oxides and sulphides also have a high conductivity and would be unsuitable for the same reason.

Cryolite, sodium fluoride, lithium fluoride, boron oxide and zinc sulphide are volatile but they are also hygroscopic, and although it is likely that thick insulating films can be deposited, the stability of components made with these materials would be doubtful.

Bismuth oxide[6] and magnesium fluoride[7] can both be deposited readily, but the grains become large as the film thickness increase much beyond 2000Å, and recrystallization can occur when high base temperatures are used[8].

Silicon monoxide, tungsten trioxide and molybdenum trioxide are very volatile. They can be deposited to form amorphous layers with small grain size, and good adhesion to glass. They are not hygroscopic and are chemically stable at low oxygen pressures. Of all the simple chemical compounds that have been studied in thin film form, probably silicon monoxide has the most suitable physical properties for making electrically insulating layers. Silicon monoxide has been studied extensively by Hass[9] who found that the optical constants and the physical structure of films varied considerably with the rate of evaporation and the residual gas pressure, at low rates of evaporation or high residual gas pressure a film is deposited whose optical constants are nearer to those of silica, whereas at high evaporation rates and low gas pressures, the deposit contains excess silicon.

2. The evaporation of glasses

Some borates, phosphates, and silicates, which can exist in a glass-like state, can be evaporated in vacuum, but many such compounds are hygroscopic. One of the exceptions is calcium silicate which has been evaporated with iron oxide (Fe_2O_3) from tungsten filaments to make optically absorbing films of neutral density. Holland, Moutou, and Hacking[19] found that Fe_2O_3 was reduced to the magnetic oxide, and that a hard glassy layer of mixed oxide and silicate was deposited. This is probably the earliest reference to the evaporation of a glass. The melting points of calcium silicate (1540 °C) and magnetite (1565 °C) are very similar, thus it is possible that the mixture was evaporated without undue separation of the components.

Vol. 9 59/60

Hanlein[11] has proposed a method of depositing films of glass by evaporation of the components from separate sources. Mixtures of materials of very different vapour pressures, which would normally separate by fractionation can be deposited to make a film of a given composition. Hanlein describes a method of coating aluminium foil with a flexible insulating film of glass by a continuous process. The foil is passed from atmosphere through vacuum locks to the coating chamber, where it is first cleaned by ionic bombardment in a glow discharge. It is then passed over the various sources, and is conduction cooled by water-cooled cheeks. The same process is described in a patent specification by Siemens–Schukertwerke[20]. It is claimed that the glassy acid network—forming oxides of silicon, boron or phosphorous can be deposited on a metal tape by evaporation. Upon heating the coated metal tape in air, the metal surface is oxidized and forms the appropriate glassy metal silicate, borate or phosphate combustion with the deposited coating. The evaporation of an alkali or alkaline earth oxide from a separate source is also described, thus it is not necessary to rely on the metal foil to provide the basic oxides.

Glass films have also been deposited for making coloured absorbing coatings on glass lenses[21]. Coloured films of up to 20 μ thick were deposited by the evaporation of the bulk coloured glass from a single tungsten crucible. No reference to the composition of the deposit was made.

When considering the possibility of evaporating a glassy mixture of oxides, it is necessary to have some data on the vapour pressure of different oxides, and some comparison of their stability in vacuum at high temperature. The stability of an oxide is determined by the free energy of its formation from the metal in the presence of excess oxygen at a given temperature. The stability of an oxide in vacuum is complicated by the fact that the partial pressure of oxygen in the chamber may be less than the dissociation pressure of the oxide (i.e. the pressure of oxygen required for its stable existence). Since most oxides are exothermic, the free heat of formation decreases considerably with increasing temperature so that the possibility of dissociation becomes greater. Most metal oxides also have rather high melting points, thus it is likely that some decomposition (or reaction with the source) will take place before evaporation commences.

Table I shows the principal acid and basic oxides that are used in glasses, together with their melting points and some vapour pressure data, collected from three different texts[24, 25, 26]. The values of free energy of formation of the oxides at the temperature indicated (usually the melting point) are also given in Table I, and can be compared. The highest free energies of formation at the melting point are possessed by the acid forming oxides of phosphorous and boron and the basic oxides of aluminium, vanadium and lanthanum. The thermodynamic calculations have been carried out from the collected data given by Kubaschewski and Evans[22] and by Kubaschewski and Hopkins[23]. Some of the free energy calculations are only approximate, because heat capacities have been neglected where they were not known. The latent heat of fusion of the oxide is not included in the free energy value. Some of the vapour pressure data have been calculated from the Clapeyron–Clausius equation. When the latent heat of evaporation was not known, this was calculated assuming that the oxide in question obeyed Trouton's rule.

The table has been roughly divided into three sections. The first section shows the acid oxides, of which all except silica are very volatile. Silica deserves some attention since it is the principal constituent of many glasses. From the vapour pressure data it can be seen that a temperature of nearly 1700 °C will be required to obtain rapid evaporation. At this temperature the heats of formation of silica and silicon monoxide are nearly equal and at about 1800 °C, they are exactly the same ($\Delta G_{2073} = 120$ Kcal/mole). The

TABLE I

Oxide	M.P. °C	B.P. °C	Vapour Pressure Data		Free Energy of Formation	
			mm Hg	Temp. °C	Kcal/mole	Temp. °C
$2B + 3/2\ (O_2) \rightleftharpoons B_2O_3$	450	1500	116	1000	−316	450
$2P + 5/2\ (O_2) \rightleftharpoons P_2O_5$	570	591	10	442	−265	570
$Si + 1/2\ (O_2) \rightleftharpoons SiO$	Subl.	2300	—	—	−115	1710
$SiO + 1/2\ (O_2) \rightleftharpoons SiO_2$*	1710	3500	7.6	1710	−124	1710
$2Na + 1/2\ (O_2) \rightleftharpoons Na_2O$	920	1600	—	—	− 37.6	1227
$2K + 1/2\ (O_2) \rightleftharpoons K_2O$	—	—	—	—	− 27.8	1227
$Pb + 1/2\ (O_2) \rightleftharpoons PbO$	890	1472	10	1085	− 31.5	890
$2Li + 1/2\ (O_2) \rightleftharpoons Li_2O$	Subl.	1300	10	1056	−117.7	727
$2Sb + 3/2\ (O_2) \rightleftharpoons Sb_2O_3$	656	1425	10	666	−123.3	656
MoO_3*	795	1480	10	1043	−116.1	727
V_2O_5*	670	1730	10	1206	−312.1	670
Al_2O_3*	2050	3250	1	2148	−255.0	1727
$Ba + 1/2\ (O_2) \rightleftharpoons BaO$	1923	—	0.1	1742	−109.7	727
$Ca + 1/2\ (O_2) \rightleftharpoons CaO$	2572	3400	0.1	2271	− 96.9	1727
CeO_2*	—	—	—	—	−216	727
$2La + 3/2\ (O_2) \rightleftharpoons La_2O_3$	2320	—	—	—	−329.7	1227
$Mg + 1/2\ (O_2) \rightleftharpoons MgO$	2640	2800	—	—	− 78.8	1727
$Sr + 1/2\ (O_2) \rightleftharpoons SrO$	2430	3000	1	2068	−116.0	727

*The free energies of formation refer to the reaction with the lower oxide.

heat of formation of SiO is steadily increasing and that of SiO_2 is decreasing with increase in temperature. At 1700 °C the probability of silica dissociating to form the lower oxide is thus quite high, although the reaction can be controlled by providing a high partial pressure of oxygen in the evaporation chamber as pointed out by Holland[2]. It is likely that the evaporation of silica at temperatures below the melting point is possible only because of the dissociation reaction,

$$2SiO_2 \rightleftharpoons 2SiO + O_2.$$

The other two sections of Table I show the basic oxides, roughly divided into groups having high and low vapour pressures respectively. The factors involved in evaporating a mixture of oxides can now be fully understood. Let us consider the evaporation of a typical soda-lime glass and a typical borosilicate glass of the " Pyrex " type. When a soda-lime glass is heated, the reaction

$$2Na_2O \rightarrow Na_2O_2 + 2Na$$

would start at about 450 °C, and sodium metal would diffuse to the surface and evaporate. The sodium would be free to combine with the residual gas in the chamber, and the deposited film could consist of oxide, hydroxide and carbonate (after exposure to atmosphere). At about 1000 °C it can be safely assumed that the sodium and potassium oxides have dissociated and that the higher oxide and the free metal have evaporated. Evaporation of the remaining components SiO_2, CaO, Al_2O_3 and MgO, would not take place until the temperature of the source was at least 1700 °C. Fractionation of the free SiO_2 would occur, leaving the lower vapour pressure oxides of calcium, aluminium, and magnesium on the evaporation source.

Borosilicate glasses do not usually contain sodium or potassium, thus boric oxide is the most volatile component with melting point at 450 °C and a calculated vapour pressure of over 100 mm Hg. at 1000 °C. The first layer deposited would contain a very high percentage of boric oxide, which rapidly takes up water vapour to make boric acid. Separation of the remaining oxides could occur in the same way as in the heating of soda glass. Apart from the separation of the components there are also the problems of reaction with the source and partial dissociation of the oxides, either of which may result in the deposition of layers containing free metal. Such layers would be energy-absorbing, giving high values of absorption coefficient or loss angle.

3. Some electrical properties of glasses

Morey[10] states that better condensers can be made from suitable glasses than from any other material, with the possible exception of mica which can be divided into thin sheets. In view of this statement and the recent work on the deposition of glass films by simultaneous evaporation of the components[11] the manufacture of vacuum deposited capacitors using glass is theoretically and practically possible. It is necessary to know the differences between the electrical properties of the basic groups of glasses, in order to select those having most suitable electrical and evaporation properties for use in vacuum deposited capacitors. The term " glass " can cover a very wide range of different mixtures or compounds, but for simplicity, this discussion deals particularly with glasses based on mixtures or compounds containing silica, boron oxide and certain metallic oxides.

Electrical conductivity

The surface of some glasses can absorb varying quantities of water, due to the presence of hygroscopic silicates[13], thus the surface conductivity is appreciably greater than the value indicated by the bulk conductivity. Guyer[14] has given the changes in volume resistivity of several Corning glasses as a function of temperature, and Fulda[15] has studied the effect of composition on the surface resistivity of a range of glasses. The general conclusions to be obtained from a study of the extensive literature are that fused silica has the highest values of volume and surface resistivity (up to 10^{15} ohm cm) and that additions of metallic ions, notably sodium can decrease the resistivity to values of the order of a few ohm cm. The difference is most marked at temperatures above about 500 °C when the mobility of the Na^+ ions is high. The addition of calcium oxide to a glass can reduce its conductivity. Borosilicate glasses also have low conductivity. Kirby[16] reviews much of the work that has been carried out on the electrical conductivity of glass.

Dielectric properties

Guyer[14] has also studied the variation of power factor* and dielectric constant with both frequency and temperature of several different types of glass, Strutt[17] has carried out similar measurement on five different glasses, one of which corresponds to " Pyrex " borosilicate glass. Stevels[18] has examined the effect of composition on the dielectric losses of a wide range of glasses.

Generally it is observed that over a very wide range of frequency the dielectric constant of glasses increases slowly with increasing temperature. The tangent of the loss angle increases approximately exponentially with temperature. For low frequencies, the displacement current is rapidly masked by the conduction current as the temperature rises. At frequencies below 1 Kc/s Morey suggests that 80 °C is the limit of stability for soda–lime glasses and 120 °C for borosilicate types. Above 10 Kc/s soda–lime glasses would be useful up to 140 °C and the borosilicates up to 240 °C.

The value of loss angle tangent (tan δ) at 25 °C, for borosilicate types increases from about 0.004 at 1 Mc/s to 0.01 at 1 Kc/s, most glasses have a value of tan δ at 25 °C lying between 0.01 and 0.03 at 1 Kc/s, but there is often a factor of 2 between the results of different observers for identical glass compositions.

The dielectric constant of glasses varies from about 3.78 for fused silica to about 8 for high density lead glasses. Although the dielectric constant of a glass can be increased by the addition of metallic oxides, this advantage is often outweighed by the increase in the loss angle, particularly at the higher temperature when the metallic ions have a high mobility.

Capacitors made from soda–lime glass would be useless for tuned circuits above about 100 °C due to the conduction current which would have a damping effect on a resonant circuit.

* For small values of loss angle, tan δ is very nearly equal to the power factor cos $(\pi/2 - \delta)$.

Vol. 9 959/60

Part 2. Some Dielectric Properties of Evaporated Silicon Oxides

It has been shown in the earlier part of this work that the composition of a thin dielectric film deposited by evaporation in high vacuum is generally different from the bulk. The evaporation of complex compounds or mixtures introduces many variables, due to the different state of oxidation of the separate components, and the changes in composition which occur.

Apart from investigating the possible production of insulating films for capacitors by evaporation, the aim of this experimental work was to obtain data on the electrical properties of thin dielectric films. In order to relate these to the bulk properties it was decided to limit the scope of the investigation to one material. Silica was chosen because of its good electrical properties at temperatures approaching 200 °C. It is also known that silica can be deposited readily by the slow evaporation of the monoxide. Silica is the principle component of many useful glasses and the properties of such glasses depend upon the presence of other acid or basic oxides. A study of the electrical properties of silica glass films made by evaporating the monoxide at varying rates has therefore been made as a first step in a general investigation of insulating films for capacitors.

1. Deposition technique

Plant

A vacuum coating plant having a 12 in. *dia.* " Pyrex " glass bell jar was used for making the conducting electrodes and the dielectric films. This bell jar could be evacuated to a pressure of 0.1 μHg in less than 10 min. A 750 W radiant heater working at 110 V was fitted inside the chamber, and was capable of raising the glass substrates to 300 °C in 15 min. Temperature was measured to within $\pm$10 °C by means of a chromel-alumel thermocouple. An H.T. supply of 50 mA at 3 kV was used for ionic bombardment cleaning and a shielded two electrode system as recommended by Holland[27] was fitted. This system was arranged to prevent direct bombardment of the work by high energy electrons, which Holland has shown can cause decomposition of hydrocarbons in the residual vapours thereby contaminating the work surface. Two independent L.T. power supplies for heating the filaments were used. It was therefore possible to control the temperature of two different sources at the same time.

Vapour sources

Tungsten foil boats were used for evaporating the silicon monoxide. The cross-section of the foil was 12.5 $\times$ 0.25 mm and a current of 200 A at 10 V was available for heating the foil to about 1700 °C. This temperature was necessary for evaporating at very high rates of the order 30 Å/sec. Silicon monoxide* lump was bound to the tungsten heater with thin tungsten wire. Aluminium for the capacitor electrodes was evaporated from helical coils of 3-strand 0.5 mm *dia.* tungsten wire. A current of 60 A at 12 V was available for heating the filament.

Method of making capacitors

At least two methods of making capacitors by evaporation are possible. In one method the dielectric film is deposited directly on a thin metal foil followed by a top metal electrode ; in the other method a metal/dielectric/metal multilayer is deposited on a glass or ceramic base. The second method was used throughout this work. The first experiments were made with multi-layers of aluminium/silicon oxide/aluminium deposited on ordinary soda-glass microslides measuring 3 in. $\times$ 1 in. The evaporation of silicon monoxide was carried out at a pressure lower than 0.1 μHg because silicon monoxide evaporated at a high pressure is likely to have a porous structure, making the films soft and non-adherent to the glass. The gettering effect during the evaporation is very marked, showing the rapid absorption of residual gases.

Electrical contacts of colloidal silver $\frac{1}{4}$ in. wide were baked on each end of a microslide, which was afterwards washed in a detergent then in water and followed by vapour degreasing in iso-propyl alcohol for 10 min. The slide was placed in a masking jig to prevent the first aluminium film from connecting both silver contacts. Glow-discharge cleaning was carried out for 4 min. before each evaporation. A charge of 3 in. of 20 s.w.g. 99.95 per cent pure aluminium wire was evaporated completely to make each capacitor electrode, the distance from source to substrate being 10 in. The thickness of the aluminium films was of the order 1500Å. After each evaporation, the masks were adjusted to give the desired " interleaving ". There was no evidence of bad contact between the aluminium and the silver contact strip, provided that a very thin film of silver paint was brushed on, and that the silver film was burnished after firing. It is known that bad contacts can occur between a silver contact strip and a very thin evaporated layer but this trouble did not arise with thick layers of aluminium.

Single-layer dielectric films of silicon oxide always had a number of low resistance leakage paths which gave the capacitor a fairly high conductivity. These faults were found to be due to three principal causes.

(*a*) Diffusion of aluminium round the edge of the plate causing short circuiting.

(*b*) Pinholes in the film.

(*c*) The occurrence of a weak point in the dielectric at the sharp step in the bottom aluminium film.

The diffusion of aluminium round the edges of the plate was overcome by masking a 1/16 in. strip along the edge during the second aluminium evaporation. The effect of pinholes was reduced by using a double layer of silicon oxide and burnishing the first layer with a clean " Selvyt " polishing cloth. Later in the programme however the two layer method of overcoming pinholes was not used because pinholes could be rendered ineffective by discharging a 4 μF paper capacitor several times across the aluminium electrodes.

Fig. 1(*a*) illustrates the effect of a sharp step in the lower aluminium film, and the diagrams shows the obvious weak point in the dielectric. Good capacitors could be made by evaporating a top layer of aluminium which did not cross the edge of the lower aluminium film, but it was difficult to make

* Silicon monoxide containing 95 per cent SiO is manufactured by the Union Carbide Co.

Vo 9 1959

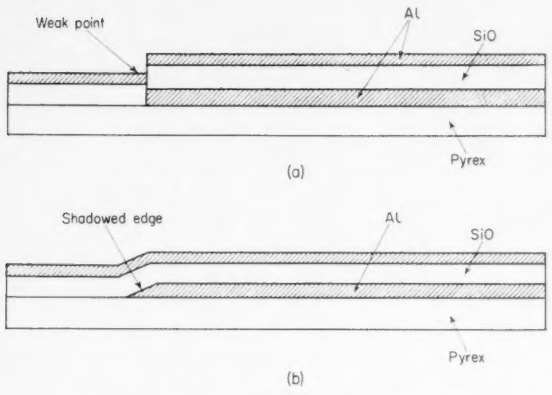

FIG. 1. The construction of a thin film capacitor deposited on a glass base. (*a*) shows a sharp step with the corresponding weak point in the dielectric and (*b*) shows a shadowed step.

contact to the top electrode of such a capacitor. This method was also not considered suitable because it would prevent the deposition of multilayers of alternate conductor and insulator to obtain very high values of capacitance, a technique which might be used in production. Aluminium films having a diffuse edge, rather than a sharp step were deposited. It was found that by supporting the mask about 1 mm away from the glass plate, a gradual decrease in thickness was obtained. No further trouble was experienced with breakdown at the edge of the lower aluminium film when the shadowing method was used, as shown in Fig. 1(*b*).

Thick layers of silicon monoxide (10,000Å) on soda–lime glass peeled or " crinkled " after a short period of exposure to atmosphere, the length of time varying from a few seconds

FIG. 2. A poorly adherent film may crinkle due to the relief of stresses set up during deposition. This effect is shown in the photomicrograph at 60 × magnification.

to a few days. This effect is shown in Fig. 2 at 60 × magnification. It was assumed that stresses were set up in the film during its deposition[18], and when the film became thick the stresses were great enough to tear the film from the base. This was often observed in thick films, and was prevented by annealing the film to remove the stresses. This was done by heating the substrate during deposition or by heating the total film combination after deposition. (*Note* : the annealing method is not always successful for thick films if there is also a big difference between the temperature coefficients of expansion of the film and base.) Although heat treatment at 250 °C prevented some films peeling from soda glass, it merely delayed the effect in others. It was observed that the silicon oxide peeled first where it came into contact with the glass itself.

It is known that the surface of soda glass may contain hygroscopic silicates and hydroxides[13] and the reaction between soda glass surfaces and heat-oxidized titanium films has already been studied in this laboratory[20]. It is probable that the hygroscopic components absorb water vapour from the atmosphere thus destroying the adhesion of the silicon oxide film. It was also observed that peeling always started at the edge of the film, and could be enhanced by body-heat or moisture, when holding a slide at the edges. When " Pyrex " glass slides were used and the silicon oxide films were annealed at 250 °C during deposition, peeling was a very rare occurrence.

The films were allowed to cool in vacuum to 100 °C before removal from the chamber. Fig. 3 is a photograph of two typical capacitors on " Pyrex " glass slides 3 in. × 1 in.

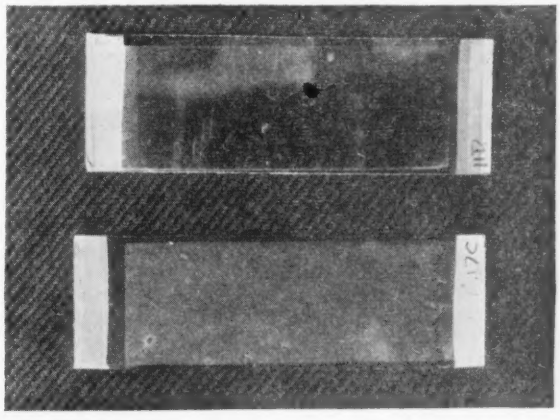

FIG. 3. A photograph of two typical capacitors deposited on Pyrex glass slides 3 in. long by 1 in. wide.

2. Measurements

Optical

The thickness of the insulating films was measured by multiple beam interferometry using Tolansky's technique[30]. The Fizeau fringe system was obtained with monochromatic light. (λ = 5460Å) and examined in reflection. An accuracy of measurement of ±5 per cent was obtained for thick films above 1000Å. Some difficulty was at first experienced in measuring films several half-wavelengths thick. During each evaporation a selected piece of $\frac{1}{4}$ in. thick plate glass was placed on the work surface, and was suitably masked to give the step for thickness measurement. It was necessary to make an oblique step by shadowing the edge slightly, otherwise at a sharp step it was difficult to follow the fringe system and find the order of interference (coincidence of fringes is obtained for a step of $\lambda/2$ or a multiple, because the fringes are $\lambda/2$ apart).

Some of the optical test plates, partly coated with an oxide

film were also used for measurements of refractive index. These measurements were made to provide a rough check on the calculated values of dielectric constant rather than to establish any relationship between the optical and electrical constants.

The refractive index of the film was measured very simply by Abeles' method[31]. A piece of the $\frac{1}{4}$ in. plate glass having half of one surface coated with a film of oxide, was placed on a goniometer table and illuminated by a collimated beam of monochromatic light. A polarizing element was placed in the collimator. The division between film and glass was viewed by means of a telescope with the eye-piece removed. The polarizer was rotated to give a minimum reflectance from the glass, and the table and telescope were rotated to obtain equal reflectance from glass and film. The reflectance from each half changed rapidly in opposite sense, and the polarizing angle could be obtained accurately within a few minutes of angle of movement, from direct readings of the scale on the goniometer table. It can be shown that when the reflectance of the coated and uncoated parts of the specimen are equal then the corresponding angle of incidence φ bears a simple relationship to the refractive index of the film so that,

$$\tan \varphi = n/n_o$$

Where n_o is the refractive index of air, which was taken to be unity. There is some uncertainty in Abeles' method for measuring thick slightly absorbing films, and for films of index much greater than that of the support, but great accuracy was not required in these measurements, which were made only to confirm the general tendency towards higher values of dielectric constant with increasing rate of deposition.

Capacitance and loss angle

Effective parallel capacitance (C) and tangent of the loss angle ($\tan \delta$) were measured directly with a Marconi Universal Bridge type TF 868/1. Measurements with the bridge could be made at frequencies of 1 Kc/s and 10 Kc/s, and it was also established that the voltage across the component under test did not exceed 12 V peak at 1 Kc/s and 1.5 V peak at 10 Kc/s in the worst out of balance condition on one range. Values of effective parallel capacitance could be obtained with an accuracy of ± 1 per cent and values of $\tan \delta$ could be obtained to about ± 5 per cent. For values of $\tan \delta$ below .001 the accuracy was as low as ± 10 per cent, particularly at 10 Kc/s. This was not very important however, because in the high temperature range the values of $\tan \delta$ were much higher.

A small oven capable of holding two capacitors was used for baking to high temperatures. A chromel-alumel thermocouple was used to measure up to 500°C. A three-terminal method of measuring capacitance was used, and the inner steel case of the oven was connected to the earth point on the bridge. The capacitors were not provided with guard rings (although these could have been also deposited by evaporation). It was assumed that edge effects could be neglected where the separation of the conductors was small compared with their area. It was also assumed that the simple expression for the capacitance of a parallel plate system would be accurate enough for calculating the values of dielectric constant.

Electrical losses in the measuring system

It can be seen from Figs. 1 and 3 that a very short distance separates the lower aluminium film from the contact strip connected to the top aluminium electrode. The surface conductivity of glass increases with temperature, so that conduction across this gap could be responsible for part of the observed dielectric losses. The conductivity of the insulating material which separated the measuring leads into the oven was also considered, but the distance between the leads was much greater (2 in.). The conductivity of the oven insulating material was determined first. The oven was raised to 500°C with no capacitors connected. A 12 V battery and a microammeter were put in series with the lead-through terminals. No current was detectable using an instrument of 25 μA full scale deflexion. This was a rough test, but was sufficient for the purpose, because the d.c. current flowing in a typical capacitor at 500°C was greater than 100 μA. The a.c. losses were not measured directly but were observed to be negligible when the bridge was connected to measure the capacitance of the leads.

A pair of parallel silver contact strips were baked on a "Pyrex"-glass slide and on a soda-glass slide to leave a gap 1/8 in. wide by 1 in. long. These slides were put into the oven and the leads were connected in series with the battery and the microammeter. Measurements of the current flowing were made at temperatures up to 460°C.

Dielectric strength and leakage resistance

A simple comparison of the break-down strength of different films was made by counting the number of defects occurring at a given applied voltage. Voltage was increased in 12 V steps by means of batteries, and an approximate value of the number of faults occurring at each voltage was obtained by counting the voltage pulses across a fixed resistor in the battery circuit. The time constant of the CR network was arranged to be less than 0.2 μsec. The pulses were counted using a Cintel μsec. counter which had a rise time less than 1 μsec and could count at a repetition rate of up to 1 Mc/s. This counter resolved pulses of amplitude 15 V spaced apart by 1 μsec or greater. It was found in practice that the counter could respond to pulses made with a 12 V battery, and although very few breakdowns were observed at 12 V several pulses were recorded on first switching on the battery. The type of switch used was important. Best results were obtained with a microswitch which produced up to 5 spurious pulses for one operation, compared with 200 pulses when contact was made by touch. Although the resolution time of the counter was short, it was not short enough to resolve all the pulses, because some were coincident and probably variable in duration. Therefore the results could be used only for comparison of different capacitors.

The d.c. conductivity of the dielectric was measured using a microammeter (25 μA F.S.D.) and a 12 V battery in series across the capacitor electrodes. A series of shunting resistors could be switched across the meter in order to extend the range. The meter was protected from serious overload by a series resistor of 10 KΩ.

Vo
9
1959

3. Results

Surface conductivity of the substrate glasses.

Values of the current flowing between two silver contact strips 1 in. long separated by 1/8 in. have been plotted against temperature in Fig. 5. The potential difference was maintained by a 12 V battery. The results are shown for " Pyrex " (borosilicate) and for " Chance " microslide glass (soda-lime). At 460°C a current of 35 μA passes between the silver electrodes on the soda glass compared with less than 1 μA on the " Pyrex " glass. The superiority of " Pyrex " was established definitely by this experiment.

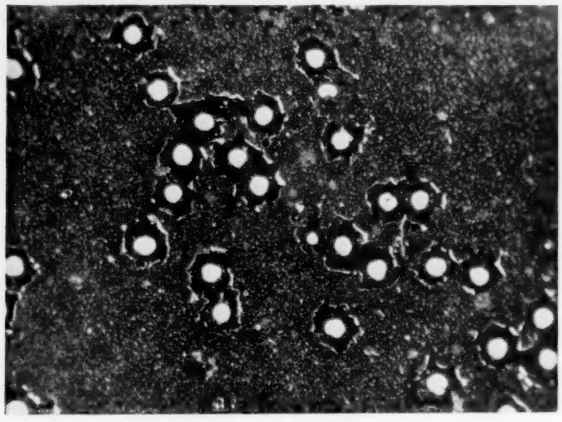

FIG. 4. The photomicrograph at 60 × magnification shows the effect of breakdown through the dielectric.

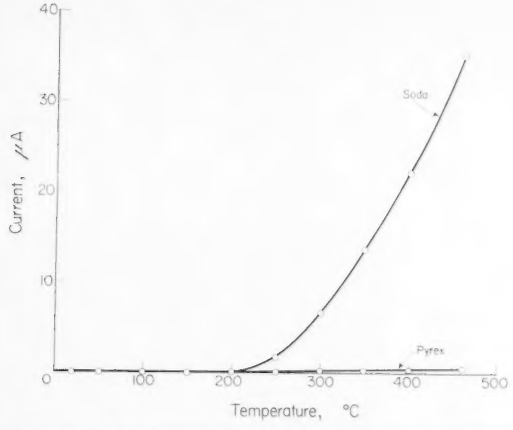

FIG. 5. The surface resistance of two types of glass on which capacitors were deposited is given in terms of the current flowing with a potential of 12 V across two parallel silver contacts 1 in. long separated by 1/8 in. The results are shown for temperatures up to 460°C.

Variation of dielectric constant with rate of deposition

The complete results for 14 batches of 4 capacitors are shown in Table II. The rate of deposition was varied in the production of these batches, from 0.55Å/sec to 29.5Å/sec. The average values of capacitance of four slides have been calculated similarly the thickness shown is the average of four measurements. The dielectric constant has been calculated from average values of thickness and capacitance using the simple expression for a parallel plate capacitor. The average area of each capacitor was 12.5 cm^2 and the necessary correction to bring C to practical units was made. The increase of dielectric constant and refractive index with rate of deposition is shown in Fig. 6.

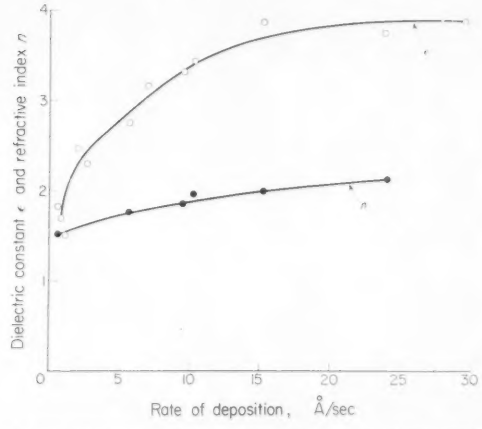

FIG. 6. The dielectric constant and refractive index of vacuum deposited silicon oxide films are plotted against rate of deposition.

Variation of dielectric losses with rate of deposition

The measurements of loss angle tangent (tan δ) were made at 20°C after the major faults had been cleared by

TABLE II

Rate of Deposition Å/sec	Thickness Å	Capacitance μF 1 Kc/s	Capacitance μF 10 Kc/s	Tangent of Loss Angle Tan δ 1 Kc/s	Tangent of Loss Angle Tan δ 10 Kc/s	Tangent of Loss Angle Tan δ 1 Kc/s (After baking)	Dielectric Constant ϵ	Refractive Index n
0.55	2910	.072	.070	.010	.008		1.81	1.51
0.83	6020	.031	.0305	.015	.013		1.68	
1.14	1370	.120		.018			1.48	
2.01	14,450	.019	.0185	.012	.008	.001	2.46	
2.65	9560	.027	.026	.014	.029		2.29	
5.7	8190	.037		.014		.002	2.74	1.75
7.05	6500	.051		.033			3.16	
9.5	17,200	.019	.0182	.037	.016	.003	3.31	1.83
10.3	13,600	.028	.027	.037	.019	.002	3.43	1.94
15.1	5560	.077	.076	.040	.018		3.84	1.98
24.0	10,100	.041	.0395	.042	.028	.0015	3.74	2.11
29.5	14,200	.030	.0293	.037	.018	.001	3.86	

discharging a 4 μF standard paper capacitor across the dielectric, but before any heat treatment was carried out. The loss angle represents the combined effect of the dielectric absorption losses and the d.c. resistivity, and it has been assumed that the inconsistent results are mainly due to variations in the d.c. resistivity of the capacitor, caused by the presence of high resistance paths across the dielectric and not necessarily by its bulk conductivity.

However, it was possible to draw rough curves which are shown in Fig. 15. The dielectric losses increased with rate of evaporation and were higher at 1 Kc/s than at 10 Kc/s. These results are in agreement with the observed variation of optical absorption with rate of evaporation. The higher losses at the lower frequency are characteristic of glasses and many other dielectric materials.

Dielectric strength

The comparison of dielectric strength obtained by measuring the number of breakdown pulses in a given time has already been discussed. The results for 5 capacitors at 20 °C are shown in Fig. 7. The number of pulses resolved

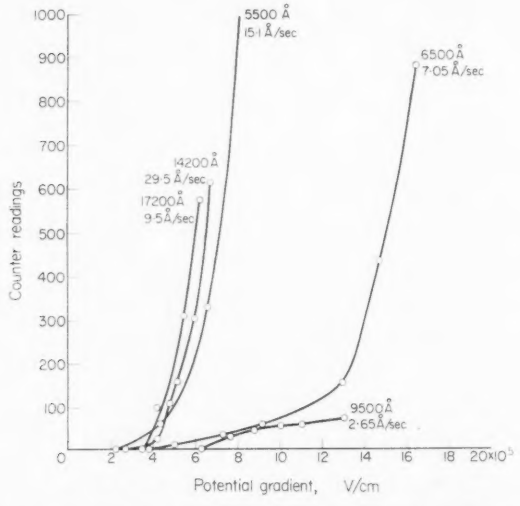

FIG. 7. The number of breakdown pulses recorded by means of an electronic counting circuit during the first 30 sec are plotted against applied voltage. The results are given for 5 capacitors.

by the counter in the first 30 sec at each applied voltage step is given, but in order to present the results more clearly, the applied voltage and thickness have been used to calculate the potential gradient. The thickness and rate of deposition are shown for each capacitor. Within the thickness range considered (5500–17,200Å) it is clear that slowly deposited silicon oxide films possess a greater dielectric strength. Insufficient results have been obtained to give definite limiting values of field strength, but it can be stated that breakdown becomes serious in the region 2×10^5–4×10^5 V/cm for films deposited at deposition rates above 10Å/sec. The breakdown strength can be improved by a factor of 2 when the deposition rate is reduced to 2Å/sec.

Fig. 8 shows how the number of breakdown pulses for a typical capacitor decreased with time of applied voltage at 20 °C. No breakdown pulses were recorded at 36 V. This

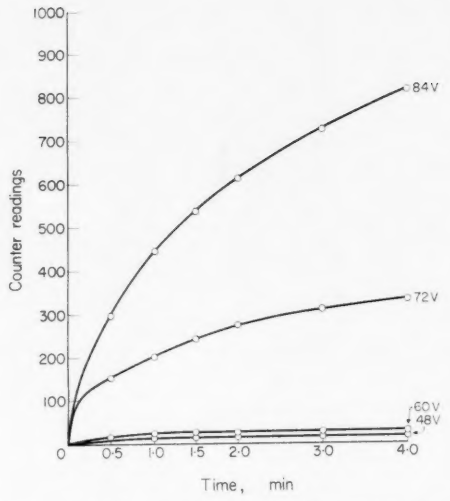

FIG. 8. The number of breakdown pulses counted for a typical capacitor are plotted against time for various applied voltages. The thickness of the dielectric was 14,200 Å and the film was deposited at the rate of 29.5 Å/sec.

capacitor had a dielectric thickness of 14,200Å deposited at 29.5Å/sec. The results show that breakdown occurred only during the first 60 sec at voltages up to 60 V. At 84 V the breakdown rate was greater during the first 30 sec and the total number of pulses continued to increase.

Leakage current

The changes in conductivity of capacitors at room temperature were very marked during the first minute. After the first impulse of charging current, the conductivity was observed to decrease quickly for the first 15 sec and rather more slowly up to 60 sec. After 120 sec the conductivity was decreasing slowly but was near enough to the final value for a reasonably accurate result to be obtained. The steady value was obtained only after a period of several hours.

The results of tests at 20 °C with 5 capacitors are shown in Fig. 9. Leakage current (μA) has been plotted against applied voltage, and the appropriate thickness and deposition rates are shown for each curve.

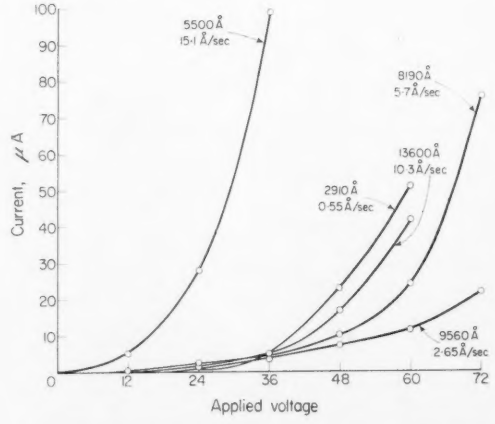

FIG. 9. The leakage current observed in 5 different capacitors at 20 °C is given as a function of applied voltage. The thickness and deposition rate are shown.

Variation of dielectric properties with temperature

Upon heating some of the capacitors to 430°C and holding them at 430°C for 30 min several permanent changes were recorded. There was always a permanent decrease in capacitance and loss angle after the heating cycle had been carried out. The changes occurring during a second heating cycle were very small compared with the changes occurring in the first cycle. The change in capacitance varied from about 23 per cent for rapidly deposited (10–30Å/sec) silicon oxide films to about 6 per cent for slowly deposited films (0.5–10Å/sec.) The changes in loss angle were greater. The tangent of the loss angle decreased from about 0.04 to 0.002 for rapidly deposited films compared with a decrease from about 0.015 to 0.001 for slowly deposited films (at 1 Kc/s).

The permanent changes in leakage current after temperature cycling were variable, usually a slight improvement was obtained. The baking temperature of 430°C was chosen because at higher temperatures (450–500°C) some of the top aluminium films were oxidized right through.

The variation of dielectric properties of some capacitors with temperature is shown in Figs. 10, 11, 12 and 13. These results were taken during the cooling cycle from 430°C to room temperature, after the permanent changes had taken place. Fig. 10 shows the percentage change in capacitance of 3 slides measured at 1 Kc/s. The capacitors are fairly stable up to 200°C and show a temperature coefficient of capacitance of 0.01 per cent/°C in the range 20–200°C for the slowly deposited films compared with 0.04 per cent/°C for the film deposited at 10.2Å/sec. The values of tan δ

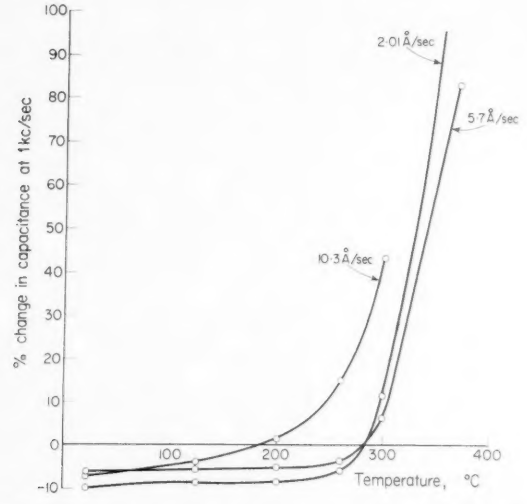

FIG. 10. The percentage change of capacitance of 3 different capacitors has been calculated at several temperatures in the cooling cycle from 430°C.

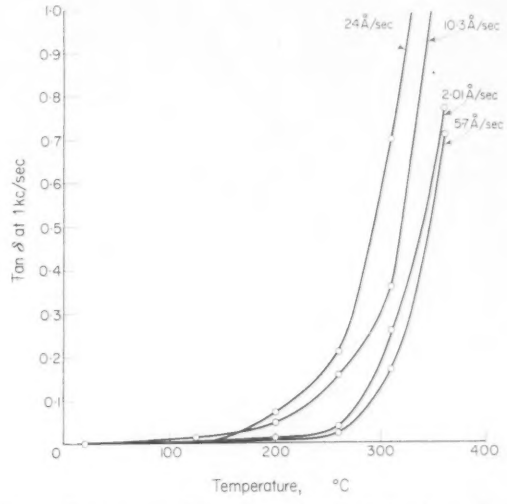

FIG. 11. The tangent of the loss angle (tan δ) has been measured for 4 films at 1 Kc/s as the temperature falls from 430°C to room temperature.

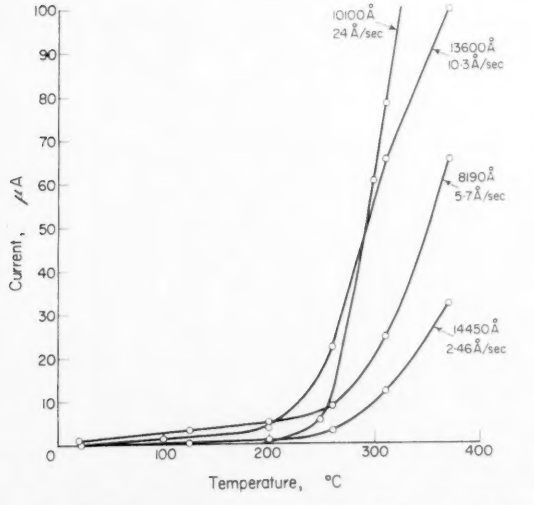

FIG. 12. The leakage current in four capacitors at 12 V is shown during the cooling cycle from 430°C.

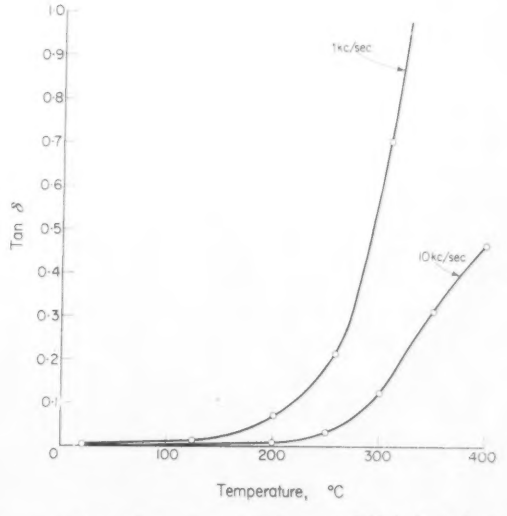

FIG. 13. Values of tan δ at 1 Kc/s and 10 Kc/s have been plotted against temperature for a film deposited at the rate of 24 Å/sec.

shown in Fig. 11 were also taken at 1 Kc/s during the cooling cycle. At 200°C tan δ is less than 0.02 for the slowly deposited films. Slowly deposited films (up to 5.7Å/sec) also have a lower leakage current (measured at 12 V) at temperatures above 200°C as shown in Fig. 12.

Variation of dielectric properties with frequency

The values of tan δ (Table II) were less at 10 Kc/s than at 1 Kc/s, but the difference was greater for the high deposition rates. Capacitance was always less at 10 Kc/s*, showing that there was some dispersion of the value of dielectric constant with frequency, Fig. 13 gives the variation of tan δ with temperature (during cooling from 430°C). These measurements were made on a dielectric film deposited at the rate of 24Å/sec.

Discussion

Leakage resistance

The observed conductivity could be attributed to three causes :—

(*a*) The ionic conductivity of the dielectric.

(*b*) Slow polarization effects.

(*c*) The aggregate current arising from a number of small leakage paths.

The ionic conductivities of silica films calculated from measurements of leakage current at 20°C, were much greater than the values for glasses in general. It was also difficult to explain the leakage currents in terms of polarization. Polarization could account partly for the observed decay of leakage current with time. The long polarization and relaxation times of many dielectrics have been explained by Maxwell[32] and Wagner[33] on the assumption of an inhomogeneous structure, but the rapid decay of leakage current in the silicon oxide films occurring when a capacitor was connected to a battery and microammeter was probably due to a decrease in the number of leakage paths rather than a marked polarizing effect. It seems likely that polarization and the normal ionic conductivity were masked by the leakage current for films measured at 20°C, however the great increase of leakage current at 250°C shown in Fig. 9 was explained in terms of increased ionic mobility at that temperature.

Figs. 7, 9, and 12 show that the leakage current depended more upon the deposition rate than upon the thickness. The leakage current was higher for the faster rates of depositions and this was attributed to a greater number of defects occurring in rapidly deposited films. An examination of the film defects likely to cause leakage was essential.

Microscopic examination of film defects

Defects were present in the dielectric films after deposition, because breakdown occurred in most capacitors. Immediately after taking the finished capacitor from the coating plant the resistance was often as low as 10Ω due to major faults (e.g. pinholes) in the insulating film. These faults were cleared by charging a 4 μF capacitor at voltages up to 100 V (by means of a battery) and discharging it across the experimental capacitor. A very small spark was observed at each defect, and the top aluminium film was removed over a small area around the original pinhole. This "self-healing" effect is very clearly shown in the optical micrograph (Fig. 4) at about 60 × magnification. The experimental capacitor was illuminated by transmission and by reflection. Holes appear as bright white spots, and some surface detail is also visible. The bottom aluminium film is removed only over the area of the pinhole, but the top aluminium film is removed over a wider area, and the curled up edges can be clearly seen. The micrograph also shows some finer detail. The very small white dots are holes which have been self-healed and probably are due to small faults in the structure of the dielectric.

The optical microscope does not reveal the existence of small holes or defects of corresponding size in the oxide film before breakdown, and it is possible that either the structural faults were too small to be seen or that breakdown was due to a local modification of the dielectric strength of the film, caused by adsorbed water vapour or other impurity. The electron microscope was used to examine the surface at high magnification. The electron micrograph shown in Fig. 14 at 28,000 × magnification is taken from a carbon

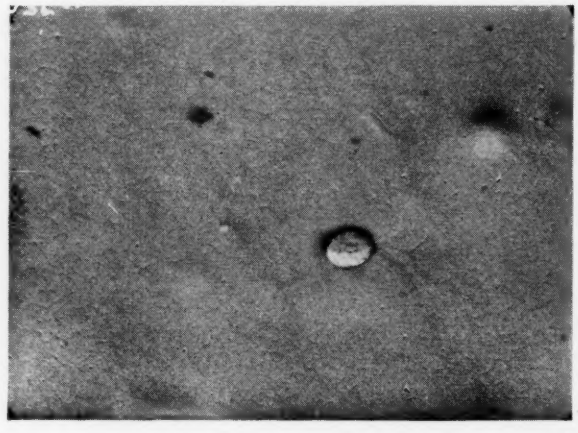

FIG. 14. The electron micrograph shows a shadowed replica of the silicon oxide surface at 28,000 × magnification. Some evidence of a broken structure in the film can be seen.

replica of a silicon oxide film deposited at 15Å/sec on glass. The replica has been shadowed with gold/palladium alloy, and the grain of the oxide film is indistinguishable from that of the shadowing metal. Although some irregular structure of about $\frac{1}{2}$ μ *dia.* is visible, it could have been artificially produced by aggregation of the metal film in the electron beam. High resolution micrographs of oxide films shown in Figs. 16 and 17 at 800,000 × magnification are also inconclusive.[38] These micrographs were made from

* Mr. K. J. Close of The Polytechnic, Regent Street, London, W.1, has confirmed the variation of tan δ with frequency in the range 1 Kc/s to 10 Kc/s with greater accuracy.

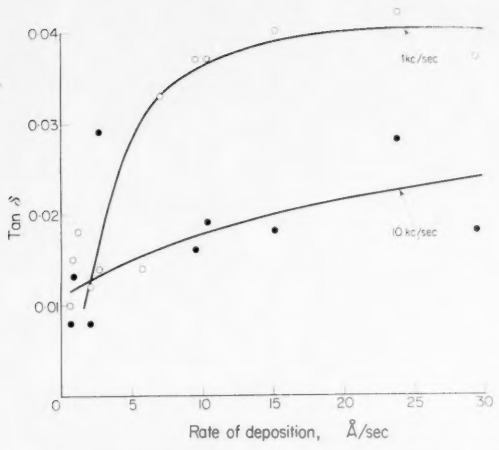

FIG. 15. Values of tan δ measured at 1 Kc/s and at 10 Kc/s have been plotted against rate of deposition. Rough curves have been drawn, which show that the losses are usually higher at 1 Kc/s.

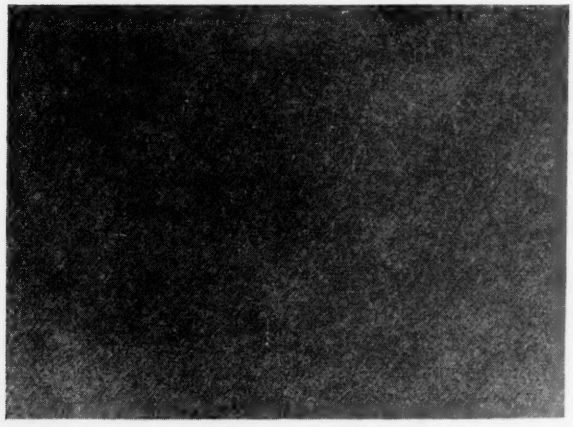

FIG. 16. Electron micrograph × 800,000, platinum/carbon replica from the surface of a silicon oxide film deposited at about 14 Å/sec.

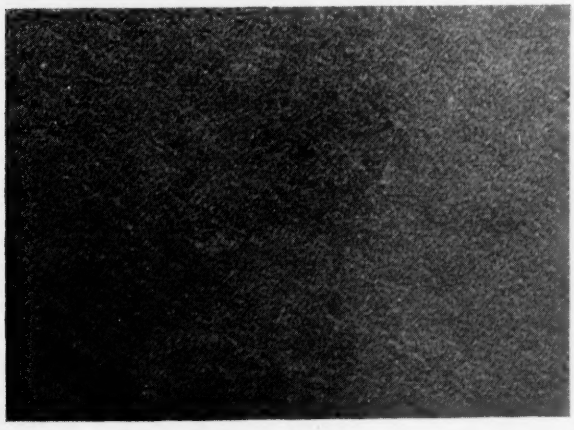

FIG. 17. Electron micrograph × 800,000, platinum/carbon replica from the surface of a silicon oxide film deposited at about 1 Å/sec.

platinum/carbon replicas using a technique due to Bradley.[37] The visible structure is 10–15Å *dia.* and the grain size of the shadowing material and the oxide film are comparable. This degree of resolution is within the limit of the modern electron microscope, but structure of 10Å can be confused by astigmatism. Fig. 17 shows traces of an ordered structure some 10 or 20 times the grain size, but no significant differences between oxide films deposited at high and low rates could be detected. Fig. 16 is modified by astigmatism but the grain size is approximately the same as in Fig. 17.

Optical or electron micrographs showed no structure in silicon oxide films before breakdown, that could account for the large number of very small defects observed for example in Fig. 4. Thus it seems that breakdown can be caused by two types of defect. Firstly by pinholes arising from dust or faulty cleaning or "spitting" from the evaporation source, and secondly by dielectric faults not visible by microscopic examination.

Dielectric strength

Values of dielectric strength based on the minimum breakdown voltage in a capacitor were not realistic in view of the film defects which existed. The defects in most capacitors could be overcome by self-healing, but part of the residual conductivity in some capacitors could be explained only by remaining faults or faults incompletely broken down. Fig 8 shows that in a typical capacitor the number of breakdown pulses at low voltage tended towards a limit within several minutes. Then a voltage was reached at which the number of breakdown pulses steadily increased. This condition implied that the field strength was approaching the dielectric strength of the insulating film. Although definite values of dielectric strength could not be calculated, the tendency towards limiting values of field strength was observed.

Refractive index

The measurements of refractive index compare with those of Hass[3]. From electron diffraction studies Hass has shown that slowly evaporated silicon monoxide is approaching silica in structure and properties. This is also in agreement with the free energy data given in Table I. At relatively low temperatures (1300–1400 °C) the monoxide is much less stable than the dioxide, which combined with the low rate of evaporation at this temperature, would favour the deposition of the dioxide. Conversely, at high temperatures (1700–1800 °C) when the stabilities of the two oxides are comparable, the high rate of evaporation would limit the oxidation of the monoxide to silica in a low partial pressure of oxygen. Some dissociation of the oxide to free silicon would also be expected. This is partly confirmed by the high values of refractive index, dielectric constant and loss angle which have been observed at high rates of deposition.

Dielectric constant

The values of dielectric constant at low rates of deposition shown in Fig. 3 and Table II are about half the published values for silica (3.7–3.8). Thus it seems likely that the density of slowly deposited silicon monoxide films is less than that of bulk silica. The reduction in density can be estimated from the reduction in value of dielectric constant from that of bulk silica. Lichtenecker[34] has found that the dielectric constant of a mixture of dielectric materials of

Vol. 9 959/60

dielectric constant ε_1, ε_2, ε_3, . . . ε_r and volume concentration n_1, n_2, n_3 . . . n_r is given by the empirical relationship :

$$\log \varepsilon = n_1 \log \varepsilon_1 + n_2 \log \varepsilon_2 + \ldots n_r \log \varepsilon_r$$

If it assumed that the film is an inhomogeneous mixture of air and silica (i.e. a grainy film) then by applying Lichtenecker's empirical result, the volume concentration of silica is found to be 53 per cent. A value of the volume concentration can also be obtained assuming the equivalent dielectric to consist of solid silica with an air-space. It can be shown that

$$\frac{\varepsilon}{d} = \frac{\varepsilon_0 \varepsilon_1}{\varepsilon_0 d_1 + \varepsilon_1 d_0}$$

where ε_0 and ε_1 are the dielectric constants and thicknesses of the air-space and silica respectively. From this the volume concentration of silica is found to be 68 per cent for an inhomogeneous film of dielectric constant $\varepsilon = 2$. Provided that the original thickness measurements were correct, and that the slowly evaporated oxide films have the structure of silica, then it is assumed that the density of a film deposited at the rate of about 1Å/sec, lies between 53 per cent and 68 per cent of the bulk density, i.e. between the values obtained by considering the two extreme cases.

The changes of capacitance measured after baking could be caused either by a decrease in the dielectric constant or an increase in film thickness. An increase in film grain size would increase the effective film thickness, alternatively a decrease in dielectric constant could be due to the oxidation of some free silicon atoms.

Dielectric losses

The decrease of dielectric losses observed after baking could be due partly to the oxidation of free silicon atoms and partly to changes in the chemisorbed impurities existing at the surface of the silicon oxide film. It is known that freshly deposited silica films are rapidly contaminated by chemisorbed substances. For example Holland[27] has shown that freshly deposited silica films can be contaminated by the silicone molecules existing in a kinetic pumping system in 3 mins for pumps using silicone fluid M.S. 704 and 1 min for pumps using M.S. 703. These results can be related directly to the vapour pressures of the fluids.

Thus contamination could be caused partly by silicone molecules and partly by chemisorbed water vapour from the residual gases of the chamber. Upon heating to 430 °C in air it is likely that the water molecules were released and evaporated. The further effects of atmospheric humidity have not been considered here, but some results have already been published for dielectric films of silicon oxides[35] in which it has been shown that encapsulation is necessary to obtain stability.

Importance of the base

A study of the properties of resistance films produced by evaporation[36] has shown that the base has a marked effect in deciding the final characteristics of the complete resistor. It is equally important to discuss an evaporated capacitor in terms of the base, the conducting films, and the dielectric. It has been shown that the base can itself introduce losses, and can cause " crinkling " of the deposited film. A simple expression is derived in the appendix, which shows that the temperature coefficient of capacitance depends partly on the temperature coefficient of expansion of the base. In the temperature range 0–300 °C the coefficient of linear expansion of " Pyrex " glass is about 3.5×10^{-6} per °C. Compared with the observed temperature coefficient of capacitance, the expansion of the borosilicate base is insignificant. The expansion of a metal base could contribute significantly to the temperature coefficient of capacitance.

Conclusions

The first part of this report shows that there is very little probability of depositing useful insulating films by evaporating a glass from the bulk. Generally the composition of the film will be different due partly to the widely different vapour pressures of the components of common glasses and partly to the dissociation of the oxides or their reaction with the source. Stable compounds, for example calcium silicate, or mixtures of stable oxides whose vapour pressures are similar should be chosen. However, the evaporation of mixtures of materials with widely different vapour pressures can be carried out using separate evaporation sources. In this way a given composition can be maintained.

The work with silicon monoxide in the second part of the report, shows that good dielectric layers can be made by evaporation. It is established that the rate of deposition has a significant effect on the electrical properties of silicon oxide films. It is necessary to deposit the oxide at less than about 5Å/sec in order to keep the value of loss angle tangent below 0.02 at 1 Kc/s and 200 °C. The use of low deposition rates also increases the value of electric field strength at which repeated breakdown occurs. Breakdown becomes frequent at field strengths between 2×10^5 and 4×10^5 V/cm for films deposited at the rate of 10Å/sec or above. These figures are improved by a factor of 2 for deposition rates of the order 2Å/sec.

The dielectric constant of slowly deposited films (2Å/sec) is less than that of bulk silica due to the lower density of the films. Higher values of dielectric constant at deposition rates of the order 20Å/sec could be due to the presence of free silicon.

After heating to 430 °C in air for 30 min and cooling again to room temperature, a permanent decrease in capacitance of between 6 per cent and 24 per cent is observed. The values of loss angle tangent are also reduced from values lying between 0.01 and 0.04 to values less than 0.002 measured at 25 °C and 1 Kc/s.

A capacitance of 0.01 μF/cm^2 of film area can be obtained for dielectrics of thickness about 1400Å, but such a capacitor will withstand a maximum applied voltage of 12 V d.c. It is necessary to increase the thickness by a factor of between 5 and 10 if a working voltage of 60 V d.c. is needed. The capacitance is then reduced to about 0.001 μF/cm^2.

The rates of deposition which give the most desirable electrical properties are too low for production purposes. Some of the basic properties of silicon oxide films have now been established. It is possible that, using silica as the principal component, the electrical properties of dielectric

films of glass may be improved by the addition of metallic oxides such as calcium which are known to decrease the ionic conductivity, and the rate of deposition increased by the addition of boron oxide or other volatile oxides such as lead or arsenic oxides. The technical problems involved would include the control of the rate of evaporation of materials from separate sources.

Acknowledgements

The author wishes to thank Mr. A. S. D. Barrett, Technical Director of Edwards High Vacuum Ltd., for permission to publish this work ; also Mr. L. Holland for many helpful discussions, Mr. A. W. Agar and Mr. M. A. Silva of Aeon Laboratories for making and interpreting the electron micrograph, and Messrs. Mullard Ltd. for the use of a Cintel counter.

References

[1] L. Holland and K. Hacking ; *Elect. Eng.* **26**, 296 (1954).
[2] L. Holland ; *Vacuum Deposition of Thin Films*, Chapman and Hall, London (1957).
[3] G. Hass, *Vacuum* **2**, 331 (1952).
[4] L. Hiesinger and H. Koenig ; *Festschrift* 100 *Jahre Heraeus Platinschmelze*, p. 376 (Hanau 1951).
[5] G. Hass, J. B. Ramsey, and R. Thun ; *J. Opt. Soc. Amer.* **48**, 324 (1958).
[6] L. Holland and G. Siddall ; *Vacuum* **3**, 375 (1953).
[7] L. Holland and E. W. Van Dam ; *J. Opt. Soc. Amer.* **46**, 773 (1956).
[8] H. S. Colman, A. F. Turner, and O. A. Ullrich ; *J. Opt. Soc. Amer.* **37**, 522 (1947).
[9] G. Hass ; *J. Amer. Ceram. Soc.* **33**, 353 (1950).
[10] G. W. Morey ; *The Properties of Glass*, 2nd Edition, Reinhold Publ. Co. N.Y. (1954).
[11] W. Hanlein ; *Production of thin flexible glass films by evaporation of glass in high vacuum*, paper VIII–2, IV[e] Congrès International du Verre.
[12] O. S. Heavens and S. D. Smith ; *J. Opt. Soc. Amer.* **47**, 469 (1957).
[13] H. Konig, H. J. Loffler, and F. Lappe ; *Glastech. Berichte* **28**, 131 (1955).
[14] E. M. Guyer ; *Proc. I.R.E.* **32**, 743 (1944).
[15] M. Fulda ; *Sprechsaal* **60**, 769, 789, 810, 831 (1927).
[16] P. L. Kirby ; *Brit. J. Appl. Phys.* **1**, 193 (1950).
[17] M. J. O. Strutt ; *Arch. Elektrotech.* **25**, 715 (1931).
[18] J. M. Stevels ; *J. Soc. Glass Tech.* **30**, 31 (1946).
[19] L. Holland, C. Moutou, and K. Hacking ; *Rev. d'Opt.* **31**, 209 (1952).
[20] Siemens Schuckertwerke, *Brit. Pat.* 738,357 (Oct. 1955).
[21] Metal-Lux, *Brit. Pat.* 705,253 (March 1954).
[22] O. Kubaschewski and E. Evans, LL. ; *Metallurgical Thermochemistry*, Butterworth-Springer, London (1951).
[23] O. Kubaschewski and B. E. Hopkins ; *Oxidation of Metals and Alloys*, Butterworth, London (1953).
[24] S. Dushman ; *Scientific Foundations of Vacuum Technique*, Wiley, N.Y. (1949).
[25] Metals Reference Book, 2nd Edition, Butterworth, London (1955).
[26] Chemical Engineers Handbook, 3rd Edition, McGraw Hill, N.Y. (1950).
[27] L. Holland, *Brit. J. Appl. Phys.* **9**, 410 (1958).
[28] R. W. Hoffman, R. D. Daniels, and E. C. Crittenden, Jr. ; *Proc. Phys. Soc. Lond. B*, **67**, 497 (1954).
[29] L. Holland, T. Putner, and S. K. Bateman ; *J. Opt. Soc. Amer.* **47**, 668 (1957).
[30] S. Tolansky ; *Multiple Beam Interferometry of Surfaces and Films*, Clarendon, Oxford (1948).
[31] F. Abelès ; *C.R. Acad. Sci.* **228**, 553 (1949).
[32] C. Maxwell ; *Electricity and Magnetism*, p. 328, Oxford (1873).
[33] K. W. Wagner ; *E.T.Z.* **36**, 111, 121, 135 (1946).
[34] K. Lichtenecker ; *Z. Phys.* **27**, 115 (1926).
[35] R. F. Hoeckelman, C. W. Hoornstra, and M. Yang ; *Micronic Capacitor*, W.A.D.C. Tech. Rep. 57–22 (1957).
[36] G. Siddall and G. Smith ; *Brit. J. Appl. Phys.* **10**, 35 (1959).
[37] D. E. Bradley ; *Brit. J. Appl. Phys.* **10**, 198 (1959).
[38] M. A. Silva ; *Aeon Laboratories*, Report No. 107 (1959).

APPENDIX

The relationship between the temperature coefficient of capacitance and the temperature coefficient of dielectric constant can be obtained by differentiation of the expression for the capacitance of a parallel plate capacitor.

$$C = \frac{A\epsilon}{4\pi d}$$

Differentiating with respect to temperature T,

$$\frac{\delta C}{\delta T} = \frac{1}{4\pi d^2}\left[\delta\epsilon\frac{\delta A}{\delta T} + dA\frac{\delta\epsilon}{\delta T} - A\epsilon\frac{\delta d}{\delta T}\right]$$

$$\therefore \quad \frac{1}{C}\frac{\delta C}{\delta T} = \frac{1}{A}\frac{\delta A}{\delta T} + \frac{1}{\epsilon}\frac{\delta\epsilon}{\delta T} - \frac{1}{d}\frac{\delta d}{\delta T}$$

Neglecting second order differences,

$$\frac{1}{A}\frac{\delta A}{\delta T} = 2\alpha$$ where α is the t.c. linear expansion of the base

and $$\frac{1}{d}\frac{\delta d}{\delta T} = \alpha'$$ where α' is the t.c. linear expansion of the dielectric.

$$\therefore \quad \frac{1}{C}\frac{\delta C}{\delta T} = \frac{1}{\epsilon}\frac{\delta\epsilon}{\delta T} + 2\alpha - \alpha'$$

This simple treatment assumes that the expansion of the area of the dielectric is limited by the base. The total effect on the thickness of the dielectric remains uncertain.

Measurements on the Properties of a Simple Omegatron

D. S. STARK

Services Electronics Research Laboratory, Baldock, Herts
(Received 19 June 1959)

Measurements have been made on a simple omegatron mass spectrometer, to show the effect of various parameters on the sensitivity, resonant frequency, resolution and background ion current. Increase of magnetic field has been shown to cause a marked improvement in peak-to-background ratio, and to improve resolution approximately as predicted by the simple theory. The range has been extended to include Hg, the height of Hg peaks having been shown to be proportional to the pressure of Hg vapour present. Using the results it has been possible to make a practical appraisal of the sensitivity of the omegatron as a leak detector. This leads to less optimistic sensitivity values than have been quoted on theoretical grounds.

1. Introduction

Since the omegatron was first used by Sommer, Thomas and Hipple[1] for measuring the charge-to-mass ratio of ions, it has been increasingly applied, in modified form, to problems of analysis and leak detection[2, 3, 4, 5]. The present paper presents some results of measurements with a simple omegatron which are of relevance in assessing its suitability as a mass spectrometer and as a leak detector, and also points out some of the experimental difficulties encountered.

2. Description of the gauge

These are described in detail by Sommer, Thomas and Hipple[1], and by Berry[6]. Briefly, molecules to be analysed are ionized by a fine beam of electrons parallel to a magnetic field, H. The ions (mass m, charge e) rotate with frequency $f = eH/2\pi m$, in orbits of very small radius. If an alternating, spatially uniform electric field of frequency close to f, is applied perpendicular to the magnetic field, then the ions of mass m will gain energy continuously, spiralling outwards till they reach a suitably placed collector. By varying either the electric or the magnetic field, ions of different mass can be made to resonate in turn. Thus a plot of ion collector current against either field will contain peaks, the position and height of these indicating the molecules present and their abundance.

3. Apparatus

The design of omegatron used is shown in Fig. 1. The R.F. field is produced by applying about 1 V from a signal generator, across two flat parallel plates, whose ends are folded in as described by Bell[5] to improve the uniformity of the field. The two ends of the interaction chamber are closed with flat sheets, containing holes to let through the electron beam. To prevent the resonant ions from drifting to the end plates during their outward spiral, and so being lost, the end plates are biased from zero to 1 V positive with respect to the lower R.F. plate. This bias is referred to as the trapping potential.

The ion collector is a thin strip of metal, parallel to the electron beam, close to the lower R.F. plate, and welded to the end of a wire passing through a hole in this plate. It is usually necessary to bias this collector between zero and to 1 V positive with respect to the lower R.F. plate, in order to deter non-resonant ions from reaching it and producing a spurious " background " current which is independent of the R.F. field.

The electron emission is produced by a few mm of 0.004 in. tungsten filament, about 70 V negative with respect to the interaction chamber. A beam of a few μA, strongly focused by the magnetic field, is accelerated through a 0.020 in. wide slit at right angles to the filament. After passing through a hole at the opposite end of the chamber, the electrons are removed by a collector about 70 V positive with respect to the chamber.

All parts of the omegatron which are in the magnetic field, are made from ferry. These are supported from a sintered glass pinch at the end of a nilo-K tube welded into a stainless steel flange. This flange is demountably jointed (using copper ring gaskets) to a metal pumping system (Fig. 2), so that the omegatron protrudes inside a non-magnetic stainless steel pipe of rectangular cross-section fitting between the poles of the magnet. On one system a permanent magnet providing 2400 oersted is used (proton resonance 3.65 Mc/s), and on another an electromagnet is used which provides up to 7000 oersted. On removal of the magnet, the system is bakable.

The filament supply and all d.c. electrode potentials are provided by batteries, these and all leads being screened to reduce electrical interference and stray capacitance effects. This is very important as currents down to 10^{-14} A have to be measured.

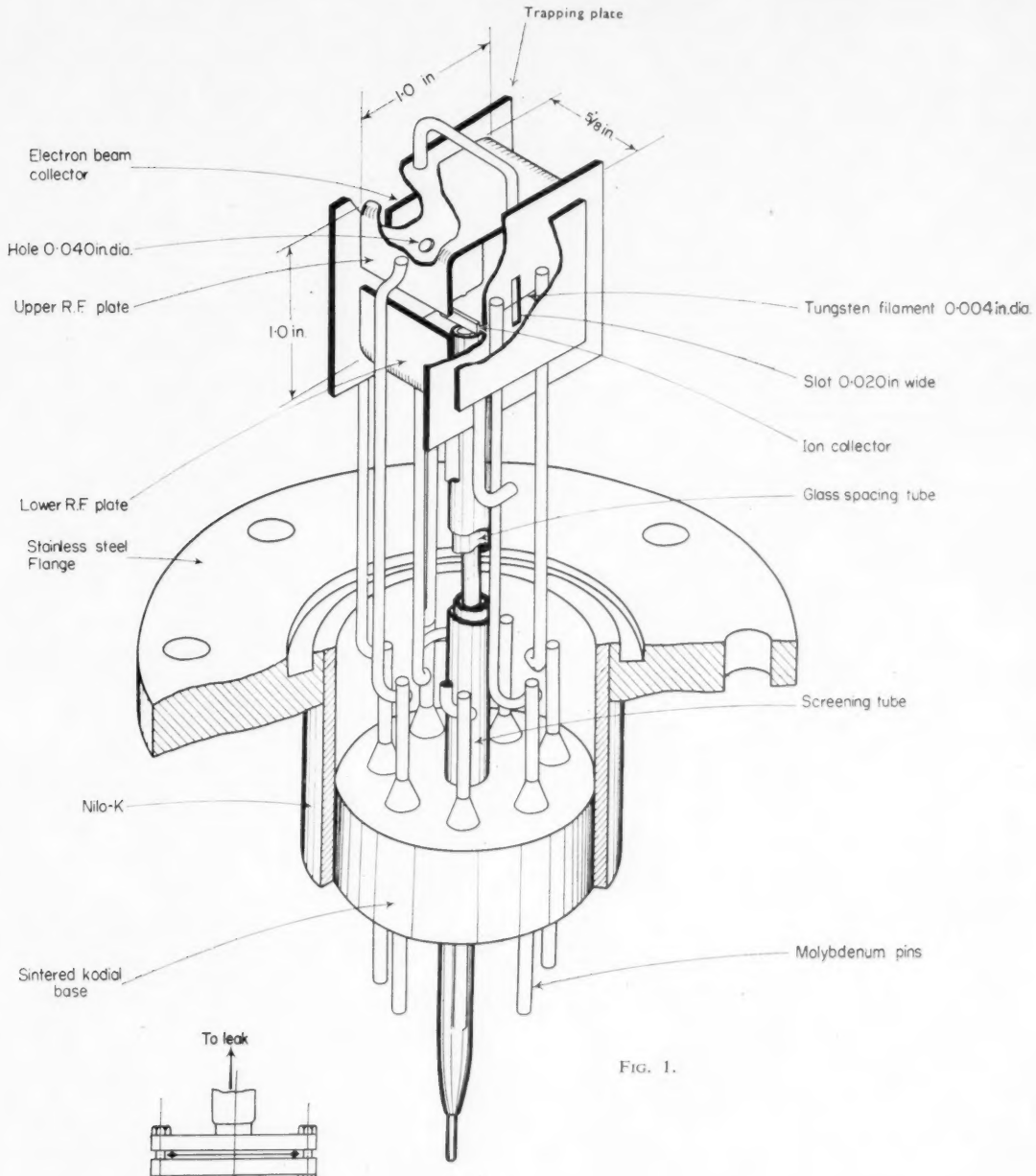
Trapping plate
1·0 in
5/8 in
Electron beam collector
Hole 0·040in.dia.
Upper R.F. plate
1·0 in
Tungsten filament 0·004in.dia.
Slot 0·020in wide
Ion collector
Glass spacing tube
Lower R.F. plate
Stainless steel Flange
Screening tube
Nilo-K
Molybdenum pins
Sintered kodial base

FIG. 1.

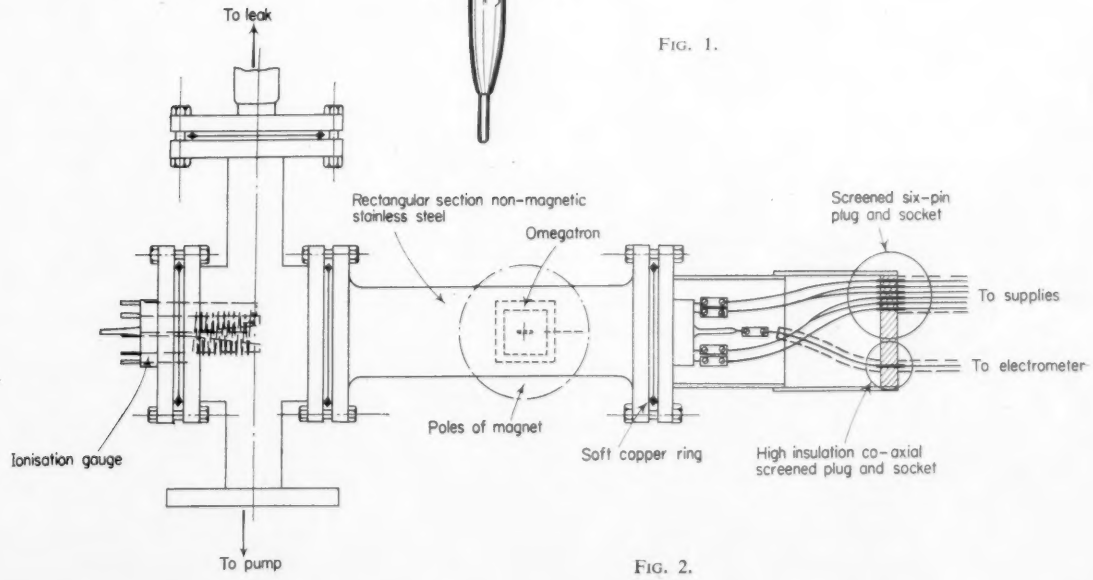
To leak
Rectangular section non-magnetic stainless steel
Omegatron
Screened six-pin plug and socket
To supplies
To electrometer
Poles of magnet
Soft copper ring
High insulation co-axial screened plug and socket
Ionisation gauge
To pump

FIG. 2.

4. Performance

General

The principal characteristics by which the performance of the omegatron can be judged are (a) sensitivity, i.e. the ratio of peak ion current to ionizing current, per mb pressure of selected gas, (b) constancy of resonant frequency, (c) resolution of adjacent peaks, i.e. peak frequency ÷ peak width at half height, (d) spurious background current received by ion collector in absence of R.F. field.

The principal parameters determining the performance of the instrument are (a) R.F. field, (b) ionizing electron current, (c) total pressure, (d) magnetic field, (e) trapping potential, (f) ion collector bias, (g) upper R.F. plate bias.

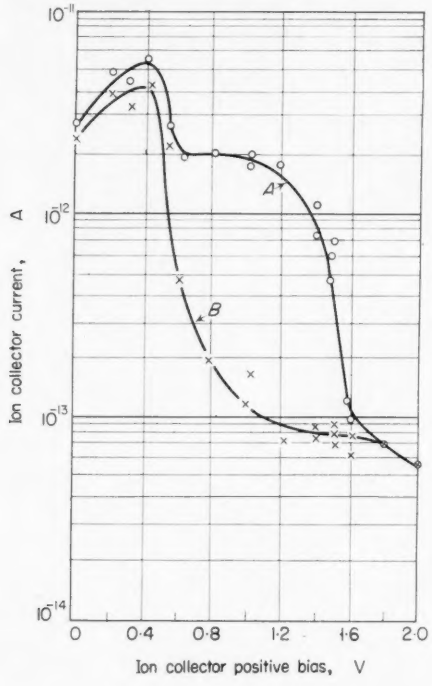

FIG. 3.

Of these parameters, the last three (d.c. electrode potentials) were the most critical, in that quite small variations in their values could radically alter the peaks. Their optimum values had to be determined by experiment, and were not necessarily the same on consecutive days. Consequently, for any quantitative use, it was necessary to make a sensitivity calibration shortly before the measurement. The optimum settings of the electrode potentials were constant, at any given time, for wide variations of the first four parameters. These four were found to affect the performance of the instrument in a regular manner, and an account of their effect is now given.

Background current

The causes of this are not altogether certain, but three experimental facts suggest that it is largely due to non-resonant ions reaching the ion collector, i.e. it is independent of the R.F. field, and it is roughly proportional to the ionizing current and to total pressure. Moreover, it is reduced by increasing the ion collector positive bias, or the upper R.F. plate negative bias, both of which would tend to prevent the arrival of un-accelerated ions. Up to a point, this can be done without reducing the peak height appreciably, but neither of these potentials can usually be raised above about 1 V, before the peak height starts to drop rapidly—this is despite the fact that the collection energy of He ions, for example, is about 70 V, with the values used. The exact behaviour varies from one omegatron to another, but Figs. 3 and 4 show typical variation both of peak height (He) and background current against ion collector positive bias. In Fig. 3, taken at 2×10^{-6} mb pressure (of which about half was He), the ion collector bias could not be raised above about 1.2 V before drastic reduction of the peak height, and at this value the background current was still about 10^{-13} A. Fig. 4, taken at 6×10^{-7} mb (including roughly 4×10^{-7} mb of He) gives similar curves for five values of upper R.F. plate bias. Here, because of the lower pressure, it was possible to reduce the background to a much smaller value before peak fall-off set in.

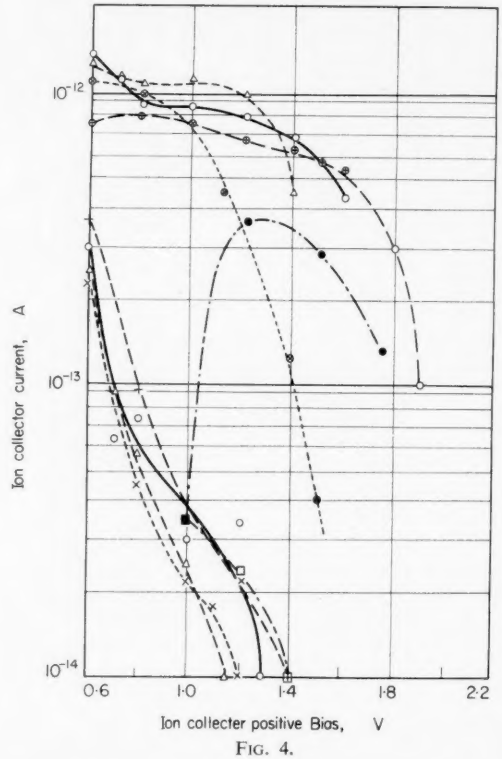

FIG. 4.

It was found that increasing the magnetic field reduced the background in a striking manner. As shown in Fig. 5, the background current at 3×10^{-6} mb pressure was reduced by a factor of a hundred when the field was increased from 2350 to 6900 oersted. This was done without any reduction in the heights of those peaks present.

Sensitivity

The requirements of sensitivity and resolution are to some extent in conflict. They are, therefore, adjusted to very different values depending on the particular application.

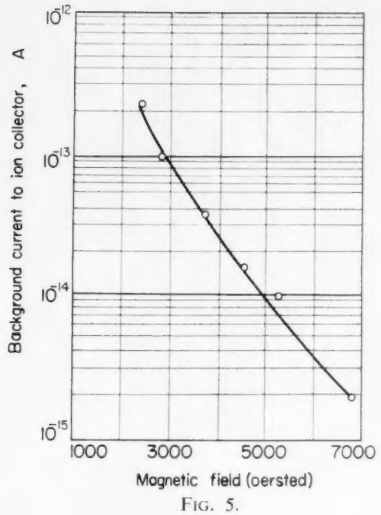

FIG. 5.

In our experiments the maximum sensitivity has usually been about half that of a typical ionization gauge, that is, about 5 to 10 ions/electron/mb for N_2. The sensitivities for H_2 and He are lower, in about the same proportion as for the ionization gauge (respectively, 40 per cent and 15 per cent of the N_2 sensitivity).

The variation of peak ion current with ionizing current was found to be linear, at least up to 6 μA ionizing current, for a field of about 2400 oersted. At 5000 oersted, the variation was roughly parabolic, with a maximum at 1 to 2 μA ionizing current. Edwards[4] who reports a similar effect, suggests that it is due to the potential depression of an ion formed in a dense electron beam.

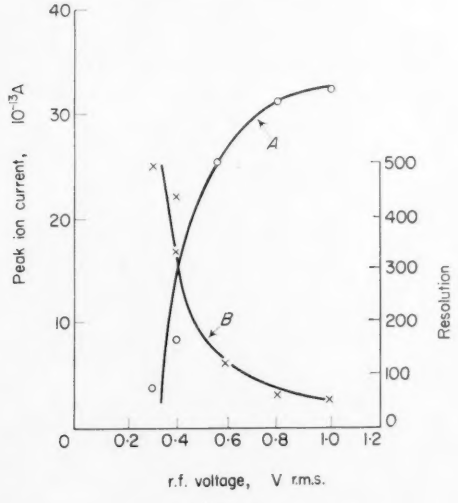

FIG. 6.

Fig.6(A) shows the normal variation of peak current with R.F. volts. For low R.F. volts the sensitivity is reduced, presumably because with the longer time of flight to the collector, a greater proportion of the ions drift out of the interaction space and are lost. For high R.F. volts, the peaks approximate to the flat-topped, parallel-sided shape predicted from the simple theory given by Sommer, Thomas and Hipple[1] which assumed 100 per cent collection efficiency. Hence the levelling-off of the curve at higher volts.

Constancy of resonant frequency

The resonant frequency for a given mass was usually within 3 per cent of the value $eH/2\pi m$, and the variation with $1/m$ was linear.

Sommer, Thomas and Hipple showed that if a small radial field E_r is present at radius r, the resonant frequency is shifted by an amount $E_r/2\pi Hr$, hence as all the electrode potentials must affect the radial field, they may be expected to alter the resonant frequency. This was found to be so, in practice. For example, with 2400 oersted, changing the ion collector bias from 0.6 to 1.0 V shifted the He peak by 0.4 per cent, while changing the R.F. input from 1 to 0.5 V moved the resonances for A and molecular N_2 by about $1\frac{1}{2}$ per cent. The shift of frequency with ionizing current was much smaller than this, and no shift with pressure was found below 10^{-6} mb.

Resolution

The simple theory[1] predicts a resolution given by $R = erH^2/2Em$, where E is the R.F. field and r is the maximum radius of the resonant ions. Table I compares the experimentally measured and theoretically predicted resolutions for a number of gases, at 2400 and 4800 oersted. It can be seen that the resolution decreases with increasing ion mass, and increases rapidly with magnetic field. However, as these measurements were made at widely different times and with different d.c. electrode potentials, it is not possible to deduce from them the exact variation of resolution with ion mass and magnetic field predicted from the equation above. In many cases the measured resolution appears to be better than the theoretical. However, the theoretical peaks have parallel sides, while the experimental peaks are broader at the base so that for equal peak widths at half height, the theoretical peaks would give better discrimination

TABLE I

Comparison of theoretical and measured values of resolution

Ion	Mass (a.m.u.)	Resolution (2400 oersted)		Resolution (4800 oersted)	
		Theoretical	Measured	Theoretical	Measured
H_2	2	270		1075	450 to 650
He	4	135	105	538	880
N_2	14	38.5		154	
O_2 or CH_4	16	33.7	55	135	200
H_2O	18	30	55 to 65	120	
N_2	28	19.3	41	77	
O_2	32	16.8	36 to 66	67	145
Hg	100.3	5.25	9.4	21	33
Hg	200.6	2.62	3.1	10.5	

The theoretical values were calculated assuming the maximum radius of the ion spirals was 1.1 cm, and that the R.F. electric field was produced by applying 1.0 V r.m.s. across plates 2.5 cm apart.

Vol. 9 959/60

between adjacent masses. The resolution was found to increase as the R.F. field was reduced, a rough inverse proportionality existing (Fig. 6 (B)). However, the resolution could not be increased indefinitely in this manner, owing to the rapid loss of sensitivity at lower R.F. fields (Fig. 6 (A)).

With a 2400 oersted magnetic field, it was easily possible to separate adjacent masses up to the water peak (18 atomic mass units), and to resolve A (40 a.m.u.) from CO_2 (44 a.m.u.) —Fig. 7. Fig. 8 (A and B) shows typical peaks for singly

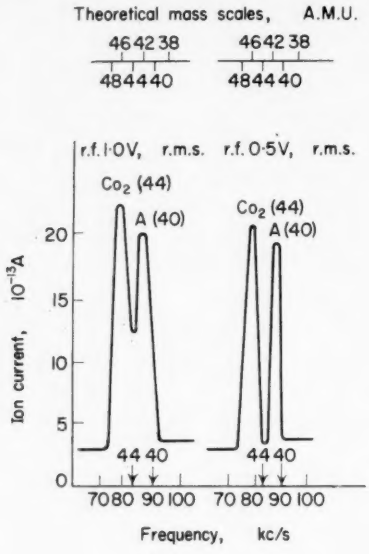

FIG. 7.

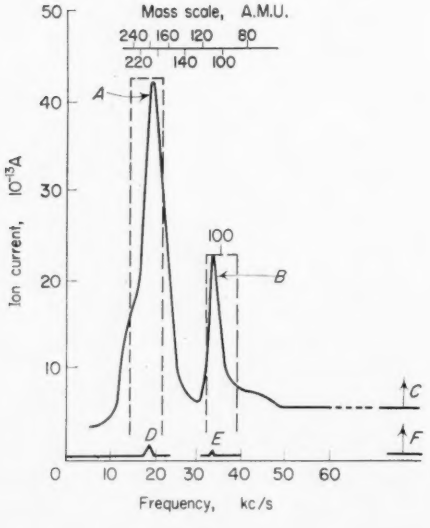

FIG. 8.

and doubly charged Hg ions (200 and 100 a.m.u. respectively, and Fig. 9 shows typical He peaks, all these being for 2400 oersted. With 4800 oersted, the resolution is sufficient to separate masses adjacent to CO_2. The peak for doubly charged Hg ions (100 a.m.u.), obtained using 4800 oersted, is shown in Fig. 10. In Figs. 8 to 10 the theoretically predicted peaks are marked by dotted lines.

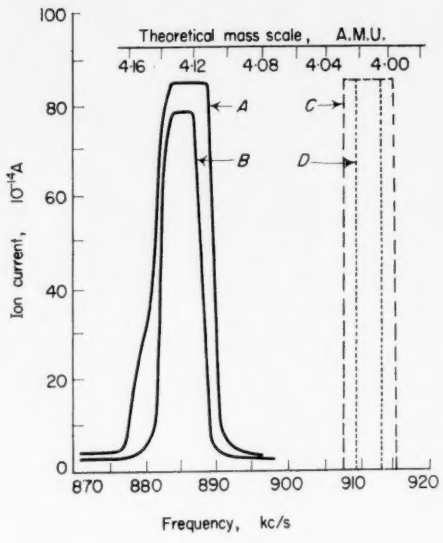

FIG. 9.

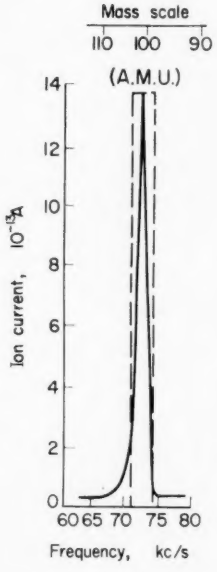

FIG. 10.

5. The omegatron as an analytical instrument

The following points should be noted when assessing the value of the omegatron as an analytical instrument for low pressures. Firstly, as the d.c. electrode potentials may have to be re-set from day to day, particularly after baking or opening to the atmosphere, the peak frequencies and sensitivities cannot be relied on to remain fixed for long periods. For quantitative work, therefore, a calibration should be made shortly before the required measurement—unless only relative pressure changes are required over short periods.

Secondly, the resolution R is inversely proportional to ion mass. This is particularly unfortunate, as the fractional separation of adjacent masses decreases with increasing mass, so that even a constant resolution would have produced a

poorer discrimination between adjacent higher masses. To be able to resolve adjacent masses throughout the range, would require the resolution to be proportional to mass. Thus, for Hg (200 a.m.u.) the present set-up can only be used when it is known that no other molecules of comparable mass are present. It can be shown that as the resolution is proportional to the square of the magnetic field, with the present instrument about 21,000 oersted would be necessary to resolve the peak at 200 a.m.u. from its immediate neighbours.

Examples of the performance for heavy ions are shown in Figs. 8 and 10. Hg was introduced into the system from a pellet at the end of a few cm length of $3\frac{1}{2}$ mm dia. glass tube sealed on to the system above the vapour trap. The pressure of Hg vapour was varied by controlling the temperature of this pellet. In Fig. 8, taken at 2400 oersted, *A* and *B* are the peaks for singly and doubly charged ions when the Hg was at room temperature (total equivalent N_2 pressure in system 2.4×10^{-6} mb). The line C gives the height of the water peak at the same time. After the pellet had been immersed in liquid air for 2 min (total equivalent N_2 pressure 2.4×10^{-7} mb) the Hg peaks fell to about 3 per cent of their former height (*D* and *E*)—these residual peaks no doubt being due to Hg condensed on the walls of the apparatus and Hg passing through the vapour trap. At the same time, the water peak was only slightly reduced (*F*). This fact showed that the Hg pellet was not a major contributor to the water vapour pressure in the system so that the drop in ion gauge reading on freezing the globule could be equated to the fall in partial pressure of the Hg vapour. Fig. 11 shows the

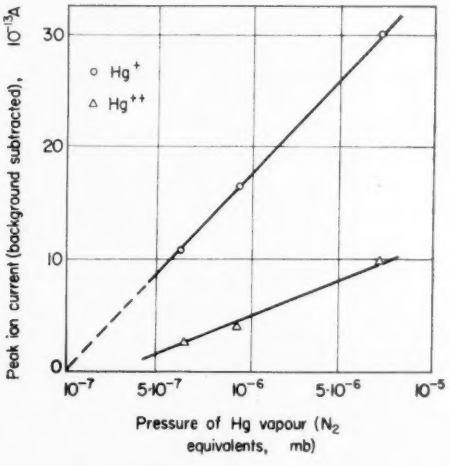

FIG. 11.

effect on peak height of varying the temperature of the pellet. For each temperature, the peak heights (singly and doubly charged ions) and ion gauge reading were noted, and from these were subtracted the peak heights and ion gauge reading obtained when the pellet was in liquid air. The net height of each peak shows a linear variation with the partial pressure of Hg. (These values are the equivalent N_2 pressures.)

6. Leak detection

As pointed out by Bell[5] the omegatron has great advantages as a leak detector. It is small, simple and easily outgassed, so that the speed at which the omegatron-leak combination is pumped can be much reduced without a large build-up of pressure. Thus, if the minimum partial pressure which the omegatron can detect is P_m ,and the pumping speed is S, then the minimum detectable leak is given by $Q_m = P_m S$. Hence the advantage of being able to reduce the pumping speed.

There are, however, a few further points to be borne in mind when assessing the value of the omegatron as a leak detector.

Firstly, the measured sensitivity of the omegatron (as of the ionization gauge) has for He about 15 per cent of its value for air, i.e. of the order 1.5 rather than 10 ions/electron/mb. Hence, as He is the only really satisfactory probe gas, the minimum detectable leak is seven times greater than normally quoted.

Compared with air, He will flow through a molecular leak faster in the ratio of the square roots of the molecular weights of air and He. However, it will also be pumped faster by the same factor, so that the partial pressure of leaking gas is the same for air and He. If the system is shut off from the pump, then, of course, the He will produce a pressure roughly 2.8 times greater than air.

Secondly, there is the question of what maximum pressure can be allowed to build up during use. This will limit (i) the reduction of pumping speed, and therefore the sensitivity of leak detection, (ii) the time for which the system can be isolated from the pump, to allow He to accumulate, (iii) the minimum pumping and baking time.

Using several models of the omegatron described, with 2400 oersted, it was found that although good peaks were obtained even when the background pressure was greater than 10^{-6} mb, the background ion current was then too high to allow the use of the electrometer on its most sensitive range. This background could be considerably reduced by increasing the ion collector bias or the upper R.F. plate bias, but if these were increased beyond certain values, the peak current was rapidly reduced unless the total pressure was kept quite low. This effect is shown in Fig. 3. Here at 2×10^{-6} mb total pressure, and 2.5 μA ionizing current, it was not possible to reduce the background current to a value permitting the use of the 3×10^{-14} A range of the electrometer. In Fig. 4, however, using the same ionizing current, but a pressure of 6×10^{-7} mb, this electrometer range was easily obtained.

In general, with 10 μA ionizing current, the pressure had to be kept below 2×10^{-7} mb to be sure of retaining the full sensitivity of the omegatron. With this ionizing current, therefore, taking the sensitivity to He as 1.5 mb^{-1} the minimum measurable current as 10^{-14} A, the minimum detectable pressure of He is approximately 6×10^{-10} mb. If the omegatron-leak combination has a volume of 0.3 l, and is isolated from the pump for 1 h, the He leak which would give this minimum detectable pressure is 5×10^{-14} l.mb/s. Air would diffuse through such a leak at about 2×10^{-14} l.mb/s.

Vol. 9 959/60

This is true provided the total pressure stays below 2×10^{-7} mb throughout. If it exceeded this pressure, the detector would still operate, but the minimum detectable leak would be greater. Comparing the 6×10^{-10} mb He pressure with the 2×10^{-7} mb background, we see that when looking for the smallest He leak, the maximum outgassing rate must not be more than about 350 times the leak. This background to signal ratio applies when a field of 2400 oersted is used, but, as already explained, stepping up the field to 6900 oersted reduced the background by a factor of a hundred.

7. Leak location

Isolating the system for 1 h, as suggested by Bell[5], may be reasonable for establishing whether a leak exists or not, but if it has to be located, the ion current response must be obtained within a few seconds of covering the leak with He—otherwise scanning the whole tube with a fine He jet would consume too much gas and time. This sets a lower limit to the sensitivity gain obtained by reducing the pumping speed, as is now described.

It is easily shown that at a time t after a gas has started to cover a leak, Q, the partial pressure of the gas is given by :—

$$P = \frac{Q}{S}\left[-1 - \exp\left(-\frac{St}{v}\right)\right] \qquad (1)$$

where the pumping speed is S and the volume being pumped is v. Here v/S is the " time constant " of the system, i.e. the time for the partial pressure to rise to a fraction $(1 - 1/e)$ of its final equilibrium value Q/S.

For our system then, assuming P_m is about 6×10^{-10} mb for He and $v = 0.3$ l, the minimum locatable leak, is given by $Q_m = S(6 \times 10^{-10}) = v/\lambda(6 \times 10^{-10})$ l.mb/s, where λ is the time constant. (Actually, Q_m will be slightly greater, because we are only letting the pressure build up to a fraction $1 - 1/e$ of its full equilibrium value.) Hence, if $\lambda = 1$, 3 or 10 sec, $Q_m = 2 \times 10^{-10}$, 6×10^{-11} or 2×10^{-11} l.mb/s, corresponding values of S being 0.3, 0.1, and 0.03 l/s.

Obviously, the greater the time constant that can be tolerated, the smaller the value to which S can be reduced, and the smaller Q_m. However, it might be argued that we are not obliged to wait until the partial pressure is $(1 - 1/e)$ of its final equilibrium value, as a leak may be located when the He peak has risen to a smaller fraction, x, of the final pressure. Hence, for a given tolerable time, t, we can use a smaller value of S, and therefore detect a smaller Q_m. However, it is easily shown that most of what is gained by decreasing S, is lost because, by not letting the peak build up so far, we are now using a smaller fraction (x) of the pressure which Q_m is capable of producing.

From (1) :—

$$x = 1 - \exp\left(-\frac{St}{v}\right)$$

Therefore minimum pumping speed :—

$$S = -\frac{v}{t}\log(1 - x)$$

Therefore minimum locatable leak :—

$$Q_m = \frac{Sp_m}{x} = -\frac{vp_m}{t} \cdot \frac{\log(1 - x)}{x}$$

Now :—

$$-\frac{\log(1 - x)}{x} = 1 + \frac{x}{2} + \frac{x^2}{3} \quad . \quad . \quad . \quad . \quad .$$

This is obviously not significantly decreased by reducing x from $\frac{1}{2}$ to 0, and its minimum value is 1.

Therefore the minimum locatable leak is :—

$$\frac{vp_m}{t} \qquad (2)$$

For $t = 3$ sec, $v = 0.3$ l and $p_m = 6 \times 10^{-10}$ mb, the minimum locatable He leak is therefore 6×10^{-11} l.mb/s. Air would enter such a leak at about 2×10^{-11} l.mb/s.

The minimum *locatable* leak is thus of the order of 2000 times greater than the figure given by Bell on theoretical grounds for the minimum leak which could be shown to be present but not located.

Even this sensitivity is only reliably obtained if the pressure is kept below 2×10^{-7} mb.

Acknowledgements

The author is indebted to the Admiralty for permission to publish this paper, and to Mr. J. Pollard for much valuable comment throughout the work.

References

[1] H. Sommer, H. A. Thomas, and J. A. Hipple ; *Phys. Rev.* **82**, 687 (1951).
[2] W. A. Morgan, G. Jernakoff, and K. P. Lanneau ; *Amer. Chem. Soc.*, Symposium on Process Instrumentation, Chicago (Sept. 1953).
[3] D. Alpert and R. S. Buritz ; *J. Appl. Phys.* **25**, 202 (1954).
[4] A. G. Edwards ; *Brit. J. Appl. Phys.* **6**, 44 (1955).
[5] R. L. Bell ; *J. Sci. Instrum.* **33**, 269 (1956).
[6] C. E. Berry ; *J. Appl. Phys.* **25**, 28 (1954).

Vo
9
1959

Book Reviews

VACUUM METALLURGY. Edited by R. F. Bunshah. xviii-472 pp. (Reinhold), New York : 1958. 100s.

TWENTY YEARS ago the term ' Vacuum Metallurgy ' would have conjured up a picture of laboratory techniques such as vacuum-melting as a prelude to experimental studies of properties and constitution, vacuum fusion for the analysis of gas content, and vacuum-furnaces for use where oxidation or other contamination was to be avoided, as in the heat-treatment of reactive metals like titanium and zirconium. More processes could be included in this list, but they would all have in common, first their small scale, and second the special skill of their operators, since with the techniques then available they were able to produce and maintain the necessary vacua. Today the position is very different. Vacuum techniques have so improved and have become so reliable that it is natural to talk of vacuum engineering, whilst vacuum metallurgy is applied on a large scale to steel as well as to the more reactive metals. Thus vacuum metallurgy now includes the melting of both steel and titanium on a tonnage basis ; vacuum degassing of molten steel for ingots of up to 250 tons weight ; vacuum melting and casting as a production process for special alloys ; melting by induction, by arc and by electron bombardment, all with the aid of vacuum techniques ; vacuum sintering of compacted powdered metals, and vacuum distillation. The change in emphasis is mainly due to the realization that has come in recent years of the important effects that relatively minor impurities may have upon the properties of metals, and of the need to control those impurities if the metallurgist is to meet the ever-increasing demands made upon him for alloys with special properties for exacting applications.

The new stature of vacuum metallurgy is well illustrated by the book under review. It consists of 27 lectures, by experts in different branches of the subject, that made up a one-week course in vacuum metallurgy organised by the College of Engineering of New York University in 1957. It is perhaps indicative of the value of the book, and a promise for the future development of the subject that twice as much space is devoted specifically to thermodynamics of vacuum processes as to vacuum equipment. Particularly commendable are the chapters on ' Thermodynamics and Kinetics in Vacuum Metallurgy ' by T. B. King, and on ' Distillation of Metals under Reduced Pressures ' by H. W. St. Clair. Thermodynamic considerations play an integral part in many chapters whether they deal with chemistry or processes, and it is clear that the development of large scale vacuum melting, for example, has been a scientific, not a rule-of-thumb process. A very high standard is maintained throughout, and the fact that the treatment of degassing of steel is already out-of-date (see J. Iron and Steel Institute, Nov., Dec., 1958, and Jan., Feb., 1959) is indicative of the rate at which the subject is advancing rather than a criticism of the book.

All those experienced in the use of vacuum techniques for the improvement of metallurgical products will welcome this book and are likely to learn from it, but for the newcomer too, it has much to offer. The basic ground work and principles are adequately treated, and attention is drawn to possible pitfalls. Thus the dangers of attaching too much importance to the reading of the vacuum gauge are dealt with in a section of ' Induction Melting of Ingot Products ', where W. E. Jones discusses the importance of leak-rate, and its influence on the mechanical properties of the vacuum-melted product.

On the whole the text is commendably free from errors, but the dangers of dictating MSS. are surely illustrated on p. 157, where ' 10 to 50 or 10 to 100 atmospheres ' is almost certainly intended to be ' 10^{-50} or 10^{-100} atmospheres '.

The book is excellently produced and illustrated and can be thoroughly recommended.

A. G. QUARRELL.

Vacuum Notes

FOLLOWING the INSTITUTE OF PHYSICS' London Conference on high vacua held in April last, various suggestions were made for arranging regular British meetings on vacuum science and technology, and for British participation in international conferences in this field.

As a result of informal discussions between societies and institutes in this country a ' Joint British Committee for Vacuum Science and Technology ' has now been formed. The committee consists of representatives from each of the following bodies :—

The Institute of Biology
The Institution of Chemical Engineers
The Royal Institute of Chemistry
The Institution of Electrical Engineers
The Iron and Steel Institute
The Institution of Mechanical Engineers
The Institute of Metals
The Institute of Petroleum
The Physical Society
The Institute of Physics

Its objects are :—

(a) To co-ordinate and help to initiate meetings in the whole field of vacuum science and technology arranged by constituent bodies and

(b) to act in the collective interest of the constituent bodies by maintaining liaison with the International Organization for Vacuum Science and Technology and with National vacuum societies, and otherwise.

The Institute of Physics has agreed to provide the secretariat for the joint committee ; communications should be addressed to the Secretary of the joint British committee at its headquarters, 47, Belgrave Square, S.W.1.

Conferences and Symposia

American Vacuum Society

General Information :

THE AMERICAN VACUUM SOCIETY has for its objective the promotion of communication among people interested in Vacuum Science and Engineering.
The Sixth National Symposium on Vacuum Technology was held October 7, 8, and 9, 1959 at the Sheraton Hotel, Philadelphia, Pennsylvania.
An excellent program of broad interest was arranged as follows :

I — The Role of Spectroscopy in Vacuum Science
II — High and Ultra High Vacuum Systems
III — Vacuum Measuring Techniques
IV — Vacuum System Applications I
V — Vacuum System Applications II
VI — Applications of Vacuum in Science
VII — Thin Films and Vaporizing Sources
VIII — Vacuum System Components
IX — Ionic Pumping

1959 Programme Committee :

GEORGE H. BANCROFT, Consolidated Vacuum Corp.
LOUIS PENSAK, Radio Corporation of America
LUTHER E. PREUSS, Edsel B. Ford Institute for Medical Research
H. W. SCHLEUNING, Brooklyn Polytechnic Institute
H. A. STEINHERZ, NRC Equipment Corp.
C. ROBERT MEISSNER, Georgia Institute of Technology, *Program Chairman*

Vo
9
1959

Abstracts :

The following papers were presented :

1. Mass spectrographic studies of impurities on surfaces by A. J. Ahearn, Bell Telephone Laboratories, Incorporated, Murray Hill, New Jersey

The detection and identification of increasingly small concentrations of impurities has become progressively important in solid state physics and engineering. Mass spectroscopy is one of the new analytical tools that has been employed with increasing frequency to meet this need.

A mass spectrograph designed and built at Bell Telephone Laboratories will be described. This is a double focusing instrument of the Mattauch type that uses a vacuum spark as its source of positive ions. The instrument was built primarily for the study of bulk impurities in solids which it can detect at concentrations below 10^{-7} atomic fraction. Moreover the instrument distinguishes between bulk impurities and surface contaminants. The latter can be detected and identified at concentrations of less than the equivalent of 0.01 monatomic layer.

Typical studies of surface contaminants on semiconductors and on insulators will be presented.

2. The vacuum microbalance and omegatron spectrometer : Study of the interaction of oxygen and clean germanium surfaces by S. P. Wolsky and E. J. Zdanuk, Research Division, Raytheon Manufacturing Company, Waltham, Massachusetts

An investigation of the interaction of oxygen with atomically clean germanium and silicon surfaces has been performed with a very sensitive quartz microbalance housed in an ultra-high vacuum system. Since such studies necessitate rigorous conditions of cleanliness, an Omegatron Spectrometer has been developed to provide a continuous analysis of the gaseous ambient. Considerable information has been obtained concerning the species introduced into the ambient due to bakeout, ion-bombardment, and other necessary experimental procedures involving the heating of metal, pyrex, and quartz regions. The apparatus and techniques are described. The oxidation and thermal restoration of germanium surfaces is discussed. Correlation of weight changes and the gaseous species participating in a reaction provides a means of determining reaction mechanisms.

3. The adsorption spectrometer as an analytic tool in ultra-high-vacuum investigations by P. A. Redhead, Radio and Electrical Engineering Division, National Research Council, Ottawa, Canada

Chemically active gases adsorbed onto a metal filament at room temperature will desorb at characteristic temperatures when the filament is heated. After adsorption of the residual gases in an ultra-high-vacuum system the filament is heated slowly and the changes in pressure in the system recorded, a desorption spectrum is thus produced which allows an approximate analysis of the residual gases in the system. The results obtained with tungsten filaments will be discussed with particular reference to the predominant active gases in UHV systems (H_2 and CO). The systems used were pumped by getter-ion pumps and the desorption spectra compared with the corresponding mass spectra.

It is shown that the adsorption spectrometer is capable of analysing the residual gases in UHV systems with a sensitivity greater than that obtainable with a mass spectrometer. The use of the adsorption spectrometer for studying gas–solid reactions will also be described.

4. The ionization of adsorbed gas by impact of slow electrons by G. E. Moore, Bell Telephone Laboratories, Incorporated, Murray Hill, New Jersey

A. J. Dempster using a mass spectrometer, showed in 1918 that

bombardment of a metal surface by slow electrons caused contaminants to leave the surface as positive ions.

In the present work, a molybdenum filament is used as the experimental surface. It can be cleaned at will by flashing. It is mounted in the mass spectrometer itself, directly behind the ionization chamber; therefore the behavior of gas adsorbed to its surface can be followed as the surface is either struck by electrons or directly heated. The energy of the impinging electrons is too low for appreciable heating of the surface or to transfer appreciable momentum to an adsorbed molecule in a collision. Any ion leaving the adsorbed layer must do so, therefore, as a result of excitation to a higher electronic state in which the molecule or one of its atoms is unstable on the surface.

When CO is adsorbed to the Mo surface, 0^+ ions are the most abundant species leaving, although a few CO^+ ions are apparently present. No C^+ ions or negative ions of any kind leave the surface. Figures for efficiency and threshold energy are being obtained and other adsorbents will be investigated.

5. Ultra high vacuum studies with a small bakeable mass spectrometer by Richard E. Honig, Radio Corporation of America, Princeton, New Jersey

For the study of residual gases in an ultra high vacuum system, a commercially available mass spectrometer source has been mounted in a bakeable glass envelope. The Hg-pumped system includes a dry ice trap, two liquid N_2 traps in series, an ionization gauge, and the mass spectrometer components with masses between 2 and 200 a.m.u. can be identified, and their partial pressures measured down to between 10^{-10} to 10^{-11} mm Hg. The concentration of gaseous components has been determined as a function of degassing procedures.

6. Residual gases in vacuum systems by A. Klopfer, Allgemeine Deutsche Philips Industrie, G.m.b.H., Zentrallaboratorium, Laboratorium Aachen, Germany

Investigations with the omegatron of the gas-composition in sealed-off high and ultra-high vacuum systems have shown that the gas liberation rate of the materials and the interactions between the surfaces and the gases, such as adsorption, chemisorption, chemical reaction and exchange reactions, determine the nature of the residual gases. The results obtained on radio tubes, T.V. picture tubes and on systems which consist only of glass and metal, are given. It is possible to classify the composition of residual gases according to the conditions prevailing in such systems.

7. Experimental study of an ion resonance mass spectrometer of the omegatron type by D. Charles and R. J. Warnecke, Centre de Physique Electronique et Corpusculaire, Compagnie Générale de T.S.F., France

The lecture is devoted to the experimental study of a mass spectrometer of the omegatron type, two different models of which are described.

The first model is used for the quantitative analysis of light gas mixtures ($m < 100$) under low pressure ($P < 10^{-5}$ Torr).

The authors consider the influence on the apparatus characteristics, of various parameters such as the amplitude of the applied electric field, the ionizing current intensity, the electron collector potential and the bias voltage magnitudes.

The ion source efficiency, the spectrometer sensitivity and luminosity are calculated; figures concerning the accuracy of measurement are given.

The second model is used to detect leaks in high vacuum envelopes. After demonstrating that the use of argon as a testing gas was preferable from the point of view of the measurement sensitivity, a number of experimental results are given, proving that the apparatus sensitivity is comparable to the existing helium leak detectors.

8. The production of ultra high vacuum in metal systems larger than 1000 liters by I. Farkass and G. F. Vanderschmidt, National Research Corporation, Cambridge, Massachusetts

Methods for the production of a pressure of 10^{-9} mm Hg in metal vacuum chambers of volumes greater than 1000 liters are described. The following pumping methods are analyzed: mechanical pumps, getter pumps, ion-getter pumps, diffusion pump-trap systems, and cryogenic pumps. Experimental results on these pumping methods are presented: the conclusion is that the best method for pumping large chambers below 10^{-9} mm Hg is the diffusion pump and trap system. Promising supplementary methods are cryogenic pumping and getter pumping.

Seals for use in large metal systems are described; the seals include metal gasket compression seals useful to 6-inch diameter large semipermanent seals, and large (3 ft. diam.) easily opened and closed seals.

(This work was supported in part by the Army Ballistic Missile Agency.)

9. An ultra high vacuum chamber for space simulation by John C. Simons, Jr., National Research Corporation, Cambridge, Massachusetts

Criteria for large ultrahigh vacuum systems, particularly for space simulation applications, are reviewed. Physics and engineering problems faced in the design of such equipment are considered and a design approach formulated.

A 40 cubic foot vacuum chamber designed by this method to operate at 10^{-9} mm Hg is described. This facility has been built and is operating in the NRC research laboratories. The pumping system consists of a 10-inch oil diffusion pump, a water-cooled baffle, and two liquid nitrogen cooled traps in series. The chamber itself is $3\frac{1}{2}$ feet in diameter and is made of stainless steel. A removable door forms one end of the chamber. Results obtained from experimental operation of the chamber are described.

Engineering and economic compromises necessary in the design of still larger ultrahigh vacuum facilities (for example, 1000 cu. ft. volume) are discussed. Design recommendations for a large system are made.

(This work was sponsored in part by the Army Ballistic Missile Agency.)

10. A differentially pumped ultra high vacuum system by Michael P. Rivera, Vacuum Equipment Division, The New York Air Brake Company, Camden 11, New Jersey

A differentially pumped vacuum system for operation in the range of 10^{-9} Torr is described. This unit is a vacuum system operating in a pressure range lower than has heretofore been available for common vacuum evaporators.

The system contains fittings commonly found in most vacuum evaporators such as high current electrodes, rotary motions, high voltage electrodes as well as two windows for observation.

The theory of the differentially pumped system is presented in order to show its deviations from standard pumping systems.

The system consists of an inner ultra high vacuum chamber evacuated by a 6-inch diffusion pump, pumping through a chevron type trap and an outer chamber evacuated by a trapped 4-inch diffusion pump.

11. Ultra-high-vacuum pumping by vibrating membrane by Helmut Schwarz, Semiconductor and Materials Division, Radio Corporation of America, Somerville, New Jersey

Calculations will be given concerning a radically new type of noncontaminating ultra-high-vacuum pump. A diaphragm or membrane is driven into high-frequency vibration so as to drive gas molecules selectively in a particular direction, i.e., perpendicular to the diaphragm surface. Analysis has shown that, as the membrane peak velocity approaches the mean thermal velocity of the gas molecules, the speed of a pump, in which the membrane and openings have special geometrics, should approach the theoretical maximum. Thus, the pump, if operated in conjunction with conventional pumps to maintain a low forepressure, potentially could approach an ideal one-way valve. Since the thermal velocities of molecules decrease with molecular

Vol. 9 959/60

weight, the pump should be increasingly effective for heavier gases.

12. An oil free ultra high vacuum system for the deposition of thin films by Hollis L. Caswell, International Business Machines Corporation, Research Laboratory, Poughkeepsie, New York

The construction of an all metal vacuum system will be described which utilizes liquid helium and electromagnetic pumping to obtain low pressures for the deposition of thin films without the use of oil or mercury pumps. Data on design, consumption, and speed of liquid helium cooled traps will be given together with the advantages and disadvantages of this type of pumping. Results of measurements on residual gases present in this system together with other data obtained with a mass spectrometer incorporated in the system will be presented.

13. Diffusion pumps of large suction speeds for pressures lower than 10^{-8} Torr by H. G. Nöller, G. Reich, W. Bächler, E. Leybold Nachfolder, Cologne, Germany

When observing certain operating techniques with suitable diffusion pumps and baffles or traps, one may reliably attain about the same suction speeds in the ultra-high vacuum range than at ordinary high vacuum pressures. The following arrangements of pump systems have been tried out :

Mercury Diffusion Pumps, CO_2— and liquid nitrogen trapped ; Oil Diffusion Pumps with water—, CO_2—, Freon and liquid nitrogen-cooled baffles. It turned out that—in compliance with theoretical reasoning—the suction speeds remain almost constant down to the lowest measured intake pressure of $<10^{-9}$ Torr. Pressures of the order of 10^{-12} Torr may be attained by means of a glass mercury diffusion pump and a manifold cold trap filled with liquid nitrogen. But the suction speed, due to the high impedance in the cold trap, is only 10 l/sec approx. Much higher suction speeds, such as some 100 l/sec at ultimate pressures of 10^{-9} Torr may be reached by metal oil diffusion pumps with liquid nitrogen traps. Gauges employed are Alpert Ionization Gauges and Omegatron Mass Spectrometer.

14. New method for vacuum measurements in the molecular range of pressures by N. A. Florescu, School of Applied Physics, The University of New South Wales, Kensington, Sydney

A method has been developed for vacuum measurements in the molecular range of pressures which consists in admitting the same rate of gas flow successively at two distinct cross sections of a tube attached to a pump. The pressures beyond these sections are indicated by an uncalibrated gauge having linear response. Intrinsic and apparent speeds, as well as gauge sensitivity are obtained in absolute values from a single experiment, as functions of gauge readings, metered gas flow, and the conductance of the tube limited by the two sections. Testing and calibration of variable leaks can also be performed.

The paper gives the theory of the method, describes the experimental arrangement, and discusses the measuring accuracy. Some experimental results are also included.

15. Advances in the design of vacuum gauges using radioactive sources by J. R. Roehrig and G. F. Vanderschmidt, National Research Corporation, Cambridge, Massachusetts

Tritium, the radioactive isotope of hydrogen, is advantageously used in radiological vacuum gauges. The tritium gas is absorbed in a thin layer of titanium, forming a stable compound at room temperature. Because of the complete absence of penetrating radiation, high intensity sources may be used to permit convenient measurement of pressures down to 10^{-5} mm Hg, with essentially no hazard to personnel.

A fundamental problem in the design of simple, portable radiological vacuum gauges is the difficulty of measuring the small current from such gauges. A method which makes use of the time of discharge of a capacitor permits a simple direct measurement of the current ; the method provides an output which is ideally suited for telemetering, and makes the gauges especially useful for high-altitude meteorological measurements.

16. The theory and design of subminiature ionization gauge tubes by R. L. Ramey, University of Virginia, Charlottesville, Virginia

Subminiature ionization gauge tubes offer advantages in reduced size, weight, and power requirements over conventional tubes of this type. The theory and design of subminiature ionization gauge tubes of the Bayard-Alpert type is discussed. The conditions for linear operation are developed and explored.

Although the standard sensitivity $S=I_+/I_-P$ is small compared to conventional ionization gauge tubes, this is easily offset by a compensating increase in collector current amplifier gain. By proper operation, the decade sensitivity $\delta \log I_+/\delta \log P$ may be made equal to unity so that linear collector current-pressure characteristics are attained.

17. A multi-point electronic manometer system for low pressure hypersonic wind tunnels by Paul L. Vitkus, NRC Equipment Corporation, Newton Highlands 61, Massachusetts

An adaptation of a radio-active ionization vacuum gauge provides multiple point instrumentation for hypersonic wind tunnels. The system provides fast, accurate, reproducible analog outputs suitable for insertion into a digital recording system.

This paper discusses design considerations of a special Alphatron (R) pressure sensing head and plug-in type electrometer amplifier. Accuracies of $\pm 2\%$ of reading from 1 to 30 mm Hg and $\pm 5\%$ from .1 to 0.99 mm Hg are achieved in two ranges, 0—3 mm Hg and 0—30 mm Hg, with equilibrium times of 1 and 4 seconds respectively.

Use of the multi-channel system should greatly reduce wind tunnel delays encountered with present liquid manometer systems.

18. An ultra sensitive mass spectrometer leak detector and its application to vacuum technology by John L. Peters, Crosby Vacuum Research Division, Teletronics Corporation, Syosset, New York

A new and improved type of mass spectrometer leak detector is described which has a sensitivity for helium of 10^{-13} standard cubic centimeters per second with a signal-to-noise ratio of 1 or better. Operating pressure is in the 10^{-5} or 10^{-6} mm Hg range, time for 2/3 of final response is 2 seconds or less and operating characteristics are similar to those of present helium sensitive mass spectrometer leak detectors. This greatly improved sensitivity has several important applications in vacuum tube technology which are briefly outlined.

19. An improved helium-only sensitive method for calibrating silica membrane helium leaks by Charles Bicknell, Consolidated Electrodynamics Corporation, Pasadena, California

A new technique for measuring the accumulated gas that leaks through a silica membrane helium leak has been developed. Though the basic principle of gas accumulation into a known volume is employed, the present method differs from that of others in that a mass spectrometer is utilized for the purpose of sensing only helium, while discriminating against all other outgassed materials thereby providing a distinct advantage over the use of the conventional ion gauge, McLeod gauge, and other total-pressure measuring devices.

The test apparatus fabricated for this investigation exhibited no tendency to " hang up " helium, and pumped " helium-free " after each test, thereby eliminating the necessity for zero corrections, etc.

Results obtained indicate that the overall accuracy achieved by using this technique and equipment was $\pm 5\%$ of the actual leak rate for leaks ranging from 1×10^{-9} atm cc/sec of helium to 5×10^{-6} atm cc/sec of helium. On the basis of the work recently completed, it seems feasible to measure leaks in the range of 1×10^{-11} atm cc/sec of helium.

20. Relations between size of vacuum chamber, outgassing rate, and required pumping speed by B. B. Dayton, Rochester Division, Consolidated Vacuum Corp., Rochester 3, New York

Equations are presented for the pressure in a vacuum system as a function of time during pump down in the presence of various modes of outgassing and for the ultimate pressure. Formulas are given for estimating the required pumping speed. Data on the outgassing characteristics of various materials is reviewed and techniques of measuring outgassing rates are discussed.

21. Vacuum treatment of milk by Carl W. Hall, Department of Agricultural Engineering, Michigan State University, East Lansing, Michigan

The objective of vacuum treatment of milk is to remove the undesirable flavors and odors usually associated with some feeds to obtain a uniform fluid milk product throughout the year.

Milk is subjected to vacuum in one or two chambers ; the first of which is a low vacuum (about 10 mm Hg) and the second chamber, a high vacuum (about 20 mm Hg). Air or steam is used for scrubbing the milk in the first chamber. Proper control of milk flow, steam flow and vacuum are required to avoid dilution or concentration of the product. The ratio of steam condensed in the first chamber to the water vaporized in the second chamber determines the change in concentration of the product. To avoid change in concentration, assuming no heat loss from the chambers, a 1 : 1 ratio between temperature increase in the first chamber and temperature decrease in the second chamber is required. To provide heat for vaporization and removal of components and to account for heat losses from the unit, the outlet temperature must be lower than the inlet temperature. The outlet is usually maintained about 3 to 5 °F below the inlet temperature to maintain the desired density. An analysis of heat losses is presented.

The methods of connecting the vacuum equipment to a HTST pasteurizing system are presented. The changes of temperature, heat flow, vacuum, state and removal of vapors are presented. The control mechanism for maintaining desired condition is discussed.

22. Equipment for hot rolling strip in vacuum by Morse Hill, Roger Holman and Edmond Kulinski, Republic Steel Corporation, Research Center, Cleveland 31, Ohio

Description of vacuum equipment used for hot rolling titanium under one micron pressure. The process involved consisted of heating titanium powder compacts to 2000 °F, rolling at 100 f.p.m. and then cooling while continuously under vacuum. The equipment consisted essentially of entrance and exit chambers, furnace, rolling mill, and pumping system. Tests showed that there was no significant contamination during this process.

23. Pressure simulation of high altitudes by D. J. Santeler, General Electric Company, Schenectady, New York

Altitude chambers have been used for years for testing aircraft equipment. As it becomes desirable to simulate higher altitudes a number of questions arise as to just what constitutes true simulation, and how it can be obtained. If a vessel contains 10^{-7} mm of atmospheric gas and 10^{-5} mm of alien gas, such as hydrocarbons, what equivalent altitude is simulated ? If a test chamber is capable of pressures as low as 10^{-7} mm, but 50% of the outgassing of a test item is returned after collision with the chamber walls, what altitude is simulated ? These problems arise due to several changing effects. As the pressure decreases the mean free path increases and the effects of the confining chamber walls become more predominate. With decreased pressures the gross pressure effects disappear and we must be concerned with the individual surface effects of different types of molecules. At low pressures the gas flow in a chamber is not random and we must consider the directional transfer of gas from one surface to another. When designing a high altitude chamber we must weigh the following four questions. What is simulation ? Why simulate ? How can we obtain simulation ? How do we classify the degree of simulation in a particular chamber ?

24. A new type of boiler that permits improvements in the performance of oil diffusion pumps by Donald L. Stevenson, Consolidated Vacuum Corporation, Rochester Division, Rochester 3, New York

A new type of diffusion pump boiler is described which furnishes useful heat to both the liquid and the vapor phase of the pump fluid. The effectiveness of this type of boiler contributes to major improvements in the performance characteristics.

The design allows approximately twice the normal heater input to be incorporated in the pump, and a relatively constant temperature is maintained within the nozzle assembly over a wide range of heater input. This has resulted in better stability of the ultimate pressure in the very high vacuum range (10^{-6}—10^{-9} mm Hg) and major improvements in speed, throughput, and limiting forepressure characteristics so that the performance surpasses in every respect that of conventional pumps.

The development of an experimental nominal four inch pump is described. It has a speed factor (or Ho Coefficient) of over 50%, as compared to 30—35% for conventional pumps. It is much smaller and more compact than conventional pumps of comparable performance.

Experimental pumps of other sizes, incorporating this type of boiler, have achieved the same high degree of efficiency. A new term, " speed efficiency " is introduced as an aid in comparing the speed of pumps in terms of their bore size. The performance of the new pumps is used to demonstrate the validity of this method of efficiency evaluation.

25. Relationship of diffusion pump performance to the thermodynamics of the pumping fluid by Hugh R. Smith, Lawrence Radiation Laboratory, University of California, Berkeley, California

Theoretical considerations of the changes in state and rates of state change of the pump fluid in a diffusion pump has led to a more basic understanding of pump operation. Many of the anomalous results observed by experimenters in this field are clarified when analyzed in the light of these new considerations.

Experimental data have confirmed the theoretical predictions. Application of these principles to existing pumps has markedly improved performance with regard to pump speed, amount of backstreaming and ultimate pressure obtained. Data indicating the range of variation of critical pump parameters are presented.

A procedure, based on these thermodynamic principles, for the design of diffusion pumps is outlined.

26. Recent developments of ultra high vacuum systems using oil diffusion pumps by W. K. Huber and E. A. Trendelenburg, Geraetebau-Anstalt Balzers, Principality of Liechtenstein

Part I.—A modified Alpert type ultra high vacuum system was connected with a bakeable glass mass spectrometer having a partial pressure sensitivity of about 1×10^{-13} mm Hg as described by Reynolds. In accordance with investigations by W. Lange (Westinghouse Research Labs.) which were done with a less sensitive instrument it could be shown that the main constituents of the residual atmosphere are H_2 and CO and that there are no higher masses than 45 detectable as long as the copper trap is not saturated. The mass spectra in the unsaturated and in the saturated state are discussed.

Part II.—A metal pump system using a rotary fore pump, a 120 l/sec diffusion pump and a 650 l/sec diffusion pump in the final stage with a following bakeable baffle and liquid air trap arrangement was built. A vacuum of about 1×10^{-9} mm Hg could be maintained for 2 weeks without refrigerating the liquid air trap. A hydraulically operated all metal valve suitable for this system will also be described.

27. The vacuum system of a 3-Bev proton synchrotron by L. Seidlitz, T. Tang, D. L. Collins, M. Szekely, Princeton-Pennsylvania Accelerator, Department of Physics, Princeton University, Princeton, New Jersey

The main features of the 3-Bev proton synchrotron being con-

Vol. 9 959/60

structed by Princeton University and the University of Pennsylvania are described and illustrated. The principal component of the vacuum system is the vacuum chamber in which the protons circulate during the acceleration cycle. The design of the chamber was partly determined by boundary conditions set by the experimental uses of the accelerator, by environmental factors such as high energy nuclear radiation and rapidly varying magnetic fields and by restrictive spatial conditions, as well as by the required operating pressure of 2×10^{-6} mm Hg. The unusual features of the resultant solution are detailed. The pumping system, consisting of 24 modular units, and the complement of instrumentation are presented. The control system, which permits remote operation and indication of most of the vacuum system components, is described. The manner in which the vacuum control system interlocks with other accelerator components is discussed.

28. A high pumping rate system at 10^{-6} mm Hg pressure by W. W. Balwanz, U.S. Naval Research Laboratory, Washington 25, D.C.

Studies of the exhaust of chemical rockets at simulated altitudes are now achieved at vacuums down to about one millimeter using conventional pumping techniques. A material further reduction in the ambient pressure, while maintaining the high gas release rate of the rocket exhaust, is impractical with the usual mechanical and diffusion pumps. A study is being conducted to determine the limits of utility of various pumping methods such as, the use of the mass transport energy of the rocket exhaust for compressing the gases, the condensation of gases, the trapping of non-condensables and the use of electrical pumping methods. Preliminary experimental investigations have demonstrated that multifold increases in the pumping rates may be achieved.

29. Sputtering of metals and semiconductors by low energy argon ions by N. Laegreid and G. K. Wehner, Mechanical Division of General Mills, Incorporated, Minneapolis, Minnesota

Sputtering yields for polycrystalline semiconductor and metal targets under normally incident A^+ ion bombardment were measured in the energy range from 30 to 800 ev. The measurements were made in a low pressure (2—5 micron) high density argon plasma created in a demountable low voltage hot cathode discharge tube. The yields (number of atoms removed/incident ion) were determined by measuring the weight loss of spherical targets immersed like large negative Langmuir probes in the plasma.

The yields are independent of gas pressure (below $p=30\mu$), ion current density and target temperature. At 100 ev ion energy the yields range from 0.06 atoms/ion for Si to 0.6 atoms/ion for Ag. The curves are discussed in terms of the ion parameters.

(This work was supported in part by the Office of Naval Research contract.)

30. Evaluation and use of large diffusion pumps and traps for the ultra high vacuum system of the model C-stellarator by W. G. Henderson, G. S. Geiger and J. T. Mark, Radio Corporation of America, Lancaster, Pennsylvania

The Radio Corporation of America under contract to Princeton University and the Atomic Energy Commission has conducted engineering investigations in ultra high vacuum to determine the design parameters of large ultra high vacuum pumping systems. In this work many techniques have been developed and much design data has been obtained that will enable engineers designing new systems to approach u.h.v. in a straightforward manner. Following these set rules and techniques, he can be assured of success without the need of experimentation or guess work. This paper described the choice of a pump, the trap, the gauge, how to leak check, bake, when to and how to cool his system, and the do's and don'ts of maintaining u.h.v. in a continuously pumped system for months on end.

31. Ultra high vacuum systems developments for the model C-stellarator by J. T. Mark and W. G. Henderson, Radio Corporation of America, Lancaster, Pennsylvania

The Radio Corporation of America under contract to Princeton University and the Atomic Energy Commission has designed and built the ultra high vacuum system for the first phase of the Model C-Stellarator fusion test by Princeton University's Forrestal Laboratories. Many developments resulting from this work are unique and the first of their kind. This paper describes developments of : an eight-inch opening hydraulicly operated and bakeable ultra high vacuum valve, high conductance ultra high vacuum liquid nitrogen traps of very low liquid consumption, large size demountable gold seal joints, four-inch diameter sapphire viewing ports, and many other developments of interest to advancing the science of high vacuum engineering.

32. Research and production potentialities of electron bombardment evaporation by David Wm. Moore, Servomechanisms, Incorporated, Goleta, California

The nature of electron bombardment evaporation and its use in both the laboratory and the production line is discussed by this paper. Advantages of electron bombardment heating, including the ability to vaporize practically any material and to do so without contamination, are presented. Practical examples of electron bombardment equipment are illustrated by examples from the research laboratories of the author's company. Means for supporting the material to be evaporated and for handling non-conductors are discussed as well as methods for controlling the ionization of the gas in the evaporation chamber.

The application of electron bombardment evaporation to high quality production is stressed, with particular emphasis on continuous operation and day to day reliability.

33. Electron beams in vacuum processes by E. S. Candidus, M. H. Hablanian, and H. A. Steinherz, NRC Equipment Corporation, Newton Highlands 61, Massachusetts.

In recent years several new industrial processes utilizing electron bombardment as the source of heat have been developed. High power electron beams are used for evaporation, melting, joining, refining, and sintering.

Each process has characteristic requirements for equipment design. Electron sources, types of electron guns and power supplies, voltage, current and power ranges for the above applications are discussed. Melting, ingot conditioning, and welding of refractory metals are considered in further detail.

Technical and economic advantages, performance and operational characteristics of electron bombardment processes are described.

34. A new electron gun for the vacuum evaporation of metals and dielectrics by R. Thun and J. B. Ramsey, U.S. Army Engineer Research and Development Laboratories, Fort Belvoir, Virginia

The production of complex film elements in narrow tolerances requires a better control of the deposition parameters and a lower impurity level than presently obtainable. The use of electron guns as evaporation sources promises a reduction of the sample contamination and an accurate control of the deposition rate. A new electron gun is described which focusses the electron beam by a spherical field between cathode and anode. The advantages of such a design over a conventional gun with grid cylinder are greater ruggedness and simplicity, higher energy output and the possibility of a full analytical treatment of its characteristic. The evaporation of difficult materials such as silicon is possible.

35. Adsorption of gases on mercury at 77 °K by G. E. Becker, Bell Telephone Laboratories, Murray Hill, New Jersey

A study has been made of the adsorption of gases on freshly condensing mercury in a cold trap used with a mercury diffusion pump. The object was to determine the contribution of this process to the pumping speed of the pump-trap combination in the pressure range below 1×10^{-6} mm of Hg. It has been found that adsorption in the cold trap makes no significant contribution to the pumping speed for molecular H_2, O_2, N_2, and CO. An approximate upper limit of 1×10^{-5} may be placed on

the sticking probability of these molecules on clean mercury at 77 °K. On the other hand, a sticking coefficient between 0.1 and unity for atomic hydrogen on mercury at 77 °K is compatible with the data.

36. The application of the pumping time equation in vacuum technique by Th. Kraus, Geraetebau-Anstalt Balzers, Principality of Liechtenstein (to be presented by O. Winkler, Balzers, Liechtenstein)

In an earlier publication a general pumping time equation was derived which determines the pressure-time dependence of the pumping process in a vacuum plant in the pressure range below about 0.1 Torr.

Besides the dimension of the inner surface of the plant and the pumping speed the pumping time which is needed to attain a defined pressure is determined by the specific value of the gas emission of the internal surface and the final pressure which is reached after infinite time.

A method was developed which allows a reliable determination of the constant which characterizes the gas emission (delivery?) of materials. A few examples show in how far this constant depends on the surface quality and previous treatment. With the help of the pumping time equation it is possible to find out quickly and with only a few measuring points the attainable final pressure as well as existing leaks or other additional gas sources in an isothermal high vacuum system.

37. Apparatus for electron optical study of low-density gas Flow by S. R. Mielczarek, D. C. Schubert, and L. Marton, National Bureau of Standards, Washington, D.C.

An apparatus has been developed and built at the National Bureau of Standards to study low-density ($\sim 10^{14}$ particles/cm^3 or $\sim 10^{-4}$ mm Hg) gas flow. This is an electron-optical schlieren technique which depends on the scattering of electrons in collision with individual gas molecules or atoms to form a dark field image of the gas. The apparatus consists of a bakeable stainless steel low-pressure chamber and other chambers containing brass and glass electron optical components which are not baked. The low-pressure chamber ($\sim 10^{-8}$ mm Hg) is connected to three other chambers ($\sim 10^{-6}$ mm Hg) through two small apertures and a slit. Metal gaskets are used on the bakeable chamber. The system is pumped by four oil diffusion pumps each with a liquid nitrogen trap. A small liquid helium trap (~ 1.5 liters) will be used to decrease the residual pressure from 10^{-7} mm Hg to 10^{-8} mm or better.

(This work was supported by the Office of Naval Research.)

38. Nitride, oxide, and silicide evaporated films for the electronic industry by E. H. Layer, Battelle Memorial Institute, Columbus, Ohio

Nitride, oxide, and silicide evaporated films exhibit properties which promise to further advance the developments recently begun in the electronics industry by metal and metal alloy evaporated films. These advances are exemplified by the recent graduation of precision film resistors, high resolution film potentiometers, high speed storage elements, fast response resistance thermometers, and 'two-dimensional' microwave resistors from 'technically feasible' to 'in use' in many types of today's electronic equipment. Primarily, the materials for these devices are metals or metal alloys. Simultaneously, with these advancements, thin film devices of the nitrides, oxides, and silicides of various metals have been developed, and more are expected to follow, which promise to extend the range of usefulness of the evaporated film concept. These materials are generally harder, and more refractory than metals and alloys, and further offer an even greater range of properties by selected combination than available from alloying of metals alone. These differences lead to improvements in device properties, for example, higher operating temperature, or longer life, and also may lead to greater versatility in circuit design. This paper will discuss these new film materials and the ways in which the inherent advantages of vacuum deposition are used to prepare superior films.

39. Evaporation of thin cathodoluminescent films by J. P. Reames, Massachusetts Institute of Technology, Cambridge 39, Massachusetts

A new method of evaporating in vacuum simultaneously ZnS and Mn to obtain a cathodoluminescent thin film is described. The ZnS and Mn are evaporated from separate evaporators which meter the amount of material evaporated by measuring the ionized atoms from each evaporator. The range of luminescent color versus Mn concentration is shown and qualitative dependence on substrate temperature is demonstrated. The equipment is described in detail with some remarks on methods of cleaning glass substrates for evaporation.

40. Evaporated Cr films on hot substrates by D. Hoffman and J. Riseman, International Resistance Company, Philadelphia, Pennsylvania

The electrical properties of thin Cr films have been shown to depend primarily on the conditions and method of preparation. By the proper choice of evaporating conditions, it has been possible to prepare Cr films with properties which closely approach that of the bulk metal.

41. Gas absorption by vacuum evaporated magnetic films by F. R. Gleason, J. H. Greiner and L. R. Yetter, International Business Machines Corporation, Owego, New York

Mass spectrometric determinations have been made of the types and amounts of gases absorbed during the deposition of vacuum evaporated magnetic thin films. Films were evaporated under varying conditions which included: 10^{-4} to 10^{-6} mm of Hg pressure, with and without liquid nitrogen trapping, with either oil or mercury diffusion pumping and various deposition rates.

Analyses have been made of gas samples collected by outgassing the source material, outgassing evaporated films, and by sampling the bell jar atmosphere during the evaporation.

It will be shown that the gas absorbed in the films is much greater than that present in the starting charges and is due to dissociation of vapor backstreaming from the oil diffusion pump. The gas molecules absorbed per metal atom degassed are independent of the film thickness indicating that the gas is trapped in the film structure as well as on the surface.

The experimental apparatus and techniques employed for this gas analysis study are described.

42. The use of sensitization methods for study of distillation source images by L. E. Preuss and C. E. Anthony, Department of Physics, Edsel B. Ford Institute for Medical Research, Detroit 2, Michigan

An unique and sensitive method for image formation of vacuum distillation sources has been developed using the surface sensitization principle. It consists of the condensation of a tenuous *latent image* made up of sensitizer metal atoms. This is done with the simple distillation camera. This image is *developed* by means of a second evaporation of a metal which ordinarily has a low sticking coefficient for the substrate. The combination of developer, substrate, and sensitizer is critical. The principle involves the changing of the accommodation factor of the developer for the condensing surface by the sensitizer deposit. The method appears to exhibit better experimental reach than the radioautographic methods. A number of source types studied by this system are described.

43. Large-area sources and two-source control by Klaus H. Behrndt, International Business Machines Corporation, Federal Systems Division, Kingston, New York

For industrial applications of thin films, it is very essential to have uniform thickness of the deposit over a large substrate area. Rods have been considered as evaporation sources, and several arrangements of rods have been theoretically investigated as to the uniformity of the deposit which can be expected. The highest thickness uniformity is still obtained from a ring source.

Vol. 9 59/60

If an alloy is to be deposited, its chemical composition can be easily varied by simultaneous evaporation from two concentric sources of the constituents. Crystal oscillators are used to control the evaporation of both sources. This procedure is discussed together with theoretical and experimental results.

44. Evaporation from a controlled planar source by J. R. Walker and B. R. Eichbaum, Product Development Laboratory, International Business Machines Corporation, Kingston, New York

A new method of reproducing, uniform, high quality " thin films " by vacuum deposition has been accomplished through evaporation from a controlled planar source. Important factors which contribute to its success are ; the planar source which is larger than the substrate, and the instrumentation to control the temperature of this source. Three major considerations in reproducing uniform films are : the control of evaporation rate, the exposure time and the physical configuration of the source and aperture. In this indirect method the control of film reproducibility and uniformity is based on a temperature-time relationship since the geometric parameters are fixed. By this method films of similar thickness and uniformity were produced on several runs in a (12-inch) PW-400 vacuum system at 8×10^{-6} mm Hg.

45. A simple film thickness gauge utilizing Newton's rings by A. W. Winston, C. A. Baer, and L. R. Allen, National Research Corporation, Cambridge, Massachusetts

A simple film thickness gauge based on Newton's rings has been constructed to measure the thickness of evaporated films. Briefly, it consists of a light filter whose wave-length transmission varies linearly with its position with respect to a slit, a micrometer feed for moving the filter, a plano-convex lens whose convex surface is coated with a semitransparent Inconel coating, and a support for positioning the lens without scratching the film or lens coating.

Its advantages are : (1) lack of ambiguity in determining fringe shift ; (2) ease of adjustment ; (3) not so complex as the usual multiple beam interferometer.

46. A demountable ultra-high vacuum glass-system and its components by Klaus H. Behrndt, International Business Machines Corporation, Federal Systems Division, Kingston, New York

A special glass system has been constructed whose body consists of $2\frac{3}{4}$-inch diameter pyrex tubing. The system is demountable by means of knife-edge seals. A liquid metal ultra-high vacuum valve allows us to disconnect the ultra-high vacuum chamber from the diffusion pump. Additional pumping is performed by a liquid helium pump. A protection circuit provides safe operation of the unattended system. Nickel-iron films are evaporated. They can be observed by the magneto-optical Kerr effect while still contained in the ultra-high vacuum chamber. The components of the system, the procedure to obtain pressures in the 10^{-10} mm Hg region, and the evaporation of the films are discussed.

47. Results with ultra-high vacuum metal system including windows, evaporators and lead-ins by H. Ehlers and J. Moll, Leybold Hochvakuum Anlagen, GMBH, Köln Bayental, Germany (to be presented by G. W. Oetjen)

Subject of this paper is an ultra-high vacuum metal system which is provided with window, rotary transmission, current lead-in, evaporator, etc., and which is used, for instance, to carry out metallization processes. The design of the different parts of the system is such that reliable and reproducible vacuum tightness is given. In this way a wearisome leak detection with expensive instruments is avoided. The system can be readily opened and closed. It can be baked out at a sufficiently high temperature and enables a quick attainment of the ultimate vacuum pressure and thus short cycle times. The experiences gained with this system will be described. Especially, a number of metallization processes were carried out in the ultra-high vacuum pressure range the results of which will likewise be set forth.

48. A large bakeable vacuum valve by Thomas H. Batzer, Lawrence Radiation Laboratory, University of California, Livermore, California

The development and design of a large bakeable valve based on a unique seat arrangement and a novel motion seal will be described.

The seat sealing is accomplished through the use of high pressure fluid actuation of an annular pinch gasket. Experimental data on seat closure performance, and the specific design features to achieve successful closures are presented.

The bakeable motion seal utilizes a stainless steel bellows sleeving over an inner concentric actuating shaft. This shaft is bent at 90° to the axis of rotation and is free to rotate relative to the bellows. There is no apparent size limitation to this type of actuation.

The design of a 10-inch gate valve utilizing these principles is described.

49. Corrosion-resistant roots pumps by H. Bode, E. Leybold, Nachfolger, Cologne, Germany

Impellers and housing of roots pumps may be protected from corrosion without major difficulty. This includes also protection against hydrofluoric acids. For the protection of bearings and gears two methods are possible :

They should either be made of corrosion-resistant material, or the gears are located in casings carefully sealed off against the aggressive substance. In the following we give a description of tests which have brought about acceptable solutions.

50. Ultra low temperature mechanical refrigeration systems for high vacuum traps and baffles by Hugh R. Smith and Patrick B. Kennedy, Lawrence Radiation Laboratory, University of California, Berkeley, California

Current techniques in mechanical refrigeration are described for the attainment of temperatures in the range of −150 °F to −240 °F in vacuum system traps and baffles.

Particular emphasis is directed to the application of refrigeration systems for the replacement of liquid nitrogen cooled installations.

Three types of systems are described : (1) A 2 stage mixed refrigerant system, (2) A double cascade with 2 stages per cascade, (3) A triple cascade with single stages per cascade. In addition to system schematics, the pertinent assembly, test, and operational procedures are described in detail.

Design features such as the selection of refrigerants, sizing of compressors, modification of commercial components, and compatability of the mechanical and refrigeration design of traps and baffles are discussed.

51. Ceramic, sapphire, and glass seals for the C-stellarator test facility by J. A. Zollman, John A. Powell and I. E. Martin, Radio Corporation of America, Electron Tube Division, Lancaster, Pennsylvania

This paper will cover the theory, calculations, and results adapting the basic Super Power Tube compression seal for use with ceramic cylinders up to 20-inch diameter and sapphire viewing windows up to 4-inch diameter into the stainless steel vacuum vessel for the Model C-Stellarator Test Facility. The properties of the metals selected and their heat-treating schedules will be given, together with the results of alternate sapphire-to-metal sealing methods. The design, fabrication, and stress isolation techniques of 4-inch and 7-inch diameter flat glass observation windows capable of 450 °C bakeout will be described.

52. Improved reliability of soft glass to metal vacuum tight seals by F. A. Loughridge and W. S. Wong, Sylvania Electric Products, Incorporated, Salem, Massachusetts

Modern high speed manufacturing methods together with increasing demands for reliability have created a statistical sampling problem in many lines of electronic lamp manufacturing. This situation can be improved by better methods of examination. Detailed methods for examination of finished

dumet seals are described in this paper which have been helpful to the authors in diagnosing manufacturing problems accurately and have permitted prompt corrective action. The helium mass-spectrometer type of leak detector and the research metallograph are used extensively in this work. The discussion of methods of examination is followed by a description of the common faults found in seals along with recommended corrective action. It is possible by use of these methods to build a higher quality product which is of great help in the sampling and inspection problem. Trial and error type of corrective action can be avoided in many cases saving time and unnecessary expense.

53. Design and operating potentials of work accelerated electron emission sources for electron beam welding by T. H. Crane, High Vacuum Equipment Corporation, Hingham, Massachusetts
In the *work accelerated gun system* focal spot size may be varied from a uselessly small point to wide areas of relatively low power density suitable for heat treatment, vacuum soldering and vacuum brazing. The same gun may be refocused by changing the grid potential to allow welding of such metals as tungsten and tantalum. In our experience with the work accelerated gun system, we have encountered problems due to the tremendous field gradient which is characteristic of this system. We have developed the concept of a mono-gradient field to use this gun in general welding work so that not too much attention need be given to the work geometry. The gun structure must be designed to minimize fields in directions other than the desired welding direction or there will be intense corona discharge rather than effective welding power. This system has several limitations in that a gas burst from the work results in a degeneration to ion conduction. Some work geometries make the fairly short focus of this gun system difficult to use from an operator's point of view. We have found, however, that these circumstances constitute only a minor portion of the welding we have thus far seen.

vol. 9 59/60

54. The behavior of titanium in a high vacuum by J. Morrison, Bell Telephone Laboratories, Incorporated, Murray Hill, New Jersey
The behavior of titanium in a high vacuum is of interest because of its use in vacuum tubes and in vapor-ion pumping. Contrary to its gettering properties at elevated temperatures, and pressures in the micron range, titanium was found to be a source of large quantities of hydrogen and small amounts of other gases at temperatures of about 200 °C and pressures in the 10^{-5} mm to 10^{-6} mm range. The evolution of gas was affected greatly by the pre-processing treatment given the titanium.

Evolution rates of hydrogen from titanium which was purposely loaded with hydrogen at 1000 °C in a gas pressure of one hundred millimeters were also determined. Titanium which has been treated in this way could serve as a practical source of hydrogen in small quantities.

The vapor pressure of titanium was determined by measuring evaporation rates in the temperature range of interest in the processing of vacuum tube components. This temperature range is lower than many published previously. The emissivity of titanium was determined experimentally in the temperature range used for these evaporation rate studies.

55. Properties of a small titanium-ion-pump by A. Klopfer, Allgemeine Deutsche Phillips Industrie, G.m.b.H., Zentrallaboratorium, Laboratorium Aachen, Aachen, Germany
A small getter-ion-pump is described which has a capacity of several Torr-liter for chemically active gases. The maximum pump speed for CO is 50 l/sec. The lowest pressure obtained with this pump is less than 10^{-10} Torr. The composition of the residual gases during the process of evacuation has been measured. The factors determining the lowest pressure that can be obtained are discussed.

56. A method for greatly enhancing the pumping action of a Penning discharge by Wilson M. Brubaker, Research Division, Consolidated Electrodynamics Corporation, Pasadena 1, California
Although the Penning discharge has long been used as a vacuum gauge, it is well known that it exhibits a pumping action; recently this phenomenon has been used to make a vacuum pump. However, the various ideas expressed in the literature on the nature of this pumping action are not in agreement. In the present work mass spectrometric methods showed that argon and other noble gases are pumped at the cathode of the discharge.

We have found that the addition of a third electrode ot the usual diode Penning structure eliminates the most serious shortcomings of the simple Penning discharge as a vacuum pump for the noble gases. The mechanism whereby the third electrode greatly enhances the pumping action of the discharge is described. Experimental data is presented which compares the pumping behavior of the discharge in the two and the three electrode structures.

57. Design considerations for high speed getter-ion pumps by Renn Zaphiropoulos and William A. Lloyd, Varian Associates, Palo Alto, California
Following a brief review of the basic principles of operation of getter-ion pumps, the recent evolution of relatively large pumps is described. In particular the design and construction features of a 5000 liter per second VacIon* pump are presented. Operating procedures and performance characteristics are given, and methods of testing are discussed. Designs of still larger pumps are presented briefly.

58. Some studies of getter-ion pumped vacuum systems by Irving Ames and R. L. Christensen, International Business Machines Corporation, Research Laboratory, Poughkeepsie, New York
Vacuum phenomena in several small, bakeable glass-metal systems, evacuated by getter-ion pumps, have been investigated. The systems were evacuated by various combinations of water-aspiration, cryogenic pumping, and getter-ion pumping. Various degrees of baking were employed. These ranged from heating of localized portions, through mild baking of the entire system while at the " fore " pressure of the liquid helium pump, to hard baking at high vacuum. The composition and behavior of the residual gases were examined by means of an omegatron. Ultimate pressures of about 1×10^{-10} mm Hg and 5×10^{-9} mm Hg (equivalent N_2 pressures) have been attained respectively with and without bakeout.

59. The actual knowledge of gases's adsorption on barium getters by Paolo Della Porta, S.A.E.S., Getters Research Laboratory, Milan, Italy
The apparatus and techniques are described which have been used at S.A.E.S., Getters Research Laboratories to study gettering by evaporated Barium films. Particular attention is given to the influence of ionizing current and hot filaments. Results obtained for N_2, H_2 and CO sorption are compared. The various processes which contribute to the complex sorption phenomena are indicated. It would appear that parallel mechanisms control the sorption of different gases by Barium films. Data are given on the mobility of molecules of different gases on the surface and within the films. Finally the technique is given for studying barium films by electron microscopy.

*Registered S.S. Patent Office.

AMERICAN VACUUM SOCIETY

Special Notice—1960 Symposium

TENTATIVE PLANS are being made to hold the Seventh National Vacuum Symposium in the Cleveland, Ohio Area in October 1960. Those wishing to contribute papers to the Cleveland Symposium *should submit their proposals to any member of the* 1960 *Program Committee.*

Such proposals (in triplicate, please) should be in the form of abstracts of 100—150 words in length and be in the hands of the Committee Members on or before June 15, 1960. The manuscripts will be due on or before August 15, 1960. An early submittal is earnestly requested.

1960 Program Committee

C. ROBERT MEISSNER, *Chairman*, Georgia Institute of Technology, Engineering Experiment Station, Atlanta, Georgia
GEORGE H. BANCROFT, Consolidated Vacuum Corp., 1775 Mt. Read Boulevard, Rochester 3, New York
LOUIS PENSAK, Radio Corporation of America, Princeton, New Jersey
LUTHER E. PREUSS, Department of Physics, Edsel B. Ford Institute for Medical Research, Henry Ford Hospital, Detroit 2, Michigan
H. W. SCHLEUNING, Brooklyn Polytechnic Institute, 333 Jay Street, Brooklyn 1, New York
H. A. STEINHERZ, NRC Equipment Corp., 6 Charlemont Street, Newton Highlands 61, Massachusetts

International Conference on Structure and Properties of Thin Films

THIS CONFERENCE, sponsored by Air Force Office of Scientific Research, Air Research and Development Command, and General Electric Research Laboratory, was held at the Sagamore Hotel, Bolton Landing, Lake George, New York, September 9—11 1959. The following papers were presented :

FORMATION OF THIN FILMS

G. A. Bassett, J. W. Menter, and D. W. Pashley, *Tube Investments Research Laboratories.*—Review Paper : The Nucleation, Growth and Microstructure of Thin Films.

Current Research Papers :

J. A. Allen, C. C. Evans, and J. W. Mitchell, *University of Bristol.*—Evidence for the Structure of Thin Films of Copper from Adsorption Measurements.

W. Buckel, *University of Göttingen.*—Some Remarks on Crystal Growth in Thin Films.

J. A. Bennett, *British Scientific Instrument Research Association.*—An Investigation into the Binding Energy of Thin Films.

H. Hashimoto, T. Naiki, M. Mannami, and K. Fujita, *Kyoto Technical University.*—Electron Microscopic Study by Cine Film on the Formation of Thin Oxide Films.

T. N. Rhodin, *Cornell University.*—Oxide Nucleation on Magnesium.

B. M. Siegel and C. C. Peterson, *Cornell University.*—Studies on the Nucleation, Growth and Oxidation of Evaporated Copper Films with a High Vacuum Electron Diffraction Camera.

CHARACTERIZATION OF THIN FILMS

J. W. Menter and D. W. Pashley, *Tube Investments Research Laboratories.*—Review Paper : The Microstructure and Mechanical Properties of Thin Films.

Current Research Papers :

H. G. F. Wilsdorf, *Franklin Institute.*—On the Multiplication of Dislocations in Thin Metal Films.

J. Silcox and M. J. Whelan, *University of Cambridge.*—Direct Evidence of the Annealing of Dislocation Loops and of Climb of Dislocations in Quenched Aluminum.

J. W. Beams, *University of Virginia.*—Mechanical Properties of Thin Films of Gold and Silver.

R. B. Nicholson, *University of Cambridge.*—Phase Transformations in Alloys.

D. W. Pashley and A. E. B. Presland, *Tube Investments Research Laboratories.*—The Study of Ordering and the Arrangement of Domains in Thin Films of Copper Gold Alloy.

M. Blackman and A. E. Curzon, *Imperial College.*—On the Size Dependence of the Melting and Solidification Temperatures of Small Particles of Tin.

H. E. Farnsworth and H. H. Madden, *Brown University.*—Chemisorption of Oxygen by Evaporated Nickel Films Deposited on a (100) Face of a Nickel Crystal.

ELECTRICAL PROPERTIES

H. Mayer, *Bergakademie Clausthal.*—Review Paper : Recent Developments in Optical and Conduction Phenomena in Thin Metal Films.

Current Research Papers :

R. Nossek and H. Mayer, *Bergakademie Clausthal.*—Separate Experimental Determination of the Relaxation Time Due to Lattice Vibrations and to Lattice Imperfections

A. Colombani, *University of Caen.*—Electromagnetic Properties of Thin Films of Bismuth.

C. C. Evans and J. W. Mitchell, *University of Bristol.*—The Influence of the Adsorption of Gases on the Resistivity of Thin Films of Copper.

R. Suhrmann, G. Wedler, and G. Schumicki, *Technische Hochschule Hannover.*—Influence of Hydrogen on the Electrical Resistance of Evaporated Palladium Films.

E. C. Crittenden, Jr., *Space Technology Laboratories, Inc. and U.S. Naval Postgraduate School.*—Critical Currents in Superconducting Thin Films.

M. Tinkham, *University of California.*—The Energy Gap in Thin Superconducting Films.

W. Shockley, *Shockley Transistor Corporation.*—Thin Diffused Layers on Semiconductors.

MAGNETIC PROPERTIES

C. P. Bean, *General Electric Research Laboratory.*—Review Paper : Magnetic Properties of Thin Films.

Current Research Papers :

C. A. Neugebauer, *General Electric Research Laboratory.*—The Saturation Magnetization of Nickel Films of Thickness Less Than 100Å.

Vo. 9 1959

K. H. Rosette and R. W. Hoffman, *Case Institute of Technology*.—Spontaneous Magnetization of Iron Films.

D. O. Smith, *Lincoln Laboratory, Massachusetts Institute of Technology*.—Some Structure-Sensitive Magnetic Properties of Permalloy Films.

P. E. Tannenwald, *Lincoln Laboratory, Massachusetts Institute of Technology*.—Some Properties of Magnetic Films by Microwave Resonance.

A. Colombani, *University of Caen*.—The Hall Effect in Thin Films of Nickel-Experimental Results.

R. D. Heidenreich and F. W. Reynolds, *Bell Telephone Laboratories*.—Magnetic Anisotropy and Microstructure of Magnetic Metal Films.

H. J. Juretschke, *Polytechnic Institute of Brooklyn*.—Magnetic and Galvanomagnetic Properties of Thin Ferromagnetic Films.

O. S. Heavens and R. F. Miller, *Royal Holloway College*.—Faraday Rotation in Thin Epitaxially Grown Nickel Films.

CHEMICAL INTERACTION AT SURFACES

G. Ehrlich, *General Electric Research Laboratory*.—Review : Molecular Processes at the Gas-Solid Interface.

Current Research Papers :

E. W. Müller, *Pennsylvania State University*.—Field Ion Microscope Studies of Surface Corrosion, of Interstitials, Vacancies and *a*-Irradiation Damage by Controlled Field Evaporation of Atomic Layers.

H. Raether, *University of Hamburg*.—The Structure of Thin Films of Iron and Its Oxides.

P. W. Selwood, *Northwestern University*.—Chemisorption on Superparamagnetic Nickel.

S. R. Logan and C. Kemball, *Queen's University of Belfast*.—The Relation Between Catalytic Activity and Weight of Metal Films Used for the Decomposition of Ammonia.

L. Pensak, *Radio Corporation of America Laboratories*.—Effect of Gases on the High Voltage Photovoltaic Effect.

D. D. Eley and P. R. Wilkinson, *University of Nottingham*.—Kinetics of Oxidation of Aluminum Films.

Panel on Theory of Surfaces.—*Chairman*—C. Herring, *Bell Telephone Laboratories. Members:*—V. Heine, *University of Cambridge* ; H. J. Juretschke, *Polytechnic Institute of Brooklyn* ; W. Shockley, *Shockley Transistor Corporation.*

Summary of Conference.—J. C. Fisher.

GENERAL DISCUSSION

The full proceedings of this conference will be published by John Wiley & Co. Ltd.

Vol. 9 959/60

Vacuum Metallurgy

THE NEW YORK University has announced that a Conference on Vacuum Metallurgy is to be held on 2—3 June, 1960, under the Chairmanship of Dr. R. F. BUNSHAH. Papers are invited for presentation at this Conference on new research or advanced engineering information. Authors desirous of submitting papers should send a 20 line abstract to Dr. R. F. BUNSHAH no later than *February* 10, 1960. The time for presentation of the papers will be 30 to 40 minutes. The proceedings of the Conference will be published in a Transactions volume. The Conference will be held on the University Heights Campus of New York University, Bronx 5, New York.

Classified Abstracts

Classification System

I. General Vacuum Science and Engineering

(Books, review articles, bibliographies, summaries, general techniques, articles on basic vacuum physics)

10. Vacuum Technology

11. Production of Low Pressures

12. Measurement of Low Pressures

13. Vacuum Applications

14. Kinetic Theory of Gases (transport phenomena, diffusion through vapors, molecular flow of gases, etc.)

15. Fluid Dynamics (turbulent and viscous flow of gases, flow through nozzles, boundary layer flow, etc.)

16. Gases and Solids (sorption, diffusion through solids, permeation, etc.)

17. Thermodynamics (compression, temperature, reactions, vaporization, dissociation, vapor pressure, cryogenics, etc.)

18. Gaseous Electronics (ionization, discharges, plasma, emission, etc.)

19. Radiation (light, heat, X-rays, microwave radiation, etc.)

II. Vacuum Apparatus and Auxiliaries

(Design, testing, operation, performance and techniques of using individual apparatus for the production, measurement, and control of low pressures)

20. Pumping Systems (plant)

21. Pumps and Pump Fluids (mechanical pumps, vapor pumps, getter-ion pumps, cryopumps, etc.)

22. Gauges (including mass spectrometer types)

23. Plumbing (joints, pipe, gaskets, fittings, flanges, glass-to-metal seals, shaft seals, etc.)

24. Valves (stopcocks, variable leaks, gas introducing devices, needle valves, etc.)

25. Baffles, Traps, and Refrigeration Equipment

26. Automatic Protective and Control Equipment (cut-offs, switches, liquid level controls, manostats, etc.)

27. Leak Detectors and Leak Detection

28. Heating Equipment (ovens, resistance heating units, induction heating units, etc.)

29. Miscellaneous

III. Vacuum Applications

30. Evaporation and Sputtering (to form solid coatings)

31. Evacuation and Sealing (electronic tubes, switches, lamps, vacuum insulation, gas-filled devices)

32. Nucleonics (particle accelerators, counters, plasma machines, isotope separation, etc.)

33. General Physics and Electronics (electron tube physics, electron microscopy, diffraction camera, field emission microscope, spectroscopes, X-ray tubes, low temperature physics, etc.)

34. High Altitude and Space Technology (test chambers, ion propulsion, etc.)

35. Impregnation and Potting

36. Drying, Degassing and Concentration (including freeze-drying, glass processing, evaporation of solvents, etc.)

37. Metallurgy, Inorganic Chemistry, Analytical Chemistry (production and analysis of metals and inorganic chemicals, melting, casting, annealing, sintering, degassing in molten state, vacuum fusion gas analysis, mass spectrometer analysis of inorganic materials, etc.)

38. Distillation, Organic Chemistry, Isotopic Gas Analysis

39. Miscellaneous Applications (fumigation, etching, forming, surface area measurement, etc.)

IV. Materials and Techniques Used in Vacuum Technology

(Properties, composition, purification and use of materials ; fabrication and processing techniques)

VO.
9
1959

40. Gases and Vapors

41. Metals and Alloys (including mercury)

42. Glass and Ceramics

43. Plastics and Elastomers

44. Waxes, Lubricants, Cements, Lacquers, Paints, Oils

45. Soldering, Welding, Brazing

46. Glass Blowing, Glass-to-metal and Ceramic-to-metal Sealing Techniques

47. Outgassing Data, Vapor Pressure Data, Gettering Data

48. Heating, Refrigeration, Ultrasonics, Centrifuging

49. Miscellaneous Materials and Techniques

V. **Basic Science and Engineering**
(For cross reference purposes)

50. Mathematics

51. Physics, Astronomy, Geophysics

52. Physical Chemistry

53. Metallurgy, Ceramics, Inorganic Chemistry

54. Biology, Biochemistry, Pharmaceutics, Toxicology, Organic Chemistry

55. Chemical Engineering

56. Electrical Engineering, Electronic Circuits

57. Mechanical Engineering

58. Nucleonics

59. Miscellaneous

Vol.
9
959/60

Abstracts

General Vacuum Science and Engineering

13. Vacuum Applications

13 : 30 : 37

347. Proceedings of the Fourth Conference on Magnetism and Magnetic Materials.
United States. Published as a supplement to Volume 30 of the Journal of Applied Physics, this book contains the 143 papers presented at a conference held in Philadelphia in November, 1958. Subjects covered include ferrites, computer components, micromagnetics, magnetic properties of metals and alloys, fine particles, amplifiers and microwave applications, resonance, metallurgical considerations, fundamental interactions, instrumentation, thin films, neutron diffraction and irradiation, garnets and other compounds, and anisotropy. C. R. M.

13 : 30 : 37

348. Sputtered Resistors Make High Component-Density Possible.
United States. Exceedingly small and sharply defined thin film resistors have been made by sputtering refractory metals. A special masking technique is used permitting resistive conductors as narrow as .001 in. and spaced .001 in. apart. This could be called the *lost-copper* method whereby the substrate is coated with vapor deposited copper. Standard photo etching methods are used to transmit the required pattern on to the substrate and subsequently stripping the copper from the *useful* areas. Refractory metal is subsequently vapor deposited over the entire substrate. This is followed by a second etching step which attacks the copper and thus removes also its overlay of refractory metal. In this manner the refractory metal is left only in the *useful* areas. The thinness of the copper film permits the transmittal of fine detail. Unusually compact circuit configurations have been produced with components and interconnexions of a material formed at the same time. C. R. M.

D. A. McLean, *Bell Lab. Rec.*, Sept. 1959.

14. Kinetic Theory of Gases

14 : 16 : 30 : 40

349. The Diffusion of Impurities into Evaporating Silicon.
United States. Following a brief review of the fundamental characteristics of semi-conductors the concept of solid state diffusion of intentional materials into silicon is introduced. In this doping process the concentration of the intentional material or impurity is found to be a non linear function of depth of penetration. The diffusion is carried out in a vacuum by the accurately controlled rate of evaporation of the parent material and rates of deposition of the impurity or impurities from the vapor phase(s). By selection of the type of impurity in the silicon body to be of a different group in the atomic table than that added by the vapor deposition a junction of opposing polarities is obtained. This junction occurs within the parent material at a region where the impurity concentrations of parent and of added materials are equal. A method is outlined for adjusting the rate of silicon evaporation to the rates of diffusion of the doping materials. The elements discussed are boron, aluminum, gallium and indium from Group III of the periodic table to produce a *p*-type silicon. On the other hand phosphorus, arsenic, antimony, and bismuth are quoted from Group V for producing *n*-type silicon. Diffusion experiments were conducted with phosphorus, gallium, arsenic and indium. Excellent control of the surface concentrations of these diffusants has been obtained within the range of 7×10^{19} to 5×10^{15} at./cc. Single and double diffused transistor structures have been obtained with an α-cut-off frequency of 70 Mc/sec. The apparatus is described and illustrated. C. R. M.

R. L. Batdorf and F. M. Smits, *Bell Lab. Rec.*, 330–333, Sept. 1959.

16. Gases and Solids

16

350. Oxide Nucleation and the Substructure of Iron.
Electron optical studies were made of the initial stage of reaction of oxygen with pure iron. Oxidation occurred in a discontinuous manner with the oxide structure orienting to the metal grain. The sites for oxide nucleation depend on the initial pretreatment atmosphere. Thus, a vacuum annealing treatment showed a random arrangement of nucleation sites, while a hydrogen annealing treatment showed a highly ordered arrangement of nucleation sites. Since iron was embrittled by annealing in dry and moist hydrogen and not by vacuum annealing, the nucleation sites probably show the substructure of iron responsible for embrittlement. (Author)

E. A. Gulbransen and K. F. Andrew, *J. Electrochem. Soc.*, **106**, 511–515, June 1959.

16

351. Enhanced Surface Reactions. III. Adsorption of Gases on Prepared Ruthenium Surfaces.
United States. Rates of adsorption of H_2, CO, and O_2 on $Ru.Al_2O_3$ catalyst surfaces prepared by pre-adsorption of gases were studied. Pre-adsorption of CO increases the rate and extent of H_2 adsorption. Adsorption of CO and of O_2 irreversibly poisons the surface. The Elovich equation is applicable to the data. The results are discussed in terms of a site-creation mechanism. It is found that the pre-adsorption of a gas may influence both the initial and the ambient rates of adsorption to various and at times opposite extents, resulting in several types of " poisoning." (Author)

M. J. D. Low and H. A. Taylor, *J. Electrochem. Soc.*, **106**, 138–142, Feb. 1959.

16 : 14 : 30 : 40

The Diffusion of Impurities into Evaporating Silicon. See Abstr. 349.

17. Thermodynamics

17

352. Equilibrium Reduction of Tungsten Dioxide by Hydrogen.
United States. A study has been made of the heterogeneous equilibrium involving H_2–W–WO_2–H_2O in the temperature range 500°–1000 °C, using a static equilibrium–type of apparatus. The standard heat of formation and entropy of WO_2, as calculated from the equilibrium data, was found to be $\triangle H^\circ = -135.0\pm0.3$ kcal and $17.1\pm$ 1.0e.u. The heats of formation of WO_2 and the two higher sub-oxides were determined by direct combustion. $\triangle H^\circ$ of $W_{18}O_{49}$ ($WO_{2.72}$) $= -183\pm1$ kcal/mole W, $\triangle H^\circ$ of

$W_{20}O_{58}$ ($WO_{2.90}$) = -193 ± 1 kcal/mole W, and $\triangle H^\circ$ of WO_2 = -137 ± 1 kcal/mole W. (Author)

R. C. Griffis, *J. Electrochem. Soc.*, **105**, 398–402, July 1958.

17 : 36

353. Sublimation Freeze–Drying Without Vacuum.

H. T. Meryman, *Science*, **130**, 3376, 628–629, 11 Sept. 1959.

19. Radiation

19 : 51

354. Phase Charge on Reflection from Evaporated Chromium Films.

C. Weaver, R. M. Hill, and J. E. S. Macleod, *J. Opt. Soc. Amer.*, **49**, 992–997, Oct. 1959.

Vacuum Apparatus and Auxiliaries

21. Pumps and Pump Fluids

21

355. On the Pumping Speed of Oil Diffusion Pumps.

Italy. The measurements of the jet breakdown pressure of an oil diffusion pump have been taken in respect of the heat input, and those of the pumping speed S have been taken both in relation to heat input and forepressure, both for air and for hydrogen. It was found that :

(1) the breakdown pressure of the jet is the same for air and hydrogen and increases when the heat imput increases ;
(2) the pumping speed both for air and hydrogen is independent of the forepressure :
(3) the pumping speed for air is nearly constant in relation to heat input, while for hydrogen it has a distinct maximum for which the ratio $S(H_2)/S(A)$ is equal to 1.34. Such a value agrees with the calculations which may be made using the theory of R. Jaeckel.

At the end, the plan for the apparatus for measuring the pumping speed of a diffusion pump has been referred to.

S. Petralia and U. Valdrè, *Il Nuovo Cimento*, **12**, No. 6, 16 Giugno 1959.

27. Leak Detectors and Leak Detection

27 : 37 : 40 : 47

356. Materials and Processes of Electron Devices.

United States. The unusual interest in the subject of electron devices is evidenced by the fact that the dust jacket of this book is printed in four languages, although the text is entirely in English. Fourteen chapters cover the preparation and working of materials used in electron devices, finishing techniques such as degassing and getter procedures, and the production of solid state devices. An unusually detailed table of contents supplements the subject index. A bibliography of about 2300 references gives some indication of the thoroughness with which this text was prepared. In addition to the quantity of excellent black and white illustrations, the book contains four color plates showing stress patterns in glass-metal sealings and in a glass tube, leak detectors at different pressures, and the degassing of a graphite anode. C. R. M.

Max Knoll assisted by B. Kazan, *J. Franklin Inst.*, **268**, Aug. 1959.

28. Heating Equipment

28

357. Microfurnace for Thermal Microscopy and Studies at High Temperatures.

United States. A small laboratory furnace is described for use in high-temperature microscopy and for determining chemical compatibility, wetting, sintering, and temperatures of apparent melting up to 3000 °C (5433 °F). The furnace shell is a water-cooled, 5-in. copper tee and is of such construction as to afford a controlled atmosphere. Water-cooled electrodes are designed to hold refractory metal strip heaters (either plain or with a wedge for better black body conditions) or special-machined graphite heaters. Stepless power input is provided by variac-controlled, saturable core reactor. (Author)

W. A. Lambertson and G. Lewis, *J. Electrochem. Soc.*, **106**, 124–126, Feb. 1959.

Vol. 9 959/60

Vacuum Applications

30. Evaporation and Sputtering

30

358. Tungsten Coils for Vacuum Metallizing.
United States. The most suitable shapes and sizes of tungsten coils for evaporation of aluminum are discussed on the basis of extensive experience in this field. Similar considerations are valid for the evaporation of other metals for which accepted heaters are tabulated. Tungsten is the choice in 83 per cent of the cases cited, because it has a high melting point, low vapor pressure, sufficient mechanical strength, and is readily 'wetted by Al and many other metals. It is common practice to use multi-strand tungsten wires which are wound into coils from which aluminum flags, or staples are suspended, or into which a one-piece charge is inserted. Uniform coverage of the coil by Al is necessary if adequate coil life—repeated charges—is expected. Three-wire strand made from 0.020, 0.025, or 0.030 in. *dia.* wire in most cases gives the best combination of good holding capacity and longest life. A coil used for evaporating 35 mg Al on to certain lamp bulbs may last 50 c, but, in evaporating 250 mg Al from a similar coil in aluminizing TV picture tubes, the life may be only 7 or 8 c. Metallurgical considerations determine the practical performance of the coil. Tungsten recrystallizes when heated to 1500 °C and becomes brittle. Al diffuses into tungsten and dissolves 3 per cent tungsten by volume. The compound formed is evaporated and redeposited on neighbouring turns of the coil and adjacent surfaces. Non-uniform heating may result from this effect as it does from nonuniform wetting of the Al on initial melting, leading to hot spots and burnouts. W. H. K.

R. P. Ranger and W. G. Matheson, *Sylvania Technol.*, **12**, 37–40, Apr. 1959.

30

359. Reflecting Coatings for the Extreme Ultraviolet.
United States. Evaporated aluminium films are the most frequently used for coating first surface mirrors because of their good adherence and high reflectance. They are particularly suitable for optical components to be used in the extreme ultraviolet because the reflectance of evaporated Al is higher than that of any other single film in the wavelength region between 1250 and 2000 A. Interest in the optical properties of films in this spectral region has been stimulated by the increasing number of research problems using vacuum ultraviolet spectroscopy. In the extreme ultraviolet the reflectance of evaporated Al films is influenced by the evaporation and storage conditions. The most important factor is the rate of evaporation. Full reflecting and opaque mirror films (600–700 A) should be deposited in less than 2 s and 1 μ thick coatings for gratings should be deposited in less than 15 s. The Al should be very pure and the substrate temperature should be less than 50 °C. A diagram of the evaporation chamber is reproduced. Graphs showing the effect of residual gas pressure, evaporation rate, ageing, purity and substrate temperature on reflectance are shown. The preparation of bloom-free 1 μ thick Al films for grating blanks is described, and the effect of thin oxide films on the efficiency of ruled gratings is discussed. Results of measurements on other films are also given, and it is shown that better ageing and higher reflectance can be obtained with materials such as platinum, zinc sulphide and aluminium oxide at wavelengths below 1200 A. Also given are the methods of preparation and the reflecting properties of various multilayer film combinations suitable for reducing the reflectance of mirrors and gratings in the visible and the near ultra-violet, while at the same time preserving a high reflectance in the extreme ultraviolet. A 250 A thick layer of magnesium fluoride evaporated on Al immediately after its deposition was found both to raise the reflectance to about 80 per cent at wavelengths down to 1200 A and to retard the effects of ageing.

G. Hass and R. Tousey, *J. Opt. Soc. Amer.*, **49**, 593, June 1959.

30

360. Optical and Photoelectric Properties of Thin Metallic Films in the Vacuum Ultraviolet.
United States. Measurements have been made on evaporated thin films of Al, Sn, In, Bi, Au, Ag, and Cd in order to correlate optical transmission, reflection, and photoemission in the far ultraviolet. Thin unbacked films prepared outside the spectrograph and glass-backed films prepared inside the spectrograph were used. The frequency at which the films change from a reflecting medium to a transmitting medium has been compared with the plasma frequency predicted by Bohm and Pines and also with electron energy eigenlosses in metals observed by Marton et al. Some new absorption transitions have been observed and related to X-ray absorption edges. A qualitative correlation between the photoelectric yields and corresponding optical properties has been attempted. (Author)

W. C. Walker, O. P. Rustgi, and G. L. Weissler, *J. Opt. Soc. Amer.*, **49**, 471, May 1959.

30

361. Improved Metallic Coatings by Vacuum, Vapor Plating.
Note. Anon., *Mat. Design Engr.*, **50**, 132–134, Aug. 1959.

30 : 34

362. Temperature Stabilization of Highly Reflecting Spherical Satillites.
G. Hass, L. F. Drummeter, Jr., and M. Schach, *J. Opt. Soc. Amer.*, **49**, 918–924, Sept. 1959.

30

363. Growth of Molybdenum, Tungsten and Columbium Crystals by Floating Zone Melting in Vacuum.
E. Buehler, *Bell System Monograph*, 3223. B.S.T.J. Vol. 38, No. 6, September 1959, 1332.

30 : 13 : 37

Proceedings of the Fourth Conference on Magnetism and Magnetic Materials. See Abstr. 347.

30 : 13 : 37

Sputtered Resistors Make High Component-Density Possible. See Abstr. 348.

30 : 14 : 16 : 40

The Diffusion of Impurities into Evaporating Silicon. See Abstr. 349.

31. Evacuation and Sealing

31 : 49

364. Titanium Coatings on Molybdenum Wire.
United States. To take advantage of the favorable properties of titanium as a grid material in electron tubes (low primary emission) and overcome its inadequate hot strength, titanium-coated molybdenum wire is used for the grid laterals. A method is described by which Ti is evaporated from a tungsten coil wrapped with fine Ti wire on to a Mo wire mounted on the axis of this coil in a vacuum tube. W. H. K.

R. L. Bronnes, *J. Electrochem. Soc.*, **106**, 272–273, Mar. 1959.

32. Nucleonics

32 : 34

365. Stratospheric Carbon-14, Carbon Dioxide, and Tritium.
F. Hagemann, J. Gray, J. L. Machta and A. Turkevich, *Science*, **130**, 542–552, Sept. 1959.

32

366. Which Approach to Controlled Fusion—The Machine Called DCX.
This article discusses the type of controlled fusion apparatus being developed at Oak Ridge National Laboratory, Oak Ridge, Tennessee. Included is a brief description of the vacuum apparatus. A dual type of system is used with separate pumping units

for the outer tank and the inner system or linear. A static vacuum pressure of about 10^{-8} Torr can be obtained. A. G.

H. C. Hay, *Mech. Eng.*, **81**, 55–57, Aug. 1959.

33. General Physics and Electronics

33

367. Studies of the Effect of Anode Materials on Oxide Cathode Performance.

United States. Experimenters in the area of physical electronics have come to realize in recent years that the components of an electron tube must be considered as a whole, and not singly, when aiming for optimum performance and stability throughout life. An example of this interaction is the influence of the anode material on cathode emission which is the subject of the experimental study carried out by Wolk. He finds that impurities present in minute amounts in so called pure nickel, such as Driver-Harris 499 nickel, a passive nickel, have a marked effect on the emission obtained from oxide-coated cathodes made from one of the purest cathode nickels, i.e. Wiggin HPM. If the anode is made also from HPM, emission from the cathode is essentially constant throughout life (2000 h). Anodes made from 499 nickel, nickel-plated steel (NPS), or Sylvania N4-nickel result in substantially higher emission levels, both initially and throughout life, showing a peak after 50 h and then dropping off, the maximum being about four times larger than corresponding emission with HPM anodes. Similar trends are observed in different combinations of cathode/anode materials. W. H. K.

B. Wolk, *Sylvania Technol.*, **12**, 41–45, Apr. 1959.

33

368. Infrared Vacuum Spectrometer with Prism Grating Double Monochrometer.

United Kingdom.

C. S. C. Tarbet and E. F. Daly, *J. Opt. Soc. Amer.*, **49**, 603, June 1959.

34. High Altitude and Space Technology

34 : 51

369. Research in Space.

Anon., *Science*, **130**, 195–202, 24 July 1959.

34 : 51

370. Effect of the Solar Wind on the Lunar Atmosphere.

J. R. Herring and A. L. Licht, *Science*, **130**, 226–268, 31 July 1959.

34 : 30

Temperature Stabilization of Highly Reflecting Spherical Satellites. See Abstr. 362.

34 : 32

Stratospheric Carbon-14, Carbon Dioxide, and Tritium. See Abstr. 365.

36. Drying, Degassing and Concentration

36 : 17

Sublimation Freeze-Drying Without Vacuum. See Abstr. 353.

37. Metallurgy, Inorganic Chemistry, Analytical Chemistry

37

371. Vacuum Casting Steel.

Digest of "The Importance of Vacuum Casting in the Steel Industry".

Z. Eminger, F. Kinsky, and Z. Kletecka, *Czechoslovak Heavy Industry*, No. 2, 3–20, 1957. Note by F. W. Boulger, *Metal Progress*, **76**, 142–148, Aug. 1959.

37

372. Vacuum Melted Metals and Alloys.

This article summarizes the status of vacuum melting. A cost comparison between conventional and vacuum melting is made. Vacuum induction melting, vacuum arc melting and vacuum degassing are discussed. Applications of these processes and the effects on the physical properties of various materials, including superalloys, magnetic materials and bearing materials, are discussed. A. G.

John L. Everhard, *Mater. Design Eng.*, **50**, 89–97, Aug. 1959.

37 : 13 : 30

Proceedings of the Fourth Conference on Magnetism and Magnetic Materials. See Abstr. 347.

37 : 13 : 30

Sputtered Resistors Make High Component-Density Possible. See Abstr. 348.

37 : 27 : 40 : 47

Materials and Processes of Electron Devices. See Abstr. 356.

Vol. 9 959/60

Materials and Techniques used in Vacuum Technology

40. Gases and Vapours

40

373. Separation of Gas Mixtures in a Supersonic Jet.
In 1954, E. W. Becker and co-workers in Marburg, Germany, discovered that large composition gradients existed in the supersonic jet generated by expanding a gas mixture through a Laval nozzle. Further experimental observations of this effect are presented for the mixtures A-N_2, O_2-N_2, and N_2-C_2H_4, showing characteristics of the phenomenon not previously reported. A quantitative theory based on free-molecule kinetics is suggested, and gives reasonable agreement with the experimental results in several respects. (Author)
P. C. Waterman and S. Alexander Stern, *J. Chem. Phys.*, **31**, 405–419, Aug. 1959.

40

374. Thermal Conductivity of Nitrogen-Carbon Dioxide Mixtures. Note by Richard S. Brokaw, *J. Chem. Phys.*, **31**, 571–572, Aug. 1959.

40

375. Adsorption of Nitrogen on Tungsten at very low Pressures.
Italy. Adsorption measurements of nitrogen on a thin tungsten ribbon in the pressure range of 10^{-8}–2×10^{-7} Torr, and at temperatures lying between 90 and 481°K, have been performed by using a new technique. The amount of adsorbed nitrogen is practically independent of the pressure in the range investigated. The adsorption rate is proportional to the pressure. At room temperature a fraction of the surface is covered by an irreversible film. At 90 °K, beside the above film, two other types of adsorption were found: the first irreversible at 481°K, and the second reversible below 160 °K. The sticking probability is independent of the pressure and almost constant until a high coverage is reached. Its value at low degrees of coverage (about 0.03) is rather lower than the values found by other authors, which however show quite large differences with each other. Some possible sources of such a scattering of data are analysed and discussed.
G. Saini, F. Ricca, and A. Nasini, *La ricerca scientifica*, Anno 29 °, No. 7, Luglio 1959.

40 : 14 : 16 : 30

The Diffusion of Impurities into Evaporating Silicon. See Abstr. 349.

40 : 27 : 37 : 47

Materials and Processes of Electron Devices. See Abstr. 356.

41. Metals and Alloys

41

376. Tungsten Zone Melting by Electron Bombardment.
United States. An apparatus for refining tungsten in vacuum by the floating zone method is described. It consists of four components : vacuum system, power supply, anode support, and traversing cathode. Included is a brief résumé on the theory of refining by this technique. Spectrographic analyses along the length of a purified tungsten rod indicate that molybdenum may not be removed by zone refining, but rather by volatilization. Further, X-ray diffraction studies show that tungsten rods purified in this manner are single crystals and these crystals as grown from the melt do not exhibit preferential growth. It is demonstrated, by bending one of the single crystals, that the purified tungsten rods have relatively high ductility. (Author)
R. G. Carlson, *J. Electrochem. Soc.*, **106**, 49–53, Jan. 1959.

42. Glass and Ceramics

42

377. Ceramic Electrical Insulating Materials.
United States. A review is presented of the relative merits of various ceramic insulating materials, particularly electrical porcelain, steatite, and alumina, which is illustrated by a series of microphotographs taken both by optical and electron microscopes. These photographs strikingly illustrate the difference in microstructure, the presence or absence of a glassy phase, and of voids. The following tables, taken from the author's paper, demonstrate the effect of composition and structure on physical and mechanical properties (dielectric properties measured at 1 Mc) :

TABLE I. Properties of Ceramic Materials

	Single crystal Al_2O_3	Glass or porcelain	Steatite	Alumina ceramic
Dielectric loss	2×10^{-5}	1000×10^{-5}	50×10^{-5}	50×10^{-5}
Resistivity at 500 °C	1×10^{11}	1×10^{5}	1×10^{10}	1×10^{10}
Tensile strength	65,000	5,000	10,000	25,000
Flexural strength	115,000	8,000	18,000	50,000
Compressive strength	300,000	50,000	65,000	200,000

Graphs are given for the variation of dielectric constant and loss tangent with temperature (25–500 °C) and frequency (1 Kc–10 KMc) for low-loss steatite. W. H. K.
M. D. Rigterink, *J. Amer. Ceram. Soc.*, **41**, 501–506, Nov. 1958.

TABLE II. Some Properties of High Alumina Ceramic Materials

Material		Mechanical		Electrical		Thermal	
	% Al_2O_3	Compressive strength (lb/in.², 25 °C)	Tensile strength (lb/in.², 25 °C)	Dielectric constant (1 mc., 25 °C)	Dissipation factor (1 mc., 25 °C)	Coefficient of linear expansion (25° to 700 °C)	Softening temperature (°C)
Sapphire (single crystal)	100	30×10^4	6.5×10^4	10.3	0.00004	8.5×10^{-6}	2040
Alumina *A*	99	42×10^4	3.4×10^4	10.0	0.0001	8.0×10^{-6}	>1600
Alumina *B*	97	28×10^4	2.7×10^4	9.5	0.0001	9.0×10^{-6}	>1600
Alumina *C*	96	30×10^4	2.6×10^4	9.0	0.0003	9.0×10^{-6}	>1600
Alumina *D*	94	19×10^4	1.5×10^4	9.2	0.0004	7.3×10^{-6}	>1600
Alumina *E*	85	20×10^4	1.8×10^4	8.2	0.0009	7.9×10^{-6}	1400

42

378. Young's Modulus of Various Refractory Materials as a Function of Temperature.

United States. Young's modulus as a function of temperature was determined by a dynamic method for single-crystal sapphire and ruby and for polycrystalline aluminum oxide, magnesium oxide, thorium oxide, mullite, spinel, stabilized zirconium oxide, silicon carbide, and nickel-bonded titanium-carbide. For the single crystals, Young's modulus was found to decrease linearly with increasing temperature from 100 °C to the highest temperature of measurement. For all the polycrystalline materials, except silicon carbide, stabilized zirconium oxide, and spinel, Young's modulus was found to decrease approximately linearly with increasing temperature until some temperature range characteristic of the material was reached in which Young's modulus decreased very rapidly and in a nonlinear manner with increasing temperature. This rapid decrease at high temperature is attributed to grain-boundary slip. Stabilised zirconium oxide and spinel were found to have the same rapid decrease in Young's modulus at high temperature, but they also had a decidedly nonlinear temperature dependence at low temperature.

(Author)

J. B. Wachtman, Jr., and D. G. Lam, Jr., *J. Amer. Ceram. Soc.*, **42**, 254–260, May 1959.

42

379. Thermal Expansion of Al_2O_3, BeO, MgO, B_4C, SiC, and TiC above 1000 °C.

United States. Thermal-expansion data on Al_2O_3, BeO, MgO, B_4C, SiC, and TiC were obtained to the temperatures where permanent deformation begins, due to sintering or other causes. The thermal expansion for these materials was found to be approximately linear over the measured temperature range. But as a linear extrapolation to room temperature was not possible, the coefficient of thermal expansion is not a constant over this temperature range. The results are compared with the latest published data for each material. The average coefficients of linear thermal expansion are given as follows :

Material	$\times 10^{-6}$	Temp. range (°C)
Al_2O_3	7.5 ± 0.4	1000–1600
BeO	10.1 ± 0.6	1000–2000
MgO	12.6 ± 0.5	1000–2000
B_4C	6.02 ± 0.51	1000–2400
SiC	5.68 ± 0.11	1000–2400
TiC	8.31 ± 0.68	1000–2600

All BeO specimens which were heated to above 2050 °C had a very large expansion. Visual examination of the cooled specimens revealed that they had bent and cracked, the physical dimensions had enlarged, and the color had changed to a bright milky white. A brief discussion of the probable reasons for these changes is given. In the attempt to extend the expansion measurements, the melting point of BeO was obtained. A specimen of hot-pressed BeO melted at 2450 °—30 °C, where as a slip-cast BeO specimen melted at 2470 °—20 °C. (Author)

C. J. Engberg and E. H. Zehms, *J. Amer. Ceram. Soc.*, **42**, 300–305, June 1959.

42

380. Rate of Thermal Dehydration of Muscovite.

United States. The very widespread use of natural mica for vacuum tube spacers warrants a brief abstract of this paper although the experiments on dehydration were carried out in air, not in vacuo. Muscovite contains 4.5 per cent water (b. wt) in its crystal lattice. Unless this water is driven out before using the mica in a vacuum tube, low pressure levels cannot be attained on the pump. It is common practice to fire mica spacers in a hydrogen atmosphere at about 600 °C. Temperatures as high as 900 °C are used in special cases, such as target plates in iconoscopes. 'Between 940 and 980 °C, the muscovite structure is destroyed. If the temperature is kept below 940 °C, no phase change occurs, and the dehydration consists entirely of the expulsion of the hydroxyl ions.' The authors have studied this dehydration in the temperature range 738 to 817 °C by a thermogravimetric method and found that the weight loss Δw is a linear function of the logarithm of time. A derived equation approximating a first-order reaction serves as a good representation of the experimental data. W. H. K.

J. B. Holt, I. B. Cutler, and M. E. Wadsworth, *J. Amer. Ceram. Soc.*, **41**, 242–246, July 1958.

44. Waxes, Lubricants, Cements, Lacquers, Paints, Oils

44

381. Health Legislation Concerning Paint Ingredients.

H. Preuss, *Metal Finishing*, **57**, 68–71, Aug. 1959.

44

382. Exciting Developments in Better Finishing Facilities.

E. A. Zahn, *Indus. Finishing*, 22–32, Aug. 1959.

45. Soldering, Welding, Brazing

45

383. Wetting of Original and Metallized High-Alumina Surfaces by Molten Brazing Solders.

United States. An apparatus using the sessile-drop method is described for determining surface tension and wettability data of liquid-solid systems at elevated temperatures in vacuum and in controlled atmospheres. The relative merits of some of the current methods of metallizing alumina ceramics are evaluated in terms of solder wetting. The wetting by molten brazing metals and alloys is reported as a function of time in terms of contact angle on surfaces of high-alumina ceramics with and without various types of high-temperature metal coatings. The wetting of molten brazing solders on original and metallized surfaces of alumina ceramics has been expressed quantitatively in terms of the angle of contact as a function of time. Complete wetting in all cases by the solders on the sintered nickel layer is attributed to the high surface free energy of solid nickel with respect to the surface energies of the molten solders and the probably lower interfacial free energy between the molten solders and sintered nickel. Consistently lower values of contact angles for the solders on molybdenum-manganese metallizing are due to the solubility of manganese in the brazing metals. In some instances this promoted extensive alloying between the solder and metallizing which often destroyed the bond between the ceramic and base metallizing. Copper solders in combination with tungsten-iron metallizing appears to have a reaction that is sensitive to temperature, within the range investigated, which in turn influences the wetting behavior. The recommendation of a solder and base metallizing combination is not attempted. The choice of a system is referred to the user from the engineering data presented. No one system appears capable of meeting all design applications. There are applications requiring complete wetting in order to cover large areas, as in the case of shielding or in the early stages of producing certain printed circuit patterns. In some sealing operations, however, although adherence is still required, only a nominal wetting may be desired in order better to confine the brazing solder to a limited area. The lack of surface free energy data and incomplete knowledge of the metallurgical reactions involved in these systems make it difficult to interpret their wetting behaviors more fully at this time.

(Author)

J. C. Williams and J. W. Nielsen, *J. Amer. Ceram. Soc.*, **42**, 229–235, May 1959.

Vol. 9 959/60

46. Glass Blowing, Glass-to-metal and Ceramic-to-metal Sealing Techniques

46

384. Fundamentals of Glass-to-Metal Bonding : IV, Wettability of Gold and Platinum by Molten Sodium Disilicate.

United States. Further studies were made on the effect of the nature of the atmosphere on the wetting of gold and platinum by sodium disilicate at 1000 °C. The gases were oxygen, nitrogen, carbon dioxide, helium, argon, water vapor, carbon monoxide, hydrogen, and several mixtures of some of these gases. Data reported were obtained in the pressure range 10^{-5} Torr to approximately 1 Torr. A special experimental apparatus was constructed for this purpose. In this pressure range the results showed that the wetting of gold was unaffected by these atmospheres. The platinum-sodium disilicate contact angle, on the other hand, depended on the nature and pressure of the gas. This angle was affected most by atmospheres of water vapor, carbon monoxide, hydrogen, and oxygen. Water vapor was found to be easily displaced from the metal by oxygen. The results were interpreted on the basis of selective adsorption of the gases at the various metal interfaces and of absorption of oxygen and hydrogen by platinum. (Author)

M. L. Volpe, R. M. Fulrath, and J. A. Pask, *J. Amer. Ceram. Soc.*, **42**, 102–106, Feb. 1959.

46

385. Tension Stresses in Glass Coatings and in Glass-Metal Seals in the Annealing Range.

United States. The strength of glass coatings applied to metals was found to decrease with time at temperatures in the lower annealing range. This decrease is caused by the well-known decrease in volume which glasses undergo at these temperatures. Glasses applied to a metal surface are constrained in directions parallel to the surface, and the decrease in volume thus produces tension strains in these directions. In this temperature range, the production of tension stress due to density increase is partly offset by stress release due to viscous flow. These effects, calculated from measurements of density variation and of stress release in the glass used for coating, were found to indicate variations in glass strength which agreed approximately with values measured by a cross-bending test. Significant tension stresses of similar origin were observed to appear in glass-metal seals during baking in the lower annealing range. (Author)

This investigation was carried out on strips of 430 metal (AISI-430), a glass-sealing alloy containing 16 to 18% Cr, 1% Mn, 0.75% Si, 0.5% Ni, and balance iron. Heavy-gauge strip was coated on one side with thin coatings of glass and then subjected to a bending test, both at room temperature and at 425°C. The smallest tension stress which produced cracks in the glass was observed. In addition to Pittsburgh Plate Glass Company glass No. 5533, used commonly for face plates of TV bulbs, two experimental high-alumina glasses were tested. The reader who is concerned with these effects, which have great practical importance, will find a more recent paper by L. F. Oldfield of great interest. He discusses 'The effects of heat treatments on the thermal expansions of some borosilicate glasses and iron-nickel-cobalt alloys and their significance in the behaviour of glass to metal seals.' (Glastech. Ber., **32K**, V, 1959, V/16-V/25.)

W. H. K.

J. C. Turnbull, *J. Amer. Ceram. Soc.*, **41**, 372–376, Sept. 1958.

47. Outgassing Data, Vapour Pressure Data, Gettering Data

47

386. Carbon as an Indicator of Gas Content of Metallic Tube Elements.

United States. It is shown in this experimental investigation that the gas evolution from anode materials used in the construction of electron tubes is a nearly linear function of the carbon content of these materials. It is thus desirable to keep the carbon content as low as possible, 0.01 or 0.005 per cent being practical values. The main benefit derived from more rigorous outgassing treatment in a reducing atmosphere, such as dry or wet hydrogen, is reflected in greater stability of the tube during life. Prolonged firing of metal parts made from sheet stock results in excessive softening of the material and deterioration of its surface finish. Carbonized anodes cannot be fired for long periods at high temperatures because carbon is then dissolved in the base metal, nickel or steel. Wet hydrogen cannot be used for the firing of carbonized parts as the carbon is lost by reaction with water vapor. It is thus recommended to fire the metal stock in heavier gauges and then roll to final size and carbonize. Tests have shown that this finishing treatment, rolling or carbonizing, has no adverse effect on the gas content. Graphs are presented which show the beneficial effect of prolonged firing in wet hydrogen (1 h at 1000 °C) for plain and nickel-plated steel, both in terms of lower carbon content and lower gas pressure during life. Values for emission from oxide-coated cathodes and transconductance of the tubes made from components so treated were uniformly higher on 500 h life tests when compared with control lots without such specially prepared materials. Gas evolution was measured by the method described in Abstract No. 387. W. H. K.

D. R. Kerstetter, *Sylvania Technol.*, **12**, 26–29, Apr. 1959.

47

387. Measurements of Gas Evolution or Sorption of Anode Materials Under Simulated Life Conditions.

United States. An experimental procedure is described which allows monitoring gas evolution and sorption of electron tube anode materials over prolonged periods of time. A corrugated strip of the material under study is supported by a Kovar wire on a soft-glass header and sealed into a T-9 soft-glass bulb which is sealed on to a trolley exhaust system. A Bayard-Alpert-type ion gauge is attached to the tube containing the sample and both are sealed off after suitable heat treating and pumping. A thermocouple is attached to the sample which is maintained at a temperature of 600 °C during the simulated life test by focusing the beam from a projector lamp with an internal reflector on it while keeping the bulb temperature at 50 °C by forced air cooling. Pressure variation is recorded for a 500 h period for plain steel and nickel-plated steel. For a tube not containing a metal sample, the pressure remains essentially at the 10^{-6} Torr level for the first 10 h, increasing slightly thereafter. Plain steel reaches a maximum pressure of 10^{-4} Torr in about 50 h and then resorbs some of the gas initially released. Nickel-plated steel evolves less gas after some initial bursts in the first few hours and attains a lower pressure after being on test for some 50 h than the one observed initially. W. H. K.

C. H. Rehkopf, *Sylvania Technol.*, **11**, 114–116, Oct. 1958.

47 : 27 : 37 : 40

Materials and Processes of Electron Devices. See Abstr. 356.

49. Miscellaneous Materials and Techniques

49

388. Surface Phenomena Associated with Application of Organic Films to Phosphor Screens.

United States. The use of aluminized cathode ray tube screens has become almost universal in the manufacture of television picture tubes and to a lesser extent in the manufacture of instrument and radar tubes. The well-known technique of aluminizing screens involves the production of a temporary organic barrier layer or film upon which the reflecting aluminum coating may be deposited, usually by evaporation in vacuum. The success of the aluminizing process depends largely on the production of this organic film free from variations in thickness and imperfections which would allow the aluminum to penetrate round the phosphor crystals and so cause local undesirable reductions in the light output from the screen. It is also necessary for this layer to be extremely thin (less than 1 μ) and to be composed of a material

that may be removed from the screen during subsequent baking treatment. Nitrocellulose and methacrylic resins have been found to be suitable film forming materials. Defects in this film produce undesirable blemishes on the finished screen. Certain inherent defects encountered when employing a 'flow filming' technique are described, and the fundamental factors governing their formation and prevention are considered. (Author)

R. W. Dudding and D. J. Finnett, *J. Electrochem. Soc.*, **105**, 388–392, July 1958.

49

389. A Study of the Molded Nickel Cathode.
United States. Molded nickel cathodes have been used as electron emitters in various electron tubes where they offer advantages over conventional oxide-coated cathodes when severe operating conditions are encountered. They can intermittently be exposed to air (as required in demountable systems) and do not suffer unduly from ion bombardment when operated in a poor vacuum or in the presence of intense electric fields. The details of the manufacturing process for a particular type of a molded cathode are described in this paper. The cathode pellet, which is attached to a cylindrical nickel sleeve, consists of two layers. The lower layer, about 0.045 in. thick, contains nickel powder and an activator (ZrH_2) in the weight proportions 99 : 1. The upper part of the pellet, which is 0.003 to 0.005 in. thick, contains nickel powder (69 per cent by weight), alkaline earth carbonates (30 per cent) and an activator (1 per cent). The nickel-powder is fired at 600 °C for 15 min in a hydrogen atmosphere (−10°C dew point). All powders are thoroughly dried before use. The cathode pellet is formed and pressed into the sleeve at a pressure of 80 tons/in.² in a single step by use of a hardened steel die and hydraulic press. Active material is then removed from the edge of the cathode sleeve by rubbing with aluminum-oxide paper. The most important step in the processing of the cathode is sintering. After sintering, the cathodes are stored in evacuated ampules until ready for use. Data on pulsed emission are presented which indicate that 17 a/cm² was obtained in a test diode with a 0.015-in. cathode-to-anode spacing when 1000V was applied to the anode while the cathode was maintained at a brightness temperature of 850 °C. These values are equivalent to an emission of about 2 to 10 a/cm² under field-free conditions. W. H. K.

C. P. Hadley and W. G. Rudy, *J. Electrochem. Soc.*, **105**, 395–398, July 1958.

49 : 31

Titanium Coatings on Molybdenum Wire. See Abstr. 364.

Vol. 9 959/60

Basic Science and Engineering

51. Physics, Astronomy, Geophysics

51

390. Experimental Determination of the Oscillator Strength of the First Negative Bands of N_2^+.
R. G. Bennett and F. W. Dalby, *J. Chem. Phys.*, **31**, 434–441, Aug. 1959.

51 : 19

Phase Charge on Reflection from Evaporated Chromium Films. See Abstr. 354.

51 : 34

Research in Space. See Abstr. 369.

51 : 34

Effect of the Solar Wind on the Lunar Atmosphere. See Abstr. 370.

56. Electrical Engineering, Electronic Circuits

56

391. Design of Broadband Ceramic Coaxial Output Windows for Microwave Power Tubes.
United States. Special demands upon output windows are imposed by broad-band microwave power tubes. Ceramic materials with relatively high dielectric constants, such as aluminum oxide bodies, have favorable mechanical, thermal, and dielectric loss properties for coaxial output seals. However, constant-Z_0 matching methods, in which the diameter of the center conductor is drastically undercut as it passes through the window, lead to much reduced power-handling capability. Broadband matching of coaxial ceramic windows is accomplished by undercutting the center conductor much less than required for constant Z_0, and extending the undercut a significant distance each side of the ceramic. Analysis of such a design is described. Calculated and experimental data show that extremely broad frequency bands with low VSWR, together with high power-handling capability, can be obtained with useful ceramic thickness. Examples of 7/8-in. coaxial output window design for d.c. to S-band frequencies are presented, with indicated maximum VSWR's of 1.2 or less. (Author)

R. R. Moats, *Sylvania Technol.*, **11**, 86–90, July 1958.

Papers to be Published in Future Issues

D. J. Santeler. Vacuum process evaluation.

H. Batey. Carbon contamination of glassware used for vacuum purposes.

R. Hawley. Vacuum as an insulator.

J. D. Mellor and D. F. Ohye. An ampoule freeze-dryer for microbiological research.

N. A. Florescu. Theoretical developments of the vapour vacuum pump.

K. G. Gunther. Ein Partialdruckvakuummeter nach dem Prinzip des elektrischen Massenfilters.

W. Becker. Reibungsvakuummeter " R E V A ".

A. M. Samarin. Vacuum Metallurgy.

R. N. Bloomer. On the general principles of chemical and ionic pumping.

Klaus H. Behrndt and Richard A. Jones. A comparison between the evaporation characteristics of a crucible and a ring source.

EDITORIAL NOTE

The index to the articles and the abstracts for Volume IX will be issued as a loose leaflet with the publication of Volume X. Being a loose leaflet, it can then be bound with the corresponding numbers of the current volume.

Vo
9
1959

END OF VOL.

Vol.
9
959/60